UNIVERSIDAD COMPLUTENSE DE MADRID

FACULTAD DE FARMACIA

TESIS DOCTORAL

Diseño y síntesis de compuestos basados
en indol contra la leishmaniasis

Design and synthesis of indole-based
compounds against leishmaniasis

MEMORIA PARA OPTAR AL GRADO DE DOCTORA

PRESENTADA POR

Miriam Gómez Benmansour

DIRIGIDA POR

José Carlos Menéndez Ramos
Simone Lucarini

© Miriam Gómez Benmansour, 2026

UNIVERSIDAD COMPLUTENSE DE MADRID

FACULTAD DE FARMACIA

Programa de doctorado de Química Médica (D9A9)

TESIS DOCTORAL

DISEÑO Y SÍNTESIS DE COMPUESTOS BASADOS EN INDOL CONTRA LA LEISHMANIASIS

DESIGN AND SYNTHESIS OF INDOLE-BASED COMPOUNDS AGAINST LEISHMANIASIS

MEMORIA PARA OPTAR AL GRADO DE DOCTORA

PRESENTADA POR

MIRIAM GÓMEZ BENMANSOUR

DIRECTORES:

José Carlos Menéndez Ramos

Simone Lucarini

Madrid, 2025

TABLE OF CONTENTS

“What you do makes a difference,
and you have to decide what kind of difference you want to make.”

Jane Goodall

“Nothing in life is to be feared;
it is only to be understood.”

Marie Curie

A mis dos ángeles de la guarda,
que me cuidan desde el cielo,
la abuelita Tere y Mamie

AGRADECIMIENTOS

Jamás pensé que llegaría el momento de agradecer a todas las personas que me han acompañado en esta aventura de la tesis. Gracias a todos los que habéis formado parte en mayor o menor medida estos años, a todos con los que he reído y compartido momentos bonitos y sobre todo a los que han estado en los momentos duros. Gracias a todos los que me habéis ayudado con cualquier cosa. Gracias Madrid, por tu buen ambiente y por tus noches interminables. Grazie Urbino, dovevi solo essere un posto di passaggio ma sei entrata nel mio cuore e ti ci porterò per sempre.

En primer lugar, me gustaría empezar agradeciendo a mis directores de tesis, José Carlos y Simone Lucarini. **José Carlos**, ya tuve la oportunidad de conocerte mientras hacía el TFM, y gracias a ti he podido hacer esta tesis doctoral. Gracias por tener siempre la puerta de tu despacho abierta para lo que podamos necesitar. Gracias por estar siempre dispuesto a encontrar un sentido a las locuras que salían de mis reacciones, y listo para consultar los libros más polvorientos de la biblioteca para encontrar una explicación lógica a mis mecanismos. Gracias por las innumerables cañas siempre que había algo que celebrar, y por abrirnos las puertas de tu casa. Mucha gente querría tener un jefe como tú. Grazie al prof. **Lucarini** per avermi accolto senza appena conoscermi e darmi l'opportunità di fare la tesi di dottorato nel suo laboratorio.

Tengo que agradecer también a muchos otros profesores de la universidad. **Maite**, gracias por tu tranquilidad y la paz que transmites, y por ser esa compañía desde el despacho cuando las tardes del laboratorio se convertían en noches. Gracias **Pilar** por la energía que desprendes y la alegría que transmites. Gracias **Mercedes** por ser esa persona con la que hablar y criticar a cualquier hora, y por ser tan cañera (de tomar cañas) como yo. Gracias **María** por ser fuente inagotable de chocolate. Grazie al prof. **Piersanti** per gli aperitivi per qualsiasi motivo. Grazie **Francesca Bartoccini** per averci supportato (soprattutto quando dovevamo chiedere solventi e reagenti). Grazie **Michele Retini**, sei una persona incredibile con un cuore immenso, grazie per essere una persona così a la mano e grazie per essere sempre disponibile per dare una mano, anche quando tutto il resto andava male. Ti auguro davvero il meglio nella tua vita, perché te lo meriti.

Claramente el trabajo de laboratorio no sería posible sin el trabajo de los técnicos. **Marisa** y **Rocío**, gracias por no salir corriendo cada vez que iba a pediros cosas y gracias por tener

siempre lo que necesito. Gracias a todos los técnicos del **CAI de RMN**, por hacerme todas esas muestras interminables que ocupaban noches enteras y por tener que venir más de una vez por mi culpa a poner el inyector. Gracias a los técnicos del **CAI de masas**, por confirmarme las locuras que salían de mis reacciones. Grazie **Giulia** per darmi mille volte le chiavi degli armadietti e soprattutto per farmi capire che non aveva senso lavorare male se potevamo avere quello che serviva. Grazie **Anna** e **Pontellini**, ormai un team inseparabile, per tutti i protoni e carboni fatti (che non sono pochi).

Lo más difícil de un doctorado no son los días interminables en el laboratorio, ni la frustración cuando los experimentos no salen, lo más difícil del doctorado es sin duda la burocracia. La burocracia casi me deja sin doctorado allá por diciembre de 2022 y la burocracia casi me deja sin cotutela en más de una ocasión. Me he encontrado a lo largo de estos tres años con gente de distintas secretarías muy poco empática y con pocas ganas de trabajar. Sin embargo, dos personas se han salvado de esta generalización. Grazie **Eugenio Pieri**, se oggi sono qui è sicuramente grazie a te, grazie delle migliaia di chiamate e e-mail, e grazie di avere la risposta per ogni singolo dubbio burocratico con cui mi trovavo. Gracias también a **Macarena**, por hacer del terrible proceso de depositar la tesis un camino un poco más fácil.

Si miro hacia atrás y busco dónde empezó mi vida de laboratorio, me toca viajar a Estrasburgo, al TFG. Merci **Mustafa Terezen**, tu as été le premier à m'aider dans un laboratoire. Merci pour ta patience et pour tout ce que j'ai appris.

Mi siguiente experiencia en el laboratorio fue en el TFM. Tengo clarísimo que mi vida no hubiera sido igual si al llegar al laboratorio, el "marrón" de encargarse de la chica esa a la que no le salía nada del molino, no te hubiera caído a ti, **Cris**. Gracias por la paciencia, por pasar horas y días perdiendo tiempo a mi lado cuando no salía nada. Gracias por compartir mi pasión por la mayonesa. Gracias por haber llorado conmigo (cero dramas, era solo bromoacetato), por las horas delante del molino, por tu alegría y sobre todo por tu sinceridad. Eres genial, y esta tesis no hubiera sido posible si no hubiera dado mis primeros pasos contigo.

Después del TFM, la vida me lanzó a la aventura del doctorado, en un país nuevo, lleno de gente nueva. Aunque los últimos años los había pasado fuera de mi ciudad, todo lo nuevo

comienza con un poco de miedo. Quando sono arrivata ad Urbino, la paura è passata subito. Ho trovato gente incredibile, sia a casa che al lab.

Grazie Viale Federico Comandino per tutte le coinquiline che ho avuto. Grazie **Sara**, per tutte le chiacchierate, pianti, risate e ore passate a guardare TikTok insieme. Grazie per essere la mia fedele compagna di feste e dire di sì al Bunker ogni giovedì e ogni sabato per tutto un anno (se conoscevamo a memoria tutte le canzoni e addirittura l'ordine, c'era un motivo). Grazie per farmi ridere quando c'era bisogno, e grazie anche di sapere usare sempre le parole giuste quando tutto andava un po' peggio. Ti voglio tanto bene. Grazie **Giulia**, anche tu fedele compagna di feste e balletti di TikTok, grazie di saper trasmettere agli altri la felicità. Grazie anche di tutte le ricette che trovavi su Instagram e facevano del pranzo della domenica un ristorante Michelin (devi ancora migliorare i falafel…). Sei una persona incredibile. Grazie **Cesaria** di portare a casa un po' di pulizia e sistemazione e di essere un po' la nostra mamma, ma grazie anche di tutte le risate quando partiva la follia che c'è dentro di te. A voi tre, grazie di essermi venute a trovare a Valencia, ma preferirei non rivedere i vostri piedi…**Leti**, la dolce Leti, grazie della tua dolcezza, di essere naturale e di avere un grande cuore. **Maria Sara**, grazie delle feste e di tutte le risate insieme, sei incredibile.

Nel mio secondo anno, sempre a Federico Comandino sono arrivate Marghe, Bea e Imma. **Marghe**, grazie di essere sempre il nostro fornitore di tisane (con e senza melatonina) e della nostra relazione per il WiFi. **Bea**, grazie di tutte le serate ma soprattutto di truccarmi sempre perché sai che sono completamente incapace. Grazie **Imma** di essere stata la nostra mamma, grazie di tutti i piatti della domenica che rimettevano a posto tutta la settimana.

Ma non solo a casa ho trovato gente incredibile, anche al lab ho trovato colleghi che sono diventati amici. Grazie **Alessandro Buono**, fedele compagno in questa avventura del dottorato, grazie di essere stato il primo a farmi vedere Urbino, e di avermi fatto vedere come sei. Grazie di tutte le conversazioni e risate in lab, soprattutto quando la follia e la disperazione sembravano vincere. Grazie di non avermi mai ucciso anche se mi tenevo tutti i palloni e la mia parte della cappa non era del tutto sistemata… Dal primo giorno fino all'ultimo, mi mancherai, compagno di cappa, ti auguro il meglio. **Michele Verboni**, da te ho imparato tante cose, che non potrei mai scriverle tutte. Grazie delle tue conoscenze sulle

parolacce, ma anche sui bisindoli e soprattutto grazie alle tue conoscenze di zuccheri. Non ti scordare mai, TT. Grazie **Diego Olivieri** della tua serietà nei momenti in cui c'era bisogno, ma di fare sempre morire da ridere nei contesti sociali. So che per te uscire dal tuo lab e venire a lavorare con noi è stato traumatico, ma io mi tengo un ricordo molto bello di questo periodo. Grazie di essere sempre disponibile per tutto. A voi tre, mi porto il VG nel cuore.

Sempre nel lab12, ho avuto l'opportunità di incontrare altre belle persone. **Cece**, te sei incredibile, ma i tuoi dolci lo sono anche di più. Grazie di averci tenuti sempre saziati, di portare sempre cibo con qualsiasi scusa e di essere rimasto vicino anche quando la tesi era finita. Ora non più Cece, ma prof. Cece, ti auguro il meglio in questa avventura che inizia. Ho avuto l'opportunità di conoscere molto brevemente **Martina C**, ma anche se poco tempo, ho sentito che ci capivamo dal primo giorno, grazie di aprirmi le porte di casa tua e anche a te, grazie degli infiniti piatti e dolci che hai cucinato in appena un mese che sono stata lì. Voi due mi avete dato tanto da mangiare, ma il regalo più incredibile me l'ha dato senza dubbi **Martina B**, grazie della piccola famiglia di Dinoventosa, il mio dinosauro è stato un fedele compagno di scrittura di tesi e me lo porterò ovunque vada, grazie.

Insieme a me, altri pazzi hanno deciso di iniziare il percorso del dottorato, i miei colleghi del XXXVIII ciclo. Grazie **Francesca Diotallevi** per condividere tutte le mie idee folle, essere sempre pronta a fare qualsiasi scherzo e per tutte le pause caffè. Grazie **Giovanni Leoni** per la tua follia, sempre garanzia di rissate. Grazie, **Vittorio Ciccone**, per le interminabili notti girando tutti i bar di Urbino, sono ancora impressionata. Grazie **Adrrrrrriano Rechia** di tutti i Camparini bevuti e della tua gentilezza. Spero ti piaccia quanto a me questo periodo a Madrid. Grazie **Matteo Gregori** di tutti i viaggi al Gala per gli Italian Brainroots e di tutti i passaggi ad Urbino quando ci siamo trasferiti in mezzo al nulla.

In mezzo tra l'Italia e la Spagna si trovano diverse persone. Grazie **Sara Sasso** (ormai il tuo cognome), per le lunghe giornate insieme (literalmente codo a codo) e per il tuo supporto quando credevo di impazzire. Grazie delle lunghe chiacchiere girando Valencia e delle serate a Madrid. Non ti ringrazio però dell'incendio che ci ha fatto pulire tutta una mattinata. Grazie **Regina**, nell'ambito lavorativo grazie a te il mio capitolo 3 ha molto più senso. Non ti dimenticare mai, non avere risultati, sono risultati. Grazie di tutto il tuo lavoro. Fuori dal lab, grazie di tutte le serate che non finivano mai e di essere sempre pronta a tutto. Grazie, **Chiara**, di essere sempre pronta a fare festa e a qualsiasi piano. Grazie di avermi fatto

scoprire il persichetto, tornerò a Terni per riprenderlo. Grazie **Olga**, la persona più fredolosa al mondo che ha deciso di passare l'inverno a Madrid… Grazie di tutte le tue focacce, che mi facevano sentire ancora vicino all'Italia.

Durante el TFM en Madrid conocí a gente increíble, con quien tuve la suerte de coincidir dos años más tarde. **Jose**, gracias por ser una de las personas más importantes de este último periodo en Madrid, y gracias por todas las fuerzas que me dabas cuando estaba fuera. Gracias por el increíble fin de semana en Valencia sin parar de hablar y por haberme dejado conocerte un poco más. Gracias también por toda la ayuda química que me has dado.

Josemi, fiel compañero del lab2, durante el TFM y también durante la tesis. Gracias por todas las ideas y planes locos y por decir siempre sí a todo (era el verano del sí). No te agradezco haberme dejado medio calva allá por agosto de 2022, pero sí te agradezco las horas pasadas delante de mis espectros, para intentar entender qué había salido esta vez de mi reacción.

Gracias **Ángel**, una persona que desde fuera puede dar un poco de miedo (y cuando lo conoces también), pero que siempre está dispuesto a echar una mano o una cerveza. Gracias **Noe**, por las conversaciones sobre absolutamente cualquier cosa, por las visitas a Pescara y también a Urbino, espero que este nuevo periodo te traiga la tranquilidad que necesitas. Mi querido **Manolito**, muchas gracias por ser fiel compañía hasta tarde cada vez que se me iba de las manos alguna columna y por estar siempre disponible para escuchar mis quejas, te mando muchos ánimos en este final de tesis. Gracias **Olmo**, durante la tesis no pude compartir laboratorio contigo, pero sí largas charlas filosóficas sobre la vida.

La mejor persona que os podréis encontrar en este laboratorio es sin duda **Álvaro**. Gracias por tu corazón puro, por ser tan buena persona y por estar disponible siempre que lo necesitara. Te deseo lo mejor en esta futura etapa de papá.

Cuando llegué esta vez al laboratorio, tuve la oportunidad de conocer algunas personas nuevas: Gracias, **Ana,** por las noches de fiesta y por estar siempre abierta a cualquier plan. Gracias también por tus croquetas españolas y holandesas y por todos los cafés de media mañana contemplando las montañas.

Gracias **Marta**, compi del lab2 hasta el final, cuando todos los demás nos habían abandonado. Gracias por no matarme en esos últimos meses estresantes de tesis, cuando mi cabeza era lo único que estaba en su sitio. **Isa** y **Paula**, pack inseparable, gracias por traer energía y alegría al laboratorio. Isa (ahora que por fin te diferencio) mucho ánimo en esta etapa que empiezas, tú puedes con todo. **Mario**, gracias por ser como eres y no odiarnos a todos cuando nos metíamos contigo, que el doctorado no te haga cambiar, eres una persona increíble. Gracias **Masi** por tener siempre una sonrisa para todos, te deseo lo mejor en esta etapa de doctorado, mucho ánimo!

Gracias también a esos compis del lab5, **Merchán**, gracias por ser como eres y que te dé todo exactamente igual, de mayor quiero ser como tú. Gracias **Dani Gorras** por tu compañía y conversación en las largas tardes/noches de laboratorio.

Gracias también a toda esa gente que ha pasado más brevemente por los laboratorios pero que han hecho los días más amenos: Oscar, Dani Bolas, Giada, Francesco Rossi…

Aunque estos años he estado muy ocupada con esta tesis, he tenido un poquito de tiempo para pasarlo con mi gente. Gracias a los **Castores III** por encontrar un ratito para vernos, aunque cada uno haya acabado en un lugar distinto, es para mí un honor ser el segundo Castor doctor, mucho ánimo a los que están en el proceso. A mis compis **Piratas**, gracias por ser la desconexión que necesitaba en los momentos más estresantes de la tesis, nos vemos pronto, en Madrid, Cuenca, Navalconcejo o en nuestra casa, el Pirata.

Gracias a mis **Place**, **Vicky** y **Ana**, a mi lado desde el instituto. Gracias por todas las discomóviles, los planes de heladito y Harry Potter, todas las cervezas con bravas y por los festis juntas.

Gracias **Elena**, por abrirnos las puertas de tu casa, en Madrid y en Bilbao, y por cuidarnos y cocinarnos siempre como la mami del grupo que eres.

En este punto llegan para mí, las personas más importantes de estos últimos años. A vosotros, esta tesis es tan vuestra como mía:

Gracias **Ana**, por estar a mi lado desde el principio de la carrera hasta hoy, cuando por fin acaba esta etapa. Gracias por ser la mejor compi para todo, de piso, de fiestas, de lloros, de festis, de chismes y de planes aleatorios. Gracias por estar siempre a mi lado, aunque

a mí se me dé muy bien eso de irme a muchos kilómetros de distancia, te siento siempre cerca. Gracias por todos esos consejos que nos vendemos pero que luego para nosotras no tenemos. Gracias por ser la mejor.

A mis **padres**, los culpables de que hoy esté donde estoy. Gracias por haberme enseñado las maravillas del mundo de la ciencia (aunque me haya acabado yendo a la competencia de la orgánica). Gracias por haberme dado, durante toda mi formación académica, la tranquilidad de tener que pensar solo en estudiar. Gracias por los sacrificios, por llevarme a cualquier hora a cualquier sitio, incluso a Estrasburgo o a Urbino.

Grazie **Ale**, fedele compagno di vita questi ultimi due anni, di tutto. Avrei bisogno di scrivere altre 300 pagine e ancora mi mancherebbe spazio per ringraziarti per tutto quello che hai fatto per me. Grazie di stare quando va tutto male, di saper portarmi su, ma grazie anche di fare parte dei miei momenti più belli. Grazie della tua passione per la chimica e di tutto quello che mi hai insegnato. Grazie anche alla tua famiglia, di farmi sentire a casa. Grazie della pazienza, che a me manca sempre. Grazie di starmi vicino anche a 6000 km, ma torna presto.

A todos, también a los que pueda haberme olvidado en estos agradecimientos, si estoy hoy donde estoy es por vosotros.

GRACIAS

Miriam

LIST OF ABBREVIATIONS

AD: Alzheimer's Disease

AFR: African Region

AmB: Amphotericin B

AMR: Region of the Americas

ATL: American Tegumentary Leishmaniasis

BBB: brain-blood barrier

BRS-3: Bombesin receptor subtype-3

CADD: Computer-Aided Drug Discovery

CDC: cross-dehydrogenative coupling

*Cen*1: *Centrin* 1

CFR: Case Fatality Rate

CL: Cutaneous Leishmaniasis

CRK12: cycle-2-related kinase 12

CYP: cytochrome P

DCL: Diffuse Cutaneous Leishmaniasis

DCM: dichloromethane

DDs: diazadienes

DDT: Dichlorodiphenyltrichloroethane

DIC: Disseminated Intravascular Coagulation

DIM: diindolylmethane

DMF: dimethylformamide

DNA: Deoxyribonucleic Acid

DNDi: Drugs for Neglected Diseases Initiative

EMR: Eastern Mediterranean Region

ENSO: El Niño Southern Oscillation

EtOAc: ethyl acetate

FCCT: fluorescent cell coculture assay

Fe-SOD: Fe-superoxide dismutase

GI: gastrointestinal

HAT: Human African Trypanosomiasis

HECT-CL: Hand-Held Exothermic Crystallisation Therapy for CL

HFD: high-fat diet

HIV: Human Immunodeficiency Virus

HLH: hemophagocytic lymphohistiocytosis

HMBC: Heteronuclear Multiple-Bond Correlation

HMQC: Heteronuclear Multiple-Quantum Coherence

HR: histamine receptors

HTS: High-Throughput Screening

I3C: indole-3-carbinol

ICZ: Indolo(3,2-b)carbazole

IUPAC: International Union of Pure and Applied Chemistry

LAmB: Liposomal Amphotericin B

LCL: Localised Cutaneous Leishmaniasis

LN: Lipid Nano-capsule

MA: Meglubine Antimoniate

MCL: Mucocutaneous Leishmaniasis

MeOH: methanol

MF: Miltefosine

MRSA: methicillin-resistant *Staphylococcus aureus*

MYA: Millions of years ago

NBS: *N*-bromosuccinimide

NMR: nuclear magnetic resonance

NOE: nuclear Overhauser effect

PAHO: Pan American Health Organisation

PD: Pentamidine

PKDL: Post-Kala-azar Dermal Leishmaniasis

PM: Paromomycin

PN: Polymeric Nanoparticle

RFHT: Radio-Frequency-Induced Therapy

RNA: Ribonucleic Acid

ROS: Reactive Oxygen Species

RTB: rotatable bond number

SAR: Structure-Activity relationship

SDS: sodium dodecyl sulphate

SEAR: South-East Asia Region

SL: Sphingolipid

SNAP: S-Nitroso-N-Acetyl Penicillamine

SSG: Sodium Stibogluconate

THF: tetrahydrofuran

THP-1: Human Leukemia Monocytic Cell Line

TosMIC: tosylmethyl isocyanide

TPSA: topological polar surface area

TryR: Trypanothione reductase

VL: Visceral Leishmaniasis

VZV: varicella Zoster virus

WHO: World Health Organisation

ENGLISH SUMMARY

Leishmaniasis is a neglected tropical disease produced by *Leishmania* protozoan parasites, transmitted by the bite of infected female sandflies. The disease infects more than 12 million people worldwide and threatens additional hundreds of millions of people, primarily in the tropics and subtropics. Leishmaniasis manifests in a variety of clinical forms, ranging from self-healing cutaneous leishmaniasis to the fatal visceral form if untreated. Despite decades of use, current chemotherapy is limited to a few drugs such as pentavalent antimonials, amphotericin B, miltefosine, and paromomycin. However, these drugs typically have serious drawbacks such as relevant side effects, high costs, long treatment duration, and, most importantly, an increasing prevalence of drug-resistant strains. Thus, the search for new, effective, and safe therapeutic agents is an urgent need.

Among the many chemical scaffolds that have been screened for antiparasitic activity, indole derivatives are worth noting for their rich spectrum of biological activities and ability to bind to many biological targets. Over the last decade, several studies have reported the promising activity of indole-based molecules against different *Leishmania* species. Natural indole alkaloids, as well as synthetic derivatives such as bisindoles, indole-imidazoles, and others, have demonstrated potent antileishmanial effects both in vitro and in vivo. Therefore, the design and synthesis of new indole-derived compounds is a rational and attractive option in the search for new antileishmanial drugs.

In this context, the present thesis aims at identifying new antileishmanial compounds by designing, synthesising, and biologically investigating three groups of indole-based analogues: indole-imidazole hybrids, bisindoles, and indole-isoindolinones.

Different indole-imidazoles have been synthesised following a previously reported procedure in the literature. However, this route presents limitations in the variability of imidazole substituents. In order to improve this limitation, two other synthetic routes were investigated. The first one, based on the Van Leusen reaction, resulted in a single analogue due to insurmountable limitations of the methodology. A new optimised

procedure involving the alkylation of preformed imidazoles with 3-(2-iodoethyl)-1*H*-indole allowed the synthesis of new derivatives, increasing the covered chemical space.

Four different families of bisindoles have been synthesised to evaluate their biological activity against leishmaniasis. These families are: amines, amides, esters, and carboxylic acids. The introduction of glycosylated substituents has been performed in order to improve pharmacokinetics and activity.

The chemistry of indole-isoindolinone derivatives has been studied, allowing synthesising three different families of compounds: di-substituted, imines and di-substituted alkoxy derivatives.

A graphical abstract of this thesis is presented below:

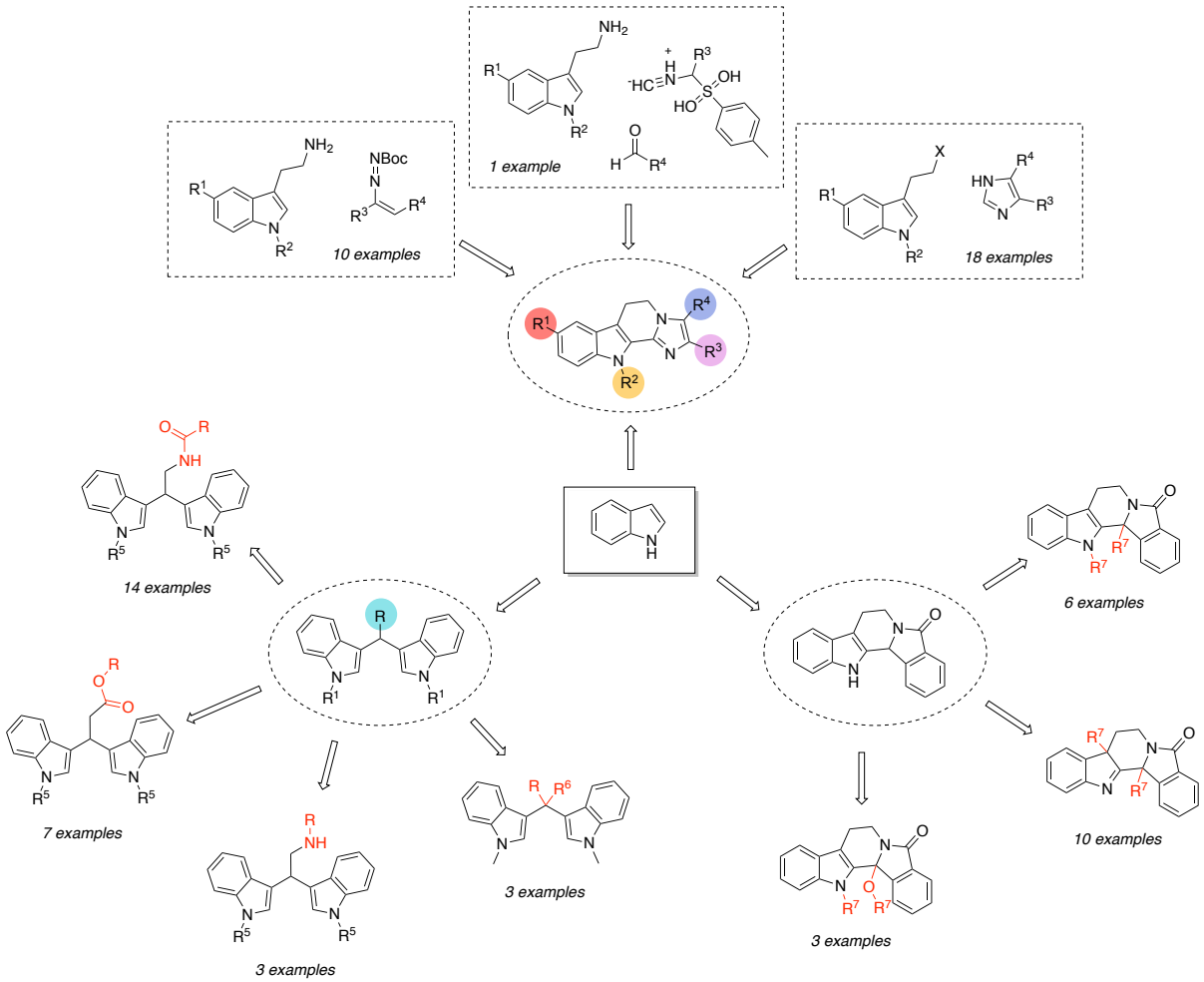

RESUMEN EN ESPAÑOL

La leishmaniasis es una enfermedad tropical desatendida causada por el parásito protozoario *Leishmania*, transmitida por la picadura de la hembras infectadas de mosquitos flebotominos. Afecta a más de 12 millones de personas en todo el mundo y amenaza a cientos de millones más, principalmente en las regiones tropicales y subtropicales. La leishmaniasis se presenta con diversas formas clínicas, desde la leishmaniasis cutánea autolimitada hasta la forma visceral, que resulta mortal si no se trata. La quimioterapia actual se limita a unos pocos fármacos, como los antimoniales pentavalentes, la anfotericina B, la miltefosina y la paromomicina. Sin embargo, estos suelen tener efectos secundarios graves, un alto costo, una larga duración del tratamiento y, lo que es más importante, su uso ha dado lugar a un progresivo desarrollo de cepas resistentes. Por lo tanto, la búsqueda de agentes terapéuticos nuevos, eficaces y seguros es una necesidad urgente.

Entre las numerosas estructuras químicas evaluadas por su actividad antiparasitaria, los derivados del indol destacan por su amplio espectro de actividades biológicas y su capacidad para unirse a múltiples dianas biológicas. Durante la última década, diversos estudios han reportado la prometedora actividad de moléculas basadas en indol contra diferentes especies de *Leishmania*. Los alcaloides indólicos naturales, así como derivados sintéticos como los bisindoles, los indolimidazoles y otros, han demostrado potentes efectos antileishmania tanto in vitro como in vivo. Por lo tanto, el diseño y la síntesis de nuevos compuestos derivados del indol constituyen una opción racional y atractiva en la búsqueda de nuevos fármacos antileishmania. En este contexto, la presente tesis tiene como objetivo identificar nuevos compuestos antileishmania mediante el diseño, la síntesis y la investigación biológica de tres grupos de análogos basados en indol: híbridos de indol-imidazol, bisindoles e híbridos indol-isoindolinonas.

Se han sintetizado diferentes indol-imidazoles siguiendo un procedimiento previamente descrito en la literatura. Sin embargo, esta ruta presenta limitaciones en la variabilidad de los sustituyentes del imidazol. Para superar esta limitación, se investigaron dos rutas sintéticas alternativas. La primera, basada en la reacción de

Van Leusen, dio como resultado un único análogo. Un nuevo procedimiento optimizado, que involucra 3-(2-yodoetil)-1*H*-indol e imidazoles preformados, permitió la síntesis de nuevos derivados, ampliando el espacio químico.

Se sintetizaron cuatro familias diferentes de bisindoles para evaluar su actividad biológica contra la leishmaniasis. Estas familias son: aminas, amidas, ésteres y ácidos carboxílicos. La introducción de sustituyentes glicosilados se ha realizado para mejorar la farmacocinética y la actividad.

Se ha estudiado la química de los derivados de indol-isoindolinona, lo que ha permitido sintetizar tres familias diferentes de compuestos: derivados disustituidos, iminas y alcoxi disustituidos.

A continuación se presenta un resumen gráfico de esta tesis:

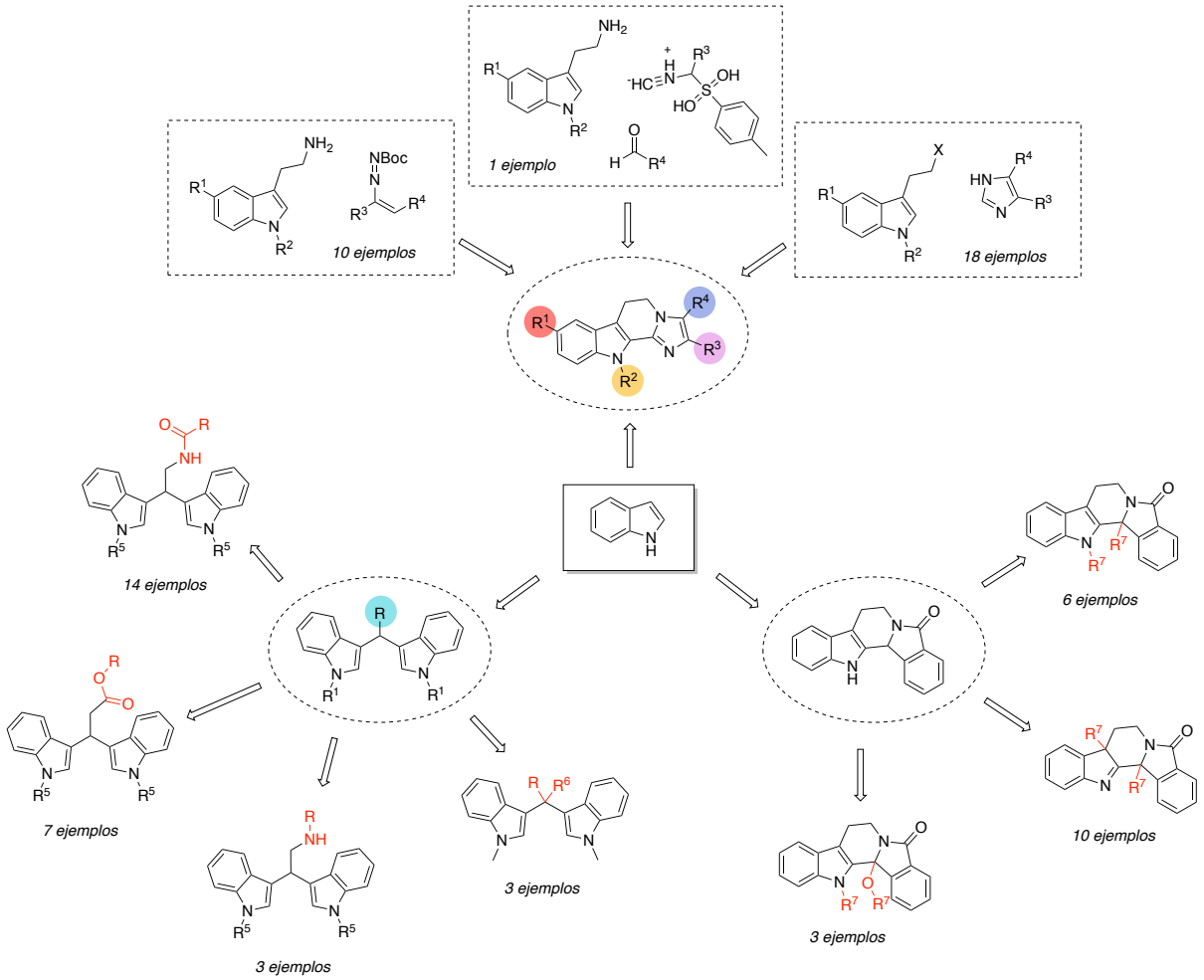

RIASSUNTO IN ITALIANO

La leishmaniosi è una malattia tropicale trascurata causata da protozoi del genere *Leishmania*, trasmessa attraverso la puntura di femmine infette di flebotomi. La malattia colpisce oltre 12 milioni di persone nel mondo e ne minaccia centinaia di milioni, soprattutto nelle regioni tropicali e subtropicali. Essa si manifesta con diverse forme cliniche, che spaziano dalla leishmaniosi cutanea, generalmente autolimitante, alla forma viscerale, letale se non trattata. L'attuale chemioterapia contro la leishmaniosi si basa su un numero limitato di farmaci, tra cui gli antimoniali pentavalenti, l'amfotericina B, la miltefosina e la paromomicina. Tuttavia, tali trattamenti presentano numerosi svantaggi, tra cui gravi effetti collaterali, costi elevati, lunga durata della terapia e, soprattutto, la crescente insorgenza di ceppi resistenti ai farmaci. Pertanto, la ricerca di nuovi agenti terapeutici efficaci, sicuri e accessibili rappresenta una priorità nella chimica farmaceutica e nella scoperta di nuovi farmaci antileishmaniosi. Tra i numerosi scaffold chimici la cui attività antiparassitaria è stata analizzata, i derivati indolici sono degni di nota per il loro ricco spettro di attività biologiche e la capacità di legarsi a numerosi bersagli biologici. L'anello indolico è un'impalcatura eterociclica privilegiata nella maggior parte dei prodotti naturali e delle molecole biologicamente attive, ed è di particolare interesse in chimica farmaceutica.

Nell'ultimo decennio, diversi studi hanno riportato la promettente attività di molecole a base di indolo contro diverse specie di *Leishmania*. Gli alcaloidi indolici naturali, così come i derivati sintetici come bisindoli, indolo-imidazoli e altri, hanno dimostrato potenti effetti antileishmaniali sia in vitro che in vivo. Pertanto, la progettazione e la sintesi di nuovi composti derivati dall'indolo rappresentano un'opzione razionale e interessante nella ricerca di nuovi farmaci antileishmaniali. In questo contesto, la presente tesi mira a identificare nuovi composti antileishmaniaci attraverso la progettazione, la sintesi e lo studio biologico di tre gruppi di analoghi a base di indolo: ibridi indolo-imidazolo, bisindoli e isoindolinoni indolici.

Diversi derivati indolo-imidazoli sono stati sintetizzati seguendo una procedura precedentemente riportata in letteratura. Tuttavia, tale metodologia presenta alcune limitazioni in termini di variabilità dei sostituenti sull'anello imidazolico. Per superare questa restrizione, sono state esplorate due ulteriori vie sintetiche. La prima, basata

sulla reazione di Van Leusen, ha consentito purtroppo l'ottenimento di un solo analogo. Una nuova procedura ottimizzata, che impiega il coupling tra il 3-(2-iodoetil)-1*H*-indolo e imidazoli preformati, ha invece permesso la sintesi di nuovi derivati, ampliando significativamente il loro spazio chimico.

Sono state inoltre sintetizzate quattro diverse famiglie di bisindoli al fine di valutarne l'attività biologica contro la *Leishmania*. Le classi di composti preparate comprendono ammine, ammidi, esteri e acidi carbossilici. Sono stati inoltre sintetizzati alcuni bisindoli glicosilati per migliorare le loro proprietà farmacocinetiche e farmacodinamiche.

Infine, è stata approfondita la chimica dei derivati indolo–isoindolinonici, come bioisosteri degli indolo–imidazoli, che ha offerto la possibilità di ottenere tre diverse famiglie di questi composti da testare: derivati disostituiti, alcossi-disostituiti e immine.

Di seguito è riportato un abstract grafico riassuntivo della presente tesi:

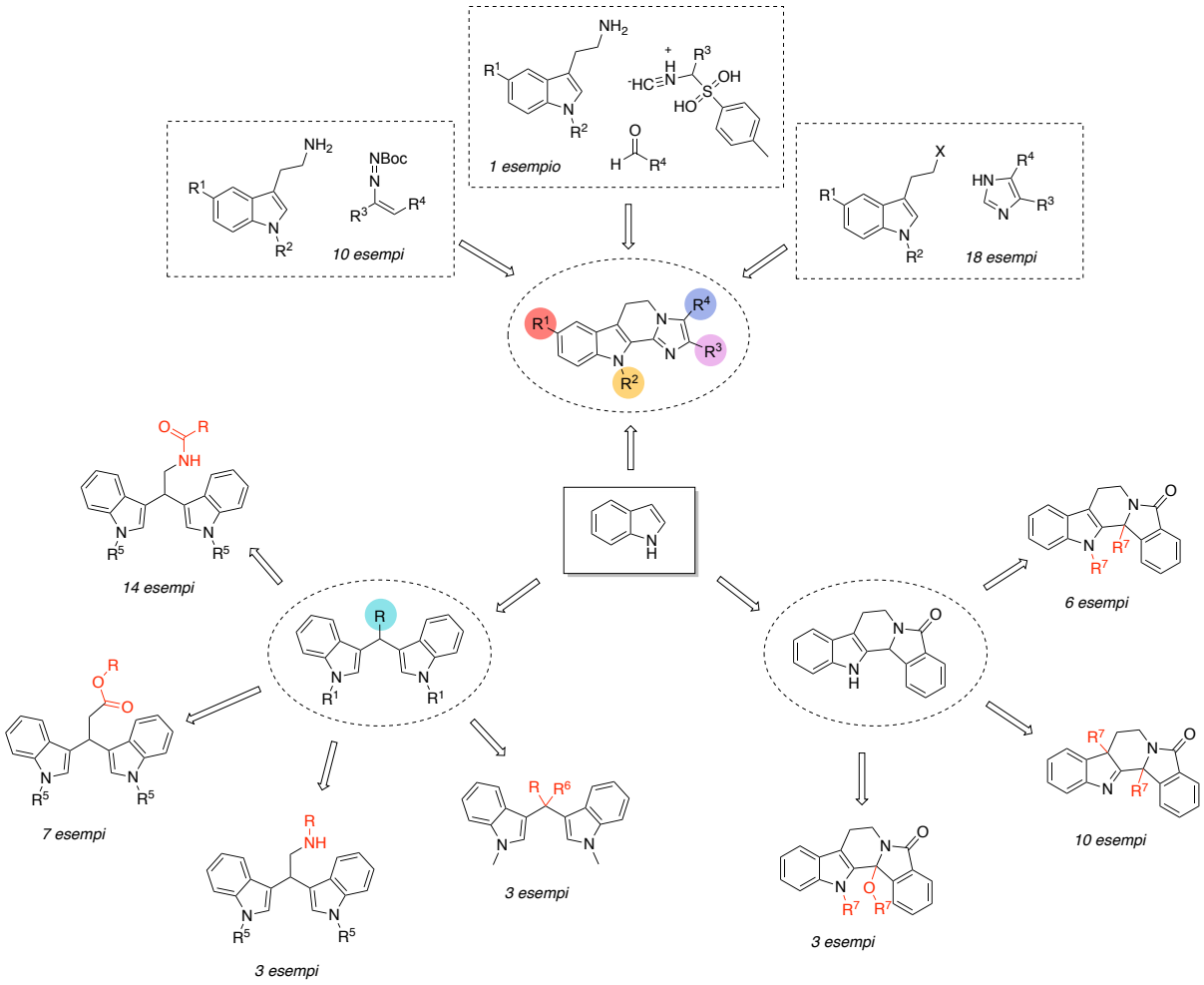

CHAPTER 1. INTRODUCTION

1.1. LEISHMANIASIS

Leishmaniasis is a neglected parasitic disease, second only to malaria for mortality, endemic in almost 100 countries. The most severe form of this disease, visceral Leishmaniasis (VL), also known as kala-azar, infects 300.000 patients per year, out of which 40.000 die worldwide. So far, no vaccine against human Leishmaniasis is on the market. Current treatments[1] are very limited and are based on only a few drugs, which often exhibit important side effects, high production costs and, except for oral miltefosine and topical paromomycin, require parenteral administration and therefore hospitalisation of the patient. Furthermore, drug resistance is frequent and threatens the effectiveness of chemotherapy. The discovery of new anti-leishmanial drugs is, thus, essential.

1.1.1. History of Leishmaniasis

Fossil evidence confirms the existence of *Leishmania*-like parasites in the prehistoric Era. Various stages of *Paleoleishmania proterus* were found inside a 100-million-year-old burmese amber containing an extinct sand fly. *Paleoleishmania neotropicum* in *Lutzomyia adiketis* was found in a Dominican amber dated 20-30 million years ago (MYA). This finding supports a digenetic life cycle involving vertebrates, suggesting that *Leishmania* parasites evolved during the Mesozoic era, probably before the breakup of Pangea.[2]

There are three main hypotheses about the geographical origin of *Leishmania*. The Palearctic hypothesis proposes its origin in Eurasia during the Palaeocene with a further spread to the Nearctic through the Bering land bridge.[3] The Neotropical hypothesis suggests a South American origin, but fossil and evolutionary data do not support this hypothesis.[4,5] The supercontinent hypothesis advocates an evolution of *Leishmania* in Godwana with further differentiation across Africa and South America after continental separation.[6]

Leishmania has a long human history. Its presence has been described in ancient Mesopotamian texts, and deoxyribonucleic acid (DNA) was found in the analysis of ancient Egyptian mummies.[7] A description of a skin disease that could correspond to

Leishmaniasis has also been found in the Eber papyrus, around 1550 BC, and in America, there is evidence of Leishmaniasis in ceramic and skeletal remains in pre-Columbian cultures.[8,9]

From the 16th century forward, diverse forms of Leishmaniasis were observed. Reports from the Middle East described Cutaneous Leishmaniasis (CL) with detailed clinical descriptions.[10] In the Americas, Spanish chroniclers described Mucocutaneous Leishmaniasis (MCL).[11] Visceral Leishmaniasis (VL) was not described until the 19th century in India, where kala-azar became a big epidemic.[12]

In 1900, pathologist William Boog Leishman found ovoid bodies in spleen samples of a dead soldier but mistakenly identified them as trypanosomes.[13] A few weeks later, the Irish physician Charles Donovan published a paper about similar ovoid bodies found in other spleen samples but from native Indian individuals.[13] In 1903, the medical doctor Donald Ross concluded that the ovoid bodies found previously by Leishman and Donovan were a novel protozoan organism that he proposed to call *Leishmania donovani*.[14]

1.1.2. Etiology

1.1.2.1 Etiologic agent

Leishmaniasis is a parasitic disease found in over 100 countries worldwide.[15] It is caused by different protozoan parasites belonging to the family *Trypanosomatidae* and the genus *Leishmania*.[16] To date, around 30 different species of *Leishmania* protozoa have been identified, of which 20 are pathogenic to mammals, and 18 of those have zoonotic potential.[16]

1.1.2.2 Responsible species

As mentioned, 18 species of *Leishmania* cause a clinical disease. Table 1.1[2] lists these species, indicating their geographical distribution and the clinical forms that they cause.

Table 1.1. Overview of the clinical disease-causing Leishmania species, their respective disease and distribution.[2]

SUBGENUS	SPECIES	OLD/NEW WORLD	CLINICAL DISEASE	DISTRIBUTION
Leishmania	*L. aethiopica*	OW	LCL, DCL	East Africa (Ethiopia, Kenya)
	L. amazonensis	NW	LCL, DCL, MCL	South America (Brazil, Venezuela, Bolivia)
	L. donovani	OW	VL, PKDL	Central Africa, South Asia, Middle East, India, China
	L. infantum (syn. *L. chagasi*)	OW, NW	VL, CL	Mediterranean countries (North Africa and Europe), Southeast Europe, Middle East, Central Asia, North, Central and South America (Mexico, Venezuela, Brazil, Bolivia)
	L. major	OW	CL	North and Central Africa, Middle East, Central Asia
	L. mexicana (syn. *L. pifanoi*)	NW	LCL, DCL	USA, Ecuador, Venezuela, Peru
	L. tropica	OW	LCL, VL	North and Central Africa, Middle East, Central Asia, India
	L. venezuelensis	NW	LCL	Northern South America, Venezuela
	L. waltoni	NW	DCL	Dominican Republic
Viannia	*L. braziliensis*	NW	LCL, MCL	Western Amazon Basin, South America (Guatemala, Venezuela, Brazil, Bolivia, Peru)
	L. guyanensis	NW	LCL, MCL	Northern South America (French Guinea, Suriname, Brazil, Bolivia)
	L. lainsoni	NW	LCL	Brazil, Bolivia, Peru
	L. lindenbergi	NW	LCL	Brazil
	L. naiffi	NW	LCL	Brazil, French Guinea
	L. panamensis	NW	LCL, MCL	Central and South America (Panama, Columbia, Venezuela, Brazil)
	L. peruviana	NW	LCL, MCL	Peru, Bolivia
	L. shawi	NW	LCL	Brazil
Mundinia	*L. martiniquensis*	NW, OW	LCL, VL	Martinique, Thailand

1.1.2.3 Vector

The only vector responsible for transmitting Leishmaniasis is the female sand fly (Figure 1.1).[15,17]

Figure 1.1. Sand fly that transmits Leishmaniasis.[18]

Only 98 of the more than 800 known sand fly species have been proven as vectors for the disease. These vectors belong to the genera Phlebotomus (42) and Lutzomyia (53). Sand flies undergo metamorphosis with four life stages (Figure 1.2): egg, larva, pupa and adult.[15] The eggs hatch between 4 and 20 days after oviposition and give bith to larvae that have 4 stages (instars I to IV). This larva stage usually lasts for 20-30 days. After that, pupae take from 6 to 13 days to emerge.[19] They are usually active during night-time, and they have limited ability to move.[17]

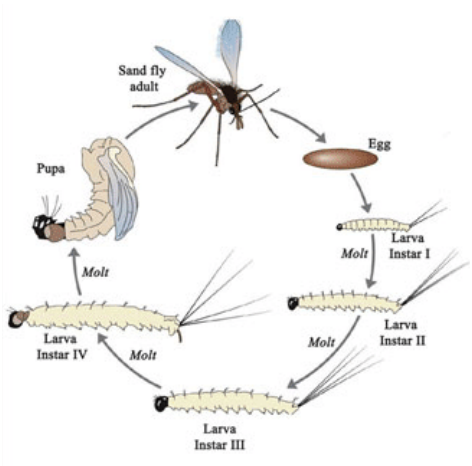

Figure 1.2. Lifecycle stages of sand fly.[20]

1.1.2.4 Parasite morphology

There are two forms of *Leishmania* parasites: amastigotes and promastigotes. Promastigotes are extracellular, elongated, motile and are found in the gut of sand flies, while amastigotes are intracellular, round-shaped, aflagelate, non-motile and reside in macrophages of vertebrates.[21]

The first differentiation step (Figure 1.3) occurs soon after the ingestion of contaminated blood by the sand flies. Due to changes in some of the conditions, amastigotes differentiate into procyclic promastigotes. After 48 hours, these procyclic promastigotes slow their replication and differentiate into strong motile forms called nectomonad promastigotes that later on differentiate into shorter parasite forms called leptomonad promastigotes. At this moment, two things can happen: eventually leptomonad can differentiate into a less studied form called haptomonad promastigotes or into metacyclic promastigotes. Metacyclic promastigotes have a small body and a long flagellum, which allows fast motility. At this point, the sand fly will probably have a new intake of blood, which will give nutrients for metacyclic promastigotes to differentiate into retroleptomonads, which are replicative. Then, they re-differentiate into the metacyclic promastigote form, increasing the quantity and quality of these promastigotes.[19]

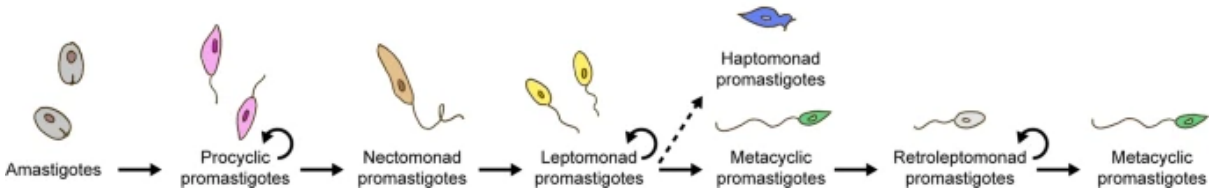

Figure 1.3. Linear life cycle of the different forms of the Leishmania parasites. Circular arrows mark the replicative parasite forms.[19]

1.1.2.5 Biological cycle

Leishmania has a digenetic life cycle (Figure 1.4). One stage takes place as an extracellular stage in the invertebrate host, as explained in the precedent section. The other stage of *Leishmania* is intracellular in the vertebrate host. In this stage, when *Leishmania* enters the human host, macrophages try to attack it by forming reactive oxygen and nitrogen species,[17] but the *Leishmania* parasite produces a protease that

lowers the macrophage activity. Once these promastigotes are phagocytosed, they differentiate into amastigote form, which proliferates, invading different parts of the body such as the spleen, liver, lymph node and other tissues.[16,22]

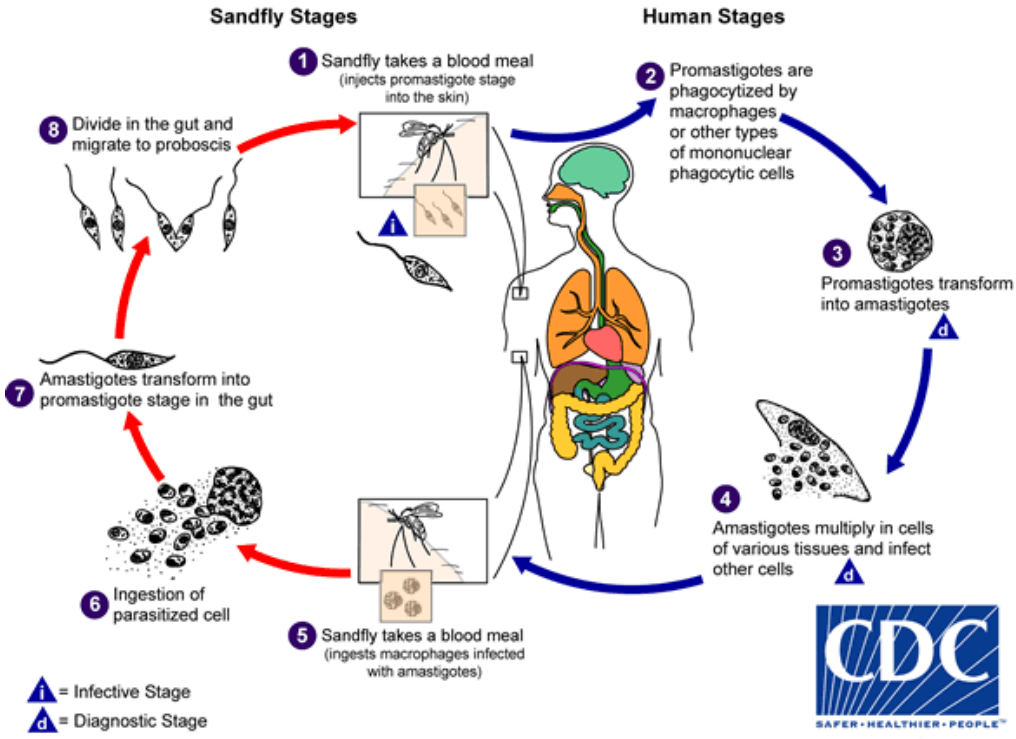

Figure 1.4. Digenetic life cycle of Leishmania.[23]

1.1.2.6 Reservoirs

Attending to the reservoir of *Leishmania*, infection can be zoonotic or anthroponotic. Humans are the only source of parasite transmission for anthroponotic infection.[15] They are considered a prime parasite reservoir in East Africa and South East Asia.[24] The zoonotic infection occurs when animals are the reservoirs of the parasite. These include rock hyraxes, dogs, cats, foxes, rodents, monkeys and other domestic animals.[16]

1.1.2.7 Transmission mechanisms

The main mode of transmission of *Leishmania* species is through the bite of blood-feeding female *Phlebotomine* sand flies.[25] This transmission depends on the moment in the life cycle of the parasite. Transmission through non-sand fly vectors is unlikely to happen except in specific canine maintenance environments.[16]

1.1.3. Epidemiology

1.1.3.1 Clinical forms and their symptoms

Leishmaniasis can usually be categorised into three different forms: Cutaneous Leishmaniasis (CL), Mucocutaneous Leishmaniasis (MCL) and Visceral Leishmaniasis (VL).

a) Cutaneous Leishmaniasis:

Cutaneous Leishmaniasis is the mildest and most common form of Leishmaniasis. It usually affects areas of the body exposed to insect bites.[16,17] The infection can either remain asymptomatic or have an incubating period of 1 to 12 weeks.[26] CL is caused by different *Leishmania* species, and two different groups of pathologies are found: Localised Cutaneous Leishmaniasis (LCL) and Diffuse Cutaneous Leishmaniasis (DCL).[27]

In LCL, the number of lesions varies between 1 and 20.[16,17] It usually begins with localised swelling and itching where the bite has taken place. The lesion may evolve to a papule, then a vesicle and finally a pustule.[16] When this pustule breaks, it creates a round ulcer with thick borders and a necrotic base. These ulcers range from 0.5 to 3 cm and are usually painless, but secondary infections may cause pain.[28] CL can be considered acute or chronic depending on the lesions. Acute CL lasts less than 30 days, and lesions are insect bite-like. Chronic CL lasts more than 30 days and includes infection of the lesion. The progression of the ulcer depends on species, parasite load and immunocompetency of the patient. Without the appropriate treatment, these lesions tend to take months to heal.[27]

DCL is characterised by anergy, which means a lack of cellular immune response to parasite antigens.[16] This lack of antigens allows the spread of the parasite through tissue, lymph and blood, resulting in lesions in the majority of the skin. The formed nodules may or may not ulcerate, beginning on the face and spreading to the extremities. Lymphedema and lymphadenopathy can also be symptoms of DCL.[16]

b) Mucocutaneous Leishmaniasis:

Mucocutaneous Leishmaniasis usually emerges after more than 5 years of evolution of CL. This progression is only observed in 1-10 % of CL patients and is influenced by genetic factors being prevalent in immunocompromised patients as dissemination from the bite site to the mucosa typically occurs via the lymphatic system.[26,29] MCL is characterised by progressive ulceration and destruction of the oral, nasal and pharyngeal mucosa affecting in some cases the soft palate, larynx, and throat, and causing facial deformations.[30] MCL does not affect the bones, but if untreated, it can cause diarrhoea, pneumonia and tuberculosis that can lead to death.[31] Some of the most common symptoms are nasal discharge, inflammation and stuffiness, respiratory complications and mucosal bleeding. Unlike CL, MCL requires treatment.[32]

c) Visceral Leishmaniasis:

Visceral Leishmaniasis (also known as kala-azar) is the most fatal form of leishmaniasis, with a mortality rate of 95 % if untreated.[33] The term "*kala-azar"*, also known as "*black sickness*", is mostly used in the South Asia region, deriving from the grey discolouration of the skin that some patients develop, probably due to an increase in the levels of adrenocorticotropic hormone.[34] *L. donovani, L. infantum, L. tropica* and *L. martiniquensis* cause visceral Leishmaniasis.[35]

The incubation phase usually lasts between 3 and 8 months, but it can be extended up to 24 months.[16] Symptoms of VL depend on the interaction between the infectious features and the host immune response, and can go from mild to moderate to severe clinical symptoms.[36] Moreover, VL may also behave as asymptomatic or latent and may not manifest until years later if an immunodeficiency develops.

Clinical manifestations include: fever, loss of appetite, weight loss, splenomegaly, hepatomegaly, high liver enzymes, hypoalbuminemia, hypergammaglobulinemia,[36–38] and pancytopenia, which is related to prolonged illness.[39] Fever is usually remittent with two spikes per day, but can be intermittent. 45 % of children with VL have splenic nodules.[40] If untreated, VL typically causes mortality, either from the disease or through its side effects. These can include disseminated intravascular coagulation

(DIC), hemophagocytic lymphohistiocytosis (HLH), post-kala-azar dermal Leishmaniasis (PKDL) and hepatic failure.

DIC is a condition characterised by the simultaneous formation of small blood vessel clots and widespread bleeding.[41] HLH is a potentially fatal disorder caused by the overactivation and proliferation of T lymphocytes and macrophages. It affects up to 28 % of VL patients.[42,43] PKDL affects 5-10 % of kala-azar patients and may appear months to years after VL infection. Its main symptoms are macular, papular or nodular rashes in the face, upper arms, trunk or other areas.[44,45]

1.1.3.2 Geographic distribution

Leishmaniasis is endemic in 99 countries (Figure 1.5): in 90 countries for CL (Figure 1.6) and 80 countries for VL (Figure 1.7), while in 71 countries both clinical forms (CL and VL) are endemic.[46] These countries include many regions of Africa, the Americas, the Middle East and central Asia, with cutaneous and visceral Leishmaniasis being the most common forms.[47]

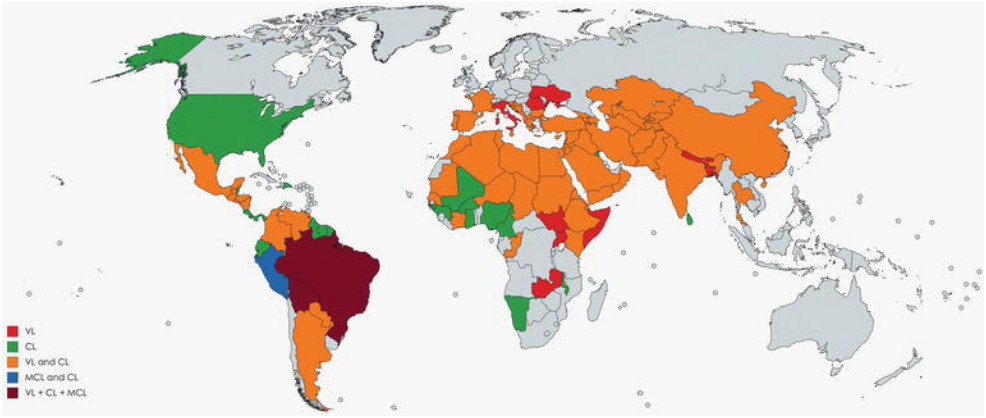

Figure 1.5. World distribution of VL, CL and MCL.[48]

Several countries in East Africa, namely Sudan, Ethiopia, Kenya, Uganda and Somalia are severely affected by VL. Sudan had the biggest number of reported cases of VL in 2023 (Figure 1.9).[38,49] In West Africa, diverse forms of Leishmaniasis have been reported. Cutaneous Leishmaniasis is endemic in Mauritania, Gambia, Nigeria, Senegal, Cameroon and Ghana. In Senegal, only MCL has been reported and in Togo and Burkina Faso, only VL.[50]

In the Middle East, Syria has historically been endemic for CL. During the last years, there has been a significant increase in CL cases also in Afghanistan and Pakistan, with these countries together accounting for more than 70 % of global CL cases (Figure 1.8), and nearly 200.000 reported cases in 2023.[49,50]

The Indian subcontinent has a high incidence of VL, with cases in India, Bangladesh and Nepal.[15] In Europe, the number of cases of VL and CL remains low, with most cases reported in Spain and Italy.[49]

While CL is endemic in the United States, VL is not considered endemic.[50] Across the rest of the American continent, a general reduction in the cases of CL and VL has been observed over the last years. However, there is a notable rise in VL cases in Argentina and Paraguay, while CL cases have increased in Argentina, Costa Rica, Ecuador, Mexico and Suriname.[46,51] MCL remains a major public health challenge in some South American countries with the highest number of reported cases since 2012, especially in Peru, Bolivia and Paraguay. Despite the overall decline in VL and CL, VL remains a serious concern in Brazil, which has accumulated more than 90 % of the VL cases in the Americas (Figure 1.9). Additionally, Brazil and Peru accumulate more than 50 % of CL cases in the Americas (Figure 1.8).[49,51]

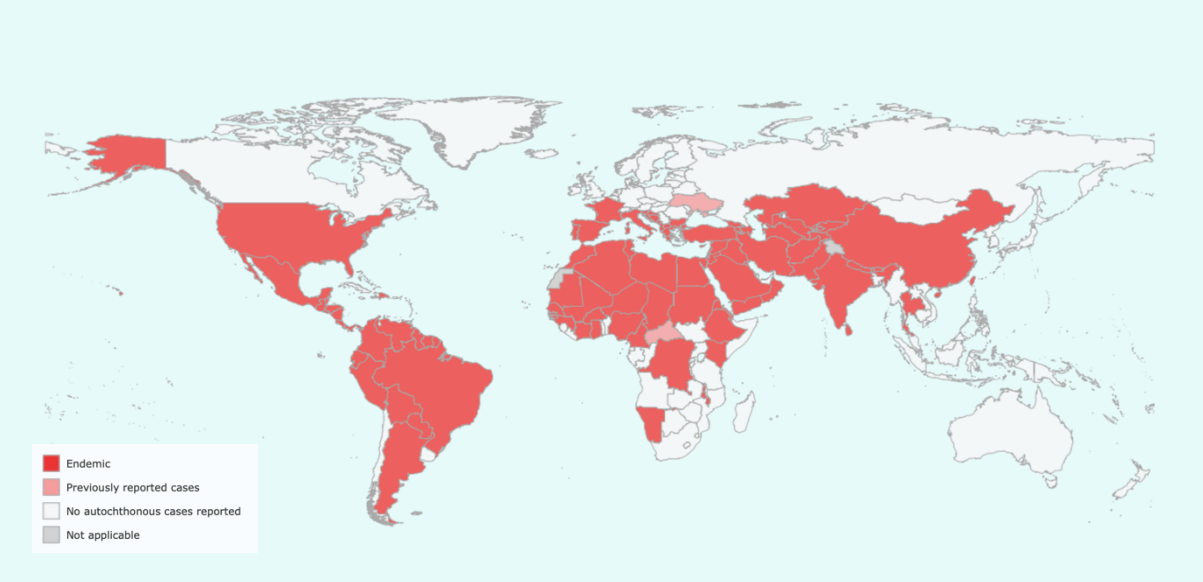

Figure 1.6. Status of endemicity of Cutaneous Leishmaniasis in 2023.[49]

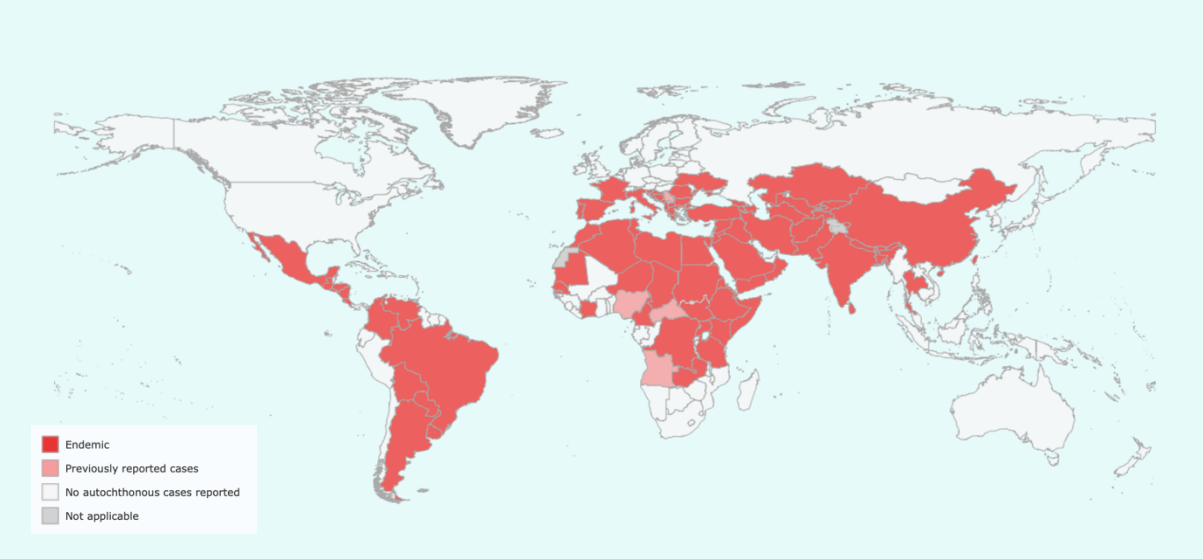

Figure 1.7. Status of endemicity of Visceral Leishmaniasis in 2023.[49]

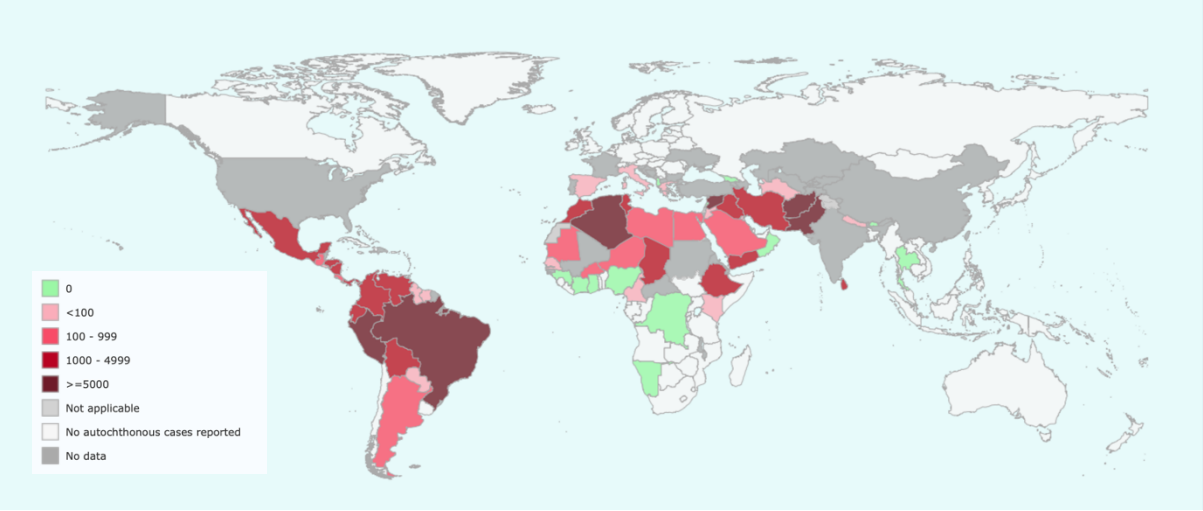

Figure 1.8. Number of cases of Cutaneous Leishmaniasis reported in 2023.[49]

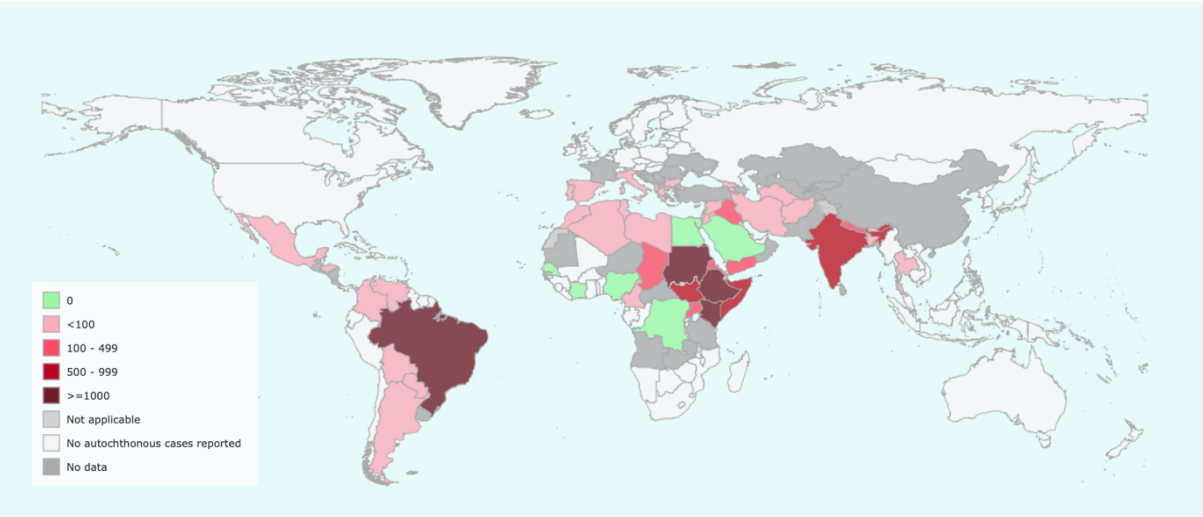

Figure 1.9. Number of cases of Visceral Leishmaniasis reported in 2023.[49]

1.1.3.3 High-risk population

Leishmaniasis mostly occurs in developing countries and is influenced by demographic, environmental, and socioeconomic factors.[15,16,27,50] Adults are more susceptible than children, mainly due to increased outdoor exposure. In particular, young adult males are also more frequently affected because of biological and immunological differences.[27,52–55]

Specific occupations such as agriculture and farming are associated with higher exposure, particularly in environments near rice fields or where animals are kept close to humans. Farmers often wear clothing that leaves a high area exposed to sand fly bites.[56,57]

Infection risks are also increased by poor housing and inadequate sanitary conditions.[16,50] In many rural areas, inadequate sanitation, including poor waste management, sewage disposal, and drainage, creates environments favourable for sand flies.[27,50] Houses built with mud walls or grass roofing that can be found in poor communities often serve as sand fly habitats. Also, overcrowded living spaces attract sand flies as they offer a large biomass.[27]

Socioeconomic data reflect the vulnerability as a large proportion of VL patients live below the poverty line (with a daily income under 1 US$).[58]

Even though adults are more affected, children under 10 years of age are among those at risk due to an underdeveloped immune system, lack of acquired immunity and higher rates of malnutrition.[34]

Co-infection of Leishmaniasis and human immunodeficiency virus (HIV) also poses a serious clinical challenge. This co-infection has been reported in more than 45 countries in 2021, with high burdens in Brazil, Ethiopia and Bihar (India).[50] Individuals co-infected with HIV and Leishmaniasis face a significant risk of developing full-blown disease along with higher mortality rates.[49,50]

This situation is due to the immune suppression, which contributes to the reactivation of latent infections and increases the vulnerability to new infections.[27] Leishmaniasis and HIV reinforce one another, creating a clinical challenge to the treatment as they lead to higher drug toxicity, the need for specialised medical services, long-term follow-up and limited treatment options.[38,51]

In the Americas, the rate of VL-HIV co-infection has been increasing since 2018, with a peak in 2023, accounting for 19 % of VL cases.[51]

1.1.3.4 Environmental factors

Leishmaniasis is a climate-sensitive disease as vectors, pathogens and hosts are influenced by environmental and ecological changes. Changes in temperature, precipitation and humidity directly affect the transmission dynamics and disease distribution.[27,50,59]

Fluctuations in temperature can either inhibit or enhance the development of *Leishmania* promastigotes and may help in the spread of the disease in previously non-endemic areas.[27,50]

The seasonality of sand flies plays a crucial role in the transmission of the disease. For example, *Phlebotomus argentipes*, a major vector in India, is most active from June to September, when temperatures are around 27 and 31°C.[60,61] Unfortunately, some *Leishmania* species, such as *L. braziliensis* and *L. infantum,* may complete their

life cycles across a broad range of temperatures as long as the sand fly survival is not compromised.[62]

In Colombia, Panama and Brazil, sand fly densities and CL incidences were related to El Niño Southern Oscillation (ENSO), showing a relation between Leishmaniasis and interannual climate events.[63,64]

Ecological disturbances, such as urbanisation, deforestation or expansion of agriculture into arid or semi-arid areas, have been directly related to an increase in Leishmaniasis risk. In regions with dense vegetation, there is a higher risk of transmission, probably due to the abundance of rodent reservoirs and sand fly breeding sites.[65,66]

Furthermore, long-term climate change has provoked the geographical expansion of leishmaniasis. For example, in northern Italy, previously non-endemic areas have become endemic because of the colonisation of the sand fly vectors.[67]

1.1.3.5 Trends over time and outbreaks

Among the 99 countries considered endemic for Leishmaniasis, a number of high-burden countries contribute disproportionately to the global sum, considering high-burden countries those that report more than 2500 CL cases or 100 VL cases per year. Pertaining to this classification, we can find 25 countries: 14 that focus on VL and 12 on CL, with Brazil included in both.[68]

The geographical distribution of Leishmaniasis shows “hotspots”. In 2023, there were 272.098 new CL cases reported (mainly autochthonous) and 11.922 new VL cases (also mostly autochthonous). The Eastern Mediterranean Region (EMR) stands as the epicentre of CL, accounting for 81 % of all global cases.[69] For VL, EMR together with the African Region (AFR) account for 79 % of cases globally.[69]

Historical data show varying trends in Leishmaniasis incidence over the years. Over the past 25 years, as shown in Figure 1.10, there has been an overall increasing trend for CL cases, reaching a maximum of cases in 2019. The COVID-19 pandemic caused

a temporary decrease in reported cases, but during the following years the number of cases returned near to pre-pandemic values.[49,69]

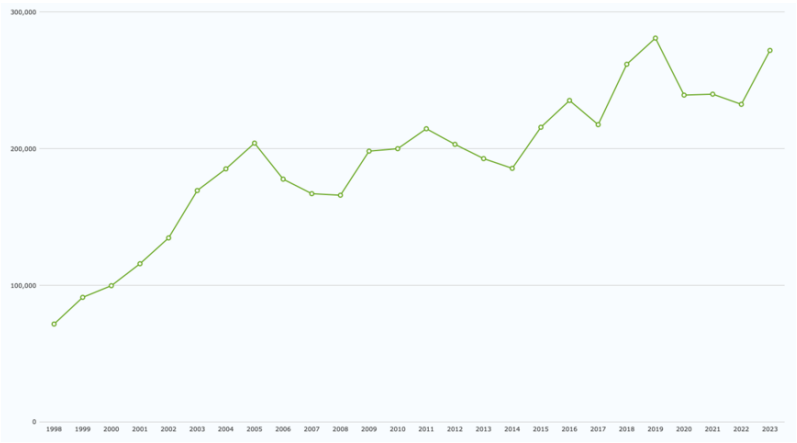

Figure 1.10 Number of CL cases reported worldwide from 1998 to 2023.[49]

For VL, the global trend shows a reduction of 62 % of cases from 2014 (Figure 1.11). This reduction is especially marked in the South-East Asia Region (SEAR), where there has been a reduction of 90 % of cases since 2014 (Figure 1.12), thanks to the elimination initiatives. On the contrary, the AFR has shown a recent light increase in VL from 2020 (Figure 1.12).[49,70]

As mentioned before, the majority of reported cases were autochthonous; however, there is a small but important fraction of imported cases. In 2023, these imported cases represented 0.14 % of global CL cases and 1.3 % of global VL cases. The majority (94 %) of the imported CL cases were reported from EMR (81 %) and the Region of the Americas (AMR) (13 %).[69]

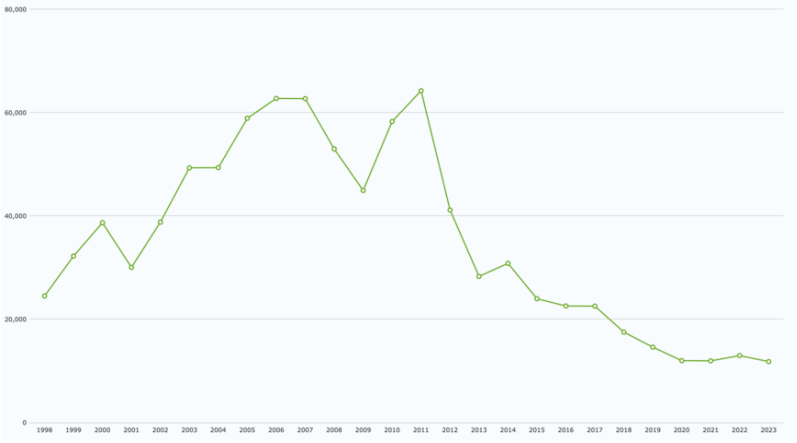

Figure 1.11. Number of VL cases reported worldwide from 1998 to 2023.[49]

Outbreaks remain a concern. In 2006, an outbreak of more than 1000 VL cases was reported in the Bakool region.[71] In 2014, for the first time, AFR reported more VL cases than SEAR (Figure 1.12) due to outbreaks in Kenya and South Sudan.[68] In 2022, a suspected outbreak among the nomadic population was reported from South Omo (Ethiopia) with 239 cases, where 59.4 % of the infected people were under 15 years of age. Also in 2022, an outbreak of CL was reported in Balochistan (Pakistan) with more than 8000 cases in just a few days.[70]

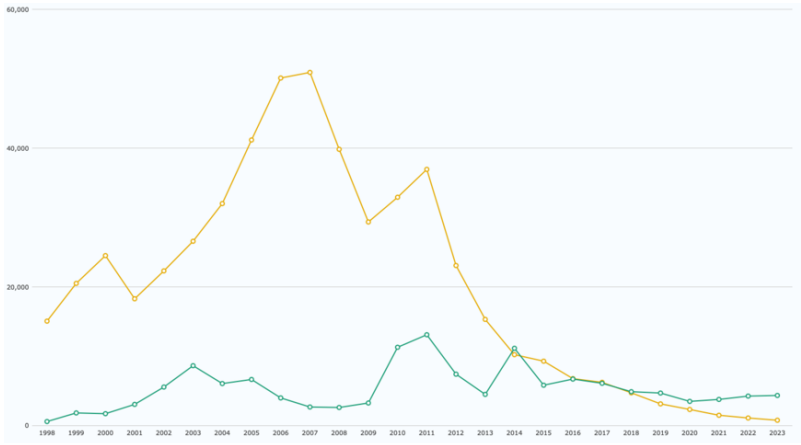

Figure 1.12. Number of VL cases reported in the AFR (green) and the SEAR (yellow) from 1998 to 2023.[49]

1.1.3.6 Mortality rate

A total of 4383 deaths were reported between 2014 and 2023, of which 374 were reported in 2023 in all types of VL patients. These deaths came from 14 countries, with Brazil (174), Sudan (94) and Ethiopia (37) being the most affected.[69] In 12 of these countries, the case fatality rate (CFR) was over 2 %, being the highest in Mexico (33 % 1/3) and Paraguay (26 % 25/95).[69]

In contrast, in 2022, 450 deaths due to VL were reported, with Brazil (165), Sudan (92), Ethiopia (43) and India (43) being the countries with the highest number of deaths. In 11 of the reporting countries, the CFR was higher than 2 % with the highest found in Brazil (9.8 % 165/1684) and Bolivia (9.1 % 2/22).[70]

Regarding available detailed information from 5 countries of 353 deaths between 2015 and 2019, 80 % of these deaths were in males of a mean age of 35 years. All of these countries reported deaths in children under 5 years, with an overall mortality rate of

15 % in children under 15 years of age. In many cases, deaths were associated with delays in treatments and concomitant illnesses such as anaemia, tuberculosis and HIV.[70]

1.1.3.7 Control and prevention measures

Vector control through the use of second-generation pesticides in endemic areas has shown a decrease in Leishmaniasis cases, but the development of resistance cannot be dismissed, as it has already been documented for dichlorodiphenyltrichloroethane (DDT) in some sand fly populations.[15,72]

Although no vaccine exists against Leishmaniasis, there are several prevention methods to reduce the risk of infection. These include avoiding outdoor areas in endemic zones during peak vector activity hours (night-time hours), using insect repellents, sleeping above the ground level and under bed nets.[17]

Given the zoonotic nature of VL and the critical role of dogs as reservoirs, control efforts must target these animals.[16] Recommended strategies include the use of protective collars, using mosquito-proof meshes in dog kennels and conducting serological surveillance, advising compassionate euthanasia in case of positive results to prevent further spread of the parasite.[17,27]

An effective vector control requires strategies that comprehend the vector's behaviour.[27] Insecticides may be effective at reducing the sand fly density, and insecticide-treated materials such as bed nets have also shown results, but long-term success depends on consistent re-treatment and community compliance.[17,27,73]

1.2. TREATMENTS FOR LEISHMANIASIS

1.2.1. Systemic pharmacological treatments

MCL and VL can be fatal if untreated; therefore, they require systemic treatment. Adequate systemic treatment of CL may reduce the risk of suffering from MCL. In the case of CL, choosing the use of systemic treatment may rely on different factors, such as the skin condition or the patient's characteristics.[74] Current systemic treatments have shown high toxicity and reduced efficacy.[75] The most common pharmacological treatments and their main characteristics are summarised in Table 1.2.

1.2.1.1 Pentavalent antimonials

In 1912, Dr Gaspar Viana successfully used the tartar emetic trivalent antimonial (Sb^{III}) for the first time in the therapy of American Tegumentary Leishmaniasis (ATL), marking the beginning of antimonial use for the treatment of Leishmaniasis.[76] Between 1920 and 1930, pentavalent antimonials (Sb^{V}) were introduced for the treatment of VL, reducing therapy duration from 3-4 months to some weeks.[76]

In the 1940s, new formulations of pentavalent antimonials such as meglubine antimoniate (MA) and sodium stibogluconate (SSG) appeared (Figure 1.13). These remain in clinical use today.[76,77] The precise mode of action of pentavalent antimonials is not completely understood. It is believed that they produce their effects through multiple mechanisms that include the inhibition of trypanothione reductase (TryR) and topoisomerase I.[78–80]

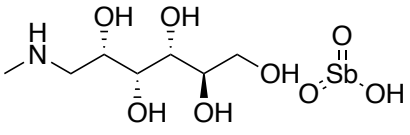

Meglumine Antimoniate

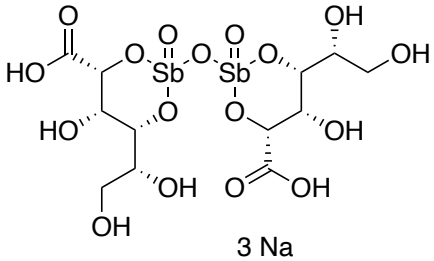

Sodium Stibogluconate

Figure 1.13. Chemical structure of pentavalent antimonials in clinical use today.

Pentavalent antimonials are usually administered in 20 mg kg^{-1} day^{-1} doses for 20-30 days when used as monotherapy.[81,82]

Despite advances in antileishmanial drugs, antimonials are still considered the first option for therapy in many endemic regions.[17,76] This is mainly due to their affordability and the documented efficacy.[83,84] However, treatment with pentavalent antimonials is often painful, requires intramuscular or intravenous injection, and may require hospitalisation.[26] Moreover, there is a high risk of adverse side effects such as cardiotoxicity and toxic effects in the pancreas, liver and kidneys.[82,85]

Drug resistance is a significant concern as VL has been reported as resistant to SSG in the Indian subcontinent, where, from the 1970s, dosage was increased, and treatments were prolonged to overcome this resistance.[86,87] Nevertheless, SSG is no longer recommended in India as failure rates ahave risen up to 60 %.[88,89]

1.2.1.2 Amphotericin B

Amphotericin B (AmB, Figure 1.14) is an antifungal drug discovered in 1955, produced by *Streptomyces nodosus*. Originally used for combating systemic fungal infections, it was repurposed as an anti-leishmanial drug around 1960.[76,90] AmB is the drug of choice in cases of antimonial resistance.[91] It works by binding to ergosterol, which is the main component of the leishmanial membrane, developing pores and thus allowing ions, water and glucose molecules through the membrane, ultimately leading to the death of the cell.[92–94] Amphotericin B also showed effectiveness via auto-oxidation, releasing Reactive Oxygen Species (ROS).[78]

AmB has major side effects, including hypokalemia, myocarditis, nephrotoxicity and infusion reactions. To overcome these problems, in the 1990s, the liposomal formulation of amphotericin B (LAmB), known as AmBisome, was developed.[88,90,95] This formulation has several advantages over the conventional AmB, such as reduced toxicity, enhanced solubility and stability, the ability to target and accumulate in the disease site, and an increase in bioavailability as the persistence in the body is longer.[90,96,97] Both AmB and LAmB require intravenous administration.

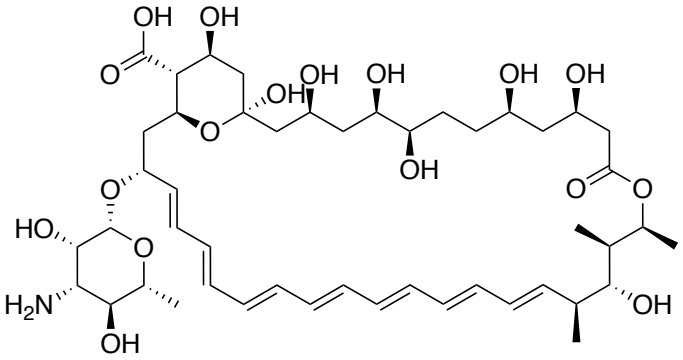

Amphotericin B

Figure 1.14. Amphotericin B structure.

Unfortunately, the price of this drug is too high and requires a strict cold chain, making it an unfeasible treatment for remote areas.[88,94,98] In 2010, the effectiveness of a single dose of LAmB against *L. donovani* in patients between 2 and 65 years of age, with a comparable efficacy to the treatment with a 1-month duration, was demonstrated.[82]

1.2.1.3 Miltefosine

Miltefosine (MF) (Figure 1.15) is an alkyl phosphocholine compound originally developed as an antineoplastic drug for the treatment of breast cancer in the 1980s.[76,82] It is the only oral medication approved against Leishmaniasis, and it is used for the three forms of Leishmaniasis: VL, CL and MCL.[99,100] Miltefosine is given as 50-100 mg day^{-1} for 4 weeks.[90] The exact leishmanicidal mode of action of MF is not known, but it is believed to cause an apoptosis-like death of the parasite that could be elicited by an interference with phosphatidylcholine synthesis, causing a destabilisation of the mitochondrial membrane and the inhibition of cytochrome-C oxidase.[78,101,102]

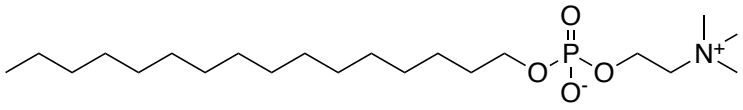

Miltefosine

Figure 1.15. Structure of miltefosine.

Miltefosine has a long half-life, which, together with inadequate use, has led to the development of parasitic resistance.[103,104] Moreover, MF can induce teratogenicity and

has some additional uncomfortable gastrointestinal adverse effects, such as diarrhoea and vomiting.[88,98,105]

1.2.1.4 Pentamidine

Pentamidine (PD) (Figure 1.16) is an aromatic diamidine with protozoal and antifungal activity, synthesised for the first time in the late 1930s and first used to treat African trypanosomiasis. PD was mostly used to treat antimonial-resistant VL during the 1980s and early 1990s and less frequently to treat CL.[77,90] The administration consists of injections every day or every other day for 4-7 days for CL and 15 days for VL. [106]

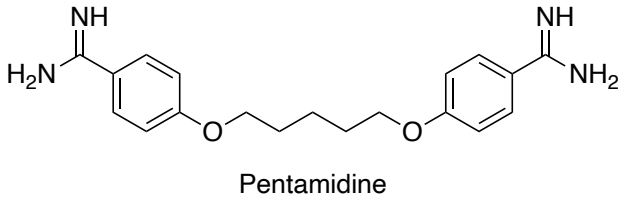

Figure 1.16. Pentamidine structure.

Even if its mechanism of action is not clear, it is believed to have multiple mechanisms. PD disrupts the synthesis of ribonucleic acid (RNA) polymerase, reducing RNA synthesis, and it alters the synthesis of nucleic acids, phospholipids, polyamines and folate.[90] Moreover, PD inhibits the active transport system and the mitochondrial topoisomerase II, leading eventually to the parasitic death.[107]

Pentamidine displays high levels of toxicity, low incidence of recovery and serious cardiac and gastrointestinal toxicity issues; therefore, it is not considered a drug of choice.[108,109]

1.2.1.5 Paromomycin

Paromomycin (PM) (Figure 1.17) is an aminoglycoside antibiotic isolated from *Streptomyces rimosus* that was originally used for the treatment of intestinal infections.[77] The anti-leishmanial activity of PM was discovered in the 1960s.[110] The administration of paromomycin is intramuscular for the case of VL due to poor absorption, which is a major drawback, and topical for the treatment of CL.

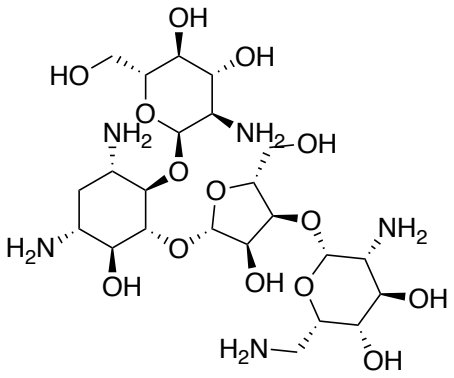

Paromomycin

Figure 1.17. Paromomycin structure.

Although its precise mechanism of action is unknown, PM inhibits protein synthesis by binding to the 30S ribosomal subunit and alters the mitochondrial membrane, both mechanisms causing the death of the cell.[111,112]

Paromomycin's pharmacokinetic properties have huge limitations, as it is rapidly eliminated from the body, prompting a need for frequent dosing, which in turn can lead to accumulation in the organs, hepatotoxicity, nephrotoxicity and ototoxicity.[113] However, in countries with fewer resources PM is used because of its low price and medium toxicity.[27]

Table 1.2. Summary of commercial anti-leishmanial drugs and their main characteristics.

Commercial drug	Period of use	Leishmaniasis treated	Main adverse effects	Form of administration	Typical treatment duration
Pentavalent Antimonials (Sodium stibogluconate, meglumine antimoniate)	Since 1912 (tartar emetic) Sb^V 1920-1930 Actual MA and SSG 1940s	VL, CL, MCL	Cardiotoxicity, liver, pancreas and kidney toxicity	Intramuscular or intravenous	20-30 days
Amphotericin B (AmB and LAmB)	1960 for AmB 1990s for LAmB	VL (come activity in CL)	Hypokalaemia, myocarditis, nephrotoxicity	Intravenous	AmB: 1 month LAmB: from 1 single dose to 1 month
Miltefosine	1980s	VL, CL and MCL	Teratogenicity and gastrointestinal symptoms	Oral	4 weeks
Pentamidine	1980s-1990s	VL mainly, CL	Cardiac and gastrointestinal toxicity	Intravenous or intramuscular	4-7 days (CL) 15 days (VL)
Paromomycin	1960s	VL, CL	Ototoxicity, hepatic and nephritic toxicity	Intramuscular (VL) or topical (CL)	3-4 weeks

1.2.1.6 Other drugs

Several compounds have been tested over the last years, with some of them showing promising results.[76] Repurposing strategies have also been useful, as the information about pharmacokinetic and safety profiles is already available if the drug already exists.[114,115] Some of these compounds are: azoles, tamoxifen, protease inhibitors, nitroimidazoles, pyrazolopyrimidines, imidazopyrimidines, triazolopyrimidines, oxaboroles, oligonucleotides and aminopyrazoles.[116]

a) Azoles

Oral antifungal azoles such as ketoconazole, fluconazole and itraconazole (Figure 1.18) have been evaluated against Leishmaniasis. These drugs were found to inhibit the multiplication of *Leishmania* promastigotes and amastigotes in murine macrophage tumour cells.

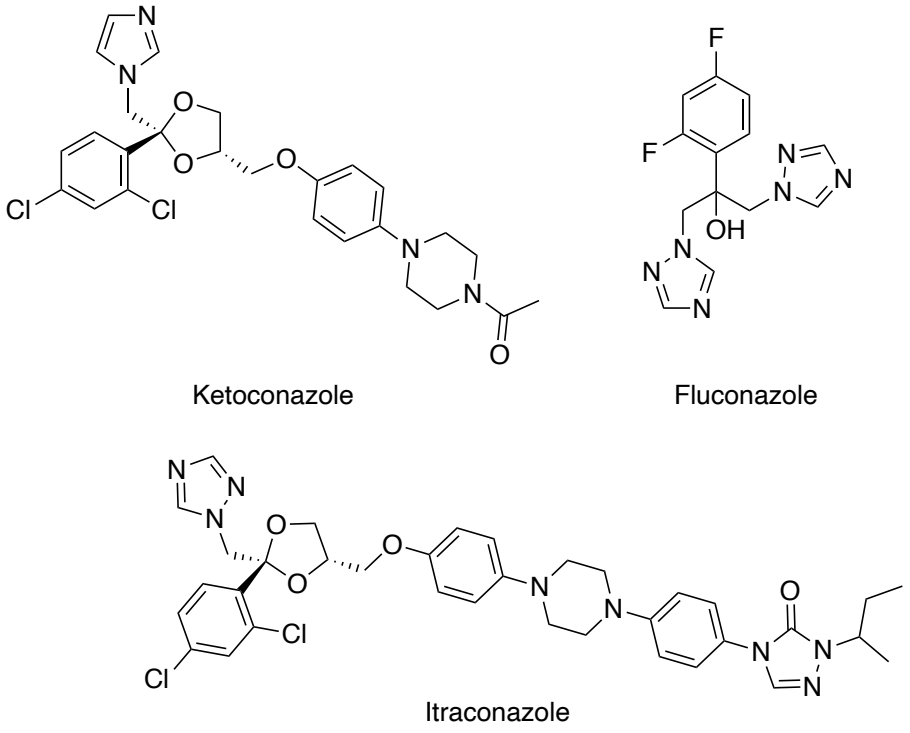

Figure 1.18. Azoles derivatives studied as potential anti-leishmanial agents.

The mechanism of azoles is believed to be related to the blocking of the biosynthesis of ergosterol by inhibition of the sterol 14α-demethylase enzyme.[77] However, azoles, as well as other Leishmaniasis therapies, appear to be effective only in certain specific

regions,[116] and have shown some important side effects such as hepatotoxicity and agranulocytosis.[36]

b) Tamoxifen

Tamoxifen (Figure 1.19) is an anticancer drug used for the treatment of breast cancer. It is a multi-target drug believed to interfere with sphingolipid (SL) metabolism.[117] SLs are an essential part of the *Leishmania* membrane, mediating cell processes such as cell growth or apoptosis.[118] Diverse *in vivo* studies have shown activity of tamoxifen against *Leishmania*, with non-significant side effects.[119]

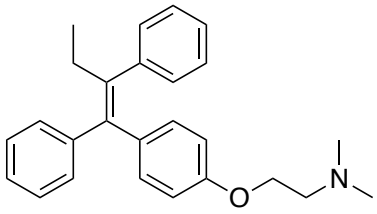

Figure 1.19. Tamoxifen structure.

c) Protease inhibitors

The efficacy of some protease inhibitors such as nelfinavir, ritonavir and saquinavir (Figure 1.20) has been evaluated against different *Leishmania* species.[120] These molecules were found to reduce the survival rate of the parasites in human leukemia monocytic cell line THP-1 macrophages and human primary monocyte-derived macrophages. Unfortunately, they did not show inhibition of the growth of *L. infantum* promastigotes in culture.[120,121]

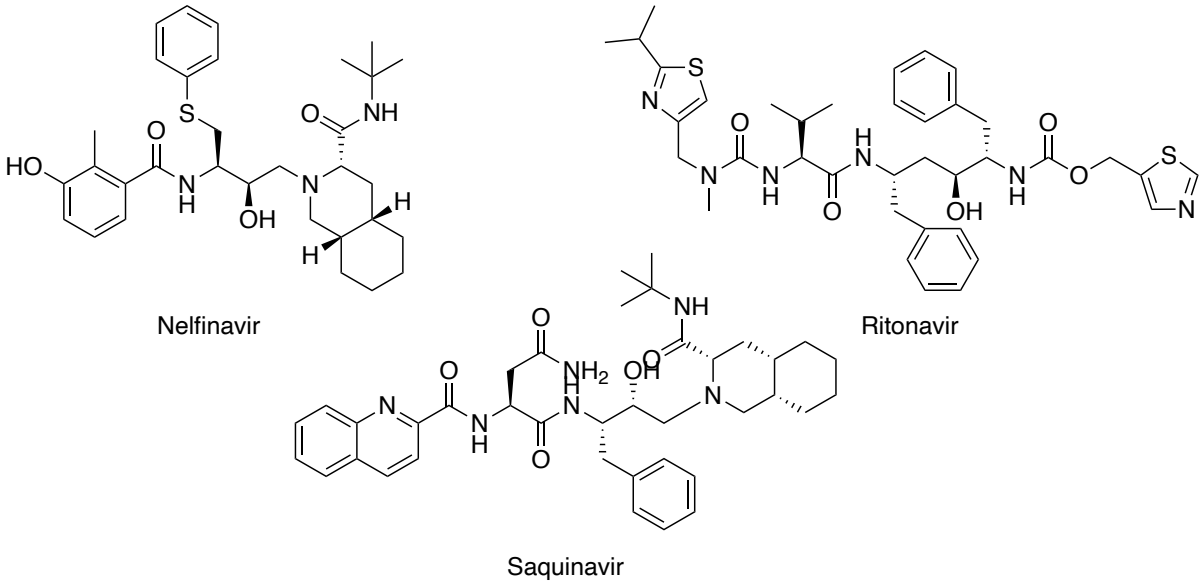

Figure 1.20. Protease inhibitors studied as potential anti-leishmanial agents.

d) Nitroimidazoles

Nitroimidazoles, including nitroimidazo-oxazoles and nitroimidazo-oxazines, are a class of molecules known for having activity against anaerobic bacterial and parasitic infections.[122,123] For example, Fexinidazole (Figure 1.21), a DNA synthesis inhibitor, showed good results in *in vivo* studies as its sulfoxide and sulfone metabolites were efficacious against *L. donovani*.[124] However, fexinidazole showed better results against other neglected diseases such as human African Trypanosomiasis (HAT) and Chagas' disease.

Some compounds developed by the Drugs for Neglected Diseases Initiative (DNDi) have shown promising results. Compound DNDi-0690 (Figure 1.21) was identified from a library of 70 imidazole compounds and showed excellent activity in *in vitro* studies for both VL and CL. DNDi-0690 was nominated as a preclinical candidate in September 2015 and entered Phase I studies in 2020, obtaining a safety profile in single-dose administration. Unfortunately, biological abnormalities were found when ascending the dose, and the clinical development was placed on hold.[125]

Previously, compound DNDi-VL-2098 (Figure 1.21) was identified as a potent and safe molecule that showed efficacy in acute and chronic VL animal models with oral dosing.

Unfortunately, the candidate was not moved forward due to the finding of testicular toxicity.[126]

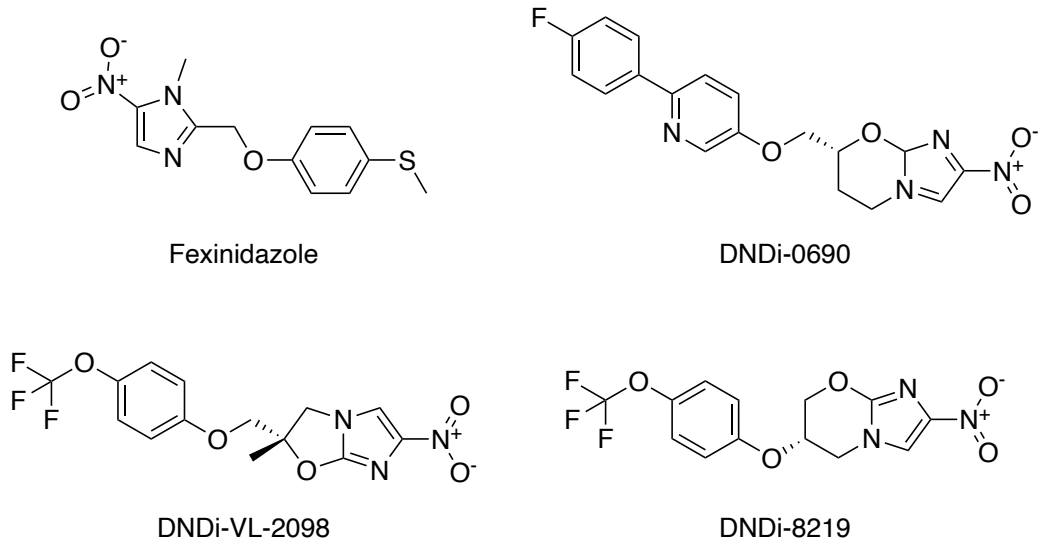

Figure 1.21. Nitroimidazole derivatives studied as potential anti-leishmanial candidates.

The nitroimidazole derivative DNDi-8219 (Figure 1.21) was identified from a 900-compound library screening showing excellent activity against *L. infantum* and with good solubility, becoming a promising compound to enter clinical trials.[127,128]

e) GSK899

From a high-throughput *in vitro* screening and after a compound optimisation, compound GSK899 (Figure 1.22) was developed, showing good values of EC_{50} and good selectivity against THP-1 host cells.[84,127] Moreover, GSK899 has good bioavailability while not having undesirable toxic effects.[129]

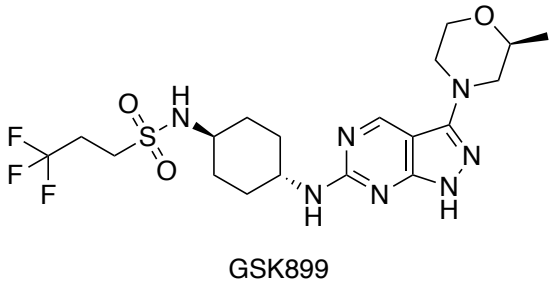

Figure 1.22. GSK899's structure.

It is believed to act by targeting mainly the cycle-2-related kinase 12 (CRK12) receptor, but has also shown interaction with other kinase receptors (CRK6 and CRK3). GSK988 entered Phase I clinical trials in 2019.[114,130]

f) GSK245

From the same high-throughput screening that led to the discovery of GSK899, GSK245 (Figure 1.23) was also identified.[116] This molecule had excellent activity in an intramacrophage in vitro assay, and further studies indicated good physicochemical properties, oral bioavailability and a good safety profile.[131]

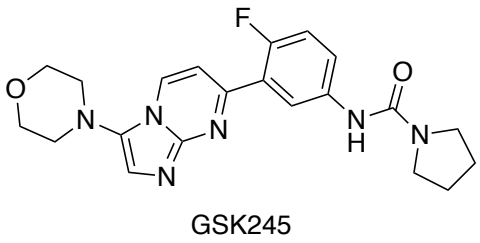

GSK245

Figure 1.23. GSK245's structure.

GSK245 entered phase I clinical trials in 2019 and successfully completed them in 2024. It was found to act through a selective inhibition of the β_5 subunit of the proteasome, and therefore was classified as a proteasome inhibitor.[131,132]

g) LXE-408

After the chemical validation of a Novartis team, establishing the parasite's proteasome as a promising target, LXE-408 (Figure 1.24) was obtained from a lead optimisation of a family of triazolopyrimidines.[133] LXE-408 showed a selective inhibition of the parasite proteasome when orally dosed in mouse disease models, with a comparable efficacy to that of AmB.[134]

After completing phase I clinical trials successfully in 2021, LXE-408 started phase II clinical trials in 2022 in India and Ethiopia. The phase II clinical trials are expected to finish in 2025, and results will be available results in 2026.[135,136]

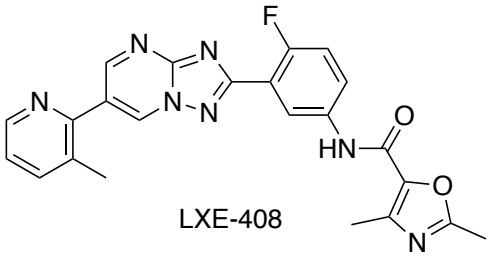

Figure 1.24. LXE-408's structure.

h) Oxaboroles

Over the last years, there has been an evolution in the boron-based compounds as potential therapeutic agents. The screening of Anacor's oxaboron class led to the discovery of many potential compounds for different diseases such as Chagas' disease, Leishmaniasis and sleeping sickness.[137] These are promising compounds for the inhibition of some hydrolytic enzymes because they can form covalent bonds with nucleophiles and boron mimics carbon.[138]

Among these compounds, DNDi-6148 (Figure 1.25) has shown promising results for the treatment of leishmaniasis.[116] DNDi-6148 completed the pharmacology and toxicology studies and showed promising *in vitro* results. In 2020, the phase I single ascending dose clinical trials began and were completed through 2022, when multiple ascending dose studies started in India. Unfortunately, the trials were placed on hold due to reproductive toxicity signals.[137]

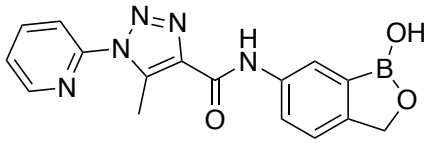

DNDi-6148

Figure 1.25. DNDi-6148's structure.

1.2.2. Local treatments

Local treatments are mainly indicated for uncomplicated cases of CL. These treatments try to eradicate the parasite at the infection site. Local treatments include

thermal treatments (thermotherapy and cryotherapy), surgical excision or infiltrations.[26,76]

1.2.2.1 Thermotherapy

The species causing cutaneous Leishmaniasis are heat-sensitive and cannot survive temperatures over 39°C. Therefore, thermotherapy is a potential treatment for CL.[139] For decades, local heat has been applied to lesions either by using caustic materials (oil, hot brown sugar) or hot metal objects (knives, spoons).[27]

However, thermotherapy has local adverse effects such as bacterial superinfection, erythema and pain.[140] Some of the thermotherapy methods include: applying local heat with an infrared lamp in two sessions,[141] using a device called Hand-Held Exothermic Crystallisation Therapy for CL (HECT-CL) which delivers controlled conduction heat allowing determined heat cycles, using a photosensitizer and irradiating light with the adequate wavelength (which can be day light) generating photodynamic therapy[142] or using radio-frequency-induced therapy (RFHT) by applying electrodes locally in the lesion for 30-60s.[140]

1.2.2.2 Cryotherapy

Cryotherapy involves applying liquid nitrogen to a lesion. It works by inducing the formation of ice crystals that alter the cell membrane, leading to the parasite's death.[143] Cryotherapy has shown promising results in some studies, and the side effects observed were not considered important, as they were redness, itching and hypo or hyperpigmentation.[144,145]

1.2.2.3 Intralesional Injections

Whenever the systemic treatment is not suitable, the Pan American Health Organisation (PAHO) recommends the treatment of CL with intralesional antimonials.[146] These infiltrations allow local maximum concentration in the lesions, but are not able to reach metastatic Leishmaniasis. Both sodium stibogluconate and meglumine antimoniate can be administered intralesional and have shown a high efficacy with minor side effects such as local pain and swelling.[143] In one study, the

effect of intralesional pentamidine was evaluated, showing comparable cure rates to intralesional antimonials.[147]

1.2.2.4 Topical local treatments

Topical ointments containing paromomycin have been developed for the treatment of CL. There are different formulations for these treatments. A combination of 15 % paromomycin with 12 % methylbenzethonium chloride had good cure success, but also local severe irritation and intolerance from the majority of patients.[148] A combination of paromomycin (15 %) and urea (10 %) seems to be more effective but also causes some adverse reactions, such as more local inflammation.[149] A cream containing paromomycin sulphate (15 %) and gentamicin sulphate (0.5 %) had the same results as the one containing only paromomycin.[148]

1.2.2.5 Other treatments

Other local treatments have been used for the treatment of cutaneous Leishmaniasis, such as laser (CO_2, argon, pulsed dye) or topical nitric oxide.[150]

CO_2 laser treatment is cost-effective and is a great option for the primary therapy of CL.[142] It works by performing thermolysis on damaged tissue and has shown successful outcomes in diverse studies.[151,152]

There are opposing results regarding studies involving nitric oxide (NO). Initial studies showed promising results after using an ointment containing S-nitroso-N-acetyl penicillamine (SNAP), a nitric oxide precursor, which could inhibit cell growth and cause cell death of the parasites.[153] However, a study that applied transdermal patches for the continuous delivery of NO found the treatment to be ineffective.[154] Despite this, the low rate of adverse effects and the convenience of the administration support the need for further research.

1.2.3. Combined therapies

Different drug-drug and drug-physical therapy combinations have been evaluated in order to find more successful treatments.

1.2.3.1 Drug-drug Combinations

Multidrug therapy seems a promising approach in many zones as it allows the reduction of drug doses and duration of the therapy, consequently reducing costs, adverse effects and the development of drug resistance.[88] Many different combinations have been studied:

a) Sodium stibogluconate & paromomycin:

Clinical trials showed that the combination of SSG and PM was effective and safe, with the benefits of reducing the treatment from 30 days to 17 days. Moreover, this combination of drugs seems to be less likely to cause resistance.[155,156] This treatment has been recommended by the World Health Organisation (WHO) in East Africa since 2010 and is still used nowadays.[157]

b) Paromomycin & miltefosine

Miltefosine and paromomycin combination therapy has good efficacy in South Asia and has successfully overcome Phase II clinical trials for its use in East Africa. It is considered as effective as the SSG+PM treatment but with the need for fewer injections, shorter duration and most importantly, with no life-threatening cardiotoxicity. The WHO is reviewing the study results in East Africa in order to update the treatment guidelines.[158,159]

c) Liposomal amphotericin B & miltefosine

The treatment of miltefosine combined with liposomal amphotericin B attained complete cure of the patients, showing a dramatic decline of the parasite load at mid-treatment and no reports of relapse in the 18 months following the treatment. Moreover, only some vomiting was observed as an adverse effect. A control study with miltefosine as monotherapy showed a gradual progression of parasite load that led to residual parasite load after the treatment.[160]

d) Pentavalent antimony & pentoxifylline

The combination of pentavalent antimony and pentoxifylline has been evaluated for the treatment of mucocutaneous Leishmaniasis. A study published in 2007 showed that the treatment of MCL with a combination of pentavalent antimonials and pentoxifylline reduced the healing time significantly and prevented the need for further courses of pentavalent antimonials.[161] As a second study in 2022 suggests, the effect of pentoxifylline could be related to the inhibition of TNF, a cytokine produced in high levels in MCL cases. This study showed that patients treated with the combination of these two drugs healed significantly faster and had lower failure rates.[162]

1.2.3.2 Drug-Physical Therapy Combinations

Some drug and physical therapy combinations have also been studied to analyse the efficacy compared to the *solo* treatment.

a) Miltefosine & thermotherapy

Miltefosine and thermotherapy treatment combination was evaluated, obtaining better results in the combined therapy rather than only thermotherapy, with cure rates of 80.3 and 57.8 % respectively.[163]

b) Cryotherapy & pentavalent antimonials

A study from 1990 evaluated the combination of Sodium stibogluconate and cryotherapy, showing a 100 % cure rate.[164] Another study from 2004 evaluated the combination of Meglumine antimoniate with cryotherapy, showing that the combined treatment was more effective than either treatment alone.[165]

1.2.4. Treatment approaches based on geographic variations

As Leishmaniasis is caused by different parasites that vary through the regions, the treatment also varies to adapt to resistances, effectiveness and availability. Treatment recommendations depending on regions are summarised in Table 1.3.

Table 1.3. Treatment recommendations attending to geographic variations.

REGION	**DRUG** (in order of choice)
Mediterranean region	LAmB
	SSG or MA
	AmB deoxycholate
	LAmB+MF
	MF
	PM
Middle East and Central Asia region	SSG or MA
	AmB deoxycholate
	LAmB
	PM
	MF
Indian Subcontinent and South Asia region	LAmB
	MF+PM
	AmB emulsion
	MF
	AmB deoxycholate
East Africa Region	SSG+PM
	SSG or MA
	LAmB
Latin American Region	LAmB
	SSG or MA
	AmB deoxycholate

1.2.4.1 Mediterranean region

In the Mediterranean region, Visceral Leishmaniasis is caused by *L. infantum*, and the treatments recommended by WHO are LAmB as first choice, pentavalent antimonials as second choice and AmB deoxycholate as third choice.[166] However, the evidence of the effect of pentavalent antimonials is not very strong and varies between countries. On one side, Morocco, Tunisia, Turkey and Israel have antimonials as their first-line treatment. On the other side, Portugal, Spain, and Greece have both antimonials and AmB preparations as first-line treatments. Meanwhile, in France, Italy, and Cyprus, LAmB is the first-line option.[27]

There is little information about the effect of pentamidine and paromomycin in the Mediterranean region. There is no experience with miltefosine's effectiveness in this region; however, its oraladministration mode makes it an attractive possibility.[27]

1.2.4.2 Middle East and Central Asia Region

Clinical trials specific to the Middle East and Central Asia have not been developed to evaluate the efficacy of each treatment in this region. However, for more than 70 years, antimonials have been the drug of choice in this region. Currently, due to drug resistance and toxicity issues, LAmB, MF, and PM are also being used.[27]

1.2.4.3 Indian Subcontinent and South Asia Region

Due to the high resistance to antimonials in the Indian Subcontinent and South Asia Region, and the good results obtained with amphotericin B, it is established as one of the drugs of choice for VL treatment in this region. Due to its efficacy and lower toxicity, LAmB is preferred over AmB deoxycholate.[167,168] Pentamidine was considered an efficient therapy until the 1990s, when the rate of response started to decrease.[169] Paromomycin has also been tested with high cure rates but toxicity.[170] Miltefosine was proposed as a first-line treatment; however, some studies have revealed an increase in the relapse rate in recent years.[103,171] Some drug-drug combined therapies have obtained favourable results, such as the combination of miltefosine and paromomycin.[172,173]

For the treatment of PKDL, miltefosine is the first drug of choice, followed by AmB deoxycholate injection.[174]

1.2.4.4 East Africa Region

In Africa, the first studies evaluating the effect of pentavalent antimonials were done in 1983.[175] Later, in the 1990s, studies showed higher cure rates when combined with paromomycin, which is still the first-line treatment option nowadays.[176–178] Pentavalent antimonials as monotherapy are still considered a good treatment option, as well as LAmB. However, studies suggest that to reach better results, the treatment with LAmB should be done in higher doses than in the Indian Subcontinent.[179,180]

1.2.4.5 Latin America Region

In the Latin American region, there is a large number of cases of mucocutaneous Leishmaniasis. For its treatment, pentavalent antimonials as monotherapy or in

combination with pentoxifylline are recommended. For VL, even if there is low evidence, there is a strong recommendation to use LAmB as the first treatment option. The treatment with pentavalent antimonials or amphotericin B deoxycholate is also suggested.[181]

1.2.5. Special Treatment Considerations

Some considerations must be made regarding the election of the treatment depending on the conditions of the patient and possible comorbidities.

1.2.5.1 HIV co-infection

Patients with coexisting HIV and Leishmaniasis are more likely to experience parasite dissemination, clinical polymorphism and atypical or more severe forms of the disease.[182] Whenever possible, immunosuppressive treatment should be paused until complete healing of the skin lesions in case of MCL-HIV coinfection.[183] The combination of MCL-HIV with VL has been reported in these groups of patients.

For the treatment of VL in immunosuppressed patients, LAmB is the preferred therapy. Alternative therapies include amphotericin B deoxycholate, SSG or miltefosine. In the case of CL or MCL, the preferred treatment is pentavalent antimonials or LAmB, as an alternative, miltefosine, topical paromomycin, intralesional SSG, or local heat therapy.[182]

1.2.5.2 Pregnancy

There is scarce information about the treatment of VL during pregnancy. Not treating pregnant patients can mean a risk for both mother and foetus, higher than the toxicity risk of the treatment. VL can cause spontaneous abortion, small-for-birth date and congenital Leishmaniasis.[184,185]

Among the different options for treatment during pregnancy, the best seems to be amphotericin B or its liposomal form. AmB and LAmB have not shown congenital transmission nor spontaneous abortion.[186,187] Pentavalent antimonials are contraindicated for use among pregnant women as they may have teratogenic effects.[188,189] Miltefosine is teratogenic and therefore contraindicated during

pregnancy.[188] Paromomycin is an aminoglycoside able to cross the placental barrier and is therefore not recommended during pregnancy.[190]

1.2.5.3 Paediatric patients

Liposomal amphotericin B can be used in children of any age; some studies have confirmed its safety from 3 months of age.[191] It is widely used, especially in severe cases of VL. Treatment with miltefosine is recommended for children above 12 years old, even if it can be used in children over 2, adjusting the dose.[192] Pentavalent antimonials are safe to use in children, but some studies have shown less effectiveness in children under 5 years.[157] Paromomycin has not been extensively studied in young patients, and it should be avoided because of possible toxicity.

1.2.6. Advances and New Perspectives

The increase of resistant strains to conventional drugs, together with the high toxicity, co-infections, and limitation in therapeutic options, has led researchers to seek new strategies. Here are some of the recent advances and new strategies for Leishmaniasis therapy.

1.2.6.1 Immunomodulatory therapies

Leishmania parasites have developed different mechanisms to survive inside the host. A promising approach to combat Leishmaniasis is the use of substances that promote the restoration of the immune response against the parasite.[193] Immunomodulators play an important role in the treatment of some diseases. Some immunomodulators have shown efficacy in the treatment of Leishmaniasis, including SSG, arabinosylated lipoarabinomannan and glycyrrhizic acid (Figure 1.26).[194]

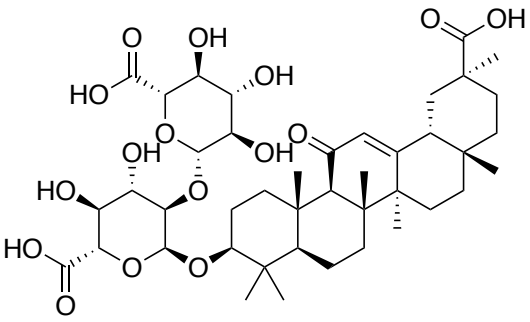

Figure 1.26. Glycyrrhizic acid's structure.

1.2.6.2 Targeted Drug Delivery Systems

Targeted drug delivery can be an interesting approach for the treatment of Leishmaniasis as it can increase bioavailability, reduce toxicity and allow reaching precise tissues or cells such as macrophages, where *Leishmania* parasites live.[17]

Reaching and getting into these specific tissues can be challenging; therefore, diverse nanotechnological carriers are used:

a) Liposomes

Liposomes are nano-sized spherical vesicles that are made of bilayer phospholipids that allow the support for the adhesion of both hydrophilic and lipophilic medicines. Liposomes allow sustained drug release, which can reduce the administration frequency.[195] An example is liposomal amphotericin B, a formulation of amphotericin B that has reduced the adverse effects of AmB.[196] Some other liposomes, such as mannose functionalized or 4-sulfated acetyl galactosamine, have shown inhibitory effects against *Leishmania* parasites.[197]

b) Lipid nano-capsules

Lipid nano-capsules (LNs) are nanocarriers that imitate lipoproteins and measure between 20 and 100 nm.[198] LNs are structures created from a combination of liposomes and polymeric Nano-capsules. They allow greater bioavailability and stability and allow a dose reduction.[199]

c) Metallic nanoparticles

Diverse metallic nanoparticles have been assayed for anti-leishmanial activity, showing low toxicity and high efficacy.[200] Amphotericin B was encapsulated in an iron oxide (Fe_3O_4) nanoparticle measuring 10-15 nm, lowering the parasite load in treated spleen.[201] Some zinc oxide nanoparticles have also been developed, showing a cytotoxic effect on amastigote cells; therefore, reducing the proliferation and inhibiting the parasite's activity.[202] Another study analysed silver nanoparticles, demonstrating a toxic effect against promastigotes and amastigotes.[203]

d) Polymeric nanoparticles

Polymeric nanoparticles (PNs) are made of biocompatible and biodegradable colloidal particles. Their size ranges from 1 to 1000 nm.[204] They are known to improve bioavailability, cellular dynamics, biodegradability and controlled drug delivery.[205] PNs containing AmB have been tested in mice with VL, obtaining promising results.[206]

e) Nanotubes

Nanotubes are cylindrical hollow structures made of inorganic and metallic materials that have been studied for their potential as nanocarriers.[143] Diverse nanotube structures have been explored as carriers of AmB, showing better results than AmB.[207]

1.2.6.3 In Silico Approaches to Improved Drug Discovery

Traditional drug discovery processes are lengthy and costly. There has been a development of new methods accelerating the process of drug discovery while reducing the cost and effort.[208]

Other powerful approaches include computer-aided drug discovery (CADD), overcoming time and cost limitations of the traditional methods. CADD works by identifying drug targets, performing virtual screening of chemical libraries and doing in silico assessment of potential toxicity.[209]

1.2.6.4 High-throughput screening

High-throughput screening (HTS) has advanced drug discovery thanks to the rapid evaluation of large libraries of compounds. Other automation techniques, such as microplate readers or imaging software and hardware, have helped enhance HTS' efficiency.[210]

1.2.6.5 Vaccines

Since a strong immunity against reinfection has been observed after recovery from CL or VL, vaccines seem to be a promising development.[26] "*Leishmanization*" or the use of live parasites to cause localised lesions to prevent sickness, was used during the 1980s.[211] Although this technique showed good results, it is no longer used because of the risk of spread. Even if many vaccines have arrived at the preclinical stage, there have not been successful candidates yet.[212]

a) First-generation vaccines

These include vaccines developed using whole-killed or live-attenuated parasites to induce broad immunity.[213] The first-generation vaccines studied for Leishmaniasis were mainly whole-killed parasites, as they are cheaper and easier to develop.

i. Whole-killed parasites:

Three different vaccines of this type were further evaluated, reaching Phase I and II of clinical trials. However, some showed to induce immunity for a short period of time, and others needed to increase their efficacy.[214–216]

ii. Live-attenuated parasites:

There are two different classifications based on the attenuation procedure: genetically defined or undefined parasites. Undefined attenuation can result in a reduced capacity to induce protective immunity, while genetically defined modification allows for the selection of parasites that are lacking essential genes associated with virulence or long-term survival.[217] The gene modified in *Leishmania* is usually *centrin* 1 (*Cen*1).

This gene does not seem to impact promastigotes but inhibits the growth of amastigotes.[218]

b) Second-generation vaccines

These refer to vaccines based on recombinant *Leishmania* antigens; peptides or polypeptides produced by the use of genetically engineered viruses and bacteria.[219] These types of vaccines are cost-effective and have excellent reproducibility. Many have been designed for canine Leishmaniasis to control one of the vectors of the disease.[220] Many second generations have been developed for humans; however, results found in animal models were not consistently reproduced in humans.[221–223]

c) Third-generation vaccines

These vaccines have formulations containing nucleic acids based either on DNA or RNA. Only DNA vaccines have been developed for leishmaniasis, having, however, different outcomes probably due to differences in formulations.[224] These vaccines are inexpensive, stable and seem to be effective, but still need further investigations about safety.[225]

1.3. BIBLIOGRAPHY

1. A.S. Nagle, S. Khare, A.B. Kumar, et al. Recent Developments in Drug Discovery for Leishmaniasis and Human African Trypanosomiasis. *Chem Rev* **2014**, 114 (22), 11305–11347.

2. D. Steverding. The history of leishmaniasis. *Parasit Vectors* **2017**, 10 (1), 82.

3. A.J. Lysenko. Distribution of leishmaniasis in the Old World. *Bull World Health Organ* **1971**, 44 (4), 515–520.

4. H. Noyes. Implications of a Neotropical Origin of the Genus Leishmania. *Mem Inst Oswaldo Cruz* **1998**, 93 (5), 657–662.

5. R. Lainson, J. Shaw. Evolution, classification and geographical distribution.; Academic Press, London, **1987**; pp 1–120.

6. H. Momen, E. Cupolillo. Speculations on the origin and evolution of the genus Leishmania. *Mem Inst Oswaldo Cruz* **2000**, 95 (4), 583–588.

7. A.R. Zink, M. Spigelman, B. Schraut, et al. Leishmaniasis in Ancient Egypt and Upper Nubia. *Emerg Infect Dis* **2006**, 12 (10), 1616–1617.

8. R. Lainson, J.J. Shaw. New World Leishmaniasis. In *Topley & Wilson's Microbiology and Microbial Infections*; **2010**.

9. F.F. Tuon, V. Amato Neto, V. Sabbaga Amato. *Leishmania*: origin, evolution and future since the Precambrian. *FEMS Immunol Med Microbiol* **2008**, 54 (2), 158–166.

10. A. Russell. The natural history of Aleppo, and parts adjacent; Printed for A. Millar, London, **1756**.

11. R. Lainson. The Neotropical Leishmania species: a brief historical review of their discovery, ecology and taxonomy. *Rev Panamazonica Saude* **2010**, 1 (2).

12. W. TWINING. Observations on Diseases of the Spleen, particularly on the vascular engorgement of that organ, common in Bengal. **1828**.

13. W.B. Leishman. On the possibility of the occurrence of trypanosomiasis in India. *BMJ* **1903**, 2 (2238), 1376–1377.

14. R. Ross. Further notes on Leishman's bodies. *BMJ* **1903**, 2 (2239), 1401–1401.

15. N. Tiwari, A. Kumar, A.K. Singh, et al. Leishmaniasis control: limitations of current drugs and prospects of natural products. In *Discovery and Development of Therapeutics from Natural Products Against Neglected Tropical Diseases*; Elsevier, **2019**; pp 293–350.

16. M. Pal, I. Ejeta, A. Girma, K. Dave, P. Dave. Etiology, Clinical Spectrum, Epidemiology, Diagnosis, Public Health Significance and Control of Leishmaniasis: A Comprehensive Review. *Acta Scientific Microbiology* **2022**, 110–121.

17. M. Güran. An Overview of Leishmaniasis: Historic to Future Perspectives. In *Vectors and Vector-Borne Zoonotic Diseases*; IntechOpen, **2019**.

18. Understanding Your Risk for Leishmaniasis | Leishmaniasis | CDC https://www.cdc.gov/leishmaniasis/risk-factors/index.html (accessed Apr 15, 2025).

19. P. Cecílio, A. Cordeiro-da-Silva, F. Oliveira. Sand flies: Basic information on the vectors of leishmaniasis and their interactions with Leishmania parasites. *Communications Biology 2022 5:1* **2022**, 5 (1), 1–12.

20. A. Amro, O. Hamarsheh. Epidemiology of Leishmaniasis in Palestine. *Handbook of Healthcare in the Arab World* **2020**, 1–17.

21. L. Pacakova, K. Harant, P. Volf, et al. Three types of Leishmania mexicana amastigotes: Proteome comparison by quantitative proteomic analysis. *Front Cell Infect Microbiol* **2022**, 12, 1022448.

22. Leishmania Parasites - Epidemiology, Immunopathology and Hosts; Almeida-Souza, F., de Oliveira Cardoso, F., Lucia Abreu-Silva, A., da Silva Calabrese, K., Eds.; IntechOpen, **2024**.

23. CDC - DPDx - Leishmaniasis https://www.cdc.gov/dpdx/leishmaniasis/index.html (accessed Apr 16, 2025).

24. I. Rohousova, D. Talmi-Frank, T. Kostalova, et al. Exposure to Leishmania spp. and sand flies in domestic animals in northwestern Ethiopia. *Parasit Vectors* **2015**, 8 (1), 360.

25. G. Baneth, S.E. Shaw. Chemotherapy of canine leishmaniosis. *Vet Parasitol* **2002**, 106 (4), 315–324.

26. A. Rafique, S.S. Sani, S. Sultana, et al. Cutaneous Leishmaniasis. *Leishmania Parasites - Epidemiology, Immunopathology and Hosts* **2023**.

27. F. Bruschi, L. Gradoni. The leishmaniases: Old neglected tropical diseases. *The Leishmaniases: Old Neglected Tropical Diseases* **2018**, 1–245.

28. Wallace. Peters, R. Killick-Kendrick. The Leishmaniases in biology and medicine. **1987**.

29. P. Mansueto, A. Seidita, G. Vitale, A. Cascio. Leishmaniasis in travelers: a literature review. *Travel Med Infect Dis* **2014**, 12, 563–581.

30. C.R. Davies, R. Reithinger, D. Campbell-Lendrum, et al. The epidemiology and control of leishmaniasis in Andean countries. *Cad Saude Publica* **2000**, 16 (4), 925–950.

31. E.A. Llanos-Cuentas, P.D. Marsden, E.L. Lago, et al. Human mucocutaneous leishmaniasis in Três Braços, Bahia - Brazil: an area of Leishmania braziliensis braziliensis transmission. II. Cutaneous disease. Presentation and evolution. *Rev Soc Bras Med Trop* **1984**, 17 (4), 169–177.

32. D.R. Mans, A.D. Kent, R. VPF Hu, H.D. Schallig. Epidemiological, Biological and Clinical Aspects of Leishmaniasis with Special Emphasis on Busi Yasi in Suriname. *J Clin Exp Dermatol Res* **2017**, 08 (02).

33. Leishmaniasis https://www.who.int/news-room/fact-sheets/detail/leishmaniasis (accessed Aug 5, 2025).

34. D. Kimberlin. Red Book: 2018-2021 report of the committee on infectious diseases. **2018**.

35. P.J. Guerin, P. Olliaro, S. Sundar, et al. Visceral leishmaniasis: current status of control, diagnosis, and treatment, and a proposed research and development agenda. *Lancet Infect Dis* **2002**, 2 (8), 494–501.

36. N. Aronson, B.L. Herwaldt, M. Libman, et al. Diagnosis and Treatment of Leishmaniasis: Clinical Practice Guidelines by the Infectious Diseases Society of America (IDSA) and the American Society of Tropical Medicine and Hygiene (ASTMH). *Clin Infect Dis* **2016**, 63 (12), 1539–1557.

37. C. Bern, A.W. Hightower, R. Chowdhury, et al. Risk Factors for Kala-Azar in Bangladesh. *Emerg Infect Dis* **2005**, 11 (5), 655.

38. K.K. Mahto, P. Prasad, M. Kumar, et al. Visceral Leishmaniasis: An Overview and Integrated Analysis of the Current Status, Geographical Distribution and Its Transmission. *Leishmania Parasites - Epidemiology, Immunopathology and Hosts* **2023**.

39. N. Varma, S. Naseem. Hematologic Changes in Visceral Leishmaniasis/Kala Azar. *Indian J Hematol Blood Transfus* **2010**, 26 (3), 78–82.

40. F. Melchionda, S. Varani, F. Carfagnini, et al. Spleen nodules: A potential hallmark of Visceral Leishmaniasis in young children. *BMC Infect Dis* **2014**, 14 (1), 1–5.

41. M. Levi, S. Sivapalaratnam. Disseminated intravascular coagulation: an update on pathogenesis and diagnosis. *Expert Rev Hematol* **2018**, 11 (8), 663–672.

42. M. Scalzone, A. Ruggiero, S. Mastrangelo, et al. Hemophagocytic lymphohistiocytosis and visceral leishmaniasis in children: case report and systematic review of literature. *J Infect Dev Countries* **2016**, 10 (01), 103–108.

43. E.F. Daher, L.L.L. Lima, A.P.F. Vieira, et al. Hemophagocytic Syndrome in Children With Visceral Leishmaniasis. *Pediatr Infect Dis J* **2015**, 34 (12), 1311–1314.

44. E.E. Zijlstra, A.M. Musa, E.A.G. Khalil, I.M. El Hassan, A.M. El-Hassan. Post-kala-azar dermal leishmaniasis. *Lancet Infect Dis* **2003**, 3 (2), 87–98.

45. N.K. Das. Post kala-azar dermal leishmaniasis. *Indian J Dermatol* **2020**, 65 (6), 450–451.

46. Leishmaniasis - PAHO/WHO | Pan American Health Organization https://www.paho.org/en/topics/leishmaniasis (accessed Aug 6, 2025).

47. M.A. McDowell, S. Rafati, M. Ramalho-Ortigao, A. Salah. Leishmaniasis: Middle East and North Africa Research and Development Priorities. *PLoS Negl Trop Dis* **2011**, 5 (7), e1219.

48. S. Esteves, I. Costa, C. Amorim, et al. Biomarkers in Leishmaniasis: From Basic Research to Clinical Application. *Biomarker - Indicator of Abnormal Physiological Process* **2018**.

49. WHO | World Health Organization https://apps.who.int/neglected_diseases/ntddata/leishmaniasis/leishmaniasis.html (accessed Aug 6, 2025).

50. S. Kyari, S. Kyari. Epidemiology of Leishmaniasis. *Leishmania Parasites - Epidemiology, Immunopathology and Hosts* **2024**.

51. O.P. de la Salud. Leishmaniasis: Informe epidemiológico de las Américas. Núm. 13, Diciembre del 2024. *Leishmaniases: Epidemiological Report of the Americas;* **2024**.

52. A. Amarasinghe, S. Wickramasinghe. A Comprehensive Review of Cutaneous Leishmaniasis in Sri Lanka and Identification of Existing Knowledge Gaps. *Acta Parasitol* **2020**, 65 (2), 300–309.

53. L.S. Galgamuwa, B. Sumanasena, L. Yatawara, S. Wickramasinghe, D. Iddawela. Clinico-Epidemiological Patterns of Cutaneous Leishmaniasis Patients Attending the Anuradhapura Teaching Hospital, Sri Lanka. *Korean J Parasitol* **2017**, 55 (1), 1–7.

54. P.K. Mandal, R.R. Wagle, S. Uranw, A.K. Thakur. Risk factors for visceral leishmaniasis in selected high endemic areas of Morang, Nepal: A case control study. *Journal of Kathmandu Medical College* **2020**, 9 (4), 188–196.

55. Y. Terefe, B. Afera, A. Bsrat, Z. Syoum. Distribution of Human Leishmaniasis (VL) and Its Associated Risk Factors, in Metemma, Ethiopia. *Epidemiol Res Int* **2015**, 2015 (1), 630812.

56. U.S. Rajapaksa, R.L. Ihalamulla, C. Udagedera, N.D. Karunaweera. Cutaneous leishmaniasis in southern Sri Lanka. *Trans R Soc Trop Med Hyg* **2007**, 101 (8), 799–803.

57. R.R. Ranawaka, H.S. Weerakoon. Randomized, double-blind, comparative clinical trial on the efficacy and safety of intralesional sodium stibogluconate and intralesional 7% hypertonic sodium chloride against cutaneous leishmaniasis caused by L. donovani. *J Dermatolog Treat* **2010**, 21 (5), 286–293.

58. M. Boelaert, F. Meheus, A. Sanchez, et al. The poorest of the poor: a poverty appraisal of households affected by visceral leishmaniasis in Bihar, India. *Trop Med Int Health* **2009**, 14 (6), 639–644.

59. G.R. Awab, G.R. Awab. Leishmaniasis Epidemiology and Psychosocial Aspect. *Leishmania Parasites - Epidemiology, Immunopathology and Hosts* **2023**.

60. C. Parmesan. Ecological and evolutionary responses to recent climate change. *Annu Rev Ecol Evol Syst* **2006**, 37, 637–669.

61. G.S. Bhunia, V. Kumar, A.J. Kumar, P. Das, S. Kesari. The use of remote sensing in the identification of the eco-environmental factors associated with the risk of human visceral leishmaniasis (kala-azar) on the Gangetic plain, in north-eastern India. *Ann Trop Med Parasitol* **2010**, 104 (1), 35–53.

62. J. Hlavacova, J. Votypka, P. Volf. The Effect of Temperature on Leishmania (Kinetoplastida: Trypanosomatidae) Development in Sand Flies. *J Med Entomol* **2013**, 50 (5), 955–958.

63. R.A.F. de Souza, R.V. Andreoli, M.T. Kayano, A.L. Carvalho. American cutaneous leishmaniasis cases in the metropolitan region of Manaus, Brazil: association with climate variables over time. *Geospat Health* **2015**, 10 (1), 40–47.

64. L.F. Chaves, J.E. Calzada, A. Valderrama, A. Saldaña. Cutaneous leishmaniasis and sand fly fluctuations are associated with el niño in panamá. *PLoS Negl Trop Dis* **2014**, 8 (10).

65. A.R. de Araujo, N.C. Portela, A.P.S. Feitosa, et al. Risk factors associated with american cutaneous leishmaniasis in an endemic area of Brazil. *Rev Inst Med Trop Sao Paulo* **2016**, 58 (0).

66. A. Oryan, M. Akbari. Worldwide risk factors in leishmaniasis. *Asian Pac J Trop Med* **2016**, 9 (10), 925–932.

67. M. Maroli, L. Rossi, R. Baldelli, et al. The northward spread of leishmaniasis in Italy: evidence from retrospective and ongoing studies on the canine reservoir and phlebotomine vectors. *Trop Med Int Health* **2008**, 13 (2), 256–264.

68. Global leishmaniasis update, 2006–2015: a turning point in leishmaniasis surveillance. *Weekly epidemiological record* **2017**, 38 (92), 557–572.

69. S. Jain, S. Madjou, J.F. Virrey Agua, et al. Global leishmaniasis surveillance updates 2023: 3 years of the NTD road map. *Weekly Epidemiological Record* **2024**, No. 45, 653–669.

70. J.A. Ruiz Postigo, S. Jain, S. Madjou, et al. Global leishmaniasis surveillance, 2022: assessing trends over the past 10 years. *Weekly Epidemiological Report* **2023**, No. 40, 471–487.

71. J. Alvar, I.D. Vélez, C. Bern, et al. Leishmaniasis Worldwide and Global Estimates of Its Incidence. *PLoS One* **2012**, 7 (5), e35671.

72. M. Coleman, G.M. Foster, R. Deb, et al. DDT-based indoor residual spraying suboptimal for visceral leishmaniasis elimination in India. *Proc Natl Acad Sci U S A* **2015**, 112 (28), 8573–8578.

73. U. González, M. Pinart, D. Sinclair, et al. Vector and reservoir control for preventing leishmaniasis. *Cochrane Database Syst Rev* **2015**, 2015 (8).

74. M. Shmueli, S. Ben-Shimol. Review of Leishmaniasis Treatment: Can We See the Forest through the Trees? *Pharmacy* **2024**, 12 (1), 30.

75. R.R. Patil, P.K. Chatterjee, R.R. Patil, P.K. Chatterjee. Epidemiology of Visceral Leishmaniasis in India. *National Medical Journal of India* **2023**, 12 (2), 62–68.

76. F. Almeida-Souza, A.L. Abreu-Silva, K. da S. Calabrese, et al. Introductory Chapter: Leishmania Parasites – Epidemiology and Immunopathogenesis. *Leishmania Parasites - Epidemiology, Immunopathology and Hosts* **2024**.

77. R. Pal, G. Teli, M.J. Akhtar, G.S.P. Matada. Synthetic product-based approach toward potential antileishmanial drug development. *Eur J Med Chem* **2024**, 263, 115927.

78. V. Soni, S. Chandel, V. Pandey, et al. Novel Therapeutic Approaches for the Treatment of Leishmaniasis. *Biomaterials and Bionanotechnology* **2019**, 263–300.

79. R. Pal, G. Teli, M.J. Akhtar, G.S.P. Matada. The role of natural anti-parasitic guided development of synthetic drugs for leishmaniasis. *Eur J Med Chem* **2023**, 258, 115609.

80. S. Sundar, A. Singh. Chemotherapeutics of visceral leishmaniasis: present and future developments. *Parasitology* **2018**, 145 (4), 481–489.

81. M. Akbari, A. Oryan, G. Hatam. Application of nanotechnology in treatment of leishmaniasis: A Review. *Acta Trop* **2017**, 172, 86–90.

82. S. Scarpini, A. Dondi, C. Totaro, et al. Visceral Leishmaniasis: Epidemiology, Diagnosis, and Treatment Regimens in Different Geographical Areas with a Focus on Pediatrics. *Microorganisms*. MDPI October 1, **2022**.

83. G.A.S. Romero, D.L. Costa, C.H.N. Costa, et al. Efficacy and safety of available treatments for visceral leishmaniasis in Brazil: A multicenter, randomized, open label trial. *PLoS Negl Trop Dis* **2017**, 11 (6), e0005706.

84. F. Alves, G. Bilbe, S. Blesson, et al. Recent development of visceral leishmaniasis treatments: Successes, pitfalls, and perspectives. *Clin Microbiol Rev* **2018**, 31 (4), 1–30.

85. C. SL, Y. V. Chemotherapy of leishmaniasis. *Curr Pharm Des* **2002**, 8 (4), 326–330.

86. A. Hefnawy, M. Berg, J.C. Dujardin, G. De Muylder. Exploiting Knowledge on Leishmania Drug Resistance to Support the Quest for New Drugs. *Trends Parasitol* **2017**, 33 (3), 162–174.

87. S. Rijal, V. Yardley, F. Chappuis, et al. Antimonial treatment of visceral leishmaniasis: are current in vitro susceptibility assays adequate for prognosis of in vivo therapy outcome? *Microbes Infect* **2007**, 9 (4), 529–535.

88. S. Sundar, Om, P. Singh, et al. Molecular Diagnosis of Visceral Leishmaniasis. *Mol Diagn Ther* **2018**, 22 (4), 443–457.

89. S. Burza, S.L. Croft, M. Boelaert. Leishmaniasis. *The Lancet* **2018**, 392 (10151), 951–970.

90. V.K. Singh, R. Tiwari, N. Rajneesh, et al. Advancing Treatment for Leishmaniasis: From Overcoming Challenges to Embracing Therapeutic Innovations. *ACS Infect Dis* **2025**, 11 (1), 47–68.

91. J. Torre-Cisneros, J.L. Prada, J.L. Villanueva, F. Valverde, P. Sánchez-Guijó. Successful treatment of antimony-resistant cutaneous leishmaniasis with liposomal amphotericin B. *Clin Infect Dis* **1994**, 18 (6), 1024–1025.

92. K.C. Gray, D.S. Palacios, I. Dailey, et al. Amphotericin primarily kills yeast by simply binding ergosterol. *Proc Natl Acad Sci* **2012**, 109 (7), 2234–2239.

93. N. Mbongo, P.M. Loiseau, M.A. Billion, M. Robert-Gero. Mechanism of amphotericin B resistance in Leishmania donovani promastigotes. *Antimicrob Agents Chemother* **1998**, 42 (2), 352–357.

94. S. Sasidharan, P. Saudagar. Leishmaniasis: where are we and where are we heading? *Parasitol Res* **2021**, 120 (5), 1541–1554.

95. O. Gupta, T. Pradhan, R. Bhatia, V. Monga. Recent advancements in anti-leishmanial research: Synthetic strategies and structural activity relationships. *Eur J Med Chem* **2021**, 223, 113606.

96. M. Solomon, S. Baum, A. Barzilai, et al. Liposomal amphotericin B in comparison to sodium stibogluconate for cutaneous infection due to Leishmania braziliensis. *J Am Acad Dermatol* **2007**, 56 (4), 612–616.

97. J. Mishra, A. Saxena, S. Singh. Chemotherapy of Leishmaniasis: Past, Present and Future. *Curr Med Chem* **2007**, 14 (10), 1153–1169.

98. P. Mazire, V. Agarwal, A. Roy. Road-map of pre-clinical treatment for Visceral Leishmaniasis. *Drug Dev Res* **2022**, 83 (2), 317–327.

99. S.L. Croft, R.A. Neal, W. Pendergast, J.H. Chan. The activity of alkyl phosphorylcholines and related derivatives against Leishmania donovani. *Biochem Pharmacol* **1987**, 36 (16), 2633–2636.

100. S. Sundar, J. Chakravarty. Investigational drugs for visceral leishmaniasis. *Expert Opin Investig Drugs* **2015**, 24 (1), 43–59.

101. C. Paris, P.M. Loiseau, C. Bories, J. Bréard. Miltefosine Induces Apoptosis-Like Death in Leishmania donovani Promastigotes. *Antimicrob Agents Chemother* **2004**, 48 (3), 852–859.

102. N.K. Verma, C.S. Dey. Possible mechanism of miltefosine-mediated death of Leishmania donovani. *Antimicrob Agents Chemother* **2004**, 48 (8), 3010–3015.

103. S. Rijal, B. Ostyn, S. Uranw, et al. Increasing Failure of Miltefosine in the Treatment of Kala-azar in Nepal and the Potential Role of Parasite Drug Resistance, Reinfection, or Noncompliance. *Clin Infect Dis* **2013**, 56 (11), 1530–1538.

104. V. Ramesh, R. Singh, K. Avishek, et al. Decline in Clinical Efficacy of Oral Miltefosine in Treatment of Post Kala-azar Dermal Leishmaniasis (PKDL) in India. *PLoS Negl Trop Dis* **2015**, 9 (10), e0004093.

105. D. Kumari, S. Perveen, R. Sharma, K. Singh. Advancement in leishmaniasis diagnosis and therapeutics: An update. *Eur J Pharmacol* **2021**, 910, 174436.

106. W. Charney, L. Rose, P. Quinlan. Pentamidine. *Handbook of Modern Hospital Safety, Second Edition* **2023**, 15-1-15–24.

107. M. Basselin, F. Lawrence, M. Robert-Gero. Pentamidine uptake in Leishmania donovani and Leishmania amazonensis promastigotes and axenic amastigotes. *Biochem J* **1996**, 315 (2), 631–634.

108. M. Paul, R. Durand, Y. Boulard, et al. Physicochemical Characteristics of Pentamidine-Loaded Polymethacrylate Nanoparticles: Implication in the Intracellular Drug Release in Leishmania Major Infected Mice. *J Drug Target* **1998**, 5 (6), 481–490.

109. T.K. Jha. Evaluation of diamidine compound (pentamidine isethionate) in the treatment of resistant cases of kala-azar occurring in North Bihar, India. *Trans R Soc Trop Med Hyg* **1983**, 77 (2), 167–170.

110. R.A. Neal. The effect of antibiotics of the neomycin group on experimental cutaneous leishmaniasis. *Ann Trop Med Parasitol* **1968**, 62 (1), 54–62.

111. M. Shalev-Benami, Y. Zhang, H. Rozenberg, et al. Atomic resolution snapshot of Leishmania ribosome inhibition by the aminoglycoside paromomycin. *Nature Com* **2017**, 8 (1), 1–9.

112. M. Maarouf, F. Lawrence, S.L. Croft, M. Robert-Gero. Ribosomes of Leishmania are a target for the aminoglycosides. *Parasitol Res* **1995**, 81 (5), 421–425.

113. S. Sundar, J. Chakravarty. Paromomycin in the treatment of leishmaniasis. *Expert Opin Investig Drugs* **2008**, 17 (5), 787–794.

114. C. Bustamante, R. Ochoa, C. Asela, C. Muskus. Repurposing of known drugs for leishmaniasis treatment using bioinformatic predictions, in vitro validations and pharmacokinetic simulations. *J Comput Aided Mol Des* **2019**, 33 (9), 845–854.

115. R.L. Charlton, B. Rossi-Bergmann, P.W. Denny, P.G. Steel. Repurposing as a strategy for the discovery of new anti-leishmanials: the-state-of-the-art. *Parasitology* **2018**, 145 (2), 219–236.

116. A.C. Pinheiro, M.V.N. de Souza. Current leishmaniasis drug discovery. *RSC Med Chem* **2022**, 13 (9), 1029–1043.

117. S.A.F. Morad, M.C. Cabot. Tamoxifen regulation of sphingolipid metabolism—Therapeutic implications. *Biochimica et Biophysica Acta (BBA) - Molecular and Cell Biology of Lipids* **2015**, 1851 (9), 1134–1145.

118. K.A. Zewdie, H.G. Hailu, M.A. Ayza, B.A. Tesfaye. Antileishmanial Activity of Tamoxifen by Targeting Sphingolipid Metabolism: A Review. *Clin Pharmacol* **2022**, 14, 11.

119. D.C. Miguel, R.C. Zauli-Nascimento, J.K.U. Yokoyama-Yasunaka, et al. Tamoxifen as a potential antileishmanial agent: efficacy in the treatment of Leishmania braziliensis and Leishmania chagasi infections. *J Antimicrob Chemother* **2009**, 63 (2), 365–368.

120. R. Diaz-Gonzalez, F.M. Kuhlmann, C. Galan-Rodriguez, et al. The Susceptibility of Trypanosomatid Pathogens to PI3/mTOR Kinase Inhibitors Affords a New Opportunity for Drug Repurposing. *PLoS Negl Trop Dis* **2011**, 5 (8), e1297.

121. J. Alvar, P. Aparicio, A. Aseffa, et al. The relationship between leishmaniasis and AIDS: The second 10 years. *Clin Microbiol Rev* **2008**, 21 (2), 334–359.

122. A.M. Thompson, P.D. O'Connor, A. Blaser, et al. Repositioning Antitubercular 6-Nitro-2,3-dihydroimidazo[2,1-b][1,3]oxazoles for Neglected Tropical Diseases: Structure-Activity Studies on a Preclinical Candidate for Visceral Leishmaniasis. *J Med Chem* **2016**, 59 (6), 2530–2550.

123. A.M. Thompson, P.D. O'Connor, A.J. Marshall, et al. 7-Substituted 2-Nitro-5,6-dihydroimidazo[2,1-b][1,3]oxazines: Novel Antitubercular Agents Lead to a New Preclinical Candidate for Visceral Leishmaniasis. *J Med Chem* **2017**, 60 (10), 4212–4233.

124. T.A.C.B. Souza, D.M. Trindade, C.C.C. Tonoli, et al. Molecular adaptability of nucleoside diphosphate kinase b from trypanosomatid parasites: stability, oligomerization and structural determinants of nucleotide binding. *Mol Biosyst* **2011**, 7 (7), 2189.

125. DNDI-0690 | DNDi https://dndi.org/research-development/portfolio/dndi-0690/ (accessed Aug 12, 2025).

126. VL-2098 | DNDi https://dndi.org/research-development/portfolio/vl-2098/ (accessed Aug 12, 2025).

127. R.M. Reguera, Y. Pérez-Pertejo, C. Gutiérrez-Corbo, et al. Current and promising novel drug candidates against visceral leishmaniasis. *Pur Appl Chem* **2019**, 91 (8), 1385–1404.

128. A.M. Thompson, P.D. O'Connor, A.J. Marshall, et al. Development of (6 R)-2-Nitro-6-[4-(trifluoromethoxy)phenoxy]-6,7-dihydro-5 H -imidazo[2,1- b] [1,3]oxazine (DNDI-8219): A New Lead for Visceral Leishmaniasis. *J Med Chem* **2018**, 61 (6), 2329–2352.

129. M. De Rycker, I. Hallyburton, J. Thomas, et al. Comparison of a high-throughput high-content intracellular Leishmania donovani assay with an axenic amastigote assay. *Antimicrob Agents Chemother* **2013**, 57 (7), 2913–2922.

130. S. Wyllie, M. Thomas, S. Patterson, et al. Cyclin-dependent kinase 12 is a drug target for visceral leishmaniasis. *Nature* **2018**, 560 (7717), 192–197.

131. S. Wyllie, S. Brand, M. Thomas, et al. Preclinical candidate for the treatment of visceral leishmaniasis that acts through proteasome inhibition. *Proc Natl Acad Sci* **2019**, 116 (19), 9318–9323.

132. GSK245 (DDD1305143) | DNDi https://dndi.org/research-development/portfolio/gsk245/ (accessed Aug 12, 2025).

133. S. Khare, A.S. Nagle, A. Biggart, et al. Proteasome inhibition for treatment of leishmaniasis, Chagas disease and sleeping sickness. *Nature* **2016**, 537 (7619), 229–233.

134. A. Nagle, A. Biggart, C. Be, et al. Discovery and Characterization of Clinical Candidate LXE408 as a Kinetoplastid-Selective Proteasome Inhibitor for the Treatment of Leishmaniases. *J Med Chem* **2020**, 63 (19), 10773–10781.

135. LXE408 Novartis for CL | DNDi https://dndi.org/research-development/portfolio/lxe408-novartis-for-cutaneous-leishmaniasis/ (accessed Aug 12, 2025).

136. LXE408 Novartis for VL DNDi https://dndi.org/research-development/portfolio/lxe408-novartis-visceral-leishmaniasis/ (accessed Aug 12, 2025).

137. DNDI-6148 | DNDi https://dndi.org/research-development/portfolio/dndi-6148/ (accessed Aug 12, 2025).

138. S. Thareja, M. Zhu, X. Ji, B. Wang. Boron-based small molecules in disease detection and treatment (2013-2016). *Heterocycl Comm* **2017**, 23 (3), 137–153.

139. S. Pradhan, R.A. Schwartz, A. Patil, S. Grabbe, M. Goldust. Treatment options for leishmaniasis. *Clin Exp Dermatol* **2022**, 47 (3), 516–521.

140. J.A. Cardona-Arias, I. Darío Vélez, L. López-Carvajal. Efficacy of Thermotherapy to Treat Cutaneous Leishmaniasis: A Meta-Analysis of Controlled Clinical Trials. *PLoS One* **2015**, 10 (5), e0122569.

141. A. Jabbar, N. Junaid. Treatment of cutaneous leishmaniasis with infrared heat. *Int J Dermatol* **1986**, 25 (7), 470–472.

142. B.M. Valencia, D. Miller, R.S. Witzig, A.K. Boggild, A. Llanos-Cuentas. Novel Low-Cost Thermotherapy for Cutaneous Leishmaniasis in Peru. *PLoS Negl Trop Dis* **2013**, 7 (5), e2196.

143. S. Sundar, J. Singh, V.K. Singh, N. Agrawal, R. Kumar. Current and emerging therapies for the treatment of leishmaniasis. *Expert Opin Orphan Drugs* **2024**, 12 (1), 19–32.

144. J. Chakravarty, S. Sundar. Current and emerging medications for the treatment of leishmaniasis. *Expert Opin Pharmacother* **2019**, 20 (10), 1251–1265.

145. E. Negera, E. Gadisa, J. Hussein, et al. Treatment response of cutaneous leishmaniasis due to Leishmania aethiopica to cryotherapy and generic sodium stibogluconate from patients in Silti, Ethiopia. *Trans R Soc Trop Med Hyg* **2012**, 106 (8), 496–503.

146. Pan American Health Organization. Directrices para el tratamiento de las leishmaniasis en la Región de las Américas. Segunda edición.

147. J. Soto, D. Paz, D. Rivero, et al. Intralesional Pentamidine: A Novel Therapy for Single Lesions of Bolivian Cutaneous Leishmaniasis. *Am J Trop Med Hyg* **2016**, 94 (4), 852–856.

148. A. Ben Salah, N. Ben Messaoud, E. Guedri, et al. Topical paromomycin with or without gentamicin for cutaneous leishmaniasis. *N Engl J Med* **2013**, 368 (6), 524–532.

149. A.D.M. Bryceson, A.H. Moody, A. Murphy. Treatment of “Old World” cutaneous leishmaniasis with aminosidine ointment: results of an open study in London. *Trans R Soc Trop Med Hyg* **1994**, 88 (2), 226–228.

150. M. Omidian, M. Jadbabaei, E. Omidian, Z. Omidian. The effect of Nd:YAG laser therapy on cutaneous leishmaniasis compared to intralesional meglumine antimoniate. *Postepy Dermatol Alergol* **2019**, 36 (2), 227–231.

151. B.M. Scorza, E.M. Carvalho, M.E. Wilson. Cutaneous Manifestations of Human and Murine Leishmaniasis. *Int J Mol Sci* **2017**, 18 (6).

152. S. Shamsi Meymandi, S. Zandi, H. Aghaie, A. Heshmatkhah. Efficacy of CO(2) laser for treatment of anthroponotic cutaneous leishmaniasis, compared with combination of cryotherapy and intralesional meglumine antimoniate. *J Eur Acad Dermatol Venereol* **2011**, 25 (5), 587–591.

153. P. López-Jaramillo, C. Ruano, J. Rivera, et al. Treatment of cutaneous leishmaniasis with nitric-oxide donor. *Lancet* **1998**, 351 (9110), 1176–1177.

154. P. López-Jaramillo, M.Y. Rincón, R.G. García, et al. A controlled, randomized-blinded clinical trial to assess the efficacy of a nitric oxide releasing patch in the treatment of cutaneous leishmaniasis by Leishmania (V.) panamensis. *Am J Trop Med Hyg* **2010**, 83 (1), 97–101.

155. SSG&PM (East Africa) | DNDi https://dndi.org/research-development/portfolio/ssg-pm/ (accessed Aug 13, 2025).

156. A. Musa, E. Khalil, A. Hailu, et al. Sodium Stibogluconate (SSG) & Paromomycin Combination Compared to SSG for Visceral Leishmaniasis in East Africa: A Randomised Controlled Trial. *PLoS Negl Trop Dis* **2012**, 6 (6), e1674.

157. W.E.C. on the C. of the Leishmaniases, W.H. Organization. Control of the leishmaniases: report of a meeting of the WHO Expert Commitee on the Control of Leishmaniases, Geneva, 22-26 March 2010. **2010**.

158. Miltefosine + Paromomycin combination (Africa) | DNDi https://dndi.org/research-development/portfolio/miltefosine-paromomycin-combo/ (accessed Aug 13, 2025).

159. A.M. Musa, J. Mbui, R. Mohammed, et al. Paromomycin and Miltefosine Combination as an Alternative to Treat Patients With Visceral Leishmaniasis in Eastern Africa: A Randomized, Controlled, Multicountry Trial. *Clin Infect Dis* **2023**, 76 (3), e1177–e1185.

160. V. Ramesh, K.K. Dixit, N. Sharma, R. Singh, P. Salotra. Assessing the Efficacy and Safety of Liposomal Amphotericin B and Miltefosine in Combination for Treatment of Post Kala-Azar Dermal Leishmaniasis. *J Infect Dis* **2020**, 221 (4), 608–617.

161. P.R.L. Machado, H. Lassa, M. Lessa, et al. Oral pentoxifylline combined with pentavalent antimony: A randomized trial for mucosal leishmaniasis. *Clin Infect Dis* **2007**, 44 (6), 788–793.

162. C. Cincura, R.S. Costa, C.M.F. De Lima, et al. Assessment of Immune and Clinical Response in Patients with Mucosal Leishmaniasis Treated with Pentavalent Antimony and Pentoxifylline. *Trop Med Infect Dis* **2022**, 7 (11).

163. L. López, B. Valencia, F. Alvarez, et al. A phase II multicenter randomized study to evaluate the safety and efficacy of combining thermotherapy and a short course of miltefosine for the treatment of uncomplicated cutaneous leishmaniasis in the New World. *PLoS Negl Trop Dis* **2022**, 16 (3), e0010238.

164. M.A. El Darouti, S.M. Al Rubaie. Cutaneous leishmaniasis. Treatment with combined cryotherapy and intralesional stibogluconate injection. *Int J Dermatol* **1990**, 29 (1), 56–59.

165. A. Asilian, A. Sadeghinia, G. Faghihi, A. Momeni. Comparative study of the efficacy of combined cryotherapy and intralesional meglumine antimoniate (Glucantime®) vs. cryotherapy and intralesional meglumine antimoniate (Glucantime®) alone for the treatment of cutaneous leishmaniasis. *Int J Dermatol* **2004**, 43 (4), 281–283.

166. W. Health Organization Regional Office for Europe. Manual on case management and surveillance of the leishmaniases in the WHO European region. **2017**.

167. S. Sundar, J. Chakravarty, D. Agarwal, M. Rai, H.W. Murray. Single-Dose Liposomal Amphotericin B for Visceral Leishmaniasis in India. *N Engl J Med* **2010**, 362 (6), 504–512.

168. Government of Nepal Ministry of Health and Population. National Guideline on Kala-azar Elimination Program. **2019**.

169. M. Mishra, U.K. Biswas, D.N. Jha, A.B. Khan. Amphotericin versus pentamidine in antimony-unresponsive kala-azar. *Lancet* **1992**, 340 (8830), 1256–1257.

170. P.K. Sinha, T.K. Jha, C.P. Thakur, et al. Phase 4 Pharmacovigilance Trial of Paromomycin Injection for the Treatment of Visceral Leishmaniasis in India. *J Trop Med* **2011**, 2011, 645203.

171. T.P.C. Dorlo, S. Rijal, B. Ostyn, et al. Failure of miltefosine in visceral leishmaniasis is associated with low drug exposure. *J Infect Dis* **2014**, 210 (1), 146–153.

172. S. Sundar, P.K. Sinha, M. Rai, et al. Comparison of short-course multidrug treatment with standard therapy for visceral leishmaniasis in India: an open-label, non-inferiority, randomised controlled trial. *Lancet* **2011**, 377 (9764), 477–486.

173. New VL treatments (South Asia) | DNDi https://dndi.org/research-development/portfolio/new-vl-treatments-south-asia/?utm_source=chatgpt.com (accessed Aug 14, 2025).

174. Operational Guidelines on Kala-Azar (Visceral Leishmaniasis) Elimination in India - 2015). *National Center for Vector Borne Diseases Control* **2015**.

175. G.M. Anabwani, G. Dimiti, J.A. Ngira, A.D.M. Bryceson. Comparison of two dosage schedules of sodium stibogluconate in the treatment of visceral leishmaniasis in Kenya. *Lancet* **1983**, 1 (8318), 210–212.

176. SSG&PM (East Africa) | DNDi https://dndi.org/research-development/portfolio/ssg-pm/ (accessed Aug 14, 2025).

177. R.N. Davidson, J. Seaman, D. Pryce, et al. Epidemic visceral leishmaniasis in Sudan: a randomized trial of aminosidine plus sodium stibogluconate versus sodium stibogluconate alone. *J Infect Dis* **1993**, 168 (3), 715–720.

178. Republic of Kenya Ministry of Health. Prevention, diagnosis and treatment of visceral leishmaniasis (kala-azar) in Kenya, **2017**

179. J. Seaman, C. Boer, R. Wilkinson, et al. Liposomal amphotericin B (AmBisome) in the treatment of complicated kala-azar under field conditions. *Clin Infect Dis* **1995**, 21 (1), 188–193.

180. S. Sundar, H. Mehta, A. Chhabra, et al. Amphotericin B colloidal dispersion for the treatment of indian visceral leishmaniasis. *Clinical Infectious Diseases* **2006**, 42 (5), 608–613.

181. Guideline for the Treatment of Leishmaniasis in the Americas. Second Edition. *Guideline for the Treatment of Leishmaniasis in the Americas. Second Edition* **2022**.

182. J. Van Griensven, E. Carrillo, R. López-Vélez, L. Lynen, J. Moreno. Leishmaniasis in immunosuppressed individuals. *Clin Microbiol Infect* **2014**, 20 (4), 286–299.

183. A.L.C. Neumayr, G. Morizot, L.G. Visser, et al. Clinical aspects and management of cutaneous leishmaniasis in rheumatoid patients treated with TNF-α antagonists. *Travel Med Infect Dis* **2013**, 11 (6), 412–420.

184. P.M. Nyakundi, R. Muigai, J.B.O. Were, et al. Congenital visceral leishmaniasis: case report. *Trans R Soc Trop Med Hyg* **1988**, 82 (4), 564.

185. I.A. Eltoum, E.E. Zijlstra, M.S. Ali, et al. Congenital kala-azar and leishmaniasis in the placenta. *Am J Trop Med Hyg* **1992**, 46 (1), 57–62.

186. E.A. Figueiró-Filho, G. Duarte, P. El-Beitune, S.M. Quintana, T.L. Maia. Visceral leishmaniasis (kala-azar) and pregnancy. *Infect Dis Obstet Gynecol* **2004**, 12 (1), 31–40.

187. M. Mueller, M. Balasegaram, Y. Koummuki, et al. A comparison of liposomal amphotericin B with sodium stibogluconate for the treatment of visceral leishmaniasis in pregnancy in Sudan. *J Antimicrob Chemother* **2006**, 58 (4), 811–815.

188. J.E. Kaplan, C. Benson, K.H. Holmes, et al. Guidelines for prevention and treatment of opportunistic infections in HIV-infected adults and adolescents: recommendations from CDC, the National Institutes of Health, and the HIV Medicine Association of the Infectious Diseases Society of America. *MMWR Recomm Rep* **2009**, 58 (RR-4).

189. F.J.R. Paumgartten, I. Chahoud. Embryotoxicity of meglumine antimoniate in the rat. *Reprod Toxicol* **2001**, 15 (3), 327–331.

190. R.N. Davidson, M. den Boer, K. Ritmeijer. Paromomycin. *Trans R Soc Trop Med Hyg* **2009**, 103 (7), 653–660.

191. L. Di Martino, R.N. Davidson, R. Giacchino, et al. Treatment of visceral leishmaniasis in children with liposomal amphotericin B. *J Pediatr* **1997**, 131 (2), 271–277.

192. S. Sundar, P.L. Olliaro. Miltefosine in the treatment of leishmaniasis: Clinical evidence for informed clinical risk management. *Ther Clin Risk Manag* **2007**, 3 (5), 733.

193. Y. Taslimi, F. Zahedifard, S. Rafati. Leishmaniasis and various immunotherapeutic approaches. *Parasitology* **2018**, 145 (4), 497–507.

194. R. Hazra, C.R. MR, S.K. Mahapatra. A brief report on eugenol oleate is an oral immunomodulatory molecule against visceral leishmaniasis. *Ind J Physiol All Sci* **2023**, 75 (02), 84–88.

195. A. Momeni, M. Rasoolian, A. Momeni, et al. Development of liposomes loaded with anti-leishmanial drugs for the treatment of cutaneous leishmaniasis. *J Liposome Res* **2013**, 23 (2), 134–144.

196. R.G. Maggi, F. Krämer. A review on the occurrence of companion vector-borne diseases in pet animals in Latin America. *Parasites & Vectors* **2019**, 12 (1), 1–37.

197. R. Kumar, K. Pandey, G.C. Sahoo, et al. Development of high efficacy peptide coated iron oxide nanoparticles encapsulated amphotericin B drug delivery system against visceral leishmaniasis. *Mat Sci Eng* **2017**, 75, 1465–1471.

198. K. Georgopoulou, D. Smirlis, S. Bisti, et al. In Vitro Activity of 10-Deacetylbaccatin III against Leishmania donovani Promastigotes and Intracellular Amastigotes. *Planta Med* **2007**, 73 (10), 1081–1088.

199. J.R. Fanti, F. Tomiotto-Pellissier, M.M. Miranda-Sapla, et al. Biogenic silver nanoparticles inducing Leishmania amazonensis promastigote and amastigote death in vitro. *Acta Trop* **2018**, 178, 46–54.

200. A. Sazgarnia, A.R. Taheri, S. Soudmand, et al. Antiparasitic effects of gold nanoparticles with microwave radiation on promastigotes and amastigotes of Leishmania major. *Int J Hyperther* **2013**, 29 (1), 79–86.

201. M. Khatami, H. Alijani, I. Sharifi, et al. Leishmanicidal Activity of Biogenic Fe3O4 Nanoparticles. *Scientia Pharmaceutica* **2017**, 85 (4), 36.

202. M. Delavari, A. Dalimi, F. Ghaffarifar, J. Sadraei. In Vitro Study on Cytotoxic Effects of ZnO Nanoparticles on Promastigote and Amastigote Forms of Leishmania major (MRHO/IR/75/ER). *Iran J Parasitol* **2014**, 9 (1), 6.

203. A.M. Allahverdiyev, E.S. Abamor, M. Bagirova, et al. Antileishmanial effect of silver nanoparticles and their enhanced antiparasitic activity under ultraviolet light. *Int J Nanomedicine* **2011**, 6, 2705–2714.

204. A. Zielinska, F. Carreiró, A.M. Oliveira, et al. Polymeric Nanoparticles: Production, Characterization, Toxicology and Ecotoxicology. *Molecules* **2020**, 25 (16), 3731.

205. R. Tiwari, R.P. Gupta, V.K. Singh, et al. Nanotechnology-Based Strategies in Parasitic Disease Management: From Prevention to Diagnosis and Treatment. *ACS Omega* **2023**, 8 (45), 42014–42027.

206. D. Barros, S.A.C. Lima, A. Cordeiro-Da-Silva. Surface Functionalization of Polymeric Nanospheres Modulates Macrophage Activation: Relevance in Leishmaniasis Therapy. *Nanomedicine* **2015**, 10 (3), 387–403.

207. P. Saudagar, V.K. Dubey. Carbon nanotube based betulin formulation shows better efficacy against Leishmania parasite. *Parasitol Int* **2014**, 63 (6), 772–776.

208. B. Shaker, S. Ahmad, J. Lee, C. Jung, D. Na. In silico methods and tools for drug discovery. *Comput Biol Med* **2021**, 137, 104851.

209. J. Vamathevan, D. Clark, P. Czodrowski, et al. Applications of machine learning in drug discovery and development. *Nature Rev Drug Disc* **2019**, 18 (6), 463–477.

210. F. Annang, G. Pérez-Moreno, R. García-Hernández, et al. High-Throughput Screening Platform for Natural Product–Based Drug Discovery Against 3

Neglected Tropical Diseases: Human African Trypanosomiasis, Leishmaniasis, and Chagas Disease. *SLAS Discovery* **2015**, 20 (1), 82–91.

211. F. Modabber. Experiences with vaccines against cutaneous leishmaniasis: of men and mice. *Parasitology* **1989**, 98 Suppl (S1), S49–S60.

212. S. Zutshi, S. Kumar, P. Chauhan, et al. Anti-Leishmanial Vaccines: Assumptions, Approaches, and Annulments. *Vaccines* **2019**, 7 (4).

213. E.A.G. Khalil. Vaccines for Visceral Leishmaniasis: Hopes and Hurdles. In *Leishmaniases as Re-emerging Diseases*; InTech, **2018**.

214. J. Convit, M. Ulrich, O. Zerpa, et al. Immunotherapy of american cutaneous leishmaniasis in Venezuela during the period 1990-99. *Trans R Soc Trop Med Hyg* **2003**, 97 (4), 469–472.

215. I.N. Satti, H. Y. Osman, N.S. Daifalla, et al. Immunogenicity and safety of autoclaved Leishmania major plus BCG vaccine in healthy Sudanese volunteers. *Vaccine* **2001**, 19 (15–16), 2100–2106.

216. M.S.S. Araújo, R.A. de Andrade, L.R. Vianna, et al. Despite Leishvaccine and Leishmune® trigger distinct immune profiles, their ability to activate phagocytes and CD8+ T-cells support their high-quality immunogenic potential against canine visceral leishmaniasis. *Vaccine* **2008**, 26 (18), 2211–2224.

217. A. Ayala, A. Llanes, R. Lleonart, C.M. Restrepo. Advances in Leishmania Vaccines: Current Development and Future Prospects. *Pathogens* **2024**, 13 (9), 812.

218. M.J. Abbaszadeh Afshar, S. Elikaee, R. Saberi, S. Mohtasebi, M. Mohebali. Expression analysis of centrin gene in promastigote and amastigote forms of leishmania infantum iranian isolates: a promising target for live attenuated vaccine development against canine leishmaniasis. *BMC Vet Res* **2021**, 17 (1), 1–7.

219. R.N. Coler, S.G. Reed. Second-generation vaccines against leishmaniasis. *Trends Parasitol* **2005**, 21 (5), 244–249.

220. R. Velez, M. Gállego. Commercially approved vaccines for canine leishmaniosis: a review of available data on their safety and efficacy. *Trop Med Inte Health* **2020**, 25 (5), 540–557.

221. J. Chakravarty, S. Kumar, S. Trivedi, et al. A clinical trial to evaluate the safety and immunogenicity of the LEISH-F1 + MPL-SE vaccine for use in the prevention of visceral leishmaniasis. *Vaccine* **2011**, 29 (19), 3531–3537.

222. Study Details | A Study of the Efficacy and Safety of the LEISH-F2 + MPL-SE Vaccine for Treatment of Cutaneous Leishmaniasis | ClinicalTrials.gov https://clinicaltrials.gov/study/NCT01011309 (accessed Aug 17, 2025).

223. R.N. Coler, M.S. Duthie, K.A. Hofmeyer, et al. From mouse to man: safety, immunogenicity and efficacy of a candidate leishmaniasis vaccine LEISH-F3+GLA-SE. *Clin Transl Immunology* **2015**, 4 (4), e35.

224. A.R. da S. Melo, L.S. de Macêdo, M. da C.V. Invenção, et al. Third-Generation Vaccines: Features of Nucleic Acid Vaccines and Strategies to Improve Their Efficiency. *Genes* **2022**, 13 (12), 2287.

225. R. Dinc. *Leishmania* Vaccines: the Current Situation with Its Promising Aspect for the Future. *Korean J Parasitol* **2022**, 60 (6), 379–391.

CHAPTER 2. OBJECTIVES

In the general context of the synthesis of pharmacologically relevant indole-derived heterocycles with potential antileishmanial activity, we have pursued the following objectives:

I. Synthesis of a family of rigid indole-imidazole compounds from the coupling of tryptamine derivatives with diazadialkenes, followed by a palladium-catalysed cross-dehydrogenative Coupling.

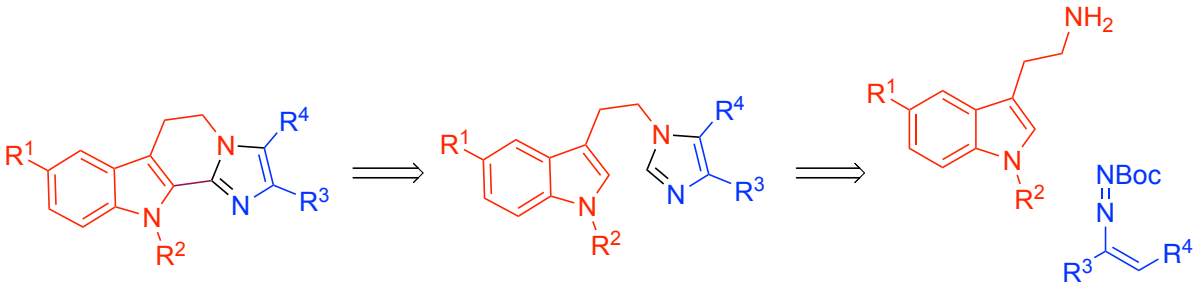

II. Development and optimisation of alternative methodologies for extending the scope of the rigid indole-imidazole derivatives.

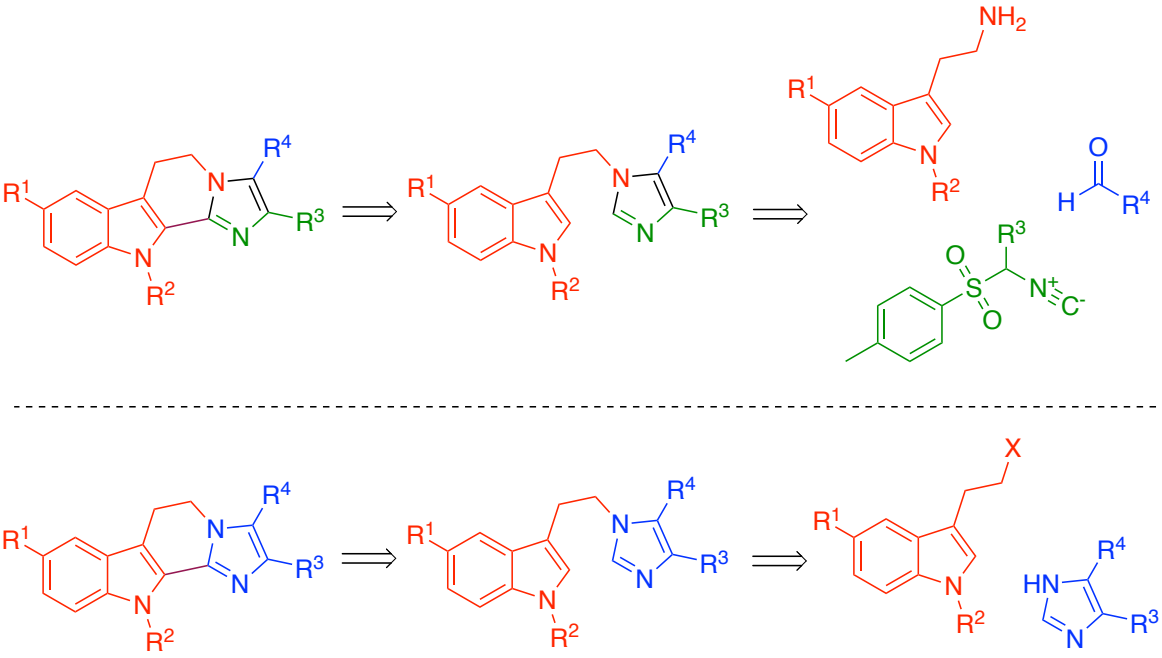

III. Design and synthesis of bisindole compounds with particular emphasis on the study of the effect of the ethylenic chain on the activity.

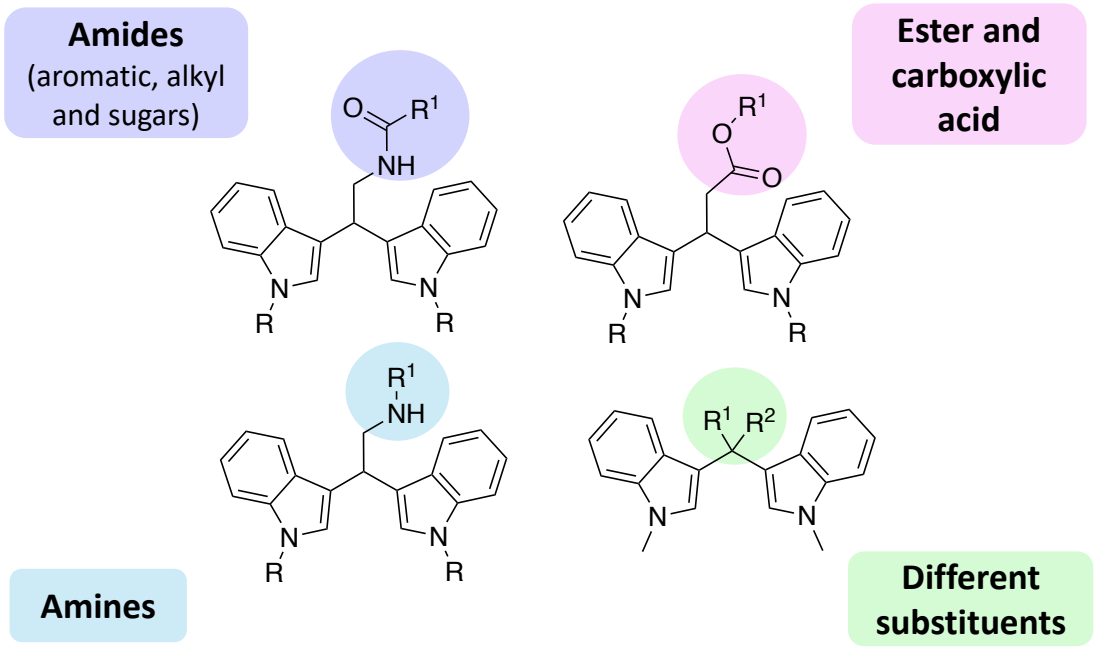

IV. Development of methodologies for the synthesis of indole-isoindolinone derivatives as potential antileishmanial agents, including the understanding of the reaction mechanisms involved.

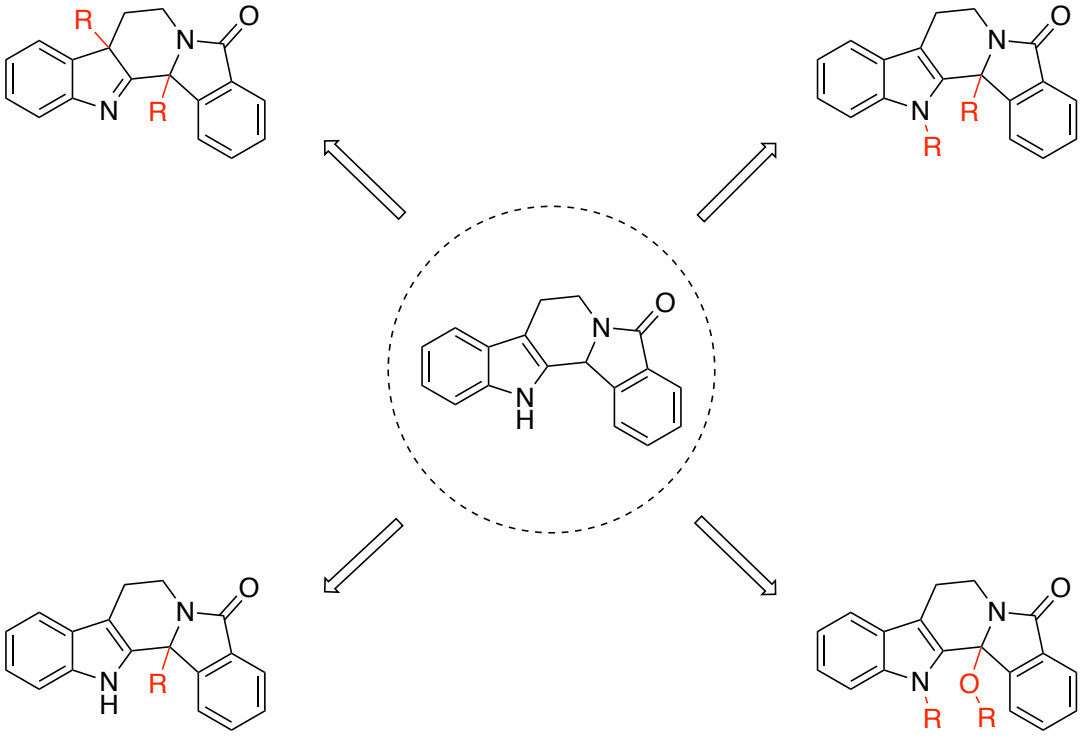

V. Antileishmanial biological evaluation of the synthesised compounds and study of the results for the development of structure-activity relationships (SAR).

A graphic overview of the objectives of this thesis is provided below.

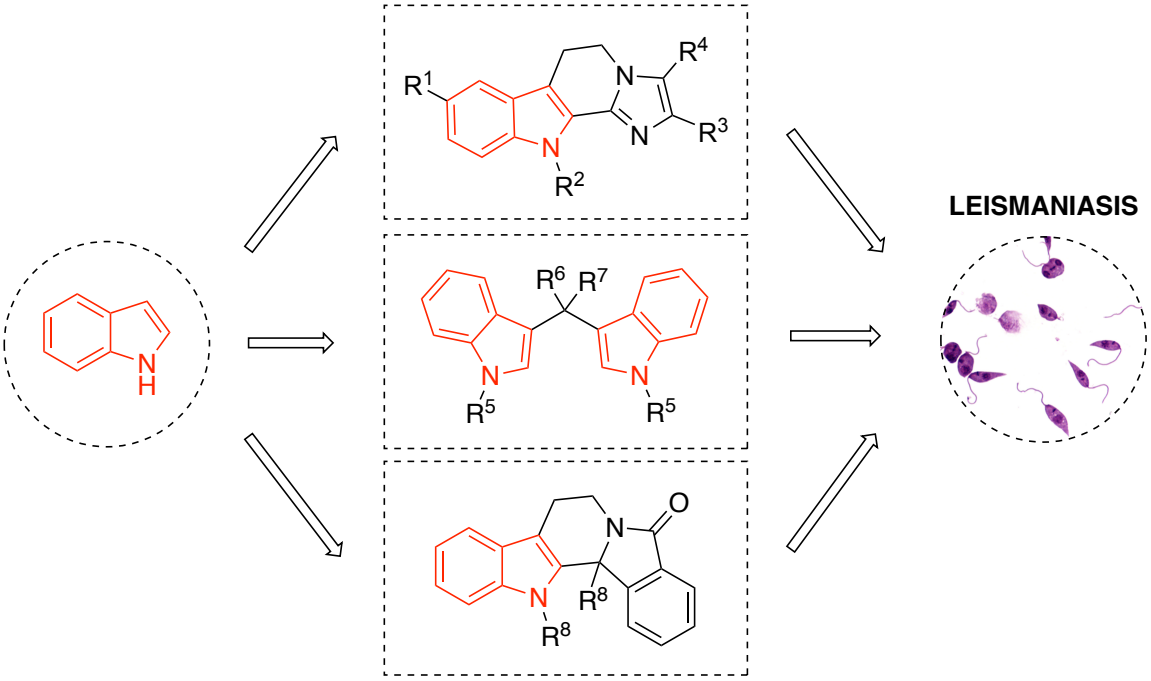

CHAPTER 3. DESIGN, SYNTHESIS AND BIOLOGICAL EVALUATION OF NEW RIGID INDOLE-IMIDAZOLE AS POTENTIAL ANTILEISHMANIAL AGENTS

3.1. INTRODUCTION

3.1.1. Indoles

Indole is one of the most important heterocyclic systems that are indole moieties are highly prevalent in natural products. Indole derivatives have gained growing importance in drug discovery as privileged scaffolds eliciting a wide variety of biological activities.

3.1.1.1 Natural products

Diverse natural products containing the indole moiety have been discovered and studied for their diverse biological activities (Figure 3.1). 7-Hydroxyspeciociliatine was isolated from the fruits of *Mitragyna speciosa Korth* and showed opioid-agonistic activity, with a weak stimulatory effect on μ-opioid receptors.[1] Brassinin and cyclobrassinin were found in plants of the family Brassicaceae.[2] Brassinin inhibits the proliferation in different human cancer cell lines,[3–5] and together with cyclobrassicin, they both have chemopreventive activity.[6] Caulilexins A–C were extracted from florets of cauliflower (*Brassica oleracea* var. *botrytis*) and all showed antifungal properties.[7] From *Malassezia furfur* yeast, pityriazepin, a natural indoloazepine, was isolated and found to be a potent AhR ligand.[8] The natural alkaloid macrolepiotin extracted from Macrolepiota neomastoidea was found to be active against multiple human cancer cell lines.[9] From the myxobacterium *Labilithrix luteola,* two secondary metabolites were found, labindole A and B. These compounds were found to have antimicrobial and antiviral activity.[10] Legonimide was isolated from the extracts of *Streptomyces* sp. CT37 and showed moderate antimicrobial activity.[11] From the akuamma tree (*Picralima nitida*), akuammine was isolated and tested, showing micromolar activity at the mu opioid receptor.[12]

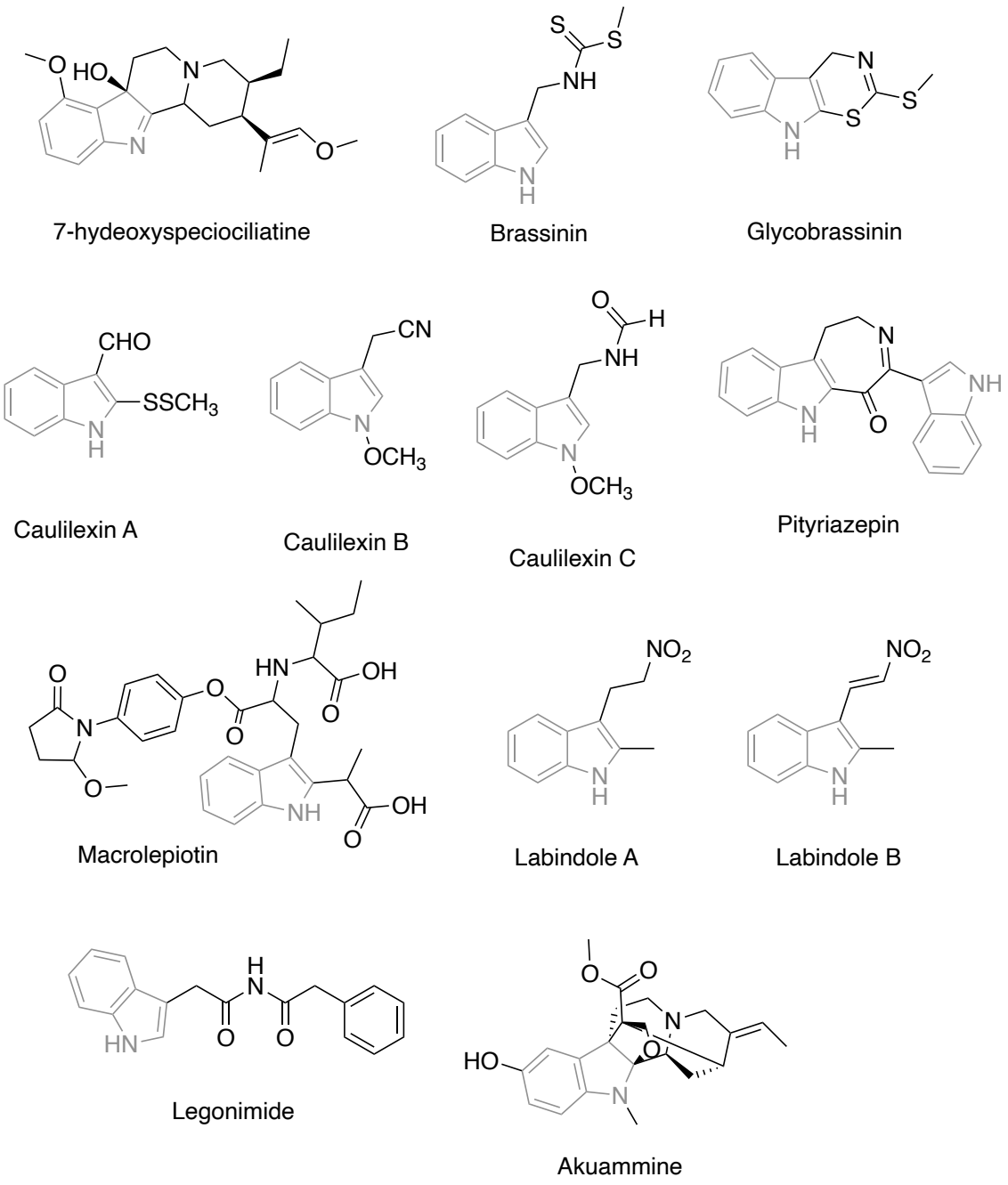

Figure 3.1. Examples of natural products containing the indole moiety (in grey) with biological activity.

3.1.1.2 Biological activities

The indole ring is known as a privileged scaffold in drug discovery as it is present in compounds with antibacterial, anticancer, antifungal, anti-tubercular, antiviral, antimalarial and anti-leishmanial activities among others. Only a selection of compounds is shown for each biological activity as the total number of molecules is too large to display.

a) Antibacterial activity

Abo-Ashour and co-workers[13] synthesised a family of indole-thiazolidinone conjugates, finding compound **1** (Figure 3.2) as the one with the highest broad-spectrum antibacterial activity against the tested Gram-positive and Gram-negative bacteria. The structure-activity relationship (SAR) suggested the importance of the methyl and Cl substituents for the activity. Mane *et al.*[14] synthesised and evaluated different 5-substituted indole-2-carboxamide derivatives (**2**), finding that the *para*-fluoro and *meta*-chloro substituents were important for the activity, as well as the free nitrogen in the indole. In 2016, Yadav *et al.*[15] synthesised a series of 1,2,3,5-substituted indoles, finding compound **3** as the one with the best antimicrobial activity, suggesting the importance of *N*-substituted carbamate in the 2 position of the indole ring. Shaikh and Debebe synthesised novel *N*-substituted indoles, finding compound **4** as the one with the best antimicrobial activity, suggesting the importance of the butyl substituent. Gani *et al.* synthesised diverse 1-cyclopropyl-3-ethoxycarbonyl-2-methylindole-5-(1-methylethoxyaceticacidhydrazide) derivatives (**5a-c**) showing that these compounds were the ones with highest antimicrobial activity due to the effect of electron-withdrawing groups such as NO_2 and electron-donating groups such as OH and the thiazole moiety. These molecules are represented in Figure 3.2.

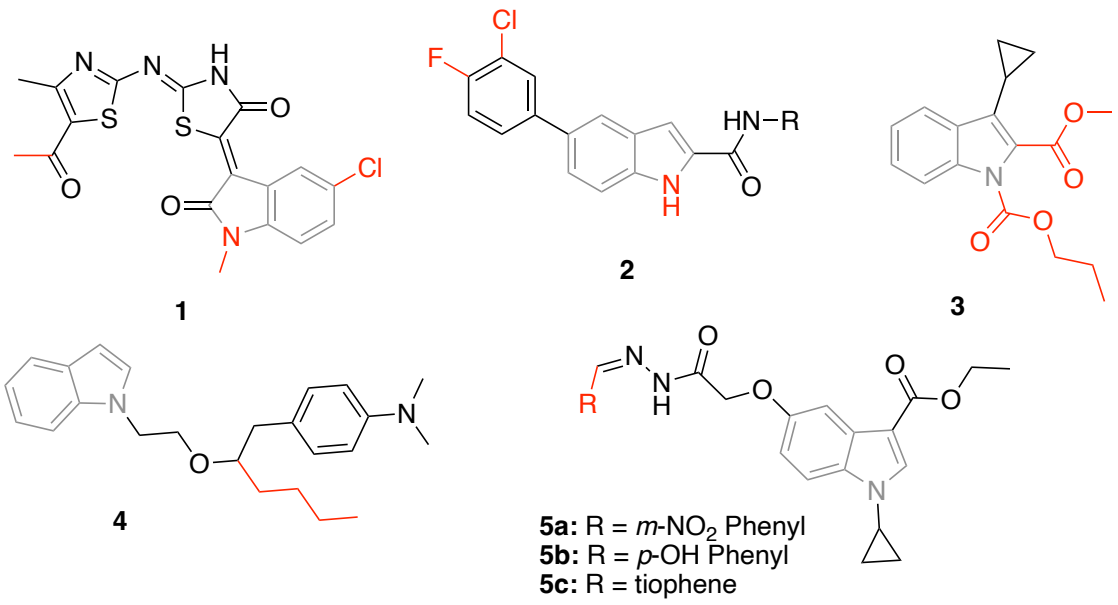

Figure 3.2. Indole derivatives with antimicrobial activity. Relevant substituents for the structure-activity relationship are marked in red.

b) Anticancer activity

Diverse indole derivatives have been designed as anticancer agents over the last years. They act through diverse targets such as histone deacetylases (HDACs), sirtuins, DNA topoisomerase, etc.[16] Corigliano *et al.* synthesised a family of 2,4-thiazolidinedione conjugates, obtaining two derivatives (**6a,b**) with significant antiproliferative effect in two different human neoplastic cell lines. The SAR concluded that the methoxy group in the position 5 of the indole ring was the most favourable for the activity.[17] In 2018, Parkash *et al.* synthesised substituted heteroannulated indole derivatives that were evaluated for their cervical anticancer activity. It was observed that the substitution in position 5 of the indole ring was enhancing the activity, preferring electron-withdrawing groups (**7a** > **7b** > **7c** > **7d**). Also, the free amine was important, as derivatives with a sulphur in this position were found less active.[18] Bakherad and coworkers synthesised thiosemicarbazone indole-based derivatives. The SAR study concluded that methyl and hydroxy phenyl substituent enhanced the activity (**8a-c**).[19] These molecules are represented in Figure 3.3.

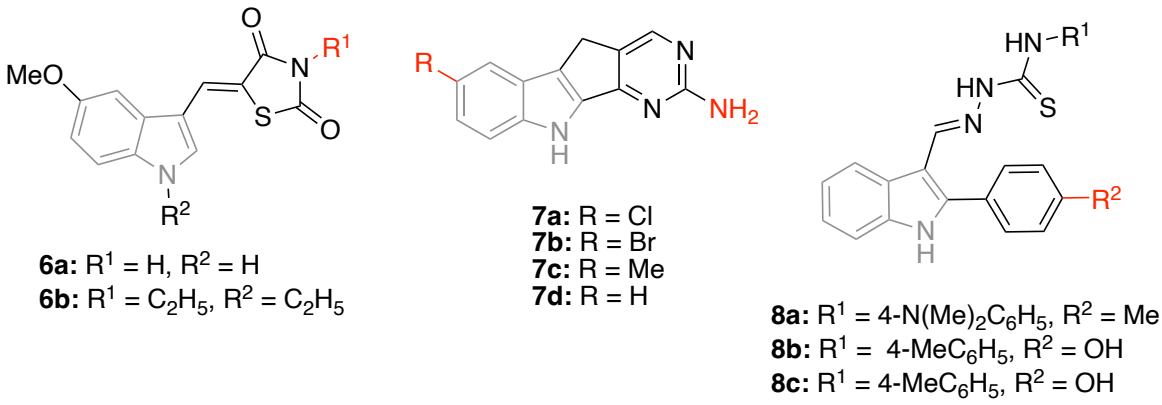

6a: R^1 = H, R^2 = H
6b: R^1 = C_2H_5, R^2 = C_2H_5

7a: R = Cl
7b: R = Br
7c: R = Me
7d: R = H

8a: R^1 = 4-$N(Me)_2C_6H_5$, R^2 = Me
8b: R^1 = 4-MeC_6H_5, R^2 = OH
8c: R^1 = 4-MeC_6H_5, R^2 = OH

Figure 3.3. Indole derivatives with anticancer activity. Relevant substituents for the structure-activity relationship are marked in red.

c) Antifungal activity

Zhang *et al.*[20] synthesised streptochlorin derivatives, these derivatives substituted the indole ring with other heterocycles, finding low to no activity, demonstrating the importance of the indole ring for the activity of streptochlorin. Xu *et al.*[21] synthesised indole-triazole molecules and observed through the SAR that the distance between the triazole and the benzyl group is not important, the *ortho*-substituent of the phenyl

ring is usually beneficial to the activity, while the activity is reduced when R^2 is an electron-withdrawing group or R^3 is substituted. In 2021, Song *et al.* synthesised pimprinine derivatives bearing a 1,3,4-oxadiazole-5-thioether moiety. Compound **10** was found to be the most active, and the structure-activity relationship showed that adding a methylene bridge between indole and thioether did not enhance the activity. These molecules are represented in Figure 3.4.

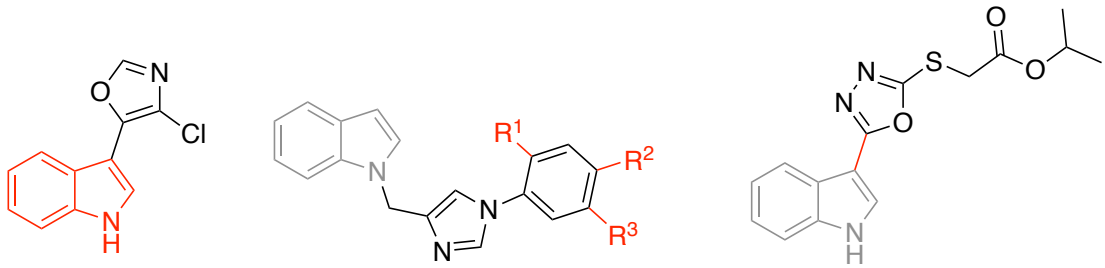

Figure 3.4. Indole derivatives with antifungal activity. Relevant substituents for the structure-activity relationship are marked in red.

d) Anti-tubercular activity

In 2013, Tehrani *et al.*[22] synthesised diverse thiocarbohydrazone and thiadiazole derivatives (**11**), observing through the activity results that the thiadiazole moiety plays a vital role in antimycobacterial activity. Khan *et al.*[23] synthesised indeno-fluorene derivatives (**12**) and analysed their anti-tubercular activity, finding that the substitution in the *para* position of the phenyl ring with a nitro group enhanced the activity.

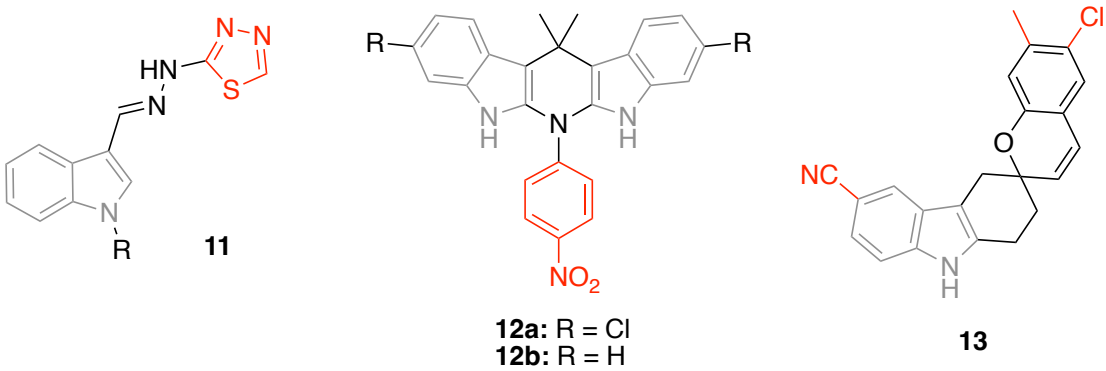

Figure 3.5. Indole derivatives with anti-tubercular activity. Relevant substituents for the structure-activity relationship are marked in red.

Dogamanti and co-workers[24] synthesised a family of indole-fused spirochromenes from which compound **13** was found to be the most potent. These molecules are shown in Figure 3.5.

e) Antiviral activity

In 2017, Scuotto *et al.*[25] synthesised arbidol derivatives and evaluated their antiviral activity. SAR indicated that changing the methoxy for the hydroxy group in the 5 position of indole enhanced the activity (**14**). Moreover, the substituent on the phenyl ring also affected the activity. Musella and co-workers[26] studied the effect of tryptamine derivatives (**15**) against the varicella Zoster virus (VZV). The SAR study showed that the presence of a biphenyl ethyl moiety and the acetylation at the amino group of tryptamines are essential for anti-VZV activity. Sanna *et al.*[27] synthesised novel indole-thiourea hybrids (**16**), which were evaluated against HIV-1. The SAR results highlighted the importance of the 4-bromophenyl moiety. The previous molecules are reported in Figure 3.6.

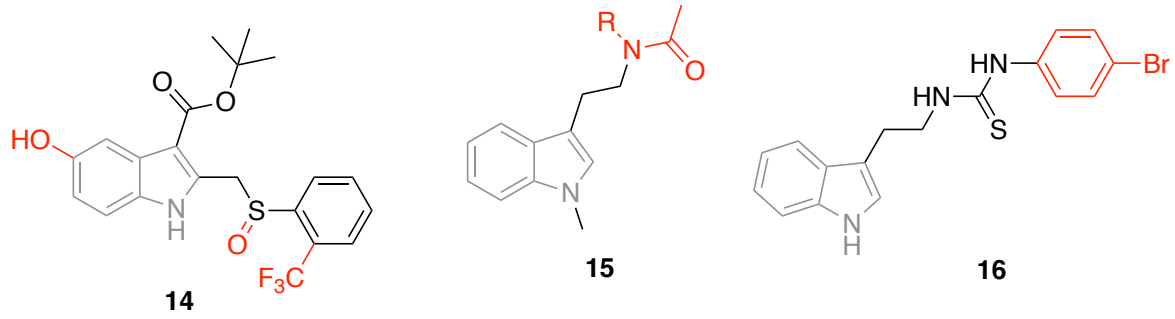

Figure 3.6. Indole derivatives with antiviral activity. Relevant substituents for the structure-activity relationship are marked in red.

f) Antimalarial activity

Santos and co-workers[28] synthesised 3-piperidin-4-yl-1*H*-indole compounds as potential antimalarials. They found the active compound **17,** and the SAR shows that 3-piperidin-4-yl-1*H*-indole does not tolerate most *N*-piperidinyl modifications. In 2014, Schuck *et al.* synthesised melatonin derivatives (**18**) against malaria. Bulky side chains at the C-3 position decrease the coordination ability of the new indole, and the methoxy group at position 5′ is important for the activity of melatonin on its receptor. These molecules are shown in Figure 3.7.

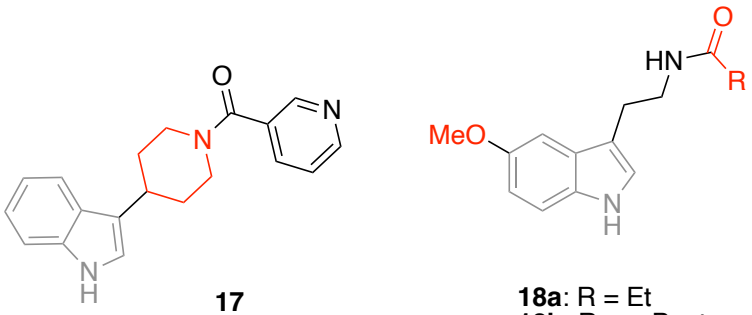

17

18a: R = Et
18b: R = *n*-Pent
18c: R = Ph

Figure 3.7. Indole derivatives with antimalarial activity. Relevant substituents for the structure-activity relationship are marked in red.

g) Anti-leishmanial activity

The antileishmanial activity of indole derivatives will be described in section 3.1.1.3.

3.1.1.3 Indoles as antileishmanial agents

Porwal and co-workers[29] synthesised and evaluated *gem*-dithioacetylated derivatives against Leishmaniasis. Their most potent compound was **19**. Removing this *gem*-dithioacetyl group resulted in loss of the activity. In the same way, changing the *p*-cianophenoxy moiety or changing the linker decreased the activity of the compounds. Félix *et al.*[30] synthesised tiopheneindole hybrids, finding **20a-c** as promising molecules. The SAR showed the importance of the cyano substituent in position 5 of the indole ring as well as the fact that bigger rings were more favourable for the activity. In 2014, Sharma's group[31] studied different triazino indole-quinoline hybrids against leishmaniasis. In this case, the activity of **21a-b** and other derivatives was strongly influenced by the length of the linker between the two pharmacophores (with 2 carbon atoms being the best length for the chain). Methylation of the indole nitrogen also increased the activity of the derivatives. Tiwari *et al.*[32] synthesised up to twenty-seven *N*-substituted derivatives, including chalcones and hydrazide-hydrazones. For the hydrazide-hidrazone derivatives, alkoxy coumarin connected through the 7 position was more active than the ones in the 4 position. The length of the chain did not affect the activity, but the substitution of the phenyl ring is important; *para*-substitution was preferred to *meta*. The indole-based molecules with antileishmanial activity are shown in Figure 3.8.

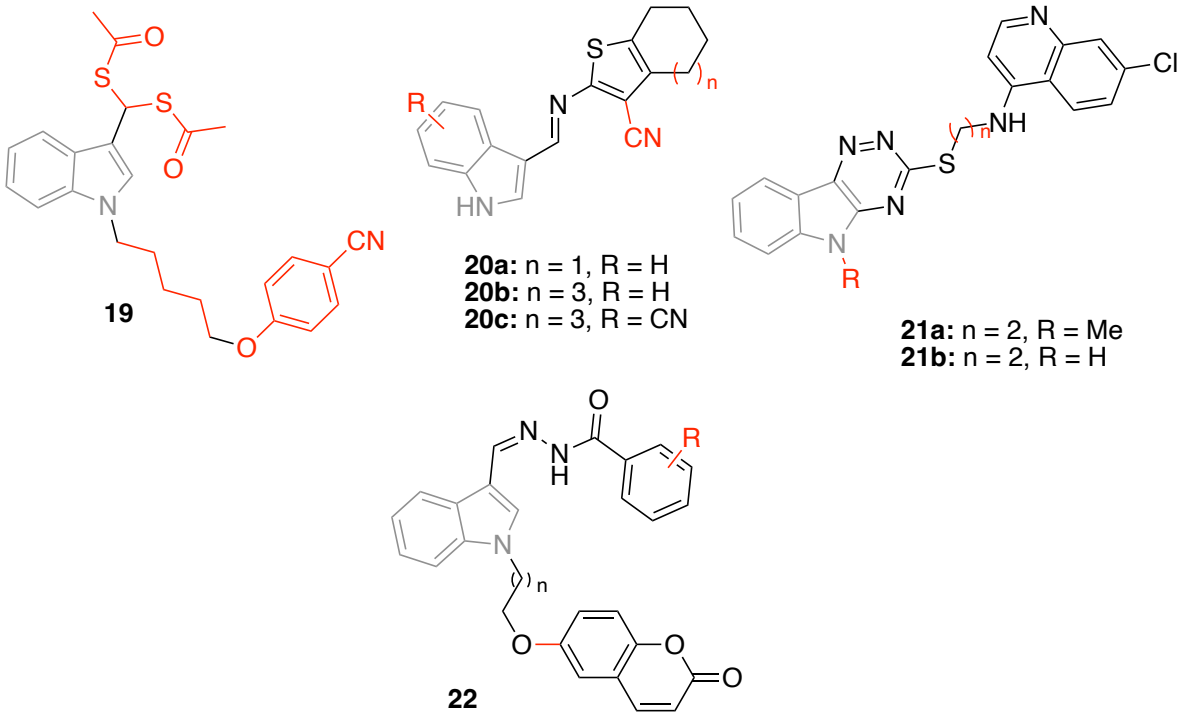

Figure 3.8. Indole derivatives with antileishmanial activity. Relevant substituents for the structure-activity relationship are marked in red.

3.1.2. Imidazoles

3.1.2.1 Natural products

Imidazole alkaloids constitute a diverse group of natural secondary metabolites containing imidazole as their structural core. These compounds are primarily found in marine sponges, marine invertebrates, microorganisms and plants. Imidazole alkaloids exhibit diverse biological activities, including cytotoxic, antimicrobial, anti-inflammatory, antiparasitic and neurotoxic. Their complexity, unique biosynthetic pathways and biological activities generate significant interest in both synthesis and drug development.[33–35]

Marine sponges are a natural source of structurally diverse alkaloids. Bromopyrrole-imidazole alkaloids (Figure 3.9) derive from a common metabolite, oroidine.[36] These alkaloids have been isolated from different sponges and exert many biological activities such as antiparasitic, antimicrobial and cytotoxic activity.[37–40]

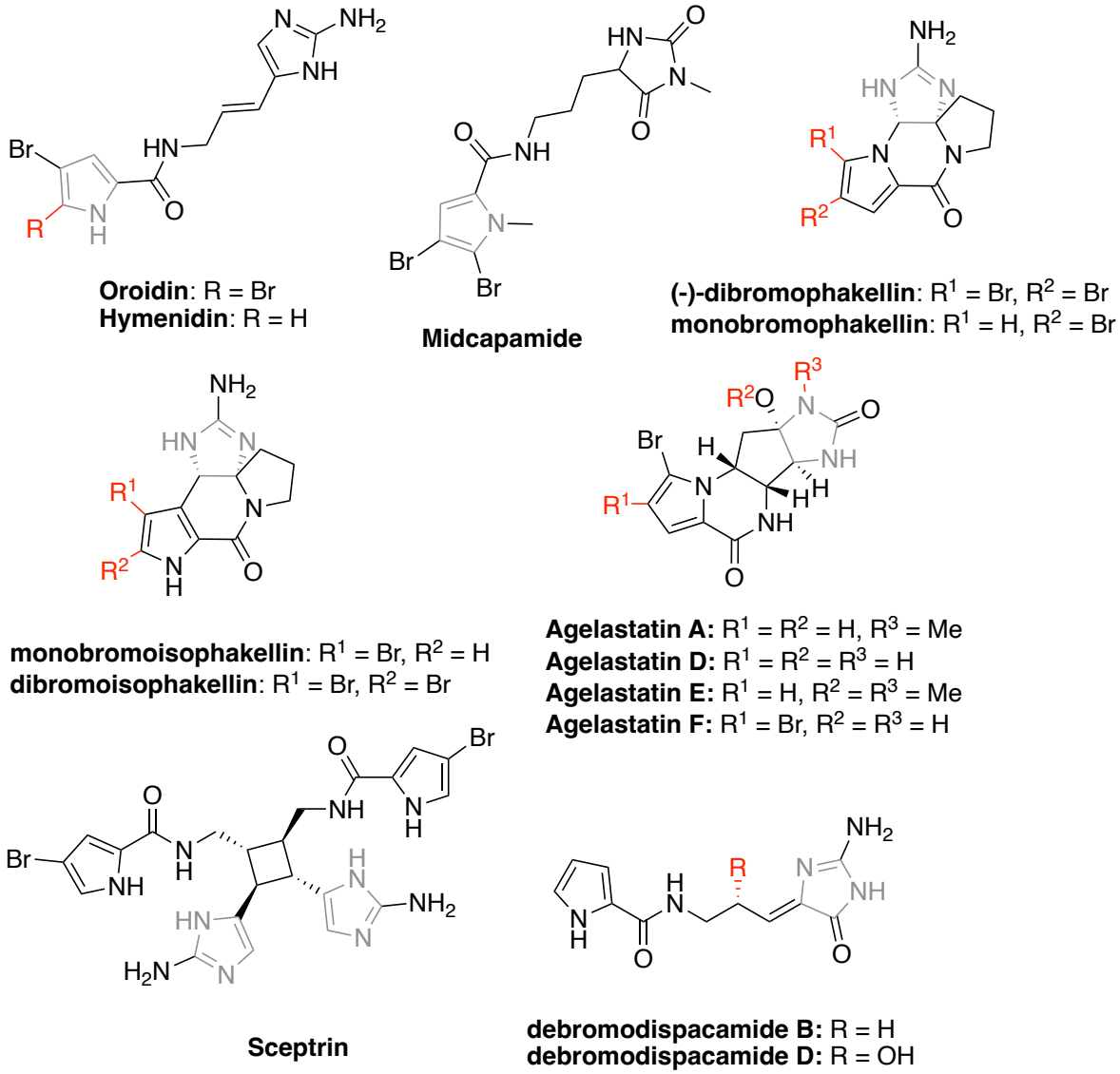

Figure 3.9. Structures of Bromopyrrole-imidazolealakloids extracted from marine sponges.

Aminoimidazole alkaloids are a group of secondary metabolites mainly extracted from the genus *Leucetta*. These molecules contain one or two imidazole/imidazolone units (Figure 3.10) and exhibit diverse biological activities such as cytotoxicity and microtubule stabilisation.[41–44]

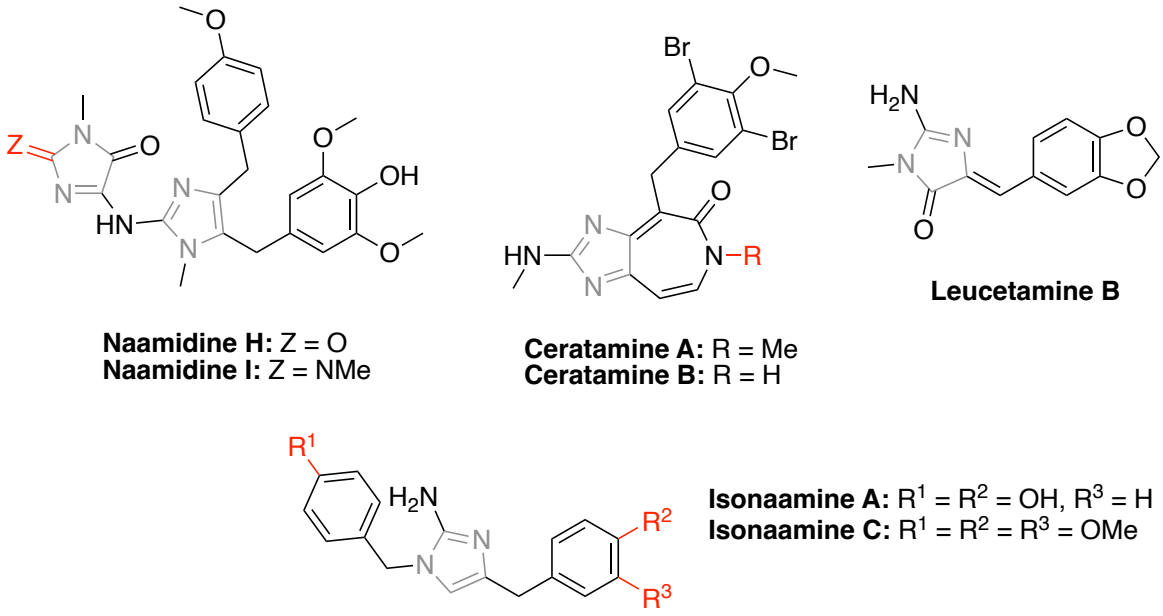

Figure 3.10. Structures of aminoimidazole alkaloids extracted from marine sponges.

Other imidazole derivatives extracted from marine sponges include spongolactams A and B, asteropterin and cribrostatin 6, among others. These derivatives exhibit diverse biological activities, including cancer-related enzyme inhibition and antimicrobial activity.[45–47]

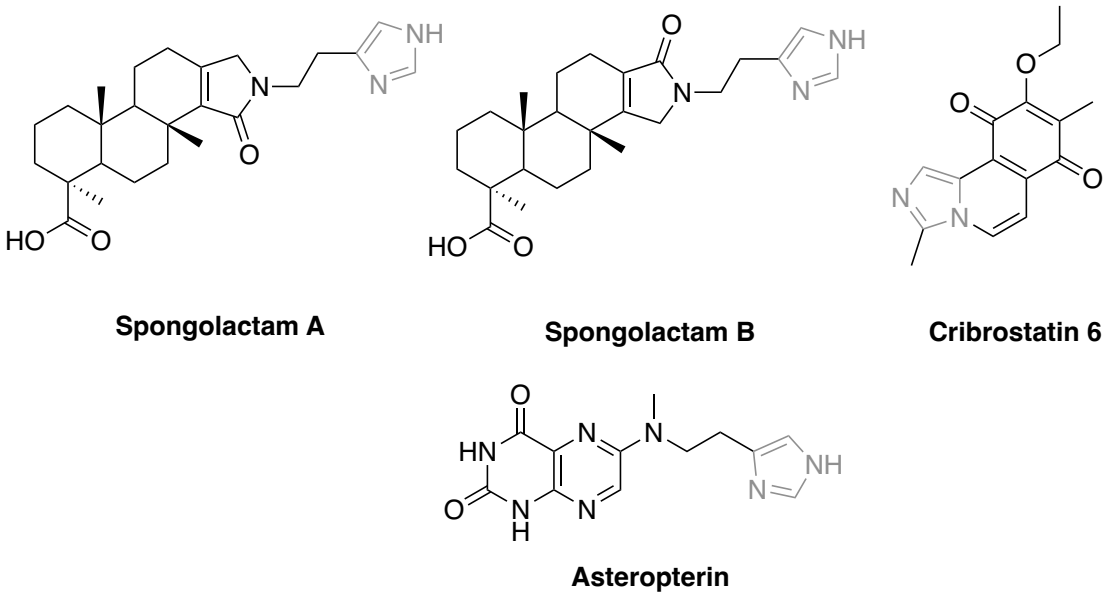

Figure 3.11. Imidazole alkaloid derivatives extracted from marine sponges.

From other marine invertebrates, such as corals, ascidians, or anemones, some imidazole derivatives have been extracted with biological activities, including kinase inhibition, antimalarial activity, or cytotoxicity.[48] (Figure 3.12)

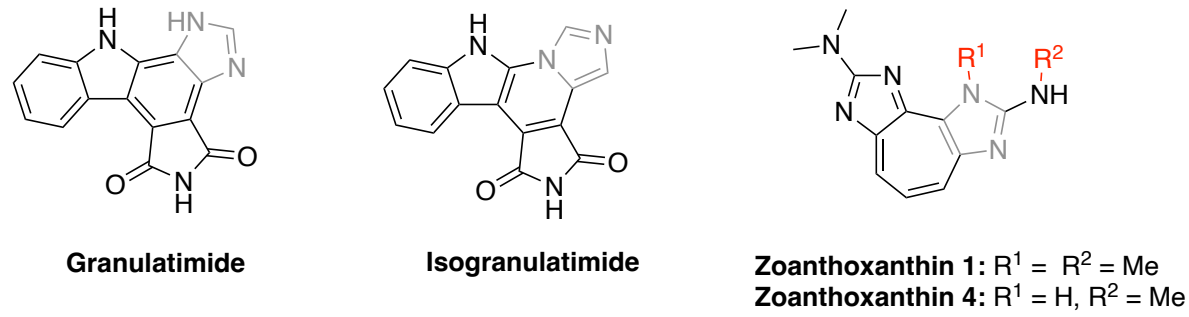

Granulatimide **Isogranulatimide**

Zoanthoxanthin 1: R^1 = R^2 = Me
Zoanthoxanthin 4: R^1 = H, R^2 = Me

Figure 3.12. Imidazole alkaloid derivatives extracted from marine invertebrates.

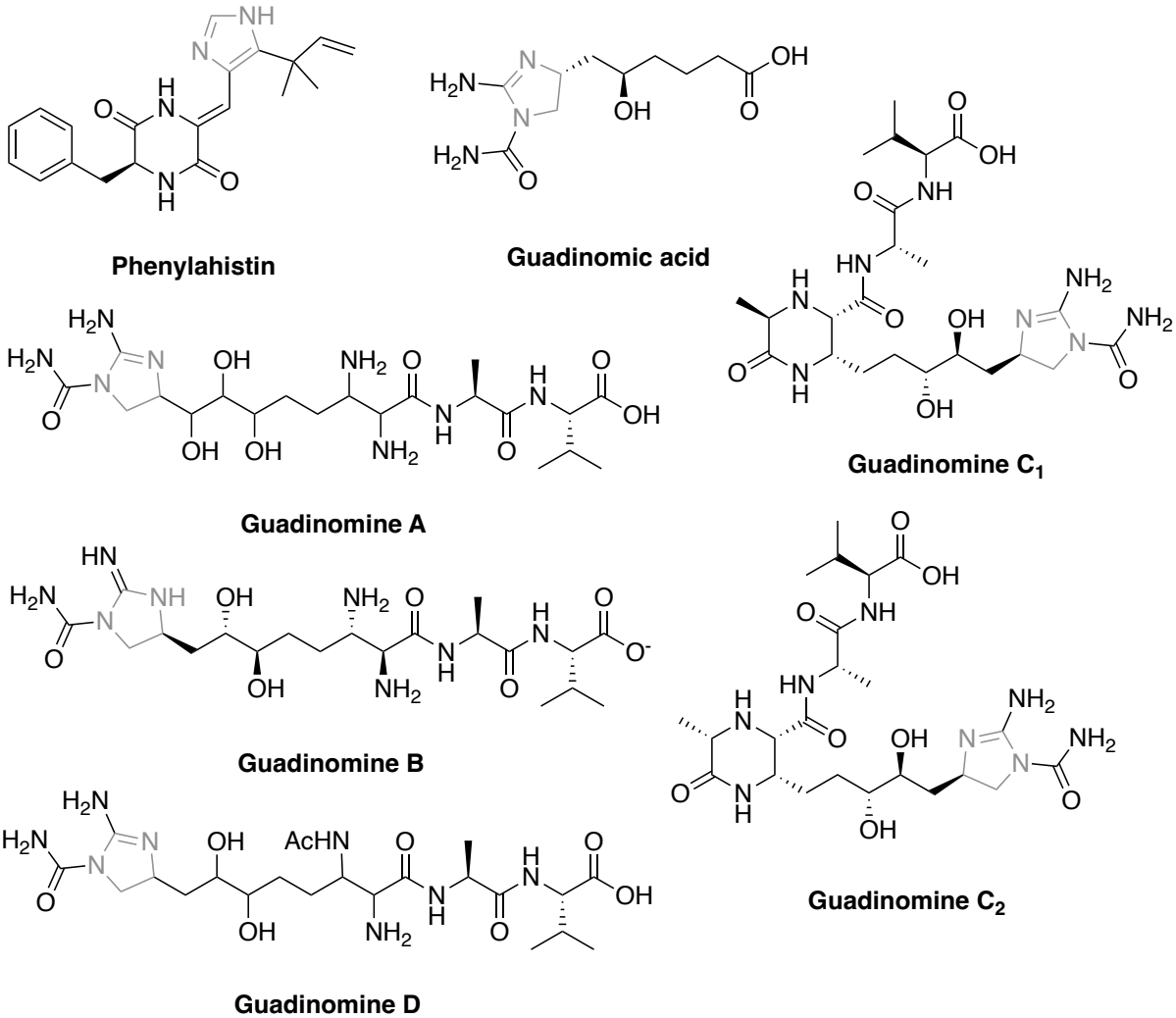

Phenylahistin **Guadinomic acid**

Guadinomine A **Guadinomine C_1**

Guadinomine B

Guadinomine D **Guadinomine C_2**

Figure 3.13. Imidazole alkaloids extracted from microorganisms.

Microorganisms, both marine and terrestrial, are a source of imidazole alkaloids (Figure 3.13); some of them show inhibition of resistant bacteria, cytotoxicity, and inhibition of lipids and kinases.[49–51]

From higher plants, bioactive cyclic peptides and imidazole alkaloids have been extracted, with representative examples shown in Figure 3.14. These compounds show biological activities, including anti-inflammatory effects, tubulin inhibition and use in the treatment of glaucoma.[52,53]

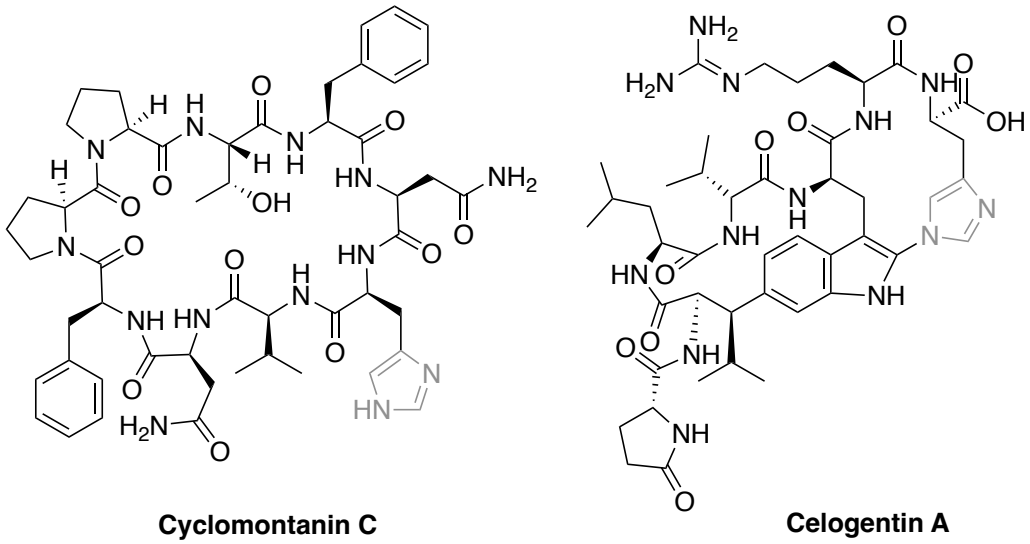

Cyclomontanin C **Celogentin A**

Figure 3.14. Bioactive cyclic peptides from higher plants containing imidazole.

3.1.2.2 Biological activity

Diverse approved pharmaceuticals, in multiple therapeutic areas, contain the imidazole nucleus. These compounds have shown diverse biological activities, including anticancer, antifungal, antimicrobial, antiviral, antitubercular, antiprotozoal, anti-inflammatory, antihistaminic, antihypertensive, antineuropathic, antiobesity, and antiparasitic properties.

a) Anticancer activity

Recent research has demonstrated the potential of imidazole derivatives as anticancer agents. Some of them have been used widely in this field, including dacarbazine, zoledronic acid, azathioprine, tipifarnib and nilotinib (Figure 3.15).[54]

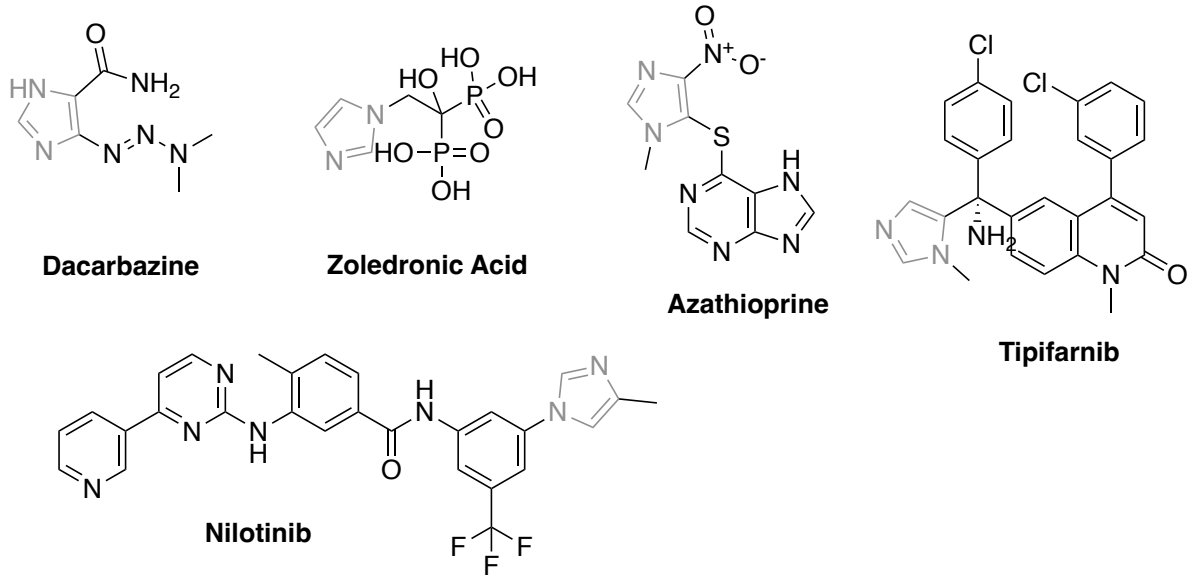

Figure 3.15. Commercial anticancer drugs containing an imidazole core.

Current efforts are focused on the discovery of new anticancer imidazole-based agents that target specifically enzymes or receptors such as topoisomerases, microtubules, cytochromes P450, kinases RAF, TGF-β, farnesyl transferase, and DNA.[55]

Some camptothecin derivatives have been evaluated as topoisomerase inhibitors. Compound **23** introduced ethyl and imidazolyl groups, obtaining a better solubility and inhibition of Topoisomerase I.[56] Compounds **24a-b** contain the imidazole group in position 20, increasing the lactone stability and reducing toxicity.[57] Toposisomerase II inhibitors include molecules such as **25**, an amsacrine derivative, which binds to DNA and blocks the cell cycle.[58] (See Figure 3.16)

Imidazole derivatives such as **26a-b** have shown to be potent inhibitors of microtubule polymerisation. Some azole CYP450 inhibitors, such as letrozole, are pharmaceutically interesting. Substitution of the triazole ring for an imidazole ring yielded compound **27**, with a better inhibitory activity.[59]

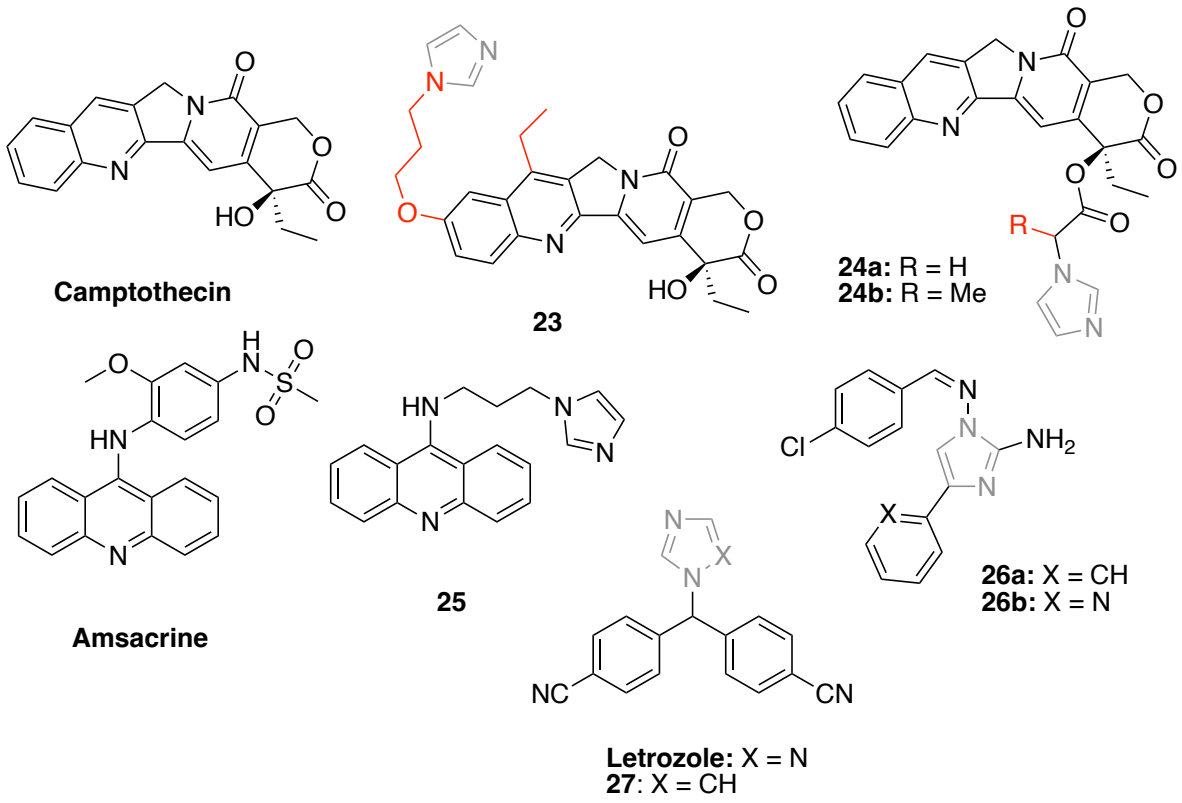

Figure 3.16. Anticancer imidazole derivatives. Relevant substituents for the structure-activity relationship are marked in red.

b) Antifungal activity

Imidazoles and triazoles are the most used class of synthetic antifungal agents.[60,61] Some commercial drugs include clotrimazole, ketoconazole and oxiconazole, among others (Figure 3.17).

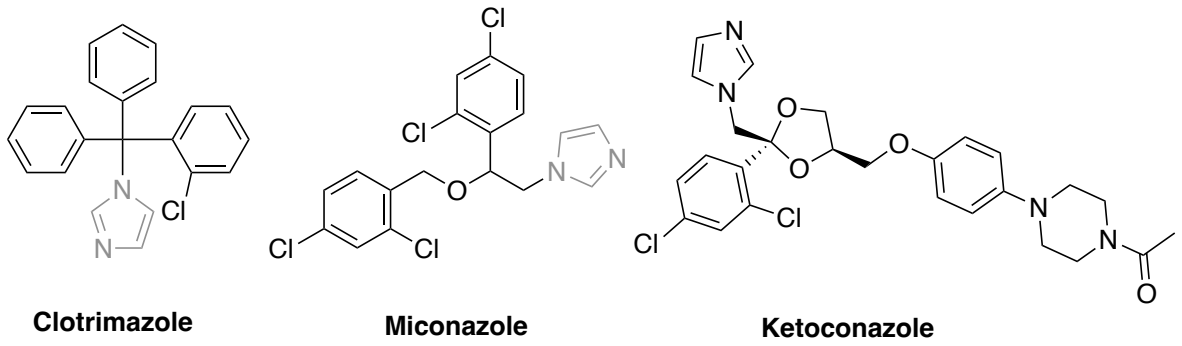

Figure 3.17. Commercial antifungal drugs.

Diverse structural modifications have been made to optimise the antifungal activity. Miconazole derivatives have been synthesised, and their biological results show that

the introduction of a chlorine substituent is favourable for the electronic effects of benzyl, enhancing the antifungal activity. Miconazole esters are promising candidates (Figure 3.18).[62,63]

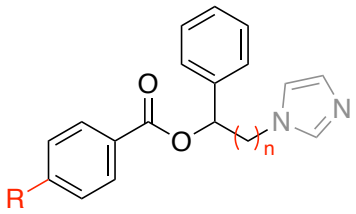

28a: n = 2, R = H
28b: n = 2, R = Cl
28c: n = 1, R = F
28d: n = 1, R = Ph

Figure 3.18. Miconazole derivatives with antifungal activity. Relevant substituents for the structure-activity relationship are marked in red.

Some new imidazole-based compounds have also been developed as antifungals. *N*-alkylimidazoles (**29a-c**) (Figure 3.19) with electron-withdrawing groups such as nitro, Br or phenyl showed an antifungal activity comparable to the one of ketoconazole against *Candida albicans, Aspergillus niger* and *Penicillium chrysogenum*. This activity was attributed to the possibility of these groups to form hydrogen bonds with key residues of CYP51.[64] Imidazole-chalcone hybrids (**30a,b**) (Figure 3.19) showed antifungal activity against *A. fumicatus,* suggesting that the presence of halogens in the molecule enhanced the antifungal activity and the radical scavenging effects.[65]

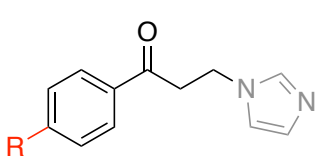

29a: R = Br
29b: R = NO_2
29c: R = Ph

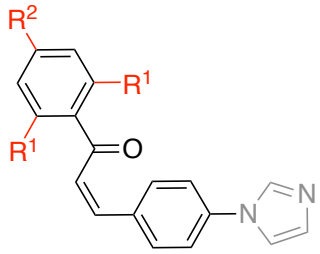

30a: R^1 = H, R^2 = Cl
30b: R^1 = Cl, R^2 = H

Figure 3.19. New imidazole-based antifungal compounds. Relevant substituents for the structure-activity relationship are marked in red.

c) Antimicrobial activity

Diverse commercial antibacterial drugs contain the imidazole moiety, such as metronidazole, ornidazole, secnidazole, nimorazole or tinidazole (Figure 3.20). Metronidazole was introduced in 1960 as a potent compound against Gram-negative anaerobic bacteria.[66]

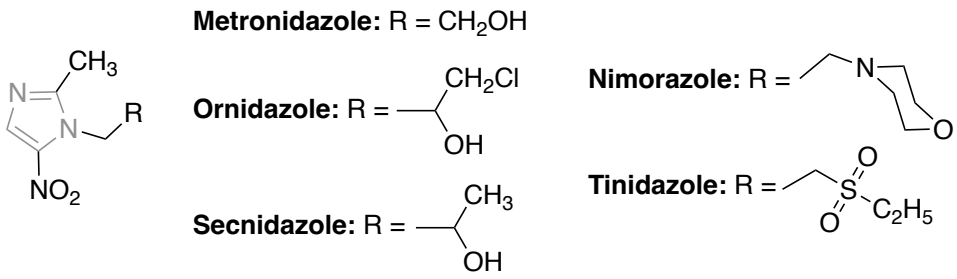

Figure 3.20. Imidazole-based commercial drugs.

During the last years, efforts in discovering new antibacterial imidazole agents have been made.[67] Introduction of an alkyl chain could be favourable for some physicochemical properties, such as water solubility or binding affinity. Compounds **31a-c** showed antibacterial activity comparable to other commercially available antibacterial drugs. The replacement of imidazole by other heterocycles reduced the antibacterial activity.[68]

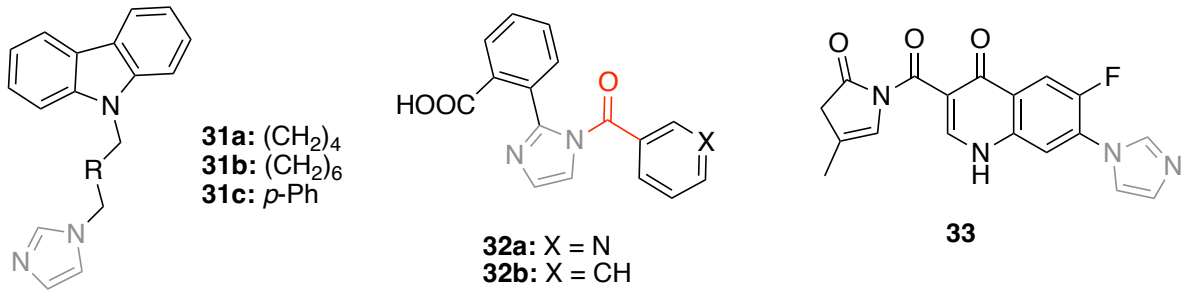

Figure 3.21. Imidazole-based antibacterial compounds. Relevant substituents for the structure-activity relationship are marked in red.

The carbonyl-linked molecules **32a-b** showed excellent antibacterial activity that was drastically reduced when the carbonyl group was removed.[69] The combination of imidazole with other heterocycles facilitates the binding of these molecules with receptors and enzymes.[70] Compound **33** gave anti-*E. coli* activity comparable to the one of ciprofloxacin. Changing the imidazole ring by piperidine, piperazine, morpholine

or pyrrolidine all harmed the biological activity, demonstrating the importance of the imidazole ring.[71]

d) Antitubercular activity

The imidazoderivative known as nitroimidazopyran PA-824 (Figure 3.22), which is in advanced stages of clinical trials has inspired the synthesis of other molecules containing imidazole moiety for the treatment of tuberculosis.[72] Pyrazinamide (PZA) is an antitubercular compound, and this prompted the synthesis of some imidazole-PZA derivatives, which have been evaluated for their antitubercular activity. Compound **34** showed promising activity and, despite being a PZA derivative, it was found to act through a mechanism of action different to the one proposed for PZA.[73] Compound **35** displayed good antitubercular activity, and the *p*-methoxy benzyl moiety proved to be important for the activity, probably due to increased lipid solubility.

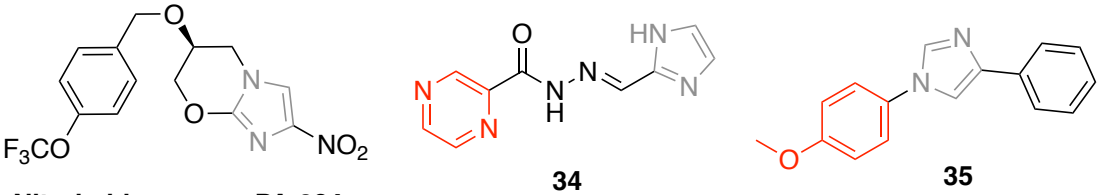

Nitroimidazopyran PA-824 **34** **35**

Figure 3.22. Imidazole-based antituberculotic compounds. Relevant substituents for the structure-activity relationship are marked in red.

e) Antihistaminic activity

The imidazole moiety is not a common core in the inhibitors of two histamine receptors (HR), H_1R and H_2R (except for cimetidine, an H_2R antagonist designed by structural manipulation of histamine itself). However, some molecules containing imidazole have been developed as current and potential H_3R and H_4R antagonists. Imetit, thioperamide, and clobenpropit (Figure 3.23) are all H_3R ligands with significant affinity also for H_4R.[74,75] Compound **36a** exhibited a good affinity for H_3R, with a selectivity index of 20 over H_4R. Whenever changing the alkyl chain (**36b-c**), the resulting molecules were selective and had very high affinity for H_3R.[76,77]

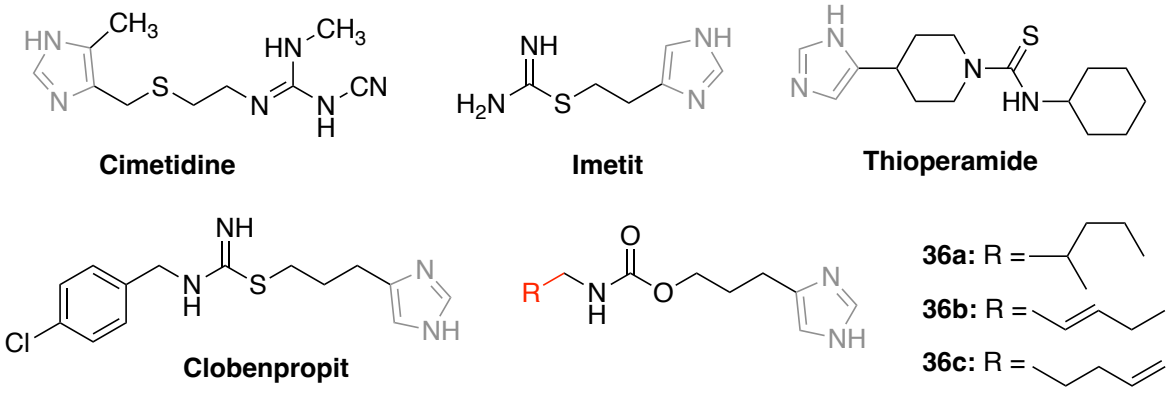

Figure 3.23. Imidazole-based antihistaminic compounds. Relevant substituents for the structure-activity relationship are marked in red.

f) Central Nervous System activity

Many Central Nervous System (CNS) active imidazole-based compounds are used, such as dexmedetomidine, and their development has been active during the last years. Numerous compounds of this family have shown good biological activities against diverse CNS disorders such as Alzheimer's disease (AD), Parkinson's, schizophrenia, epilepsy, dementia, anxiety and depression.[78,79] Nafimidone is a substituted imidazole used for the treatment of epilepsy,[80] some analogues (**37** and **38**) showed good anticonvulsant and anti-maximal electroshock seizure activity. In compound **38** the *meta*-chloro substitution was vital for the activity (Figure 3.24).[81,82]

Regarding AD, compound **39a** showed the ability to suppress γ-secretase secretion and inhibit the production of toxic Aβ-peptides and the modification of this compound led to **39b,** which is currently under clinical trials.[83,84]

Fipamezole has demonstrated positive results in phase II clinical trials, reducing L-dopa-induced dyskinesias in patients with Parkinson's disease. Compounds **40a-b** were found to be excellent nociceptin (ORL1) receptor antagonists, potentially useful for the treatment of Parkinson's disease.[85]

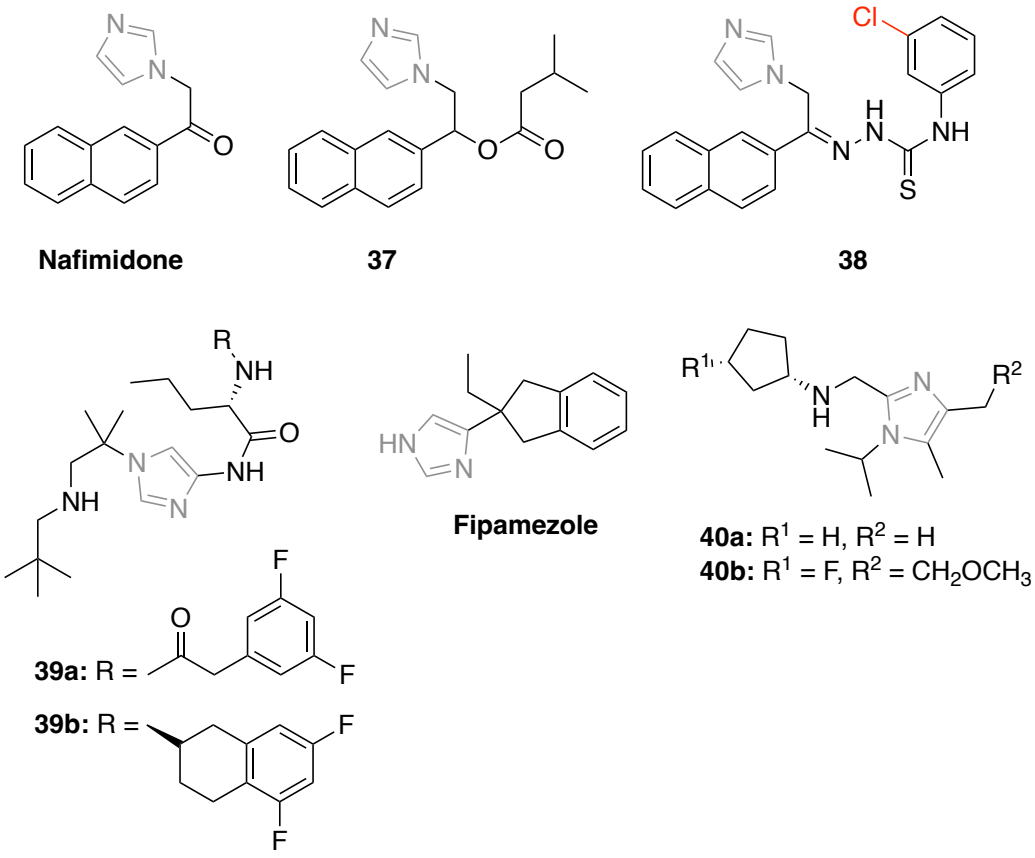

Figure 3.24. Imidazole-based CNS-active compounds. Relevant substituents for the structure-activity relationship are marked in red.

g) Antihypertensive activity

Losartan, eprosartan and olmesartan are three examples of angiotensin II receptor agonists, employed for the treatment of hypertension, that contain imidazole moieties (Figure 3.25).[86,87] Losartan analogues **41** and **42a-b** have substituents that increase the affinity for AT1 receptors, and compound **41** is highly selective due to the butyl and hydroxymethyl groups in the imidazole ring. Substitution with methyl in **42b** reduced the activity with respect to **42a**.[88,89]

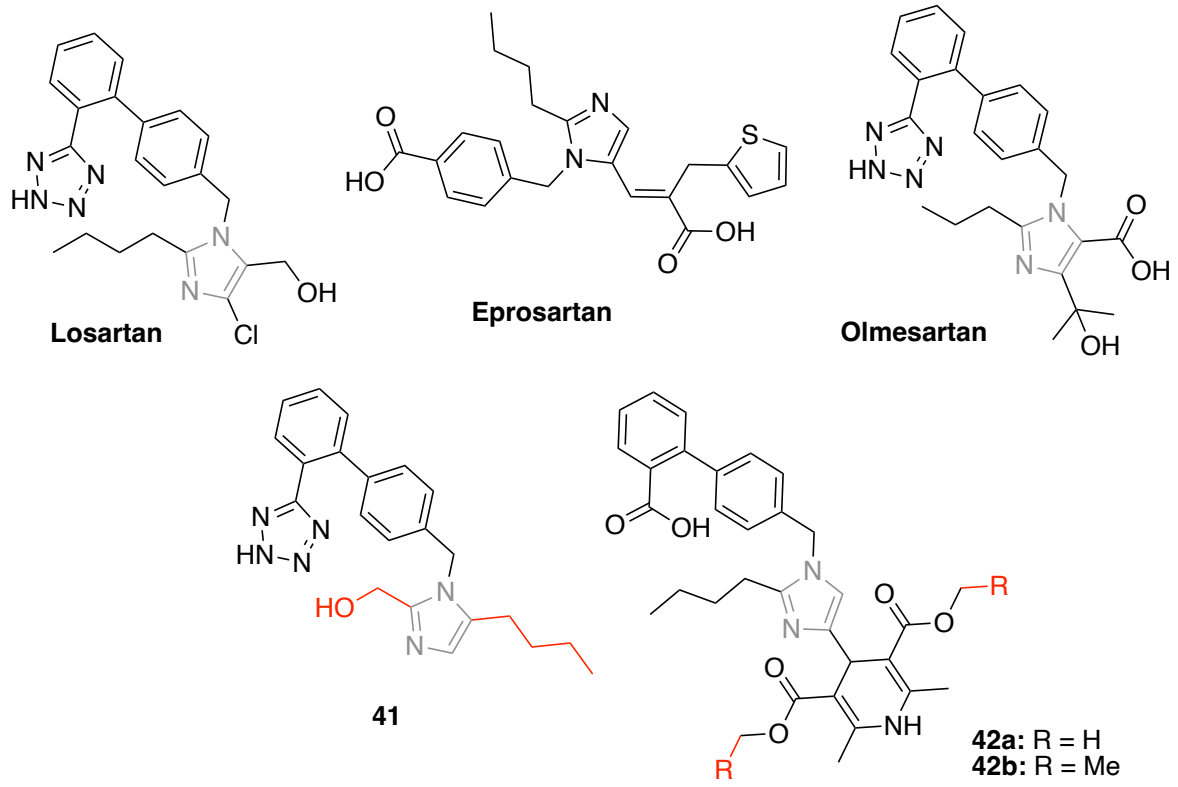

Figure 3.25. Imidazole-based antihypertension compounds. Relevant substituents for the structure-activity relationship are marked in red.

h) Anti-inflammatory activity

Some imidazoles, in particular triphenyl imidazoles, have been developed as potential anti-inflammatory compounds. Triphenyl compounds **43a-b** displayed both anti-inflammatory and antifungal activities, with the possibility of being developed as a bifunctional compound.[90] Insertion of a sulfuryl group led to compounds **44a-b,** which showed that both imidazole and sulfuryl were important for good activity.[91]

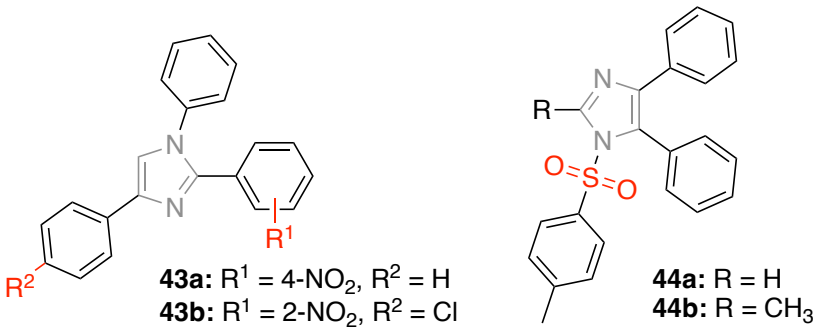

Figure 3.26. Imidazole-based anti-inflammatory compounds. Relevant substituents for the structure-activity relationship are marked in red.

i) Antiobesity activity

The CB_1 receptor is considered a potential target for the treatment of obesity. The substitution of the hydrazide moiety of the commercial drug rimonabant led to compound **45**, with high selectivity for the receptor.[92] Bombesin receptor subtype-3 (BRS-3) might also be a potential target in obesity, compounds **46a-b** target this receptor, with high potency and good pharmacokinetics profile (Figure 3.27).[93,94]

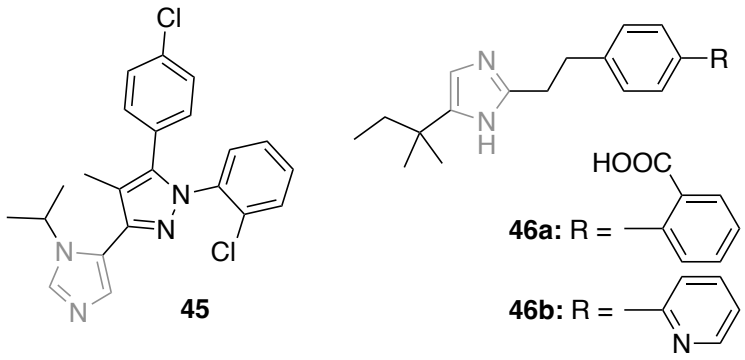

Figure 3.27. Imidazole-based antiobesity compounds.

j) Antiviral activity

Some imidazole-based compounds have shown antiviral activity.[95,96] The replacement of the triazole ring of a potent anti-HIV compound by imidazole (**48a-b**, Figure 3.28) showed remarkable anti-HIV-1 activity with higher selectivity. Molecular modelling studies suggested the importance of the naphthalene unit for the affinity.

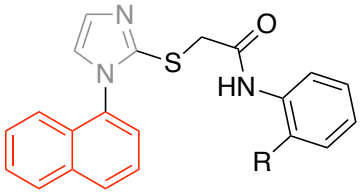

47a: R = Cl
47b: R = NO_2

Figure 3.28. Imidazole-based antiviral compounds. Relevant substituents for the structure-activity relationship are marked in red.

k) Antiparasitic activity

Megazol, benznidazole and metronidazole are traditional protozoal agents bearing the imidazole moiety (Figure 3.29). Benznidazole analogue **48** showed higher activity than the parent molecule toward *Trichomonas vaginalis*, with no cytotoxicity.[97] Phenyl nitroimidazoles **49a-b** had anti-*trypanosomal* activity comparable to that observed for megazol; moreover, **49b** showed good results in oral dosing, becoming a promising lead compound for the treatment of human African trypanosomiasis.[98] Whenever an imidazole ring was added to the flexible chain of the benzophthalazine skeleton, resulting compounds, such as compound **50** showed enhanced anti-*T. cruzi* activity.[99] Other imidazole-based antiprotozoal compounds against leishmaniasis will be described in section 3.1.2.3.

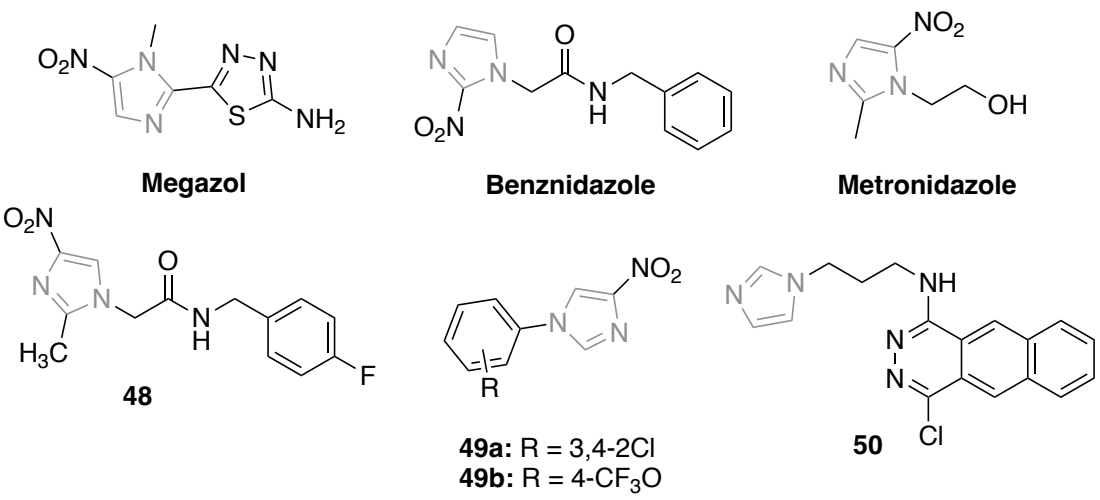

Figure 3.29. Imidazole-based antiparasitic compounds.

3.1.2.3 Imidazoles as antileishmanial agents

Drug repurposing has emerged as a promising strategy for the treatment of leishmaniasis. Diverse azole derivatives such as clotrimazole, econazole and bifonazole have been evaluated for their antileishmanial activity. Econazole has shown the best results, with activity comparable to miltefosine, a finding that suggests the repurposing of econazole for the treatment of leishmaniasis.[100] Compounds **51-53** showed the best antileishmanial activity values from a large number of derivatives studied. All reduced the infection rate significantly. Enzymatic studies confirmed that

their mode of action, at least in part, consisted of inhibiting the parasitic Fe-superoxide dismutase (Fe-SOD).[101]

Through modifications of miconazole, furyl compound **54** and diphenyl imidazole **55** were found to have both good *in vitro* and *in vivo* activity.[102,103] Tetralin imidazole derivative **56** displayed remarkable antileishmanial activity. A comparative research showed the importance of the benzyloxy group for the selectivity.[104] Cyclohexyl-bridged bis-imidazole **57** showed stronger antileishmanial activity than sodium stibogluconate and pentamidine, with high selectivity. Structure-activity relationship highlighted the importance of the methylene imidazole group.[105]

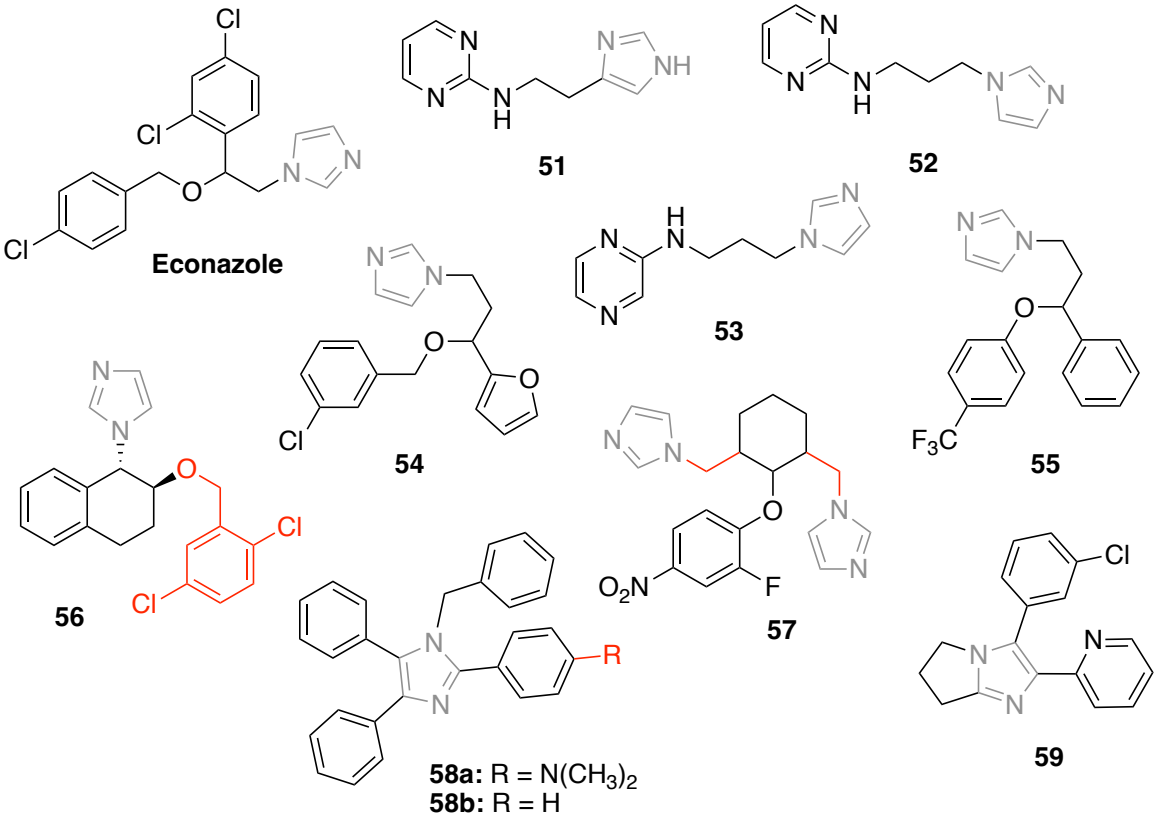

Figure 3.30. Imidazole-based antileishmanial compounds. Relevant substituents for the structure-activity relationship are marked in red.

From a study of diverse aryl-substituted imidazoles, compounds **58a-b** were found to be the ones with a better balance in activity, toxicity and selectivity. The substitution in position 2 of the imidazole ring was found to be important for the activity. A study published in 2023 proposed compound **59** as a potent antileishmanial compound and demonstrated the importance of different modifications for the activity and other

important parameters: methoxy substitution in the 6-position for the selectivity, adding new heteroatoms did not improve the selectivity index, small, lipophilic groups or anilines with polar atoms in position 3 showed moderate activity but increased size or lipophilicity reduced solubility and metabolic stability, methylation of the exocyclic nitrogen improved aqueous solubility, although it reduced selectivity.[106] The mentioned imidazole-based compounds with antileishmanial activity are represented in Figure 3.30.

3.1.3. Indole-imidazoles

The combination of two or more pharmacophore moieties in a single molecular structure has become an innovative method for creating novel bioactive substances. By using this technique, researchers in the pharmaceutical and medicinal chemistry fields can obtain a variety of diverse small molecules that are essential for discovering new drugs.[107]

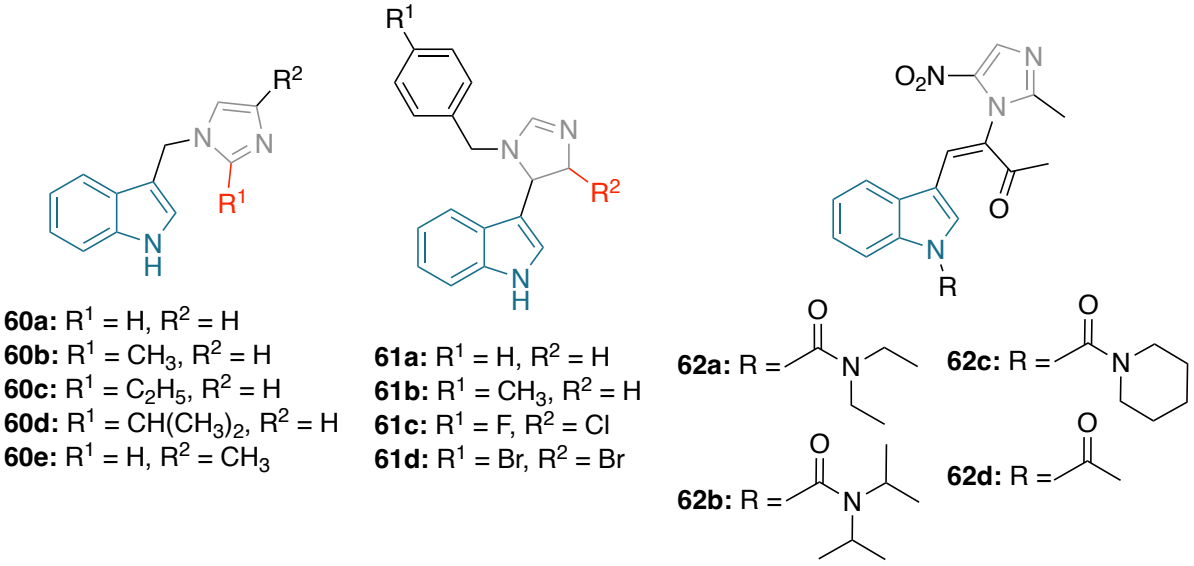

60a: R^1 = H, R^2 = H
60b: R^1 = CH_3, R^2 = H
60c: R^1 = C_2H_5, R^2 = H
60d: R^1 = $CH(CH_3)_2$, R^2 = H
60e: R^1 = H, R^2 = CH_3

61a: R^1 = H, R^2 = H
61b: R^1 = CH_3, R^2 = H
61c: R^1 = F, R^2 = Cl
61d: R^1 = Br, R^2 = Br

Figure 3.31. Indole-imidazole compounds with diverse activities. Relevant substituents for the structure-activity relationship are marked in red.

Indole-imidazole hybrids have been studied for their wide range of activities (Figure 3.31). Jasiewicz *et al.*[108] evaluated the series of indole-imidazole compounds **60a-e** for their antioxidant and antibacterial activities. Compounds with electron-donating groups **60b-e** showed higher biocompatibility, with high antioxidant activity and iron

chelation capacity. Compound **60a** was the most active against *M. luteus* and *P. fluorescens*.

Gao *et al.*[109] developed streptochlorin analogues (**61a-d**) with antifungal activity. All four compounds showed good antifungal activity, with compounds **61a-b** being especially against the *Alternaria leaf spot* pathogen and **61c-d** especially against *Rhizoctonia solani*. The introduction of a halogen in position 4 of the imidazole group (**61c-d**) increased the antifungal activity.

Li *et al.*[110] designed and synthesised a family of indole-nitroimidazole compounds from which compounds **62a-e** showed good activity against methicillin-resistant *Staphylococcus aureus* (MRSA) and other Gram-positive and Gram-negative bacteria. Compound **62a** showed a higher activity than the reference antibiotics clinafloxacin and norfloxacin. Compounds **62b-e** showed good antibacterial activity, with **62c** being the most potent against MRSA due to its interaction with DNA, causing its denaturation.

Some indole-imidazole hybrids with antileishmanial activity have also been developed (Figure 3.32). Compound **63** showed antileishmanial activity both *in vivo* and *in vitro*. This compound was especially active against *L. mexicana* and demonstrated high systemic efficacy in experiments carried out in mice, with a big decrease in parasite numbers in both spleen and liver, indicating a strong effect against visceral infection.[111] A series of indole imidazole compounds (**64a-f**) was evaluated for their antileishmanial activity. Even if they were not the most active of the ones studied in this study, all compounds were found to be active in the four *L. infantum* promastigote strains, and in particular, **64e** and **64f**, which have *N*-methylated indoles, were found to be very potent.[112]

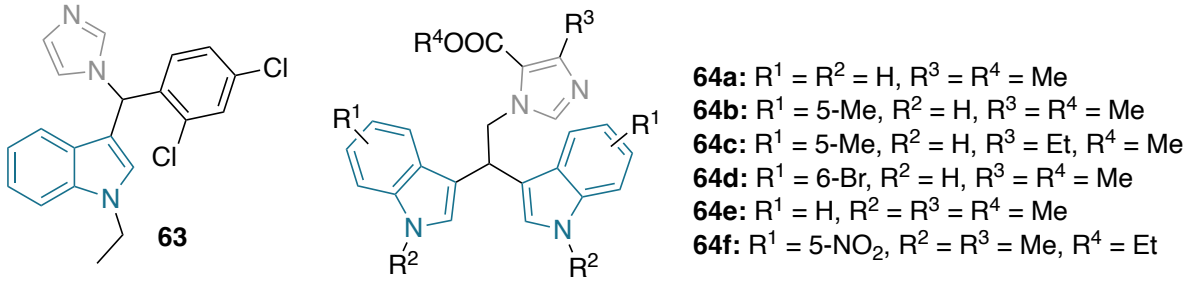

Figure 3.32. Indole-imidazole compounds with antileishmanial activity.

3.2. OBJECTIVES

The aim of this thesis chapter is the synthesis of a library of rigid indole-imidazole derivatives with potential antileishmanial activity. These derivatives will contain variations in four different substituents. We will evaluate the limitations of the previously reported synthesis and develop alternatives to achieve our objectives.

3.3. RESULTS AND DISCUSSION

Through a high-throughput screening (HTS) of molecules from the University of Urbino, molecule **65e** was found as a potential antileishmanial compound; therefore, it was decided to obtain a small library of compounds **65** in order to analyse their antileishmanial activity.

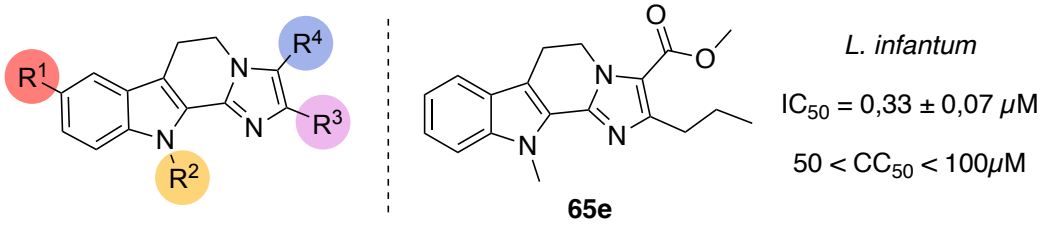

*Figure 3.33. General structure of compounds **65** and the four variable substituents. Compound **65e** found to be active against leishmaniasis in the HTS.*

3.3.1. Design and synthesis

The synthesis of derivatives of the 6,11-dihydro-5*H*-imidazo[1',2':1,2]pyrido[3,4-b]indole framework, corresponding to structure **65**, was previously reported in the literature and involved the synthesis of the advanced intermediate **66** from different

tryptamine derivatives **67** and diaza-dialkenes **68**. This intermediate was then closed using an intramolecular Pd-catalysed Cross-Dehydrogenative Coupling (CDC), leading to the corresponding compounds **65**.

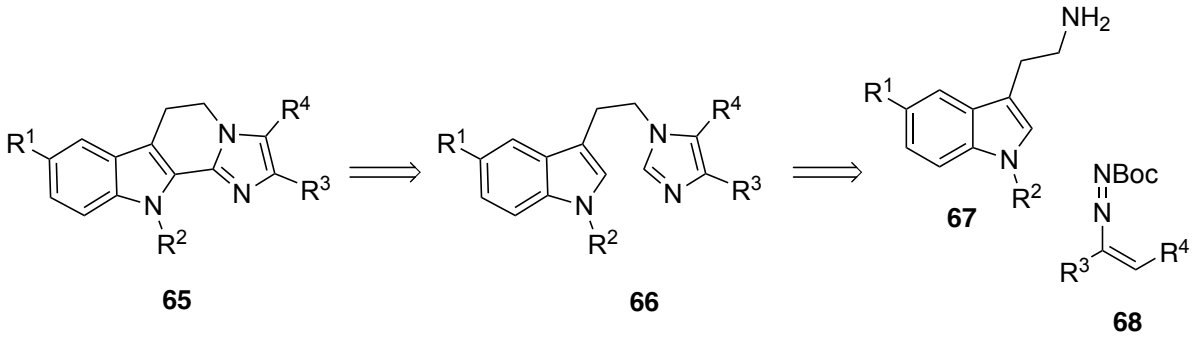

*Scheme 3.1. Retrosynthetic route for the synthesis of **65** and its derivatives.*

For the synthesis of the tryptamine derivatives, two different synthetic pathways were envisaged, depending on the availability of precursors. For non-commercially available tryptamines or those with high prices, their synthesis was developed starting from the corresponding indole. The methylation of these indoles gave intermediates **69** in moderate to high yields. Then, a TFA-promoted condensation of compounds **69a-d** with dimethylaminonitroethylene led to the intermediates **70a-d**. Reduction of compounds **70a-d** with $LiAlH_4$ led to the desired tryptamine derivatives **67a-d**. (Scheme 3.2)

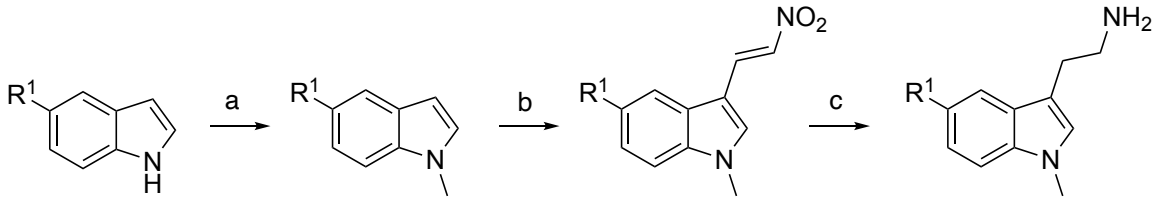

69a: R^1 = F (97%)
69b: R^1 = Cl (91%)
69c: R^1 = Me (50%)
69d: R^1 = Ph (82%)

70a: R^1 = F (80%)
70b: R^1 = Cl (87%)
70c: R^1 = Me (41%)
70d: R^1 = Ph (72%)

67a: R^1 = F (74%)
67b: R^1 = Cl (61%)
67c: R^1 = Me (76%)
67d: R^1 = Ph (71%)

Reagents and conditions: (a) NaH (60%), MeI, DMF, r.t., o.n. (b) dimethylaminonitroethylene, TFA, Ar atmosphere, r.t., 30 minutes (c) $LiAlH_4$, THF, reflux, o.n.

*Scheme 3.2. Synthesis of tryptamine derivatives **67a-d** from the corresponding indoles. Yields of each step are reported in brackets for each derivative.*

Regarding 5-Br tryptamine, whenever the reduction with $LiAlH_4$ was performed, hydrogenolysis of the bromine atom was also observed. A hydrogenation in the H-CUBE using Pd/C was attempted as an alternative, but unfortunately, with the same result. Finally, a double $NaBH_4$ reduction was also attempted, unfortunately, with the same results; therefore, the preparation of this particular this derivative was abandoned.

For commercially available tryptamines, different *N*-alkylation (**67e,f,i**) and *N*-arylation (**67g,h**) reactions were performed on the indole nitrogen, using modifications of methods reported in the literature. (Scheme 3.3)

For the case of *N*-phenyl substituted tryptamine (**67h**), we first attempted a procedure reported for the *N*-arylation of indoles using catalysts derived from CuI and *trans-N,N'*-dimethyl-1,2-cyclohexanediamine.[113] Unfortunately, this method did not work. Our second approach consisted of an *N*-arylation of nitrogen-containing heterocycles with aryl iodides, catalysed by $Cu(OAc)_2 \cdot H_2O$.[114] In this case, the reaction was reported for indoles, but we were pleased to find that the reaction also worked with tryptamines, without the need to protect the free amine. This *N*-substitution is essential for the completion of the final synthetic step

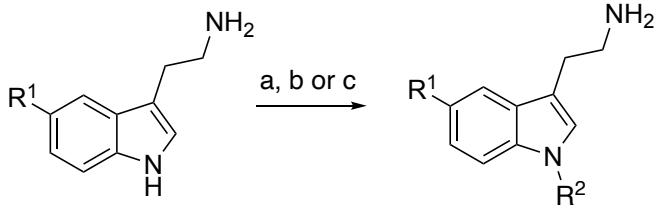

67e: R^1 = H, R^2 = Me (57%)
67f: R^1 = H, R^2 = *n*-Pr (42%)
67g: R^1 = H, R^2 = Bn (65%)
67h: R^1 = H, R^2 = Ph (70%)
67i: R^1 = OMe, R^2 = Me (42%)

(a) for 67e, 67f and 67i: RI (methyl or propyl), NaH (60%), DMF, r.t., 1-2 h
(b) for 67g: BnBr, NaH (60%), N_2 atmosphere, DMF, r.t., 1-2 h
(c) for 67h: IPh, $Cu(OAc)_2 \cdot H_2O$, Cs_2CO_3, DMF, 110 °C, 24 h

*Scheme 3.3. Synthesis of tryptamine derivatives **67e-i** from the corresponding non-substituted tryptamines. Yields are reported in brackets for each derivative.*

Next, the coupling between tryptamines **67** and 1,2-diaza-1,3-dienes (DDs) (**68a-b**) was performed to construct indolyl-ethyl imidazoles (**66**) (Scheme 3.4). The starting DDs were provided by Prof. Favi's group.

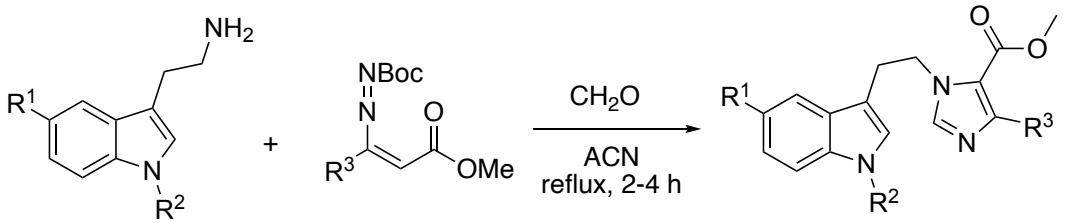

67a: R^1 = F, R^2 = Me
67b: R^1 = Cl, R^2 = Me
67c: R^1 = Me, R^2 = Me
67d: R^1 = Ph, R^2 = Me
67e: R^1 = H, R^2 = Me
67f: R^1 = H, R^2 = *n*-Pr
67g: R^1 = H, R^2 = Bn
67h: R^1 = H, R^2 = Ph
67i: R^1 = OMe, R^2 = Me

68a: R^3 = *n*-Pr
68b: R^3 = *n*-Bu

66a: R^1 = F, R^2 = Me, R^3 = *n*-Pr (45%)
66b: R^1 = Cl, R^2 = Me, R^3 = *n*-Pr (45%)
66c: R^1 = Me, R^2 = Me, R^3 = *n*-Pr (56%)
66d: R^1 = Ph, R^2 = Me, R^3 = *n*-Pr (52%)
66e: R^1 = H, R^2 = Me, R^3 = *n*-Pr (77%)
66f: R^1 = H, R^2 = *n*-Pr, R^3 = *n*-Pr (30%)
66g: R^1 = H, R^2 = Bn, R^3 = *n*-Pr (41%)
66h: R^1 = H, R^2 = Ph, R^3 = *n*-Pr (32%)
66i: R^1 = OMe, R^2 = Me, R^3 = *n*-Pr (25%)
66j: R^1 = H, R^2 = Me, R^3 = *n*-Bu (42%)

*Scheme 3.4. Synthesis of indole-containing imidazoles **66a-i** from diazadialkenes **68a-b**. Yields are reported in brackets for each derivative.*

As mentioned previously, the last step consisted of a previously reported palladium-catalysed Cross-Dehydrogenative Coupling (CDC) that led to the desired final products **65a-j (**Scheme 3.5**)**. In this reaction, the formation of side-products corresponding to the fully aromatic, dehydrogenated derivatives of compounds **65** was observed.

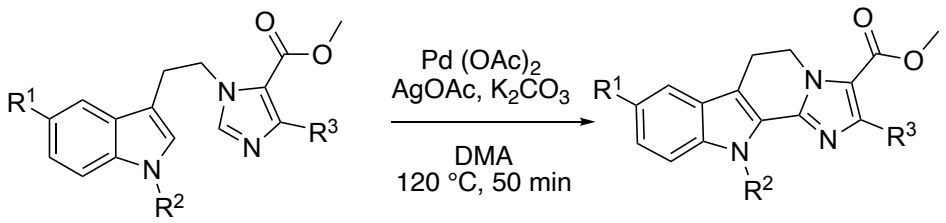

66a: R^1 = F, R^2 = Me, R^3 = *n*-Pr
66b: R^1 = Cl, R^2 = Me, R^3 = *n*-Pr
66c: R^1 = Me, R^2 = Me, R^3 = *n*-Pr
66d: R^1 = Ph, R^2 = Me, R^3 = *n*-Pr
66e: R^1 = H, R^2 = Me, R^3 = *n*-Pr
66f: R^1 = H, R^2 = *n*-Pr, R^3 = *n*-Pr
66g: R^1 = H, R^2 = Bn, R^3 = *n*-Pr
66h: R^1 = H, R^2 = Ph, R^3 = *n*-Pr
66i: R^1 = OMe, R^2 = Me, R^3 = *n*-Pr
66j: R^1 = H, R^2 = Me, R^3 = *n*-Bu

65a: R^1 = F, R^2 = Me, R^3 = *n*-Pr (54%)
65b: R^1 = Cl, R^2 = Me, R^3 = *n*-Pr (54%)
65c: R^1 = Me, R^2 = Me, R^3 = *n*-Pr (33%)
65d: R^1 = Ph, R^2 = Me, R^3 = *n*-Pr (50%)
65e: R^1 = H, R^2 = Me, R^3 = *n*-Pr (67%)
65f: R^1 = H, R^2 = *n*-Pr, R^3 = *n*-Pr (30%)
65g: R^1 = H, R^2 = Bn, R^3 = *n*-Pr (82%)
65h: R^1 = H, R^2 = Ph, R^3 = *n*-Pr (17%)
65i: R^1 = OMe, R^2 = Me, R^3 = *n*-Pr (23%)
65j: R^1 = H, R^2 = Me, R^3 = *n*-Bu (64%)

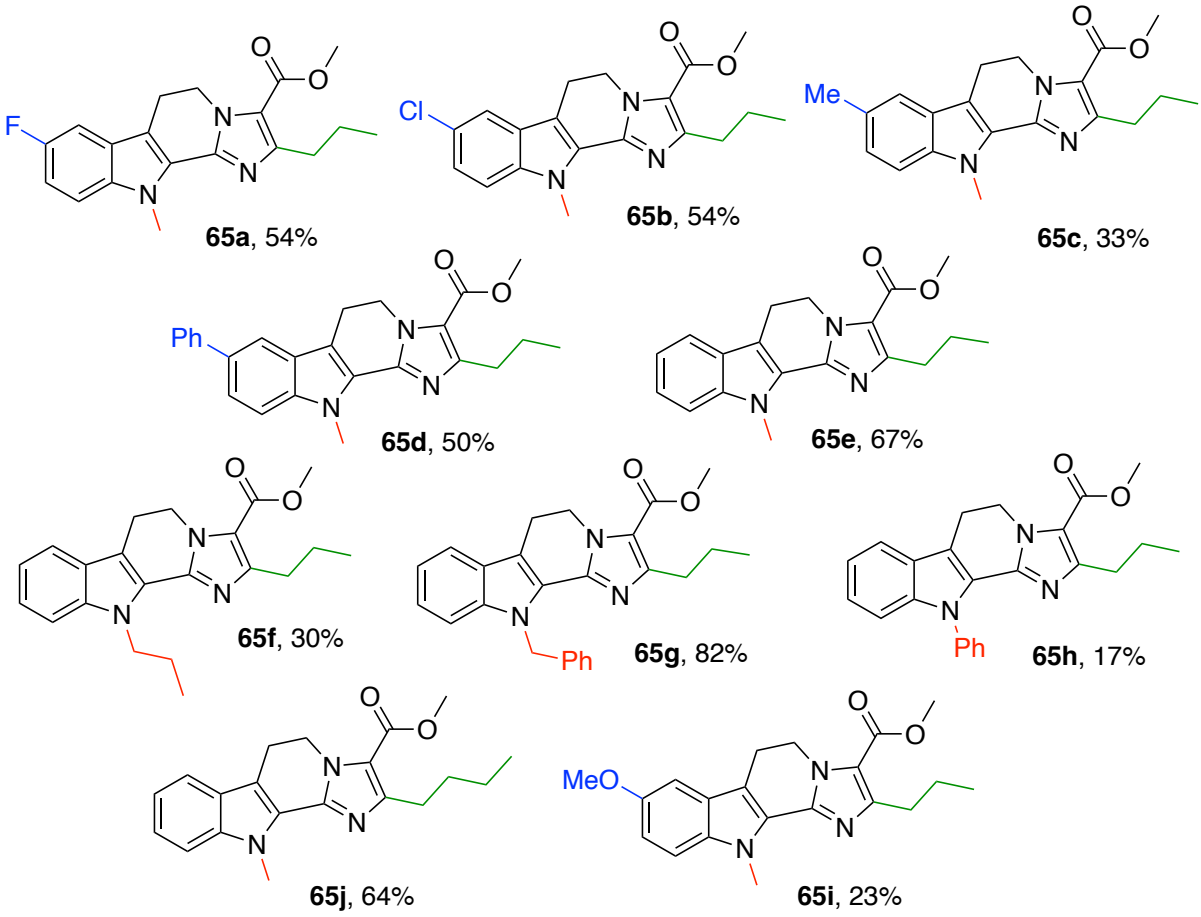

*Scheme 3.5. Synthesis of the desired final compounds **65a-j** from the corresponding open intermediates **66a-j**. Yields are reported in brackets for each derivative.*

3.3.2. Biological evaluation

Compounds from the first synthetic pathway were screened for their efficacy against *L. infantum* MHOM/TN/80/IPT1 promastigotes at a single dose of 20 μM for 72 h. Some of the intermediates **66** were also tested, as is usually performed in medicinal chemistry, but neither of them showed antileishmanial activity.

*Table 3.1. Summary of compounds **65** derivatives activity on L. infantum promastigotes and THP-1 cells. IC_{50} values are reported as mean (95 % CI (confidence interval)) from at least two experiments. Each experimental condition was conducted at least in duplicate and miltefosine (MILT) was used as a positive control.*

Compound	Inhibition of *L. infantum* at 20 μM (%)	*L. infantum* MHOM/TN/80/IPT1 IC_{50} (µM) (95 % CI)	THP-1 1:2 da 100 µM CC_{50} (µM) (95% CI)	Selectivity Index (CC_{50}/IC_{50})
MILT	96.7 %	3.6 (3.3-4.0)	36.7	10.2
65a	5.7 %	n.a.	-	-
65b	-39.5 %	n.a.	-	-
65c	-1.0 %	n.a.	-	-
65d	n.a.	n.a.	-	-
65e	85.9 %	2.0 (1.9-2.1)	-	-
65f	n.a.	n.a.	-	-
65g	-4.4 %	n.a.	-	-
65h	-5.7 %	n.a.	-	-
65i	-16.4 %	n.a.	-	-
65j	85.3 %	2.2 (2.1-2.3)	>25[a]	>11

[a]Due to solubility problems, CC50 was not determined at 50 and 100 µM

Most of the studied compounds showed low or no activity against *Leishmania* parasites (Table 3.1, Figure 3.34). Only lead compound (**65e**) and its derivative **65j** showed interesting biological activities (Figure 3.34), with IC_{50} values better than those of the positive control. Interestingly, compound **65j** is the only member of the series that features a different substituent on position 4 of the imidazole ring. This observation

suggests that modification of the imidazole substituents can significantly influence antiparasitic activity. Therefore, the newly discovered synthetic pathway can potentially provide a valuable platform for the design and synthesis of more potent derivatives.

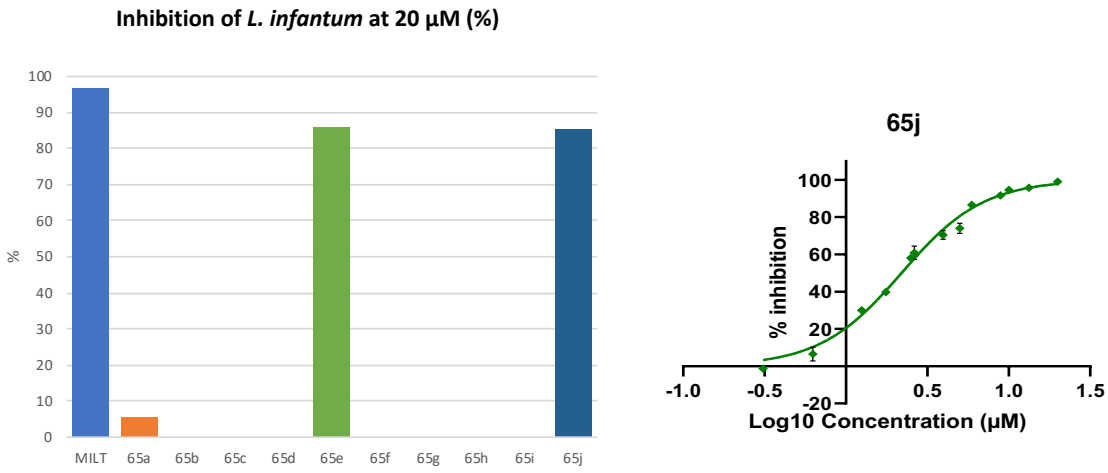

*Figure 3.34. Left: Inhibition of Leishmania infantum promastigotes at 20 µM. Right: Dose-response curve for the inhibition of L. infantum parasites by **65j**.*

The biological assay for evaluation of toxicity (CC_{50}) could not be performed in the case of compound **65j**, due to its low solubility at 50 and 100 µM; therefore, the future structural modifications should aim to improve solubility, for instance, by introducing more polar or hydrophilic substituents.

3.3.2.1 In silico study

Physicochemical, pharmacokinetic and drug-likeness properties of the synthesised derivatives **65a-j** were calculated using the SwissADME web tool.[115] As shown in Table 3.2, none of the synthesised molecules violated either Lipinsky's or Veber's rule, suggesting good oral bioavailability.

Rotatable bond number (RTB) is a useful parameter that influences not only oral bioavailability but also the binding affinity of a molecule. All the molecules synthesised in this series possess six or fewer rotatable bonds, well within the permissible limit (<10).

*Table 3.2. Physicochemical, pharmacokinetic and drug-likeness properties of indole-imidazole derivatives **65a-j***

Cmpd	MW (g/mol)	logP	HBD	HBA	RTB	TPSA (Å²)	GI Absorption	BBB Permeation
Desired Values	**<500**	**<5**	**<5**	**<10**	**<10**	**<140**		
65a	341.38	3.46	0	4	4	49.05	High	yes
65b	357.83	3.67	0	3	4	49.05	High	yes
65c	337.42	3.48	0	3	4	49.05	High	yes
65d	399.48	4.45	0	3	5	49.05	High	yes
65e	323.39	3.13	0	3	4	49.05	High	yes
65f	351.44	3.80	0	3	6	49.05	High	yes
65g	399.48	4.36	0	3	6	49.05	High	yes
65h	385.46	4.28	0	3	5	49.05	High	yes
65i	353.41	3.13	0	4	5	58.28	High	yes
65j	337.42	3.47	0	3	5	49.05	High	yes

The topological polar surface area (TPSA) is also an estimation of the tendency of a compound to traverse biological membranes. Those compounds having a TPSA value below 140 Å² can normally experience passive membrane diffusion. All of our diindolylmethane derivatives possess TPSA values below 60 Å², which indicates a very good membrane permeability.

Pharmacokinetic properties of gastrointestinal (GI) absorption and brain-blood barrier (BBB) permeability are the most significant determinants for bioavailability and distribution. Good GI absorption allows entry into systemic circulation, and sufficient lipophilicity allows potential BBB penetration. Interestingly, all the synthesised compounds exhibited good predicted GI absorption, and most were also predicted to cross the BBB. This is a desirable feature, since it would potentially allow the treatment of cerebral leishamiasis, which, although rare, leads to severe complications.[116]

*Table 3.3. Water solubility of derivatives **65** calculated in SwissADME. LogS in the table is the average value of logS calculated using three different methods*

Compound	logS	Solubility
Desired Value	0 > log S > -2	
65a	-4.51	Soluble
65b	-4.94	Soluble
65c	-4.68	Soluble
65d	-6.21	Poorly soluble
65e	-4.33	Soluble
65f	-5.06	Moderately soluble
65g	-6.18	Poorly soluble
65h	-6.08	Poorly soluble
65i	-4.44	Soluble
65j	-4.77	Soluble

Although not highly soluble, some compounds, including **65j,** are predicted to be water soluble, however, their solubility requirements for biological test (DMSO) were not met (Table 3.3).

3.3.3. *Synthetic alternatives*

Because of the limited diversity of the R^3 and R^4 substituents in diazadiene chemistry, a different retrosynthetic approach was designed to increase the chemical space of the imidazole substituents.

The alternative pathway envisioned at this point was the Van Leusen imidazole synthesis, developed in 1972 by the Dutch professor Albert Van Leusen (Scheme 3.6).[1] This reaction provides a straightforward method to synthesise imidazole-based compounds through a 1,3-dipolar cycloaddition of tosylmethyl isocyanide (TosMIC), also known as Van Leusen's reagent, and aldimidines that can be generated from the reaction between aldehydes and amines.[117]

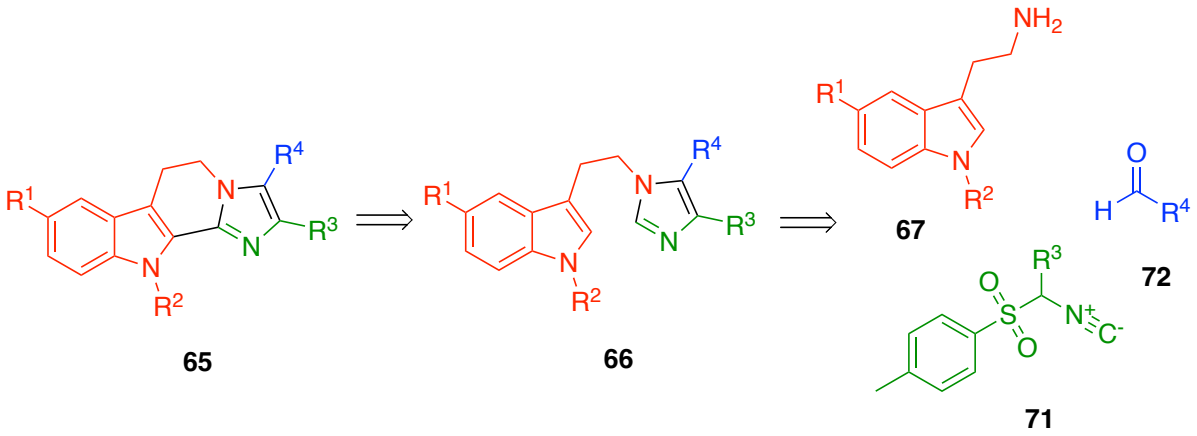

*Scheme 3.6. Proposed Van Leusen reaction for the synthesis of the advanced intermediates **66.***

Unfortunately, all the attempts to react TosMIC derivative **71a** (Scheme 3.7) with the preformed aldimine **73** from methyltryptamine and benzaldehyde, using many different conditions (Table 3.4, Scheme 3.8), proved to be unsuccessful.

[1] This work was done in collaboration with Regina Kurti as part of her Degree Thesis (Universidad Complutense de Madrid and Università di Urbino, 2024).

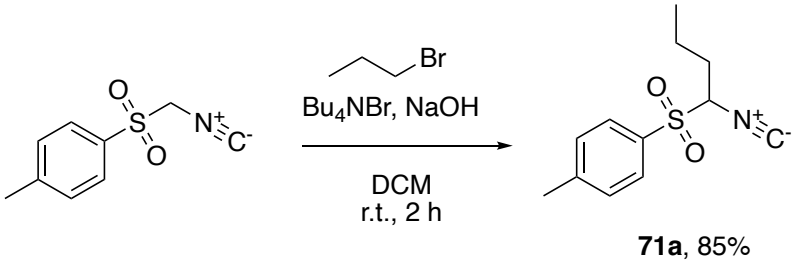

*Scheme 3.7. Synthesis of TosMIC derivative **71a**.*

Table 3.4. Screened conditions for the Van Leusen reaction represented in Scheme 3.8.

Entry	Base (1.5 equiv.)	Temp (°C)	Solvent	Time (h)
1	K_2CO_3	r.t.	MeOH	48
2	K_2CO_3	reflux	MeOH	48
3	K_2CO_3	90 (MW)	MeOH	1
4	NaH	r.t.	MeOH	24
5	NaH	0	Toluene	48
6	LHMDS	- 40	THF	48

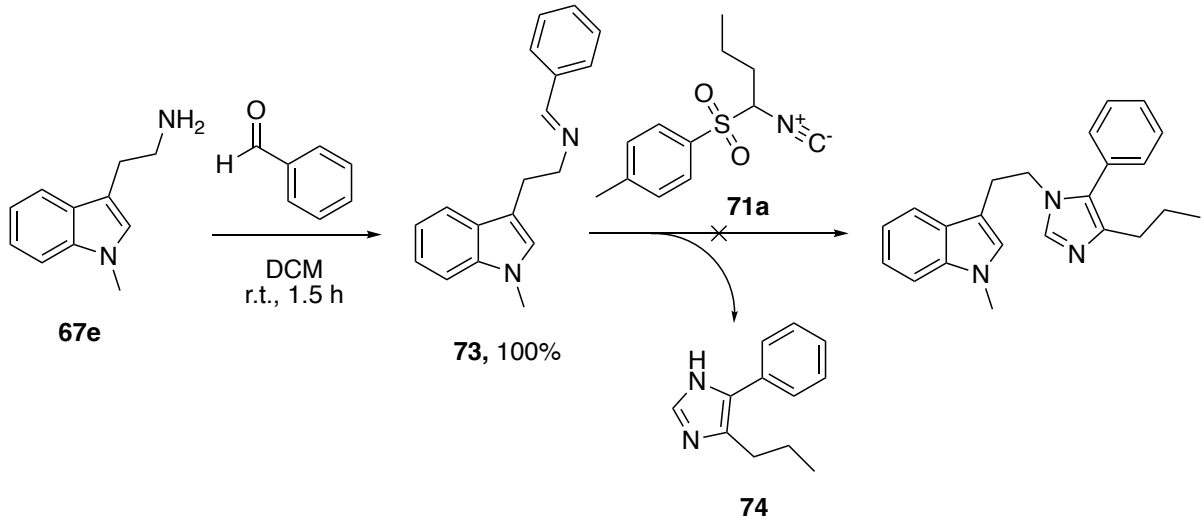

*Scheme 3.8. Attempted Van Leusen synthesis of the indole-imidazole derivatives **65**.*

All the experimental conditions assayed consistently resulted in the formation of compound **74**, arising from the loss of the *N*-methylindolylethyl fragment, as the only identifiable product, albeit in low yield (Scheme 3.8). A potential explanation involves

a base-promoted elimination reaction, favoured by the steric compression of the three adjacent imidazole substituents and the good stability of the imidazole anion as a leaving group. The only derivative that could be synthesised using this methodology was compound **65o**, which used non-substituted TosMIC (Scheme 3.9).

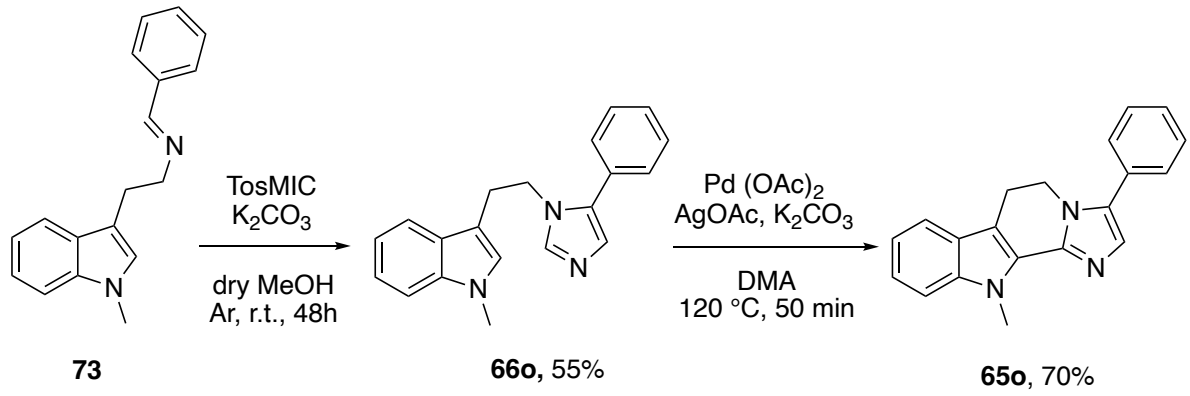

*Scheme 3.9. Synthesis of derivative **65o** using the Van Leusen reaction.*

At this point, the synthetic strategy was reoriented toward the reaction between halogenated ethyl-indole derivatives and preformed imidazoles (Scheme 3.10).

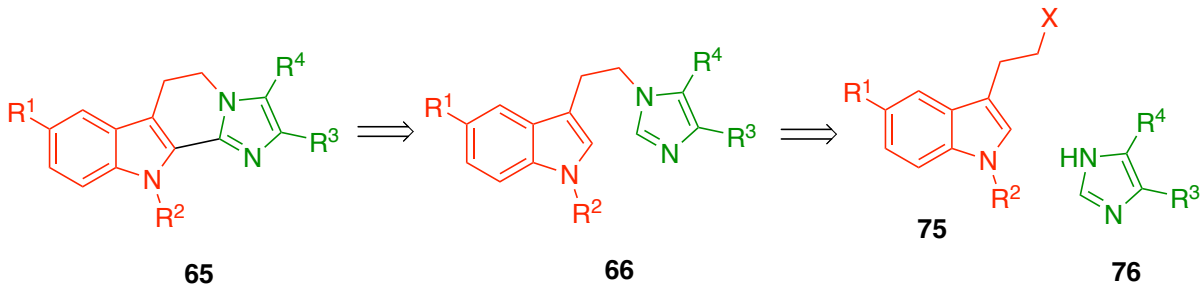

*Scheme 3.10. Proposed retrosynthetic analysis for the synthesis of derivatives **65** from ethyl-indole derivatives and preformed imidazoles.*

This synthetic approach started from the synthesis of derivatives **75** by *N*-alkylation of the commercially available iodine or bromine derivatives. However, whenever the methylation of the bromine derivative was attempted, the obtained product was a mixture of three different halogenated compounds **75a-c** (Scheme 3.11). This mixture of products likely arises from halogen-exchange processes in the reaction, where bromine comes from the original starting material, iodine from the methyl iodide reagent used for the methylation, and chlorine comes from NH_4Cl sat. solution used during the reaction work-up.

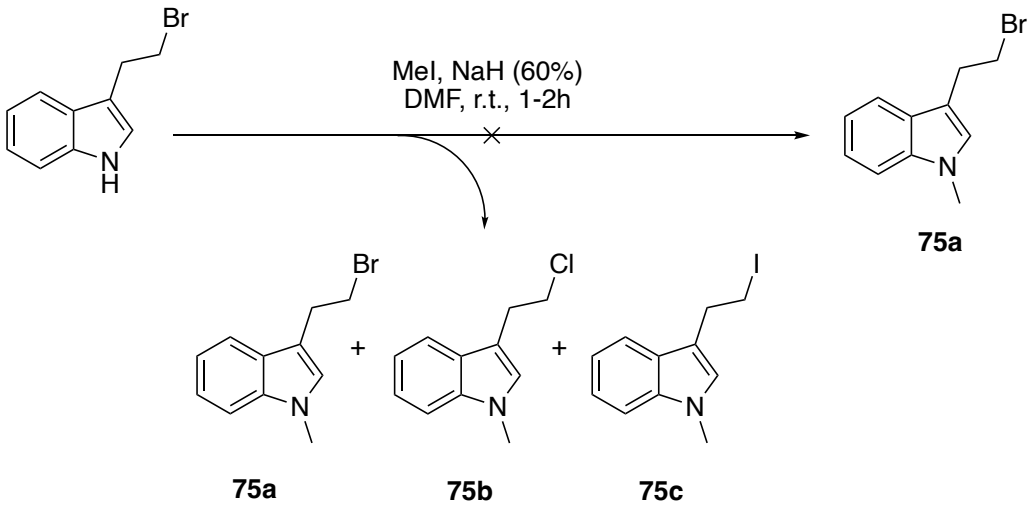

*Scheme 3.11. Formation of a mixture of halogenated products **75a-c** via halogen exchange.*

Based on the previous results, we chose to perform the reaction starting from the iodine derivative and perform a different work-up procedure so that we would avoid the possibility of halogen exchange. However, whenever this reaction was performed, the obtained product was not the expected one, but the product of the cyclopropane ring formation in position 3 of the indole (**77**) (Scheme 3.12).

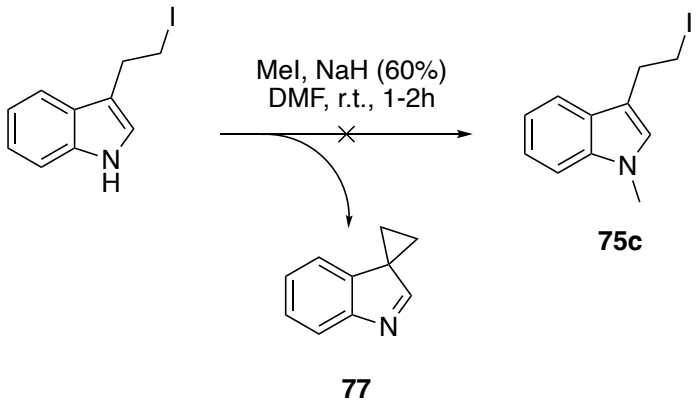

*Scheme 3.12. Formation of the cyclopropane-derived spiro compound **77**.*

In view of the difficulties associated with the synthesis of compounds **75**, our efforts were redirected toward the optimisation of the coupling reaction between the halogenated compounds and the preformed imidazoles. This meant the introduction of a further methylation step once the advanced intermediate **78** was formed (Scheme 3.13).

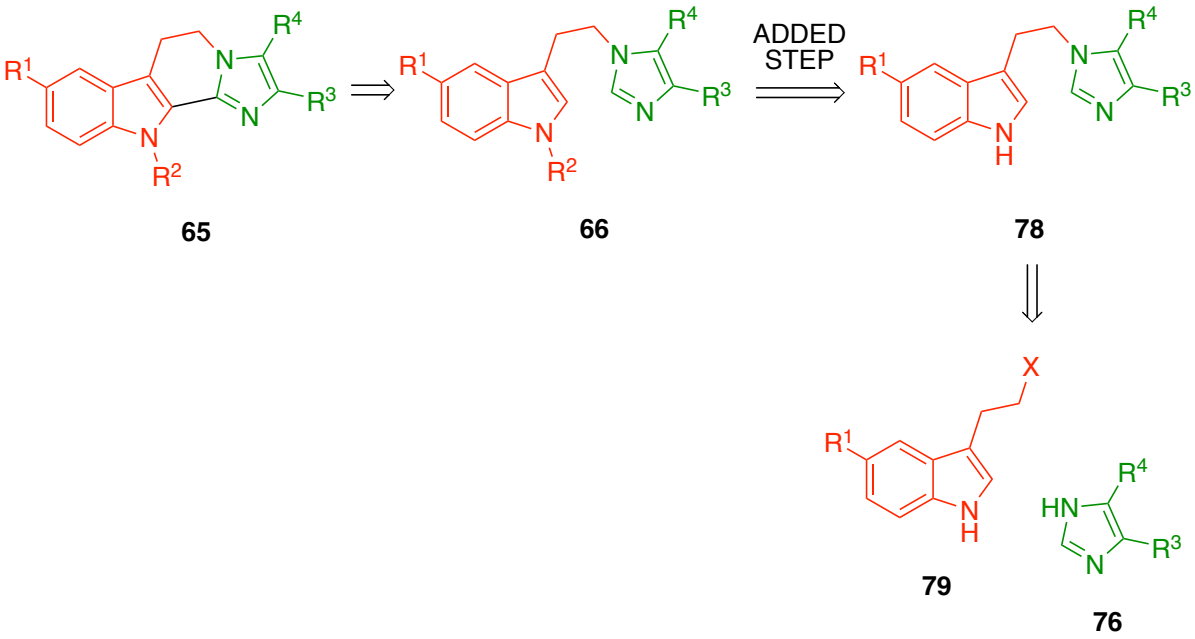

*Scheme 3.13. Proposed retrosynthetic route with alkylation step after the formation of **78**.*

Iodide derivative **79** was available commercially; however, due to pricing and availability, we decided to synthesise it from tryptophol using a previously reported Appel reaction (Scheme 3.14).

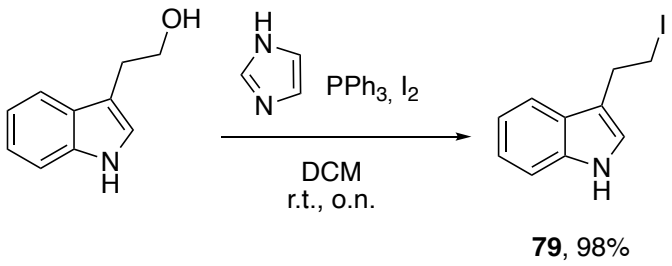

*Scheme 3.14. Synthesis of iodine ethyl-indole **79** from tryptophol.*

To explore and optimise the coupling between **79** and the different preformed imidazoles, different methodologies were employed, including traditional solution-phase synthesis, mechanochemistry and microwave-assisted synthesis.

According to International Union of Pure and Applied Chemistry (IUPAC), mechanochemical reactions are those that are directly induced by the absorption of mechanical energy from friction or grinding processes.[118] This mechanical energy produces changes in the crystalline structure, breaking bonds and thus allowing the

formation of new structures.[119,120] One of the most relevant characteristics of mechanochemistry is the fact that it is carried out in the absence of solvents, or using only very small quantities. This has led to mechanochemistry being classified within the field of green chemistry, which seeks to optimise the resources used, including reagents, solvents, energy, etc.[120]

Microwave-assisted synthesis involves reactions where heating is produced by microwave irradiation, producing efficient internal heating. This methodology allows the reduction of reaction times and can improve reaction yields.[121]

A systematic evaluation of different parameters was conducted in the three evaluated methodologies.

A series of experiments represented in Table 3.5 was conducted to optimise the coupling of halogenated indole derivatives with preformed imidazole under different bases, solvents, and concentrations. The initial reaction performed employing NaH (60 %) base at 80 °C in dimethylformamide (DMF) (c = 0.33 M) yielded the product of interest **78a** with 33 % yield (entry 1). Lowering the temperature to 70 °C and diluting the concentration to 0.15 M led to a slight increase in yield (36 %, entry 2), revealing that dilution is advantageous for the reaction efficiency. The use of ^{t}BuOK also gave low conversions, with both brominated (23 %, entry 3) and iodinated (27 %, entry 4) substrates, due presumably to partial degradation of the initial compound under strongly basic conditions.

Replacement of these bases with Cs_2CO_3 under the same conditions significantly increased the yield up to 58 % (entry 5), indicating that milder basic conditions are more suitable for this transformation. The combination of Cs_2CO_3 as base with the iodinated derivative was the most suitable balance between reactivity and stability, and thus represents the most favourable conditions, which gave the best result and provided the desired product in 62 % yield (entry 6).

*Table 3.5. Optimisation of reaction conditions for the synthesis of **78** using traditional chemistry. All reactions were performed with 1 equivalent of imidazole that was added in the presence of base and stirred for 30 minutes at r.t. before adding the indole derivative. All yields are isolated.*

Entry	Ethylindole derivative (equiv.)	Base (equiv.)	Temp (°C)	Solvent (conc.)	Time (h)	Yield (%)
1	Br (1.2)	NaH (1.0)	80	DMF (0.33 M)	16	33
2	Br (1.2)	NaH (1.0)	70	DMF (0.15 M)	16	36
3	Br (1.2)	^{t}BuOK (1.0)	70	DMF (0.15 M)	16	23
4	I (1.2)	^{t}BuOK (1.0)	70	DMF (0.15 M)	16	27
5	Br (1.2)	Cs_2CO_3 (1.0)	70	DMF (0.15 M)	16	58
6	I (1.2)	Cs_2CO_3 (1.0)	70	DMF (0.15 M)	16	62

A series of mechanochemical experiments shown in Table 3.6 was conducted to enhance the coupling of halogenated indole derivatives with preformed imidazoles under grinding auxiliaries like Celite or NaCl, varying the weight of grinding balls, base, and substrate equivalents.

In general, the mechanochemical reaction was challenging, with only low to moderate conversions obtained within the set of parameters assayed. Initial experiments with the bromide derivative and K_2CO_3 as base (entries 1-3) resulted in poor yields (21-23 %), which indicated that there is limited reactivity under solvent-free milling. Variation in the milling time (30 to 60 min) or halide stoichiometry (1.0-1.5 equiv.) did not have a measurable impact on the outcome, suggesting that the reaction is regulated either by solid–solid diffusion or by non-activation of the substrates.

Changing to ^{t}BuOK (entry 4) or increasing the loading of K_2CO_3 to 1.5 equivalents (entry 5) did not cause improvement, with yields remaining below 25 %. Similarly, using more Celite (0.6 g compared to 0.4 g) as grinding auxiliary caused a comparatively insignificant effect, with yields increasing to merely 28 % (entry 7). These results show that while improved mixing and impact efficiency provide some assistance, the overall conversion of the reaction remains limited.

Switching to the more reactive iodide as electrophile did not lead to a dramatic yield increase under otherwise similar conditions (entries 10–15). Yields in most examples were again in the range of 13-24 %, indicating that the inherent higher reactivity of the C–I bond is not entirely available under mechanochemical conditions, perhaps because molecular mobility is limited or too little heat is released during milling. Using fewer milling balls (2 × 4.0 g) instead of 30 × 0.5 g consistently resulted in lower yields due to reduced impact frequency and less efficient mixing.

Using NaCl instead of Celite as grinding auxiliary (entry 16) produced only traces of product, confirming that Celite provides a superior grinding medium, likely due to its higher surface area and porous nature, favouring dispersion of the substrate. Replacement of K_2CO_3 by Cs_2CO_3 (entries 17-19) did not improve the outcome either, with yields remaining in the 13–21 % range. Pre-mixing imidazole with the base for 30 minutes before the addition of the iodide derivative (entries 18-19) did not provide a significant advantage under these circumstances.

The inclusion of 18-crown-6 as a phase-transfer catalyst (entry 15) gave a comparable yield (24 %), suggesting minimal increase in ionic mobility or base activation within the solid phase and adding difficulty during the purification stage.

Overall, although minor variations in milling time, auxiliary type, and ball shape contributed to the outcome, no parameter combination gave any meaningful improvement, and mechanochemical yields were always below 30 %. The data indicate that, in this specific transformation, mechanochemical activation is not efficient enough, perhaps because dry milling permits limited diffusion and partial activation of these solid reagents.

*Table 3.6. Mechanochemical optimisation of reaction conditions for the synthesis of **78**. All reactions were conducted in a planetary ball mill at 600rpm using 15 mL stainless steel jars. All reactions were performed with 1 equivalent of imidazole. All yields are isolated.*

Entry	Auxiliar (g)	Balls (g)	Ethylindole derivative (equiv.)	Base (equiv.)	Time (h)[a]	Yield (%)
1	Celite (0.4)	30 (0.5)	Br (1.5)	K_2CO_3 (1.0)	30'(2')	23
2	Celite (0.4)	30 (0.5)	Br (1.5)	K_2CO_3 (1.0)	60'(2')	21
3	Celite (0.4)	30 (0.5)	Br (1.0)	K_2CO_3 (1.0)	60'(2')	21
4	Celite (0.4)	30 (0.5)	Br (1.5)	^tBuOK (1.0)	60'(2')	21
5	Celite (0.4)	30 (0.5)	Br (1.5)	K_2CO_3 (1.5)	60'(2')	19
6	Celite (0.6)	30 (0.5)	Br (1.5)	K_2CO_3 (1.0)	60'	24
7	Celite (0.6)	30 (0.5)	Br (1.5)	K_2CO_3 (1.0)	60'	28
8	Celite (0.6)	30 (0.5)	Br (1.5)	K_2CO_3 (1.0)	30'	5
9	Celite (0.6)	30 (0.5)	Br (1.5)	K_2CO_3 (1.0)	30'	12
10	Celite (0.6)	30 (0.5)	I (1.5)	K_2CO_3 (1.0)	30'(2')	24
11	Celite (0.6)	2 (4.0)	I (1.0)	K_2CO_3 (1.0)	30'(2')	13
12	Celite (0.6)	30 (0.5)	I (1.0)	K_2CO_3 (1.0)	30'(2')	5
13	Celite (0.6)	2 (4.0)	I (1.5)	K_2CO_3 (1.0)	60'(2')	20
14	Celite (0.6)	30 (0.5)	I (1.5)	^tBuOK (1.0)	60'(2')	22
15[b]	Celite (0.6)	2 (4.0)	I (1.5)	K_2CO_3 (1.0)	60'	24
16	NaCl (1.5)	2 (4.0)	I (1.5)	K_2CO_3 (1.0)	60'	traces
17	Celite (0.6)	2 (4.0)	I (1.5)	Cs_2CO_3 (1.0)	60'	21
18[c]	Celite (0.6)	30 (0.5)	I (1.5)	Cs_2CO_3 (1.0)	30'+60'	13
19[c]	Celite (0.6)	2 (4.0)	I (1.5)	Cs_2CO_3 (1.0)	30'+60'	14

[a]Time in brackets indicates the time between rotation changes
[b]18-crown-6 was used as an additive in this reaction
[c]Imidazole and base were mixed for 30 minutes before adding the iodine starting material

Diverse conditions were screened for the microwave-assisted synthesis (Table 3.7). Reactions with the bromide electrophile and NaH (entries 1-2) gave poor conversions with only 23-25 % isolated yields, despite the long reaction times. These findings demonstrate that NaH is not an efficient base for promoting this transformation, and that variation in concentration (0.05-0.2 M) has little impact on reactivity.

An improvement was observed when the iodide was used as the electrophile along with Cs_2CO_3 (entries 3-7). Irradiation for 3 hours, at 80 °C provided a reasonable yield of 42 % of the desired product (entry 3). However, in this reaction, the formation of the cyclopropane side-product (**77**) could also be observed. Pre-activation of imidazole by base and extending the reaction duration to 3-4 h achieved a yield of 64-68 % (entries 4-5). This result, therefore, clearly indicates that the preformation of the deprotonated imidazole intermediate plays a key role in enhancing the overall efficiency of the coupling.

Reaction temperature screening revealed that 70 °C is optimum, giving the highest yield (80 %) (entry 7). Higher (90 °C) and lower (60 °C) temperatures yielded lower amounts (59 % and 70 %, respectively; entries 6 and 11), showing a narrow optimal temperature window under microwave activation.

Replacement of Cs_2CO_3 with a stronger base, such as ^tBuOK, resulted in significantly decreased yields (25-37 %; entries 8, 10, 14), probably due to competitive elimination side reactions or partial substrate decomposition.

A comparison of halide leaving groups confirmed that the iodine derivative outperforms the bromine derivative under the same conditions (entries 12-13 vs. 16-17), as expected by the greater reactivity of the C–I bond towards substitution.

Experiments involving changes in the stoichiometry of the electrophile (entries 9, 15, 17) showed that 1.0 equivalent of the ethylindole derivative is capable of delivering comparable yields with 1.2 equivalents. In particular, entry 17 (iodide derivative, 1.0 equiv.) afforded 79 % yield, which is slightly below the optimum condition (81 %, entry 16) but with less reagent excess. Accordingly, entry 17 conditions were selected as

optimal, as they offer a better and cost-efficient compromise of yield and reagent consumption.

*Table 3.7. Microwave optimisation of reaction conditions for the synthesis of **78**. All reactions were performed with 1 equivalent of imidazole that was added in the presence of base and stirred for 30 minutes at r.t. before the microwave reaction. All yields are isolated.*

Entry	Ethylindole derivative (equiv.)	Base (equiv.)	Temp (°C)	Solvent (conc.)	Time	Yield (%)
1	Br (1.2)	NaH (1.0)	80	DMF (0.2 M)	30'+4 h	25
2	Br (1.2)	NaH (1.0)	80	DMF (0.05 M)	30'+4 h	23
3[a]	I (1.2)	Cs_2CO_3 (1.0)	80	DMF (0.15 M)	3	42
4	I (1.2)	Cs_2CO_3 (1.0)	80	DMF (0.15 M)	30'+3 h	64
5	I (1.2)	Cs_2CO_3 (1.0)	80	DMF (0.15 M)	30'+4 h	68
6	I (1.2)	Cs_2CO_3 (1.0)	90	DMF (0.15 M)	30'+4 h	59
7	I (1.2)	Cs_2CO_3 (1.0)	70	DMF (0.15 M)	30'+4 h	80
8	I (1.2)	^tBuOK (1.0)	80	DMF (0.15 M)	30'+4 h	25
9	I (1.0)	Cs_2CO_3 (1.0)	80	DMF (0.15 M)	30'+4 h	77
10	I (1.2)	^tBuOK (1.0)	80	DMF (0.15 M)	30'+4 h	37
11	I (1.2)	Cs_2CO_3 (1.0)	60	DMF (0.15 M)	30'+4 h	70
12	Br (1.2)	Cs_2CO_3 (1.0)	70	DMF (0.15 M)	30'+4 h	63
13	Br (1.2)	Cs_2CO_3 (1.0)	80	DMF (0.15 M)	30'+4 h	38
14	Br (1.2)	^tBuOK (1.0)	70	DMF (0.15 M)	30'+4 h	23
15	Br (1.0)	Cs_2CO_3 (1.0)	70	DMF (0.15 M)	30'+4 h	72
16	I (1.2)	Cs_2CO_3 (1.0)	70	DMF (0.15 M)	30'+4 h	81
17	I (1.0)	Cs_2CO_3 (1.0)	70	DMF (0.15 M)	30'+4 h	79

[a]Conducted without the previous mixture of imidazole with base

To summarise, from the three optimisation methods evaluated, the one considered more efficient in terms of yield, reaction times, and green chemistry is the microwave-

assisted synthesis using 1 equiv. of iodoethylindole **79**, Cs_2CO_3 (1.0 equiv) as base in DMF at 70 °C for 4 hours after the pre-activation of the imidazole.

With the optimised conditions in hand, we decided to explore the general applicability of the method by studying various imidazole derivatives as substrates. It should be noted that if the substitution pattern of the imidazole ring is non-symmetric ($R^3 \neq R^4$), the reaction could give two regioisomeric products, corresponding to the incorporation of the substituents at either of the two positions available on the imidazole.

The regiochemistry of most products was determined using two-dimensional nuclear magnetic resonance (2D NMR) techniques like HMBC (Heteronuclear Multiple-Bond Correlation) and HMQC (Heteronuclear Multiple-Quantum Coherence). The HMBC experiments allowed the correlation of proton signals with the carbon atoms two or three bonds away, and this proved instrumental in substituent position assignments at the heterocyclic ring. One-bond couplings were employed to directly correlate proton and carbon signals using HMQC experiments to set up the connectivity in the molecule.

In a few cases where 2D NMR by itself was insufficient to distinguish the regioisomers unequivocally, selective nuclear Overhauser effect (NOE) experiments were conducted. By irradiating certain proton signals and observing the enhancement of spacially adjacent protons, the experiments provided useful insight into substituents' proximity in space, which made the absolute assignment of product configuration feasible.

As each reaction gave two products in most of the cases, the yield corresponding to the reaction is the sum of the yields of both regioisomers represented in brackets.

Looking into the obtained results (Scheme 3.15), we can see a great difference in the formation of regioisomers in three cases, **78o**, **78r'** and **78s**. While the nitrogen atoms of imidazole are electronically equivalent by resonance when deprotonated, substituents in the ring can have a strong influence on the ratio of tautomers. In the case of 4(5)-nitroimidazole, the tautomer ratio is highly skewed, much favouring 4-nitroimidazole by a rough ratio of 400:1.[122] This is due to the electron-withdrawing nitro

group stabilising this tautomer by delocalisation of electron density and affecting the relative acidity of the nitrogen atoms, imposing a significant bias towards one of the tautomers in practice. This could explain the formation of **78s'** in a much bigger proportion, as it is the regioisomer that contains the nitro group in position 4 of the imidazole ring. This can probably also explain the case of the major formation of regioisomer **78r'**. The electron-donating character of the methyl substituent, together with the electron-withdrawing character of the aldehyde, may favour the formation mainly of **78r'**. In the case of **78o'**, probably this regioisomer is the only product observed due to the possibility to stabilise the negative charge through delocalisation in the phenyl ring when in position 4 of the imidazole ring.

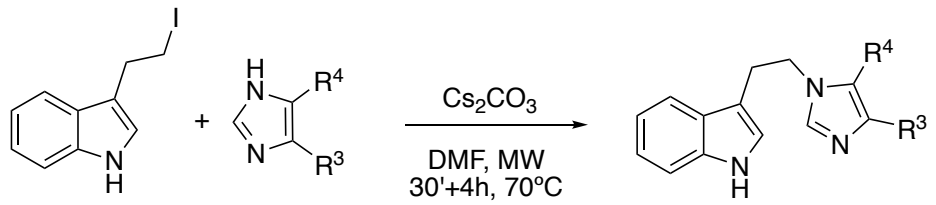

79 **78**

Two molecules if $R^3 \neq R^4$

78k: R^3 = H, R^4 = H (79%)
78l: R^3 = H, R^4 = COOMe (26%) **78l'**: R^3 = COOMe, R^4 = H (29%)
78m: R^3 = Br, R^4 = Me (28%) **78m'**: R^3 = Me, R^4 = Br (24%)
78n: R^3 = H, R^4 = CHO (36%) **78n'**: R^3 = CHO, R^4 = H (35%)
78o: R^3 = H, R^4 = Ph (not observed) **78o'**: R^3 = Ph, R^4 = H (43%)
78p: Benzimidazole (67%)
78q: R^3 = H, R^4 = COOEt (27%) **78q'**: R^3 = COOEt, R^4 = H (36%)
78r: R^3 = CHO, R^4 = Me (23%) **78r'**: R^3 = Me, R^4 = CHO (not observed)
78s: R^3 = H, R^4 = NO_2 (8%) **78s'**: R^3 = NO_2, R^4 = H (51%)
78t: R^3 = Me, R^4 = NO_2 (mix 59%) **78t'**: R^3 = NO_2, R^4 = Me (mix 59%)
78u: 6-NO_2-Benzimidazole (33%) **78u'**: 5-NO_2-Benzimidazole (40%)

Scheme 3.15. Scope of molecules synthesised using optimised conditions.

As mentioned previously, the determination of the configuration of the regioisomer was possible thanks to 2D NMR experiments. In Figure 3.35 and Figure 3.36 are shown two representative examples of regioisomers elucidation.

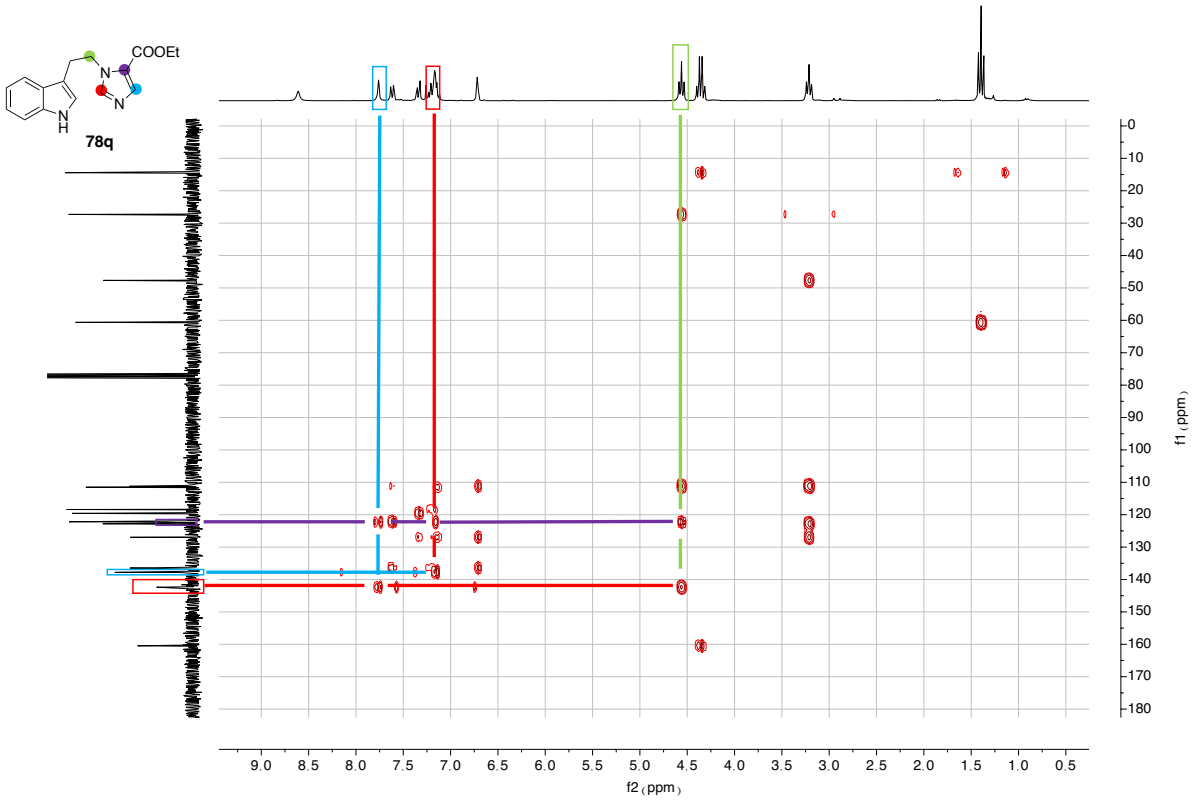

*Figure 3.35. 2D NMR HMBC of compound **78q**.*

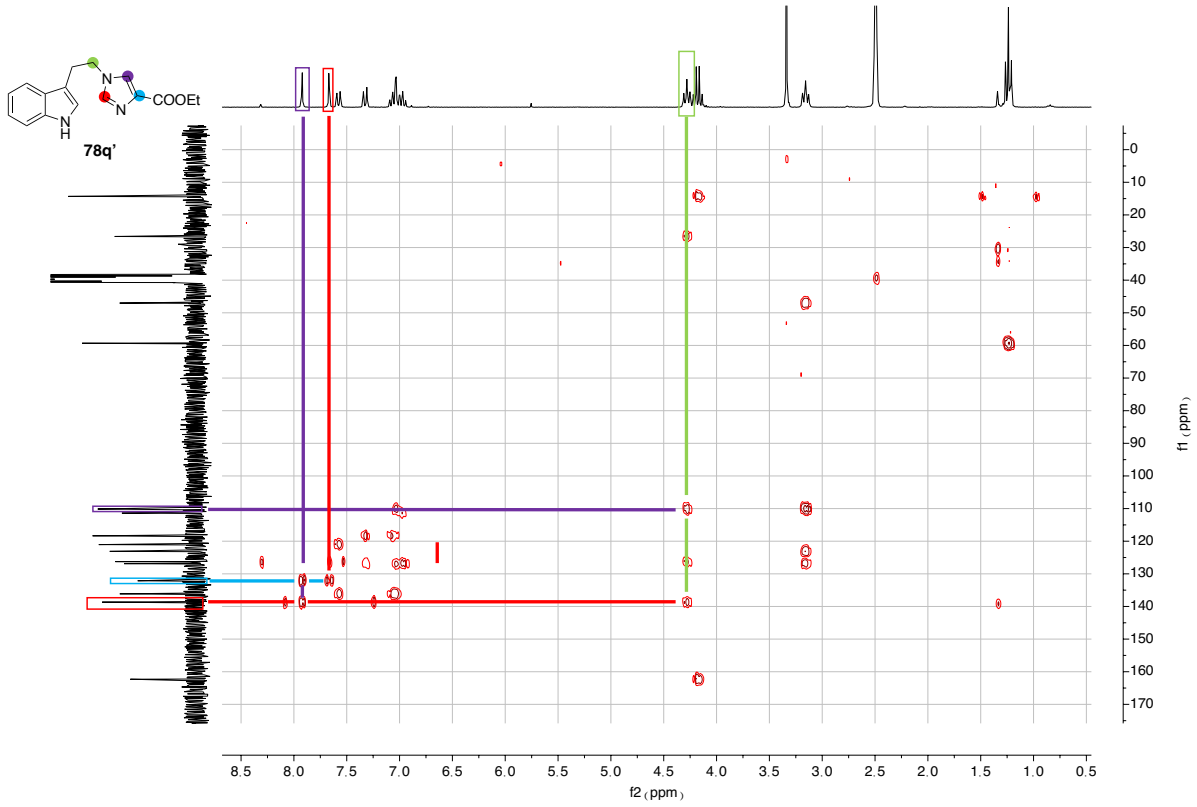

*Figure 3.36. 2D NMR HMBC of compound **78q'**.*

In Figure 3.35 we can observe that the proton in the CH_2 from the ethylenic chain (represented in green) is correlated with the carbon corresponding to the CH in position 2 of imidazole (represented in red) and a quaternary carbon, which corresponds to position 5 of the imidazole ring (represented in purple). The regiochemistry seems to be clear with this experiment, as the proton in the ethylenic chain does not correlate with the carbon in position 4 of the imidazole (represented in blue); however, HMBC of the corresponding regioisomer was also performed to confirm the analysis (Figure 3.36). In Figure 3.36 the proton of the CH_2 from the ethylenic chain (represented in green) does not correlate with the quaternary carbon where the ester is linked (represented in blue), indicating that the ester is situated in position 4 (represented in blue) of the imidazole ring.

Due to a lack of time, methylation of compounds **78** to obtain the advanced open derivatives **66** was only performed in some examples, as shown in Scheme 3.16. The yields were lower than expected in many cases, but allowed us, however, to obtain sufficient amounts of the desired products.

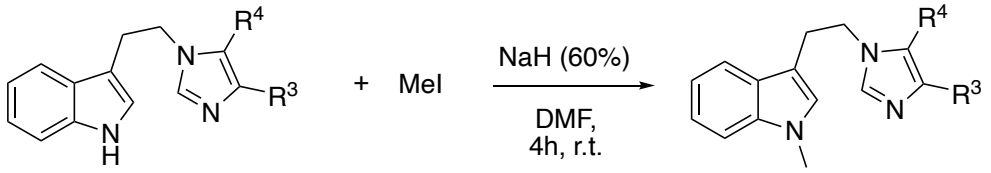

66k: R^3 = H, R^4 = H (92%)
66l: R^3 = H, R^4 = COOMe (39%) **66l'**: R^3 = COOMe, R^4 = H (30%)
66m: R^3 = Br, R^4 = Me (50%) **66m'**: R^3 = Me, R^4 = Br (49%)
66n: R^3 = H, R^4 = CHO (56%) **66n'**: R^3 = CHO, R^4 = H (54%)
66o': R^3 = Ph, R^4 = H (31%)
66p: Benzimidazole (3%)

*Scheme 3.16. Methylation of compounds **78** to produce the advanced intermediates **66**.*

As in the previous case, whenever positions 4 and 5 of the imidazole were substituted, the elucidation was done using a selective NOE experiment, as represented in Figure 3.37.

When the imidazole methyl substituent was irradiated selectively, both CH_2 of the ethylenic chain could be observed, suggesting that the methyl substituent was in

position 5 of the imidazole ring. Avogadro predictions (Figure 3.38) showed that whenever the methyl substituent was in position 5 (**66m**), the distance to the protons in the ethylenic chain would be 2.612 Å for the closest CH_2 of the ethylenic chain and 4.830 Å for the furthest. In contrast, if the methyl substituent is in position 4 of the imidazole ring (**66m'**), the distance to the protons in the ethylenic chain would be 5.367 Å for the closest CH_2 of the ethylenic chain and 6.518 Å for the furthest, not observable through NOE experiments.

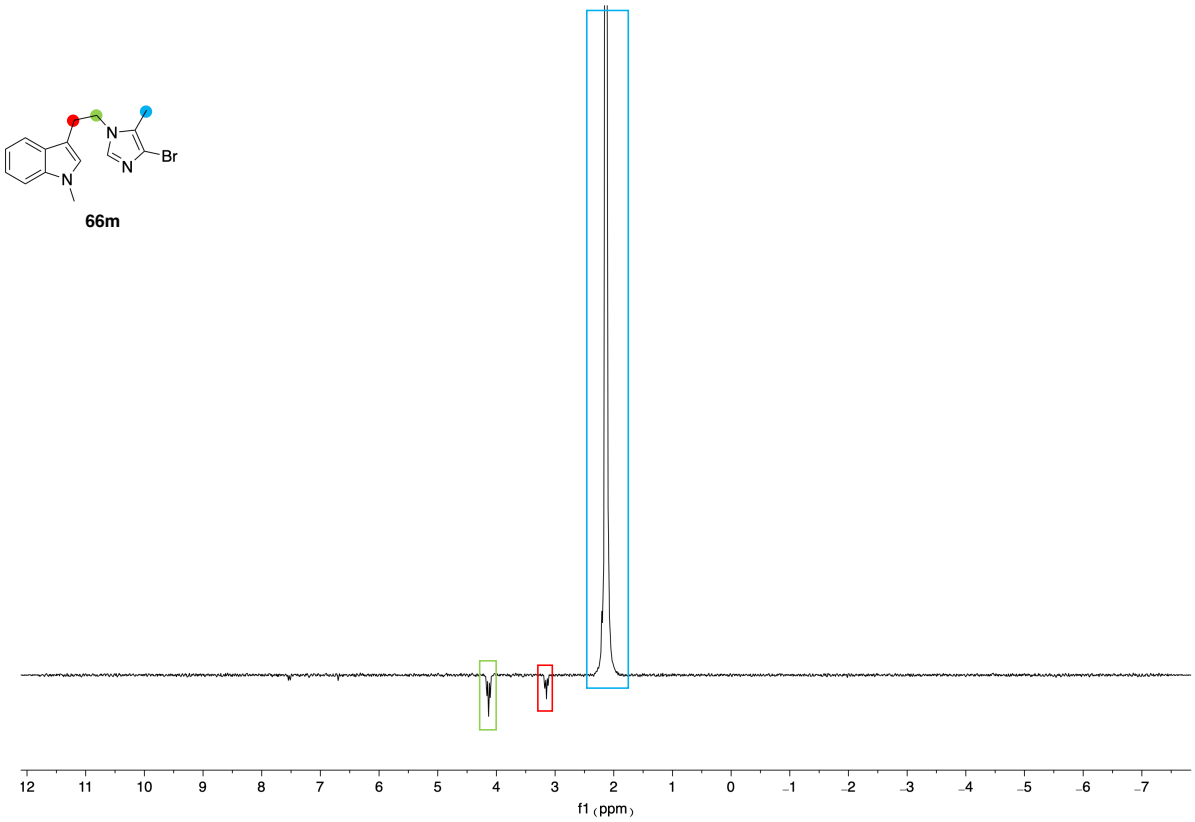

*Figure 3.37. Selective NOE 1D experiment of compound **66m**.*

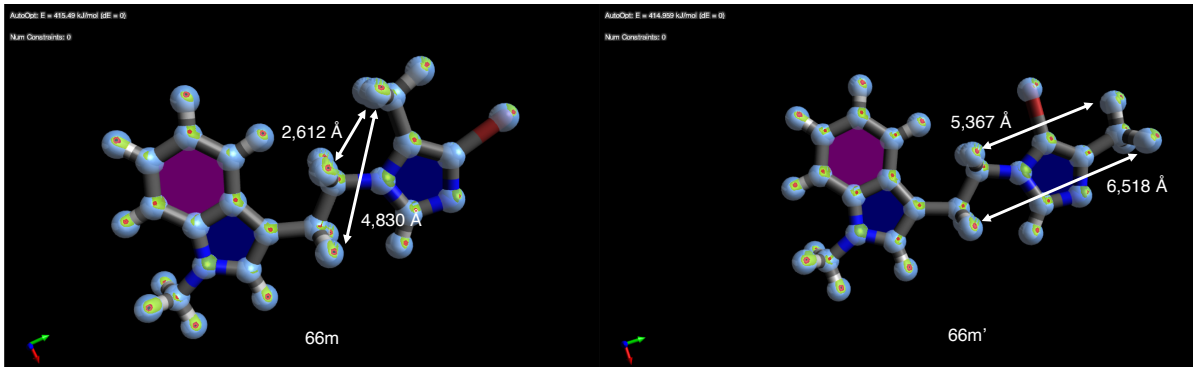

*Figure 3.38. Avogadro auto optimised compounds **66m** and **66m'** using UFF as force field with 4 steps per update and steepest descent algorithm.*

To complete the synthetic pathway, the cyclisation of molecules **66k-p** was considered by analogy with the synthesis of compounds **65a-j**. Due to time constraints, unfortunately, just compound **65l** (Scheme 3.17) from this second pathway was prepared. Nevertheless, this result proves the feasibility of the cyclisation reaction for the new derivatives.

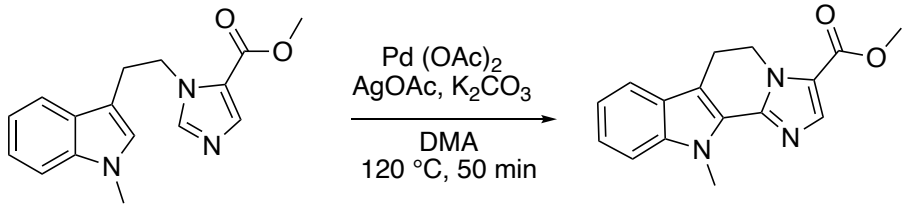

66l **65l**, 28%

*Scheme 3.17. Synthesis of compound **65l** from **66l**.*

3.4. EXPERIMENTAL SECTION

3.4.1. General experimental information

For experimental procedures developed in the Università di Urbino, all reagents and solvents were of commercial quality and were used as received. Column chromatography purifications were performed under “flash” conditions using Merck 230–400 mesh silica gel. Thin-layer chromatography (TLC) was carried out on Merck silica gel 60 F254 plates, which were visualised by exposure to ultraviolet light. ^{1}H NMR and ^{13}C NMR were recorded on a Bruker Avance 400 spectrometer (^{1}H: 400 MHz, ^{13}C: 101 MHz), or on a Bruker Avance Neo 600 spectrometer (^{1}H: 600 MHz, ^{13}C: 151 MHz) using MeOD, DMSO-*d*$_6$ or $CDCl_3$ as solvent. Chemical shifts are reported in the δ scale relative to residual MeOH (s, 4.87 ppm), $CHCl_3$ (s, 7.26 ppm) or DMSO (p, 2.50 ppm) for ^{1}H NMR and to the central line of MeOH (49.5 ppm), $CDCl_3$ (77.16 ppm) or DMSO-*d*$_6$ (39.52 ppm) for ^{13}C NMR. ^{13}C NMR were recorded with ^{1}H broadband decoupling. The following abbreviations were used to report the multiplicities: br = broad, s = singlet, d = doublet, t = triplet, q = quartet, hept = heptet, dd = doublet of doublets, ddd = doublet of doublets of doublets, m = multiplet. Coupling constants (*J*) are reported in Hertz (Hz). ESI-MS spectra were recorded on Waters Micromass ZQ 4000, using electrospray ionisation techniques, with samples dissolved in MeOH. HRMS spectra were performed by slow direct infusion (5 µL/min) of ≈ 0.1 µg/mL solution (methanol), using Orbitrap Exploris 240 mass spectrometer.

For experimental procedures developed in the Universidad Complutense de Madrid, all reagents (Aldrich, Fischer, Alpha Aesar) and solvents (Scharlau, Fischer) were of commercial quality and were used as received. Reactions were monitored by TLC on aluminium plates coated with silica gel and fluorescent indicator (Macherey-Nagel Xtra SIL G/UV254). Mechanochemical reactions were carried out in a planetary ball mill Retsch PM 100, using grinding jars and balls of stainless steel with different volumes and diameters. Microwave-assisted reactions were performed on an Anton Paar (Microwave 400) focused microwave reactor. Separations by flash chromatography were performed using a Combiflash Teledyne automated flash chromatograph or on conventional silica gel columns (Scharlau 40–60 µm, 230–400 mesh ASTM). NMR

spectroscopic data were recorded using a Bruker Avance 250 spectrometer operating at 250 MHz for ^{1}H NMR and 63 MHz for ^{13}C NMR, Bruker AVIII HD 300 MHz BACS-60 operating at 300 MHz for ^{1}H NMR and 76 MHz for ^{13}C NMR or Bruker NEO 300MHz SampleXpress Lite operating at 300 MHz for ^{1}H NMR and 76 MHz for ^{13}C NMR (Unidad de Resonancia Magnética Nuclear, Universidad Complutense); Topspin or Mestrenova software packages were used throughout for data processing; chemical shifts are given in ppm and coupling constants in Hertz. Elemental analyses were determined by the Unidad de Microanálisis Elemental, Universidad Complutense, using a Leco 932 combustion microanalyzer. Exact mass data were recorded with a high-resolution mass spectrometer FTMS Bruker APEX Q IV coupled to 2DLC-NS-ESI-MALDI (Mass range: 200-10.000 uma) and a time-of-flight mass spectrometer MALDI-TOF/TOF Bruker ULTRAFLEX coupled to MALDI (Mass range: 300-150000 uma), operated by the Unidad de Espectrometría de Masas, Universidad Complutense.

- PART 1 –

*3.4.2. Synthesis of N-methyl-1H-indoles (**69**)*

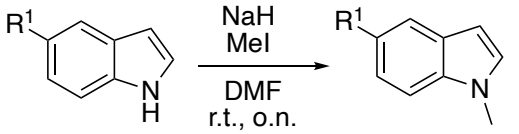

69a: R^1 = F
69b: R^1 = Cl
69c: R^1 = Me
69d: R^1 = Ph

General procedure for the synthesis of 1-methyl-1*H*-indoles (69a-d) GP1

According to the reported synthesis in the literature,[123] the indole derivative (1.0 equiv.) was dissolved in dry DMF (c = 0.25 M). At 0 °C, NaH (1.6 equiv, 60 % dispersion in mineral oil) was added portion-wise. When the addition was finished, the ice bath was removed, and the reaction mixture was stirred at room temperature. After 30 minutes methyl iodide (1.2 equiv.) was added dropwise at 0 °C. Afterwards the reaction mixture was warmed to room temperature and stirred overnight. Water was added and the aqueous phase was extracted with dichloromethane (DCM) (3 x 20 mL). The combined organic layers were washed with brine, dried using Na_2SO_4, and after filtration, the solvent was removed in vacuo. If needed, further purification was performed by flash chromatography on silica gel.

5-Fluoro-1-methyl-1*H*-indole **(69a)**:

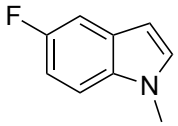

According to GP1 5-fluoro-1*H*-indole (1 g, 7.4 mmol, 1.0 equiv.), NaH (474 mg, 11.84 mmol, 1.6 equiv.) and iodomethane (0.55 mL, 8.88 mmol, 1.2 equiv.) in DMF (29.6 mL) provided, after cyclohexane/ethyl acetate (95:5) column chromatography, the desired compound **69a** (1.07 g, yield 97 %) as a white solid.

The physicochemical data are consistent with those reported in the literature.[123]

^{1}H NMR (400 MHz, $CDCl_3$, 25 °C): δ = 7.27 (dd, 1H, J_1 = 2.5 Hz, J_2 = 9.0 Hz), 7.23 (ddt, 1H, J_1 = 1.0 Hz J_2 = 4.5 Hz, J_3 = 9.0 Hz), 7.09 (d, 1H, J_1 = 3.0 Hz), 6.97 (dd, 1H, J_1 = 2.5 Hz, $J_2 \approx J_2$ = 9.0 Hz), 6.44 (dd, 1H, J_1 = 1.0 Hz, J_2 = 3.0 Hz), 3.79 (s, 3H).

5-Chloro-1-methyl-1*H*-indole **(69b)**:

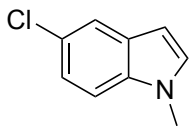

According to GP1 5-chloro-1*H*-indole (1 g, 6.6 mmol, 1.0 equiv.), NaH (422 mg, 10.55 mmol, 1.6 equiv.) and iodomethane (0.5 mL, 7.92 mmol, 1.2 equiv.) in DMF (24.6 mL) provided, after cyclohexane/ethyl acetate (95:5) column chromatography, the desired compound **69b** (998 mg, yield 91 %) as a yellow oil.

The physicochemical data are consistent with those reported in the literature.[124]

^{1}H NMR (400 MHz, $CDCl_3$, 25 °C): δ = 7.59 (dd, 1H, J_1 = 1.0 Hz, J_2 = 2.0 Hz), 7.23 (d, 1H, J = 8.5 Hz), 7.17 (dd, 1H, J_1 = 2.0 Hz, J_2 = 8.5 Hz), 7.07 (d, 1H, J_1 = 3.0 Hz), 6.43 (dd, 1H, J_1 = 1.0 Hz, J_2 = 3.0 Hz), 3.78 (s, 3H).

1,5-Dimethyl-1*H*-indole **(69c)**:

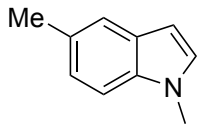

According to GP1 5-methyl-1*H*-indole (600 mg, 4.57 mmol, 1.0 equiv.), NaH (293 mg, 7.32 mmol, 1.6 equiv.) and iodomethane (345 mL, 5.49 mmol, 1.2 equiv.) in DMF (18.3 mL) provided, after cyclohexane/ethyl acetate (95:5) column chromatography, the desired compound **69c** (333 mg, yield 50 %) as yellow oil.

The physicochemical data are consistent with those reported in the literature [123].

^{1}H NMR (400 MHz, $CDCl_3$, 25 °C): δ = 7.21 (d, 1H, J = 9.0 Hz), 7.10 (d, 1H, J = 2.5 Hz), 7.02 (d, 1H, J = 3.0 Hz), 6.89 (dd, 1H, J_1 = 2.5 Hz, J_2 = 9.0 Hz), 6.40 (dd, 1H, J = 3.0 Hz), 3.86 (s, 3H), 3.77 (s, 3H).

1-Methyl-5-phenyl-1*H*-indole **(69d)**:

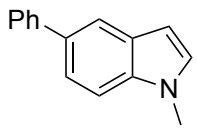

According to a modification of GP1 5-phenyl-1*H*-indole (130 mg, 0.67 mmol, 1.0 equiv.), NaH (40 mg, 1.1 mmol, 1.5 equiv.) and iodomethane (53 mL, 0.82 mmol, 1.3 equiv.) in THF (2.2 mL)

provided, after cyclohexane/ethyl acetate (95:5) column chromatography, the desired compound **69d** (114 mg, yield 82 %) as a white solid.

The physicochemical data are consistent with those reported in the literature.[125]

^{1}H NMR (400 MHz, $CDCl_3$, 25 °C): δ = 7.85 (dd, 1H, J_1 = 1.0 Hz, J_2 = 2.0 Hz), 7.67 (dd, 2H, J_1 = 1.0 Hz, J_2 = 8.5 Hz), 7.50 (dd, 1H, J_1 = 2.0 Hz, J_2 = 8.5 Hz), 7.47 – 7.42 (m, 2H), 7.39 (dt, 1H, J_1 = 1.0 Hz, J_2 = 8.5 Hz), 7.34 – 7.29 (m, 1H), 7.09 (d, 1H, J = 3.0 Hz), 6.55 (dd, 1H, J_1 = 1.0 Hz, J_2 = 3.0 Hz), 3.83 (s, 3H).

*3.4.3. Synthesis of 1-methyl-3-(2-nitrovinyl)-1H-indoles (**70**)*

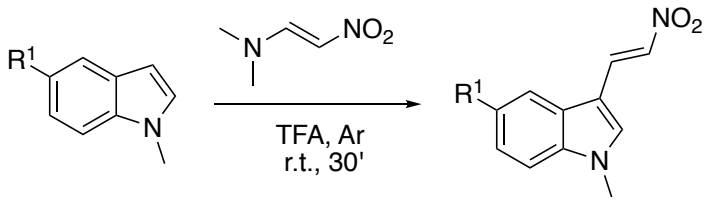

69a: R^1 = F
69b: R^1 = Cl
69c: R^1 = Me
69d: R^1 = Ph

70a: R^1 = F
70b: R^1 = Cl
70c: R^1 = Me
70d: R^1 = Ph

General procedure for the synthesis of 1-methyl-3-(2-nitrovinyl)-1*H*-indoles (70a-d) GP2

According to the method reported in the literature,[126] under an argon atmosphere, TFA was added to a mixture of substituted indole (1 equiv.) and dimethylaminonitroethylene (1 equiv.) at room temperature. After 30 mins of stirring, the reaction was quenched by adding dropwise a solution of saturated aqueous $NaHCO_3$, and the resultant slurry mixture was extracted with EtOAc (3 x 20 mL). The combined organic layers were then washed with water, dried using Na_2SO_4, and after filtration, the solvent was removed *in vacuo* to give the target indolyl nitroalkene as a solid. The pure product was obtained by crystallisation (MeOH).

5-Fluoro-1-methyl-3-(2-nitrovinyl)-1*H*-indole **(70a)**:

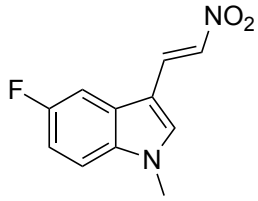

According to GP2, TFA (0.55 mL) added to 5-fluoro-1-methyl-1*H*-indole (145 mg, 0.97 mmol, 1.0 eq) and dimethylamino nitroethylene (113 mg, 0.97 mmol, 1.0 eq) provided, after recrystallization from MeOH the desired compound **70a** (170 mg, yield 80 %) as a yellow solid.

Compound is known, but physicochemical data have not been reported in the literature.

^{1}H NMR (400 MHz, DMSO-d_6, 25 °C): δ = 8.35 (d, 1H, J = 13.5 Hz), 8.27 (s, 1H), 8.04 (d, 1H, J = 13.5 Hz), 7.89 (dd, 1H, J_1 = 2.5 Hz, J_2 = 9.5 Hz), 7.63 (dd, 1H, J_1 = 4.5 Hz, J_2 = 9.5 Hz), 7.20 (ddd, 1H, J_1 = 2.5 Hz, $J_2 \approx J_3$ = 9.5 Hz), 3.88 (s, 3H).

^{13}C NMR (101 MHz, DMSO-d_6, 25 °C): δ = 158.8 (d, J = 236.0 Hz), 140.3, 134.8, 133.6, 131.5, 125.7 (d, J = 10.5 Hz), 112.6 (d, J = 10.0 Hz), 111.3 (d, J = 26.0 Hz), 107.1 (d, J = 4.5 Hz), 106.2 (d, J = 25 Hz), 33.6.

5-Chloro-1-methyl-3-(2-nitrovinyl)-1*H*-indole **(70b)**:

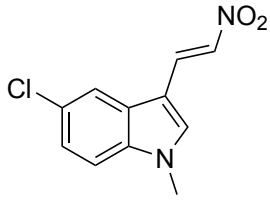

According to GP2, TFA (0.47 mL) added to 5-chloro-1-methyl-1*H*-indole (135 mg, 0.82 mmol, 1.0 eq) and dimethylamino nitroethylene (95 mg, 0.82 mmol, 1.0 eq) provided, after recrystallization from MeOH the desired compound **70b** (169 mg, yield 87 %) as a yellow solid.

Compound is known, but physicochemical data have not been reported in the literature.

^{1}H NMR (400 MHz, DMSO-d_6, 25 °C): δ = 8.35 (d, 1H, J = 13.5 Hz), 8.27 (s, 1H), 8.13 (d, 1H, J = 2.0 Hz), 8.09 (d, 1H, J = 13.5 Hz), 7.63 (d, 1H, J = 9.0 Hz), 7.35 (dd, 1H, J_1 = 2.0 Hz, J_2 = 9.0 Hz), 3.87 (s, 3H).

^{13}C NMR (101 MHz, DMSO-d_6, 25 °C): δ = 139.9, 136.7, 133.3, 131.9, 127.1, 126.2, 123.3, 119.9, 112.9, 106.7, 33.5.

1,5-Dimethyl-3-(2-nitrovinyl)-1*H*-indole **(70c)**:

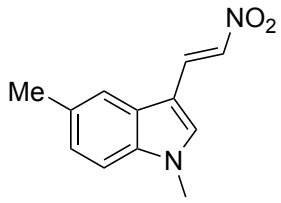

According to GP2, TFA (3.94 mL) added to 5,1-dimethyl-1*H*-indole (1 g, 6.9 mmol, 1.0 eq) and dimethylamino nitroethylene (800 mg, 6.9 mmol, 1.0 eq) provided, after recrystallization from MeOH the desired compound **70c** (609 mg, yield 41 %) as a brown solid.

^{1}H NMR (400 MHz, DMSO-d_6, 25 °C): δ = 8.34 (d, 1H, J = 13.5 Hz), 8.16 (s, 1H), 8.01 (d, 1H, J = 13.5 Hz), 7.81 (br s, 1H), 7.48 (d, 1H, J_1 = 8.5 Hz), 7.17 (dd, 1H, J_1 = 1.0 Hz, J_2 = 8.5 Hz), 3.84 (s, 3H), 2.46 (s, 3H).

^{13}C NMR (101 MHz, DMSO-d_6, 25 °C): 139.6, 136.7, 134.4, 131.6, 130.7, 125.2, 124.9, 120.5, 110.9, 106.9, 33.3, 21.0.

5-Phenyl-1-methyl-3-(2-nitrovinyl)- 1*H*-indole (**70d**)

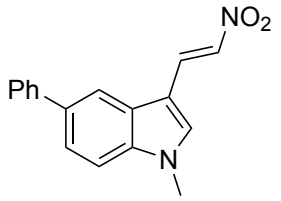

According to GP2, TFA (0.65 mL) added to 5-phenyl-1-methyl-1*H*-indole (200 mg, 0.97 mmol, 1.0 eq) and dimethylamino nitroethylene (113 mg, 0.97 mmol, 1.0 eq) provided, after recrystallization from MeOH the desired compound **70d** (195 mg, yield 72 %) as a yellow solid.

^{1}H NMR (400 MHz, DMSO-d_6, 25 °C): δ = 8.42 (d, 1H, J = 13.5 Hz), 8.26 (s, 1H), 8.20 (dd, 1H, J_1 = 1.0 Hz, J_2 = 2.0 Hz), 8.16 (d, 1H, J = 13.5 Hz), 7.84 – 7.79 (m, 2H), 7.69 (dd, 1H, J_1 = 1.0 Hz, J_2 = 8.5 Hz), 7.65 (dd, 1H, J_1 = 1.5 Hz, J_2 = 8.5 Hz), 7.51 – 7.45 (m, 2H), 7.38 – 7.33 (m, 1H), 3.91 (s, 3H).

^{13}C NMR (101 MHz, DMSO-d_6, 25 °C): δ = 140.8, 139.6, 137.7, 134.8, 133.9, 131.5, 128.7, 127.3, 126.9, 125.8, 122.7, 118.5, 111.7, 107.6, 33.5.

*3.4.4. Synthesis of 2-(1-methyl-1H-indol-3-yl)ethan-1-amine (**67**)*

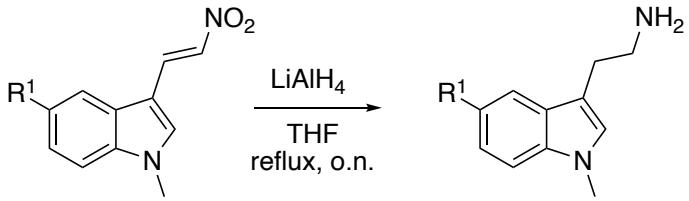

70a: R^1 = F
70b: R^1 = Cl
70c: R^1 = Me
70d: R^1 = Ph

67a: R^1 = F
67b: R^1 = Cl
67c: R^1 = Me
67d: R^1 = Ph

General procedure for the synthesis of 2-(1-methyl-1*H*-indol-3-yl)ethan-1-amine from nitrovinyl derivatives (67a-d) GP3

According to the method reported in the literature,[127] to a solution of the appropriate nitroolefin (1 equiv.) in freshly distilled tetrahydrofuran (THF) (c = 0.125 M) with ice-bath cooling, lithium aluminium hydride powder (8 equiv.) was added cautiously. Stirring was continued at 0 °C for 30 minutes, then the reaction was heated under reflux overnight. When the nitroolefin was completely consumed (TLC check), the reaction was cooled to 0 °C and carefully quenched by adding potassium sodium tartrate (Rochelle's salt). After stirring for 30 min, the solution was extracted with DCM (3 x 20 mL), dried over Na_2SO_4, filtered and concentrated in vacuo. The crude material was purified by flash chromatography.

2-(5-Fluoro-1-methyl-1*H*-indol-3-yl)ethan-1-amine (**67a**):

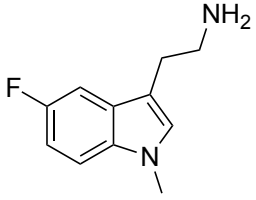

According to GP3, 5-fluoro-1-methyl-3-(2-nitrovinyl)-1*H*-indole (950 mg, 4.3 mmol, 1.0 eq) in THF (34.5 mL) with lithium aluminium hydride (1.308 g, 34.5 mmol, 8.0 eq) provided, after DCM/MeOH (95:5) with 1% of ammonia column chromatography, the desired compound **67a** (608 mg, yield 74 %) as a light yellow oil.

The physicochemical data are consistent with those reported in the literature.[127]

^{1}H NMR (400 MHz, $CDCl_3$, 25 °C): δ = 7.22 (dd, 1H, J_1 = 2.5 Hz, J_2 = 9.0 Hz), 7.18 (dd, 1H, J_1 = 4.5 Hz, J_2 = 9.0 Hz), 6.95 (ddd, 1H, J_1 = 2.5 Hz, $J_2 \approx J_3$ = 9.0 Hz), 6.94 (br s, 1H), 3.74 (s, 3H), 3.01 (t, 2H, J = 6.5 Hz), 2.88 (t, 2H, J = 6.5 Hz).

2-(5-Chloro-1-methyl-1*H*-indol-3-yl)ethan-1-amine **(67b)**:

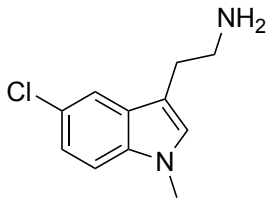

According to GP3, 5-chloro-1-methyl-3-(2-nitrovinyl)-1*H*-indole (900 mg, 3.8 mmol, 1.0 eq) in THF (30 mL) with lithium aluminium hydride (1.15 g, 30.4 mmol, 8.0 eq) provided, after DCM/MeOH/ammonia (94:5:1) column chromatography, the desired compound **67b** (480 mg, yield 61 %) as a light yellow oil.

Compound is known, but physicochemical data have not been reported in the literature.

^{1}H NMR (400 MHz, $CDCl_3$, 25 °C): δ = 7.55 (d, 1H, J = 2.0 Hz), 7.20 (d, 1H, J = 8.5 Hz), 7.16 (dd, 1H, J_1 = 2.0 Hz, J_2 = 8.5 Hz), 6.91 (s, 1H), 3.73 (s, 3H), 3.00 (t, 2H, J = 6.5 Hz), 2.85 (t, 2H, J = 6.5 Hz).

2-(1,5-Dimethyl-1*H*-indol-3-yl)ethan-1-amine **(67c)**:

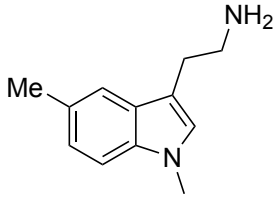

According to GP3, 1,5-dimethyl-3-(2-nitrovinyl)-1*H*-indole (150 mg, 0.7 mmol, 1.0 eq) in THF (5.6 mL) with lithium aluminium hydride (210 mg, 5.6 mmol, 8.0 eq) provided, after DCM/MeOH (9:1) with 1 % of ammonia column chromatography, the desired compound **67c** (100 mg, yield 76 %) as a yellow oil.

Compound is known, but physicochemical data have not been reported in the literature.

^{1}H NMR (400 MHz, $CDCl_3$, 25 °C): δ = 7.37 (d, 1H, J = 1.5 Hz), 7.18 (d, 1H, J = 8.5 Hz), 7.05 (dd, 1H, J_1 = 1.5 Hz, J_2 = 8.5 Hz), 6.85 (s, 1H), 3.72 (s, 3H), 3.01 (t, 2H, J = 6.5 Hz), 2.87 (t, 2H, J = 6.5 Hz), 2.46 (s, 3H).

2-(5-Phenyl-1-methyl-1*H*-indol-3-yl)ethan-1-amine (**67d**):

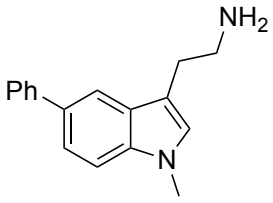

According to GP3, 5-phenyl-1-methyl-3-(2-nitrovinyl)-1*H*-indole (180 mg, 0.65 mmol, 1.0 eq) in THF (34.5 mL) with lithium aluminium hydride (196 mg, 5.17 mmol, 8.0 eq) provided, after DCM/MeOH (95:5) with 1 % of ammonia column chromatography, the desired compound **67d** (115 mg, yield 71 %) as a light yellow oil.

Compound is known, but physicochemical data have not been reported in the literature.

^{1}H NMR (400 MHz, $CDCl_3$, 25 °C): δ = 7.80 (dd, 1H, J_1 = 0.5 Hz, J_2 = 2.0 Hz), 7.69 – 7.65 (m, 2H), 7.49 (dd, 1H, J_1 = 2.0 Hz, J_2 = 8.5 Hz), 7.48 – 7.42 (m, 2H), 7.35 (dd, 1H, J_1 = 1.0 Hz, J_2 = 8.5 Hz), 7.34 – 7.29 (m, 1H), 6.93 (s, 1H), 3.77 (s, 3H), 3.06 (t, 2H, J = 6.5 Hz), 2.95 (t, 2H, J = 6.5 Hz), 2.00 (s, 2H).

^{13}C NMR (101 MHz, $CDCl_3$, 25 °C): δ = 142.8, 136.8, 132.6, 128.8, 128.5, 127.8, 127.5, 126.4, 121.6, 117.7, 112.6, 109.6, 42.5, 32.8, 29.1.

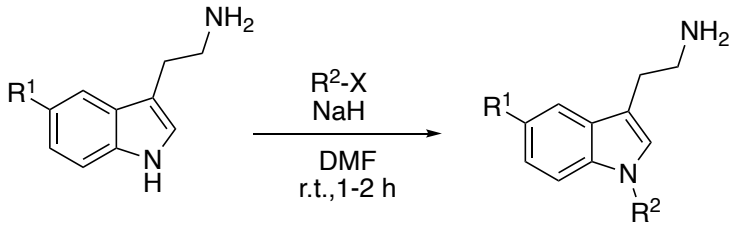

67e: R^1 = H, R^2 = Me
67f: R^1 = H, R^2 = *n*-Pr
67g: R^1 = H, R^2 = Bn
67h: R^1 = H, R^2 = Ph
67i: R^1 = OMe, R^2 = Me

General procedure for the methylation of preformed tryptamines for the for the synthesis of 2-(1-methyl-1*H*-indol-3-yl)ethan-1-amines (67e-i) GP4

According to a method reported in the literature for indole derivatives lacking the aminoethyl chain,[128] the appropriate tryptamine derivative (1.0 equiv.) was dissolved in DMF (c = 0.17 M) and cooled to 0 °C. NaH 60 % suspension in mineral oil (1.2 equiv.) was then added portion-wise and the mixture was stirred for 30 min. The

suitable alkyl halide RX (1.1 equiv.) was added dropwise to the mixture. Then the mixture was left stirring at room temperature for 1-2 h. The reaction was then quenched with a saturated aqueous solution of NH_4Cl and extracted with EtOAc (3 x 20 mL). The combined organic layers were dried over anhydrous Na_2SO_4, filtered, and concentrated under reduced pressure. The crude product was purified using column chromatography.

2-(1-Methyl-1*H*-indol-3-yl)ethan-1-amine **(67e)**:

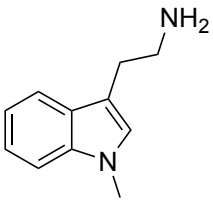

This molecule was synthesised with a modification of GP4. According to the reported method,[129] a solution of tryptamine (270 mg, 1.69 mmol, 1.0 equiv.) in anhydrous DMF (3 mL, c = 0.5 M) was added dropwise to a 60 % suspension of sodium hydride in mineral oil (74 mg, 1.85 mmol, 1.1 eq) in anhydrous DMF (5 mL, c = 0.33 M) at room temperature. The mixture was stirred at r.t. for 30 min, cooled to 0 °C, and MeI (115 µL, 1.85 mmol, 1.1 eq) was added dropwise. The resulting mixture was stirred at r.t. overnight. Then, water was added, and the resulting solution was extracted with EtOAc (6 x 20 mL). The combined organic phases were dried over Na_2SO_4, filtered, and dried under reduced pressure to afford a crude compound, which was purified by flash chromatography DCM/MeOH/ammonia (94:5:1) to provide the desired compound **67e** (169 mg, yield 57 %) as a yellow oil.

The physicochemical data are consistent with those reported in the literature.[129]

^{1}H NMR (400 MHz, $CDCl_3$, 25 °C): δ = 7.60 (ddd, 2H, $J_1 \approx J_2$ = 1.0 Hz, J_3 = 8.0 Hz), 7.30 (ddd, 2H, $J_1 \approx J_2$ = 1.0 Hz, J_3 = 8.0 Hz), 7.23 (ddd, 1H, J_1 = 1.0 Hz, J_2 = 7.0 Hz, J_3 = 8.0 Hz), 7.10 (ddd, 1H, J_1 = 1.0 Hz, J_2 = 7.0 Hz, J_3 = 8.0 Hz), 6.90 (s, 1H), 3.75 (s, 3H), 3.02 (t, 2H, J = 6.5 Hz), 2.91 (t, 2H, J = 6.5 Hz).

2-(1-propyl-1*H*-indol-3-yl)ethan-1-amine **(67f)**:

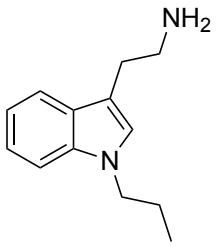

According to GP4, tryptamine (400 mg, 2.5 mmol, 1.0 equiv.) in DMF (14 mL) after addition NaH (120 mg, 3 mmol, 1.2 equiv.) and 1-iodopropane (268 µL, 2.7 mmol, 1.1 equiv.) provided, after DCM/MeOH/ammonia (94:5:1) column chromatography, the desired compound **67f** (210 mg, yield 42 %) as a light yellow oil.

Compound is known, but physicochemical data have not been reported in the literature.

^{1}H NMR (400 MHz, $CDCl_3$, 25 °C): δ = 7.60 (ddd, 1H, $J_1 \approx J_2$ = 1.0 Hz, J_3 = 8.0 Hz), 7.32 (ddd, 1H, $J_1 \approx J_2$ = 1.0 Hz, J_3 = 8.5 Hz), 7.20 (ddd, 1H, J_1 = 1.0 Hz, J_2 = 7.0 Hz, J_3 = 8.5 Hz), 7.09 (ddd, 1H, J_1 = 1.0 Hz, J_2 = 7.0 Hz, J_3 = 8.0 Hz), 6.95 (s, 1H), 4.04 (t, 2H, J = 7.5 Hz), 3.03 (t, 2H, J = 6.5 Hz), 2.93 (t, 2H, J = 6.5 Hz), 2.00 (br s, 2H), 1.85 (h, 2H, J = 7.5 Hz), 0.93 (t, 3H, J = 7.5 Hz).

2-(1-benzyl-1*H*-indol-3-yl)ethan-1-amine **(67g)**:

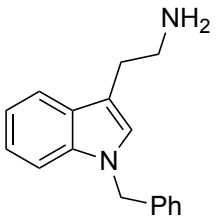

This molecule was synthesised with a modification of GP4. According to the reported method,[130] to a solution of NaH (180 mg, 4.49 mmol, 1.2 equiv.) in DMF (9 mL, c = 0.4 M) was added a solution of tryptamine (600 mg, 3.74 mmol, 1.0 equiv.) in DMF (9 mL, c = 0.4 M) at 0 °C under N_2 atmosphere. The mixture was stirred at room temperature for 30 min. To this mixture, benzyl bromide was added (405 µL, 4.11 mmol, 1.1 eq) at 0 °C, and the mixture was stirred at room temperature for 2 h. The reaction was quenched by addition of water, then the residue was extracted with ethyl acetate (3 x 30 mL). The combined organic extracts were dried over anhydrous Na_2SO_4, filtered, and concentrated in vacuo. The crude was purified by flash chromatography DCM/MeOH/ammonia (94:5:1) to provide the desired compound **67g** (609 mg, yield 65 %) as a white solid.

The physicochemical data are consistent with those reported in the literature.[130]

^{1}H NMR (400 MHz, $CDCl_3$, 25 °C): δ = 7.63 (ddd, 1H, $J_1 \approx J_2$ = 1.0 Hz, J_3 = 8.0 Hz), 7.32 – 7.26 (m, 4H), 7.18 (ddd, 1H, J_1 = 1.0 Hz, J_2 = 7.0 Hz, J_3 = 8.5 Hz), 7.14 – 7.08 (m, 3H), 6.97 (s, 1H), 5.28 (s, 2H), 3.04 (t, 2H, J = 6.5 Hz), 2.93 (t, 2H, J = 6.5 Hz).

2-(1-phenyl-1*H*-indol-3-yl)ethan-1-amine **(67h)**:

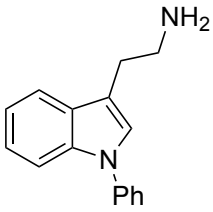

This molecule was synthesised with a modification of GP4. According to the reported method,[114] under an N_2 atmosphere, $Cu(OAc)_2{\cdot}H_2O$ (4 mg, 1 mol %) in DMF (4 mL, c = 0.5 M) was added to a solid mixture of tryptamine (320 mg, 2 mmol, 1.0 equiv.) and Cs_2CO_3 (1.303 g, 4 mmol, 2.0 equiv.). Then ArI (267 µL, 2.4 mmol, 1.2 equiv.) was also added to the resulting mixture, which was stirred at 110 °C for 24 h. When the reaction finished (TLC check), water was added, and the residue was extracted with EtOAc (3 x 20 mL). The combined organic phases were dried over anhydrous Na_2SO_4, filtered, and concentrated in vacuo. The crude mixture was purified by flash chromatography DCM/MeOH/ammonia (94:5:1) to provide the desired compound **67h** (330 mg, yield 70 %) as a light yellow oil.

The physicochemical data are consistent with those reported in the literature.[131]

^{1}H NMR (400 MHz, $CDCl_3$, 25 °C): δ = 7.67 (ddd, 2H, $J_1 \approx J_2$ = 1.0 Hz, J_3 = 8.0 Hz), 7.58 (ddd, 1H, $J_1 \approx J_2$ = 1.0 Hz, J_3 = 8.0 Hz), 7.53 – 7.48 (m, 4H), 7.37-7.31 (m, 1H), 7.25 – 7.20 (m, 2H), 7.18 (ddd, 1H, J_1 = 1.0 Hz, J_2 = 7.0 Hz, J_3 = 8.0 Hz), 3.09 (t, 2H, J_1 = 6.5 Hz), 2.97 (t, 2H, J_1 = 6.5 Hz).

2-(5-methoxy-1-methyl-1*H*-indol-3-yl)ethan-1-amine (**67i**):

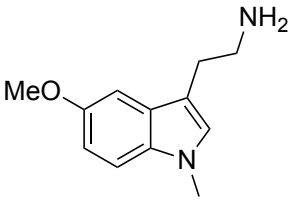

According to GP4, 5-Methoxytryptamine (300 mg, 1.6 mmol, 1.0 equiv) in DMF (9.1 mL) after addition NaH (76 mg, 1.9 mmol, 1.2 equiv) and 1-iodomethane (0.108 mL, 1.73 mmol, 1.1 equiv) provided, after DCM/MeOH/ammonia (94:5:1) column chromatography, the desired compound **67i** (210 mg, yield 42 %) as a light yellow oil.

The physicochemical data are consistent with those reported in the literature.[132]

^{1}H NMR (400 MHz, $CDCl_3$, 25 °C): δ = 7.18 (d, 1H, *J* = 9.0 Hz), 7.03 (d, 1H, *J* = 2.5 Hz), 6.88 (dd, 1H, J_1 = 2.5 Hz, J_2 = 9.0 Hz) 6.88 (br s, 1H), 3.86 (s, 3H), 3.71 (s, 3H), 3.02 (t, 2H, *J* = 6.5 Hz), 2.89 (t, 2H, *J* = 6.5 Hz).

*3.4.5. Synthesis of indole-containing imidazoles (part 1) (**66**)*

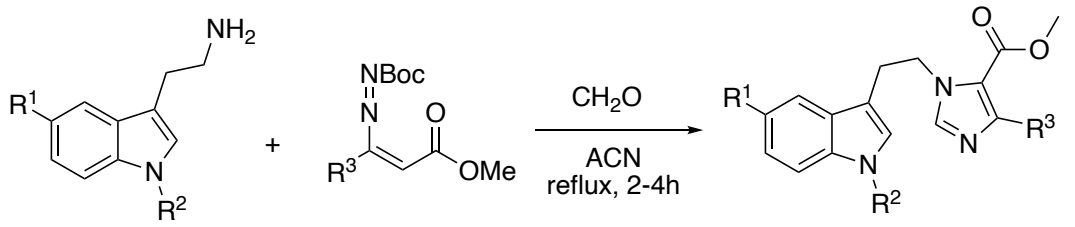

67a: R^1 = F, R^2 = Me
67b: R^1 = Cl, R^2 = Me
67c: R^1 = Me, R^2 = Me
67d: R^1 = Ph, R^2 = Me
67e: R^1 = H, R^2 = Me
67f: R^1 = H, R^2 = *n*-Pr
67g: R^1 = H, R^2 = Bn
67h: R^1 = H, R^2 = Ph
67i: R^1 = OMe, R^2 = Me

68a: R^3 = *n*-Pr
68b: R^3 = *n*-Bu

66a: R^1 = F, R^2 = Me, R^3 = *n*-Pr
66b: R^1 = Cl, R^2 = Me, R^3 = *n*-Pr
66c: R^1 = Me, R^2 = Me, R^3 = *n*-Pr
66d: R^1 = Ph, R^2 = Me, R^3 = *n*-Pr
66e: R^1 = H, R^2 = Me, R^3 = *n*-Pr
66f: R^1 = H, R^2 = *n*-Pr, R^3 = *n*-Pr
66g: R^1 = H, R^2 = Bn, R^3 = *n*-Pr
66h: R^1 = H, R^2 = Ph, R^3 = *n*-Pr
66i: R^1 = OMe, R^2 = Me, R^3 = *n*-Pr
66j: R^1 = H, R^2 = Me, R^3 = *n*-Bu

General procedure for the synthesis of indole-containing imidazoles from diazadialkenes (66a-j) GP5

According to the reported synthesis in the literature,[133] to a stirred solution of the tryptamine derivative **67** (1 equiv.) in acetonitrile (c = 0.2 M) DD derivative **68** (1 equiv.) was added at room temperature. After the disappearance of the reagents, paraformaldehyde (2 equiv.) was added, and then the resulting mixture was refluxed for 2–4 h (TLC check). The solvent was evaporated under reduced pressure and the crude residue was purified by column chromatography.

Methyl 1-(2-(5-fluoro-1-methyl-1*H*-indol-3-yl)ethyl)-4-propyl-1*H*-imidazole-5-carboxylate **(66a)**:

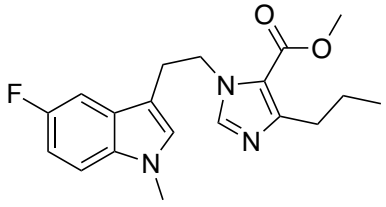

According to GP5, tryptamine derivative **67a** (200 mg, 1.04 mmol, 1 equiv.) DD derivative **68a** (266.7 mg, 1.04 mmol, 1 equiv.) and paraformaldehyde (63 mg, 2.08 mmol, 2 equiv.) in acetonitrile (5.2 mL, c = 0.2 M)

provided, after dichloromethane/methanol (95:5) column chromatography, the desired compound **66a** (159 mg, yield 45 %) as a dark orange oil.

R_f = 0.15 (1:1 cyclohexane/ethyl acetate)

^{1}H NMR (400 MHz, $CDCl_3$, 25 °C): δ = 7.24 – 7.12 (m, 3H), 6.96 (ddd, 1H, J_1 = 2.5 Hz, $J_2 \approx J_3$ = 9.0 Hz), 6.68 (s, 1H), 4.46 (t, 2H, *J* = 7.0 Hz), 3.88 (s, 3H), 3.69 (s, 3H), 3.11 (t, 2H, *J* = 7.0 Hz), 2.85 (t, 2H, *J* = 7.5 Hz), 1.70 (h, 2H, *J* = 7.5 Hz), 0.96 (t, 3H, *J* = 7.5 Hz).

^{13}C NMR (101 MHz, $CDCl_3$, 25 °C): δ = 161.6, 157.9 (d, *J* = 235.5 Hz), 152.6, 140.7, 133.8, 129.0, 127.8 (d, *J* = 9.5 Hz), 117.9, 110.3 (d, *J* = 17.0 Hz), 110.2-110.1 (m, 2C), 103.5 (d, *J* = 23.5 Hz), 51.5, 48.4, 33.0, 31.4, 27.3, 22.8, 14.1.

Methyl 1-(2-(5-chloro-1-methyl-1*H*-indol-3-yl)ethyl)-4-propyl-1*H*-imidazole-5-carboxylate **(66b)**:

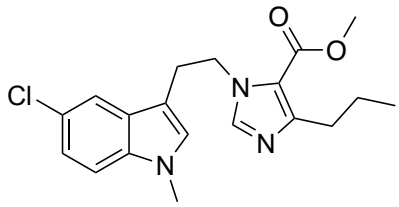

According to GP5, tryptamine derivative **67b** (46 mg, 0.18 mmol, 1 equiv.) DD derivative **68a** (38 mg, 0.18 mmol, 1 equiv.) and paraformaldehyde (11 mg, 0.36 mmol, 2 equiv.) in acetonitrile (0.9 mL, c = 0.2 M) provided, after cyclohexane/ethyl acetate (7:3) column chromatography, the desired compound **66b** (29 mg, yield 45 %) as a brown oil.

R_f = 0.2 (1:1 cyclohexane/ethyl acetate)

^{1}H NMR (400 MHz, $CDCl_3$, 25 °C): δ = 7.51 (s, 1H), 7.22 – 7.13 (m, 3H), 6.65 (s, 1H), 4.46 (t, 2H, *J* = 7.0 Hz), 3.88 (s, 3H), 3.69 (s, 3H), 3.12 (t, 2H, *J* = 7.0 Hz), 2.85 (t, 2H, *J* = 7.5 Hz), 1.70 (h, 2H, *J* = 7.5 Hz), 0.96 (t, 3H, *J* = 7.5 Hz).

^{13}C NMR (101 MHz, $CDCl_3$) δ 161.7, 152.9, 140.9, 137.2, 127.6, 127.3, 121.9, 119.2, 118.6, 117.9, 110.3, 109.5, 51.3, 48.4, 32.7, 31.5, 27.4, 22.9, 14.1.

Methyl 1-(2-(1,5-dimethyl-1*H*-indol-3-yl)ethyl)-4-propyl-1*H*-imidazole-5-carboxylate **(66c)**:

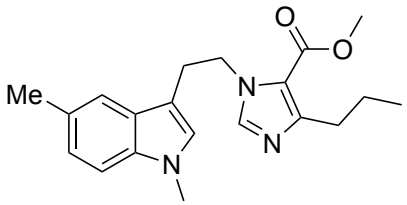

According to GP5, tryptamine derivative **67c** (150 mg, 0.8 mmol, 1 equiv.) DD derivative **68a** (204 mg, 0.8 mmol, 1 equiv.) and paraformaldehyde (48 mg, 1.6 mmol, 2 equiv.) in acetonitrile (4 mL, c = 0.2 M) provided, after cyclohexane/ethyl acetate (7:3) column chromatography, the desired compound **66c** (152 mg, yield 56 %) as a light yellow oil.

R_f = 0.22 (1:1 cyclohexane/ethyl acetate)

^{1}H NMR (400 MHz, $CDCl_3$, 25 °C): δ = 7.33 (br s, 1H), 7.18 (d, 1H, *J* = 8.5 Hz), 7.15 (s, 1H), 7.06 (d, 1H, *J* = 8.5 Hz), 6.58 (s, 1H), 4.47 (t, 2H, *J* = 7.0 Hz), 3.88 (s, 3H), 3.67 (s, 3H), 3.13 (t, 2H, *J* = 7.0 Hz), 2.85 (t, 2H, *J* = 7.5 Hz), 2.47 (s, 3H), 1.70 (h, 2H, *J* = 7.5 Hz), 0.97 (t, 3H, *J* = 7.5 Hz).

^{13}C NMR (101 MHz, $CDCl_3$, 25 °C): δ = 161.7, 153.1, 141.0, 135.7, 128.4, 127.8, 127.4, 123.5, 118.3, 117.8, 109.7, 109.2, 51.3, 48.4, 32.8, 31.6, 27.4, 22.9, 21.6, 14.1.

Methyl 1-(2-(1-methyl-5-phenyl-1*H*-indol-3-yl)ethyl)-4-propyl-1*H*-imidazole-5-carboxylate (**66d**):

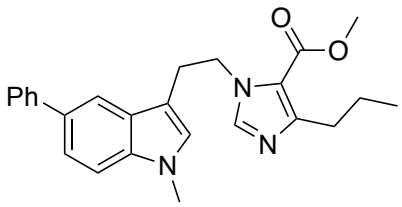

According to GP5, tryptamine derivative **67d** (105 mg, 0.42 mmol, 1 equiv.) DD derivative **68a** (108 mg, 0.42 mmol, 1 equiv.) and paraformaldehyde (25 mg, 0.84 mmol, 2 equiv.) in acetonitrile (2.1 mL, c = 0.2 M) provided, after dichloromethane/ ethyl acetate (9:1) column chromatography, the desired compound **66d** (88 mg, yield 52 %) as a white solid.

R_f = 0.18 (7:3 cyclohexane/ethyl acetate)

^{1}H NMR (400 MHz, $CDCl_3$, 25 °C): δ = 7.79 (dd, 1H, J_1 = 0.5 Hz, J_2 = 2.0 Hz), 7.71 – 7.66 (m, 2H), 7.50 (dd, 1H, J_1 = 2.0 Hz, J_2 = 8.5 Hz), 7.45 (ddd, 2H, J_1 = 1.0 Hz, J_2 = 7.0 Hz, J_3 = 8.0 Hz), 7.37 – 7.34 (m, 1H), 7.32 (ddd, 1H, J_1 = 1.0 Hz, J_2 = 7.0 Hz, J_3 = 8.0 Hz), 7.20 (s, 1H), 6.67 (s, 1H), 4.52 (t, 2H, *J* = 7.0 Hz), 3.87 (s, 3H), 3.73 (s, 3H),

3.21 (t, 2H, *J* = 7.0 Hz), 2.88 – 2.81 (m, 2H), 1.68 (h, 2H, *J* = 7.5 Hz), 0.95 (t, 3H, *J* = 7.5 Hz).

^{13}C NMR (101 MHz, $CDCl_3$) δ 161.7, 152.8, 142.6, 140.9, 136.7, 132.8, 128.8, 128.1, 128.0, 127.5, 126.5, 121.8, 117.9, 117.3, 110.7, 109.8, 51.4, 48.4, 32.9, 31.5, 27.4, 22.8, 14.1.

Methyl 1-(2-(1-methyl-1*H*-indol-3-yl)ethyl)-4-propyl-1*H*-imidazole-5-carboxylate **(66e)**:

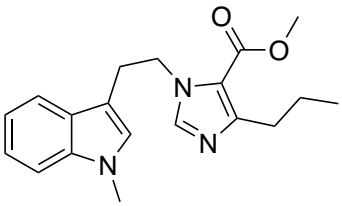

According to GP5, tryptamine derivative **67e** (74 mg, 0.29 mmol, 1 equiv.) DD derivative **68a** (50 mg, 0.29 mmol, 1 equiv.) and paraformaldehyde (17 mg, 0.57 mmol, 2 equiv.) in acetonitrile (1.45 mL, c = 0.2 M) provided, after cyclohexane/ethyl acetate (7:3) column chromatography, the desired compound **66e** (72 mg, yield 77 %) as a violet oil.

R_f = 0.17 (1:1 cyclohexane/ethyl acetate)

The physicochemical data are consistent with those reported in the literature.[133]

^{1}H NMR (400 MHz, $CDCl_3$, 25 °C): δ = 7.58 (ddd, 1H, $J_1 \approx J_2$ = 1.0 Hz, J_3 = 8.0 Hz), 7.29 (ddd, 1H, $J_1 \approx J_2$ = 1.0 Hz, J_3 = 8.0 Hz), 7.23 (ddd, 1H, J_1 = 1.0 Hz, J_2 = 7.0 Hz, J_3 = 8.0 Hz), 7.15 (s, 1H), 7.13 (ddd, 1H, J_1 = 1.0 Hz, J_2 = 7.0 Hz, J_3 = 8.0 Hz), 6.64 (s, 1H), 4.48 (t, 2H, *J* = 7.0 Hz), 3.88 (s, 3H), 3.70 (s, 3H), 3.17 (t, 2H, *J* = 7.0 Hz), 2.85 (t, 2H, *J* = 7.5 Hz), 1.71 (h, 2H, *J* = 7.5 Hz), 0.97 (t, 3H, *J* = 7.5 Hz).

Methyl 4-propyl-1-(2-(1-propyl-1*H*-indol-3-yl)ethyl)-1*H*-imidazole-5-carboxylate **(66f)**:

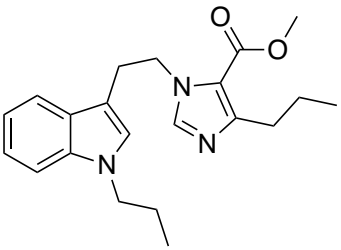

According to GP5, tryptamine derivative **67f** (188 mg, 0.93 mmol, 1 equiv.) DD derivative **68a** (239 mg, 0.93 mmol, 1 equiv.) and paraformaldehyde (56 mg, 1.86 mmol, 2 equiv.) in acetonitrile (4.7 mL, c = 0.2 M) provided, after cyclohexane/ethyl acetate (7:3) column chromatography, the desired compound **66f** (97 mg, yield 30 %) as a violet oil.

R_f = 0.34 (1:1 cyclohexane/ethyl acetate)

^{1}H NMR (400 MHz, $CDCl_3$, 25 °C): δ = 7.56 (ddd, 2H, $J_1 \approx J_2$ = 1.0 Hz, J_3 = 8.0 Hz), 7.34 – 7.29 (m, 2H), 7.21 (ddd, 1H, J_1 = 1.0 Hz, J_2 = 7.0 Hz, J_3 = 8.0 Hz), 7.11 (ddd, 1H, J_1 = 1.0 Hz, J_2 = 7.0 Hz, J_3 = 8.0 Hz), 6.67 (s, 1H), 4.53 (t, 2H, J = 7.0 Hz), 3.99 (t, 2H, J = 7.5 Hz), 3.88 (s, 3H), 3.18 (t, 2H, J = 7.0 Hz), 2.88 (t, 2H, J = 7.5 Hz), 1.80 (h, 2H, J = 7.5 Hz), 1.70 (h, 2H, J = 7.5 Hz), 0.96 (t, 3H, J = 7.5 Hz), 0.89 (t, 3H, J = 7.5 Hz).

^{13}C NMR (101 MHz, $CDCl_3$, 25 °C): δ = 161.6, 152.8, 140.8, 136.6, 127.6, 126.4, 121.7, 119.1, 118.7, 117.9, 110.0, 109.8, 51.4, 48.5, 48.0, 31.4, 27.4, 23.7, 22.9, 14.1, 11.7.

Methyl 1-(2-(1-benzyl-1*H*-indol-3-yl)ethyl)-4-propyl-1*H*-imidazole-5-carboxylate (**66g**):

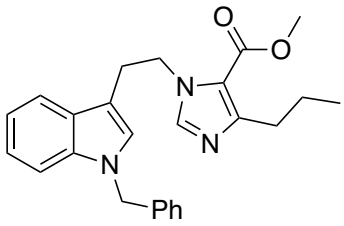

According to GP5, tryptamine derivative **67g** (200 mg, 0.8 mmol, 1 equiv.) DD derivative **68a** (205 mg, 0.8 mmol, 1 equiv.) and paraformaldehyde (48 mg, 1.6 mmol, 2 equiv.) in acetonitrile (4 mL, c = 0.2 M) provided, after cyclohexane/ethyl acetate (7:3) column chromatography, the desired compound **66g** (130 mg, yield 41 %) as a violet oil.

R_f = 0.37 (1:1 cyclohexane/ethyl acetate)

^{1}H NMR (400 MHz, $CDCl_3$, 25 °C): δ = 7.59 (ddd, 2H, $J_1 \approx J_2$ = 1.0 Hz, J_3 = 8.0 Hz), 7.33 – 7.22 (m, 5H), 7.18 (ddd, 1H, J_1 = 1.0 Hz, J_2 = 7.0 Hz, J_3 = 8.0 Hz), 7.13 (ddd, 1H, J_1 = 1.0 Hz, J_2 = 7.0 Hz, J_3 = 8.0 Hz), 7.09 – 7.05 (m, 2H), 6.73 (s, 1H), 5.23 (s, 2H), 4.54 (t, 2H, J = 7.0 Hz), 3.87 (s, 3H), 3.20 (t, 2H, J = 7.0 Hz), 2.86 (t, 2H, J = 7.5 Hz), 1.70 (h, 2H, J = 7.5 Hz), 0.95 (t, 3H, J = 7.5 Hz).

^{13}C NMR (101 MHz, $CDCl_3$, 25 °C): δ = 161.4, 151.7, 140.3, 137.5, 136.9, 128.9, 127.79, 127.76, 126.9, 126.7, 122.2, 119.6, 118.7, 118.0, 110.7, 110.1, 51.5, 50.1, 48.6, 31.0, 27.4, 22.8, 14.1.

Methyl 1-(2-(1-phenyl-1*H*-indol-3-yl)ethyl)-4-propyl-1*H*-imidazole-5-carboxylate (**66h**)

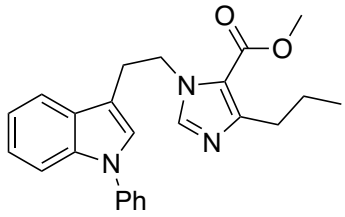

According to GP5, tryptamine derivative **67h** (225 mg, 0.95 mmol, 1 equiv.) DD derivative **68a** (244 mg, 0.95 mmol, 1 equiv.) and paraformaldehyde (57 mg, 1.9 mmol, 2 equiv.) in acetonitrile (4.8 mL, c = 0.2 M) provided, after cyclohexane/ethyl acetate (8:2) column chromatography, the desired compound **66h** (118 mg, yield 32 %) as a yellow oil.

R_f = 0.37 (1:1 cyclohexane/ethyl acetate)

^{1}H NMR (400 MHz, $CDCl_3$, 25 °C): δ = 7.64 (ddd, 1H, $J_1 \approx J_2$ = 1.0 Hz, J_3 = 8.0 Hz), 7.55 (ddd, 1H, $J_1 \approx J_2$ = 1.0 Hz, J_3 = 8.0 Hz), 7.52 – 7.46 (m, 2H), 7.45 – 7.41 (m, 2H), 7.33 (dddd, 1H, $J_1 \approx J_2$ = 1.0 Hz, $J_3 \approx J_4$= 8.0 Hz), 7.30 (s, 1H), 7.24 (ddd, 1H, J_1 = 1.0 Hz, J_2 = 7.0 Hz, J_3 = 8.0 Hz), 7.20 (ddd, 1H, J_1 = 1.0 Hz, J_2 = 7.0 Hz, J_3 = 8.0 Hz), 6.92 (s, 1H), 4.57 (t, 2H, J = 7.0 Hz), 3.87 (s, 3H), 3.25 (t, 2H, J = 7.0 Hz), 2.87 (t, 2H, J = 7.5 Hz), 1.70 (h, 2H, J = 7.5 Hz), 0.95 (t, 3H, J = 7.5 Hz).

^{13}C NMR (101 MHz, $CDCl_3$, 25 °C): δ = 161.6, 152.6, 140.7, 139.6, 136.3, 129.7, 128.5, 126.5, 126.4, 124.4, 122.8, 120.4, 118.9, 118.0, 112.7, 110.9, 51.5, 48.3, 31.3, 27.3, 22.9, 14.1.

Methyl 1-(2-(5-methoxy-1-methyl-1*H*-indol-3-yl)ethyl)-4-propyl-1*H*-imidazole-5-carboxylate (**66i**)

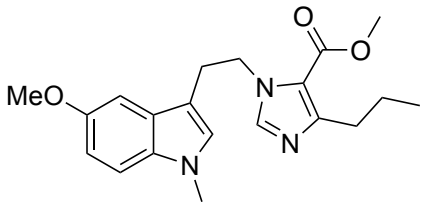

According to GP5, tryptamine derivative **67i** (200 mg, 0.98 mmol, 1 equiv.) DD derivative **68a** (251 mg, 0.98 mmol, 1 equiv.) and paraformaldehyde (58.8 mg, 1.6 mmol, 2 equiv.) in acetonitrile (4.9 mL, c = 0.2 M) provided, after cyclohexane/ethyl acetate (7:3) column chromatography, the desired compound **66i** (87 mg, yield 25 %) as a dark yellow oil.

R_f = 0.15 (1:1 cyclohexane/ethyl acetate)

^{1}H NMR (400 MHz, $CDCl_3$, 25 °C): δ = 7.25 (s, 1H), 7.17 (d, 1H, J = 9.0 Hz), 7.07 (d, 1H, J = 2.5 Hz), 6.89 (dd, 1H, J_1 = 2.5 Hz, J_2 = 9.0 Hz), 6.62 (s, 1H), 4.48 (t, 2H, J =

7.0 Hz), 3.88 (s, 3H), 3.87 (s, 3H), 3.67 (s, 3H), 3.13 (t, 2H, *J* = 7.0 Hz), 2.85 (t, 2H, *J* = 7.5 Hz), 1.70 (h, 2H, *J* = 7.5 Hz), 0.96 (t, 3H, *J* = 7.5 Hz).

^{13}C NMR (101 MHz, $CDCl_3$, 25 °C): δ = 161.6, 154.1, 152.5, 140.7, 132.6, 127.9 (2C), 117.9, 112.0, 110.3, 109.7, 100.7, 56.1, 51.4, 48.3, 32.9, 31.4, 27.5, 22.8, 14.1.

Methyl 4-butyl-1-(2-(1-methyl-1*H*-indol-3-yl)ethyl)-1*H*-imidazole-5-carboxylate **(66j)**:

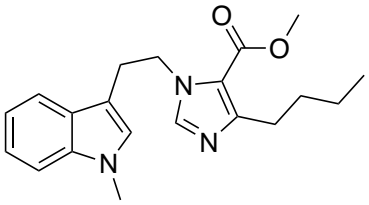

According to GP5, tryptamine derivative **66e** (95 mg, 0.55 mmol, 1 equiv.) DD derivative **68b** (155 mg, 0.55 mmol, 1 equiv.) and paraformaldehyde (33 mg, 1.1 mmol, 2 equiv.) in acetonitrile (2.7 mL, c = 0.2 M) provided, after cyclohexane/ethyl acetate (8:2) column chromatography, the desired compound **66j** (82 mg, yield 42 %) as a yellow oil.

R_f = 0.2 (1:1 cyclohexane/ethyl acetate)

^{1}H NMR (400 MHz, $CDCl_3$, 25 °C): δ = 7.56 (ddd, 2H, $J_1 \approx J_2$ = 1.0 Hz, J_3 = 8.0 Hz), 7.30 (ddd, 2H, $J_1 \approx J_2$ = 1.0 Hz, J_3 = 8.0 Hz), 7.27 (s, 1H), 7.23 (ddd, 1H, J_1 = 1.0 Hz, J_2 = 7.0 Hz, J_3 = 8.0 Hz), 7.12 (ddd, 1H, J_1 = 1.0 Hz, J_2 = 7.0 Hz, J_3 = 8.0 Hz), 6.65 (s, 1H), 4.51 (t, 2H, *J* = 7.0 Hz), 3.88 (s, 3H), 3.71 (s, 3H), 3.18 (t, 2H, *J* = 7.0 Hz), 2.89 (t, 2H, *J* = 7.5 Hz), 1.72 – 1.61 (m, 2H), 1.38 (h, 2H, J_1 = 7.5 Hz), 0.95 (t, 3H, *J* = 7.5 Hz).

^{13}C NMR (101 MHz, $CDCl_3$, 25 °C): δ = 161.5, 152.4, 140.4, 137.2, 127.5, 127.4, 121.9, 119.3, 118.6, 117.9, 110.1, 109.6, 51.5, 48.6, 32.8, 31.8, 28.9, 27.3, 22.6, 14.1.

*3.4.6. Synthesis of final indole-imidazole compounds (**65**)*

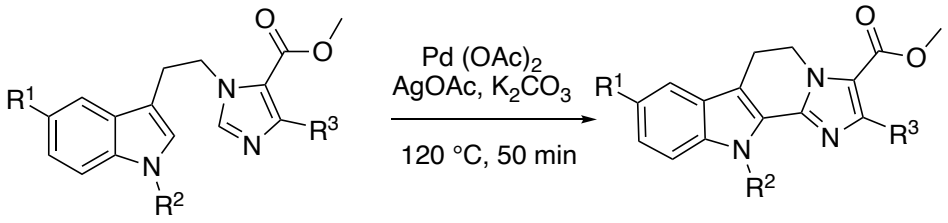

66a: R^1 = F, R^2 = Me, R^3 = *n*-Pr
66b: R^1 = Cl, R^2 = Me, R^3 = *n*-Pr
66c: R^1 = Me, R^2 = Me, R^3 = *n*-Pr
66d: R^1 = Ph, R^2 = Me, R^3 = *n*-Pr
66e: R^1 = H, R^2 = Me, R^3 = *n*-Pr
66f: R^1 = H, R^2 = *n*-Pr, R^3 = *n*-Pr
66g: R^1 = H, R^2 = Bn, R^3 = *n*-Pr
66h: R^1 = H, R^2 = Ph, R^3 = *n*-Pr
66i: R^1 = OMe, R^2 = Me, R^3 = *n*-Pr
66j: R^1 = H, R^2 = Me, R^3 = *n*-Bu

65a: R^1 = F, R^2 = Me, R^3 = *n*-Pr
65b: R^1 = Cl, R^2 = Me, R^3 = *n*-Pr
65c: R^1 = Me, R^2 = Me, R^3 = *n*-Pr
65d: R^1 = Ph, R^2 = Me, R^3 = *n*-Pr
65e: R^1 = H, R^2 = Me, R^3 = *n*-Pr
65f: R^1 = H, R^2 = *n*-Pr, R^3 = *n*-Pr
65g: R^1 = H, R^2 = Bn, R^3 = *n*-Pr
65h: R^1 = H, R^2 = Ph, R^3 = *n*-Pr
65i: R^1 = OMe, R^2 = Me, R^3 = *n*-Pr
65j: R^1 = H, R^2 = Me, R^3 = *n*-Bu

General procedure for the synthesis of final indole-imidazole closed compounds (65a-j): GP6

According to the reported synthesis in the literature,[133] the indole-imidazole derivative (1 equiv.), $Pd(OAc)_2$ (10 mol %), AgOAc (3 equiv.) and K_2CO_3 (1 equiv.), were weighed and transferred into a vial equipped with a magnetic stirrer bar. DMA (c = 0.1 M) was then added, and the mixture was stirred at 130 °C for 50 min. The remaining solvent was evaporated, and the crude mixture was then purified by column chromatography on silica gel.

Methyl 8-fluoro-11-methyl-2-propyl-6,11-dihydro-5*H*-imidazo[1',2':1,2]pyrido[3,4-b]indole-3-carboxylate (**65a**):

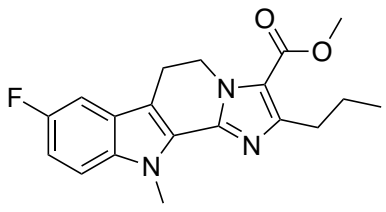

According to GP6, the indole-imidazole derivative **66a** (122 mg, 0.36 mmol, 1 equiv.), $Pd(OAc)_2$ (8 mg, 0.036 mmol, 10 mol %), AgOAc (179 mg, 1.07 mmol, 3 equiv.) and K_2CO_3 (49 mg, 0.36 mmol, 1 equiv.) in DMA (3.6 mL, c = 0.1 M) provided, after cyclohexane/ethyl acetate (9:1) column chromatography, the desired compound **65a** (66 mg, yield 54 %) as a white powder.

R_f = 0.3 (9:1 cyclohexane/ethyl acetate)

^{1}H NMR (400 MHz, $CDCl_3$, 25 °C): δ = 7.26 (dd, 1H, J_1 = 4.5 Hz, J_2 = 9.0 Hz), 7.18 (dd, 1H, J_1 = 2.5 Hz, J_2 = 9.0 H), 7.01 (ddd, 1H, J_1 = 2.5 Hz, $J_2 \approx J_3$ = 9.0 Hz), 4.65 (t, 2H, J = 7.0 Hz), 4.21 (s, 3H), 3.90 (s, 3H), 3.15 (t, 2H, J = 7.0 Hz), 2.92 (t, 2H, J = 7.5 Hz), 1.76 (h, 2H, J = 7.5 Hz), 1.02 (t, 3H, J = 7.5 Hz).

^{13}C NMR (101 MHz, $CDCl_3$, 25 °C): δ = 161.9, 158.3 (d, J = 236.5 Hz), 152.7, 142.6, 135.5, 127.6, 125.5 (d, J = 10.0 Hz), 118.1, 111.7 (d, J = 26.5 Hz), 110.8-110.5 (m, 2C), 103.9 (d, J = 23.5 Hz), 51.4, 44.2, 31.9, 31.5, 23.0, 20.8, 14.2.

HRMS (ESI-Orbitrap, *m*/*z*): calcd for $C_{19}H_{20}FN_3O_2$ $[M + H]^+$ 342.1612; found 342.1608

Methyl 8-chloro-11-methyl-2-propyl-6,11-dihydro-5*H*-imidazo[1',2':1,2]pyrido[3,4-*b*]indole-3-carboxylate (**65b**):

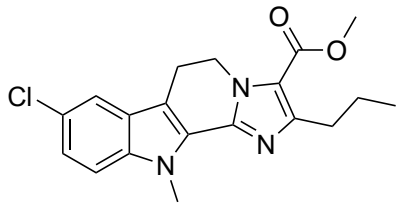

According to GP6, the indole-imidazole derivative **66b** (118 mg, 0.33 mmol, 1 equiv.), $Pd(OAc)_2$ (7 mg, 0.033 mmol, 10 mol %), AgOAc (164 mg, 0.98 mmol, 3 equiv.) and K_2CO_3 (45 mg, 0.33 mmol, 1 equiv.) in DMA (3.3 mL, c = 0.1 M) provided, after cyclohexane/ethyl acetate (9:1) column chromatography, the desired compound **65b** (64 mg, yield 54 %) as a white powder.

R_f = 0.3 (9:1 cyclohexane/ethyl acetate)

^{1}H NMR (400 MHz, $CDCl_3$, 25 °C): δ = 7.52 (d, 1H, J = 2.0 Hz), 7.27 (d, 1H, J = 9.0 Hz), 7.21 (dd, 1H, J_1 = 2.0 Hz, J_2 = 9.0 Hz), 4.65 (t, 2H, J = 7.5 Hz), 4.21 (s, 3H), 3.90 (s, 3H), 3.16 (t, 2H, J = 7.5 Hz), 2.91 (t, 2H, J = 7.5 Hz), 1.76 (h, 2H, J = 7.5 Hz), 1.01 (t, 3H, J = 7.5 Hz).

^{13}C NMR (101 MHz, $CDCl_3$, 25 °C): δ = 162.0, 152.9, 142.7, 137.2, 127.5, 126.4, 125.9, 123.4, 118.6, 118.2, 111.0, 110.2, 51.4, 44.2, 31.8, 31.6, 23.0, 20.8, 14.2.

HRMS (ESI-Orbitrap, *m*/*z*): calcd for $C_{19}H_{20}ClN_3O_2$ $[M + H]^+$ 358.1317; found 358.1312

Methyl 8,11-dimethyl-2-propyl-6,11-dihydro-5*H*-imidazo[1',2':1,2]pyrido[3,4-*b*]indole-3-carboxylate (**65c**):

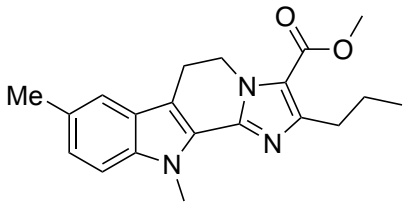

According to GP6, the indole-imidazole derivative **66c** (100 mg, 0.29 mmol, 1 equiv.), $Pd(OAc)_2$ (7 mg, 0.029 mmol, 10 mol %), AgOAc (148 mg, 0.88 mmol, 3 equiv.) and K_2CO_3 (41 mg, 0.29 mmol, 1 equiv.) in DMA (2.9 mL, c = 0.1 M) provided, after cyclohexane/ethyl acetate (9:1) column chromatography, the desired compound **65c** (32 mg, yield 33 %) as a white powder.

R_f = 0.2 (9:1 cyclohexane/ethyl acetate)

^{1}H NMR (400 MHz, $CDCl_3$, 25 °C): δ = 7.34 (d, 1H, *J* = 1.5 Hz), 7.25 (d, 1H, *J* = 8.5 Hz), 7.11 (dd, 1H, J_1 = 1.5 Hz, J_2 = 8.5 Hz), 4.63 (t, 2H, *J* = 7.5 Hz), 4.19 (s, 3H), 3.90 (s, 3H), 3.17 (t, 2H, *J* = 7.5 Hz), 2.91 (t, 2H, *J* = 7.5 Hz), 2.47 (s, 3H), 1.76 (h, 2H, *J* = 7.5 Hz), 1.02 (t, 3H, *J* = 7.5 Hz).

^{13}C NMR (101 MHz, $CDCl_3$, 25 °C): δ = 162.1, 152.9, 143.3, 137.4, 129.4, 126.4, 125.6, 125.0, 118.8, 117.9, 110.5, 109.7, 51.3, 44.3, 31.70, 31.68, 23.0, 21.6, 20.9, 14.3.

Methyl 11-methyl-8-phenyl-2-propyl-6,11-dihydro-5H-imidazo[1',2':1,2]pyrido[3,4-*b*]indole-3-carboxylate (**65d**):

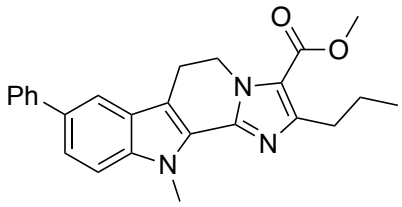

According to GP6, the indole-imidazole derivative **66d** (74 mg, 0.18 mmol, 1 equiv), $Pd(OAc)_2$ (4 mg, 0.018 mmol, 10 mol %), AgOAc (92 mg, 0.55 mmol, 3 equiv) and K_2CO_3 (26 mg, 0.18 mmol, 1 equiv) in DMA (1.8 mL, c = 0.1 M) provided, after cyclohexane/ethyl acetate (9:1) column chromatography, the desired compound **65d** (37 mg, yield 50 %) as a white powder.

^{1}H NMR (400 MHz, $CDCl_3$, 25 °C): δ = 7.76 (dd, *J* = 1.8, 0.7 Hz, 1H), 7.69 – 7.64 (m, 2H), 7.54 (dd, *J* = 8.6, 1.7 Hz, 1H), 7.48 – 7.41 (m, 3H), 7.36 – 7.30 (m, 1H), 4.68 (t, *J* = 7.5 Hz, 2H), 4.25 (s, 3H), 3.91 (s, 3H), 3.24 (t, *J* = 7.5 Hz, 2H), 2.97 – 2.88 (m, 2H), 1.84 – 1.72 (m, 2H), 1.03 (t, *J* = 7.3 Hz, 3H).

^{13}C NMR (101 MHz, $CDCl_3$, 25 °C): δ = 162.0, 152.8, 143.0, 142.3, 138.5, 133.8, 128.9, 127.5, 126.9, 126.7, 125.9, 123.2, 118.1, 117.7, 111.4, 110.3, 51.4, 44.3, 31.9, 31.6, 23.0, 20.9, 14.3.

HRMS (ESI-Orbitrap, *m*/*z*): calcd for $C_{25}H_{25}N_3O_2$ $[M + H]^+$ 400.2020; found 400.2018

Methyl 11-methyl-2-propyl-6,11-dihydro-5*H*-imidazo[1',2':1,2]pyrido[3,4-*b*]indole-3-carboxylate (**65e**):

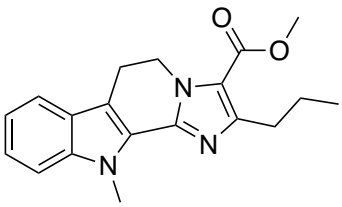

According to GP6, the indole-imidazole derivative **66e** (60 mg, 0.18 mmol, 1 equiv.), $Pd(OAc)_2$ (4 mg, 0.018 mmol, 10 mol %), AgOAc (93 mg, 0.55 mmol, 3 equiv.) and K_2CO_3 (26 mg, 0.18 mmol, 1 equiv.) in DMA (1.8 mL, c = 0.1 M) provided, after cyclohexane/ethyl acetate (9:1) column chromatography, the desired compound **65e** (36 mg, yield 67 %) as a white powder.

R_f = 0.38 (9:1 cyclohexane/ethyl acetate)

The physicochemical data are consistent with those reported in the literature [133].

^{1}H NMR (400 MHz, $CDCl_3$, 25 °C): δ = 7.57 (ddd, 1H, $J_1 \approx J_2$ = 1.0 Hz, J_3 = 8.0 Hz), 7.37 (ddd, 1H, $J_1 \approx J_2$ = 1.0 Hz, J_3 = 8.0 Hz), 7.28 (ddd, 1H, J_1 = 1.0 Hz, J_2 = 7.0 Hz, J_3 = 8.0 Hz), 7.15 (ddd, 1H, J_1 = 1.0 Hz, J_2 = 7.0 Hz, J_3 = 8.0 Hz), 4.65 (t, 2H, J = 7.5 Hz), 4.23 (s, 3H), 3.90 (s, 3H), 3.21 (t, 2H, J = 7.5 Hz), 2.91 (t, 2H, J = 7.5 Hz), 1.76 (h, 2H, J = 7.5 Hz), 1.02 (t, 3H, J = 7.5 Hz).

Methyl 2,11-dipropyl-6,11-dihydro-5*H*-imidazo[1',2':1,2]pyrido[3,4-*b*]indole-3-carboxylate (**65f**):

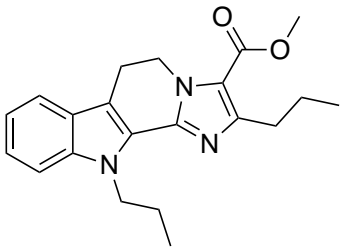

According to GP6, the indole-imidazole derivative **66f** (85 mg, 0.24 mmol, 1 equiv), $Pd(OAc)_2$ (5 mg, 0.024 mmol, 10 mol %), AgOAc (120 mg, 0.72 mmol, 3 equiv) and K_2CO_3 (33 mg, 0.24 mmol, 1 equiv) in DMA (2.4 mL, c = 0.1 M) provided, after cyclohexane/ethyl acetate (95:5) column chromatography, the desired compound **65f** (26 mg, yield 30 %) as a white powder.

R_f = 0.4 (9:1 cyclohexane/ethyl acetate)

^{1}H NMR (400 MHz, $CDCl_3$, 25 °C): δ = 7.57 (ddd, 2H, $J_1 \approx J_2$ = 1.0 Hz, J_3 = 8.0 Hz), 7.40 (ddd, 2H, $J_1 \approx J_2$ = 1.0 Hz, J_3 = 8.0 Hz), 7.28 (ddd, 1H, J_1 = 1.0 Hz, J_2 = 7.0 Hz, J_3 = 8.0 Hz), 7.14 (ddd, 1H, J_1 = 1.0 Hz, J_2 = 7.0 Hz, J_3 = 8.0 Hz), 4.74 (br t, 2H, J = 7.0 Hz), 4.68 (t, 2H, J = 7.5 Hz), 3.91 (s, 3H), 3.22 (t, 2H, J = 7.5 Hz), 2.97 (br t, 2H, J = 7.0 Hz), 1.91 – 1.82 (m, 2H), 1.82 – 1.74 (m, 2H), 1.02 (t, 3H, J = 7.5 Hz), 0.90 (t, 3H, J = 7.5 Hz).

^{13}C NMR (101 MHz, $CDCl_3$, 25 °C): δ = 161.8, 153.4, 152.1, 151.0, 138.1, 125.3, 123.1, 119.87, 119.86, 119.2, 117.8, 110.3, 51.3, 46.2, 44.1, 29.7, 23.6, 22.5, 20.8, 14.0, 11.3.

HRMS (ESI-Orbitrap, *m*/*z*): calcd for $C_{25}H_{25}N_3O_2$ $[M + H]^+$ 400.2020; found 400.2012

Methyl 11-benzyl-2-propyl-6,11-dihydro-5*H*-imidazo[1',2':1,2]pyrido[3,4-*b*]indole-3-carboxylate (**65g**):

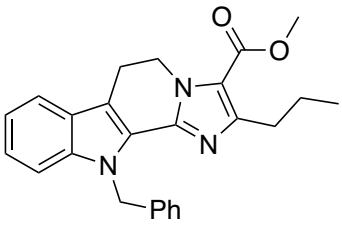

According to GP6, the indole-imidazole derivative **66g** (100 mg, 0.25 mmol, 1 equiv), $Pd(OAc)_2$ (6 mg, 0.025 mmol, 10 mol %), AgOAc (125 mg, 0.75 mmol, 3 equiv) and K_2CO_3 (138 mg, 0.25 mmol, 1 equiv) in DMA (2.5 mL, c = 0.1 M) provided, after cyclohexane/ethyl acetate (9:1) column chromatography, the desired compound **65g** (82 mg, yield 82 %) as a white powder.

Rf = 0.41 (9:1 cyclohexane/ethyl acetate)

^{1}H NMR (400 MHz, $CDCl_3$, 25 °C): δ = 7.58 (ddd, 1H, $J_1 \approx J_2$ = 1.0 Hz, J_3 = 8.0 Hz), 7.36 (d, 1H, J = 8.5 Hz), 7.24 – 7.14 (m, 6H), 7.15 (ddd, 1H, J_1 = 1.0 Hz, J_2 = 7.0 Hz, J_3 = 8.0 Hz), 6.06 (s, 2H), 4.68 (t, 2H, J = 7.5 Hz), 3.90 (s, 3H), 3.24 (t, 2H, J = 7.5 Hz), 2.91 (br t, 2H, J = 7.5 Hz), 1.73 (h, 2H, J = 7.5 Hz), 0.97 (t, 3H, J = 7.5 Hz).

HRMS (ESI-Orbitrap, *m*/*z*): calcd for $C_{21}H_{25}N_3O_2$ $[M + H]^+$ 352.2020; found 352.2010

Methyl 11-phenyl-2-propyl-6,11-dihydro-5*H*-imidazo[1',2':1,2]pyrido[3,4-*b*]indole-3-carboxylate (**65h**):

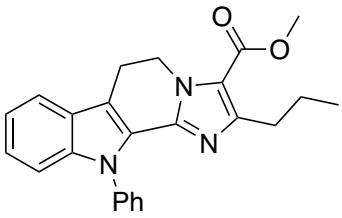

According to GP6, the indole-imidazole derivative **66h** (72 mg, 0.19 mmol, 1 equiv), $Pd(OAc)_2$ (4 mg, 0.019 mmol, 10 mol %), AgOAc (93 mg, 0.56 mmol, 3 equiv) and K_2CO_3 (26 mg, 0.19 mmol, 1 equiv) in DMA (1.9 mL, c = 0.1 M) provided, after cyclohexane/ethyl acetate (9:1) column chromatography, the desired compound **65h** (12 mg, yield 17 %) as a white powder.

Rf = 0.2 (9:1 cyclohexane/ethyl acetate)

^{1}H NMR (400 MHz, $CDCl_3$, 25 °C): δ = 7.63 (ddd, 1H, $J_1 \approx J_2$ = 1.0 Hz, J_3 = 8.0 Hz), 7.53 – 7.43 (m, 4H), 7.52 (ddd, 1H, J_1 = 1.0 Hz, J_2 = 7.0 Hz, J_3 = 8.0 Hz), 7.33 (ddd, 1H, $J_1 \approx J_2$ = 1.0 Hz, J_3 = 8.0 Hz), 7.25 – 7.18 (m, 2H), 4.73 (t, 2H, J = 7.5 Hz), 3.88 (s, 3H), 3.28 (t, 2H, J = 7.5 Hz), 2.77 (br t, 2H, J = 7.5 Hz), 1.55 (h, 2H, J = 7.5 Hz), 0.87 (t, 3H, J = 7.5 Hz).

HRMS (ESI-Orbitrap, *m*/*z*): calcd for $C_{24}H_{23}N_3O_2$ $[M + H]^+$ 386.1863; found 386.1857

Methyl 8-methoxy-11-methyl-2-propyl-6,11-dihydro-5*H*-imidazo[1',2':1,2]pyrido[3,4-b]indole-3-carboxylate (**65i**):

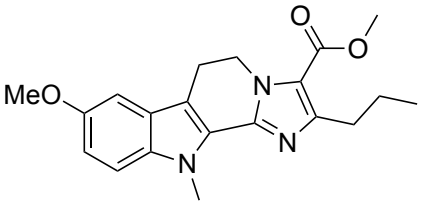

According to GP6, the indole-imidazole derivative **66i** (75 mg, 0.21 mmol, 1 equiv), $Pd(OAc)_2$ (5 mg, 0.021 mmol, 10 mol %), AgOAc (106 mg, 0.63 mmol, 3 equiv) and K_2CO_3 (29 mg, 0.21 mmol, 1 equiv) in DMA (1 mL, c = 0.1 M) provided, after cyclohexane/ethyl acetate (9:1) column chromatography, the desired compound **65i** (17 mg, yield 23 %) as a white powder.

R_f = 0.15 (9:1 cyclohexane/ethyl acetate)

^{1}H NMR (400 MHz, $CDCl_3$, 25 °C): δ = 7.26 (dd, 1H, J_1 = 1.0 Hz, J_2 = 9.0 Hz), 6.97 (dd, 1H, J_1 = 1.0 Hz, J_2 = 2.5 Hz), 6.95 (dd, 1H, J_1 = 2.5 Hz, J_2 = 9.0 Hz), 4.65 (t, 2H, J = 7.5 Hz), 4.19 (s, 3H), 3.90 (s, 3H), 3.87 (s, 3H), 3.17 (t, 2H, J = 7.5 Hz), 2.96 – 2.88 (m, 2H), 1.76 (h, 2H, J = 7.5 Hz), 1.02 (t, 3H, J = 7.5 Hz).

^{13}C NMR (101 MHz, $CDCl_3$, 25 °C): δ = 162.1, 154.6, 152.9, 143.2, 134.3, 126.8, 125.6, 117.9, 113.9, 110.8, 110.4, 100.5, 56.0, 51.4, 44.3, 31.8, 31.7, 23.0, 21.0, 14.3.

HRMS (ESI-Orbitrap, *m*/*z*): calcd for $C_{20}H_{23}N_3O_3$ $[M + H]^+$ 354.1812; found 354.1807

Methyl 2-butyl-11-methyl-6,11-dihydro-5*H*-imidazo[1',2':1,2]pyrido[3,4-*b*]indole-3-carboxylate (**65j**):

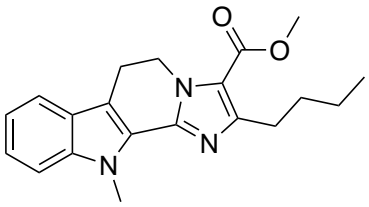

According to GP6, the indole-imidazole derivative **66j** (67 mg, 0.19 mmol, 1 equiv), $Pd(OAc)_2$ (4 mg, 0.019 mmol, 10 mol %), AgOAc (96 mg, 0.57 mmol, 3 equiv) and K_2CO_3 (26 mg, 0.19 mmol, 1 equiv) in DMA (1.9 mL, c = 0.1 M) provided, after cyclohexane/ethyl acetate (85:15) column chromatography, the desired compound **65j** (33 mg, yield 64 %) as a white powder.

R_f = 0.32 (9:1 cyclohexane/ethyl acetate)

^{1}H NMR (400 MHz, $CDCl_3$, 25 °C): δ = 7.57 (ddd, 2H, $J_1 \approx J_2$ = 1.0 Hz, J_3 = 8.0 Hz), 7.37 (ddd, 2H, $J_1 \approx J_2$ = 1.0 Hz, J_3 = 8.0 Hz), 7.29 (ddd, 1H, J_1 = 1.0 Hz, J_2 = 7.0 Hz, J_3 = 8.0 Hz), 7.16 (ddd, 1H, J_1 = 1.0 Hz, J_2 = 7.0 Hz, J_3 = 8.0 Hz), 4.66 (t, 2H, J = 7.5 Hz), 4.23 (s, 3H), 3.91 (s, 3H), 3.21 (t, 2H, J = 7.5 Hz), 2.96 (br t, 2H, J = 7.5 Hz), 1.73 (p, 2H, J = 7.5 Hz), 1.45 (h, 2H, J = 7.5 Hz), 0.98 (t, 3H, J = 7.5 Hz).

^{13}C NMR (101 MHz, $CDCl_3$) δ 162.1, 153.1, 143.2, 138.9, 126.3, 125.4, 123.2, 120.1, 119.2, 117.9, 111.0, 110.0, 51.4, 44.3, 31.9, 31.7, 29.4, 22.8, 21.0, 14.1.

HRMS (ESI-Orbitrap, *m*/*z*): calcd for $C_{20}H_{23}N_3O_2$ $[M + H]^+$ 338.1863; found 338.1859

- PART 2 -

1-((1-Isocyanobutyl)sulfonyl)-4-methylbenzene (**71a**):

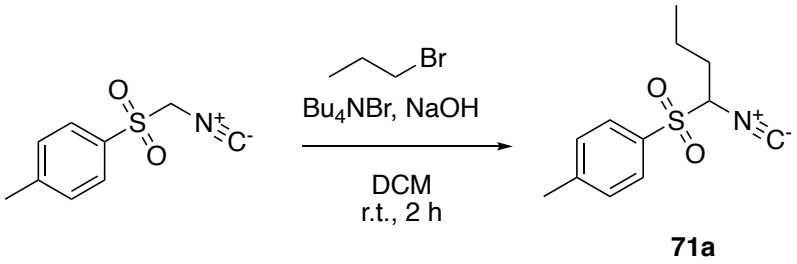

71a

TosMIC (6 mmol), Bu_4NBr (1.2 mmol) and bromopropane (12 mmol) were dissolved in 3.6 mL of DCM and 4 mL of freshly prepared NaOH 30 % solution. The reaction mixture was stirred at 0 °C and controlled by TLC with hexane:EtOAc (8:2) as eluent. After 2 hours, the reaction was quenched with H_2O (30 mL), and the resulting mixture was extracted with DCM (3 x 30 mL) and then washed with H_2O (2 x 20 mL). The organic layer was dried over anhydrous sodium sulphate, filtered and then evaporated under reduced pressure, to obtain **71a** in an 85 % yield (1.1 g) as a brown oil.

The physicochemical data are consistent with those reported in the literature.[134]

^{1}H NMR (500 MHz, CDCl3) δ 7.82 (m, 2H), 7.39 (m, 2H), 4.47 (dd, J = 10.9, 3.4 Hz, 1H), 2.52 – 2.42 (m, 3H), 1.90 – 1.64 (m, 2H), 1.59 – 1.23 (m, 2H), 1.06 – 0.93 (m, 3H).

(*Z*)-*N*-(2-(1-methyl-1*H*-indol-3-yl)ethyl)-1-phenylmethanimine (**73**):

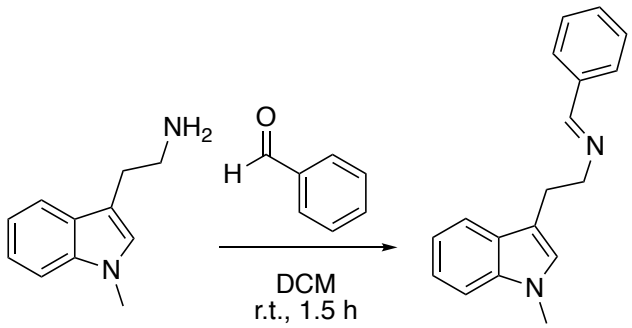

67e **73**

To a solution of *N*-methyltryptamine (2.2 mmol) in 10 mL of DCM, benzaldehyde (2 mmol) and anhydrous Na_2SO_4 (5 g) were added. The reaction mixture was stirred

at room temperature and checked by ^{1}H NMR. After 1.5 h, the mixture was filtered, and the solvent was evaporated under reduced pressure, furnishing **73** as a yellow oil in a quantitative yield.

^{1}H NMR (250 MHz, $CDCl_3$) δ: 8.22 (s, 1H), 7.76 – 7.56 (m, 3H), 7.45 – 7.42 (m, 2H), 7.34 – 7.21 (m, 3H), 7.17 – 7.10 (m, 1H), 6.90 (s, 1H), 3.95 (td, J = 7.4, 1.3 Hz, 2H), 3.73 (s, 3H), 3.18 (t, J = 7.0 Hz, 2H) ppm.

^{13}C NMR (63 MHz, $CDCl_3$) δ: 161.45, 137.04, 136.36, 130.62, 128.67, 128.15, 128.02, 126.99, 121.55, 119.16, 118.74, 112.63, 109.25, 62.48, 32.67, 26.99 ppm.

1-Methyl-3-(2-(5-phenyl-1*H*-imidazol-1-yl)ethyl)-1*H*-indole (**66o**):

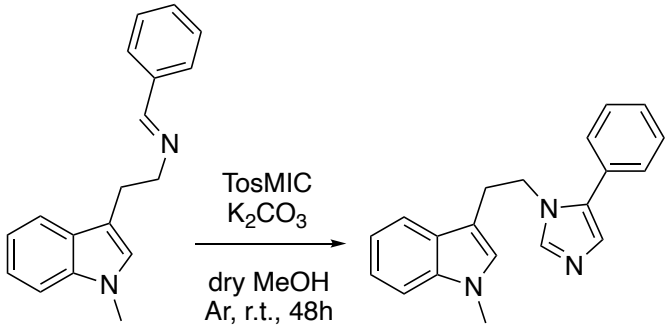

73 **66o**

To a solution of **73** (1 mmol) in dry MeOH (1.5 mL) under an Ar atmosphere, TosMIC (1.5 mmol) and K_2CO_3 (1.5 mmol) were added, and the reaction mixture was stirred for 48 h while monitored by TLC. Once the reaction was completed, 20 mL of water was added, and the mixture was extracted with DCM (3 x 40 mL). The organic phase was dried over anhydrous sodium sulphate and then evaporated under reduced pressure. The crude mixture was purified by silica gel column chromatography eluting with a gradient from DCM to 8.5:1.5 DCM:MeOH, yielding **66o** (166 mg, 55 %) of a yellow oil.

^{1}H NMR (250 MHz, $CDCl_3$) δ: 7.45 – 7.36 (m, 4H), 7.33 – 7.28 (m, 2H), 7.27 – 7.17 (m, 3H), 7.09 – 7.02 (m, 2H), 6.61 (s, 1H), 4.24 (t, J = 7.3 Hz, 2H), 3.69 (s, 3H), 3.00 (t, J = 7.3 Hz, 2H) ppm.

^{13}C NMR (63 MHz, $CDCl_3$) δ: 138.4, 137.0, 133.0, 130.2, 129.0, 128.8, 128.2, 128.1, 127.4, 127.1, 121.9, 119.1, 118.4, 109.9, 109.5, 46.1, 32.7, 27.3 ppm.

HRMS (ESI-Orbitrap, *m*/*z*): calcd for $C_{20}H_{19}N_3$ $[M + H]^+$ 302.1579; found 302.1651

11-Methyl-3-phenyl-6,11-dihydro-5*H*-imidazo[1',2':1,2]pyrido[3,4-*b*]indole (**65o**):

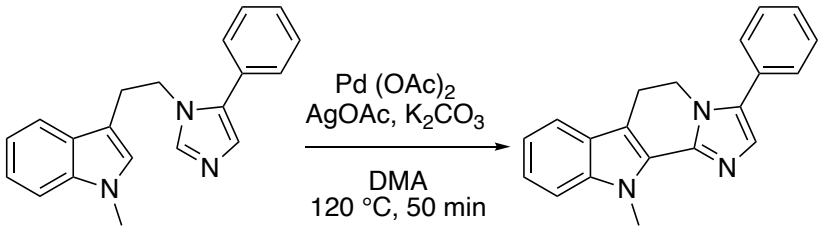

66o **65o**

According to GP6, the indole-imidazole derivative **66o** (60 mg, 0.2 mmol, 1 equiv), $Pd(OAc)_2$ (5 mg, 0.02 mmol, 10 mol %), AgOAc (100 mg, 0.6 mmol, 3 equiv) and K_2CO_3 (28 mg, 0.2 mmol, 1 equiv) in DMA (2.0 mL, c = 0.1 M) provided, after cyclohexane/ethyl acetate (85:15) column chromatography, the desired compound **65j** (63 mg, yield 70 %) as a white solid

^{1}H NMR (250 MHz, $CDCl_3$) δ: 7.56 (dt, J = 7.9, 1.0 Hz, 1H), 7.51 – 7.36 (m, 6H), 7.35 – 7.24 (m, 1H), 7.23 (s, 1H), 7.20 – 7.12 (m, 1H), 4.34 – 4.23 (m, 5H), 3.21 (t, J = 7.2 Hz, 2H) ppm.

^{13}C NMR (63 MHz, $CDCl_3$) δ: 138.6, 133.2, 129.9, 129.4, 129.0, 128.7, 128.2, 127.4, 127.3, 125.6, 122.8, 120.0, 118.9, 109.9, 109.4, 43.5, 31.7, 21.2 ppm.

HRMS (ESI-Orbitrap, *m*/*z*): calcd for $C_{20}H_{17}N_3$ $[M + H]^+$ 300.1422; found 300.1488

3-(2-Iodoethyl)-1*H*-indole (**75c**).

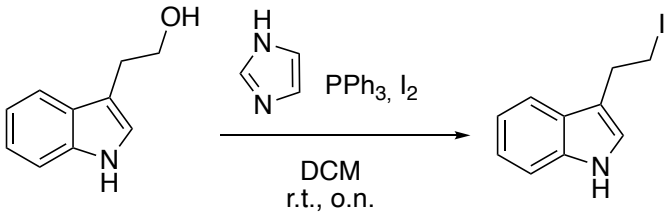

75c

According to reported synthesis in the literature[135], to a solution of imidazole (184 mg, 2.7 mmol, 1.35 equiv) in DCM (2.5 mL), I_2 (682 mg, 2.6 mmol, 1.3 equiv) was added and stirred for 5 minutes. While at 0°C, tryptophol (322 mg, 2 mmol, 1 equiv) in DCM (2 mL) was added, and the mixture was allowed to stir at room temperature overnight. After the reaction was completed, methanol (0.6 mL) was added, and the reaction was stirred for a further 30 minutes. The solution was extracted with H_2O (5 mL), the organic phase was vigorously shaken and extracted with 5 mL of a sodium hydrogen sulfite ($NaHSO_3$) solution acidified with HCl. The organic phase was then dried over Na_2SO_4 and under reduced pressure. The final compound **75c** was obtained after column chromatography (9:1 Hex:EtOAc) as a white powder (529 mg, 1.95 mmol, 97.6 %).

The physicochemical data are consistent with those reported in the literature.[136]

^{1}H NMR (300 MHz, $CDCl_3$) δ 8.01 (br s, 1H), 7.59 (ddt, *J* = 7.7, 1.6, 0.8 Hz, 1H), 7.38 (dt, *J* = 8.1, 1.1 Hz, 1H), 7.22 (ddd, *J* = 8.2, 7.0, 1.4 Hz, 1H), 7.14 (ddd, *J* = 8.1, 7.0, 1.2 Hz, 1H), 7.09 (d, *J* = 2.2 Hz, 1H), 3.48 – 3.42 (m, 2H), 3.40 – 3.33 (m, 2H).

*3.4.7. Synthesis of indole containing imidazoles (part 2) (**78,66**)*

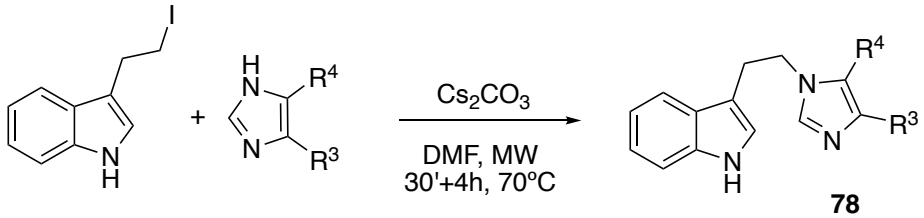

79 **76** **78**

Two molecules if R^3 R^4

76k: R^3 = H, R^4 = H
76l: R^3 = H, R^4 = COOMe
76m: R^3 = Br, R^4 = Me
76n: R^3 = H, R^4 = CHO
76o: R^3 = H, R^4 = Ph
76p: Benzimidazole
76q: R^3 = H, R^4 = COOEt
76r: R^3 = CHO, R^4 = Me
76s: R^3 = H, R^4 = NO_2
76t: R^3 = Me, R^4 = NO_2
76u: NO_2-Benzimidazole

78k: R^3 = H, R^4 = H
78l: R^3 = H, R^4 = COOMe **78l'**: R^3 = COOMe, R^4 = H
78m: R^3 = Br, R^4 = Me **78m'**: R^3 = Me, R^4 = H
78n: R^3 = H, R^4 = CHO **78n'**: R^3 = CHO, R^4 = H
78o: R^3 = H, R^4 = Ph **78o'**: R^3 = Ph, R^4 = H
78p: Benzimidazole
78q: R^3 = H, R^4 = COOEt **78q'**: R^3 = COOEt, R^4 = H
78r: R^3 = CHO, R^4 = Me **78r'**: R^3 = Me, R^4 = CHO
78s: R^3 = H, R^4 = NO_2 **78s'**: R^3 = NO_2, R^4 = H
78t: R^3 = Me, R^4 = NO_2 **78t'**: R^3 = NO_2, R^4 = Me
78u: 6-NO_2-Benzimidazole **78u'**: 5-NO_2-Benzimidazole

General procedure for the synthesis of indole-containing imidazoles from preformed imidazoles GP7

According to the optimisation of this reaction, the corresponding imidazole derivative **76** (1 equiv.) and Cs_2CO_3 (1 equiv.) were stirred for 30 minutes at room temperature in dry DMF (c = 0.15 M). Then, 3-(2-iodoethyl)-1*H*-indole (**75c**) (1 equiv.) was added, and the reaction was put in the microwave at 70 °C for 4 hours. After the time had elapsed, the solvent was evaporated under reduced pressure and the crude was purified by column chromatography to afford the desired product.

3-(2-(1*H*-Imidazol-1-yl)ethyl)-1*H*-indole (**78k**):

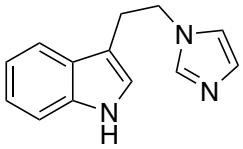

According to GP7, imidazole (21 mg, 0.3 mmol, 1 equiv), Cs_2CO_3 (98 mg, 0.3 mmol, 1 equiv) and 3-(2-iodoethyl)-1*H*-indole (81.3 mg, 0.3 mmol, 1 equiv) in dry DMF (2 mL) provided, after column chromatography 95:5 DCM:MeOH, the desired product **78k** (50 mg, 79 % yield) as a light yellow powder.

^{1}H NMR (300 MHz, DMSO-d_6) δ 10.84 (s, 1H), 7.57 – 7.52 (m, 2H), 7.33 (dt, *J* = 8.1, 1.0 Hz, 1H), 7.19 (t, *J* = 1.2 Hz, 1H), 7.10 – 7.03 (m, 2H), 6.98 (ddd, *J* = 8.0, 7.0, 1.1 Hz, 1H), 6.85 (t, *J* = 1.1 Hz, 1H), 4.23 (t, *J* = 7.4 Hz, 2H), 3.13 (ddd, *J* = 7.9, 6.9, 0.8 Hz, 2H).

^{13}C NMR (75 MHz, $CDCl_3$) δ 137.2, 136.1, 128.2, 127.0, 123.0, 121.0, 119.3, 118.3, 118.3, 111.4, 110.5, 46.6, 26.9.

Methyl 1-(2-(1*H*-indol-3-yl)ethyl)-1*H*-imidazole-5-carboxylate (**78l**):

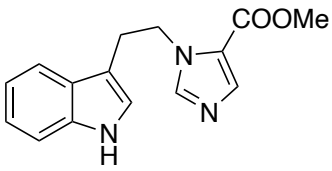

According to GP7, methyl 1*H*-imidazole-5-carboxylate (101 mg, 0.8 mmol, 1 equiv), Cs_2CO_3 (261 mg, 0.8 mmol, 1 equiv) and 3-(2-iodoethyl)-1*H*-indole (217 mg, 0.8 mmol, 1 equiv) in dry DMF (5.3 mL) provided, after column chromatography 95:5 DCM:MeOH, the desired product **78l** (55.3 mg, 25.7 % yield) as a white solid.

^{1}H NMR (250 MHz, $CDCl_3$) δ 8.43 (br s, 1H), 7.75 (s, 1H), 7.62 (ddd, *J* = 7.3, 1.5, 0.7 Hz, 1H), 7.36 – 7.32 (m, 1H), 7.25 – 7.18 (m, 1H), 7.18 – 7.11 (m, 2H), 6.72 (d, *J* = 2.4 Hz, 1H), 4.56 (t, *J* = 6.8 Hz, 2H), 3.88 (s, 3H), 3.21 (td, *J* = 6.8, 0.7 Hz, 2H).

^{13}C NMR (63 MHz, $CDCl_3$) δ 160.9, 142.5, 138.0, 136.5, 127.0, 122.8, 122.3, 119.7, 118.9, 118.4, 111.5, 111.3, 51.7, 47.7, 27.3.

Methyl 1-(2-(1*H*-indol-3-yl)ethyl)-1*H*-imidazole-4-carboxylate (**78l'**):

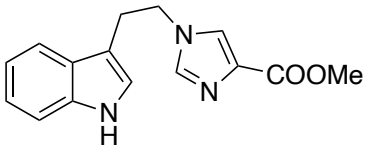

According to GP7, methyl 1*H*-imidazole-5-carboxylate (101 mg, 0.8 mmol, 1 equiv), Cs_2CO_3 (261 mg, 0.8 mmol, 1 equiv) and 3-(2-iodoethyl)-1*H*-indole (217 mg, 0.8 mmol, 1 equiv) in dry DMF (5.3 mL) provided, after column chromatography 95:5 DCM:MeOH, the desired product **78l'** (61.4 mg, 28.5 % yield) as a white powder.

^{1}H NMR (250 MHz, $CDCl_3$) δ 8.28 (s, 1H), 7.71 – 7.50 (m, 2H), 7.44 – 7.33 (m, 1H), 7.25 – 7.02 (m, 3H), 6.72 (d, *J* = 2.4 Hz, 1H), 4.26 (t, *J* = 6.7 Hz, 2H), 3.91 – 3.85 (m, 3H), 3.22 (t, *J* = 6.7 Hz, 2H).

^{13}C NMR (63 MHz, $CDCl_3$) δ 163.5, 138.2, 136.5, 133.7, 126.6, 125.2, 122.9, 122.6, 119.9, 118.1, 111.7, 110.7, 51.8, 48.2, 27.6.

3-(2-(4-Bromo-5-methyl-1*H*-imidazol-1-yl)ethyl)-1*H*-indole (**78m**):

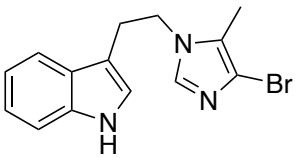

According to GP7, methyl 4-bromo-5-methyl-1*H*-imidazole (161 mg, 1 mmol, 1 equiv), Cs_2CO_3 (326 mg, 1 mmol, 1 equiv) and 3-(2-iodoethyl)-1*H*-indole (271 mg, 1 mmol, 1 equiv) in dry DMF (6.7 mL) provided, after column chromatography 95:5 DCM:MeOH, the desired product **78m** (84.2 mg, 27.8 % yield) as a light orange powder.

^{1}H NMR (250 MHz, $CDCl_3$) δ 8.24 (s, 1H), 7.60 – 7.51 (m, 1H), 7.46 – 7.37 (m, 1H), 7.27 – 7.21 (m, 1H), 7.21 – 7.15 (m, 1H), 7.14 (s, 1H), 6.80 (d, *J* = 2.4 Hz, 1H), 4.15 (t, *J* = 6.9 Hz, 2H), 3.16 (td, *J* = 6.9, 0.8 Hz, 2H), 2.12 (d, *J* = 1.2 Hz, 3H).

^{13}C NMR (63 MHz, $CDCl_3$) δ 136.5, 135.8, 126.9, 124.8, 122.8, 122.5, 119.9, 118.1, 114.0, 111.7, 111.0, 46.5, 27.2, 9.0.

3-(2-(5-Bromo-4-methyl-1*H*-imidazol-1-yl)ethyl)-1*H*-indole (**78m'**):

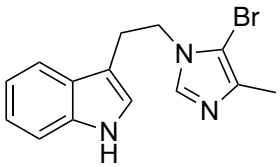

According to GP7, methyl 4-bromo-5-methyl-1*H*-imidazole (161 mg, 1 mmol, 1 equiv), Cs_2CO_3 (326 mg, 1 mmol, 1 equiv) and 3-(2-iodoethyl)-1*H*-indole (271 mg, 1 mmol, 1 equiv) in dry DMF (6.7 mL) provided, after column chromatography 95:5 DCM:MeOH, the desired product **78m'** (73.4 mg, 24.1 % yield) as a red solid.

^{1}H NMR (250 MHz, $CDCl_3$) δ 8.51 (s, 1H), 7.65 – 7.55 (m, 1H), 7.36 (dt, *J* = 8.2, 0.8 Hz, 1H), 7.25 – 7.19 (m, 1H), 7.18 – 7.17 (m, 1H), 7.13 (dd, *J* = 7.1, 1.3 Hz, 1H), 6.80 (d, *J* = 2.4 Hz, 1H), 4.16 (t, *J* = 7.1 Hz, 2H), 3.17 (t, *J* = 7.1 Hz, 2H), 2.21 (s, 3H).

^{13}C NMR (63 MHz, $CDCl_3$) δ 136.9, 136.8, 136.5, 127.0, 122.8, 122.3, 119.7, 118.3, 111.6, 111.1, 100.2, 47.1, 26.8, 13.2.

1-(2-(1*H*-Indol-3-yl)ethyl)-1*H*-imidazole-5-carbaldehyde (**78n**):

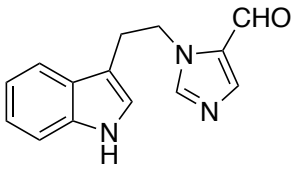

According to GP7, 1*H*-imidazole-5-carbaldehyde (77 mg, 0.8 mmol, 1 equiv), Cs_2CO_3 (261 mg, 0.8 mmol, 1 equiv) and 3-(2-iodoethyl)-1*H*-indole (217 mg, 0.8 mmol, 1 equiv) in dry DMF (5.3 mL) provided, after column chromatography 95:5 DCM:MeOH, the desired product **78n** (67.9 mg, 35.5 % yield) as a red solid.

^{1}H NMR (250 MHz, $CDCl_3$) δ 9.85 (s, 1H), 8.27 (s, 1H), 7.85 (d, *J* = 2.4 Hz, 1H), 7.67 (dd, *J* = 7.5, 2.6 Hz, 1H), 7.48 – 7.35 (m, 1H), 7.30 – 7.13 (m, 3H), 6.80 (t, *J* = 2.7 Hz, 1H), 4.61 (td, *J* = 6.9, 2.5 Hz, 2H), 3.25 (td, *J* = 6.8, 2.5 Hz, 2H).

^{13}C NMR (63 MHz, $CDCl_3$) δ 179.3, 144.1, 143.9, 136.5, 130.9, 127.0, 122.7, 122.5, 119.9, 118.5, 111.6, 111.2, 48.0, 27.0.

1-(2-(1*H*-Indol-3-yl)ethyl)-1*H*-imidazole-4-carbaldehyde (**78n'**):

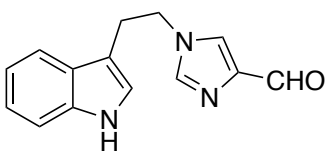

According to GP7, 1*H*-imidazole-5-carbaldehyde (77 mg, 0.8 mmol, 1 equiv), Cs_2CO_3 (261 mg, 0.8 mmol, 1 equiv) and 3-(2-iodoethyl)-1*H*-indole (217 mg, 0.8 mmol, 1 equiv)

in dry DMF (5.3 mL) provided, after column chromatography 95:5 DCM:MeOH, the desired product **78n'** (66.2 mg, 34.6 % yield) as a white powder.

^{1}H NMR (250 MHz, DMSO-d_6) δ 10.87 (br s, 1H), 9.67 (s, 1H), 8.08 (d, *J* = 1.3 Hz, 1H), 7.80 (s, 1H), 7.57 (d, *J* = 7.8 Hz, 1H), 7.34 (d, *J* = 8.0 Hz, 1H), 7.13 – 6.93 (m, 3H), 4.33 (t, *J* = 7.2 Hz, 2H), 3.19 (t, *J* = 7.2 Hz, 2H).

^{13}C NMR (63 MHz, DMSO) δ 185.2, 141.3, 139.8, 136.1, 127.6, 126.9, 123.2, 121.1, 118.4, 118.3, 111.4, 110.0, 47.2, 26.5.

3-(2-(4-Phenyl-1*H*-imidazol-1-yl)ethyl)-1*H*-indole (**78o'**)**:**

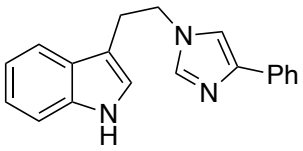

According to GP7, 4-phenyl-1*H*-imidazole (115 mg, 0.8 mmol, 1 equiv), Cs_2CO_3 (261 mg, 0.8 mmol, 1 equiv) and 3-(2-iodoethyl)-1*H*-indole (217 mg, 0.8 mmol, 1 equiv) in dry DMF (5.3 mL) provided, after column chromatography 95:5 DCM:MeOH, the desired product **78o'** (98.8 mg, 43.0 % yield) as a brown foam.

^{1}H NMR (250 MHz, $CDCl_3$) δ 8.78 (s, 1H), 7.78 (dd, *J* = 7.1, 1.9 Hz, 2H), 7.59 (d, *J* = 7.5 Hz, 1H), 7.43 – 7.26 (m, 5H), 7.25 – 7.14 (m, 3H), 6.72 (d, *J* = 2.3 Hz, 1H), 4.24 (td, *J* = 6.8, 1.9 Hz, 2H), 3.24 (td, *J* = 6.7, 1.9 Hz, 2H).

^{13}C NMR (63 MHz, $CDCl_3$) δ 142.0, 137.5, 136.4, 134.2, 128.7 (2C), 126.9, 126.8, 124.8 (2C), 122.9, 122.2, 119.6, 118.2, 114.9, 111.7, 111.1, 47.9, 27.6.

1-(2-(1*H*-Indol-3-yl)ethyl)-1*H*-benzo[*d*]imidazole (**78p**):

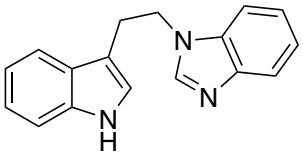

According to GP7, 1*H*-benzo[*d*]imidazole (209 mg, 0.8 mmol, 1 equiv), Cs_2CO_3 (261 mg, 0.8 mmol, 1 equiv) and 3-(2-iodoethyl)-1*H*-indole (217 mg, 0.8 mmol, 1 equiv) in dry DMF (5.3 mL) provided, after column chromatography 95:5 DCM:MeOH, the desired product **78p** (139.3 mg, 66.6 % yield) as a light pink solid.

^{1}H NMR (250 MHz, DMSO-d_6) δ 10.85 (s, 1H), 8.09 (d, *J* = 1.4 Hz, 1H), 7.68 – 7.59 (m, 2H), 7.55 (d, *J* = 7.8 Hz, 1H), 7.36 – 7.30 (m, 1H), 7.21 (pd, *J* = 7.2, 1.5 Hz, 2H),

7.11 – 7.03 (m, 2H), 6.97 (ddd, *J* = 7.9, 7.0, 1.2 Hz, 1H), 4.53 (t, *J* = 7.4 Hz, 2H), 3.23 (t, *J* = 7.3 Hz, 2H).

^{13}C NMR (63 MHz, DMSO) δ 144.0, 143.4, 136.1, 133.7, 126.9, 123.2, 122.1, 121.3, 121.0, 119.4, 118.4, 118.2, 111.4, 110.4, 110.3, 44.8, 25.5.

Ethyl 1-(2-(1*H*-indol-3-yl)ethyl)-1*H*-imidazole-5-carboxylate (**78q**):

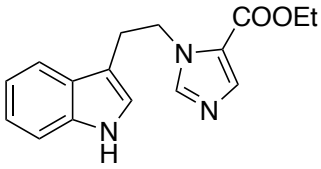

According to GP7, ethyl 1*H*-imidazole-5-carboxylate (84 mg, 0.6 mmol, 1 equiv), Cs_2CO_3 (195 mg, 0.6 mmol, 1 equiv) and 3-(2-iodoethyl)-1*H*-indole (163 mg, 0.6 mmol, 1 equiv) in dry DMF (2 mL) provided, after column chromatography 95:5 DCM:MeOH, the desired product **78q** (46.6 mg, 27.4 % yield) as a light yellow powder.

^{1}H NMR (250 MHz, $CDCl_3$) δ 8.61 (br s, 1H), 7.76 (s, 1H), 7.65 – 7.58 (m, 1H), 7.37 – 7.30 (m, 1H), 7.25 – 7.18 (m, 1H), 7.18 – 7.16 (m, 1H), 7.16 – 7.11 (m, 1H), 6.71 (d, *J* = 2.4 Hz, 1H), 4.56 (t, *J* = 6.8 Hz, 2H), 4.36 (q, *J* = 7.1 Hz, 2H), 3.21 (t, *J* = 6.8 Hz, 2H), 1.40 (t, *J* = 7.1 Hz, 3H).

^{13}C NMR (63 MHz, $CDCl_3$) δ 160.5, 142.4, 137.8, 136.5, 127.0, 122.8, 122.3, 122.2, 119.6, 118.4, 111.5, 111.2, 60.6, 47.7, 27.3, 14.4.

Ethyl 1-(2-(1*H*-indol-3-yl)ethyl)-1*H*-imidazole-4-carboxylate (**78q'**):

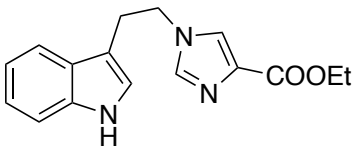

According to GP7, ethyl 1*H*-imidazole-5-carboxylate (84 mg, 0.6 mmol, 1 equiv), Cs_2CO_3 (195 mg, 0.6 mmol, 1 equiv) and 3-(2-iodoethyl)-1*H*-indole (163 mg, 0.6 mmol, 1 equiv) in dry DMF (4 mL) provided, after column chromatography 95:5 DCM:MeOH, the desired product **78q'** (61.1 mg, 35.9 % yield) as a white powder

^{1}H NMR (250 MHz, DMSO-d_6) δ 10.85 (br s, 1H), 7.92 (d, *J* = 1.3 Hz, 1H), 7.67 (d, *J* = 1.3 Hz, 1H), 7.58 (d, *J* = 7.7 Hz, 1H), 7.33 (dt, *J* = 8.2, 1.0 Hz, 1H), 7.08 (dd, *J* = 7.0, 1.3 Hz, 1H), 7.04 (d, *J* = 1.9 Hz, 1H), 6.97 (ddd, *J* = 8.0, 7.0, 1.2 Hz, 1H), 4.28 (t, *J* = 7.3 Hz, 2H), 4.18 (q, *J* = 7.1 Hz, 2H), 3.19 – 3.12 (m, 2H), 1.24 (s, 3H).

^{13}C NMR (63 MHz, DMSO) δ 162.3, 138.7, 136.1, 132.1, 126.9, 126.3, 123.1, 121.0, 118.4, 118.3, 111.4, 110.1, 59.3, 47.0, 26.6, 14.3.

1-(2-(1*H*-Indol-3-yl)ethyl)-5-methyl-1*H*-imidazole-4-carbaldehyde (**78r**):

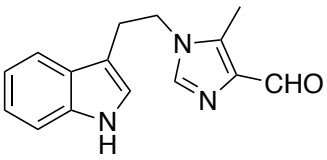

According to GP7, 4-methyl-1*H*-imidazole-5-carbaldehyde (88 mg, 0.8 mmol, 1 equiv), Cs_2CO_3 (261 mg, 0.8 mmol, 1 equiv) and 3-(2-iodoethyl)-1*H*-indole (217 mg, 0.8 mmol, 1 equiv) in dry DMF (5.3 mL) provided, after column chromatography 95:5 DCM:MeOH, the desired product **78r** (47.4 mg, 23.4 % yield) as a yellow powder.

^{1}H NMR (250 MHz, DMSO-d_6) δ 10.87 (s, 1H), 9.73 (s, 1H), 7.68 (s, 1H), 7.52 (d, J = 7.8 Hz, 1H), 7.34 (dt, J = 8.1, 1.0 Hz, 1H), 7.12 – 7.03 (m, 2H), 6.97 (ddd, J = 8.0, 7.0, 1.2 Hz, 1H), 4.22 (t, J = 7.2 Hz, 2H), 3.11 (t, J = 7.2 Hz, 2H), 2.32 (s, 3H).

^{13}C NMR (63 MHz, DMSO) δ 186.5, 139.0, 137.1, 136.9, 136.5, 127.3, 123.8, 121.5, 118.8, 118.5, 111.8, 110.4, 45.0, 26.5, 9.0.

3-(2-(5-Nitro-1*H*-imidazol-1-yl)ethyl)-1*H*-indole and 3-(2-(4-nitro-1*H*-imidazol-1-yl)ethyl)-1*H*-indole (**78s** & **78s'**):

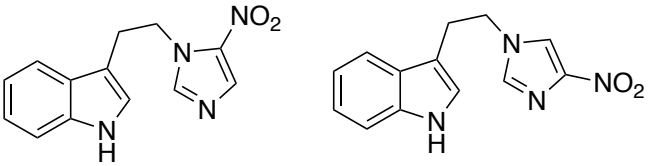

According to GP7, 5-nitro-1*H*-imidazole (90 mg, 0.8 mmol, 1 equiv), Cs_2CO_3 (261 mg, 0.8 mmol, 1 equiv) and 3-(2-iodoethyl)-1*H*-indole (217 mg, 0.8 mmol, 1 equiv) in dry DMF (5.3 mL) provided, after column chromatography 95:5 DCM:MeOH a mix of products **78s** and **78s'** (121.1 mg, 59.1 % yield) as a yellow powder.

Ratio of 0.15:1 5-nitro(*):4-nitro(") demonstrated by previously reported spectra in the literature.[137]

^{1}H NMR (300 MHz, DMSO-d_6) δ 10.89 (br s, 0.15H*), 10.87 (br s, 1H"), 8.41 (d, J = 1.5 Hz, 1H"), 8.07 (d, J = 1.1 Hz, 0.15H*), 7.80 (d, J = 1.1 Hz, 0.15H*), 7.76 (d, J = 1.5 Hz, 1H"), 7.60 – 7.54 (m, 1H"), 7.54 (d, J = 6.1 Hz, 0.15H*), 7.34 (dt, J = 8.1, 1.0 Hz, 0.15H*), 7.34 (dt, J = 8.1, 1.0 Hz, 1H"), 7.12 – 7.04 (m, 2H"), 7.11 – 7.04 (m, 0.15H*),

7.02 – 6.95 (m, 0.15H*), 7.01 – 6.94 (m, 1H"), 4.60 (t, *J* = 7.4 Hz, 0.3H*), 4.35 (t, *J* = 7.2 Hz, 2H"), 3.22 (t, *J* = 7.2 Hz, 2H"), 3.16 (t, *J* = 7.3 Hz, 0.3H*).

^{13}C NMR (75 MHz, DMSO) δ 146.8", 143.0*, 137.4", 136.2*, 136.1", 133.6*, 126.9*, 126.8", 123.5*, 123.3", 121.6*, 121.1*,6", 121.1*, 121.1", 118.5*, 118.4", 118.2", 118.0*, 111.4*, 111.4", 109.8", 109.5*, 48.0", 47.9*, 26.3", 26.2*.

3-(2-(4-Methyl-5-nitro-1*H*-imidazol-1-yl)ethyl)-1*H*-indole and 3-(2-(5-methyl-4-nitro-1*H*-imidazol-1-yl)ethyl)-1*H*-indole (**78t** & **78t'**):

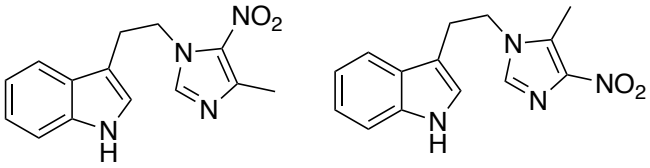

According to GP7, 4-methyl-5-nitro-1*H*-imidazole (102 mg, 0.8 mmol, 1 equiv), Cs_2CO_3 (261 mg, 0.8 mmol, 1 equiv) and 3-(2-iodoethyl)-1*H*-indole (217 mg, 0.8 mmol, 1 equiv) in dry DMF (5.3 mL) provided, after column chromatography 95:5 DCM:MeOH a mix of products **78t** and **78t'**: (128.5 mg, 59.1 % yield) as a yellow powder.

^{1}H NMR (250 MHz, DMSO-*d*6) δ 10.90 (s, 1H*), 10.90 (s, 0.3H"), 7.72 (s, 0.3H"), 7.66 (s, 1H*), 7.55 (d, *J* = 7.8 Hz, 0.3H"), 7.49 (d, *J* = 7.8 Hz, 1H*), 7.37 – 7.30 (m, 1H*), 7.37 – 7.30 (m, 1H"), 7.11 – 6.92 (m, 3H*), 7.11 – 6.92 (m, 1H"), 4.55 (t, *J* = 7.4 Hz, 0.7H*), 4.28 (t, *J* = 7.4 Hz, 2H*), 3.13 (t, *J* = 7.1 Hz, 2H*), 3.13 (t, *J* = 7.1 Hz, 0.7H"), 2.46 (s, 1H"), 2.37 (s, 3H*).

^{13}C NMR (63 MHz, DMSO) δ 144.8, 143.7, 136.2, 136.1, 135.8, 135.7, 131.64, 131.64, 126.9, 126.8, 123.5, 123.4, 121.12, 121.09, 118.46, 118.46, 118.03, 117.99, 111.49, 111.46, 109.6, 109.5, 45.79, 45.79, 25.8, 16.2, 9.92, 9.92.

1-(2-(1*H*-Indol-3-yl)ethyl)-6-nitro-1*H*-benzo[*d*]imidazole and 1-(2-(1*H*-indol-3-yl)ethyl)-5-nitro-1*H*-benzo[*d*]imidazole (**78u** & **78u'**):

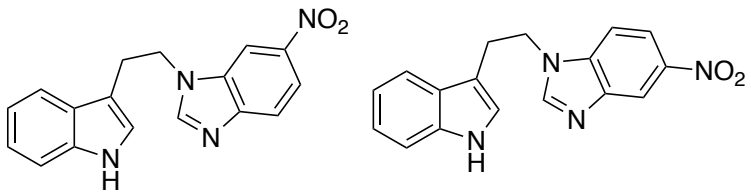

According to GP7, 6-nitro-1*H*-benzo[*d*]imidazole (102 mg, 0.8 mmol, 1 equiv), Cs_2CO_3 (261 mg, 0.8 mmol, 1 equiv) and 3-(2-iodoethyl)-1*H*-indole (217 mg, 0.8 mmol, 1 equiv) in dry DMF (5.3 mL)

provided, after column chromatography 95:5 DCM:MeOH a mix of products **78u** and **78u'** (178.4 mg, 72.8 % yield) as a light yellow powder.

Ratio of 0.8:1 6-nitro(*):5-nitro(") demonstrated by previously reported spectra in the literature.[138]

^{1}H NMR (250 MHz, DMSO-d_6) δ 10.82 (br s, 0.8H*), 10.82 (br s, 1H"), 8.51 (d, J = 2.1 Hz, 1H"), 8.50 (d, J = 2.4 Hz, 0.8H*), 8.42 (s, 1H"), 8.40 (s, 0.8H*), 8.12 (dd, J = 9.0, 2.2 Hz, 1H"), 8.06 (dd, J = 8.9, 2.3 Hz, 0.8H*), 7.80 (d, J = 2.6 Hz, 1H"), 7.76 (d, J = 2.6 Hz, 0.8H*), 7.51 (d, J = 7.2 Hz, 1H"), 7.49 (d, J = 6.7 Hz, 0.8H*), 7.33 (dt, J = 3.6, 1.0 Hz, 1H"), 7.29 (dt, J = 3.6, 1.0 Hz, 0.8H*), 7.10 – 7.00 (m, 1.6H*), 7.10 – 7.00 (m, 2H"), 6.95 (ddd, J = 8.0, 7.0, 1.1 Hz, 1H"), 6.94 (ddd, J = 8.0, 7.0, 1.1 Hz, 0.8H*), 4.79 – 4.52 (m, 2H"), 4.62 (t, J = 7.3 Hz, 1.6H*), 3.26 (t, J = 7.0 Hz, 1.6H*), 3.26 (t, J = 7.0 Hz, 2H").

^{13}C NMR (63 MHz, DMSO) δ 149.1*, 148.1", 147.7*, 142.7*, 142.6", 142.4", 138.3", 136.1", 136.1*, 133.2*, 126.8*, 126.8", 123.3", 123.3*, 121.0", 121.0*, 119.6*, 118.4*, 118.4", 118.1", 118.0*, 117.7", 116.9*, 115.6", 111.4", 111.3*, 111.0", 110.2*, 110.0", 107.7*, 45.4", 45.3*, 25.6*, 25.4".

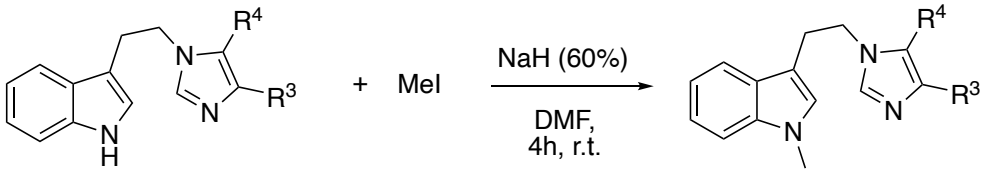

78 **66**

66k: R^3 = H, R^4 = H
66l: R^3 = H, R^4 = COOMe
66m: R^3 = Br, R^4 = Me
66n: R^3 = H, R^4 = CHO
66l': R^3 = COOMe, R^4 = H
66m': R^3 = Me, R^4 = Br
66n': R^3 = CHO, R^4 = H
66o': R^3 = Ph, R^4 = H
66p: Benzimidazole

General procedure for the synthesis of methylation of indole containing imidazoles GP8

According to a modification of a synthesis previously described in the literature,[133] to a suspension of NaH (1.2 mmol, 60 % dispersion in mineral oil) at 0°C in dry DMF (c = 0.2 M), a solution of appropriate *N*H indole bi-heterocycle derivative **78** was added

dropwise. After stirring for 30 minutes, methyl iodide (1.2 mmol) was added at 0 °C; afterwards, the reaction mixture was stirred for an additional period of 4 hours (TLC check). When finished, NH_4Cl (aq., sat.) was added, and the remaining solution was extracted. The reaction mixture was then extracted with AcOEt (3 × 10 mL). The combined organic layers were dried over Na_2SO_4, filtered, and concentrated to give the crude *N*-methyl indole derivative, which was purified by column chromatography.

3-(2-(1*H*-Imidazol-1-yl)ethyl)-1-methyl-1*H*-indole (**66k**):

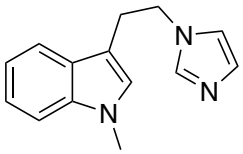

According to GP8, 3-(2-(1*H*-imidazol-1-yl)ethyl)-1*H*-indole (85 mg, 0.4 mmol, 1 equiv), NaH (60 %) (19 mg, 0.48 mmol, 1.2 equiv) and MeI (30 μL, 0.48 mmol, 1.2 equiv) in dry DMF (2 mL) provided, after column chromatography 95:5 DCM:MeOH, the desired product **66k** (83 mg, 92 % yield) as a light gold solid.

^{1}H NMR (300 MHz, $CDCl_3$) δ 7.52 (dt, *J* = 7.9, 1.0 Hz, 2H), 7.31 (ddd, *J* = 8.3, 1.3, 0.8 Hz, 1H), 7.25 (ddd, *J* = 8.0, 6.8, 1.3 Hz, 1H), 7.13 (ddd, *J* = 8.0, 6.8, 1.3 Hz, 1H), 7.07 (t, *J* = 1.2 Hz, 1H), 6.87 (t, *J* = 1.3 Hz, 1H), 6.65 (d, *J* = 0.8 Hz, 1H), 4.26 (t, *J* = 6.9 Hz, 2H), 3.72 (s, 3H), 3.21 (td, *J* = 6.9, 0.8 Hz, 2H).

^{13}C NMR (75 MHz, $CDCl_3$) δ 137.2, 136.9, 128.1, 127.4, 127.3, 122.0, 119.3, 119.2, 118.4, 109.8, 109.7, 48.1, 32.8, 27.5.

Methyl 1-(2-(1-methyl-1*H*-indol-3-yl)ethyl)-1*H*-imidazole-5-carboxylate (**66l**):

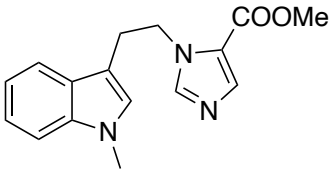

According to GP8, methyl 1-(2-(1*H*-indol-3-yl)ethyl)-1*H*-imidazole-5-carboxylate (75 mg, 0.28 mmol, 1 equiv), NaH (60 %) (13 mg, 0.33 mmol, 1.2 equiv) and MeI (21 μL, 0.33 mmol, 1.2 equiv) in dry DMF (1.5 mL) provided, after column chromatography 95:5 DCM:MeOH, the desired product **66l** (31 mg, 39.4 % yield) as a yellow oil.

^{1}H NMR (250 MHz, $CDCl_3$) δ 7.75 (s, 1H), 7.61 (dt, *J* = 7.7, 1.0 Hz, 1H), 7.31 (ddd, *J* = 8.2, 1.5, 0.8 Hz, 1H), 7.27 (d, *J* = 1.3 Hz, 1H), 7.23 (dd, *J* = 8.2, 1.3 Hz, 1H), 7.14

(ddd, *J* = 8.0, 6.7, 1.5 Hz, 1H), 6.65 (s, 1H), 4.55 (t, *J* = 6.9 Hz, 2H), 3.89 (s, 3H), 3.71 (s, 3H), 3.24 – 3.16 (m, 2H).

^{13}C NMR (75 MHz, $CDCl_3$) δ 160.6, 142.0, 137.1, 127.3, 122.1, 122.05, 122.0, 121.9, 119.2, 118.5, 109.7, 109.5, 51.6, 47.9, 32.7, 27.2.

Methyl 1-(2-(1-methyl-1*H*-indol-3-yl)ethyl)-1*H*-imidazole-4-carboxylate (**66l'**):

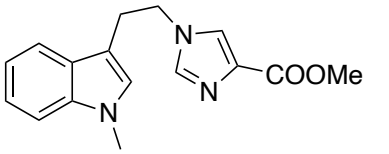

According to GP8, methyl 1-(2-(1*H*-indol-3-yl)ethyl)-1*H*-imidazole-4-carboxylate (80 mg, 0.3 mmol, 1 equiv), NaH (60 %) (14 mg, 0.36 mmol, 1.2 equiv) and MeI (22 μL, 0.36 mmol, 1.2 equiv) in dry DMF (1.5 mL) provided, after column chromatography 95:5 DCM:MeOH, the desired product **66l'** (26.1 mg, 30.2 % yield) as a light brown solid.

^{1}H NMR (250 MHz, $CDCl_3$) δ 7.57 – 7.48 (m, 2H), 7.34 – 7.22 (m, 3H), 7.14 (ddd, *J* = 8.0, 6.6, 1.4 Hz, 1H), 6.61 (s, 1H), 4.24 (t, *J* = 6.8 Hz, 2H), 3.88 (s, 3H), 3.70 (s, 3H), 3.20 (t, *J* = 6.7 Hz, 2H).

^{13}C NMR (63 MHz, $CDCl_3$) δ 163.4, 138.2, 137.2, 133.7, 127.4, 127.1, 125.2, 122.1, 119.4, 118.2, 109.7, 109.2, 51.8, 48.3, 32.8, 27.5.

3-(2-(4-Bromo-5-methyl-1*H*-imidazol-1-yl)ethyl)-1-methyl-1*H*-indole (**66m**):

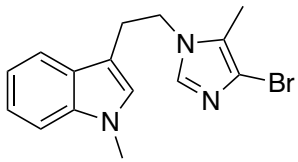

According to GP8, 3-(2-(4-bromo-5-methyl-1*H*-imidazol-1-yl)ethyl)-1*H*-indole (76 mg, 0.25 mmol, 1 equiv), NaH (60 %) (12 mg, 0.3 mmol, 1.2 equiv) and MeI (19 μL, 0.3 mmol, 1.2 equiv) in dry DMF (1.3 mL) provided, after column chromatography 95:5 DCM:MeOH, the desired product **66m** (39.6 mg, 49.8 % yield) as a yellow oil.

^{1}H NMR (250 MHz, $CDCl_3$) δ 7.50 (dt, *J* = 7.8, 1.1 Hz, 1H), 7.32 (ddd, *J* = 8.2, 1.4, 0.8 Hz, 1H), 7.26 (ddd, *J* = 8.0, 6.7, 1.4 Hz, 1H), 7.16 (s, 1H), 7.14 (ddd, *J* = 8.0, 6.7, 1.4 Hz, 1H), 6.67 (s, 1H), 4.11 (t, *J* = 7.0 Hz, 2H), 3.73 (s, 3H), 3.12 (td, *J* = 7.0, 0.7 Hz, 2H), 2.10 (s, 3H).

^{13}C NMR (63 MHz, $CDCl_3$) δ 137.5, 136.1, 127.7, 127.6, 125.1, 122.4, 119.7, 118.6, 114.2, 110.0, 109.8, 47.0, 33.1, 27.4, 9.3.

3-(2-(5-Bromo-4-methyl-1*H*-imidazol-1-yl)ethyl)-1-methyl-1*H*-indole (**66m'**):

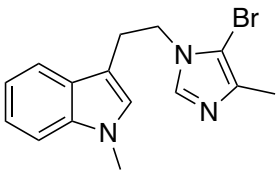

According to GP8, 3-(2-(5-bromo-4-methyl-1*H*-imidazol-1-yl)ethyl)-1*H*-indole (61 mg, 0.2 mmol, 1 equiv), NaH (60 %) (10 mg, 0.24 mmol, 1.2 equiv) and MeI (15 μL, 0.24 mmol, 1.2 equiv) in dry DMF (1 mL) provided, after column chromatography 95:5 DCM:MeOH, the desired product **66m'** (31.1 mg, 48.9 % yield) as a brown oil.

^{1}H NMR (250 MHz, $CDCl_3$) δ 7.56 (dt, *J* = 7.8, 1.0 Hz, 1H), 7.45 (s, 1H), 7.35 – 7.29 (m, 1H), 7.25 (ddd, *J* = 8.0, 6.7, 1.4 Hz, 1H), 7.14 (ddd, *J* = 8.0, 6.7, 1.4 Hz, 1H), 6.74 (s, 1H), 4.18 (t, *J* = 7.2 Hz, 2H), 3.73 (s, 3H), 3.17 (t, *J* = 7.3 Hz, 2H), 2.23 (s, 3H).

^{13}C NMR (63 MHz, $CDCl_3$) δ 137.2, 136.5, 136.0, 127.4, 122.04, 122.00, 119.3, 118.4, 109.7, 109.5, 100.7, 47.6, 32.8, 26.7, 12.8.

1-(2-(1-Methyl-1*H*-indol-3-yl)ethyl)-1*H*-imidazole-5-carbaldehyde (**66n**):

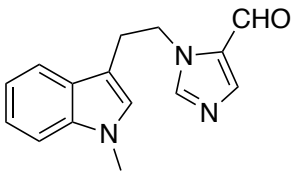

According to GP8, 3 1-(2-(1*H*-indol-3-yl)ethyl)-1*H*-imidazole-5-carbaldehyde (61 mg, 0.26 mmol, 1 equiv), NaH (60 %) (12 mg, 0.31 mmol, 1.2 equiv) and MeI (19μL, 0.31 mmol, 1.2 equiv) in dry DMF (1.3 mL) provided, after column chromatography 95:5 DCM:MeOH, the desired product **66n** (36.7 mg, 56 % yield) as a beige solid.

^{1}H NMR (250 MHz, $CDCl_3$) δ 9.81 (s, 1H), 7.84 – 7.78 (m, 1H), 7.61 (dt, *J* = 7.7, 1.0 Hz, 1H), 7.33 – 7.28 (m, 2H), 7.25 (ddd, *J* = 8.0, 6.6, 1.5 Hz, 1H), 7.14 (ddd, *J* = 8.0, 6.6, 1.5 Hz, 1H), 4.55 (t, *J* = 6.9 Hz, 2H), 3.71 (s, 3H), 3.19 (td, *J* = 6.9, 0.7 Hz, 2H).

^{13}C NMR (63 MHz, $CDCl_3$) δ 179.6, 144.3, 144.2, 137.5, 127.8, 127.7, 127.1, 122.3, 119.6, 118.9, 110.0, 109.9, 48.4, 33.1, 27.3.

1-(2-(1-Methyl-1*H*-indol-3-yl)ethyl)-1*H*-imidazole-4-carbaldehyde **66n'**:

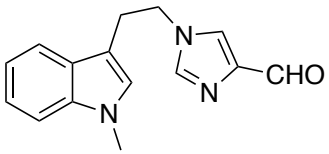

According to GP8, 3-(2-(1*H*-imidazol-1-yl)ethyl)-1*H*-indole (56 mg, 0.24 mmol, 1 equiv), NaH (60 %) (11 mg, 0.28 mmol, 1.2 equiv) and MeI (18 μL, 0.28 mmol, 1.2 equiv) in dry DMF (1.2 mL) provided, after column chromatography 95:5 DCM:MeOH, the desired product **66n'** (33 mg, 54 % yield) as a light brown solid.

^{1}H NMR (250 MHz, $CDCl_3$) δ 9.83 (s, 1H), 7.58 – 7.45 (m, 2H), 7.41 – 7.30 (m, 2H), 7.27 – 7.22 (m, 1H), 7.14 (ddd, *J* = 8.0, 6.7, 1.4 Hz, 1H), 6.62 (d, *J* = 3.6 Hz, 1H), 4.27 (dt, *J* = 8.5, 6.7 Hz, 2H), 3.71 (d, *J* = 1.6 Hz, 3H), 3.28 – 3.16 (m, 2H).

^{13}C NMR (63 MHz, $CDCl_3$) δ 186.30, 142.90, 142.36, 138.93, 127.47, 122.25, 119.51, 119.44, 118.25, 118.21, 109.83, 109.17, 48.46, 32.84, 27.56.

1-Methyl-3-(2-(4-phenyl-1*H*-imidazol-1-yl)ethyl)-1*H*-indole (**66o'**)**:**

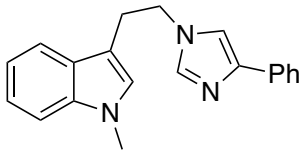

According to GP8, 3-(2-(4-phenyl-1*H*-imidazol-1-yl)ethyl)-1*H*-indole (157 mg, 0.55 mmol, 1 equiv), NaH (60 %) (26 mg, 0.65 mmol, 1.2 equiv) and MeI (41 μL, 0.65 mmol, 1.2 equiv) in dry DMF (2.75 mL) provided, after column chromatography 95:5 DCM:MeOH, the desired product **66o'** (52 mg, 31 % yield) as an orange oil.

^{1}H NMR (400 MHz, $CDCl_3$) δ 7.79 – 7.72 (m, 2H), 7.59 – 7.54 (m, 1H), 7.40 – 7.30 (m, 4H), 7.27 (d, *J* = 8.8 Hz, 1H), 7.25 – 7.20 (m, 1H), 7.19 – 7.11 (m, 2H), 6.66 (s, 1H), 4.23 (t, *J* = 7.0 Hz, 2H), 3.71 (s, 3H), 3.24 (t, *J* = 6.9 Hz, 2H).

^{13}C NMR (101 MHz, $CDCl_3$) δ 142.2, 137.5, 137.2, 134.5, 128.7, 127.4, 127.3, 126.8, 124.8, 122.0, 119.3, 118.4, 114.8, 110.0, 109.6, 48.0, 32.8, 27.6.

1-(2-(1-Methyl-1*H*-indol-3-yl)ethyl)-1*H*-benzo[*d*]imidazole (**66p**):

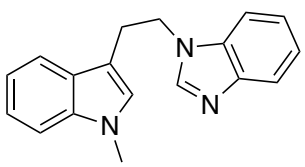

According to GP8, 1-(2-(1-methyl-1*H*-indol-3-yl)ethyl)-1*H*-benzo[*d*]imidazole (144 mg, 0.55 mmol, 1 equiv), NaH (60 %) (26 mg, 0.66 mmol, 1.2 equiv) and MeI (41 μL, 0.66 mmol,

1.2 equiv) in dry DMF (2.75 mL) provided, after column chromatography 95:5 DCM:MeOH, the desired product **66p** (5 mg, 3 % yield) as a beige solid.

^{1}H NMR (400 MHz, $CDCl_3$) δ 7.84 – 7.78 (m, 1H), 7.61 (s, 1H), 7.57 (dt, *J* = 7.9, 1.0 Hz, 1H), 7.44 – 7.37 (m, 1H), 7.34 – 7.28 (m, 3H), 7.27 (d, *J* = 2.5 Hz, 1H), 7.15 (ddd, *J* = 8.0, 6.8, 1.2 Hz, 1H), 6.54 (s, 1H), 4.46 (t, *J* = 6.9 Hz, 2H), 3.67 (s, 3H), 3.32 – 3.26 (m, 2H).

^{13}C NMR (101 MHz, $CDCl_3$) δ 144.0, 143.4, 137.3, 133.8, 127.5, 127.3, 122.9, 122.2, 122.1, 120.5, 119.3, 118.4, 110.1, 109.73, 109.70, 45.9, 32.8, 26.1.

*3.4.8. Synthesis of final indole-imidazole compounds (part 2) (**65**)*

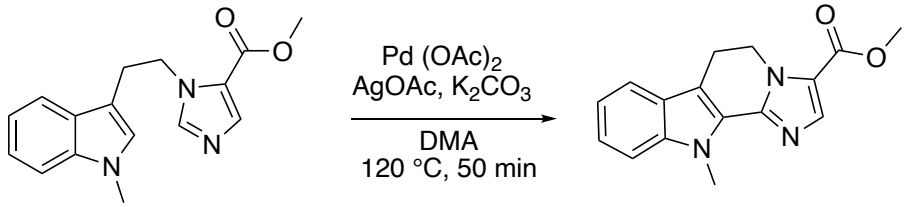

66l **65l**, 28%

According to GP6, the indole-imidazole derivative **66l** (45 mg, 0.16 mmol, 1 equiv), $Pd(OAc)_2$ (4 mg, 0.016 mmol, 10 mol %), AgOAc (80 mg, 0.5 mmol, 3 equiv) and K_2CO_3 (22 mg, 0.16 mmol, 1 equiv) in DMA (1.6 mL, c = 0.1 M) provided, after cyclohexane/ethyl acetate (95:5) column chromatography, the desired compound **65l** (13 mg, yield 28 %) as a white powder.

R_f = 0.4 (9:1 cyclohexane/ethyl acetate)

^{1}H NMR (600 MHz, $CDCl_3$) δ 7.82 (s, 1H), 7.58 (dt, *J* = 8.0, 1.0 Hz, 1H), 7.37 (dt, *J* = 8.0, 0.9 Hz, 1H), 7.32 – 7.28 (m, 1H), 7.17 (ddd, *J* = 8.0, 7.0, 1.0 Hz, 1H), 4.70 (t, *J* = 7.5 Hz, 2H), 4.21 (s, 3H), 3.89 (s, 3H), 3.24 (t, *J* = 7.5 Hz, 2H).

^{13}C NMR (151 MHz, $CDCl_3$) δ 161.2, 144.8, 138.8, 137.6, 126.1, 125.3, 123.5, 122.2, 120.2, 119.3, 111.2, 110.0, 51.7, 43.8, 31.6, 20.8.

HRMS (ESI-Orbitrap, *m*/*z*): calcd for $C_{16}H_{15}N_3O_2$ $[M + H]^+$ 282.1237; found 282.1240

3.5. BIBLIOGRAPHY

1. M. Kitajima, K. Misawa, N. Kogure, et al. A new indole alkaloid, 7-hydroxyspeciociliatine, from the fruits of Malaysian Mitragyna speciosa and its opioid agonistic activity. *J Nat Med* **2006**, 60 (1), 28–35.

2. M. Soledade, C. Pedras, A. Loukaci, F.I. Okanga. The cruciferous phytoalexins brassinin and cyclobrassinin are intermediates in the biosynthesis of brassilexin. *Bioorg Med Chem Lett* **1998**, 8 (21), 3037–3038.

3. W.-M. Yin, X.-B. Cao, S.-X. Li, et al. Brassinin inhibits proliferation and induces cell cycle arrest and apoptosis in nasopharyngeal cancer C666-1 cells. *Arab J Chem* **2022**, 15 (9).

4. M. Kello, D. Drutovic, M. Chripkova, et al. ROS-Dependent Antiproliferative Effect of Brassinin Derivative Homobrassinin in Human Colorectal Cancer Caco2 Cells. *Molecules* **2014**, 19 (8), 10877–10897.

5. T. Hong, J. Ham, J. Song, G. Song, W. Lim. Brassinin Inhibits Proliferation in Human Liver Cancer Cells via Mitochondrial Dysfunction. *Cells* **2021**, 10 (2), 332.

6. R.G. Mehta, J. Liu, A. Constantinou, et al. Cancer chemopreventive activity of brassinin, a phytoalexin from cabbage. *Carcinogenesis* **1995**, 16 (2), 399–404.

7. M.S.C. Pedras, M.G. Sarwar, M. Suchy, A.M. Adio. The phytoalexins from cauliflower, caulilexins A, B and C: Isolation, structure determination, syntheses and antifungal activity. *Phytochemistry* **2006**, 67 (14), 1503–1509.

8. N. Mexia, G. Gaitanis, A. Velegraki, et al. Pityriazepin and other potent AhR ligands isolated from Malassezia furfur yeast. *Arch Biochem Biophys* **2015**, 571, 16–20.

9. K.H. Kim, K.M. Park, S.U. Choi, K.R. Lee. Macrolepiotin, a new indole alkaloid from Macrolepiota neomastoidea. *J Antibiotics* **2009**, 62 (6), 335–338.

10. L.S. Mulwa, R. Jansen, D.F. Praditya, et al. Six Heterocyclic Metabolites from the Myxobacterium Labilithrix luteola. *Molecules* **2018**, 23 (3).

11. Q. Fang, F. Maglangit, M. Mugat, et al. Targeted Isolation of Indole Alkaloids from Streptomyces sp. CT37. *Molecules* **2020**, 25 (5), 1108.

12. S.M. Creed, A.M. Gutridge, M.D. Argade, et al. Isolation and Pharmacological Characterization of Six Opioidergic Picralima nitida Alkaloids. *J Nat Prod* **2021**, 84 (1), 71–80.

13. M.F. Abo-Ashour, W.M. Eldehna, R.F. George, et al. Novel indole-thiazolidinone conjugates: Design, synthesis and whole-cell phenotypic evaluation as a novel class of antimicrobial agents. *Eur J Med Chem* **2018**, 160, 49–60.

14. Y.D. Mane, Y.P. Sarnikar, S.M. Surwase, et al. Design, synthesis, and antimicrobial activity of novel 5-substituted indole-2-carboxamide derivatives. *Res Chem Interm* **2017**, 43 (2), 1253–1275.

15. B.P. Yadav, I. Ahmad, M. Thakur. Synthesis of some novel indole derivatives aspotential antibacterial, antifungaland antimalarial agents. *IOSR-PHR* **2016**, 6, 27–33.

16. S. Dadashpour, S. Emami. Indole in the target-based design of anticancer agents: A versatile scaffold with diverse mechanisms. *Eur J Med Chem* **2018**, 150, 9–29.

17. D.M. Corigliano, R. Syed, S. Messineo, et al. Indole and 2,4-Thiazolidinedione conjugates as potential anticancer modulators. *PeerJ* **2018**, 2018 (8), e5386.

18. B. Prakash, A. Amuthavalli, D. Edison, M.S. Sivaramkumar, R. Velmurugan. Novel indole derivatives as potential anticancer agents: Design, synthesis and biological screening. *Med Chem Res* **2018**, 27 (1), 321–331.

19. Z. Bakherad, M. Safavi, A. Fassihi, et al. Anti-cancer, anti-oxidant and molecular docking studies of thiosemicarbazone indole-based derivatives. *Res Chem Interm* **2019**, 45 (5), 2827–2854.

20. M.Z. Zhang, C.Y. Jia, Y.C. Gu, et al. Synthesis and antifungal activity of novel indole-replaced streptochlorin analogues. *Eur J Med Chem* **2017**, 126, 669–674.

21. G. Xu, J. Zhao, Y. Jiang, P. Zhang, W. Li. Design, Synthesis and Antifungal Activity of Novel Indole Derivatives Linked with the 1,2,3-Triazole Moiety via the CuAAC Click Reaction. *J Chem Res* **2016**, 40 (5), 269–272.

22. K. Haj Mohammad Ebrahim Tehrani, V. Mashayekhi, P. Azerang, et al. Synthesis and Antimycobacterial Activity of Novel Thiadiazolylhydrazones of 1-Substituted Indole-3-carboxaldehydes. *Chem Biol Drug Des* **2014**, 83 (2), 224–236.

23. G.A. Khan, J.A. War, A. Kumar, et al. A facile synthesis of novel indole derivatives as potential antitubercular agents. *JTUSCI* **2017**, 11 (6), 910–921.

24. A. Dogamanti, P. Chiranjeevi, V.K. Aamate, et al. Indole-fused spirochromenes as potential anti-tubercular agents: design, synthesis and in vitro evaluation. *Mol Divers* **2021**, 25 (4), 2137–2148.

25. M. Scuotto, R. Abdelnabi, S. Collarile, et al. Discovery of novel multi-target indole-based derivatives as potent and selective inhibitors of chikungunya virus replication. *Bioorg Med Chem* **2017**, 25 (1), 327–337.

26. S. Musella, V. di Sarno, T. Ciaglia, et al. Identification of an indol-based derivative as potent and selective varicella zoster virus (VZV) inhibitor. *Eur J Med Chem* **2016**, 124, 773–781.

27. G. Sanna, S. Madeddu, G. Giliberti, et al. Synthesis and Biological Evaluation of Novel Indole-Derived Thioureas. *Molecules* **2018**, 23 (10), 2554.

28. S.A. Santos, A.K. Lukens, L. Coelho, et al. Exploring the 3-piperidin-4-yl-1H-indole scaffold as a novel antimalarial chemotype. *Eur J Med Chem* **2015**, 102, 320–333.

29. S. Porwal, S. Gupta, P.M.S. Chauhan. gem-Dithioacetylated indole derivatives as novel antileishmanial agents. *Bioorg Med Chem Lett* **2017**, 27 (20), 4643–4646.

30. M.B. Félix, E.R. de Souza, M. do C.A. de Lima, et al. Antileishmanial activity of new thiophene–indole hybrids: Design, synthesis, biological and cytotoxic evaluation, and chemometric studies. *Bioorg Med Chem* **2016**, 24 (18), 3972–3977.

31. R. Sharma, A.K. Pandey, R. Shivahare, et al. Triazino indole–quinoline hybrid: A novel approach to antileishmanial agents. *Bioorg Med Chem Lett* **2014**, 24 (1), 298–301.

32. S. Tiwari, S. Kirar, U.C. Banerjee, et al. Synthesis of N-substituted indole derivatives as potential antimicrobial and antileishmanial agents. *Bioorg Chem* **2020**, 99, 103787.

33. B. Forte, B. Malgesini, C. Piutti, et al. A Submarine Journey: The Pyrrole-Imidazole Alkaloids. *Mar Drugs* **2009**, 7 (4), 705–753.

34. S.M. Weinreb. Some recent advances in the synthesis of polycyclic imidazole-containing marine natural products. *Nat Prod Rep* **2007**, 24 (5), 931–948.

35. D. Bialonska, J.K. Zjawiony. Aplysinopsins - Marine Indole Alkaloids: Chemistry, Bioactivity and Ecological Significance. *Mar Drugs* **2009**, 7 (2), 166–183.

36. D. Tasdemir, B. Topaloglu, R. Perozzo, et al. Marine natural products from the Turkish sponge Agelas oroides that inhibit the enoyl reductases from Plasmodium falciparum, Mycobacterium tuberculosis and Escherichia coli. *Bioorg Med Chem* **2007**, 15 (21), 6834–6845.

37. S. Tilvi, C. Moriou, M.T. Martin, et al. Agelastatin E, agelastatin F, and benzosceptrin C from the marine sponge agelas dendromorpha. *J Nat Prod* **2010**, 73 (4), 720–723.

38. C. Vergne, J. Appenzeller, C. Ratinaud, et al. Debromodispacamides B and D: Isolation from the marine sponge Agelas mauritiana and stereoselective synthesis using a biomimetic proline route. *Org Lett* **2008**, 10 (3), 493–496.

39. R.A. Davis, G.A. Fechner, M. Sykes, et al. (–)-Dibromophakellin: An α2B adrenoceptor agonist isolated from the Australian marine sponge, Acanthella costata. *Bioorg Med Chem* **2009**, 17 (6), 2497–2500.

40. T. Hertiani, R.A. Edrada-Ebel, S. Ortlepp, et al. From anti-fouling to biofilm inhibition: New cytotoxic secondary metabolites from two Indonesian Agelas sponges. *Bioorg Med Chem* **2010**, 18 (3), 1297–1311.

41. S. Tsukamoto, T. Kawabata, H. Kato, et al. Naamidines H and I, cytotoxic imidazole alkaloids from the Indonesian marine sponge Leucetta chagosensis. *J Nat Prod* **2007**, 70 (10), 1658–1660.

42. D.S. Ermolat'ev, V.L. Alifanov, V.B. Rybakov, E. V. Babaev, E. V. Van Der Eycken. A Concise Microwave-Assisted Synthesis of 2-Aminoimidazole Marine Sponge Alkaloids of the Isonaamines Series. *Synthesis* **2008**, 2008 (13), 2083–2088.

43. F. Carreaux, J. Pierre Bazureau, M. Debdab, et al. An Efficient Method for the Preparation of New Analogs of Leucettamine B under Solvent-Free Microwave Irradiation. *Heterocycles* **2009**, 78 (5), 1191.

44. M. Nodwell, J.L. Riffell, M. Roberge, R.J. Andersen. Synthesis of antimitotic analogs of the microtubule stabilizing sponge alkaloid ceratamine A. *Org Lett* **2008**, 10 (6), 1051–1054.

45. M.D. Markey, T.R. Kelly. Synthesis of cribrostatin 6. *J Org Chem* **2008**, 73 (19), 7441–7443.

46. S. Murayama, Y. Nakao, S. Matsunaga. Asteropterin, an inhibitor of cathepsin B, from the marine sponge Asteropus simplex. *Tetrahedron Lett* **2008**, 49 (26), 4186–4188.

47. D. Mori, Y. Kimura, S. Kitamura, et al. Spongolactams, farnesyl transferase inhibitors from a marine sponge: Isolation through an LC/MS-guided assay, structures, and semisyntheses. *J Org Chem* **2007**, 72 (19), 7190–7198.

48. S. Deslandes, S. Chassaing, E. Delfourne. Marine Pyrrolocarbazoles and Analogues: Synthesis and Kinase Inhibition. *Mar Drugs* **2009**, 7 (4), 754–786.

49. M. Iwatsuki, R. Uchida, H. Yoshijima, et al. Guadinomines, Type III Secretion System Inhibitors, Produced by Streptomyces sp. K01-0509. *J Antibiot* **2008**, 61 (4), 222–229.

50. N. Shangguan, M.M. Joullié. Total synthesis of isoroquefortine E and phenylahistin. *Tetrahedron Lett* **2009**, 50 (49), 6755–6757.

51. H. Kim, M.Y. Kim, J. Tae. Concise asymmetric total synthesis of ent -guadinomic acid from an epoxy alkenol. *Synlett* **2009**, 2009 (18), 2949–2952.

52. P.H. Chuang, P.W. Hsieh, Y.L. Yang, et al. Cyclopeptides with anti-inflammatory activity from seeds of Annona montana. *J Nat Prod* **2008**, 71 (8), 1365–1370.

53. B.T.Y. Li, J.M. White, C.A. Hutton. Synthesis of the Leu–Trp Component of the Celogentin Family of Cyclic Peptides Through a C–H Activation–Cross-Coupling Strategy. *Aust J Chem* **2010**, 63 (3), 438–444.

54. G.M. Cragg, P.G. Grothaus, D.J. Newman. Impact of natural products on developing new anti-cancer agents. *Chem Rev* **2009**, 109 (7), 3012–3043.

55. S. Baroniya, Z. Anwer, P. Sharma, R. Dudhe, N. Kumar. Recent advancement in imidazole as anti cancer agents: A review. *Der Pharmacia Sinica* **2010**, 1, 172–182.

56. Q.Y. Li, X.Q. Deng, Y.G. Zu, et al. Cytotoxicity and Topo I targeting activity of substituted 10--nitrogenous heterocyclic aromatic group derivatives of SN-38. *Eur J Med Chem* **2010**, 45 (7), 3200–3206.

57. Q. Li, H. Lv, Y. Zu, et al. Synthesis and antitumor activity of novel 20s-camptothecin analogues. *Bioorg Med Chem Lett* **2009**, 19 (2), 513–515.

58. S.M. Sondhi, J. Singh, R. Rani, et al. Synthesis, anti-inflammatory and anticancer activity evaluation of some novel acridine derivatives. *Eur J Med Chem* **2010**, 45 (2), 555–563.

59. W.-T. Li, D.-R. Hwang, J.-S. Song, et al. Synthesis and Biological Activities of 2-Amino-1-arylidenamino Imidazoles as Orally Active Anticancer Agents. *J. Med. Chem* **2010**, 53, 2409.

60. B. Zhai, X. Lin. Recent Progress on Antifungal Drug Development. *Curr Pharm Biotechnol* **2011**, 12 (8), 1255–1262.

61. M.K. Kathiravan, A.B. Salake, A.S. Chothe, et al. The biology and chemistry of antifungal agents: A review. *Bioorg Med Chem* **2012**, 20 (19), 5678–5698.

62. D. De Vita, L. Scipione, S. Tortorella, et al. Synthesis and antifungal activity of a new series of 2-(1H-imidazol-1-yl)-1-phenylethanol derivatives. *Eur J Med Chem* **2012**, 49, 334–342.

63. M.N. Aboul-Enein, A.A.E.S. El-Azzouny, M.I. Attia, O.A. Saleh, A.L. Kansoh. Synthesis and Anti-Candida Potential of Certain Novel 1-[(3-Substituted-3-phenyl)propyl]-1H-imidazoles. *Arch Pharm* **2011**, 344 (12), 794–801.

64. B. Lakshmanan, P. Mitra Mazumder, D. Sasmal, S. Ganguly. Biologically Active Azoles: Synthesis, Characterization and Antimicrobial Activity of Some 1-substituted imidazoles. *Pharm Lett* **2010**, 2 (4), 82–89.

65. T. Hussain, H.L. Siddiqui, M. Zia-ur-Rehman, M. Masoom Yasinzai, M. Parvez. Anti-oxidant, anti-fungal and anti-leishmanial activities of novel 3-[4-(1H-imidazol-1-yl) phenyl]prop-2-en-1-ones. *Eur J Med Chem* **2009**, 44 (11), 4654–4660.

66. S. Khabnadideh, Z. Rezaci, A. Khalafi Nezhad, M. Motazedian, M. Eskandari. Synthesis of metronidazole derivatives as antigiardiasis agents. **2007**, 15 (1), 17–20.

67. G.L.V. Damu, Q. Wang, H. Zhang, et al. A series of naphthalimide azoles: Design, synthesis and bioactive evaluation as potential antimicrobial agents. *Sci China Chem* **2013**, 56 (7), 952–969.

68. F.F. Zhang, L.L. Gan, C.H. Zhou. Synthesis, antibacterial and antifungal activities of some carbazole derivatives. *Bioorg Med Chem Lett* **2010**, 20 (6), 1881–1884.

69. D. Sharma, B. Narasimhan, P. Kumar, et al. Synthesis, antimicrobial and antiviral evaluation of substituted imidazole derivatives. *Eur J Med Chem* **2009**, 44 (6), 2347–2353.

70. B.F. Abdel-Wahab, G.E.A. Awad, F.A. Badria. Synthesis, antimicrobial, antioxidant, anti-hemolytic and cytotoxic evaluation of new imidazole-based heterocycles. *Eur J Med Chem* **2011**, 46 (5), 1505–1511.

71. S. Pattan, N. Dighe, C. Hariprasad, et al. Synthesis and evaluation of some new 6-fluro-quinolin-4 (1H)-one derivatves for their anti-microbial activities. *JPSR* **2009**, 1.

72. C.K. Stover, P. Warrener, D.R. VanDevanter, et al. A small-molecule nitroimidazopyran drug candidate for the treatment of tuberculosis. *Nature* **2000**, 405 (6789), 962–966.

73. C. H. S. Lima, M. G. M. O. Henriques, A. L. P. Candea, et al. Synthesis and antimycobacterial evaluation of N'-(E)-heteroaromaticpyrazine-2-carbohydrazide derivatives. *Med Chem* **2011**, 7 (3), 245–249.

74. E. Tiligada, E. Zampeli, K. Sander, H. Stark. Histamine H3 and H4 receptors as novel drug targets. *Expert Opin Investig Drugs* **2009**, 18 (10), 1519–1531.

75. H. G. Bhatt, Y. K. Agrawal, H. G. Raval, K. Manna, P. R. Desai. Histamine H4 receptor: a novel therapeutic target for immune and allergic responses. *Mini Rev Med Chem* **2010**, 10 (14), 1293–1308.

76. D. Łazewska, M. Wiecek, X. Ligneau, et al. Histamine H3 and H4 receptor affinity of branched 3-(1H-imidazol-4-yl)propyl N-alkylcarbamates. *Bioorg Med Chem Lett* **2009**, 19 (23), 6682–6685.

77. M. Broderick, T. Masri. Histamine H(3) receptor (H(3)R) antagonists and inverse agonists in the treatment of sleep disorders. *Curr Pharm Des* **2011**, 17 (15), 1426–1429.

78. S. Hack, B. Wörlein, G. Höfner, J. Pabel, K.T. Wanner. Development of imidazole alkanoic acids as mGAT3 selective GABA uptake inhibitors. *Eur J Med Chem* **2011**, 46 (5), 1483–1498.

79. G. Galley, H. Stalder, A. Goergler, M.C. Hoener, R.D. Norcross. Optimisation of imidazole compounds as selective TAAR1 agonists: Discovery of RO5073012. *Bioorg Med Chem Lett* **2012**, 22 (16), 5244–5248.

80. R. Drew. Pharmacology of Azole Antifungal Agents. *Antifungal Therapy* **2016**, 209–228.

81. U. Caliş, E. Septioğlu, M.D. Aytemir. Synthesis and anticonvulsant evaluation of some novel (thio)semicarbazone derivatives of arylalkylimidazole. *Arzneimittelforschung* **2011**, 61 (6), 327–334.

82. A. Karakurt, M. Özalp, Ş. Işik, J.P. Stables, S. Dalkara. Synthesis, anticonvulsant and antimicrobial activities of some new 2-acetylnaphthalene derivatives. *Bioorg Med Chem* **2010**, 18 (8), 2902–2911.

83. M.A. Brodney, D.D. Auperin, S.L. Becker, et al. Design, synthesis, and in vivo characterization of a novel series of tetralin amino imidazoles as γ-secretase inhibitors: Discovery of PF-3084014. *Bioorg Med Chem Lett* **2011**, 21 (9), 2637–2640.

84. M.A. Brodney, D.D. Auperin, S.L. Becker, et al. Diamide amino-imidazoles: A novel series of γ-secretase inhibitors for the treatment of Alzheimer's disease. *Bioorg Med Chem Lett* **2011**, 21 (9), 2631–2636.

85. Y. Sugimoto, K. Kobayashi, M. Asai, et al. Synthesis and biological evaluation of imidazole derivatives as novel NOP/ORL1 receptor antagonists: Exploration and optimization of alternative pyrazole structure. *Bioorg Med Chem Lett* **2009**, 19 (16), 4611–4616.

86. J. Prasad, M.B. Pathak, S.K. Panday. An efficient and straight forward synthesis of (5S)-1-benzyl-5-(1H- imidazol-1-ylmethyl)-2-pyrrolidinone (MM1): A novel antihypertensive agent. *Med Chem Res* **2012**, 21 (3), 321–324.

87. G. Agelis, A. Resvani, S. Durdagi, et al. The discovery of new potent non-peptide Angiotensin II AT1 receptor blockers: A concise synthesis, molecular docking studies and biological evaluation of N-substituted 5-butylimidazole derivatives. *Eur J Med Chem* **2012**, 55, 358–374.

88. G. García, I. Serrano, P. Sánchez-Alonso, et al. New losartan-hydrocaffeic acid hybrids as antihypertensive-antioxidant dual drugs: Ester, amide and amine linkers. *Eur J Med Chem* **2012**, 50, 90–101.

89. F. Hadizadeh, M. Imenshahidi, P. Esmaili, M. Taghiabadi. Synthesis and Effects of Novel Dihydropyridines as Dual Calcium Channel Blocker and Angiotensin Antagonist on Isolated Rat Aorta. *Iran J Basic Med Sci* **2010**, 13 (1), 195–201.

90. A. Husain, S. Drabu, N. Kumar. Synthesis and biological screening of di- and trisubstituted imidazoles. *Acta Pol Pharm* **2009**, 66 (3), 243–248.

91. Y.J. Ren, F.H. Wu, C.F. Shu, M. Liu. Synthesis and Potent Biological Activity of 1-Sulfonyl Substituted Imidazole and Benzo[d]imidazole Compounds. *Adv Mat Res* **2011**, 236–238, 2570–2573.

92. R.L. Dow, J.R. Hadcock, D.O. Scott, et al. Bioisosteric replacement of the hydrazide pharmacophore of the cannabinoid-1 receptor antagonist SR141716A. Part I: Potent, orally-active 1,4-disubstituted imidazoles. *Bioorg Med Chem Lett* **2009**, 19 (18), 5351–5354.

93. J. Liu, S. He, T. Jian, et al. Synthesis and SAR of derivatives based on 2-biarylethylimidazole as bombesin receptor subtype-3 (BRS-3) agonists for the treatment of obesity. *Bioorg Med Chem Lett* **2010**, 20 (7), 2074–2077.

94. S. He, P.H. Dobbelaar, J. Liu, et al. Discovery of substituted biphenyl imidazoles as potent, bioavailable bombesin receptor subtype-3 agonists. *Bioorg Med Chem Lett* **2010**, 20 (6), 1913–1917.

95. T.G. Edwards, K.J. Koeller, U. Slomczynska, et al. HPV episome levels are potently decreased by pyrrole–imidazole polyamides. *Antiviral Res* **2011**, 91 (2), 177–186.

96. A. Basu, K. Jasu, V. Jayaprakash, et al. Development of CoMFA and CoMSIA models of cytotoxicity data of anti-HIV-1-phenylamino-1H-imidazole derivatives. *Eur J Med Chem* **2009**, 44 (6), 2400–2407.

97. E. Hernández-Núñez, H. Tlahuext, R. Moo-Puc, et al. Synthesis and in vitro trichomonicidal, giardicidal and amebicidal activity of N-acetamide(sulfonamide)-2-methyl-4-nitro-1H-imidazoles. *Eur J Med Chem* **2009**, 44 (7), 2975–2984.

98. B.B. Trunz, R. Jdrysiak, D. Tweats, et al. 1-Aryl-4-nitro-1H-imidazoles, a new promising series for the treatment of human African trypanosomiasis. *Eur J Med Chem* **2011**, 46 (5), 1524–1535.

99. M. Sánchez-Moreno, A.M. Sanz, F. Gómez-Contreras, et al. In vivo trypanosomicidal activity of imidazole- or pyrazole-based benzo[g]phthalazine derivatives against acute and chronic phases of chagas disease. *J Med Chem* **2011**, 54 (4), 970–979.

100. J.T. Mesquita, T. Alves Da Costa-Silva, • Samanta, et al. Activity of imidazole compounds on Leishmania (L.) infantum chagasi: reactive oxygen species induced by econazole. *Mol Cell Biochem* **2014**, 389 (1-2), 293-300.

101. Á. Martín-Montes, K. Kolodová, C. Marín, et al. In vitro Leishmanicidal and Trypanosomicidal Properties of Imidazole-Containing Azine and Benzoazine Derivatives. *ChemMedChem* **2021**, 16 (23), 3600–3614.

102. K. Bhandari, N. Srinivas, V.K. Marrapu, et al. Synthesis of substituted aryloxy alkyl and aryloxy aryl alkyl imidazoles as antileishmanial agents. *Bioorg Med Chem Lett* **2010**, 20 (1), 291–293.

103. V.K. Marrapu, M. Mittal, R. Shivahare, S. Gupta, K. Bhandari. Synthesis and evaluation of new furanyl and thiophenyl azoles as antileishmanial agents. *Eur J Med Chem* **2011**, 46 (5), 1694–1700.

104. V.K. Marrapu, N. Srinivas, M. Mittal, et al. Design and synthesis of novel tetrahydronaphthyl azoles and related cyclohexyl azoles as antileishmanial agents. *Bioorg Med Chem Lett* **2011**, 21 (5), 1407–1410.

105. N. Srinivas, S. Palne, Nishi, S. Gupta, K. Bhandari. Aryloxy cyclohexyl imidazoles: A novel class of antileishmanial agents. *Bioorg Med Chem Lett* **2009**, 19 (2), 324–327.

106. M. Dichiara, Q.J. Simpson, A. Quotadamo, et al. Structure-Property Optimization of a Series of Imidazopyridines for Visceral Leishmaniasis. *ACS Infect Dis* **2023**, 9 (8), 1470–1487.

107. A. Dogamanti, P. Chiranjeevi, V.K. Aamate, et al. Indole-fused spirochromenes as potential anti-tubercular agents: design, synthesis and in vitro evaluation. *Mol Divers* **2021**, 25 (4), 2137–2148.

108. B. Jasiewicz, K. Babijczuk, B. Warżajtis, et al. Indole Derivatives Bearing Imidazole, Benzothiazole-2-Thione or Benzoxazole-2-Thione Moieties—Synthesis, Structure and Evaluation of Their Cytoprotective, Antioxidant, Antibacterial and Fungicidal Activities. *Molecules* **2023**, 28 (2), 708.

109. Y. Gao, D.C. Huang, C. Liu, et al. Streptochlorin analogues as potential antifungal agents: Design, synthesis, antifungal activity and molecular docking study. *Bioorg Med Chem* **2021**, 35, 116073.

110. Z.Z. Li, V.K.R. Tangadanchu, N. Battini, et al. Indole-nitroimidazole conjugates as efficient manipulators to decrease the genes expression of methicillin-resistant Staphylococcus aureus. *Eur J Med Chem* **2019**, 179, 723–735.

111. F. Pagniez, H. Abdala-Valencia, P. Marchand, et al. Antileishmanial activities and mechanisms of action of indole-based azoles. *J Enzyme Inhib Med Chem* **2006**, 21 (3), 277–283.

112. A. Diotallevi, L. Scalvini, G. Buffi, et al. Phenotype Screening of an Azole-bisindole Chemical Library Identifies URB1483 as a New Antileishmanial Agent Devoid of Toxicity on Human Cells. *ACS Omega* **2021**, 6 (51), 35699–35710.

113. J.C. Antilla, A. Klapars, S.L. Buchwald. The copper-catalyzed N-arylation of indoles. *J Am Chem Soc* **2002**, 124 (39), 11684–11688.

114. Z.-L. Xu, H.-X. Li, Z.-G. Ren, et al. Cu(OAc)2·H2O-catalyzed N-arylation of nitrogen-containing heterocycles. *Tetrahedron* **2011**, 67 (29), 5282–5288.

115. A. Daina, O. Michielin, V. Zoete. SwissADME: a free web tool to evaluate pharmacokinetics, drug-likeness and medicinal chemistry friendliness of small molecules. *Sci Rep* **2017**, 7 (1), 1–13.

116. K. Kumar Vaitheeswaran, B.K. Gupta, R. Krishnan G, et al. Neuro-leishmaniasis with cauda equina syndrome and cranial nerve palsy: a rare manifestation of recurrent atypical visceral leishmaniasis. *BMC Infect Dis* **2024**, 24 (1), 1–8.

117. A.M. Van Leusen, J. Wildeman, O.H. Oldenziel. Chemistry of sulfonylmethyl isocyanides. 12. Base-induced cycloaddition of sulfonylmethyl isocyanides to carbon,nitrogen double bonds. Synthesis of 1,5-disubstituted and 1,4,5-trisubstituted imidazoles from aldimines and imidoyl chlorides. *J Org Chem* **1977**, 42 (7), 1153–1159.

118. The IUPAC Compendium of Chemical Terminology; Gold, V., Ed.; International Union of Pure and Applied Chemistry (IUPAC), Research Triangle Park, NC, **2019**.

119. R.S. Varma. Greener and Sustainable Trends in Synthesis of Organics and Nanomaterials. *ACS Sustain Chem Eng* **2016**, 4 (11), 5866–5878.

120. M. Solares-Briones, G. Coyote-Dotor, J.C. Páez-Franco, et al. Mechanochemistry: A Green Approach in the Preparation of Pharmaceutical Cocrystals. *Pharmaceutics* **2021**, 13 (6), 790.

121. A. De La Hoz, A. Díaz-Ortiz, P. Prieto. Microwave-Assisted Green Organic Synthesis. *Green Chem* **2016**, 2016-January (47), 1–33.

122. R.A. Stockman. Heterocyclic chemistry. *Annual Reports Section "B" (Organic Chemistry)* **2007**, 103 (0), 107–124.

123. T.W. Greulich, C.G. Daniliuc, A. Studer. *N*-Aminopyridinium Salts as Precursors for N-Centered Radicals – Direct Amidation of Arenes and Heteroarenes. *Org Lett* **2015**, 17 (2), 254–257.

124. G.L. Tolnai, S. Ganss, J.P. Brand, J. Waser. C2-Selective Direct Alkynylation of Indoles. *Org Lett* **2013**, 15 (1), 112–115.

125. K.W. Quasdorf, M. Riener, K. V. Petrova, N.K. Garg. Suzuki–Miyaura Coupling of Aryl Carbamates, Carbonates, and Sulfamates. *J Am Chem Soc* **2009**, 131 (49), 17748–17749.

126. J. Xing, G. Chen, P. Cao, J. Liao. Rhodium-Catalyzed Asymmetric Addition of Arylboronic Acids to Indolylnitroalkenes. *European J Org Chem* **2012**, 2012 (6), 1230–1236.

127. H. Wang, D. Liu, H. Chen, J. Li, D.Z. Wang. $CuCl_2$/TBHP-mediated direct chlorooxidation of indoles. *Tetrahedron* **2015**, 71 (38), 7073–7076.

128. D. Liu, Z. Hu, Y. Zhang, et al. Access to Enantioenriched Spiro-*ε*-Lactam Oxindoles by an N-Heterocyclic Carbene-Catalyzed [4+3] Annulation of Flexible Oxotryptamines with Enals. *Chem Eur J* **2019**, 25 (48), 11223–11227.

129. A. V. Lygin, A. de Meijere. Synthesis of 1-Substituted Benzimidazoles from *o* -Bromophenyl Isocyanide and Amines. *European J Org Chem* **2009**, 2009 (30), 5138–5141.

130. C. Liu, Z. Sun, F. Xie, et al. Gold-catalyzed pathway-switchable tandem cycloisomerizations to indolizino[8,7- *b*]indole and indolo[2,3- *a*]quinolizine derivatives. *Chem Com* **2019**, 55 (96), 14418–14421.

131. I.I. Grandberg, N.I. Bobrova. Indoles. *Chem Heterocycl Compd* **1973**, 9 (2), 196–201.

132. M.E. Flaugh, T.A. Crowell, J.A. Clemens, B.D. Sawyer. Synthesis and evaluation of the antiovulatory activity of a variety of melatonin analogs. *J Med Chem* **1979**, 22 (1), 63–69.

133. S. Mantenuto, C. Ciccolini, S. Lucarini, et al. Palladium(II)-Catalyzed Intramolecular Oxidative C–H/C–H Cross-Coupling Reaction of C3,N-Linked Biheterocycles: Rapid Access to Polycyclic Nitrogen Heterocycles. *Org Lett* **2017**, 19 (3), 608–611.

134. A. Geißler, H. Junca, A.M. Kany, et al. Isocyanides inhibit bacterial pathogens by covalent targeting of essential metabolic enzymes. *Chem Sci* **2024**, 15 (30), 11946–11955.

135. P.L. Zhu, Z. Zhang, X.Y. Tang, I. Marek, M. Shi. Gold- and Silver-Catalyzed Intramolecular Cyclizations of Indolylcyclopropenes for the Divergent Synthesis of Azepinoindoles and Spiroindoline Piperidines. *ChemCatChem* **2015**, 7 (4), 595–600.

136. W. Wang, H. Wang, R. Dai, et al. Organocatalytic Deoxyhalogenation of Alcohols with Inorganic Halides. *ACS Catal* **2023**, 13 (13), 9033–9040.

137. V. Iaroshenko, D. Sevenard, D. Volochnyuk, et al. Facile Synthesis of Fluorinated 1-Desazapurines. *Synthesis* **2009**, 2009 (11), 1865–1875.

138. S. Kurhade, A. Rossetti, A. Dömling. Facile Synthesis of N-Substituted Benzimidazoles. *Synthesis* **2016**, 48 (21), 3713–3718.

CHAPTER 4. DESIGN, SYNTHESIS AND BIOLOGICAL EVALUATION OF NEW BISINDOLIC DERIVATIVES AGAINST LEISHMANIASIS

4.1. INTRODUCTION

As mentioned in the previous chapter, indole is a privileged scaffold relevant in medicinal chemistry. Indoles are present in a large number of commercial drugs and natural products. Moreover, the chemistry known for indoles is very explored which allows a significant amount of modifications.

4.1.1. Bisindoles

Bisindole alkaloids represent a class of secondary metabolites biosynthesised by diverse marine and terrestrial organisms. These include nortopsentins, rhopaladins, dragmacidins, vibrindole, arsindolines and topsentins, obtained from marine sponges, tunicates, actinomycetes and green algae.[1] Non-marine natural bisindoles are relatively rare, but there are some examples, such as Streptindole, isolated from human intestinal bacteria *Streptococcus faecium*.[2] (Figure 4.1)

Bisindolic compounds have shown a wide range of biological activities such as anticancer,[3] antibacterial,[4] antileishmanial,[5] anti-inflammatory, analgesic,[6] and antihyperlipidemic activity.[7]

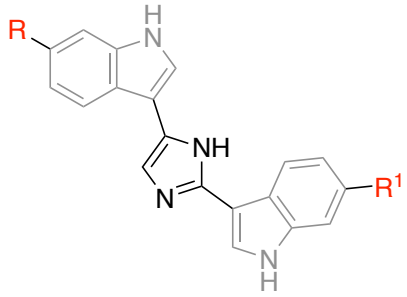

Nortopsentin

A: R = R^1 = Br
B: R = Br R^1 = H
C: R = H R^1 = Br
D: R = R^1 = H

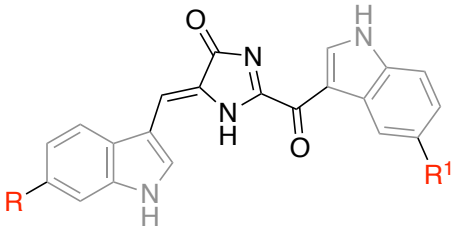

Rhopaladin

A: R = OH R^1 = Br
B: R = OH R^1 = H
C: R = H R^1 = Br
D: R = H R^1 = H

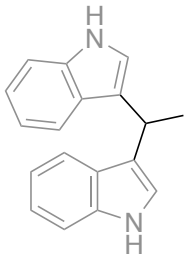

Vibrindole A

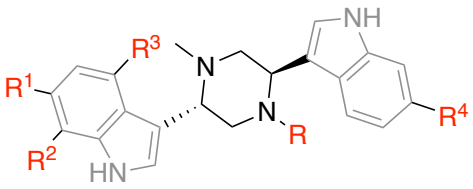

Dragmacidin

Dragmacidin: R = H R^1 = R^2 = Br R^3 = OH R^4 = Br
A: R = H R^1 = Br R^2 = R^3 = H R^4 = Br
B: R = Me R^1 = Br R^2 = R^3 = H R^4 = Br

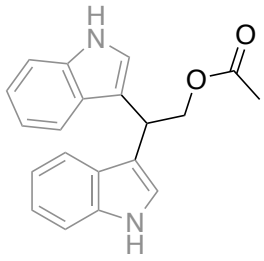

Streptindole

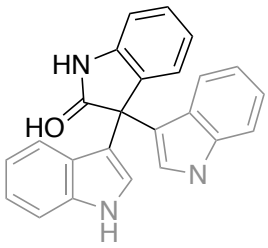

Arsindoline A

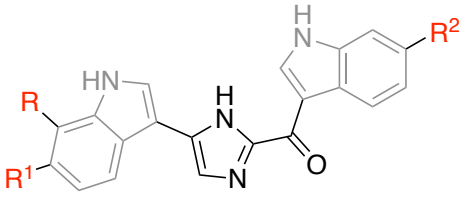

Topsentin: R = R^1 = H R^2 = OH
Bromotopsentin: R = Br R^1 = H R^2 = OH
Deoxytopsentin: R = R^1 = R^2 = H
Bromodeoxytopsentin: R = Br R^1 = R^2 = H
Isobromodeoxytopsentin: R = R^1 = H R^2 = Br

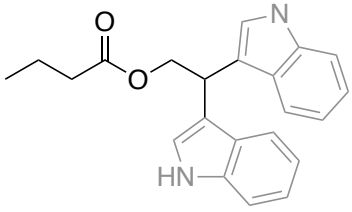

Arsindoline B

Figure 4.1. Structures of bisindoles isolated from natural sources.

4.1.1.1 Diindolylmethane and its derivatives

Diindolylmethane (DIM) is a bioactive compound derived from the metabolization of indole-3-carbinol (I3C) (Figure 4.2), present in diverse types of cruciferous vegetables such as Brussels sprouts, radish, cabbage, cauliflower, broccoli, etc.[8] After the ingestion of these cruciferous vegetables, the acidic environment of the stomach

promotes acidic condensation reactions that form a mixture of biologically active compounds, including DIM.[9]

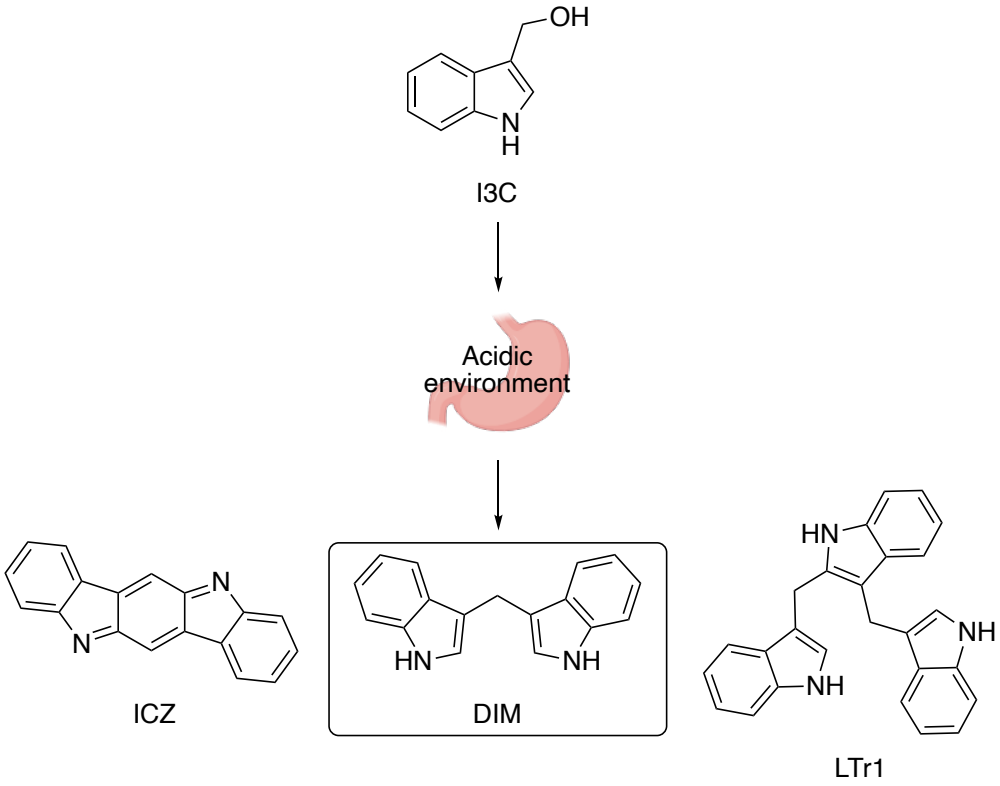

Figure 4.2. Major acid condensation products of I3C in acidic environment: Indolo(3,2-b)carbazole (ICZ), DIM and 3,3′-Diindolylmethane-derived Linear Trimer (LTr1)

DIM has been reported to have different protective effects in multiple physiological systems. In the metabolic context, DIM improves glucose regulation,[10] reduces lipid accumulation[11] and regulates adipocyte differentiation.[12,13]

In the liver, diindolylmethane exhibits hepatoprotective properties by reducing toxin-induced damage, decreasing oxidative stress, and attenuating inflammation, thereby promoting better hepatic function.[14,15]

In the nervous system, DIM has shown neuroprotective potential. It improves recovery in cerebral haemorrhage models, reduces neuroinflammation and promotes neuronal survival under hypoxic conditions.[16,17] Moreover, animal studies have shown analgesic and antidepressant properties.[18]

In addition, DIM has also been shown to be antinociceptive,[19] cardioprotectant,[20] antiplatelet, antithrombotic,[21] antiprotozoal,[22] antibacterial,[23] antiviral,[24] radioprotectant[25] and anti-inflammatory.[26]

Diindolylmethane derivatives also have a wide range of biological activities, such as antioxidant, anticancer, antimicrobial, antiinflammation, antidiabetic, antileishmanial and antihyperlipidemic, among others:

a) Antioxidant

Diindolylmethane derivatives may alleviate oxidative stress while stimulating the expression of the genes that drive the antioxidant response and protect against DNA damage through their antioxidant properties.[27] Some biological studies indicate that these compounds can reduce oxidative stress, and therefore function as antioxidants.[28]

Substituents in the positions 4-7 of the indole ring affect the antioxidant activity of the molecule, suggesting a better activity for electron-donating groups rather than non-substituted and no substitution rather than electron-accepting groups.[27]

b) Anticancer

Anticancer is a well-established pharmacological property of diindolylmethane and its derivatives.[29,30] These compounds act by modulating cancer cell cycle regulation and survival, and diindolylmethanes have been shown to inhibit cancer cell invasion and tumour neoangiogenesis.[29] In breast cancer cells, diindolylmethanes induced apoptosis, while in cultured human umbilical vein endothelial cells, they exhibited a concentration-dependent reduction in migration, proliferation, invasion and capillary tube formation.[31]

Bisindolylmethanes bearing a bromine substituent in position 5 of the indole ring were shown to be more active than non-substituted derivatives.[32]

c) Antimicrobial

The growing problem of antimicrobial resistance demands efforts to identify effective antimicrobial agents against resistant pathogenic microorganisms. Diindolylmethane derivatives containing a pyrazole moiety showed potent activity against three pathogenic microbial strains.[33] Some other derivatives were found to be potent against a broader set of bacterial microbial strains (six Gram-positive and four Gram-negative strains).[34]

Overall, the substitution of these diindolylmethane molecules in the indole ring showed that it reduced the antibacterial activity, while the modification of the methylene carbon, by adding functional groups such as furan, pyridine or sugar, enhanced the antibacterial activity of these molecules.[34]

d) Anti-inflammation

Several diindolylmethanes testedfor anti-inflammatory activity showed significant activity without having ulcerogenic liability.[35,36] Other *p*-phenyl substituted diindolylmethanes were studied for their ability to prevent neuroinflammation.[37]

The results suggested that nitro substitution in *ortho* and *meta* position produced anti-inflammatory activity.

e) Antidiabetic

The effect of diindolylmethanes to suppress diabetes has been widely studied. Some derivatives were studied for their capability to inhibit *β*-glucuronidase, which is believed to be involved in the pathogenesis of atherosclerosis.[38] Other derivatives were able to alter the carbohydrate breakdown in high-fat diet (HFD)-induced mice.[39]

f) Antileishmanial

Diindolylmethane was reported by Roy and colleagues as a potent *Leishmania donovani* topoisomerase I inhibitor. This molecule binds strongly to this enzyme.[22] Further antileishmanial activity of diindolylmethane derivatives will be commented on in the next section.

g) Antihyperlipidemic

Diindolylmethane derivatives bearing a coumarin moiety were found to be potent against hyperlipidemic activity, through reduction of cholesterol and triglycerides and an increase of the high-density lipoprotein cholesterol/triglyceride ratio.[7]

The substitution of the benzopyrone ring seems to play an important role in the activity.[7]

4.1.2. Bisindoles for leishmaniasis

Roy *et al.* studied the antileishmanial activity of DIM, suggesting that this activity could come from the fact that DIM is a class I non-competitive inhibitor of *L. donovani* topoisomerase I.[22] In 2011, they synthesised some DIM derivatives (Figure 4.3), showing antileishmanial activity in DIM-resistant parasites.[40]

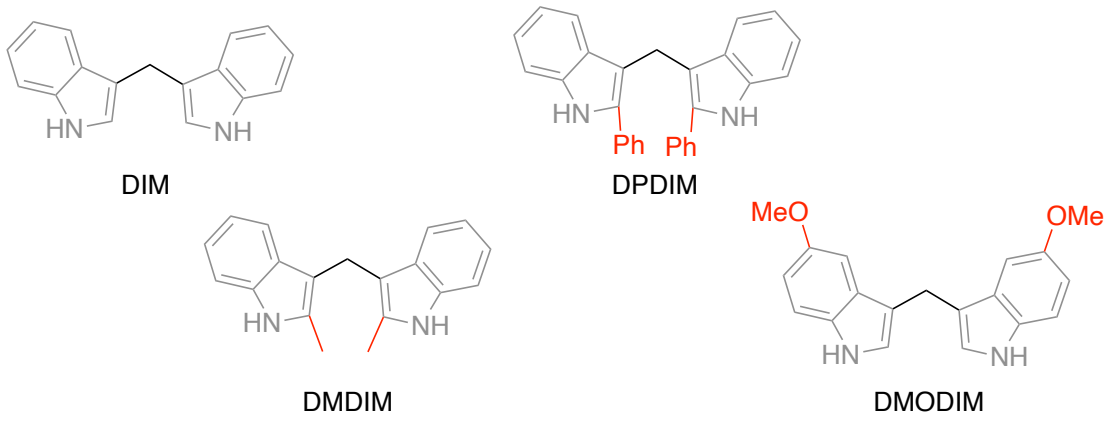

Figure 4.3. DIM and derivatives synthesised by Roy et al.[40]

In 2013, Vishwakarma *et al.*[41] synthesised and evaluated different 5-iodo, 5-methoxy (**81-83**), and non-substituted diindolylmethanes with aromatic or heteroaromatic rings (Figure 4.4) attached directly to the methylene carbon against leishmaniasis. They found that diindolylmethanes substituted with nitro-substituted aromatic or heteroaromatic moieties were the most active.[41]

In 2019, Selvaraj *et al.*[42] synthesised 27 different bisindolic molecules (**84**) (Figure 4.4) and tested them against leishmaniasis, obtaining 15 molecules with excellent inhibitory

potential. From these results, they could establish a structure-activity relationship for these molecules.

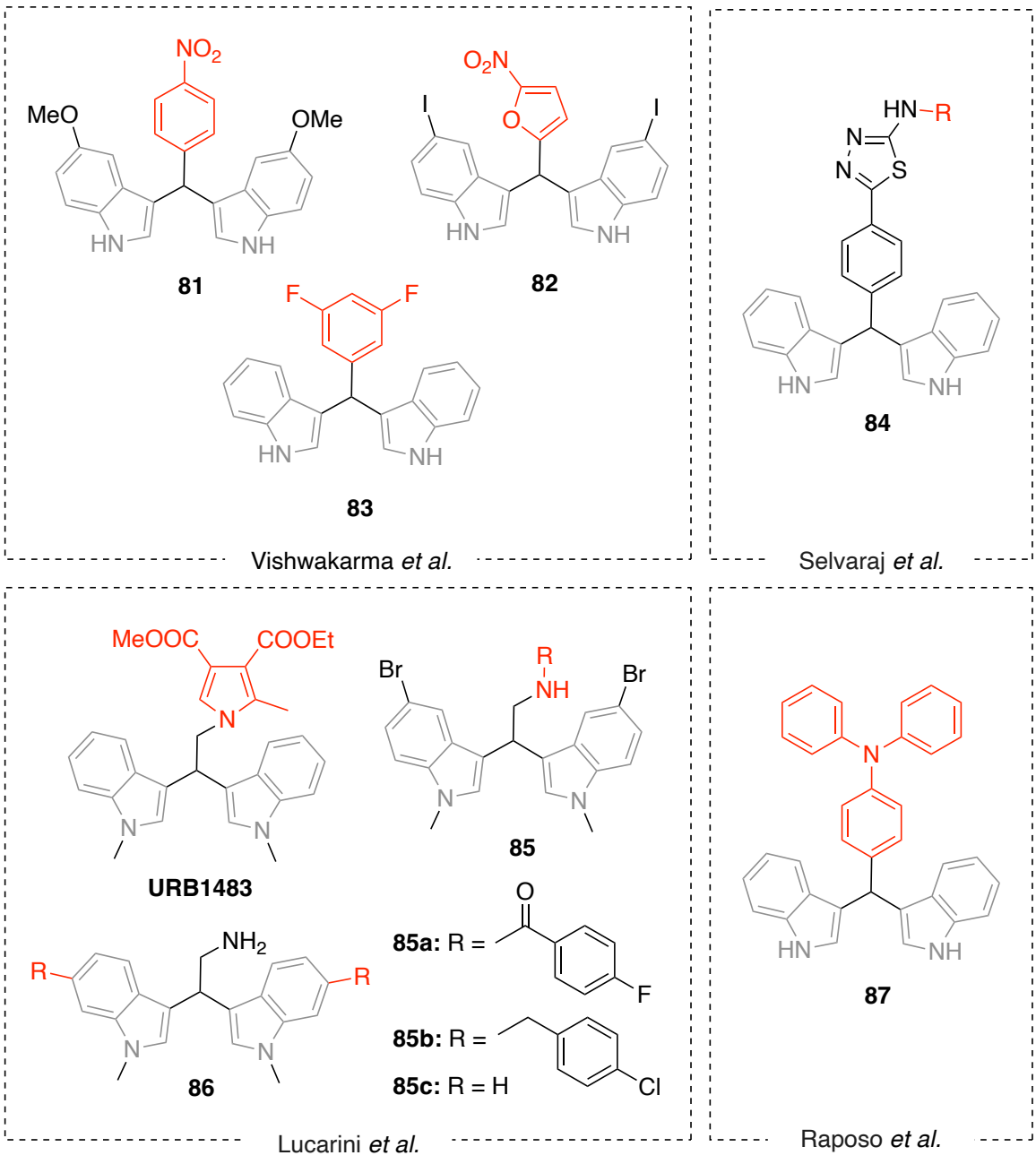

Figure 4.4. Representative examples of bisindoles studied against leishmaniasis.[5,41–45]

In 2021, our group found,[44] through phenotypical evaluation of a small library of azole-bisindole derivatives, 9 molecules with good activity on *L. infantum* MHOM/TN/80/IPT1 promastigotes. From those, URB1483 (Figure 4.4) was chosen as the best compound,

showing no cytotoxicity in mammalian cells and with an effect comparable to that of the commercial drug pentamidine.

Raposo *et al.* reported in 2023,[43] three diindolylmethane molecules (Figure 4.4), from which one (**87**) showed the highest activity of the series against both *T. brucei* and *L. major*, with an IC_{50} of 3.21 μM and 3.30 μM, respectively, and a selectivity index of around 10 for both.

In further studies developed by our group,[5] four classes of diindolylmethane derivatives more hydrophilic than URB1483 were evaluated. Compound **85b** (Figure 4.4) possessed the most active effect against *L. infantum* promastigotes with an IC_{50} of 2.7 μM. It was, however, slightly cytotoxic against human macrophage-like THP-1 cells (CC_{50} = 11.7 μM), indicating low selectivity index (SI ≈ 4). Another noteworthy member of the series is the amide **85a**, which was good in antileishmanial activity (IC_{50} < 10 μM) but was also toxic (CC_{50} = 22 μM). Another bisindole marine alkaloid, compound **85c** was active against *L. infantum* as well, yet also revealed cytotoxicity (CC_{50} < 20 μM). finding that 24 of the 26 molecules analysed were active (**85**) (Figure 4.4).

In 2025, our group developed a late-stage Suzuki-Miyaura functionalization reaction that allowed to synthesise 18 NH_2-diindolylmethane derivatives substituted in the indole ring (Figure 4.4). Most of these molecules (**86**) showed promising activity and selectivity index values.[45]

4.2. OBJECTIVES

The main aim of this part of the work was to design and synthesise new bisindole derivatives as prospective antileishmanial agents. As part of our previous work in the group, we aimed to explore different bisindole families. Particularly, we tried to assess the impact of the ethylene linker between the two indole units since their substitution pattern and length would most likely significantly influence the antiparasitic activity of the related compounds.

4.3. RESULTS AND DISCUSSION

Following previous work developed in the field of bisindoles against leishmaniasis, especially in our group, we could observe that diindolylmethane derivatives bearing a bromine in the indole ring showed higher toxicity. Moreover, we hypothesised that the methyl alkylation in the indole ring would increase the activity of the derivatives. Therefore, we decided to synthesise diindolylmethane derivatives without substituents in the indole ring, focusing mainly in the methylation of the indole nitrogen. We also decided to analyse the effect of the variation of the ethylenic chain on the activity of the molecules by synthesising different families of bisindoles.

4.3.1. Design and synthesis

We synthesised diverse families of bisindoles, including amines, amides, esters and carboxylic acids. (Scheme 4.1)

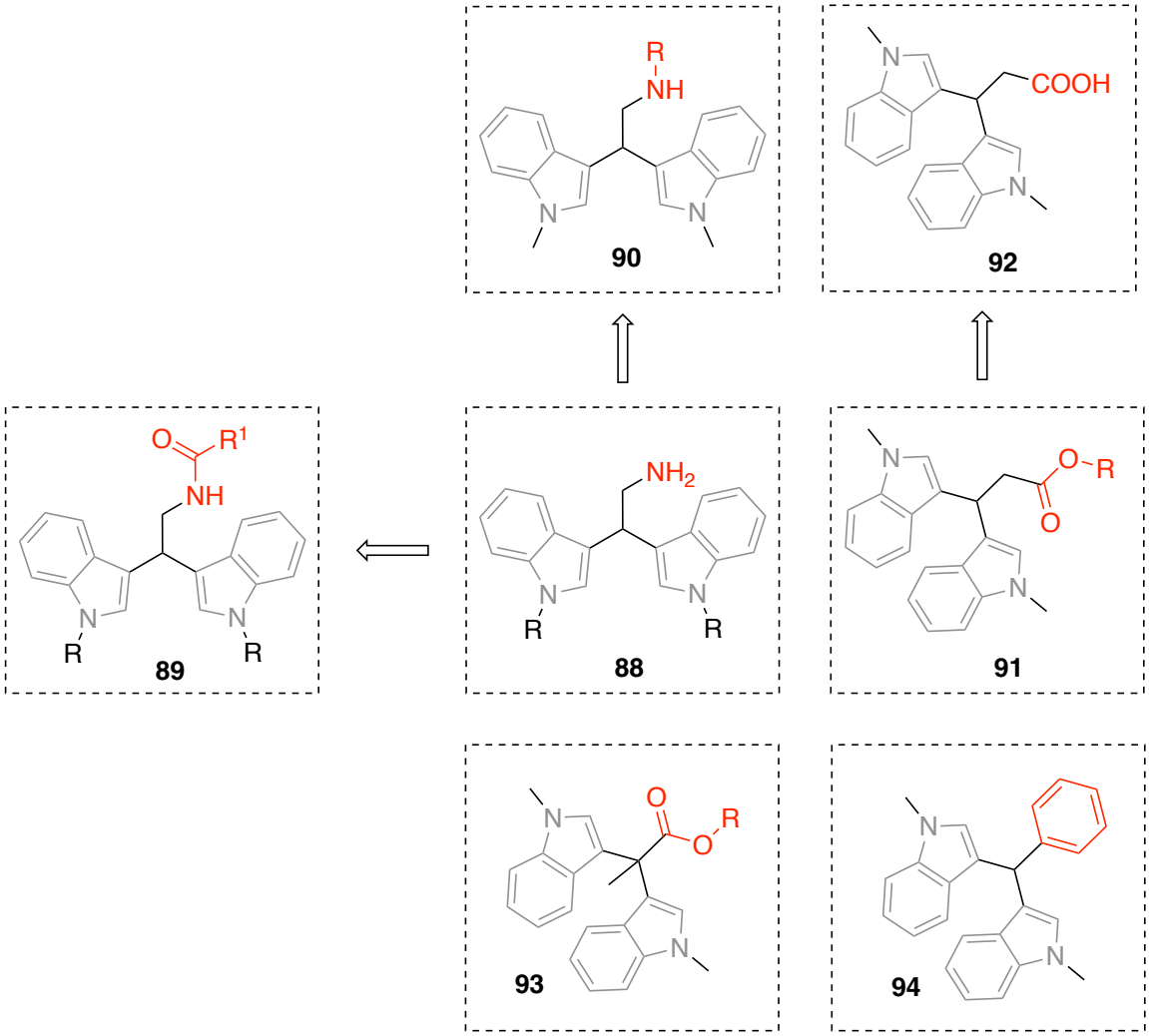

Scheme 4.1. Families of diindolylmethanes synthesised in this chapter.

Multiple synthetic methodologies have been developed for the synthesis of **88**, such as reduction from the nitro derivative with azide,[46] hypophosphites associated with Pd/C,[47] or Zn dust,[48] or heating hydroxytryptamine in a xylene/EtOH (4:1) solution at 130°C for 3 days.[49] However, we decided to use a method previously developed by our group,[50] which involves the formation of a labile amide that undergoes rapid hydrolysis (Scheme 4.2). This method has the advantage of shorter reaction times and requires only one reaction step, as the intermediate of the reaction does not need to be isolated.

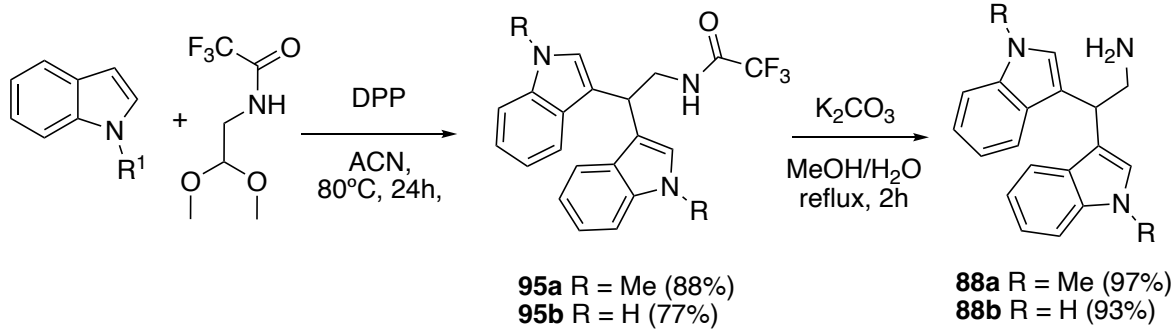

*Scheme 4.2. Synthesis of free amines **88**.*

For the synthesis of the amide derivatives **89**, a traditional amide coupling has been performed between the amines **88** and different carboxylic acids. All the amides were obtained with an excellent yield (Table 4.1), and all, except for **89bb,** were unknown in the literature.

*Table 4.1. Synthesis of amide derivatives **89**.*

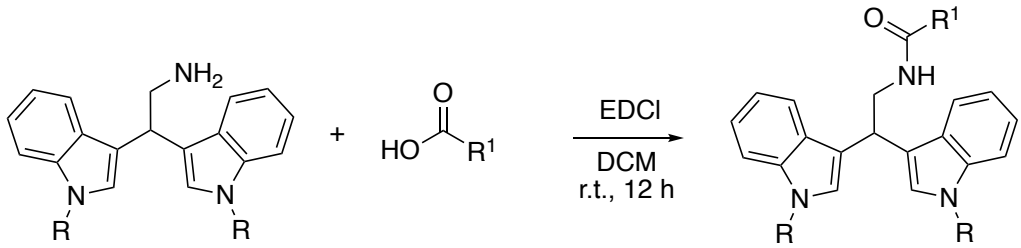

88a R = Me
88b R = H

96a R^1 = i-Pr
96b R^1 = Ph
96c R^1 = 4F-Ph
96d R^1 = 4Cl-Ph
96e R^1 = 4NO_2-Ph
96f R^1 = 4MeO-Ph
96g R^1 = Furane
96h R^1 = Tiophene

89aa R = Me R^1 = i-Pr
89ab R = Me R^1 = Ph
89ac R = Me R^1 = 4F-Ph
89ad R = Me R^1 = 4Cl-Ph
89ae R = Me R^1 = 4NO_2-Ph
89af R = Me R^1 = 4MeO-Ph
89ag R = Me R^1 = Furane
89ah R = Me R^1 = Tiophene
89ba R = H R^1 = i-Pr
89bb R = H R^1 = Ph

Entry	Molecule	R	R^1	Yield (%)
1	**89aa**	Me	i-Pr	84
2	**89ab**	Me	Ph	97
3	**89ac**	Me	4F-Ph	99
4	**89ad**	Me	4Cl-Ph	84
5	**89ae**	Me	4NO_2-Ph	91

6	**89af**	Me	4MeO-Ph	Q
7	**89ag**	Me	Furane	99
8	**89ah**	Me	Tiophene	Q
9	**89ba**	H	i-Pr	71
10	**89bb**	H	Ph	96

Q: quantitative yield

The only substituted amine synthesised was obtained by reductive amination between the free amine **88a** and *p*-chlorobenzaldehyde (Scheme 4.3). Only one amine was synthesised as this project was elaborated in collaboration with prof. Paula Kiuru from the University of Helsinki, and they were in charge of the synthesis of the substituted amine derivatives.

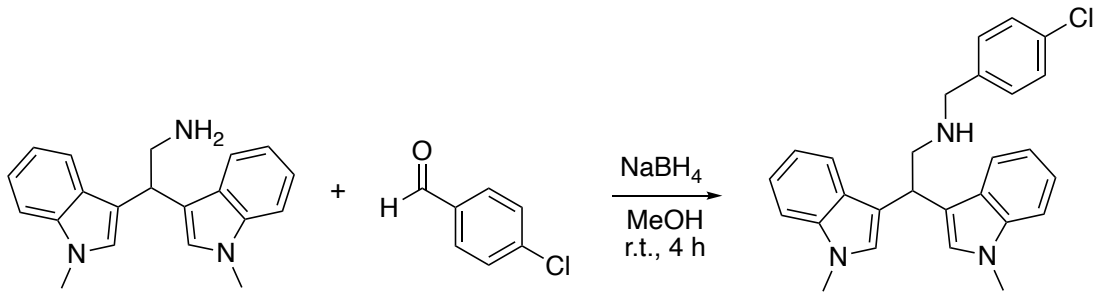

*Scheme 4.3. Synthesis of substituted amine derivative **90**.*

Many synthetic procedures have been developed for the synthesis of esters **91**. However, we decided to use a methodology in the realm of green chemistry, as the reaction required double Michael addition was performed in the presence of sodium dodecyl sulphate (SDS) as a catalyst and water as solvent (Table 4.2).[50]

*Table 4.2. Synthesis of esters and carboxylic acid derivatives **91** and **92**.*

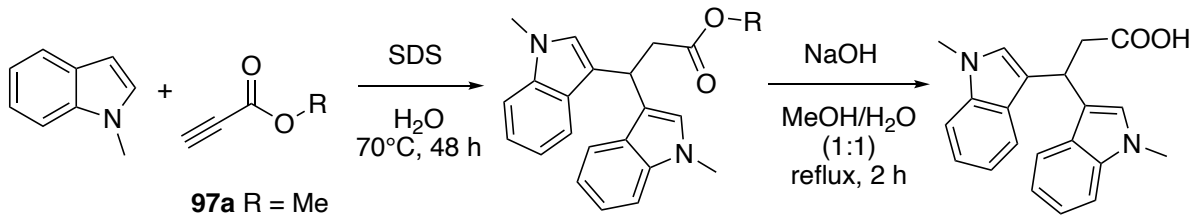

97a R = Me
97b R = Et

91a R = Me
91b R = Et

92

Entry	Molecule	R	Yield (%)
1	**91a**	Me	51
2	**91b**	Et	54
3	**92**	H	87[a]

[a] From **91b**

The carboxylic acid **92** could be obtained from the hydrolysis of any ester **91**.

The disubstituted derivatives **93**, were previously reported in the literature (Table 4.3). The carboxylic acid **93a** could have been obtained from the hydrolysis of compound **93b;** however, since the starting material required for the direct introduction of the carboxylic acid group was available to us, we decided to follow that synthetic route.

*Table 4.3. Synthesis of the disubstituted derivatives **93**.*

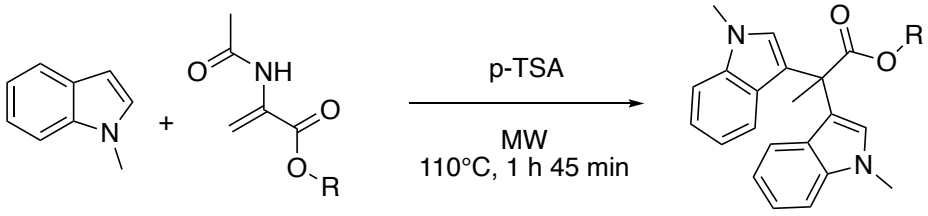

98a R = H
98b R = Me

93a R = H
93b R = Me

Entry	Molecule	R	Yield (%)
1	**93a**	H	24
2	**93b**	Me	85

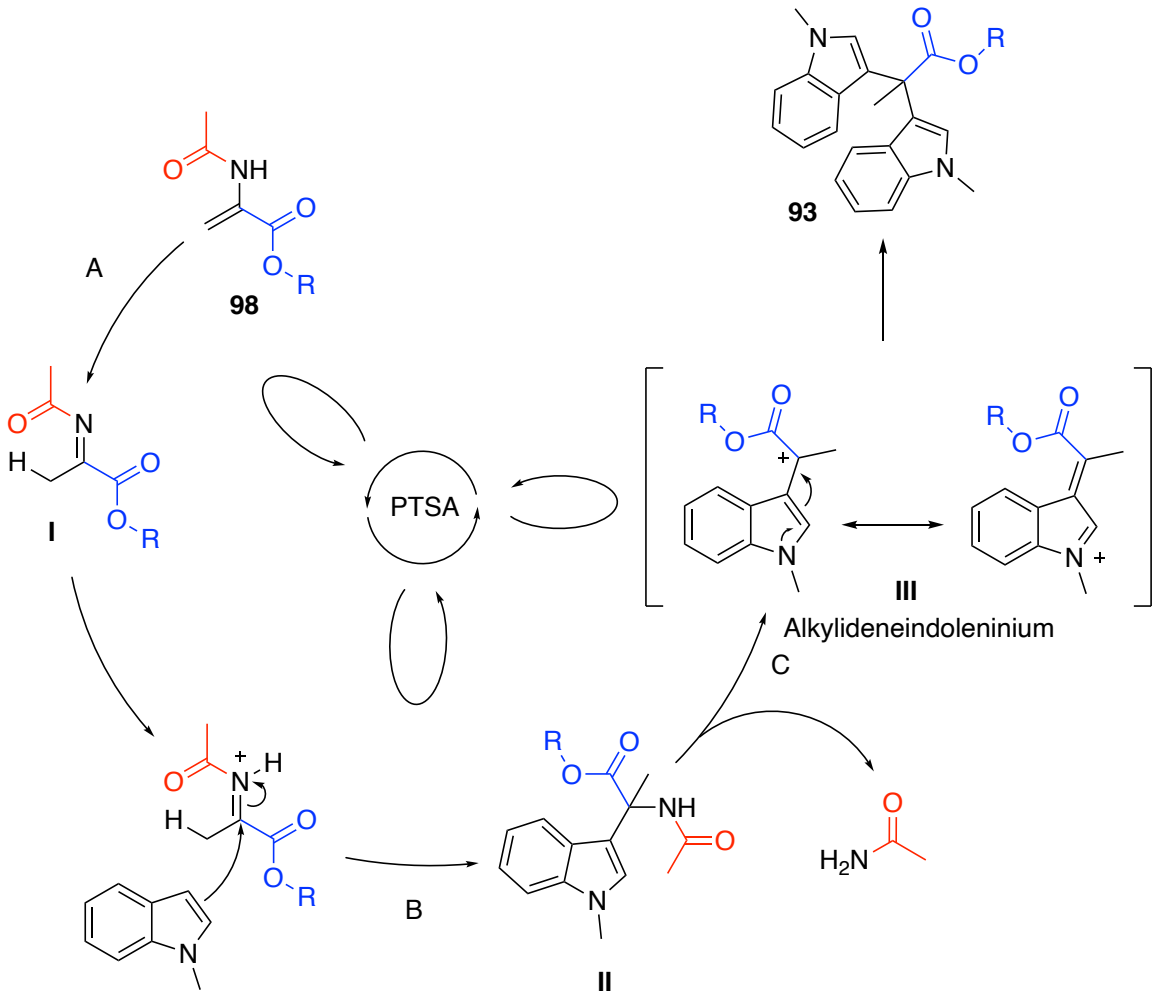

*Scheme 4.4. Reported proposed mechanism for the synthesis of derivatives **93**.[51]*

The reported proposed mechanism[51] (Scheme 4.4) considers the formation of an alkylideneindoleninium cation (**III**) after the tautomerization of the intermediate **I** (step A) through a Friedel-Crafts reaction (step B) and loss of the amide leaving group (step C). As it can be observed, the yield of our carboxylic acid derivative **93a** was significantly lower than that of the ester derivative **93b**, probably due to the formation of a subproduct resulting from the decarboxylation of the intermediate **II** instead of the loss of the amide leaving group in step C.

The last molecule of this family of diindolylmethanes synthesised was the previously reported molecule **94**, obtained through an *N*-bromosuccinimide (NBS) catalysed reaction under solvent-free conditions (Scheme 4.5).[52] The role of NBS is not clear in this reaction, but prior literature proposes that NBS could act as a source of Br^+ and

activate the carbonyl group or, alternatively, it could generate small quantities of Br_2 or HBr that would be the reaction catalyst.[53]

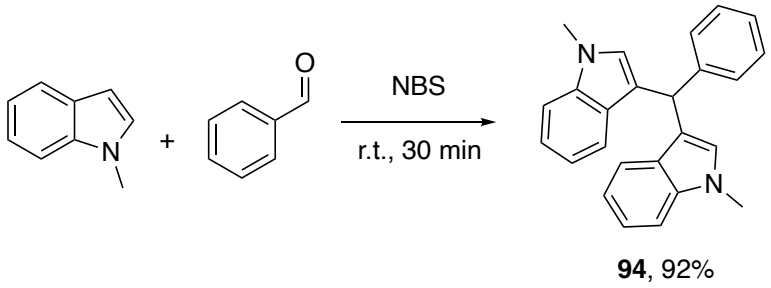

94, 92%

*Scheme 4.5. NBS catalysed reaction for the synthesis of **94**.*

4.3.2. Biological evaluation

Nineteen compounds were screened for their efficacy against *L. infantum* MHOM/TN/80/IPT1 promastigotes at a single dose of 20 μM for 72 h. All the amines, both free (**88**) and substituted (**90**), showed good inhibition values (Figure 4.5). As hypothesised, the IC_{50} values of *N*-methylated amines were better than non-substituted bisindoles, suggesting that *N*-methylation increases the activity against *L. infantum* promastigotes.

The amidic bisindoles (**89**) showed, unfortunately, moderate-to-low inhibition, except **89ab** and **89ac,** which showed IC_{50} values comparable to those of miltefosine. Moreover, toxicity values were > 50 and > 100 μM, respectively (Table 4.4), both better than miltefosine's. These results of activity and toxicity mean that these compounds have a selectivity index double and triple, respectively, that of miltefosine.

Table 4.4. Summary of bisindole derivatives activity on L. infantum promastigotes and THP-1 cells and its corresponding SI. IC_{50} and CC_{50} values are reported as mean (95% CI) from at least two experiments. Each experimental condition was conducted at least in duplicate and Miltefosine (MILT) was used as a positive control.

Compound	Inhibition of *L. infantum* at 20 μM (%)	*L. infantum* MHOM/TN/80/IPT1 IC_{50} (μM) (95% CI)	THP-1 1:2 da 100 μM CC_{50} (μM) (95% CI)	Selectivity Index (CC_{50}/IC_{50})
MILT	96.7 %	3.6 (3.3-4.0)	36.7	10.2
88a	98.0 %	4.1 (3.7-4.5)	41.6	10.1
88b	82.3 %	12.9 (11.6-14.6)	n.a	
89aa	16.5 %	n.a.		
89ab	62.8 %	2.4 (1.9-2.9)	> 50	> 20.8
89ac	76.2 %	3.4 (3.1-3.8)	> 100	> 29.4
89ad	47.1 %	n.a.		
89ae	50.9 %	n.a.		
89af	41.2 %	n.a.		
89ag	47.6 %	n.a.		
89ah	50.7 %	n.a.		
89ba	-34.2 %	n.a.		
89bb	27.6 %	n.a.		
90	98.8 %	1.7 (1.6-1.8)	18.7	11
91a	82.4 %	9.0 (7.3-11.3)	n.a.	
91b	76.7 %	n.a.		
92	14.6 %	n.a.		
93a	52.5 %	n.a.		
93b	69.0 %	17.2 (15.0-20.4)	n.a.	
94	63.3 %	n.a.		

An examination of the values of the amides **89ba** and **89bb** helped us to confirm that substitution of the indolic nitrogen increases the activity of the molecules as these two derivatives are not substituted and have lower inhibition (16.5 % and 62.8 %, respectively) compared to their *N*-methylated analogues **89aa** and **89ab** (-34.2 % and 27.6 % respectively) (Table 4.4).

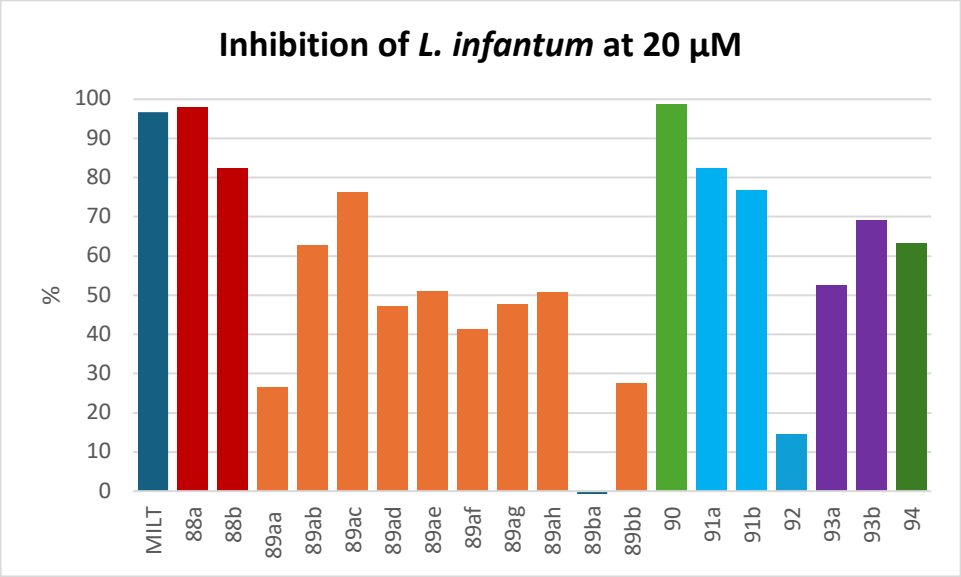

Figure 4.5. Inhibition of Leishmania infantum promastigotes at 20 µM.

Examining the esters and carboxylic acids (**91a-b, 92** and **93a-b**) we can determine that esters are better antileishmanial derivatives than carboxylic acids. The ester derivatives showed high inhibition of *L. infantum* promastigotes, while carboxylic acids had moderate to poor inhibition values.

4.3.2.1 In silico study

Physicochemical, pharmacokinetic and drug-likeness properties of the synthesised diindolylmethanes were calculated using the SwissADME web tool.[54] As shown in Table 4.5, none of the synthesised molecules (except **90**) violated either Lipinsky's or Veber's rule, suggesting good oral bioavailability.

*Table 4.5. Physicochemical, pharmacokinetic and drug-likeness properties of bisindole derivatives (**88-94**).*

Cmpd	MW (g/mol)	logP	HBD	HBA	RTB	TPSA (Å^2)	GI Absorption	BBB Permeation
Desired Values	**<500**	**<5**	**<5**	**<10**	**<10**	**<140**		
88a	303.40	3.09	1	1	3	35.88	High	yes
88b	275.35	3.03	3	1	3	57.60	High	yes
89aa	373.49	3.93	1	1	6	38.96	High	yes
89ab	407.51	4.43	1	1	6	38.96	High	yes
89ac	425.50	4.71	1	2	6	38.96	High	yes
89ad	441.95	4.91	1	1	6	38.96	High	yes
89ae	452.50	3.70	1	3	7	84.78	High	no
89af	437.53	4.39	1	2	7	48.19	High	yes
89ag	397.47	3.83	1	2	6	52.10	High	yes
89ah	413.53	4.54	1	1	6	67.20	High	no
89ba	345.44	3.89	3	1	6	60.68	High	yes
89bb	379.45	4.37	3	1	6	60.68	High	yes
90	427.97	5.21	1	1	6	21.89	High	no
91a	346.42	3.69	0	2	5	36.16	High	yes
91b	360.45	3.98	0	2	6	36.16	High	yes
92	332.40	3.29	1	2	4	47.16	High	yes
93a	332.40	3.27	1	2	3	47.16	High	yes
93b	346.42	3.68	0	2	4	36.16	High	yes
94	350.46	4.91	0	0	3	9.86	Low	no

The number of rotatable bonds (RTB) should be lower than 10, since this number not only affects the oral bioavailability but also the binding potency. Most of our synthesised compounds have 6 or fewer RTB.

The topological polar surface area (TPSA) is a measure of the ability of a drug to pass through cell membranes. A value of TPSA under 140 Å² indicates the possibility of passive transport of the molecule through membranes. All of our diindolylmethane derivatives (except **89ae**) have values under 61 Å².

The pharmacokinetic properties of a molecule depend on several factors, including GI (Gastrointestinal) absorption and BBB (Blood-Brain Barrier) permeation. These are particularly relevant because the more a dose reaches the bloodstream (mainly through GI absorption), the more it can cross the BBB. All of our compounds, except **94**, had a predicted high GI absorption, and all (except **89ab, 90** and **94**) could cross the BBB. The substituted amine derivative **90** can be absorbed from the gastrointestinal tract but cannot cross the BBB, likely due to its poor water solubility and high lipophilicity.

One of the challenges of drug discovery is the synthesis of water-soluble molecules. This observation also applies to our case, especially because the promising molecule URB1483 had as its biggest problem the low water solubility.

*Table 4.6. Water solubility of derivatives **88-94** calculated in SwissADME. LogS in the table is the average value of logS calculated using three different methods.*

Compound	logS	Solubility
Desired Value	0 > log S > -2	
88a	-4,35	Soluble
88b	-4,81	Soluble
89aa	-5,52	Moderately soluble
89ab	-6,52	Poorly soluble
89ac	-6,70	Poorly soluble
89ad	-7,12	Poorly soluble
89ae	-6,57	Poorly soluble
89af	-6,63	Poorly soluble
89ag	-5,99	Moderately soluble

89ah	-6,49	Poorly soluble
89ba	-5,98	Moderately soluble
89bb	-6,98	Poorly soluble
90	-7,20	Poorly soluble
91a	-4,94	Soluble
91b	-5,27	Moderately soluble
92	-4,60	Soluble
93a	-4,79	Soluble
93b	-5,13	Moderately soluble
94	-6,55	Poorly soluble
URB1483	-6,47	Poorly soluble

Unfortunately, most of the synthesised molecules were predicted to be poorly soluble (Table 4.6); however, most of them had better log S values than URB1483. Both free amines **89a** and **89b** have good solubility and biological results, suggesting that they can be good candidates as antileishmanial drugs.

4.3.3. Design and synthesis of glycosylated derivatives

Glycosylated bisindoles emerged in recent years as a very versatile class of bioactive compounds with broad pharmacological potential.[32,55] Glycosylation of the bisindole skeleton should entail increases in solubility and selectivity. Alteration of the electronic environment of the indole rings and the net polarity of the molecule by addition of sugar residues onto bisindolic nitrogen atoms through β-N,N′ linkages has been shown to influence their interaction with pathogenic process-involving enzymes and receptors.

In this structural family, the bisindole glycoconjugates have exhibited biological activity in a range of disease contexts. In cancer models, these derivatives initiate cell-cycle arrest and apoptosis via protein expression pathway modulation involving cellular stress responses. The glycosylic substituents confer improved hydrogen-bonding capacity and the capability to orient the indole moieties in an optimal manner within

protein binding sites, generating higher docking scores and superior binding stability compared to their non-glycosylated counterparts. In parallel, inclusion of carbohydrate fragments decreases mammalian cell unspecific cytotoxicity, suggesting that glycosylation is used for selective recognition and fewer off-target effects.[32]

The same concept of molecules can be used for parasitic systems as well. Bisindoles have been reported to inhibit essential enzymes in Leishmania, such as topoisomerase IB, which is crucial for DNA replication and the survival of parasites. Novel analogues of bromo-substituted glycosylated DIMs have demonstrated lower toxicity and higher solubility than non-glycosylated bisindoles, while maintaining their activity (Figure 4.6). Glycosylation is biased towards water solubility and biocompatibility, which is relevant for oral intake and in vivo stability, being key limitations of traditional leishmanicidal compounds.[55]

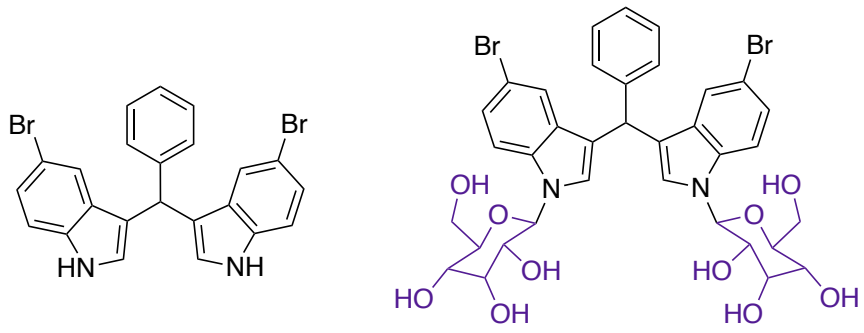

Non-glycoside
IC_{50} = 34.81 ± 1.59 μM

Glycoside
IC_{50} = 27.91 ± 1.37 μM

Figure 4.6. Comparison between glycosylated and non-glycosylated bisindoles

Further diversification is also required since, even in the case of a successful *N*-linked conjugation, functionalization of other indole ring positions could yield derivatives with different characteristics and differing modes of enzyme interaction. Differences in sugar variety could similarly influence recognition processes at the parasite-host interface. The positive correlation between glycosylation and reduced cytotoxicity, already observed in similar systems, also suggests that such modifications can produce more potent and less toxic antileishmanial leads.

Therefore, the synthesis of different glycosylated bisindole derivatives was planned (Scheme 4.6).

Derivatives obtained from the direct coupling between free amine bisindoles **88** and sugars were intended; however, although the formation of the product was observed, their purification was not possible, probably due to their instability.

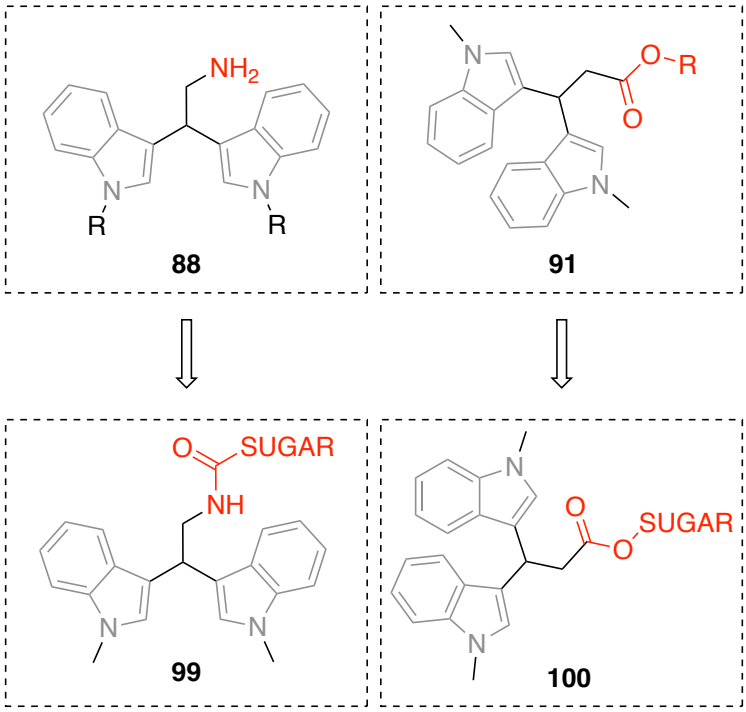

Scheme 4.6. Glycosylated bisindoles synthesised

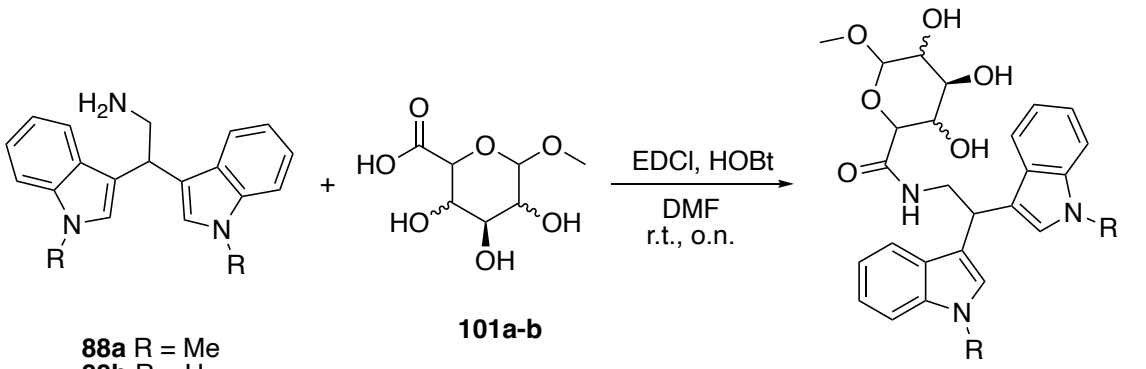

*Scheme 4.7. Synthesis of amide glycosylated bisindoles **99**.*

For the synthesis of amidic glycosylated bisindoles, first the methylated oxidised glucose and galactose **101a-b** were synthesised and then coupled with the free

bisindolic amines **88a-b** (Scheme 4.7). This led to the obtention of compounds **99** with moderate yields.

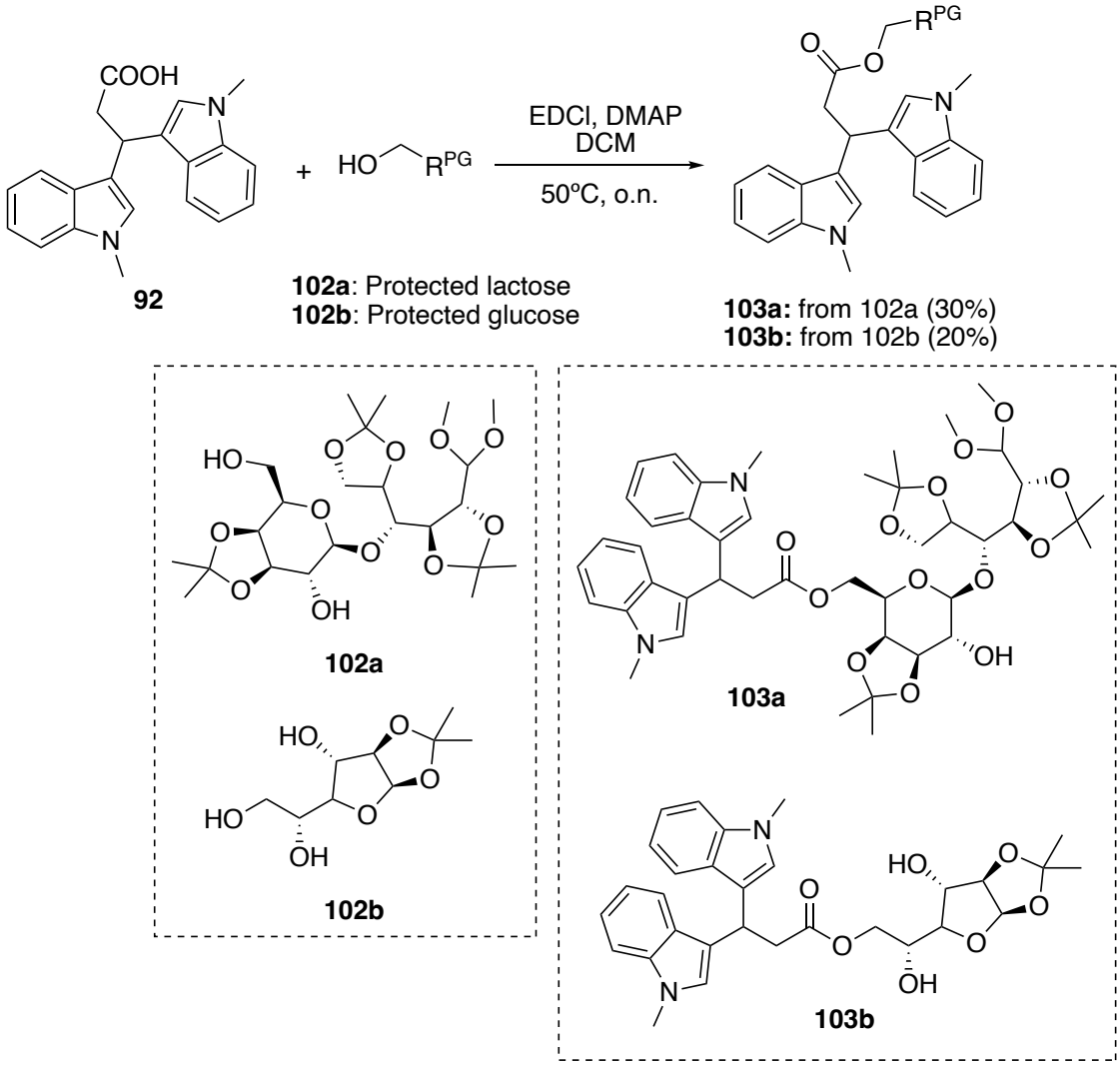

*Scheme 4.8. Synthesis of ester glycosylated-protected bisindoles **102**.*

For the synthesis of the ester glycosylated bisindoles, first, the protection of sugars was made in order to avoid undesired reactions with other hydroxylic groups of the molecule. Protected glucose was commercially available, and protected lactose was synthesised following reported procedures.[56] Then, coupling with carboxylic acid **92** was made in order to obtain intermediates **103a-b** (Scheme 4.8) that underwent an acidic deprotection, leading to the desired final compounds **100a-b** (Scheme 4.9).

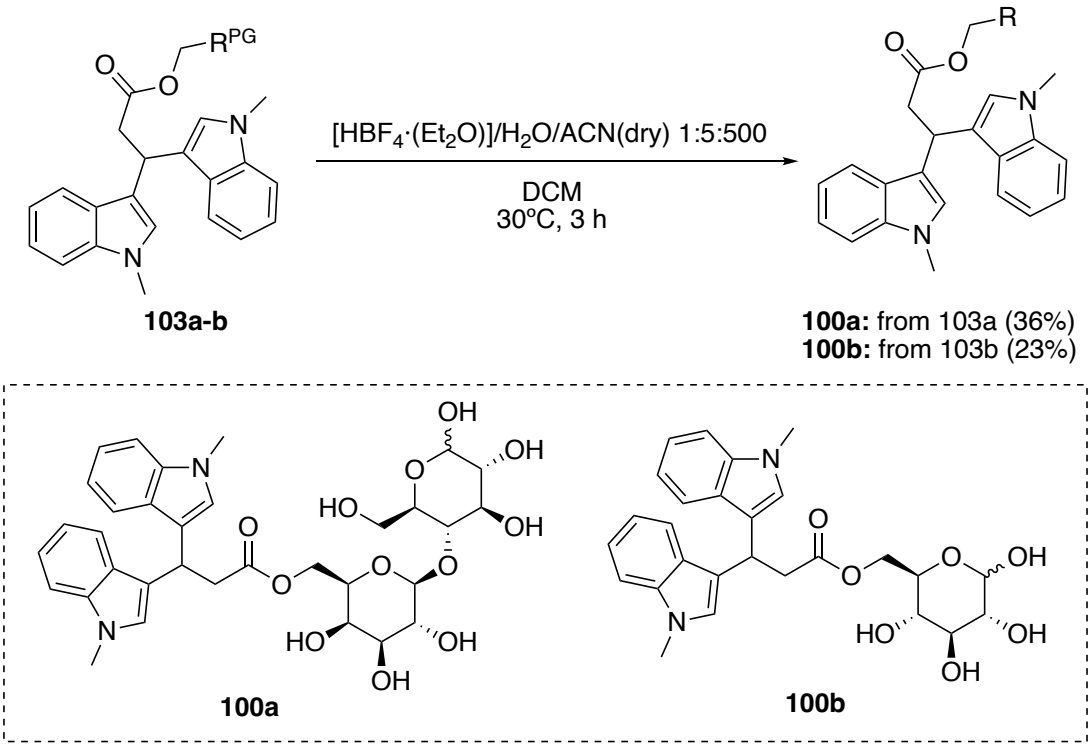

*Scheme 4.9. Deprotection of ester glycosylated bisindoles to obtain final compounds **100a-b**.*

Unfortunately, yields are not high due to the difficulties found in the purification of these molecules.

4.3.4. Biological evaluation of glycosylated derivatives

The six glycosylated bisindoles (**99aa-99bb, 100a-b**) and the two protected derivatives (**103a-b**) were screened for their efficacy against *L. infantum* MHOM/TN/80/IPT1 promastigotes at a single dose of 20 μM for 72 h (Table 4.7).

Table 4.7. Summary of glycosylated bisindole derivatives activity on L. infantum promastigotes and THP-1 cells and its corresponding SI. IC_{50} values are reported as mean (95% CI) from at least two experiments. Each experimental condition was conducted at least in duplicate and miltefosine (MILT) was used as a positive control

Compound	Inhibition of *L. infantum* at 20 *μ*M (%)	*L. infantum* MHOM/TN/80/IPT1 IC_{50} (μM) (95% CI)
MILT	96.7 %	3.6 (3.3-4.0)
99aa	15.6 %	n.a.
99ab	13.6 %	n.a.
99ba	6.5 %	n.a.
99bb	3.1 %	n.a.
100a	9.5 %	n.a.
100b	9.4 %	n.a.
103a	96.2 %	6.6 (6.2-7.0)
103b	61.2 %	21.0 (18.9-24.5)

At 20 μM screening concentration, amide-type glycosides (**99**) were weakly inhibitory, with a parasite growth inhibition of not more than 15 %. None of them reached the IC_{50} determination threshold, indicating a weak antiparasitic activity in this subgroup. The activity of this group was lower than the non-glycosilated analogues **89**. Ester glycosylated bisindoles (**100a–b**) also exhibited weak inhibition, again much lower than the non-glycosilated ester analogues **91** (Figure 4.7).

On the other hand, the protected ester derivatives (**103**) showed considerably enhanced leishmanicidal potency. Compound **103a** showed 96.2 % inhibition at 20 μM and an IC_{50} of 6.6 μM, which was near the potency of the standard drug miltefosine. Compound **103b**, although less potent, still showed good inhibition (61.2 %) and a moderate IC_{50} value. Toxicity should be studied in order to evaluate the selectivity index of these molecules.

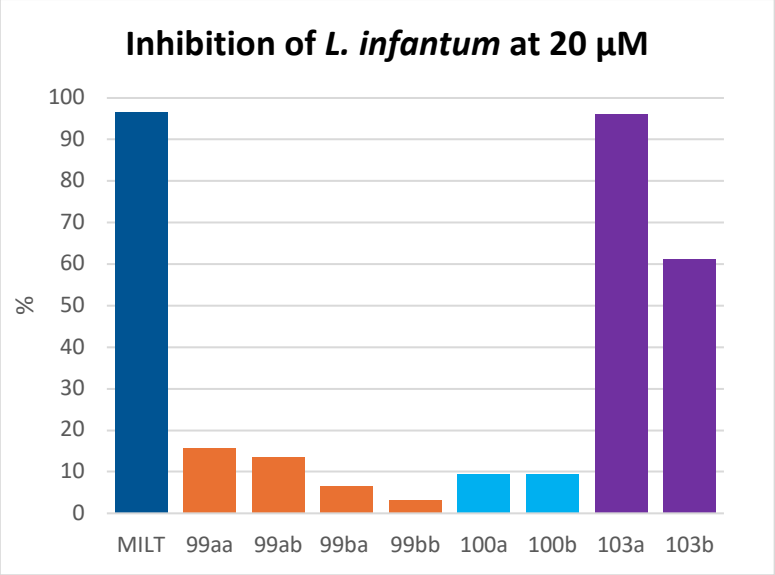

Figure 4.7. Inhibition of Leishmania infantum promastigotes at 20 µM.

The increased activity could be a result of increased lipophilicity and membrane permeability imparted by the acetyl protecting groups that could increase parasite uptake or intracellular target interaction.

These results suggest that the glycosylation of the ethylene chain in the bisindole core is not as beneficial as the reported substitution in the nitrogen of the imidazole ring.

4.3.4.1 In silico studies

Physicochemical, pharmacokinetic and drug-likeness properties of the synthesised diindolylmethanes were calculated using the SwissADME web tool.[54] As we can see in Table 4.8, most of the synthesised molecules violated either Lipinsky's or Veber's rule, suggesting that glycosylation may impair absorption.

The number of rotatable bonds (RTBs) ought to be below 10, since too much molecular flexibility goes against a good binding affinity and bioavailability. All of the **99** and **100** compounds possess an RTB value of 7 to 10, but compound **103a** is slightly worse (RTB = 14), suggesting compromised conformational stability and possibly reduced permeability through membranes.

The amide glycosylated bisindoles (**99**) have favourable TPSA values ranging between 118 and 140 Å² in accord with favourable predicted permeability. Compounds

100a (205 Å²) and **103a** (148.7 Å²), by contrast, have TPSA values outside this threshold, in accord with their predicted poor gastrointestinal (GI) absorption.

In agreement with these structural expectations, GI absorption was expected to be high for all compounds except for **100a** and **103a**, which were predicted to be low in absorption due to their higher polarity and bulkiness. These compounds are not expected to cross the blood–brain barrier (BBB) according to their polar and bulky glycosylated character.

*Table 4.8. Physicochemical, pharmacokinetic and drug-likeness properties of bisindole derivatives (**99,100,103**).*

Cmpd	MW (g/mol)	logP	HBD	HBA	RTB	TPSA (Å²)	GI Absorption	BBB Permeation
Desired Values	**<500**	**<5**	**<5**	**<10**	**<10**	**<140**		
99aa	493.55	1.46	4	6	7	118.11	High	no
99ab	493.55	1.38	4	6	7	118.11	High	no
99ba	465.50	1.32	6	6	7	139.83	High	no
99bb	465.50	1.26	6	6	7	139.83	High	no
100a	656.68	-0.20	7	12	10	205.46	Low	no
100b	494.54	1.20	4	7	7	126.31	High	no
103a	822.94	3.90	1	13	14	148.69	Low	no
103b	534.60	3.02	2	7	8	104.31	High	no

Overall, the amide glycosylated bisindoles (**99**) best fulfill the classical drug-likeness criteria, with moderate lipophilicity, limited molecular flexibility, and optimal TPSA values favouring high GI absorption. By contrast, the ester glycosylated bisindoles (**100**) and their protected analogues (**103**), with improved antileishmanial activity, have suboptimal pharmacokinetic properties, emphasising the need for balance between biological activity and physicochemical characteristics in future optimisation.

As shown in Table 4.9, most of the glycosylated bisindoles have good predicted solubility, except the acetylated analogues (**103**).

*Table 4.9. Water solubility of derivatives **99,100** and **103** calculated in SwissADME. LogS in the table is the average value of logS calculated using three different methods.*

Compound	logS	Solubility
Desired Value	0 > log S > -2	
99aa	-3,94	Soluble
99ab	-3,94	Soluble
99ba	-4,40	Soluble
99bb	-4,40	Soluble
100a	-2,48	Soluble
100b	-3,48	Soluble
103a	-6,68	Poorly soluble
103b	-5,09	Moderately soluble

Unfortunately, the compound that was found most active in the biological activity tests (**103a**) was the least soluble of the series.

4.4. EXPERIMENTAL SECTION

*4.4.1. Synthesis of trifluoroacetamide-bisindoles (**95a-b**)*

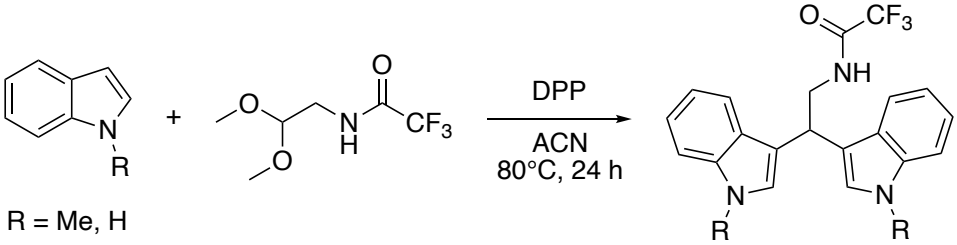

General procedure for the synthesis of trifluoroacetamide-bisindoles (95a-b) GP9

According to the literature procedure,[57] diphenyl phosphate (0.1 equiv.) was added to a solution of the appropriate indole derivative (2 equiv.) and (trifluoroacetylamino)-acetaldehyde dimethyl acetal (1 equiv., 1 M) in anhydrous acetonitrile, and the resulting mixture was stirred at 80 °C for 12-48 h in a sealed tube, monitoring the progress of the reaction by TLC. After cooling to room temperature, saturated aqueous $NaHCO_3$ and DCM were added, and the two phases were separated. The aqueous solution was extracted with DCM (3 x 20 mL). After drying over Na_2SO_4, the combined organic phases were concentrated in vacuo. The resulting crude product **95** was purified, when needed, by using column flash chromatography on silica gel.

N-(2,2-bis(1-methyl-1H-indol-3-yl)ethyl)-2,2,2-trifluoroacetamide (**95a**):

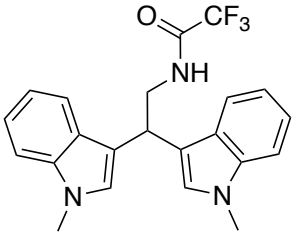

According to GP9 1-methyl-1*H*-indole (492 mg, 3.75 mmol, 2 equiv.), *N*-(2,2-dimethoxyethyl)-2,2,2-trifluoroacetamide (377 mg, 1.86 mmol, 1 equiv.), diphenyl phosphate (47 mg, 0.19 mmol, 0.1 equiv.) in ACN (3.8 mL) provided, after cyclohexane/ethyl acetate (85:15) column chromatography, the desired compound **95a** (612 mg, yield 88 %) as a white powder.

The physicochemical data are consistent with those reported in the literature. [57]

^{1}H NMR (400 MHz, $CDCl_3$, 25 °C): δ = 7.61 (ddd, 2H, $J_1 \approx J_2$ = 1.0 Hz, J_3 = 8.0 Hz), 7.33 (ddd, 2H, $J_1 \approx J_2$ = 1.0 Hz, J_3 = 8.5 Hz), 7.25 (ddd, 2H, J_1 = 1.0 Hz, J_2 = 7.0 Hz, J_3 = 8.5 Hz), 7.09 (ddd, 2H, J_1 = 1.0 Hz, J_2 = 7.0 Hz, J_3 = 8.0 Hz), 6.89 (br s, 2H), 6.40 (br s, 1H), 4.79 (dd, 1H, $J_1 \approx J_2$ = 7.0 Hz), 4.12 (dd, 2H, $J_1 \approx J_2$ = 7.0 Hz), 3.75 (s, 6H).

N-(2,2-di(1H-indol-3-yl)ethyl)-2,2,2-trifluoroacetamide (**95b**):

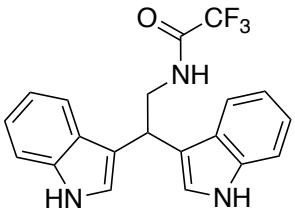

According to GP9 1*H*-indole (400 mg, 4.26 mmol, 2 equiv.), *N*-(2,2-dimethoxyethyl)-2,2,2-trifluoroacetamide (428 mg, 2.13 mmol, 1 equiv.), diphenyl phosphate (53 mg, 0.21 mmol, 0.1 equiv.) in ACN (2.1 mL) provided, after cyclohexane/ethyl acetate (85:15) column chromatography, the desired compound **95b** (609 mg, yield 77 %) as a white powder.

The physicochemical data are consistent with those reported in the literature.[57,58]

^{1}H NMR (400 MHz, $CDCl_3$, 25 °C): δ = 8.05 (br s, 2H), 7.59 (dddd, 2H, $J_1 \approx J_2 \approx J_3$= 1.0 Hz, J_4 = 8.0 Hz), 7.38 (ddd, 2H, $J_1 \approx J_2$ = 1.0 Hz, J_3 = 8.0 Hz), 7.21 (ddd, 2H, J_1 = 1.0 Hz, J_2 = 7.0 Hz, J_3 = 8.0 Hz), 7.09 (ddd, 2H, J_1 = 1.0 Hz, J_2 = 7.0 Hz, J_3 = 8.0 Hz), 7.02 (dd, 2H, J_1 = 1.0 Hz, J_2 = 2.5 Hz), 6.40 (br s, 1H), 4.81 (tt, J = 7.0, 0.9 Hz, 1H), 4.15 (dd, 2H, $J_1 \approx J_2$ = 7.0 Hz).

*4.4.1.1 Synthesis of free amines-bisindoles (**88a-b**)*

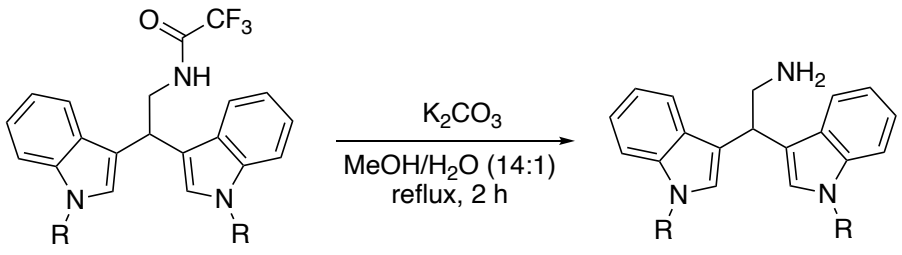

95a R = Me
95b R = H

88a R = Me
88b R = H

General procedure for the synthesis of free amine-bisindoles (5a-b) GP10

According to the literature procedure,[57] trifluoroacetamide derivative **95** (1 equiv., 0.1 M) and potassium carbonate (5 equiv.) in MeOH/H_2O (14:1) were stirred while refluxed for 2-3 h. Methanol was removed under reduced pressure after completion of

the reaction and water was added. The aqueous solution was extracted with DCM (3 x 20 mL), the combined organic phases were dried over Na_2SO_4, filtered, and concentrated in vacuo. When needed, the crude material was purified by flash chromatography on silica gel.

2,2-bis(1-methyl-1*H*-indoxl-3-yl)ethan-1-amine (**88a**):

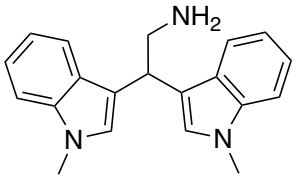

According to GP10, *N*-(2,2-bis(1-methyl-1*H*-indol-3-yl)ethyl)-2,2,2-trifluoroacetamide **95a** (569 mg, 1.42 mmol, 1 equiv.), K_2CO_3 (984 mg, 7.12 mmol, 5 equiv.) in MeOH (13 mL) and H_2O (0.9 mL) provided, after DCM/MeOH (95:5) with 1 % of ammonia column chromatography, the desired compound **88a** (420 mg, yield 97 %) as a white foam.

The physicochemical data are consistent with those reported in the literature.[58]

^{1}H NMR (400 MHz, $CDCl_3$, 25 °C): δ = 7.65 (ddd, 2H, $J_1 \approx J_2$ = 1.0 Hz, J_3 = 8.0 Hz), 7.28 (ddd, 2H, $J_1 \approx J_2$ = 1.0 Hz, J_3 = 8.5 Hz), 7.21 (ddd, 2H, J_1 = 1.0 Hz, J_2 = 7.0 Hz, J_3 = 8.5 Hz), 7.07 (ddd, 2H, J_1 = 1.0 Hz, J_2 = 7.0 Hz, J_3 = 8.0 Hz), 6.90 (br s, 2H), 4.56 (dd, 1H, $J_1 \approx J_2$ = 7.0 Hz), 3.68 (s, 6H), 3.44 (d, 2H, J_1 = 7.0 Hz).

2,2-di(1*H*-indol-3-yl)ethan-1-amine (**88b**):

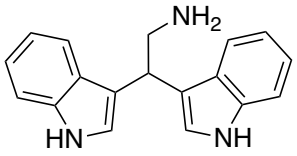

According to GP10, *N*-(2,2-di(1H-indol-3-yl)ethyl)-2,2,2-trifluoroacetamide **95b** (390 mg, 1.05 mmol, 1 equiv.), K_2CO_3 (726 mg, 5.25 mmol, 5 equiv.) in MeOH (9.6 mL) and H_2O (0.7 mL) provided, after DCM/MeOH (9:1) with 1 % of ammonia column chromatography, the desired compound **88b** (269.8 mg, yield 93.3 %) as a white foam.

The physicochemical data are consistent with those reported in the literature.[58]

^{1}H NMR (400 MHz, DMSO-d_6, 25 °C): δ = 10.80 (br s, 2H), 7.49 (d, 2H, J_1 = 8.0 Hz), 7.30 (d, 2H, J_1 = 8.0 Hz), 7.22 (d, 2H, J = 2.5 Hz), 7.00 (dd, 2H, $J_1 \approx J_2$ = 8.0 Hz), 6.87 (dd, 2H, $J_1 \approx J_2$ = 8.0 Hz), 4.41 (dd,1H, $J_1 \approx J_2$ = 7.0 Hz), 3.31 (br s, 2H), 3.28 (d, 2H, J_1 = 7.0 Hz).

*4.4.2. Synthesis of amidic-bisindoles (**89aa-ah, 89ba-bb**)*

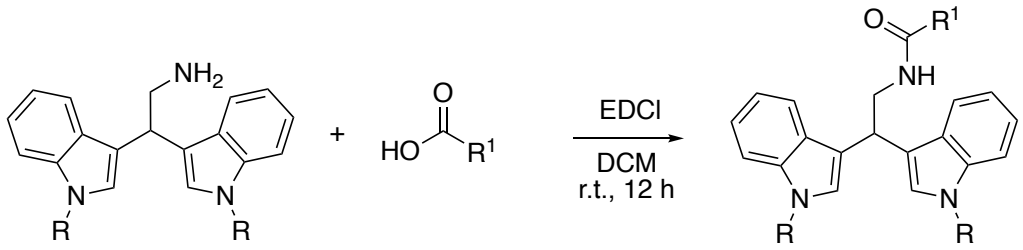

88a R = Me
88b R = H

96a R^1 = i-Pr
96b R^1 = Ph
96c R^1 = 4F-Ph
96d R^1 = 4Cl-Ph
96e R^1 = 4NO_2-Ph
96f R^1 = 4MeO-Ph
96g R^1 = Furane
96h R^1 = Tiophene

89aa R = Me R^1 = i-Pr
89ab R = Me R^1 = Ph
89ac R = Me R^1 = 4F-Ph
89ad R = Me R^1 = 4Cl-Ph
89ae R = Me R^1 = 4NO_2-Ph
89af R = Me R^1 = 4MeO-Ph
89ag R = Me R^1 = Furane
89ah R = Me R^1 = Tiophene
89ba R = H R^1 = i-Pr
89bb R = H R^1 = Ph

General procedure for the synthesis of amide-bisindoles (89aa-ah, 89ba-bb) GP11

According to the literature procedure,[59] to a solution of the corresponding 2,2-bis(indol-3-yl)ethan-1-amine **88** (1 equiv., 0.075 M) and the corresponding acid **96** (1.05 equiv.) in DCM, 1-ethyl-3-(3-dimethylaminopropyl)carbodiimide (EDCI) (1.5 equiv.) was added at 0°C. The reaction was then stirred at room temperature. After 12 h, the solution was quenched with sat. NH_4Cl aq. The resulting mixture was extracted with DCM (3 x 20 mL). The combined organic layers were dried over anhydrous Na_2SO_4, filtered, and concentrated in vacuo. The crude residue was purified by column chromatography on silica gel.

N-(2,2-bis(1-methyl-1*H*-indol-3-yl)ethyl)isobutyramide (**89aa**):

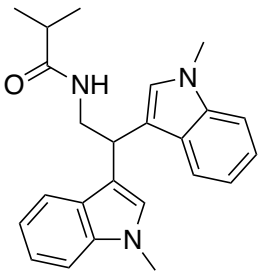

According to GP11, bisindole **88a** (80 mg, 0.26 mmol, 1 equiv.), isobutyric acid (25.8 µL, 0.28 mmol, 1.05 equiv.) and EDCI (75.8 mg, 0.40 mmol, 1.5 equiv.) in DCM (3.5 mL) provided, after purification by column chromatography using cyclohexane/ethyl acetate (7:3), the desired compound **89aa** (82.4 mg, yield 84 %) as a white solid.

R_f = 0.41 (1:1 cyclohexane/ethyl acetate)

^{1}H NMR (400 MHz, $CDCl_3$, 25 °C): δ = 7.65 (ddd, 2H, $J_1 \approx J_2$ = 1.0 Hz, J_3 = 8.0 Hz), 7.30 (ddd, 2H, $J_1 \approx J_2$ = 1.0 Hz, J_3 = 8.0 Hz), 7.22 (ddd, 2H, J_1 = 1.0 Hz, J_2 = 7.0 Hz, J_3 = 8.0 Hz), 7.07 (ddd, 2H, J_1 = 1.0 Hz, J_2 = 7.0 Hz, J_3 = 8.0 Hz), 6.87 (s, 2H), 5.54 (br t, 1H), 4.73 (dd, 1H, $J_1 \approx J_2$ = 7.0 Hz), 4.01 (dd, 2H, J_1 = 6.0 Hz, J_2 = 7.0 Hz), 3.73 (s, 6H), 2.18 (hept, 1H, J = 7.0 Hz), 1.05 (d, 6H, J = 7.0 Hz).

^{13}C NMR (101 MHz, $CDCl_3$, 25 °C): δ = 177.1, 137.5, 127.5, 127.0, 121.8, 119.9, 119.1, 115.8, 109.4, 44.0, 35.8, 34.5, 32.9, 19.7.

HRMS (ESI-Orbitrap, *m*/*z*): calcd for $C_{24}H_{27}N_3O$ $[M + Na]^+$ 396.2052; found 396.2047.

N-(2,2-bis(1-methyl-1*H*-indol-3-yl)ethyl)benzamide (**89ab**):

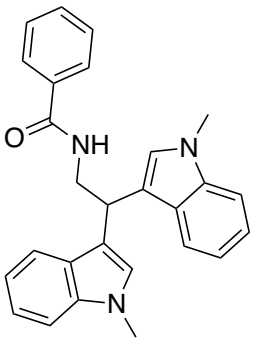

According to GP11, bisindole **88a** (50 mg, 0.16 mmol, 1 equiv.), benzoic acid (21 mg, 0.17 mmol, 1.05 equiv.) and EDCl (47.4 mg, 0.25 mmol, 1.5 equiv.) in DCM (2.1 mL) provided, after purification by column chromatography using cyclohexane/ethyl acetate (6:4), the desired compound **89ab** (65 mg, yield 97 %) as a white foam.

R_f = 0.62 (1:1 cyclohexane/ethyl acetate)

^{1}H NMR (400 MHz, $CDCl_3$, 25 °C): δ = 7.68 (ddd, 2H, $J_1 \approx J_2$ = 1.0 Hz, J_3 = 8.0 Hz), 7.58 (ddd, 2H, $J_1 \approx J_2$ = 1.5 Hz, J_3 = 7.5 Hz), 7.43 (dddd, 1H, $J_1 \approx J_2$ = 1.5 Hz, $J_3 \approx J_4$ = 7.5 Hz), 7.36 – 7.30 (m, 4H), 7.23 (ddd, 2H, J_1 = 1.0 Hz, J_2 = 7.0 Hz, J_3 = 8.0 Hz), 7.08 (ddd, 2H, J_1 = 1.0 Hz, J_2 = 7.0 Hz, J_3 = 8.0 Hz), 6.93 (s, 2H), 6.26 (br t, 1H, J = 5.5 Hz), 4.86 (dd, 1H, $J_1 \approx J_2$ = 7.0 Hz), 4.23 (dd, 2H, J_1 = 5.5 Hz, J_2 = 7.0 Hz), 3.74 (s, 6H).

^{13}C NMR (101 MHz, $CDCl_3$, 25 °C): δ = 167.6, 137.5, 134.9, 131.4, 128.6, 127.5, 127.04, 126.99, 121.9, 119.9, 119.1, 115.7, 109.5, 44.7, 34.4, 32.9.

HRMS (ESI-Orbitrap, *m*/*z*): calcd for $C_{27}H_{25}N_3O$ $[M + Na]^+$ 430.1895; found 430.1873.

N-(2,2-bis(1-methyl-1*H*-indol-3-yl)ethyl)-4-fluorobenzamide (**89ac**):

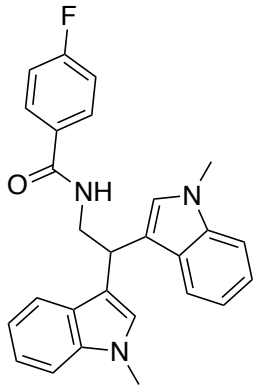

According to GP11, bisindole **88a** (50 mg, 0.16 mmol, 1 equiv.), 4-fluorobenzoic acid (24 mg, 0.17 mmol, 1.05 equiv.) and EDCl (47.4 mg, 0.25 mmol, 1.5 equiv.) in DCM (2.1 mL) provided, after purification by column chromatography using cyclohexane/ethyl acetate (8:2), the desired compound **89ac** (69.1 mg, yield 99 %) as a white foam.

R_f = 0.71 (1:1 cyclohexane/ethyl acetate)

^{1}H NMR (400 MHz, $CDCl_3$, 25 °C): δ = 7.68 (dd, J_1 = 1.5 Hz, J_2 = 8.0 Hz), 7.62-7.56 (m, 2H), 7.33 (d, 2H, J = 8.0 Hz, 2H), 7.28-7.22 (m, 2H), 7.09 (ddd, 2H, J_1 = 1.0 Hz, J_2 = 7.0 Hz, J_3 = 8.0 Hz), 7.04 – 6.98 (m, 2H), 6.94 (s, 2H), 6.32-6.21 (m, 1H), 4.91-4.83 (m, 1H), 4.25-4.19 (m, 2H), 3.74 (s, 6H).

^{13}C NMR (101 MHz, $CDCl_3$, 25 °C): δ = 166.5, 164.7 (d, 1C, $J_{C4\text{-}F}$ = 252 Hz, C4), 137.5, 131.0 (d, 1C, $J_{C1\text{-}F}$ = 3.5 Hz, C1), 129.3 (d, 1C, $J_{C2\text{-}F}$ = 9.0 Hz, C2), 127.4, 126.9, 121.9, 119.8, 119.1, 115.6, 115.5 (d, 1C, $J_{C3\text{-}F}$ = 24.5 Hz, C3), 109.5, 44.9, 34.3, 32.9.

HRMS (ESI-Orbitrap, *m*/*z*): calcd for $C_{27}H_{24}FN_3O$ $[M + Na]^+$ 448.1801; found 448.1792.

N-(2,2-bis(1-methyl-1*H*-indol-3-yl)ethyl)-4-chlorobenzamide (**89ad**):

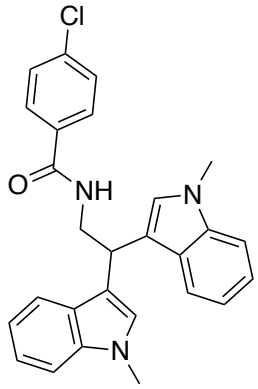

According to GP11, bisindole **88a** (50 mg, 0.16 mmol, 1 equiv.), 4-chlorobenzoic acid (27.1 mg, 0.17 mmol, 1.05 equiv.) and EDCl (47.4 mg, 0.25 mmol, 1.5 equiv.) in DCM (2.1 mL) provided, after purification by column chromatography using cyclohexane/ethyl acetate (8:2), the desired compound **89ad** (61.4 mg, yield 84 %) as needle crystals.

R_f = 0.68 (1:1 cyclohexane/ethyl acetate)

^{1}H NMR (400 MHz, $CDCl_3$, 25 °C): δ = 7.67 (ddd, 2H, $J_1 \approx J_2$ = 1.0 Hz, J_3 = 8.0 Hz), 7.53 – 7.48 (m, 2H), 7.33 – 7.29 (m, 4H), 7.24 (ddd, 2H, J_1 = 1.0 Hz, J_2 = 7.0 Hz, J_3 =

8.0 Hz), 7.08 (ddd, 2H, J_1 = 1.0 Hz, J_2 = 7.0 Hz, J_3 = 8.0 Hz), 6.92 (br s, 2H), 6.21 (br t, 1H, J = 5.5 Hz), 4.85 (dd, 1H, $J_1 \approx J_2$ = 7.0 Hz), 4.21 (dd, 2H, J_1 = 5.5 Hz, J_2 = 7.0 Hz), 3.74 (s, 6H).

^{13}C NMR (101 MHz, $CDCl_3$, 25 °C): δ = 166.5, 137.6, 137.5, 133.2, 128.8, 128.5, 127.4, 126.9, 122.0, 119.8, 119.2, 115.6, 109.5, 44.9, 34.3, 32.9.

HRMS (ESI-Orbitrap, *m*/*z*): calcd for $C_{27}H_{24}ClN_3O$ [M + Na]$^+$ 464.1506; found 464.1499.

N-(2,2-bis(1-methyl-1*H*-indol-3-yl)ethyl)-4-nitrobenzamide (**89ae**):

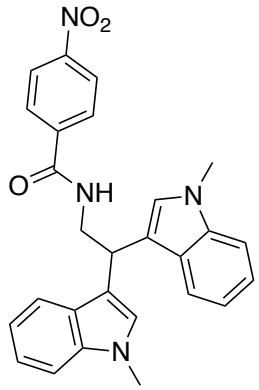

According to GP11, bisindole **88a** (50 mg, 0.16 mmol, 1 equiv.), 4-nitrobenzoic acid (28.9 mg, 0.17 mmol, 1.05 equiv.) and EDCI (47.4 mg, 0.25 mmol, 1.5 equiv.) in DCM (2.1 mL) provided, after purification by column chromatography using cyclohexane/ethyl acetate (7:3), the desired compound **89ae** (68 mg, yield 91 %) as a yellow foam.

R_f = 0.62 (1:1 cyclohexane/ethyl acetate)

^{1}H NMR (400 MHz, $CDCl_3$, 25 °C): δ = 8.20 – 8.14 (m, 2H), 7.73 – 7.68 (m, 2H), 7.66 (ddd, 2H, $J_1 \approx J_2$ = 1.0 Hz, J_3 = 8.0 Hz), 7.33 (ddd, 2H, $J_1 \approx J_2$ = 1.0 Hz, J_3 = 8.0 Hz), 7.25 (ddd, 2H, J_1 = 1.0 Hz, J_2 = 7.0 Hz, J_3 = 8.0 Hz), 7.09 (ddd, 2H, J_1 = 1.0 Hz, J_2 = 7.0 Hz, J_3 = 8.0 Hz), 6.94 (br s, 2H), 6.33 (br t, 1H, J = 6.0 Hz), 4.88 (dd, 1H, $J_1 \approx J_2$ = 7.5 Hz), 4.23 (dd, 2H, J_1 = 6.0 Hz, J_2 = 7.5 Hz), 3.75 (s, 6H).

^{13}C NMR (101 MHz, $CDCl_3$, 25 °C): δ = 165.5, 149.6, 140.4, 137.5, 128.2, 127.4, 126.9, 123.8, 122.1, 119.7, 119.3, 115.4, 109.6, 45.2, 34.2, 32.9.

HRMS (ESI-Orbitrap, *m*/*z*): calcd for $C_{27}H_{24}N_4O_3$ [M + Na]$^+$ 475.1746; found 475.1738.

N-(2,2-bis(1-methyl-1*H*-indol-3-yl)ethyl)-4-methoxybenzamide (**89af**):

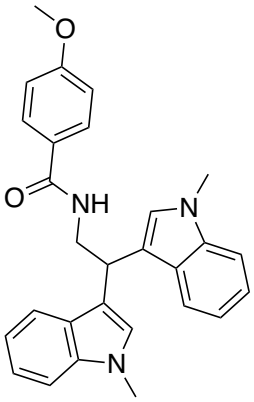

According to GP11, bisindole **88a** (50 mg, 0.16 mmol, 1 equiv.), 4-methoxybenzoic acid (26.3 mg, 0.17 mmol, 1.05 equiv.) and EDCI (47.4 mg, 0.25 mmol, 1.5 equiv.) in DCM (2.1 mL) provided, after purification by column chromatography using cyclohexane/ethyl acetate (6:4), the desired compound **89af** (72 mg, yield > 99 %) as a white solid.

R_f = 0.42 (1:1 cyclohexane/ethyl acetate)

^{1}H NMR (400 MHz, $CDCl_3$, 25 °C): δ = 7.68 (ddd, 2H, $J_1 \approx J_2$ = 1.0 Hz, J_3 = 8.0 Hz), 7.58 – 7.52 (m, 2H), 7.32 (ddd, 2H, $J_1 \approx J_2$ = 1.0 Hz, J_3 = 8.0 Hz), 7.24 (ddd, 2H, J_1 = 1.0 Hz, J_2 = 7.0 Hz, J_3 = 8.0 Hz), 7.08 (ddd, 2H, J_1 = 1.0 Hz, J_2 = 7.0 Hz, J_3 = 8.0 Hz), 6.93 (br s, 2H), 6.85 - 6.81 (m, 2H), 6.20 (br t, 1H, J = 6.0 Hz), 4.85 (dd, 1H, $J_1 \approx J_2$ = 7.0 Hz), 4.21 (dd, 2H, J_1 = 6.0 Hz, J_2 = 7.0 Hz), 3.81 (s, 3H), 3.73 (s, 6H).

^{13}C NMR (101 MHz, $CDCl_3$, 25 °C): δ = 167.1, 162.1, 137.5, 128.8, 127.5, 127.1, 127.0, 121.9, 119.9, 119.1, 115.8, 113.7, 109.4, 55.5, 44.7, 34.4, 32.9.

HRMS (ESI-Orbitrap, *m*/*z*): calcd for $C_{28}H_{27}N_3O_2$ $[M + Na]^+$ 460.2001; found 460.1979.

N-(2,2-bis(1-methyl-1*H*-indol-3-yl)ethyl)furan-2-carboxamide (**89ag**):

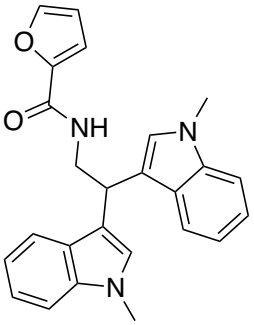

According to GP11, bisindole **88a** (50 mg, 0.16 mmol, 1 equiv.), furan-2-carboxylic acid (19.4 mg, 0.17 mmol, 1.05 equiv.) and EDCI (47.4 mg, 0.25 mmol, 1.5 equiv.) in DCM (2.1 mL) provided, after purification by column chromatography using cyclohexane/ethyl acetate (6:4), the desired compound **89ag** (65.1 mg, yield 99 %) as a white solid.

R_f = 0.46 (1:1 cyclohexane/ethyl acetate)

^{1}H NMR (400 MHz, $CDCl_3$, 25 °C): δ = 7.68 (ddd, 2H, $J_1 \approx J_2$ = 1.0 Hz, J_3 = 8.0 Hz), 7.33 – 7.29 (m, 3H), 7.23 (ddd, 2H, J_1 = 1.0 Hz, J_2 = 7.0 Hz, J_3 = 8.0 Hz), 7.09 – 7.07 (m, 1H), 7.07 (ddd, 2H, J_1 = 1.0 Hz, J_2 = 7.0 Hz, J_3 = 8.0 Hz), 6.92 (br s, 2H), 6.52 (br

t, 1H, J = 6.0 Hz), 6.44 (dd, 1H, J_1 = 2.0 Hz, J_2 = 3.5 Hz), 4.83 (dd, 1H, $J_1 \approx J_2$ = 7.0 Hz), 4.19 (dd, 2H, J_1 = 6.0 Hz, J_2 = 7.0 Hz), 3.74 (s, 6H).

^{13}C NMR (101 MHz, $CDCl_3$, 25 °C): δ = 158.6, 148.3, 143.8, 137.5, 127.4, 127.0, 121.8, 119.9, 119.1, 115.6, 114.1, 112.1, 109.4, 43.7, 34.6, 32.9.

HRMS (ESI-Orbitrap, *m*/*z*): calcd for $C_{25}H_{23}N_3O_2$ $[M + Na]^+$ 420.1688; found 420.1683.

N-(2,2-bis(1-methyl-1*H*-indol-3-yl)ethyl)thiophene-2-carboxamide (**89ah**):

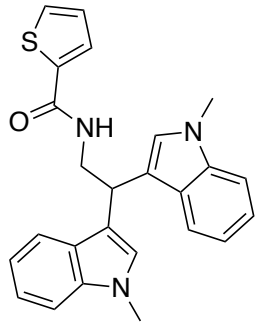

According to GP11, bisindole **88a** (50 mg, 0.16 mmol, 1 equiv.), thiophene-2-carboxylic acid (22.2 mg, 0.17 mmol, 1.05 equiv.) and EDCI (47.4 mg, 0.25 mmol, 1.5 equiv.) in DCM (2.1 mL) provided, after purification by column chromatography using cyclohexane/ethyl acetate (7:3), the desired compound **89ah** (67.8 mg, yield 99.5 %) as a white solid.

R_f = 0.71 (1:1 cyclohexane/ethyl acetate)

^{1}H NMR (400 MHz, $CDCl_3$, 25 °C): δ = 7.67 (ddd, 2H, $J_1 \approx J_2$ = 1.0 Hz, J_3 = 8.0 Hz), 7.41 (dd, 1H, J_1 = 1.0 Hz, J_2 = 5.0 Hz), 7.32 (ddd, 2H, $J_1 \approx J_2$ = 1.0 Hz, J_3 = 8.0 Hz), 7.24 (ddd, 2H, J_1 = 1.0 Hz, J_2 = 7.0 Hz, J_3 = 8.0 Hz), 7.21 (dd, 1H, J_1 = 1.0 Hz, J_2 = 3.5 Hz), 7.08 (ddd, 2H, J_1 = 1.0 Hz, J_2 = 7.0 Hz, J_3 = 8.0 Hz), 6.98 (dd, 1H, J_1 = 3.5 Hz, J_2 = 5.0 Hz), 6.93 (br s, 1H), 6.13 (br t, 1H, J = 6.0 Hz), 4.84 (dd, 1H, $J_1 \approx J_2$ = 7.0 Hz), 4.19 (dd, 2H, J_1 = 6.0 Hz, J_2 = 7.0 Hz), 3.74 (s, 6H).

^{13}C NMR (101 MHz, $CDCl_3$, 25 °C): δ = 162.0, 139.4, 137.5, 129.8, 127.9, 127.6, 127.4, 127.0, 121.9, 119.9, 119.1, 115.6, 109.5, 44.7, 34.5, 32.9.

HRMS (ESI-Orbitrap, *m*/*z*): calcd for $C_{25}H_{23}N_3OS$ $[M + Na]^+$ 448.1801; found 448.1792.

N-(2,2-di(1*H*-indol-3-yl)ethyl)isobutyramide (**89ba**):

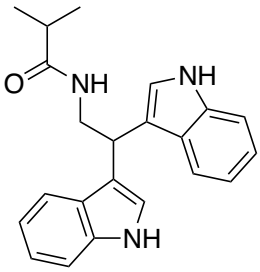

According to GP11, bisindole **88b** (80 mg, 0.29 mmol, 1 equiv.), isobutyric acid (28.4 µL, 0.31 mmol, 1.05 equiv.) and EDCl (83.5 mg, 0.44 mmol, 1.5 equiv.) in DCM (3.9 mL) provided, after purification by column chromatography using cyclohexane/ethyl acetate (25:75), the desired compound **89ba** (71.6 mg, yield 71.4 %) as a light orange powder.

R_f = 0.34 (1:1 cyclohexane/ethyl acetate)

^{1}H NMR (400 MHz, $CDCl_3$, 25 °C): δ = 8.08 (br s, 2H), 7.63 (dddd, 2H, $J_1 \approx J_2 \approx J_3$= 1.0 Hz, J_4 = 8.0 Hz), 7.37 (ddd, 2H, $J_1 \approx J_2$ = 1.0 Hz, J_3 = 8.0 Hz), 7.18 (ddd, 2H, J_1 = 1.0 Hz, J_2 = 7.0 Hz, J_3 = 8.0 Hz), 7.06 (ddd, 2H, J_1 = 1.0 Hz, J_2 = 7.0 Hz, J_3 = 8.0 Hz), 7.01 (dd, 2H, J_1 = 0.5 Hz, J_2 = 2.5 Hz), 5.56 (br t, 1H, J_1 = 6.0 Hz), 4.75 (dd, 1H, $J_1 \approx J_2$ = 7.0 Hz), 4.05 (dd, 2H, J_1 = 6.0 Hz, J_2 = 7.0 Hz), 2.19 (hept, 1H , J = 7.0 Hz), 1.05 (d, 6H, J = 7.0 Hz).

^{13}C NMR (101 MHz, $CDCl_3$, 25 °C): δ = 177.2, 136.8, 127.0, 122.3 (2C), 119.8, 119.6, 117.1, 111.3, 43.6, 35.8, 34.6, 19.7.

HRMS (ESI-Orbitrap, *m*/*z*): calcd for $C_{22}H_{23}N_3O$ $[M + Na]^+$ 368.1739; found 368.1725.

N-(2,2-di(1*H*-indol-3-yl)ethyl)benzamide (**89bb**):

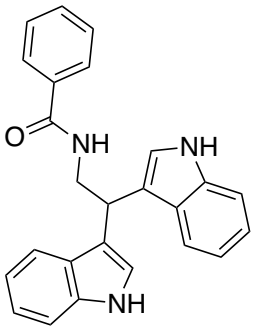

According to GP11, bisindole **88b** (50 mg, 0.18 mmol, 1 equiv.), benzoic acid (23 mg, 0.19 mmol, 1.05 equiv.) and EDCl (52.2 mg, 0.27 mmol, 1.5 equiv.) in DCM (2.4 mL) provided, after purification by column chromatography using cyclohexane/ethyl acetate (3:7), the desired compound **89bb** (65.9 mg, yield 96 %) as a white foam.

R_f = 0.49 (1:1 cyclohexane/ethyl acetate)

The physicochemical data are consistent with those reported in the literature.[60]

^{1}H NMR (400 MHz, DMSO-d_6, 25 °C): δ = 10.78 (br d, 2H, J = 2.5 Hz), 8.53 (t, 1H, J = 5.5 Hz), 7.78 – 7.71 (m, 2H), 7.53 (d, 2H, J = 8.0 Hz), 7.47 (dddd, 1H, $J_1 \approx J_2$ = 1.5 Hz, $J_3 \approx J_4$ = 7.5 Hz), 7.43 – 7.36 (m, 2H), 7.30 (d, 2H, J = 8.0 Hz), 7.22 (br d, 2H, J_1 = 2.5 Hz), 7.01 (ddd, 2H, J_1 = 1.0 Hz, J_2 = 7.0 Hz, J_3 = 8.0 Hz), 6.87 (ddd, 2H, J_1 = 1.0 Hz, J_2 = 7.0 Hz, J_3 = 8.0 Hz), 4.88 (dd, 1H, $J_1 \approx J_2$ = 7.5 Hz), 3.99 (dd, 2H, J_1 = 5.5 Hz, J_2 = 7.5 Hz).

^{13}C NMR (101 MHz, DMSO-d_6, 25 °C): δ = 166.8, 136.9, 135.2, 131.4, 128.6, 127.6, 127.4, 122.8, 121.2, 119.4, 118.5, 116.9, 111.8, 44.9, 34.0.

HRMS (ESI-Orbitrap, *m*/*z*): calcd for $C_{25}H_{21}N_3O$ [M + Na]$^+$ 402.1582; found 402.1564.

*4.4.3. Synthesis of substituted amine-bisindole (**90**)*

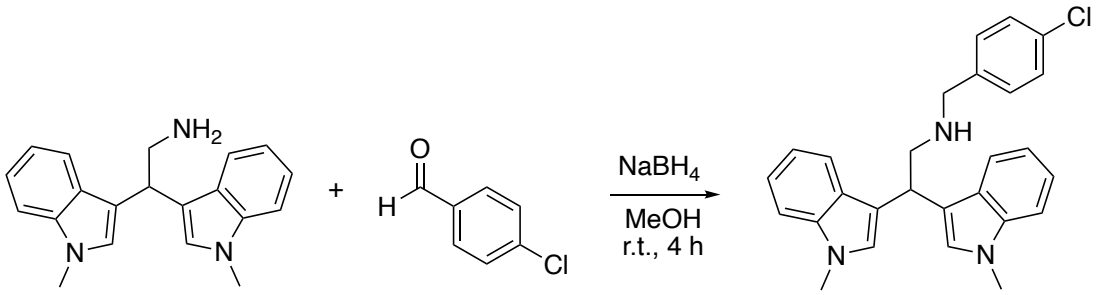

N-(4-chlorobenzyl)-2,2-bis(1-methyl-1*H*-indol-3-yl)ethan-1-amine (**90**):

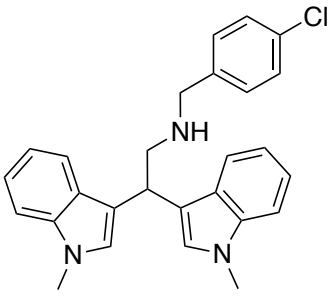

According to a modification of a synthesis reported in the literature,[61] the amine **88a** (60 mg, 0.2 mmol, 1 equiv.) and 4-chlorobenzaldehyde (28 mg, 0.2 mmol, 1 equiv.) were stirred in 0.3 mL of MeOH for 2 h. After this time, the mixture was cooled to 0°C and $NaBH_4$ (11 mg, 0.3 mmol, 1.5 equiv.) was added portion-wise. The mixture was then stirred at room temperature until the disappearance of the starting material (TLC check). The reaction was stopped, AcOH (0.1 mL) was added and the crude was evaporated under reduced pressure. The resulting slurry was dissolved in H_2O and extracted with DCM (6 x 2 mL). The combined organic phases were dried over anhydrous sodium sulphate, and the solvent was removed under reduced pressure to leave the crude

product, which was purified by chromatography over silica gel to obtain the desired product **90** (46 mg, 53 % yield).

^{1}H NMR (400 MHz, $CDCl_3$, 25 °C): δ = 7.59 (ddd, 2H, $J_1 \approx J_2$ = 1.0 Hz, J_3 = 8.0 Hz), 7.28 (ddd, 2H, $J_1 \approx J_2$ = 1.0 Hz, J_3 = 8.0 Hz), 7.24 – 7.18 (m, 4H), 7.17 – 7.12 (m, 2H), 7.05 (ddd, 2H, J_1 = 1.0 Hz, J_2 = 7.0 Hz, J_3 = 8.0 Hz), 6.85 (br s, 2H), 4.82 (dd, 1H, $J_1 \approx J_2$ = 7.0 Hz), 3.80 (s, 2H), 3.70 (s, 6H), 3.36 (d, 2H, J = 7.0 Hz).

^{13}C NMR (101 MHz, $CDCl_3$, 25 °C): δ = 139.1, 137.4, 132.5, 129.6, 128.5, 127.5, 126.9, 121.7, 119.8, 118.8, 116.6, 109.3, 53.8, 53.2, 34.5, 32.8.

*4.4.4. Synthesis of ester and carboxylic acid bisindoles (**91a-b,92**)*

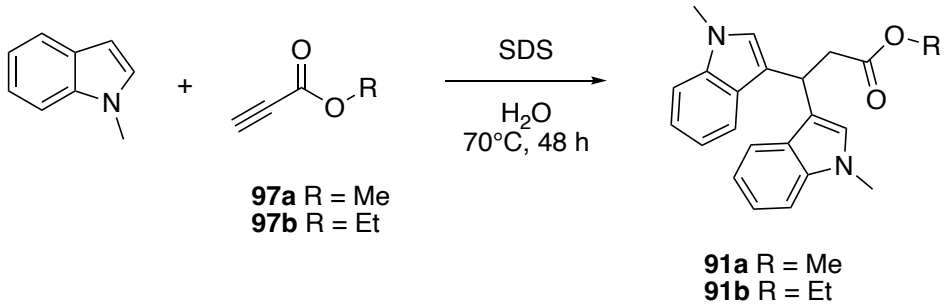

97a R = Me
97b R = Et

91a R = Me
91b R = Et

General procedure for the synthesis of 3,3-bis(-indol-3-yl)propanoates (91a-b) GP12

According to a modification of a synthesis reported in the literature,[50] sodium dodecylsulfate (0.1 equiv.), 1-methyl-1*H*-indole (1 equiv.), and water (c = 0.04 M) were stirred vigorously for 10 minutes, then the corresponding propiolate (1.2 equiv.) was added dropwise. The mixture was stirred at 70°C for 48 hours. After this time, a small amount of sodium chloride was introduced, and the reaction mixture was extracted with ethyl acetate. The combined organic phases were dried over anhydrous sodium sulphate, and the solvent was removed under reduced pressure to leave the crude product, which was purified by chromatography over silica gel.

Methyl 2,2-bis(1-methyl-1*H*-indol-3-yl)acetate (**91a**):

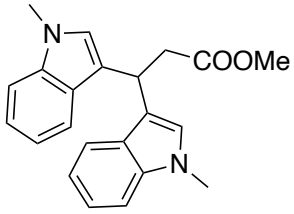

According to GP12, sodium dodecylsulphate (58 mg, 0.2 mmol, 0.1 equiv.), 1-methyl-1*H*-indole (262 µL, 2 mmol, 1 equiv) and methyl propiolate (214 µL, 2.4 mmol, 1.2 equiv) in water (50 mL) provided, after purification by column chromatography using cyclohexane/ethyl acetate (9:1), the desired compound **91a** (176 mg, yield 51 %) as a light beige powder.

The physicochemical data are consistent with those reported in the literature.[62]

^{1}H NMR (400 MHz, $CDCl_3$) δ 7.61 (dt, *J* = 8.0, 1.0 Hz, 2H), 7.29 (t dt, *J* = 8.0, 1.0 Hz, 2H), 7.21 (ddd, *J* = 8.0, 7.0, 1.0 Hz, 2H), 7.06 (ddd, *J* = 8.0, 7.0, 1.0 Hz, 2H), 6.87 (s, 2H), 5.12 (tt, *J* = 7.5, 1.0 Hz, 1H), 3.72 (s, 6H), 3.59 (s, 3H), 3.19 (d, *J* = 7.5 Hz, 2H).

Ethyl 2,2-bis(1-methyl-1*H*-indol-3-yl)acetate (**91b**):

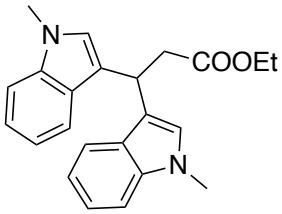

According to GP12, sodium dodecylsulphate (116 mg, 0.4 mmol, 0.1 equiv.), 1-methyl-1*H*-indole (524 µL, 4 mmol, 1 equiv) and methyl propiolate (588 µL, 4.8 mmol, 1.2 equiv) in water (100 mL) provided, after purification by column chromatography using cyclohexane/ethyl acetate (95:5), the desired compound **91b** (388 mg, yield 54 %) as a white powder.

The physicochemical data are consistent with those reported in the literature.[62]

^{1}H NMR (400 MHz, $CDCl_3$, 25 °C): δ = 7.62 (dt, *J* = 8.0, 1.0 Hz, 2H), 7.28 (dt, *J* = 8.0, 1.0 Hz, 2H), 7.23 – 7.17 (m, 2H), 7.05 (ddd, *J* = 8.0, 7.0, 1.0 Hz, 2H), 6.88 (s, 2H), 5.12 (tt, *J* = 7.5, 1.0 Hz, 1H), 4.04 (q, *J* = 7.0 Hz, 2H), 3.71 (s, 6H), 3.17 (d, *J* = 7.5 Hz, 2H), 1.11 (t, *J* = 7.0 Hz, 3H).

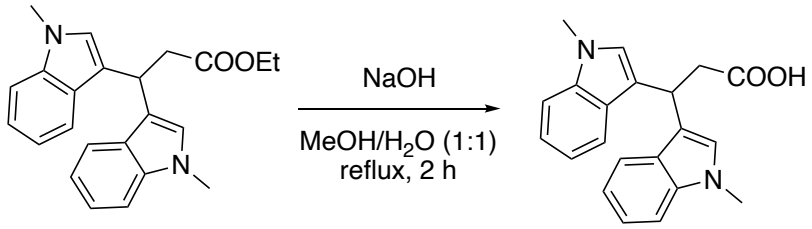

91b **94**

3,3-bis(1-methyl-1*H*-indol-3-yl)propanoic acid (**92**):

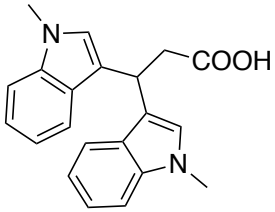

According to a procedure reported in the literature,[63] ethyl 2,2-bis(1-methyl-1*H*-indol-3-yl)acetate **91b** (830 mg, 2.3 mmol, 1 equiv.) was dissolved in a 1:1 mix of MeOH/H_2O (c = 0.0625 M). Then NaOH (461 mg, 11.5 mmol, 5 equiv.) was added and the mixture was stirred under reflux for 2 h. After the time had elapsed, the reaction was cooled to room temperature, quenched with 45 mL of water and acidified to pH 3 with 2 M aqueous HCl. The mixture was then extracted with EtOAc (3 x 40 mL). The combined organic phases were dried over anhydrous sodium sulphate, and the solvent was removed under reduced pressure to leave the crude product, which was purified by column chromatography DCM/MeOH (95:5) with 1 % of acetic acid to give the desired product **92** (605 mg, yield 83 %) as a white solid.

The physicochemical data are consistent with those reported in the literature.[63]

^{1}H NMR (400 MHz, DMSO-d_6, 25 °C): δ = 7.49 (dt, *J* = 8.0, 1.1 Hz, 2H), 7.33 (dt, *J* = 8.0, 1.0 Hz, 2H), 7.21 (s, 2H), 7.07 (ddd, *J* = 8.0, 7.0, 1.0 Hz, 2H), 6.92 (ddd, *J* = 8.0, 7.0, 1.0 Hz, 2H), 4.88 (tt, *J* = 7.5, 1.0 Hz, 1H), 3.07 (d, *J* = 7.5 Hz, 2H).

*4.4.5. Synthesis of mono and di-substituted bisindoles (**93a-b,94**)*

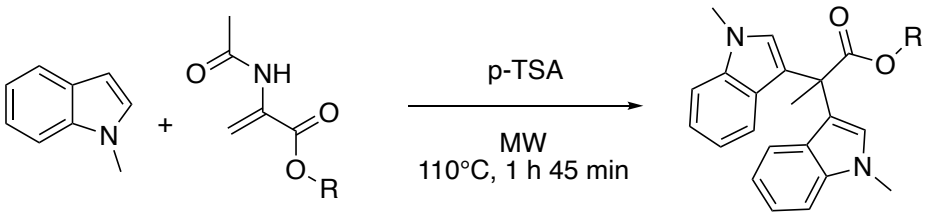

98a R = H
98b R = Me

93a R = H
93b R = Me

Methyl 2-acetamidoacrylate (**98b**):

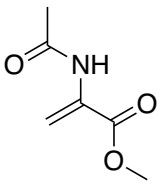

According to a described procedure,[64] to a solution of 2-acetamidoacrylic acid (258 mg, 2 mmol, 1 equiv.) in MeOH (4.76 mL, 0.42 M), Cs_2CO_3 (326 mg, 1 mmol, 0.5 equiv.) was added and the mixture was stirred at room temperature for one hour. The solution was then evaporated under reduced pressure until dry. The crude was dissolved in DMF (7.14 mL, 0.28 M), and iodomethane (0.311 mL, 5 mmol, 2.5 equiv.) was added dropwise. After 2 hours, the reaction was stopped, and the mixture was concentrated to dryness. The desired product was obtained after cyclohexane/ethyl acetate (7:3) column chromatography (196 mg, 69 %) as white needles.

The physicochemical data are consistent with those reported in the literature. [64]

^{1}H NMR (400 MHz, $CDCl_3$, 25 °C): δ = 7.71 (br s, 1H), 6.60 (s, 1H), 5.88 (d, 1H, J = 1.5 Hz), 3.85 (s, 3H), 2.13 (s, 3H).

2,2-bis(1-methyl-1*H*-indol-3-yl)propanoic acid (**93a**):

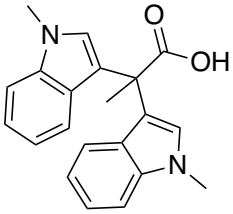

According to a described procedure,[51] a solution of 1-methyl-1*H*-indole (261 µL, 2 mmol, 2 equiv.), 2-acetamidoacrylic acid (12 mg, 1 mmol, 1 equiv.) and *p*-toluenesulfonic acid (9 mg, 0.05 mmol, 0.05 equiv.) in acetonitrile (5 mL, 0.2 M) was charged in a Pyrex microwave vial and the resulting mixture was stirred in a microwave reactor at 110°C (300 W) for 1.75 h. After cooling to room temperature, water (15 mL) was added, and the aqueous phase was extracted with ethyl acetate (5 x 20 mL). The combined organic phases were dried over anhydrous sodium sulphate and the solvent was removed under reduced pressure. The desired product **93a** was obtained after cyclohexane/ethyl acetate (8:2) column chromatography (81 mg, 24 %) as a light brown powder.

The physicochemical data are consistent with those reported in the literature. [65]

^{1}H NMR (400 MHz, $CDCl_3$, 25 °C): δ = 7.52 (ddd, 2H, $J_1 \approx J_2$ = 1.0 Hz, J_3 = 8.0 Hz), 7.31 (ddd, 2H, $J_1 \approx J_2$ = 1.0 Hz, J_3 = 8.0 Hz), 7.20 (ddd, 2H, J_1 = 1.0 Hz, J_2 = 7.0 Hz,

J_3 = 8.0 Hz), 7.01 (ddd, 2H, J_1 = 1.0 Hz, J_2 = 7.0 Hz, J_3 = 8.0 Hz), 6.91 (s, 2H), 3.73 (s, 6H), 2.15 (s, 3H).

Methyl 2,2-bis(1-methyl-1*H*-indol-3-yl)propanoate(**93b**):

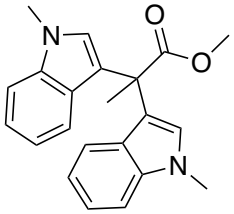

According to a described procedure,[51] a solution of 1-methyl-1*H*-indole (153 µL, 1.2 mmol, 2 equiv.), methyl 2-acetamidoacrylate (85 mg, 0.6 mmol, 1 equiv.) and *p*-toluenesulfonic acid (5 mg, 0.03 mmol, 0.05 equiv.) in acetonitrile (3 mL, 0.2 M) was charged in a Pyrex microwave vial and the resulting mixture was stirred in a microwave reactor at 110 °C (300 W) for 1.75 h. After cooling to room temperature, water (9 mL) was added, and the aqueous phase was extracted with ethyl acetate (3 x 15 mL). The combined organic phases were dried over anhydrous sodium sulphate and the solvent was removed under reduced pressure. The desired product **93b** was obtained after cyclohexane/ethyl acetate (9:1) column chromatography (175 mg, 85 %) as a white foam.

The physicochemical data are consistent with those reported in the literature. [51]

^{1}H NMR (400 MHz, $CDCl_3$, 25 °C): δ = 7.52 (ddd, 2H, $J_1 \approx J_2$ = 1.0 Hz, J_3 = 8.0 Hz), 7.31 (ddd, 2H, $J_1 \approx J_2$ = 1.0 Hz, J_3 = 8.0 Hz), 7.20 (ddd, 2H, J_1 = 1.0 Hz, J_2 = 7.0 Hz, J_3 = 8.0 Hz), 7.02 (ddd, 2H, J_1 = 1.0 Hz, J_2 = 7.0 Hz, J_3 = 8.0 Hz), 6.84 (s, 2H), 3.72 (s, 6H), 3.67 (s, 3H), 2.12 (s, 3H).

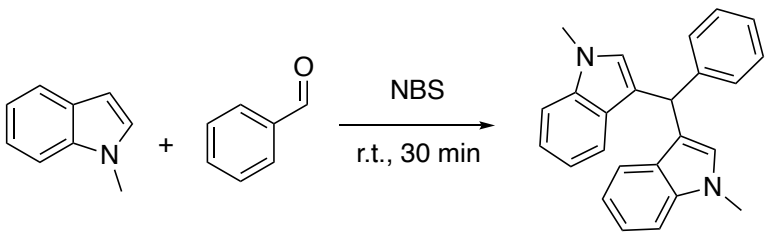

94

3,3'-(Phenylmethylene)bis(1-methyl-1*H*-indole) (**94**):

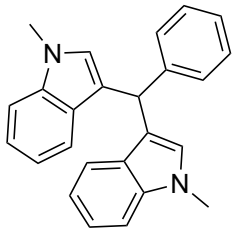

According to the reported synthesis in the literature,[52] a mixture of benzaldehyde (51 µL, 0.5 mmol, 1 equiv.) and 1-methyl-1*H*-indole (129 µL, 1 mmol, 2 equiv.) was stirred with NBS (9 mg, 0.05 mmol, 0.1 equiv.) in the absence of solvent at room temperature in a capped vial. After completion of the reaction (30 min, TLC check), a saturated aqueous solution of $NaHCO_3$ was added and was extracted with DCM (5 x 5 mL). The combined organic phases were dried over Na_2SO_4, filtered and the solvent evaporated under reduced pressure. The desired product was obtained after cyclohexane/ethyl acetate (95:5) column chromatography. (161 mg, 92 %).

The physicochemical data are consistent with those reported in the literature.[66]

^{1}H NMR (400 MHz, $CDCl_3$, 25 °C): δ = 7.38 (ddd, 2H, $J_1 \approx J_2$ = 1.0 Hz, J_3 = 8.0 Hz), 7.34 (ddd, 2H, $J_1 \approx J_2$ = 1.0 Hz, J_3 = 8.0 Hz), 7.31 – 7.26 (m, 4H), 7.23 – 7.17 (m, 3H), 6.99 (ddd, 2H, J_1 = 1.0 Hz, J_2 = 7.0 Hz, J_3 = 8.0 Hz), 6.53 (d, 2H, J = 1.0 Hz), 5.88 (s, 1H), 3.68 (s, 6H).

*4.4.6. Synthesis of amide glycosylated bisindoles (**99**)*

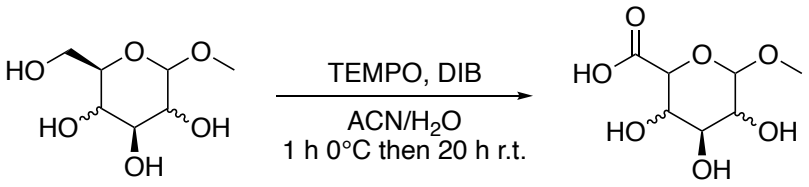

101a from methyl-glucose
101b from methyl-galactose

General procedure for the synthesis of methyl-glucoronic acid derivatives GP13

According to a previously reported synthesis in the literature,[67] the corresponding glucose pyranoside derivative (2.5 mmol) was dissolved in MeCN (11.6 mL) and water (1.9 mL) and solid 2,2,6,6-tetramethyl-1-piperidinyloxy (TEMPO) (98 mg, 0.625 mmol, 0.25 equiv.) was added. The mixture was cooled with an ice-bath and (diacetoxyiodo)benzene (DIB) (2.013 g, 6.25 mmol, 2.5 equiv.) was added portion-wise. The mixture was stirred for 1 h at 0 °C and then for 20 h at room temperature.

The reaction was quenched with MeOH and the solvent was removed under reduced pressure. Then, H_2O was added, and the aqueous phase was washed 3 times with EtOAc. The aqueous phase was then evaporated to obtain our final products **101a-b** without further purification.

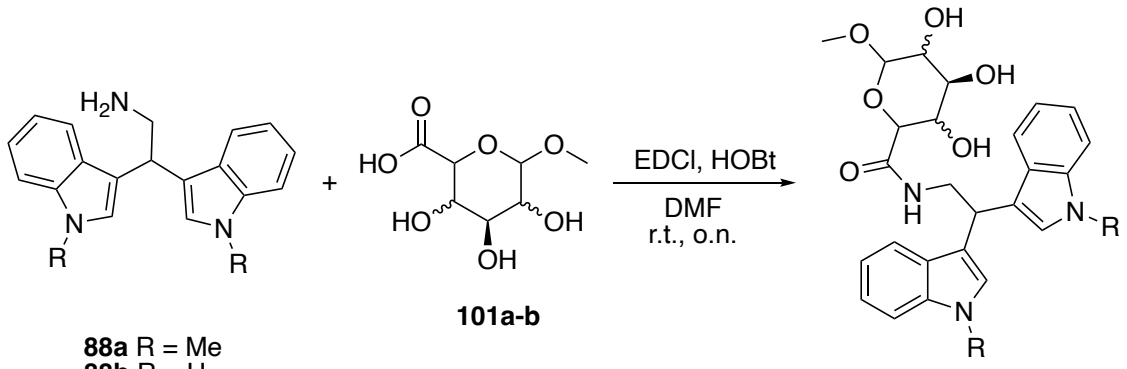

88a R = Me
88b R = H

101a-b

99aa R = Me from 101a
99ab R = Me from 101b
99ba R = H from 101a
99bb R = H from 101b

General procedure for the synthesis of glycosylated amides-bisindoles GP14

According to a modification of a synthesis previously reported in literature,[68] a mixture of the corresponding methyl oxidised sugar **101** (0.25 mmol) and HOBt (0.3 mmol) in anhydrous DMF (7.9 mL) was stirred at room temperature for 0.5 h. Then, the bisindolyl compound **88a-b** (0.3 mmol) and EDCI (0.5 mmol) were added to the solution and the mixture was stirred at room temperature overnight. Then, 30 mL of H_2O were added, and extracted with EtOAc (3 × 20 mL). The organic layers were combined, washed with brine, dried over anhydrous Na_2SO_4, and concentrated in vacuo. The resulting crude product was purified, if needed, by using column flash chromatography on silica gel.

(3*S*,4*S*,5*R*)-*N*-(2,2-bis(1-methyl-1*H*-indol-3-yl)ethyl)-3,4,5-trihydroxy-6-methoxytetrahydro-2*H*-pyran-2-carboxamide (**99aa**):

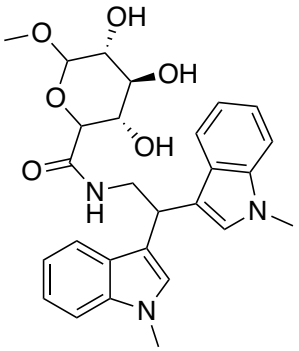

According to GP14, (3*S*,4*S*,5*R*)-3,4,5-trihydroxy-6-methoxytetrahydro-2*H*-pyran-2-carboxylic acid **101a** (52 mg, 0.25 mmol, 0.84 equiv.), HOBt (41 mg, 0.3 mmol, 1 equiv.) 2,2-bis(1-methyl-1*H*-indol-3-yl)ethan-1-amine **88a** (91 mg. 0.3 mmol, 1 equiv.) and EDCI (97 mg, 0.5 mmol, 1.68 equiv.) in DMF (7.9 mL, 0.038 M) provided, after DCM/MeOH/NH_3 (96:4:1) column chromatography, the desired compound **99aa** (80 mg, yield 64 %) as a light brown foam.

R_f = 0.57 (9:1 DCM/MeOH)

^{1}H NMR (400 MHz, MeOD, 25 °C): δ = 7.54 (dq, 2H, J_1 = 1.0 Hz, J_2 = 8.0 Hz), 7.29 (dd, 2H, J_1 = 1.0 Hz, J_2 = 8.0 Hz), 7.11 (ddd, 2H, J_1 = 1.0 Hz, J_2 = 7.0 Hz, J_3 = 8.0 Hz), 7.00 (t, 2H, J = 1.0 Hz), 6.95 (ddd, 2H, J_1 = 1.0 Hz, J_2 = 7.0 Hz, J_3 = 8.0 Hz), 4.81 (t, 1H, J = 7.5 Hz), 4.60 (d, 1H, J = 3.5 Hz), 4.03 – 3.89 (m, 2H), 3.80 (d, 1H, J = 10.0 Hz), 3.70 (d, 6H, J = 1.0 Hz), 3.57 (t, 1H, J = 9.0 Hz), 3.34 (dd, 1H, J_1 = 3.5 Hz, J_2 = 6.0 Hz), 3.21 (s, 3H).

^{13}C NMR (101 MHz, MeOD, 25 °C): δ = 172.6, 138.80, 138.78, 129.0, 128.9, 127.9, 127.8, 122.4, 120.4, 120.3, 119.6, 117.0, 116.9, 110.19, 110.17, 101.4, 74.5, 73.8, 72.8, 71.7, 56.0, 45.4, 34.8, 32.7 (2C).

HRMS (ESI-Orbitrap, *m*/*z*): calcd for $C_{27}H_{31}N_3O_6$ $[M + Na]^+$ 516.2105; found 516.2101

(3*R*,4*S*,5*R*)-*N*-(2,2-bis(1-methyl-1*H*-indol-3-yl)ethyl)-3,4,5-trihydroxy-6-methoxytetrahydro-2*H*-pyran-2-carboxamide (**99ab**):

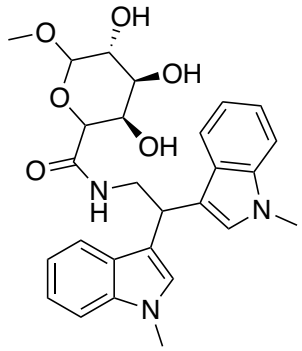

According to GP14, (3*R*,4*S*,5*R*)-3,4,5-trihydroxy-6-methoxytetrahydro-2*H*-pyran-2-carboxylic acid **101b** (52 mg, 0.25 mmol, 0.84 equiv.), HOBt (41 mg, 0.3 mmol, 1 equiv.) 2,2-bis(1-methyl-1*H*-indol-3-yl)ethan-1-amine **88a** (91 mg. 0.3 mmol, 1 equiv.) and EDCI (97 mg, 0.5 mmol, 1.68 equiv.) in DMF (7.9 mL, 0.038 M) provided, after DCM/MeOH/NH_3 (96:4:1) column chromatography, the desired compound **99ab** (63 mg, yield 51 %) as a light brown foam.

R_f = 0.49 (9:1 DCM/MeOH)

^{1}H NMR (400 MHz, MeOD, 25 °C): δ = 7.53 (ddt, 2H, J_1 = 1.0 Hz, J_2 = 2.0 Hz, J_3 = 8.0 Hz), 7.30 (ddt, 2H, J_1 = 1.0 Hz, J_2 = 2.0 Hz, J_3 = 8.0 Hz), 7.12 (dddd, 2H, J_1 = 1.0 Hz, J_2 = 2.5 Hz, J_3 = 7.0 Hz, J_4 = 8.0 Hz), 7.03 (dd, 2H, J_1 = 1.0 Hz, J_2 = 11.0 Hz), 6.95 (dtd, 2H, J_1 = 1.0 Hz, J_2 = 7.0 Hz, J_3 = 8.0 Hz), 4.81 (t, 1H, J = 7.5 Hz), 4.62 – 4.60 (m, 1H), 4.21 (q, 1H, J = 1.5 Hz), 4.14 (dd, 1H, J_1 = 7.0 Hz, J_2 = 13.0 Hz), 4.07 (d, 1H, J = 1.5 Hz), 3.83 (dd, 1H, J_1 = 8.0 Hz, J_2 = 13.0 Hz), 3.72 (d, 6H, J = 1.5 Hz), 3.71 (dd, 2H, J_1 = 1.0 Hz, J_2 = 2.0 Hz), 3.10 (s, 3H).

^{13}C NMR (101 MHz, MeOD, 25 °C): δ = 171.3, 138.82, 138.78, 129.0, 128.8, 127.9, 127.8, 122.5, 122.4, 120.4, 120.2, 119.7, 119.6, 116.94, 116.90, 110.2, 110.1, 101.6, 72.5, 71.3, 71.1, 69.6, 56.0, 45.4, 34.7, 32.74, 32.72.

HRMS (ESI-Orbitrap, *m*/*z*): calcd for $C_{27}H_{31}N_3O_6$ $[M + Na]^+$ 516.2105; found 516.2106

(3*S*,4*S*,5*R*)-*N*-(2,2-di(1*H*-indol-3-yl)ethyl)-3,4,5-trihydroxy-6-methoxytetrahydro-2*H*-pyran-2-carboxamide (**99ba**):

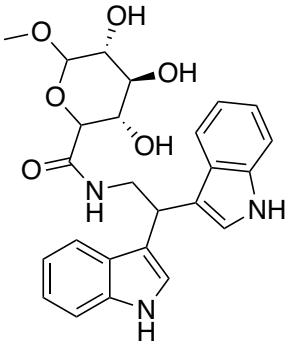

According to GP14, (3*S*,4*S*,5*R*)-3,4,5-trihydroxy-6-methoxytetrahydro-2*H*-pyran-2-carboxylic acid **101a** (52 mg, 0.25 mmol, 0.84 equiv.), HOBt (41 mg, 0.3 mmol, 1 equiv.) 2,2-di(1*H*-indol-3-yl)ethan-1-amine **88b** (83 mg. 0.3 mmol, 1 equiv.) and EDCI (97 mg, 0.5 mmol, 1.68 equiv.) in DMF (7.9 mL, 0.038 M) provided, after DCM/MeOH/NH_3 (95:5:1) column chromatography, the desired compound **99ba** (72 mg, yield 52 %) as a light brown foam.

R_f = 0.35 (9:1 DCM/MeOH)

^{1}H NMR (400 MHz, MeOD, 25 °C): δ = 7.54 (ddt, 2H, J_1 = 1.0 Hz, J_2 = 2.0 Hz, J_3 = 8.0 Hz), 7.32 (dq, 2H, J_1 = 1.0 Hz, J_2 = 8.0 Hz), 7.10 (t, 2H, J = 1.1 Hz), 7.05 (ddd, 2H, J_1 = 1.0 Hz, J_2 = 7.0 Hz, J_3 = 8.0 Hz), 6.92 (ddd, 2H, J_1 = 1.0 Hz, J_2 = 7.0 Hz, J_3 = 8.0 Hz), 4.82 (tt, 1H, J_1 = 1.0 Hz, J_2 = 7.5 Hz), 4.60 (d, 1H, J = 3.5 Hz), 4.00 (q, 1H, J = 13.0), 3.99 (q, 1H, J = 13.0) 3.80 (d, 1H, J = 9.9 Hz), 3.57 (dd, 1H, J = 9.7, 8.8 Hz), 3.36 – 3.32 (m, 2H), 3.21 (s, 3H).

^{13}C NMR (101 MHz, MeOD, 25 °C): δ = 172.6, 138.4, 138.3, 128.5, 128.4, 123.4, 123.3, 122.3, 120.2, 120.1, 119.5, 117.6, 117.5, 112.23, 112.22, 101.4, 74.5, 73.8, 72.8, 71.6, 56.0, 45.3, 35.1.

HRMS (ESI-Orbitrap, *m*/*z*): calcd for $C_{25}H_{27}N_3O_6$ $[M + Na]^+$ 488.1792; found 488.1781

(3*R*,4*S*,5*R*)-*N*-(2,2-di(1*H*-indol-3-yl)ethyl)-3,4,5-trihydroxy-6-methoxytetrahydro-2*H*-pyran-2-carboxamide (**99bb**):

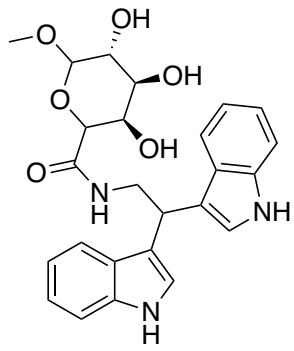

According to GP14, (3*R*,4*S*,5*R*)-3,4,5-trihydroxy-6-methoxytetrahydro-2*H*-pyran-2-carboxylic acid **101b** (52 mg, 0.25 mmol, 0.84 equiv.), HOBt (41 mg, 0.3 mmol, 1 equiv.) 2,2-di(1*H*-indol-3-yl)ethan-1-amine **88b** (83 mg. 0.3 mmol, 1 equiv.) and EDCI (97 mg, 0.5 mmol, 1.68 equiv.) in DMF (7.9 mL, 0.038 M) provided, after DCM/MeOH/NH_3 (95:5:1) column chromatography, the desired compound **99bb** (55 mg, yield 40 %) as a light brown foam.

R_f = 0.24 (9:1 DCM/MeOH)

^{1}H NMR (400 MHz, MeOD, 25 °C): δ = 7.53 (ddt, 2H, J_1 = 1.0 Hz, J_2 = 3.5 Hz, J_3 = 8.0 Hz), 7.32 (ddt, 2H, J_1 = 1.0 Hz, J_2 = 2.0 Hz, J_3 = 8.0 Hz), 7.11 (dd, 2H, J_1 = 1.0 Hz, J_2 = 7.0 Hz), 7.05 (dddd, 2H, J_1 = 1.0 Hz, J_2 = 2.5 Hz, J_3 = 7.0 Hz, J_4 = 8.0 Hz), 6.92 (dddd, 2H, J_1 = 1.0 Hz, J_2 = 5.5 Hz, J_3 = 7.0 Hz, J_4 = 8.0 Hz), 4.85 – 4.79 (m, 1H), 4.61 (t, 1H, J = 1.5 Hz), 4.21 (dd, 1H, J_1 = 8.0 Hz, J_2 = 13.0 Hz), 4.20 (s, 1H), 4.08 (d, 1H, J = 1.5 Hz), 3.84 (dd, 1H, J_1 = 8.0 Hz, J_2 = 13.0 Hz), 3.70 (dd, 2H, J_1 = 1.0 Hz, J_2 = 2.0 Hz), 3.11 (s, 3H).

^{13}C NMR (101 MHz, MeOD, 25 °C): δ = 171.3, 138.4, 138.3, 128.5, 128.3, 123.4, 123.3, 122.32, 122.30, 120.2, 120.0, 119.6, 119.5, 117.52, 117.45, 112.3, 112.2, 101.6, 72.5, 71.2, 71.1, 69.6, 56.0, 45.2, 35.0.

HRMS (ESI-Orbitrap, *m*/*z*): calcd for $C_{25}H_{27}N_3O_6$ [M + Na]$^+$ 488.1792; found 488.1790

*4.4.7. Synthesis of ester glycosylated bisindoles (**100**)*

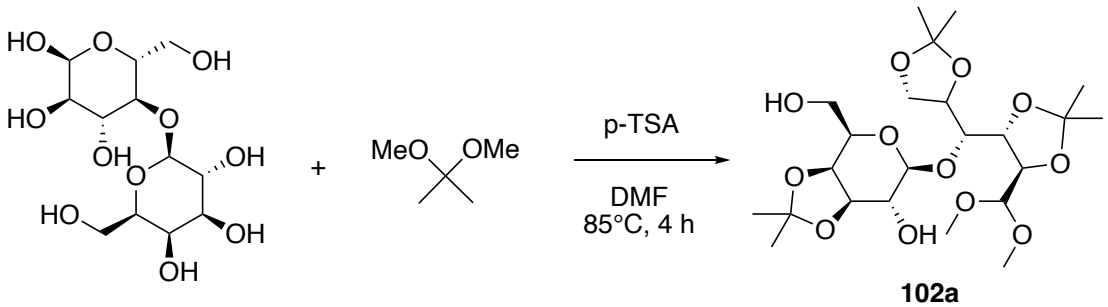

102a

(3a*S*,4*R*,6*S*,7*R*,7a*R*)-6-((1*R*)-((4*S*,5*R*)-5-(dimethoxymethyl)-2,2-dimethyl-1,3-dioxolan-4-yl)(2,2-dimethyl-1,3-dioxolan-4-yl)methoxy)-4-(hydroxymethyl)-2,2-dimethyltetrahydro-4*H*-[1,3]dioxolo[4,5-*c*]pyran-7-ol (LTA) (**102a**):

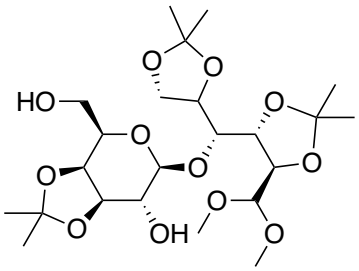

According to a modification of a procedure described in the literature,[56] lactose monohydrate (2.162 g, 6 mmol, 1 equiv.) p-toluenesulfonic acid (p-TSA) (17.1 mg, 0.09 mmol, 0.015 equiv.) and 2,2-dimethoxypropane in dimethylformamide (DMF) (15.8 mL, 129 mmol, 21.5 equiv.) were heated at 85°C for 4 hours. After this, the solution was cooled to room temperature. Amberlyst sodium salt was added and the suspension was stirred for 10 minutes. The solvent was then dried under reduced pressure. Column chromatography using cyclohexane/ethyl acetate (6:4), provided the desired compound **102a** (1.988 g, yield 65 %) as a white foam.

The physicochemical data are consistent with those reported in the literature.[56]

^{1}H NMR (400 MHz, $CDCl_3$, 25 °C): δ = 4.59 (dd, *J* = 8.0, 6.5 Hz, 1H), 4.42 (d, *J* = 8.0 Hz, 1H), 4.36 (d, *J* = 6.5 Hz, 1H), 4.33 (td, *J* = 5.0, 2.5 Hz, 1H), 4.20 (dd, *J* = 9.0, 5.0 Hz, 1H), 4.07 – 3.96 (m, 4H), 3.94 – 3.88 (m, 2H), 3.81 (dt, *J* = 9.0, 2.0 Hz, 1H), 3.65 (dd, *J* = 12.0, 2.5 Hz, 1H), 3.53 (dd, *J* = 8.5, 6.5 Hz, 1H), 3.49 (s, 3H), 3.48 (s, 3H), 1.49 (s, 6H), 1.38 (s, 6H), 1.31 (s, 3H), 1.31 (s, 3H).

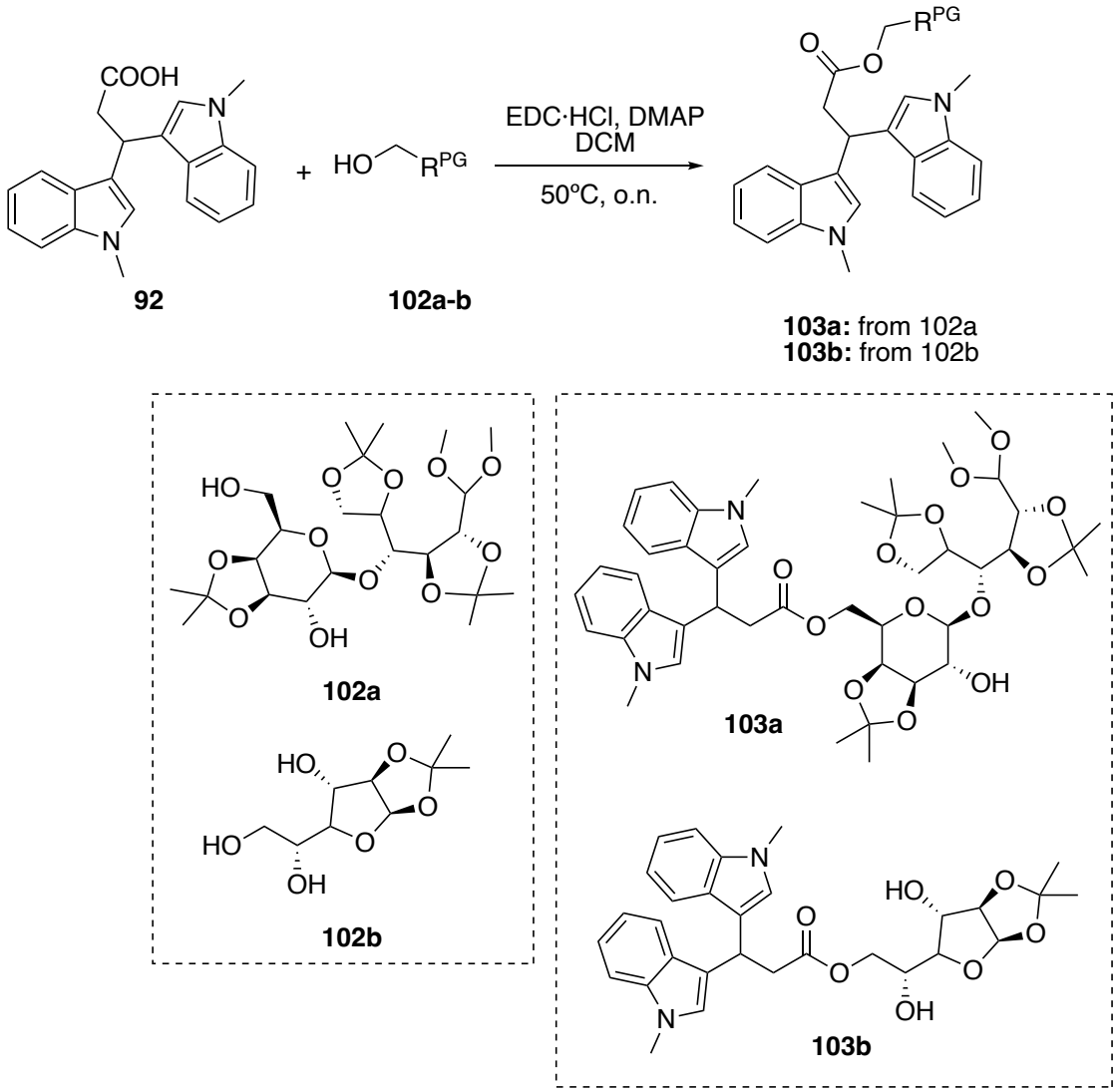

General procedure for the synthesis of ester protected glycosylated-bisindoles GP15

According to a modification of the described procedure,[69] under anhydrous conditions, 3,3-bis(1-methyl-1*H*-indol-3-yl)propanoic acid **92** (1 equiv.) was dissolved in DCM (0.06 M). EDCI (2 equiv.) and 4-(dimethylamino)pyridine (DMAP) (0.67 equiv.) were rapidly added and stirred. The protected sugar **102** (2 equiv.) was dissolved in DCM, and this solution was added to the bisindolic solution dropwise under stirring. The mixture was maintained at 50 °C and allowed to stir for 24 h. Then the reaction was cooled to room temperature, water was added, and extractions were performed 3 times with EtOAc. The organic phases were dried over Na_2SO_4, filtered and then the

solvent was removed under reduced pressure. The crude mixture was purified using column chromatography and/or crystallisation.

((3a*S*,4*R*,6*S*,7*R*,7a*R*)-6-((1*R*)-((4*S*,5*R*)-5-(dimethoxymethyl)-2,2-dimethyl-1,3-dioxolan-4-yl)(2,2-dimethyl-1,3-dioxolan-4-yl)methoxy)-7-hydroxy-2,2-dimethyltetrahydro-4*H*-[1,3]dioxolo[4,5-*c*]pyran-4-yl)methyl 3,3-bis(1-methyl-1*H*-indol-3-yl)propanoate (**103a**):

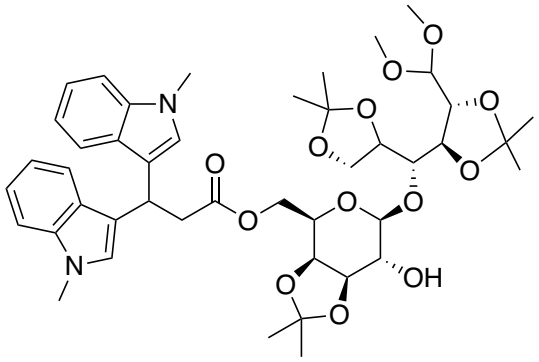

According to GP15, LTA **102a** (305 mg, 0.6 mmol, 2 equiv.), 3,3-bis(1-methyl-1*H*-indol-3-yl)propanoic acid **92** (91 mg, 0.3 mmol, 1 equiv.), DCM (5 mL, 0.06 M) EDCI (115 mg, 0.6 mmol, 2 equiv.) and DMAP (23 mg, 0.2 mmol, 0.67 equiv.) gave after purification by column chromatography 7:3 cychlohexane/ethyl acetate, the desired product **103a** (73 mg, 30 %) as a white foam.

R_f = 0.3 (1:1 cyclohexane/ethyl acetate)

^{1}H NMR (400 MHz, $CDCl_3$, 25 °C): δ = 7.64 (dt, 1H, J_1 = 1.0 Hz, J_2 = 8.0 Hz), 7.54 (dt, 1H, J_1 = 1.0 Hz, J_2 = 8.0 Hz), 7.28 (d, 2H, J = 8.0 Hz), 7.20 (dddd, 2H, J_1 = 1.0 Hz, J_2 = 6.0 Hz, J_3 = 7.0 Hz, J_4 = 8.0 Hz), 7.05 (dddd, 2H, J_1 = 1.0 Hz, J_2 = 7.0 Hz, J_3 = 8.0 Hz, J_4 = 14.0 Hz), 6.88 (dd, 2H, J_1 = 1.0 Hz, J_2 = 16.0 Hz), 5.14 – 5.06 (m, 1H), 4.42 (dd, 1H, J_1 = 6.0 Hz, J_2 = 7.5 Hz), 4.36 (d, 1H, J = 6.0 Hz), 4.33 – 4.26 (m, 2H), 4.22 (d, 1H, J = 8.0 Hz), 4.18 – 4.07 (m, 2H), 4.03 – 3.97 (m, 2H), 3.91 (dd, 1H, J_1 = 1.5 Hz, J_2 = 7.5 Hz), 3.71 (d, 7H, J = 11.5 Hz), 3.52 – 3.31 (m, 9H), 3.24 (ddd, 1H, J_1 = 2.0 Hz, J_2 = 6.0 Hz, J_3 = 7.0 Hz), 3.20 (d, 2H, J = 8.0 Hz), 1.54 (s, 3H), 1.45 (s, 3H), 1.38 – 1.34 (m, 9H), 1.20 (s, 3H).

^{13}C NMR (101 MHz, $CDCl_3$, 25 °C): δ = 172.3, 137.4, 137.3, 127.14, 127.12, 126.7, 126.3, 121.82, 121.80, 119.8, 119.7, 119.0, 118.9, 117.5, 117.4, 110.4, 110.1, 109.4, 109.3, 108.4, 105.1, 103.7, 78.9, 78.1, 77.9, 76.4, 75.1, 74.2, 72.8, 70.8, 64.7, 62.3, 56.1, 53.3, 41.7, 32.8 (2C), 31.1, 28.2, 27.4, 26.5, 26.3, 25.8, 24.4.

HRMS (ESI-Orbitrap, *m*/*z*): calcd for $C_{44}H_{58}N_2O_{13}$ [M + Na]$^+$ 845.3831; found 845.3824

(2*R*)-2-hydroxy-2-((3a*R*,6*S*,6a*R*)-6-hydroxy-2,2-dimethyltetrahydrofuro[2,3-*d*][1,3]dioxol-5-yl)ethyl 3,3-bis(1-methyl-1*H*-indol-3-yl)propanoate (**103b**):

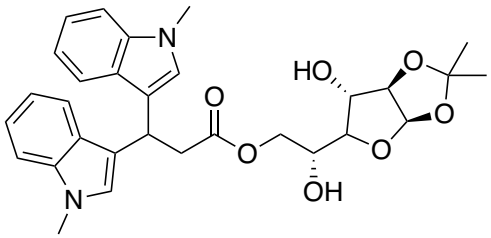

According to GP15, protected glucose **103b** (264 mg, 0.6 mmol, 2 equiv.), 3,3-bis(1-methyl-1*H*-indol-3-yl)propanoic acid **92** (183 mg, 0.3 mmol, 1 equiv.), DCM (10 mL, 0.06 M) EDC·HCl (230 mg, 0.6 mmol, 2 equiv.) and DMAP (45 mg, 0.2 mmol, 0.67 equiv.) gave, after purification by column chromatography 6:4 cychlohexane/ethyl acetate and further crystallization in MeOH, the desired product **103b** (63 mg, 20 %) as a white powder.

R_f = 0.16 (1:1 cyclohexane/ethyl acetate)

^{1}H NMR (400 MHz, $CDCl_3$, 25 °C): δ = 7.62 (ddt, *J* = 10.5, 8.0, 1.0 Hz, 2H), 7.28 (dq, *J* = 8.5, 1.0 Hz, 2H), 7.21 (ddt, *J* = 8.5, 7.0, 1.5 Hz, 2H), 7.07 (dddd, *J* = 8.0, 7.0, 3.5, 1.0 Hz, 2H), 6.89 (s, 2H), 5.89 (d, *J* = 3.5 Hz, 1H), 5.14 – 5.05 (m, 1H), 4.42 (d, *J* = 3.5 Hz, 1H), 4.32 (dd, *J* = 12.0, 2.5 Hz, 1H), 4.05 – 3.99 (m, 2H), 3.85 (dd, *J* = 7.0, 3.0 Hz, 1H), 3.75 (td, *J* = 6.5, 2.5 Hz, 1H), 3.71 (d, *J* = 2.0 Hz, 6H), 3.27 (d, *J* = 8.0 Hz, 2H), 1.46 (s, 3H), 1.30 (s, 3H).

^{13}C NMR (101 MHz, $CDCl_3$, 25 °C): δ = 172.9, 137.44, 137.40, 137.38, 127.0, 126.8, 126.6, 121.9, 121.8, 119.7, 119.6, 119.1, 117.1, 117.0, 111.9, 109.5, 105.1, 85.2, 79.3, 75.7, 69.3, 66.1, 41.6, 32.9, 31.2, 27.1, 27.0, 26.3.

HRMS (ESI-Orbitrap, *m*/*z*): calcd for $C_{29}H_{35}N_2O_7$ [M + Na]$^+$ 535.2439; found 535.2440

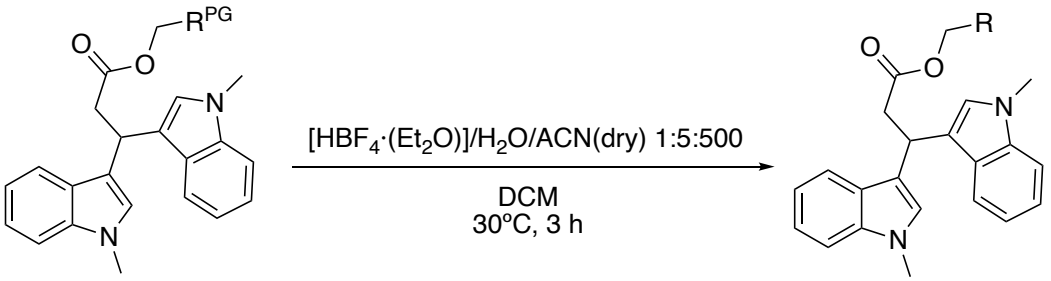

103a-b

100a: from 103a
100b: from 103b

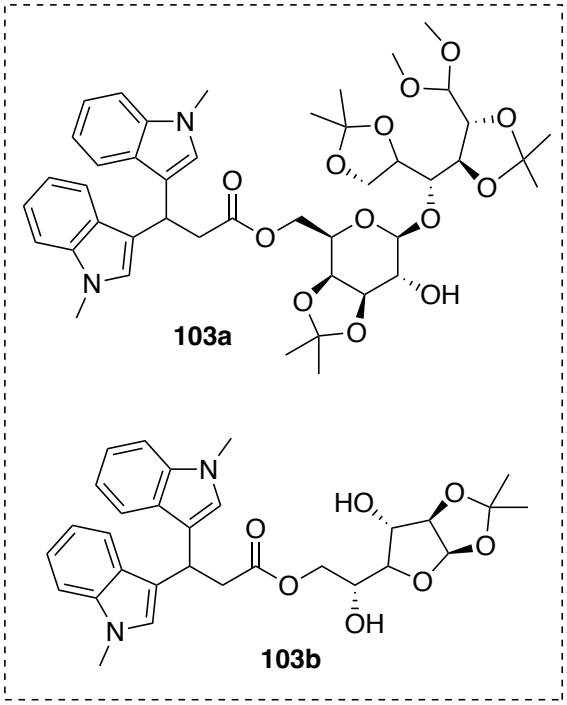

103a

103b

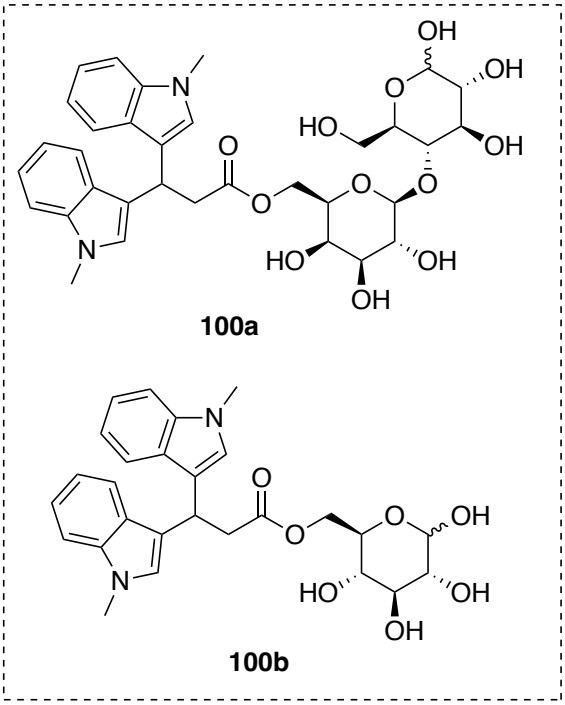

100a

100b

General procedure for the deprotection of ester protected-glycosylated-bisindoles GP16

According to a procedure described in the literature, compounds **103a-b** (1 equiv.) were dissolved in $[HBF_4(Et)_2O]/H_2O$/dry CH_3CN (c = 0.12 M, 1:5:500) and the mixture was stirred at 30 °C for 3 h. If the formation of a solid was observed, it was filtered and washed with ACN to give the desired product. If the formation of a solid was not observed, the solvent was evaporated, and the crude was purified by column chromatography.

((2*R*,3*R*,4*S*,5*R*,6*S*)-3,4,5-trihydroxy-6-(((2*R*,3*S*,4*R*,5*R*)-4,5,6-trihydroxy-2-(hydroxymethyl)tetrahydro-2*H*-pyran-3-yl)oxy)tetrahydro-2*H*-pyran-2-yl)methyl 3,3-bis(1-methyl-1*H*-indol-3-yl)propanoate (**100a**):

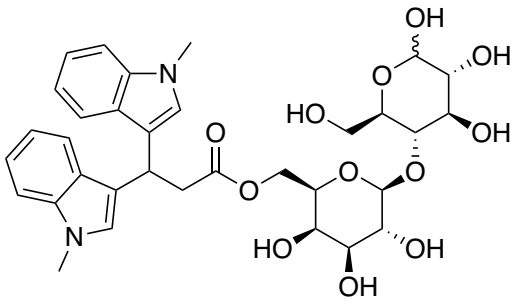

According to GP16, compound **103a** (70 mg, 0.09 mmol, 1 equiv.) in $[HBF_4(Et)_2O]/H_2O$/dry CH_3CN (1.4 µL/7 µL/0.7 mL, c = 0.12 M, 1:5:500) gave, after filtering the solid and washing with ACN, the desired product **100a** as a yellow solid (21 mg, 36 % yield).

^{1}H NMR (600 MHz, methanol-d_4, 25 °C): δ = 7.53 (ddt, *J* = 8.0, 4.8, 1.0 Hz, 1H), 7.48 (dq, *J* = 8.0, 0.9 Hz, 1H), 7.29 (dq, *J* = 8.3, 0.9 Hz, 2H), 7.13 – 7.09 (m, 2H), 7.06 (d, *J* = 1.0 Hz, 1H), 7.00 – 6.91 (m, 3H), 5.05 (t, *J* = 7.9 Hz, 1H), 4.50 (d, *J* = 7.8 Hz, 1H), 4.17 (ddd, *J* = 11.5, 5.4, 4.6 Hz, 1H), 4.13 – 4.06 (m, 2H), 3.89 – 3.85 (m, 2H), 3.82 – 3.79 (m, 2H), 3.74 (s, 3H), 3.71 (d, *J* = 1.3 Hz, 3H), 3.51 (td, *J* = 2.3, 1.0 Hz, 1H), 3.46 – 3.40 (m, 3H), 3.28 – 3.21 (m, 4H).

^{13}C NMR (151 MHz, methanol-d_4) δ 174.33 (d, *J* = 1.8 Hz), 138.78 (d, *J* = 6.4 Hz), 128.51 (d, *J* = 15.8 Hz), 127.66 (dd, *J* = 38.8, 3.9 Hz), 122.44 (d, *J* = 4.5 Hz), 120.61 – 120.09 (m), 119.58 (d, *J* = 2.6 Hz), 118.67, 118.46 (d, *J* = 3.7 Hz), 110.20 (d, *J* = 2.1 Hz), 105.29 (d, *J* = 7.1 Hz), 95.91 (d, *J* = 661.2 Hz), 82.27 (d, *J* = 29.5 Hz), 76.44 (d, *J* = 13.6 Hz), 74.83 (d, *J* = 358.7 Hz), 74.36 (dd, *J* = 14.3, 5.1 Hz), 72.23 (d, *J* = 314.0 Hz), 72.15 (d, *J* = 5.5 Hz), 69.95, 64.39 (d, *J* = 3.2 Hz), 62.23 (d, *J* = 15.3 Hz), 42.37, 32.79 (d, *J* = 5.9 Hz), 32.05.

HRMS (ESI-Orbitrap, *m*/*z*): calcd for $C_{33}H_{40}N_2O_{12}$ $[M + Na]^+$ 679.2473; found 679.2477

((2*R*,3*S*,4*S*,5*R*)-3,4,5,6-tetrahydroxytetrahydro-2*H*-pyran-2-yl)methyl 3,3-bis(1-methyl-1*H*-indol-3-yl)propanoate (**100b**):

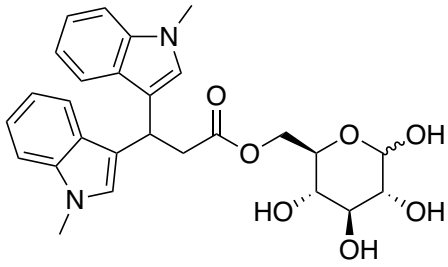

According to GP16, compound **103b** (41 mg, 0.08 mmol, 1 equiv.) in $[HBF_4(Et)_2O]/H_2O$/dry CH_3CN (1.4 µL/6.8 µL/0.68 mL, c = 0.12 M, 1:5:500) gave, after filtering the solid and washing with ACN, the desired product **100b** as a yellow solid (9 mg, 23 % yield).

^{1}H NMR (400 MHz, $CDCl_3$) δ 7.49 – 7.42 (m, 2H), 7.27 (d, *J* = 8.3 Hz, 2H), 7.10 (ddd, *J* = 8.1, 7.0, 1.1 Hz, 2H), 7.02 – 6.96 (m, 2H), 6.96 – 6.87 (m, 2H), 5.10 – 4.96 (m, 2H), 4.43 (d, *J* = 7.8 Hz, 1H), 4.32 (ddd, *J* = 22.0, 11.8, 2.1 Hz, 1H), 4.10 (ddd, *J* = 26.1, 11.8, 5.6 Hz, 1H), 3.94 – 3.83 (m, 1H), 3.80 – 3.75 (m, 1H), 3.75 – 3.68 (m, 6H), 3.63 (t, *J* = 9.3 Hz, 1H), 3.25 – 3.22 (m, 1H), 3.19 (d, *J* = 5.6 Hz, 1H), 3.16 – 3.10 (m, 1H).

^{13}C NMR (101 MHz, $CDCl_3$) δ 176.9 (d, *J* = 7.9 Hz), 141.39, 130.97, 130.1 (d, *J* = 5.6 Hz), 124.90, 122.8 (d, *J* = 4.6 Hz), 122.02, 120.9 (d, *J* = 4.0 Hz), 112.69, 98.6 (d, *J* = 429.3 Hz), 79.6 (d, *J* = 173.3 Hz), 75.55 (d, *J* = 471.7 Hz), 76.7 (d, *J* = 103.2 Hz), 74.3 (d, *J* = 14.0 Hz), 67.5 (d, *J* = 14.4 Hz), 44.8 (d, *J* = 3.3 Hz), 35.25, 34.6 (d, *J* = 2.6 Hz).

HRMS (ESI-Orbitrap, *m*/*z*): calcd for $C_{27}H_{30}N_2O_7$ $[M + Na]^+$ 517.1945; found 517.1949

4.5. BIBLIOGRAPHY

1. P.J. Praveen, P.S. Parameswaran, M.S. Majik. Bis(indolyl)methane Alkaloids: Isolation, Bioactivity, and Syntheses. *Synthesis* **2015**, 47 (13), 1827–1837.

2. T. Osawa, M. Namiki. Structure elucidation of streptindole, a novel genotoxic metabolite isolated from intestinal bacteria. *Tetrahedron Lett* **1983**, 24 (43), 4719–4722.

3. S.B. Lee, T.Y. Chang, N.Z. Lee, et al. Design, synthesis and biological evaluation of bisindole derivatives as anticancer agents against Tousled-like kinases. *Eur J Med Chem* **2022**, 227.

4. X. Yan, Y. De Tang, F. He, et al. Synthesis and assessment of bisindoles as a new class of antibacterial agents. *Monatsh Chem* **2020**, 151 (6), 971–979.

5. A. Centanni, A. Diotallevi, G. Buffi, et al. Exploring hydrophilic 2,2-di(indol-3-yl)ethanamine derivatives against Leishmania infantum. *PLoS One* **2024**, 19 (6), e0301901.

6. É.T. De Souza, D.P. De Lira, A.C. De Queiroz, et al. The Antinociceptive and Anti-Inflammatory Activities of Caulerpin, a Bisindole Alkaloid Isolated from Seaweeds of the Genus Caulerpa. *Mar Drugs* **2009**, 7 (4), 689–704.

7. K. V. Sashidhara, A. Kumar, M. Kumar, A. Srivastava, A. Puri. Synthesis and antihyperlipidemic activity of novel coumarin bisindole derivatives. *Bioorg Med Chem Lett* **2010**, 20 (22), 6504–6507.

8. R. Kakarla, P. Karuturi, Q. Siakabinga, et al. Current understanding and future directions of cruciferous vegetables and their phytochemicals to combat neurological diseases. *Phytother Res* **2024**, 38 (3), 1381–1399.

9. F. Centofanti, A. Buono, M. Verboni, et al. Synthetic Methodologies and Therapeutic Potential of Indole-3-Carbinol (I3C) and Its Derivatives. *Pharmaceuticals* **2023**, 16 (2), 240.

10. J. Poornima, S. Mirunalini. Regulation of carbohydrate metabolism by indole-3-carbinol and its metabolite 3,3′-diindolylmethane in high-fat diet-induced C57BL/6J mice. *Mol Cell Biochem* **2014**, 385 (1–2), 7–15.

11. S. Zhu, Y. Wang, Y. Li, et al. TMAO is involved in sleep deprivation-induced cognitive dysfunction through regulating astrocytic cholesterol metabolism via SREBP2. *Front Mol Neurosci* **2024**, 17, 1499591.

12. J. Lee, Y. Yue, Y. Park, S.H. Lee. 3,3′-Diindolylmethane Suppresses Adipogenesis Using AMPKα-Dependent Mechanism in 3T3-L1 Adipocytes and Caenorhabditis elegans. *J Med Food* **2017**, 20 (7), 646–652.

13. A. Lopez-Vazquez, J.J. Garcia-Banuelos, A.S. Gonzalez-Garibay, et al. IRS-1 pY612 and Akt-1/PKB pT308 Phosphorylation and Antiinflammatory Effect of Diindolylmethane in Adipocytes Cocultured with Macrophages. *Med Chem* **2017**, 13 (8), 727–733.

14. S. Tomar, M. Nagarkatti, P.S. Nagarkatti. 3,3′-Diindolylmethane attenuates LPS-mediated acute liver failure by regulating miRNAs to target IRAK4 and suppress Toll-like receptor signalling. *Br J Pharmacol* **2015**, 172 (8), 2133–2147.

15. P.B. Busbee, M. Nagarkatti, P.S. Nagarkatti. Natural Indoles, Indole-3-Carbinol (I3C) and 3,3'-Diindolylmethane (DIM), Attenuate Staphylococcal Enterotoxin B-Mediated Liver Injury by Downregulating miR-31 Expression and Promoting Caspase-2-Mediated Apoptosis. *PLoS One* **2015**, 10 (2), e0118506.

16. J. Rzemieniec, E. Bratek, A. Wnuk, et al. Neuroprotective effect of 3,3'-Diindolylmethane against perinatal asphyxia involves inhibition of the AhR and NMDA signaling and hypermethylation of specific genes. *Apoptosis* **2020**, 25 (9–10), 747–762.

17. S. Paul, E. Candelario-Jalil. Emerging neuroprotective strategies for the treatment of ischemic stroke: An overview of clinical and preclinical studies. *Exp Neurol* **2021**, 335, 113518.

18. C.A. Madison, J. Kuempel, G.L. Albrecht, et al. 3,3′-Diindolylmethane and 1,4-dihydroxy-2-naphthoic acid prevent chronic mild stress induced depressive-like behaviors in female mice. *J Affect Disord* **2022**, 309, 201–210.

19. J. Mattiazzi, M.H. Marcondes Sari, T. de B. Brum, et al. 3,3′-Diindolylmethane nanoencapsulation improves its antinociceptive action: Physicochemical and behavioral studies. *Colloids Surf B Biointerfaces* **2019**, 181, 295–304.

20. S. Hajra, A. Basu, S. Singha Roy, A.R. Patra, S. Bhattacharya. Attenuation of doxorubicin-induced cardiotoxicity and genotoxicity by an indole-based natural compound 3,3'-diindolylmethane (DIM) through activation of Nrf2/ARE signaling pathways and inhibiting apoptosis. *Free Radic Res* **2017**, 51 (9–10), 812–827.

21. K. Ramakrishna, N. Singh, S. Krishnamurthy. Diindolylmethane ameliorates platelet aggregation and thrombosis: In silico, in vitro, and in vivo studies. *Eur J Pharmacol* **2022**, 919.

22. A. Roy, B.B. Das, A. Ganguly, et al. An insight into the mechanism of inhibition of unusual bi-subunit topoisomerase I from Leishmania donovani by 3,3'-di-indolylmethane, a novel DNA topoisomerase I poison with a strong binding affinity to the enzyme. *Biochem J* **2008**, 409 (2), 611–622.

23. K. Golberg, V. Markus, B. El Kagan, et al. Anti-Virulence Activity of 3,3'-Diindolylmethane (DIM): A Bioactive Cruciferous Phytochemical with Accelerated Wound Healing Benefits. *Pharmaceutics* **2022**, 14 (5), 967.

24. L. Xue, J.J. Pestka, M. Li, G.L. Firestone, L.F. Bjeldanes. 3,3'-Diindolylmethane stimulates murine immune function in vitro and in vivo. *J Nutr Biochem* **2008**, 19 (5), 336–344.

25. S. Fan, Q. Meng, J. Xu, et al. DIM (3,3′-diindolylmethane) confers protection against ionizing radiation by a unique mechanism. *Proc Natl Acad Sci* **2013**, 110 (46), 18650–18655.

26. J.C. Han, R.S. Mi, M.L. Yeo, et al. 3,3'-Diindolylmethane suppresses the inflammatory response to lipopolysaccharide in murine macrophages. *J Nutr* **2008**, 138 (1), 17–23.

27. S.H. Benabadji, R. Wen, J. Zheng, X. Dong, S. Yuan. Anticarcinogenic and antioxidant activity of diindolylmethane derivatives. *Acta Pharmacol Sin.* **2004**, 25 (5), 666–671.

28. Z. Huang, L. Zuo, Z. Zhang, et al. 3,3′-Diindolylmethane decreases VCAM-1 expression and alleviates experimental colitis via a BRCA1-dependent antioxidant pathway. *Free Radic Biol Med* **2011**, 50 (2), 228–236.

29. S. Banerjee, D. Kong, Z. Wang, et al. Attenuation of multi-targeted proliferation-linked signaling by 3,3′-diindolylmethane (DIM): From bench to clinic. *Mut Res/Rev Mut Res* **2011**, 728 (1–2), 47–66.

30. J.R. Weng, C.H. Tsai, S.K. Kulp, C.S. Chen. Indole-3-carbinol as a chemopreventive and anti-cancer agent. *Cancer Lett* **2008**, 262 (2), 153–163.

31. X. Chang, J.C. Tou, C. Hong, et al. 3,3′-Diindolylmethane inhibits angiogenesis and the growth of transplantable human breast carcinoma in athymic mice. *Carcinogenesis* **2005**, 26 (4), 771–778.

32. D.K. Sharma, B. Rah, M.R. Lambu, et al. Design and synthesis of novel N,N′-glycoside derivatives of 3,3′-diindolylmethanes as potential antiproliferative agents. *MedChemComm* **2012**, 3 (9), 1082–1091.

33. G. Sivaprasad, P.T. Perumal, V.R. Prabavathy, N. Mathivanan. Synthesis and anti-microbial activity of pyrazolylbisindoles--promising anti-fungal compounds. *Bioorg Med Chem Lett* **2006**, 16 (24), 6302–6305.

34. S. Roy, R. Gajbhiye, M. Mandal, et al. Synthesis and antibacterial evaluation of 3,3′-diindolylmethane derivatives. *Med Chem Res* **2014**, 23 (3), 1371–1377.

35. K. Sujatha, P.T. Perumal, D. Muralidharan, M. Rajendran. ChemInform Abstract: Synthesis, Analgesic and Antiinflammatory Activities of Bis(indolyl)methanes. *ChemInform* **2009**, 40 (24), no-no.

36. S. Mani, K. Suvetha, D. Kumarasamyraja, N.L. Gowrishankar. Synthesis and biological evaluation of novel pyrazolyl bis-indolylmethane. *Int J Pharm Pharm Sci* **2012**, 4, 518–521.

37. B.R. De Miranda, J.A. Miller, R.J. Hansen, et al. Neuroprotective efficacy and pharmacokinetic behavior of novel anti-inflammatory para-phenyl substituted diindolylmethanes in a mouse model of Parkinson's disease. *J Pharmacol Exptl Ther* **2013**, 345 (1), 125–138.

38. K.M. Khan, F. Rahim, A. Wadood, et al. Evaluation of bisindole as potent β-glucuronidase inhibitors: Synthesis and in silico-based studies. *Bioorg Med Chem Lett* **2014**, 24 (7), 1825–1829.

39. P. Jayakumar, K.V. Pugalendi, M. Sankaran. Attenuation of hyperglycemia-mediated oxidative stress by indole-3-carbinol and its metabolite 3, 3′-diindolylmethane in C57BL/6J mice. *J Physiol Biochem* **2014**, 70 (2), 525–534.

40. A. Roy, S. Chowdhury, S. Sengupta, et al. Development of Derivatives of 3, 3′-Diindolylmethane as Potent Leishmania donovani Bi-Subunit Topoisomerase IB Poisons. *PLoS One* **2011**, 6 (12), e28493.

41. S.B. Bharate, J.B. Bharate, S.I. Khan, et al. Discovery of 3,3′-diindolylmethanes as potent antileishmanial agents. *Eur J Med Chem* **2013**, 63, 435–443.

42. M. Taha, I. Uddin, M. Gollapalli, et al. Synthesis, anti-leishmanial and molecular docking study of bis-indole derivatives. *BMC Chemistry* **2019**, 13 (1), 1–12.

43. R.C.R. Gonçalves, P. Peñalver, S.P.G. Costa, J.C. Morales, M.M.M. Raposo. Polyaromatic Bis(indolyl)methane Derivatives with Antiproliferative and Antiparasitic Activity. *Molecules* **2023**, 28 (23), 7728.

44. A. Diotallevi, L. Scalvini, G. Buffi, et al. Phenotype Screening of an Azole-bisindole Chemical Library Identifies URB1483 as a New Antileishmanial Agent Devoid of Toxicity on Human Cells. *ACS Omega* **2021**, 6 (51), 35699–35710.

45. A. Buono, A. Diotallevi, S. Maestrini, et al. Efficient and Rapid Arylation of NH_2-Unprotected Bromobisindole Ethanamines via Suzuki-Miyaura Coupling: Generating New Leads Against Leishmania. *Chem Eur J* **2025**, 31 (43), e202500637.

46. J. Kang, Y. Gao, M. Zhang, et al. Streptindole and Its Derivatives as Novel Antiviral and Anti-Phytopathogenic Fungus Agents. *J Agric Food Chem* **2020**, 68 (30), 7839–7849.

47. M. Baron, E. Métay, M. Lemaire, F. Popowycz. Reduction of aromatic and aliphatic nitro groups to anilines and amines with hypophosphites associated with Pd/C. *Green Chem* **2013**, 15 (4), 1006–1015.

48. S. Kandekar, R. Preet, M. Kashyap, et al. Structural Elaboration of a Natural Product: Identification of 3,3′-Diindolylmethane Aminophosphonate and Urea Derivatives as Potent Anticancer Agents. *ChemMedChem* **2013**, 8 (11), 1873–1884.

49. F.Y. Miyake, K. Yakushijin, D.A. Home. A facile synthesis of dragmacidin B and 2,5-bis(6′-bromo-3′-indolyl)piperazine. *Org Lett* **2000**, 2 (20), 3185–3187.

50. L.-T. An, J.-J. Cai, X.-Q. Pan, et al. Ga(DS)3-catalysed double hydroarylation of acetylenic esters with indoles for the synthesis of bisindolyl propanoates. *Tetrahedron Lett* **2015**, 56 (26), 3996–3998.

51. S. Lucarini, M. Mari, G. Piersanti, G. Spadoni. Organocatalyzed coupling of indoles with dehydroalanine esters: synthesis of bis(indolyl)propanoates and indolacrylates. *RSC Adv* **2013**, 3 (41), 19135.

52. H. Koshima, W. Matsusaka. *N* -bromosuccinimide catalyzed condensations of indoles with carbonyl compounds under solvent-free conditions. *J Heterocycl Chem* **2002**, 39 (5), 1089–1091.

53. B. Karimi, G.R. Ebrahimian, H. Seradj. Efficient and chemoselective conversion of carbonyl compounds to 1,3-dioxanes catalyzed with N-bromosuccinimide under almost neutral reaction conditions. *Org Lett* **1999**, 1 (11), 1737–1739.

54. A. Daina, O. Michielin, V. Zoete. SwissADME: a free web tool to evaluate pharmacokinetics, drug-likeness and medicinal chemistry friendliness of small molecules. *Sci Rep* **2017**, 7 (1), 1–13.

55. P. Kour, P. Saha, S. Bhattacharya, et al. Design, synthesis, and biological evaluation of 3,3′-diindolylmethane *N* -linked glycoconjugate as a leishmanial topoisomerase IB inhibitor with reduced cytotoxicity. *RSC Med Chem* **2023**, 14 (10), 2100–2114.

56. D.B. Sarney, H. Kapeller, G. Fregapane, E.N. Vulfson. Chemo-enzymatic synthesis of disaccharide fatty acid esters. *J Am Oil Chem Soc* **1994**, 71 (7), 711–714.

57. M. Mari, A. Tassoni, S. Lucarini, et al. Brønsted Acid Catalyzed Bisindolization of α-Amido Acetals: Synthesis and Anticancer Activity of Bis(indolyl)ethanamino Derivatives. *Eur J Org Chem* **2014**, 2014 (18), 3822–3830.

58. S. Mantenuto, S. Lucarini, M. De Santi, et al. One-Pot Synthesis of Biheterocycles Based on Indole and Azole Scaffolds Using Tryptamines and 1,2-Diaza-1,3-dienes as Building Blocks. *Eur J Org Chem* **2016**, 2016 (19), 3193–3199.

59. K. Sugimoto, I. Mori, T. Kato, et al. Guanidinium Hypoiodite-Catalyzed Intramolecular Oxidative Coupling Reaction of Oxindoles with β-Dicarbonyls. *J Org Chem* **2023**, 88 (12), 7660–7673.

60. J. Kang, Y. Gao, M. Zhang, et al. Streptindole and Its Derivatives as Novel Antiviral and Anti-Phytopathogenic Fungus Agents. *J Agric Food Chem* **2020**, 68 (30), 7839–7849.

61. Y. Wang, C. Zheng, S.L. You. Iridium-Catalyzed Asymmetric Allylic Dearomatization by a Desymmetrization Strategy. *Angew Chem Int Ed* **2017**, 56 (47), 15093–15097.

62. S. Zhang, Z. Chen, S. Qin, et al. Non-redox metal ion promoted oxidative coupling of indoles with olefins by the palladium(II) acetate catalyst through dioxygen activation: experimental results with DFT calculations. *Org Biomol Chem* **2016**, 14 (17), 4146–4157.

63. X. Wang, M.-J. Luo, Y.-X. Wang, et al. Design, synthesis, and herbicidal activity of indole-3-carboxylic acid derivatives as potential transport inhibitor response 1 antagonists. *Front Chem* **2022**, 10.

64. B. Cossec, F. Cosnier, M. Burgart. Methyl Mercapturate Synthesis: An Efficient, Convenient and Simple Method. *Molecules* **2008**, 13 (10), 2394–2407.

65. P.P. Sathieshkumar, P. Latha, R. Nagarajan. Total Synthesis of Pseudellone C. *Eur J Org Chem* **2017**, 2017 (22), 3161–3164.

66. B.S. Chinta, B. Baire. Reactivity of indole-3-alkoxides in the absence of acids: Rapid synthesis of homo-bisindolylmethanes. *Tetrahedron* **2016**, 72 (49), 8106–8116.

67. H.S. Siebe, A.S. Sardjan, S.C. Maßmann, et al. Formation of substituted dioxanes in the oxidation of gum arabic with periodate. *Green Chem* **2023**, 25 (10), 4058–4066.

68. T. Han, C. Jiang, X. Wei, et al. Design, synthesis of amide derivatives of scutellarin and their antileukemia and neuroprotective activities. *Med Chem Res* **2022**, 31 (6), 905–915.

69. V. Dhawan, G. Joshi, B. Sutariya, et al. Polysaccharide conjugates surpass monosaccharide ligands in hepatospecific targeting – Synthesis and comparative in silico and in vitro assessment. *Carbohydr Res* **2021**, 509, 108417.

CHAPTER 5. SYNTHESIS OF NEW INDOLE-ISOINDOLINONE MOLECULES AS POTENTIAL ANTILEISHMANIAL AGENTS

5.1. INTRODUCTION

A mentioned in Chapter 3, indole-based compounds are one of the most extensively studied class of compounds in medicinal chemistry, with a wide range of biological activities.

5.1.1. Isoindolinones

5.1.1.1 Natural products

Isoindole derivatives are relatively rare in nature, however, there are some examples of natural compounds containing this motif.

Indolocarbazoles are a well-characterized group of natural metabolites produced primarily by actinomycetes and certain cyanobacteria.[1,2] Staurosporine (Figure 5.1) was the first compound from the indolocarbazole alkaloid family to be discovered from *Streptomyces staurosporeus* in 1977. Staurosporine showed antimicrobial activity against fungi and yeast, and it is one of the most potent protein kinase inhibitors to date.[3,4] Over the past 35 years, more than 60 compounds from the indocarbazole alkaloid family have been isolated, either glycosides or aglycones. Holyrines A and B and K252d were isolated in 1999 from cultures of a marine actinomycete.[5]

Chilenine was the first isolated compound from the isoindolobenzazepine alkaloid family in 1982 from *Berberis empetrifolia Lam*.[6] From this same family of compounds and the same plant, lennoxamine was isolated three years later, in 1985.[7] Magallanesine, also isolated from the *Berberis* genus (*Berberis darwinii Hook.*) is the first isolated compound of the isoindolobenzazocine family.[8]

Aristolactams (Figure 5.1) were mainly isolated from *Aristolochiaceae* but can also be found in several other plant species.[9,10] Another class of isoindolinone are cularine alkaloids, such as aristoyagonine, usually found in the *Fumariaceae* family and in particular in *Sarcocapnos enneaphylla*.[11]

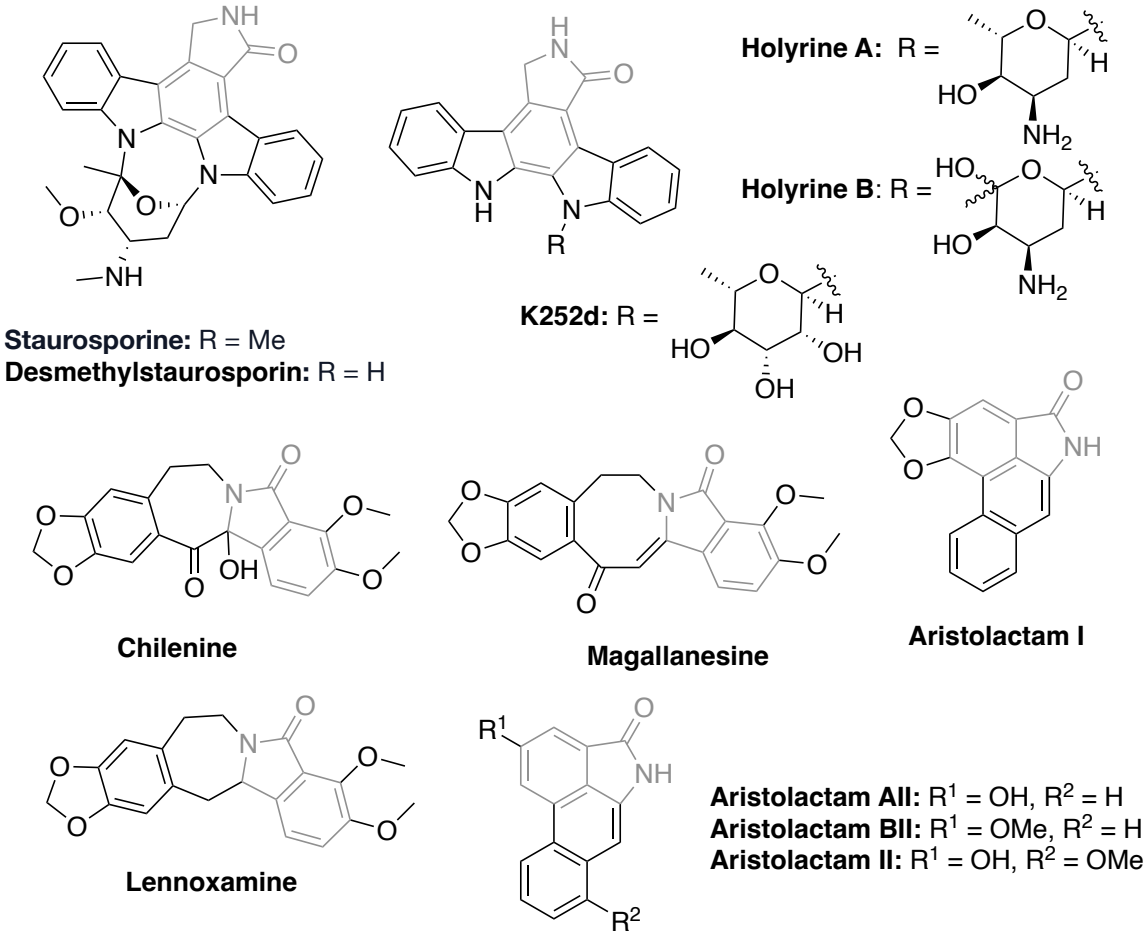

Figure 5.1. Natural products containing the isoindolinone motif (marked in grey).

5.1.1.2 Biological activities

Numerous compounds containing isoindolinone cores and endowed with different biological activities have been developed, some of them being approved drugs.

a) Anticancer activity

Jayaraj *et al.* synthesised and evaluated against two different cancer lines different isoindolinone derivatives (**104, 105**) (Figure 5.2) finding that variations in the *N*-position of **104** influenced the activity. Electron-donating groups generally enhanced the activity, while electron-withdrawing groups (except bromine) reduced the activity. Moreover, the substitution at R^2 of **105** with electron-donating groups drastically increased the activity, being the ferrocenyl derivative the most active one, with activities comparable to commercial drugs.[12]

Compound **106**, showed the highest anticancer activity of its series, showing a dose-dependent inhibitory effect. The activity pattern suggests that **106** regulates proliferation of apoptosis.[13]

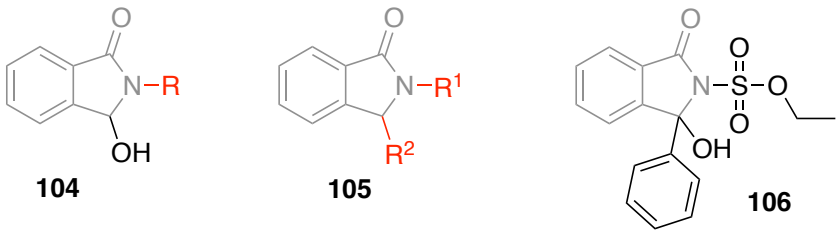

Figure 5.2. Isoindolinone-based compounds with anticancer activity. Relevant substituents for the structure-activity relationship are marked in red.

b) Anxiolytic activity

Pagoclone (Figure 5.3) is a GABA-A/BZD Site Partial Agonist from the non-benzodiazepines class of anxiolytics that was developed for the treatment of stuttering but was never approved for commercialization.[14] The closely related pazinaclone is another non-selective anxiolytic and sedative compound also from the nonbenzodiazepines class that was never approved for its commercialization.[15]

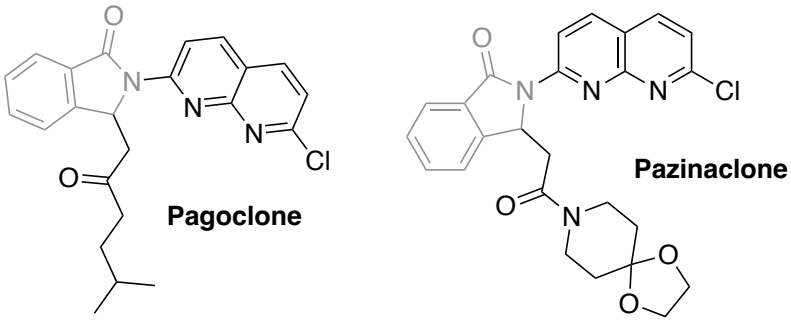

Figure 5.3. Isoindolinone-based anxiolytic compounds.

c) Antihypertensive activity

Chlorthalidone (Figure 5.4) is an approved drug patented in 1957 that is used to treat principally high blood pressure but also diabetes insipidus or renal tubular acidosis.[16,17] Zhang and colleagues,[18] reported the synthesis and evaluation of isoindolinone derivatives to treat hypertension, finding compounds **107** as potent antihypertensive agents, comparable to other drugs in clinical trials. Falipamil is a bradycardic drug

used for the treatment of sinus arrhythmia in some animals. It has potential anti-tachycardic and anti-anginal effects.[19]

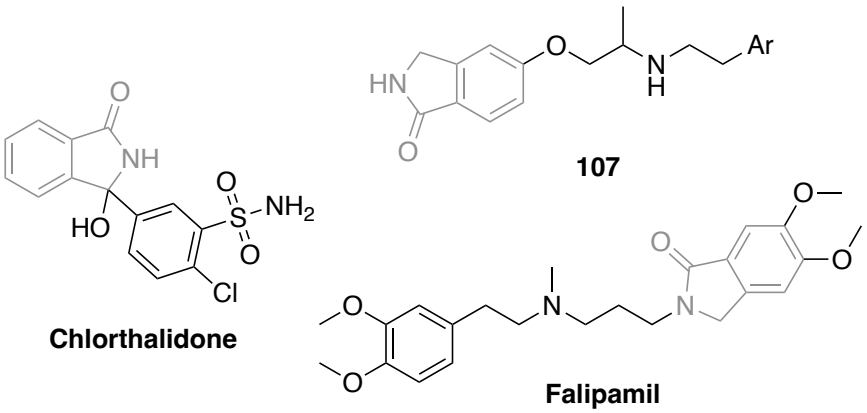

Figure 5.4. Isoindolinone-based antihypertensive compounds.

d) Antipsychotic activity

Compound **108** was the most effective compound among a series of derivatives. It exhibited antipsychotic-like effects in rats, and it is orally active, becoming a promising preclinical lead.[20] Bellioti *et al.* synthesised a series of isoindolinone derivatives, where compound PD 172938 inhibits amphetamine-stimulated locomotor activity in the rat, indicating possible antipsychotic activity.[21]

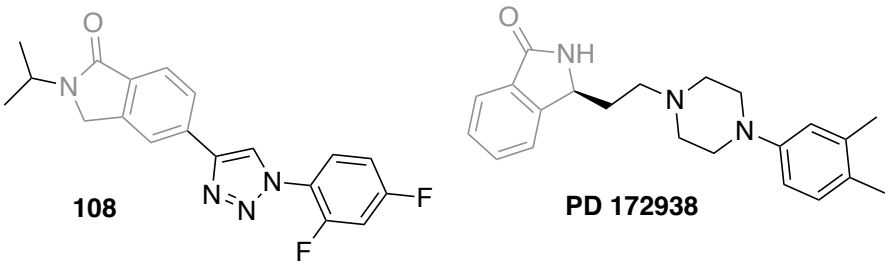

Figure 5.5. Isoindolinone-based compounds with antipsychotic activity.

5.1.2. Fused Indole-isoindolinones

As mentioned in Chapter 3, the combination of various pharmacophores is an innovative method to try to increase pharmacological activity.

5.1.2.1 Natural products

To the best of our knowledge, corallocin C, K252a, staurosporinone and tjipanazole J (Figure 5.6) together with staurosporine, desmethylstaurosporine, Holyrines A and B and K252d (represented in Section 5.1.1, Figure 5.1) are the only natural products containing both the isoindolinone and the indole moieties.

Corallocin C was reported for the first time in 2016, when it was isolated from the mushroom *Hericium coralloides*.[22] K252a is a staurosporine analogue isolated from the bacterium *Nocardiopsis*. This compound is a high inhibitor of CaM kinase and phosphorylase kinase, and at higher concentrations, it also acts as a serine/threonine kinase inhibitor.[23] Staurosporinone was isolated in 1996 from the extracts of *Lycogala epidendrum*.[24] Tjipanazole J was isolated from the extract of the cyanophyte *Tolypothrix tjipanasensis*, and it is the only compound of the Tjipanazole family to contain the indole-isoindolinone moiety.[25]

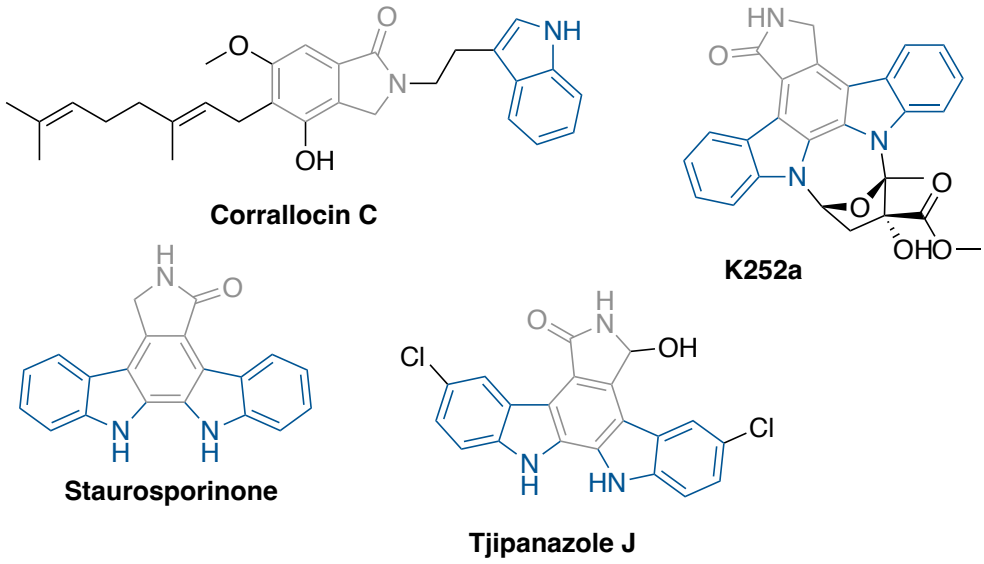

Figure 5.6. Indole-isoindolinone-based natural products.

5.1.2.2 Biological activities

Only a few compounds containing both the indole and isoindolinone moieties have been studied. Studied compounds show diverse biological activities.

a) Antimalarial activity

Pereira *et al.*[26] synthesised some indole-isoindolinone derivatives (Figure 5.7) and evaluated their antimalarial activity. The compounds were screened against a chloroquine-resistant W2 strain of *P. falciparum*, and it was observed that derivatives **109a-b**, **110**, **111a-d**, **112a-b**, and **113a-b** exhibited IC_{50} values of 1-8 µM. Compounds **109a** and **109b** exhibited the highest activity with IC_{50} values of 1-2 µM. The isoindolinone moiety was also crucial to potency, since its replacement with a pyrrolidone group resulted in loss of activity. Compounds containing a (S)-tryptophanol moiety proved to be more active than their (R)-enantiomers, indicating the importance of stereochemistry. The configuration of the stereocenter at the fusion position influenced efficacy, with **113b** being approximately four times more active than diastereomer **113a**. Liver-stage assays in Huh-7 cells confirmed considerable reduction of parasite load for all but compound **112a**. Compounds **109a**, **109b**, **110**, **111a-d**, and **113b** are the most promising for strong dual-stage antiplasmodial activity.

The same group published in 2025 a study where they evaluated 26 different compounds against malaria.[27] Compounds **114-115** (Figure 5.7) had low-mid nanomolar potency. Stereochemistry at C-13b was critical for activity, and substituents at this position regulated potency, with para-substituted aromatic rings tending to enhance antimalarial activity, whereas ortho-nitro substitutions were not favourable for activity. Increasing the *N*-alkyl chain decreased potency, while *N*-methylation of the indole nitrogen minimal effect. In vitro cytotoxicity tests with J774 and HepG2 cells indicated low toxicity, and compounds **114a**, **114c**, and **115b** displayed excellent selectivity, with compound **115b** being seven times more selective than chloroquine. Liver-stage tests indicated high inhibition of *P. berghei* infection in Huh-7 cells with negligible cytotoxicity. These results highlight **115b**, **114a**, and **114c** as the most promising dual-stage antiplasmodial candidates.

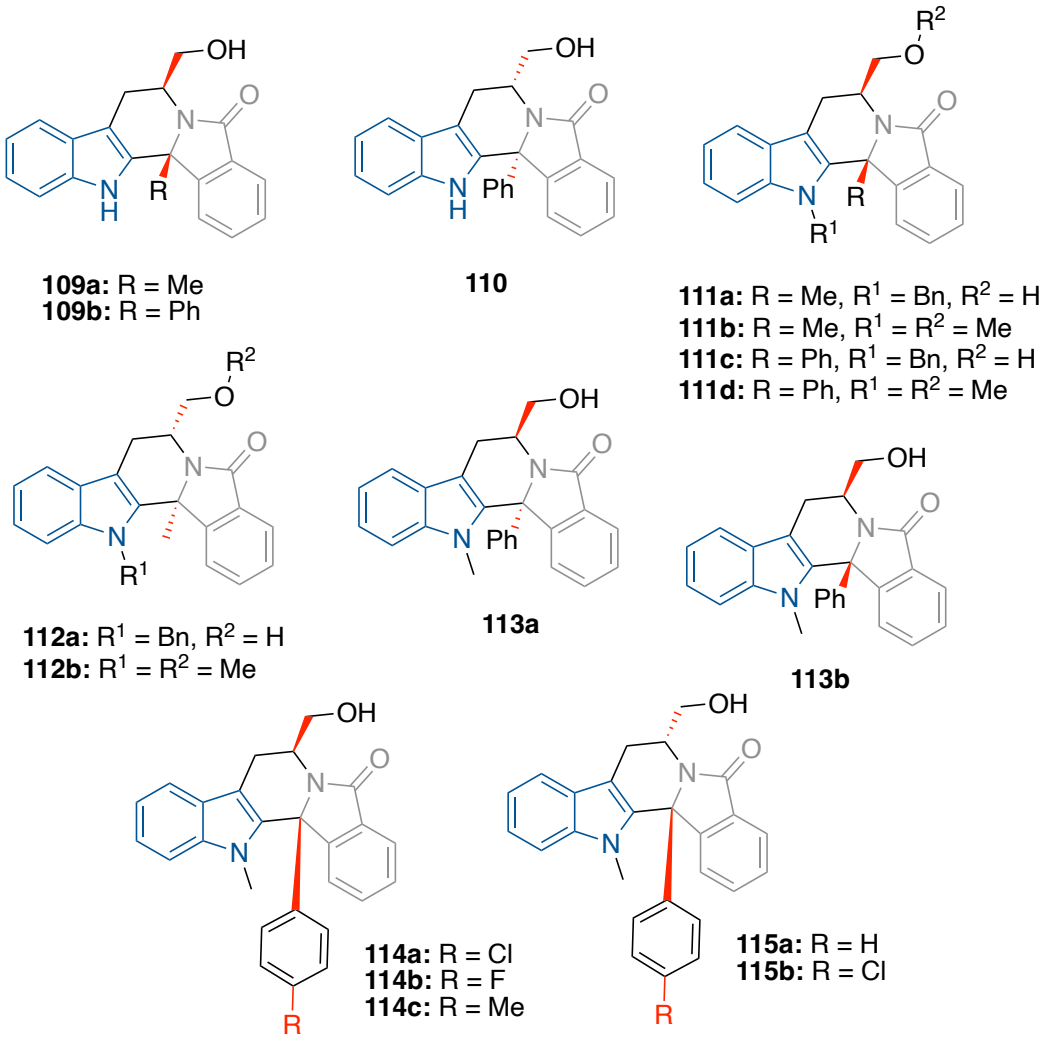

Figure 5.7. Indole-isoindolinone-based compounds with antimalarial activity. Relevant substituents for the structure-activity relationship are marked in red.

b) Anticancer activity

Compound **65D08** was discovered in a high-throughput screen of 2,491 structurally diverse natural products and derivatives in a fluorescent cell coculture assay (FCCT) that detects selective cytotoxicity against lung cancer cells. **65D08** was selectively cytotoxic in multiple dilutions and exhibited enhanced cytotoxicity against MCF7 breast cancer cells over VA13, with less toxicity toward noncancerous HEK293T cells, exhibiting a good selectivity profile. **65D08** represents a promising scaffold for optimisation in anticancer drug development due to its selective activity and suitability for high-throughput fluorescent coculture screening approaches.[28]

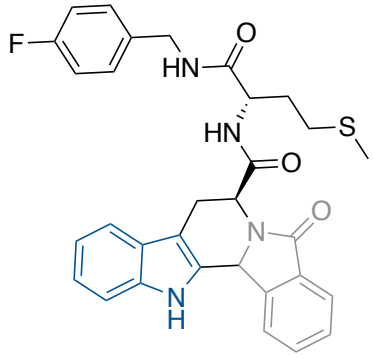

65D08

Figure 5.8. Indole-isoindolinone-based compound with anticancer activity.

5.2. OBJECTIVES

The aim of this Thesis chapter is the synthesis of indole-isoindolinone derivatives as potential antileishmanial compounds. These derivatives are chosen due to their structural similarity to indole-imidazole compounds presented in Chapter 3, and because they are scarcely studied for their biological activities.

5.3. RESULTS AND DISCUSSION

The synthesis of the indole-isoindolinone core was previously reported in the literature[29] and consisted of two steps. The first step is the nucleophilic attack of tryptamine on phthalic anhydride, obtaining compound **116** with quantitative yield (Scheme 5.1)

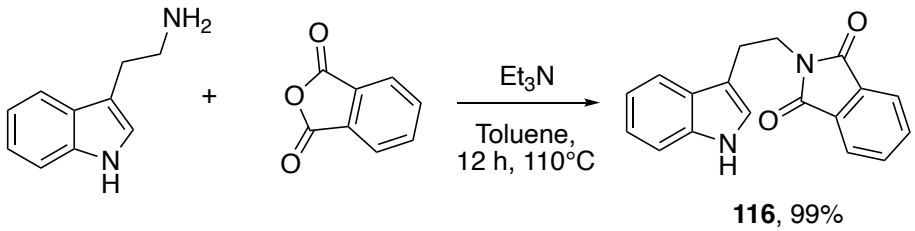

116, 99%

*Scheme 5.1. Synthesis of compound **116**.*

The second step of the synthesis begins with the protonation of one of the carbonyls of phthalimide with triflic acid, which allows cyclisation onto position 2 of the indole ring via an SAE mechanism. The subsequent acid-promoted loss of a water molecule

affords an iminium cation. Finally, after neutralisation of the excess triflic acid, this intermediate is reduced by treatment with sodium trifluoroacetoxyborohydride, generated *in situ* from sodium borohydride and trifluoroacetic acid, forming the polycyclic structure **117** in high yield (Scheme 5.2).

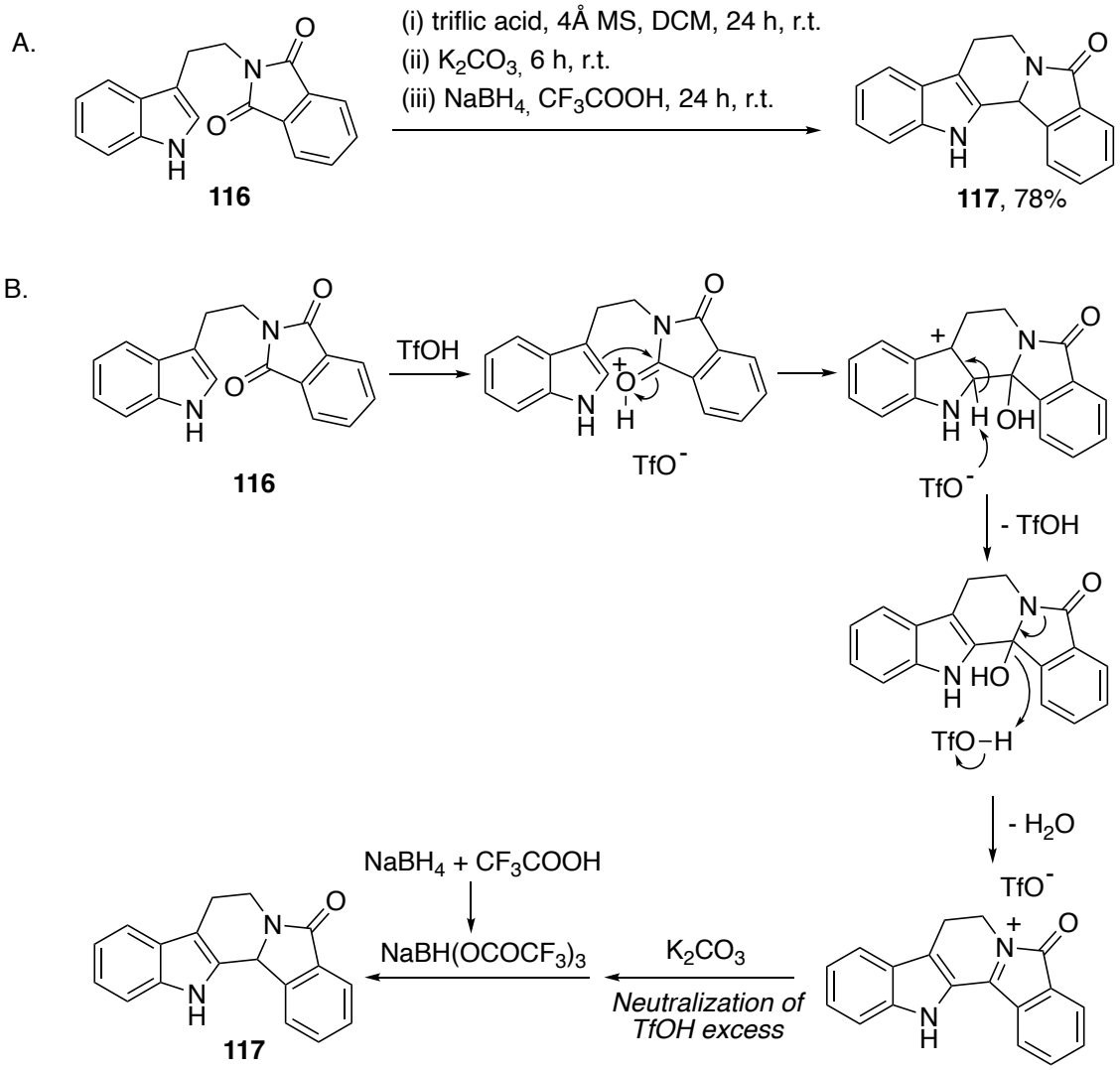

*Scheme 5.2. A) Synthesis of compound **117**. B) Proposed mechanism for the synthesis of **117**.*

In order to synthesise a small library of derivatives of this parent framework, we decided to perform different base-promoted alkylations in the indolic nitrogen, using reported procedures. However, whenever we performed this reaction, we observed the formation of two different products, neither of them being the expected *N*-monosubstituted derivative **118**. Instead, we observed the formation of the disubstitution products **119b** and **120b**, one of them containing an alkoxy substituent

(Scheme 5.3). Lowering the equivalents of base and/or alkyl halide did not lead to the formation of the mono-substituted compound, but resulted in lower overall yields.

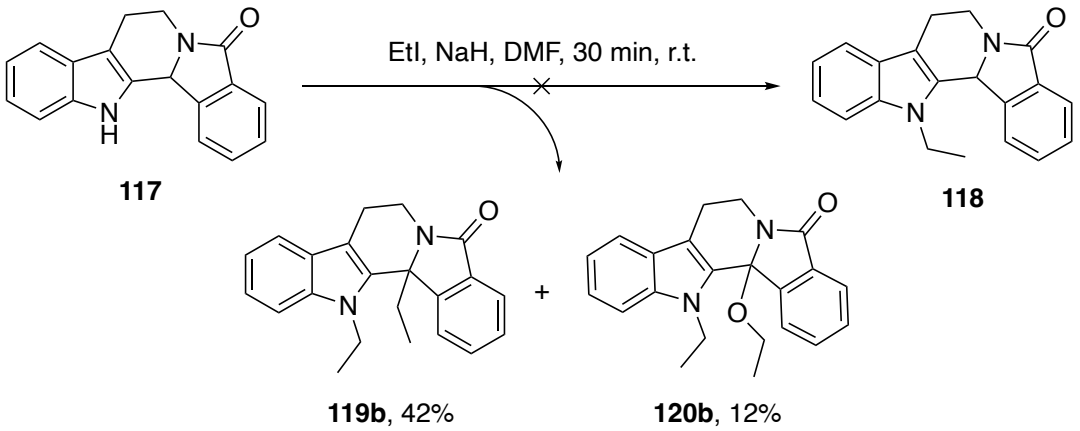

*Scheme 5.3. Alkylation of compound **117**.*

Attempting to perform the alkylation of compound **116** before the cyclisation reaction did not succeed. The formation of the disubstituted product is probably due to the fact that the two positions of the molecule marked in Figure 5.9 are subjected to deprotonation.

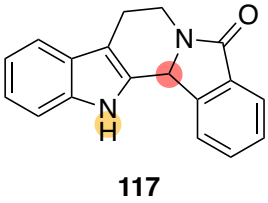

*Figure 5.9. Positions of **117** subjected to deprotonation.*

The position marked in red is particularly acidic because the generated upon deprotonation is doubly benzylic, while simultaneously being a dipole-stabilized carbanion α to an amide nitrogen. Upon loss of the proton, the lone pair can efficiently delocalize into the π-system of the indole (green arrows in Figure 5.10), the conjugating benzylic ring (blue arrows in Figure 5.10), and the lactam carbonyl (amide-type resonance) (red arrows in Figure 5.10), spreading the negative charge across a large region of the molecule and significantly lowering the energy of the carbanion. This stabilisation is also supported by cross-conjugation, since the carbanion can cross both aromatic systems simultaneously and offer multiple resonance pathways

that are stabilising. Furthermore, any electronegative substituents present nearby, such as the lactam carbonyl, are electron-withdrawing groups, which lower the pKa.

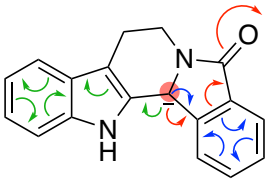

*Figure 5.10. Delocalisation upon deprotonation of the proton marked in red in **117**.*

The indole nitrogen is also acidic, as the corresponding anion can delocalize its negative charge in the indole ring (orange arrows in Figure 5.11).

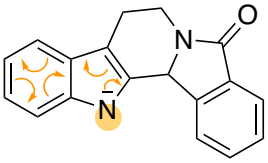

*Figure 5.11. Delocalisation upon deprotonation of the indolic nitrogen (marked in yellow) in **117**.*

As the monosubstituted compound **121** has been isolated (Scheme 5.4), we can assume that the proton marked in red is more acidic than the one of the indolic nitrogen.

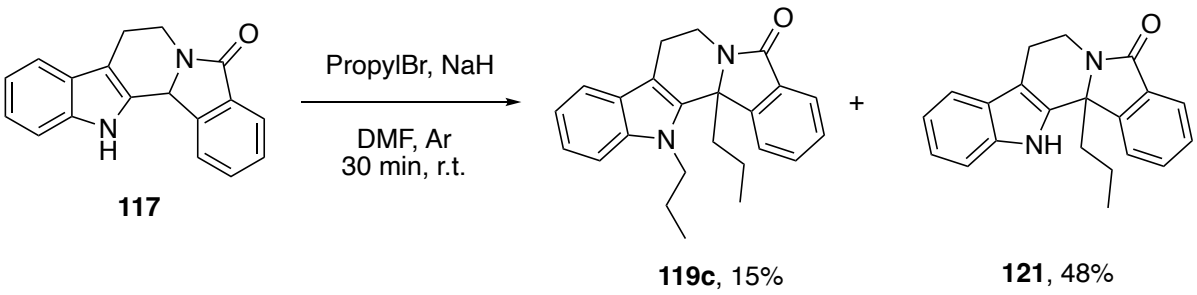

*Scheme 5.4. Obtention of monosubstituted compound **121**.*

Regarding the formation of the alkoxy derivatives, we had two different hypotheses for the origin of the oxygen atom: a) the atom was coming from the oxygen present in the air, or b) the atom was coming from the water present in the solvents. We planned an experiment under argon atmosphere where the solvent was previously degassed for half an hour in order to be sure that no oxygen was present. To this reaction, a

stoichiometric amount of water was added. Only compound **119a** was observed, so we can suppose that the oxygen of derivative **120a** was coming from the oxygen present in the air and not from possible water present in the solvent.

At this point, we decided to synthesise a small scope of molecules **119**. We used different alkylic, vinylic and benzylic substituents. However, whenever the substituents were too bulky, not only derivatives **119** were obtained, but the formation of fused 3*H*-indole derivatives **122**, bearing two all-carbon quaternary stereocenters, was also observed (Scheme 5.5).

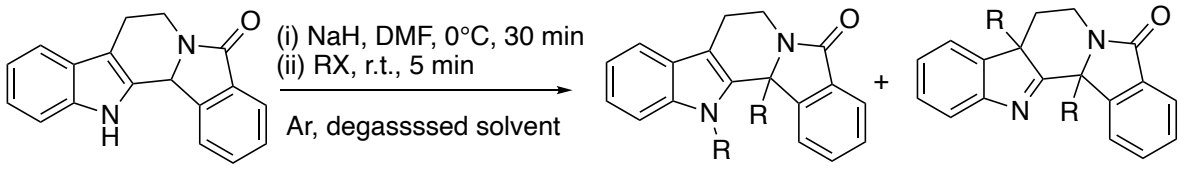

119 **122**

119a: R = Me (64%)
119b: R = Et (84%)
119c: R = Pr (15%)
119d: R = But (71%)
119e: R = n-Hex (25%) **122e:** R = n-Hex (13%)
119f: R = allyl (23%) **122f:** R = allyl (15%)
119g: R = isoprenyl (25%) **122g:** R = isoprenyl (12%)
119h: R = benzyl (34%) **122h:** R = benzyl (22%)
119i: R = 3-F benzyl (55%) **122i:** R = 3-F benzyl (29%)
119j: R = 4-F benzyl (54%) **122j:** R = 4-F benzyl (36%)

*Scheme 5.5. Synthesis of derivatives **119** and **122**.*

As mentioned before, the first substitution takes place in the carbon marked in red; therefore, whenever a substituent is too big, the indole ring C-3 position may attack the halide (Scheme 5.6).

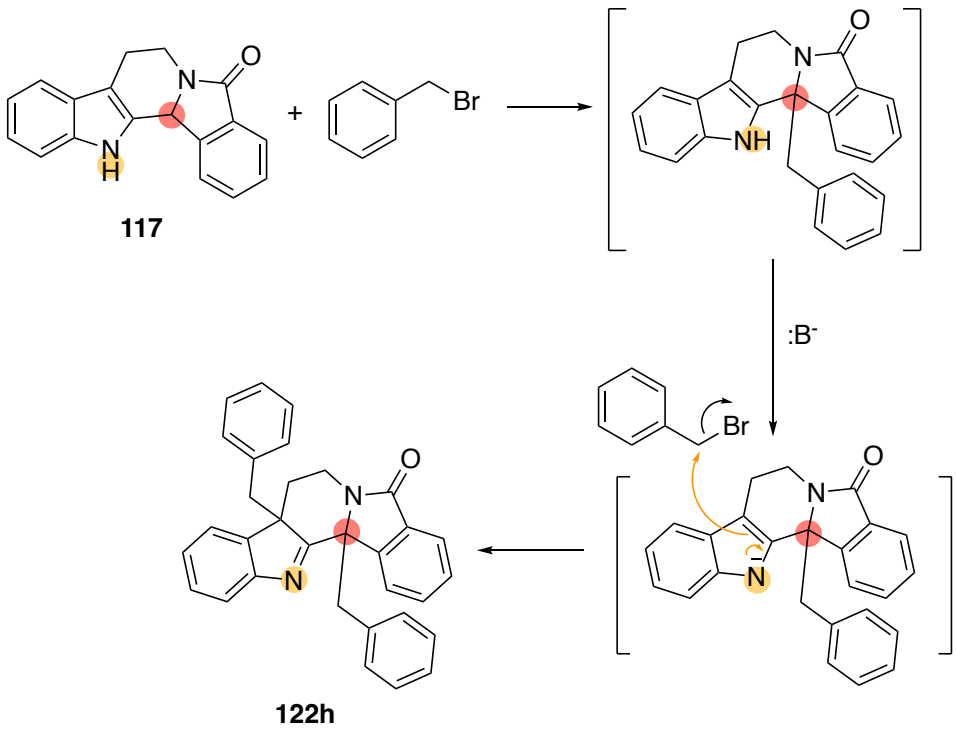

*Scheme 5.6. Proposed mechanism for the synthesis of disubstituted fused 3H-indole derivatives **122**.*

Compounds **122** were obtained as single diastereomers, and the relative configuration of their stereogenic centres must be considered. A 1D NOE NMR experiment in which the protons of the CH_2 of the isoprenyl chain of molecule **122g** were selectively irradiated was performed. No spatial proximity with the other isoprenyl chain was observed, suggesting that these chains are in a *trans* arrangement. It is reasonable to assume that, after the first substitution, a steric hindrance is generated, and this prevents the second substitution from taking place from the same face, favouring the formation of the *trans* isomer. Furthermore, calculations of the stability of both conformations using *ab initio* calculations at the 6-31G* level carried out with the Spartan 18 program, revealed that the *trans* isomer is 6.09 kJ/mol more stable than the *cis* (Figure 5.12).

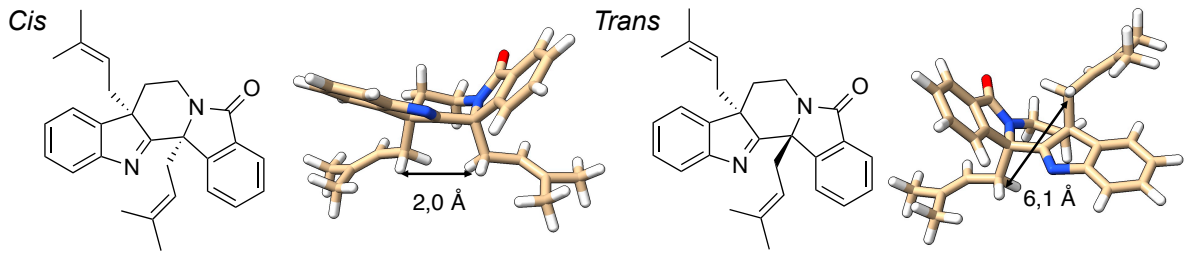

*Figure 5.12. Minimisation of cis and trans conformations of compound **122g** predicted with Spartan 18.*

To be sure that the formation of imine derivatives **122** was not influenced by thermodynamic or kinetic factors, different experiments open to air at different temperatures (-10, 0, 25 and 70°C) were performed for the *n*-hexyl derivative (**119e**, **122e**). Only minimal differences in yield or ratio between **119** and **122** were observed; however, in the reaction at -10°C, other than the desired product, the formation of compound **124** was observed from the dehydrogenation of the starting material.

Interestingly, **124** is a constitutional isomer of the natural product fascaplysin (Figure 5.13). Fascaplysin was isolated in 1988 from the Fijian sponge *Fascaplysinopsis bergquist sp*.[30] and has a wide range of biological activities, including anticancer,[31,32] analgesic,[33] antithrombotic,[34] anti-Alzheimer,[35] anti-plasmodial,[36] and antimalarial[37] activities.

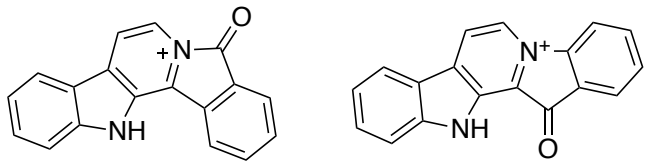

124 **Fascaplysin**

*Figure 5.13. Structures of fascaplysin and compound **124**.*

A small library of oxygen-containing derivatives (**120**) was also synthesised (Scheme 5.7) in order to compare their biological activities with compounds **119**. These derivatives have lower yields due to the fact that the reaction also generates the corresponding non-alkoxy derivative. The reaction was also performed under a stream of air in order to provide oxygen, but yields did not vary significantly.

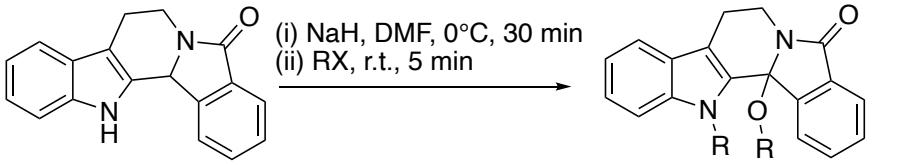

120

120a: R = Me (43%)
120b: R = Et (12%)
120c: R = benzyl (16%)

*Scheme 5.7. Synthesis of oxygen-containing derivatives **120**.*

5.4. EXPERIMENTAL SECTION

2-(2-(1*H*-Indol-3-yl)ethyl)isoindoline-1,3-dione (**116**):

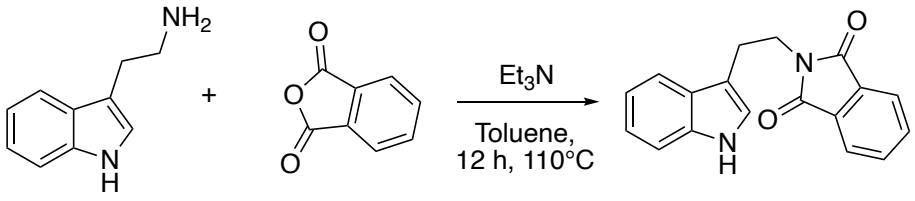

116

According to the procedure reported in the literature,[29] tryptamine (6.4 g, 0.4 mol, 1 equiv.), phthalic anhydride (7.1 g,0.48 mmol, 1.2 equiv.) and triethylamine (6.7 mL, 0.48 mmol, 1.2 equiv.) were placed in a round-bottom flask and toluene (80 mL, c = 0.5 M) was added. The mixture was stirred under reflux for 8 h. When the reaction was completed, it was cooled to room temperature and diluted with water. The crude of the reaction was filtered, the solid was washed with water and dried for 1-2 h in the oven at 100 °C, giving the corresponding product **116** (11.45 g, 99 %) as a yellow solid.

The physicochemical data are consistent with those reported in the literature.[29]

^{1}H NMR (250 MHz, $CDCl_3$) δ 8.02 (s, 1H), 7.84 (dd, *J* = 5.4, 3.1 Hz, 2H), 7.77 – 7.73 (m, 1H), 7.70 (dd, *J* = 5.5, 3.0 Hz, 2H), 7.36 (dt, *J* = 8.3, 0.9 Hz, 1H), 7.23 – 7.16 (m, 1H), 7.16 – 7.09 (m, 2H), 4.07 – 3.95 (m, 2H), 3.16 (ddd, *J* = 8.5, 6.2, 0.9 Hz, 2H).

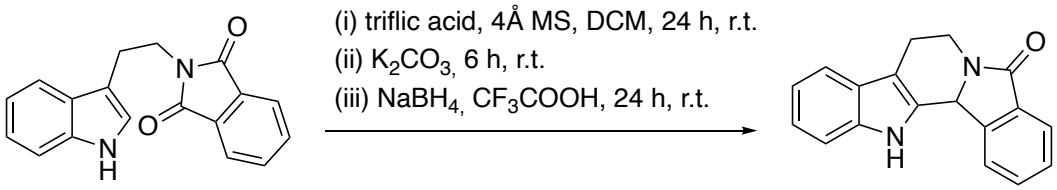

116 **117**

7,8,13,13b-Tetrahydro-5*H*-benzo[1,2]indolizino[8,7-*b*]indol-5-one (**117**):

According to a modification of the reported synthesis in the literature,[38] in a 50 mL two neck round bottom flask with a condenser and rubber septum, compound **116** (871 mg, 3 mmol, 1 equiv.), 4 Å molecular sieves (396 mg), and anhydrous

dichloromethane (158 mL, c = 0.019 M) were placed under an argon atmosphere and stirred. To this mixture, trifluoromethanesulfonic acid (2.65 mL, 30 mmol, 10 equiv.) was added and stirred at room temperature. After 12 h, the reaction mixture was neutralised with solid K_2CO_3 (4.56 g, 33 mmol, 11 equiv.). After 4 hours, to this crude reaction mixture, $NaBH_4$ (510 mg, 13.5 mmol, 4.5 equiv.) and CF_3COOH (3.1 mL, 40.5 mmol, 13.5 equiv.) were added under argon atmosphere with vigorous stirring at room temperature. After 12 h, the reaction mixture was quenched with aqueous $NaHCO_3$. The organic layer was separated, and the aqueous layer was extracted with ethyl acetate (3 x 100 mL). The combined organic layers were washed with aqueous $NaHCO_3$, dried over anhydrous Na_2SO_4 and filtered. The solvent was removed under reduced pressure. The crude mixture was used without further purification, obtaining compound **117** (640 mg, 78%) as a light-yellow solid.

The physicochemical data are consistent with those reported in the literature.[38]

^{1}H NMR (250 MHz, $CDCl_3$) δ 8.88 (s, 1H), 7.90 (ddt, *J* = 8.2, 7.2, 0.9 Hz, 2H), 7.59 (td, *J* = 7.5, 1.4 Hz, 1H), 7.52 – 7.43 (m, 2H), 7.41 – 7.34 (m, 1H), 7.18 (td, *J* = 8.0, 7.6, 1.6 Hz, 1H), 7.14 – 7.06 (m, 1H), 5.85 (s, 1H), 4.87 (ddd, *J* = 13.2, 5.7, 1.4 Hz, 1H), 3.41 (ddd, *J* = 13.1, 10.8, 5.5 Hz, 1H), 3.06 – 2.92 (m, 1H), 2.92 – 2.81 (m, 1H).

*5.4.1. Synthesis of indole-isoindolinones (**119, 122**)*

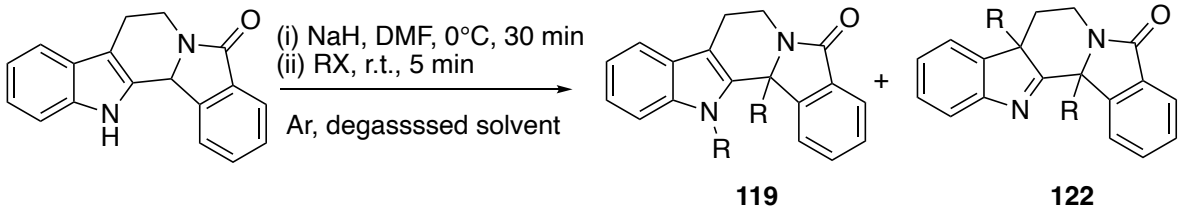

119 **122**

119a: R = Me
119b: R = Et
119c: R = Pr
119d: R = But
119e: R = n-Hex
119f: R = allyl
119g: R = isoprenyl
119h: R = benzyl
119i: R = 3-F benzyl
119j: R = 4-F benzyl

122e: R = n-Hex
122f: R = allyl
122g: R = isoprenyl
122h: R = benzyl
122i: R = 3-F benzyl
122j: R = 4-F benzyl

General procedure for the synthesis of disubstituted indole-isoindolinone GP17

7,8,13,13b-Tetrahydro-5*H*-benzo[1,2]indolizino[8,7-*b*]indol-5-one (**117**) (1 equiv.) and NaH (60 %) (6 equiv.) are added to a round-bottom flask that is purged with argon 3 times. To this mix, previously degassed DMF (1 mL, c = 0.2 M) is added while at 0°C and the mixture is stirred for 30 minutes. When the time is elapsed, the corresponding halide is added and the mixture is stirred for a further 5 minutes at room temperature, then, a saturated solution of NH_4Cl is added and the aqueous phase is extracted 3 times with EtOAc. The combined organic layers are dried over Na_2SO_4 and under reduced pressure. The crude is purified using column chromatography.

13,13b-Dimethyl-7,8,13,13b-tetrahydro-5*H*-benzo[1,2]indolizino[8,7-*b*]indol-5-one (**119a**):

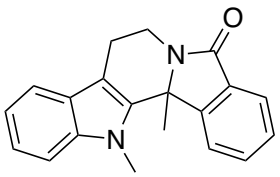

According to GP17, compound **117** (55 mg, 0.2 mmol, 1 equiv.), NaH (60 %) (48 mg, 1.2 mmol, 6 equiv.) and iodomethane (78 μL, 1 mmol, 5 equiv.) in DMF (1 mL, 0.2 M), provided after column chromatography 8:2 Hex:EtOAc the desired product **119a** (48 mg, 63.5 % yield) as an orange oil.

^{1}H NMR (300 MHz, $CDCl_3$) δ 7.98 (dt, *J* = 7.8, 0.8 Hz, 1H), 7.91 (ddd, *J* = 7.4, 1.3, 0.7 Hz, 1H), 7.62 (td, *J* = 7.6, 1.3 Hz, 1H), 7.53 – 7.45 (m, 2H), 7.31 – 7.27 (m, 1H), 7.25 – 7.19 (m, 1H), 7.10 (ddd, *J* = 7.9, 6.7, 1.3 Hz, 1H), 4.78 (ddd, *J* = 13.1, 5.9, 1.0 Hz, 1H), 4.10 (s, 3H), 3.34 (ddd, *J* = 13.0, 11.7, 4.6 Hz, 1H), 3.06 (ddd, *J* = 15.4, 11.8, 6.0 Hz, 1H), 2.86 (ddd, *J* = 15.4, 4.6, 1.0 Hz, 1H), 1.98 (s, 3H).

^{13}C NMR (75 MHz, $CDCl_3$) δ 167.9, 148.4, 137.9, 136.2, 132.2, 131.7, 128.8, 126.2, 124.5, 123.3, 122.6, 119.8, 118.9, 109.7, 109.1, 64.3, 36.0, 33.0, 25.9, 22.3.

R_f = 0.47 (1:1 Hex:EtOAc)

HRMS (ESI-Orbitrap, *m*/*z*): calcd for $C_{20}H_{18}N_2O$ $[M + H]^+$ 303.1492; found 303.1505.

13,13b-Diethyl-7,8,13,13b-tetrahydro-5*H*-benzo[1,2]indolizino[8,7-*b*]indol-5-one (**119b**):

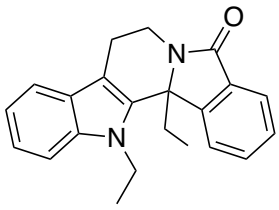

According to GP17, compound **117** (55 mg, 0.2 mmol, 1 equiv.), NaH (60 %) (48 mg, 1.2 mmol, 6 equiv.) and iodoethane (80 μL, 1 mmol, 5 equiv.) in DMF (1 mL, 0.2 M), provided after column chromatography 8:2 Hex:EtOAc the desired product **119b** (55.8 mg, 84.4 % yield) as a light yellow oil.

^{1}H NMR (300 MHz, $CDCl_3$) δ 7.92 (ddd, *J* = 7.5, 1.3, 0.7 Hz, 1H), 7.84 (dt, *J* = 7.9, 0.9 Hz, 1H), 7.62 (ddd, *J* = 7.8, 7.4, 1.3 Hz, 1H), 7.49 (td, *J* = 7.4, 0.8 Hz, 2H), 7.30 (dt, *J* = 8.2, 1.0 Hz, 1H), 7.21 (ddd, *J* = 8.3, 6.9, 1.2 Hz, 1H), 7.10 (ddd, *J* = 7.9, 6.9, 1.1 Hz, 1H), 4.77 (ddd, *J* = 12.6, 5.9, 1.0 Hz, 1H), 4.61 (q, *J* = 7.1 Hz, 2H), 3.22 (ddd, *J* = 12.6, 11.8, 4.5 Hz, 1H), 3.07 (ddd, *J* = 15.2, 11.8, 5.9 Hz, 1H), 2.85 (ddd, *J* = 15.2, 4.4, 1.0 Hz, 1H), 2.54 (dq, *J* = 14.5, 7.2 Hz, 1H), 2.31 (dt, *J* = 14.5, 7.3 Hz, 1H), 1.35 (t, *J* = 7.1 Hz, 3H), 0.58 (t, *J* = 7.3 Hz, 3H).

^{13}C NMR (75 MHz, $CDCl_3$) δ 168.5, 145.7, 136.6, 136.1, 133.6, 131.7, 128.9, 126.9, 124.5, 123.5, 122.4, 119.7, 119.0, 109.8, 109.6, 68.4, 40.4, 35.7, 30.6, 22.2, 15.6, 7.6.

R_f = 0.56 (1:1 Hex:EtOAc)

HRMS (ESI-Orbitrap, *m*/*z*): calcd for $C_{22}H_{22}N_2O$ $[M + H]^+$ 331.1805; found 331.1813.

13,13b-Dipropyl-7,8,13,13b-tetrahydro-5*H*-benzo[1,2]indolizino[8,7-*b*]indol-5-one (**119c**):

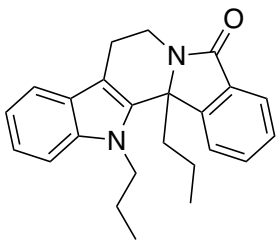

According to GP17, compound **117** (55 mg, 0.2 mmol, 1 equiv.), NaH (60 %) (48 mg, 1.2 mmol, 6 equiv.) and 1-bromopropane (91 μL, 1 mmol, 5 equiv.) in DMF (1 mL, 0.2 M), provided after column chromatography 8:2 Hex:EtOAc the desired product **119c** (10.7 mg, 14.9 % yield) as an orange oil.

^{1}H NMR (300 MHz, CDCl3) δ 7.91 (ddd, *J* = 7.5, 1.4, 0.7 Hz, 1H), 7.80 (dt, *J* = 7.9, 0.8 Hz, 1H), 7.65 – 7.58 (m, 1H), 7.52 – 7.44 (m, 2H), 7.33 – 7.27 (m, 1H), 7.23 – 7.18 (m, 1H), 7.09 (ddd, *J* = 8.0, 6.9, 1.2 Hz, 1H), 4.81 – 4.70 (m, 1H), 4.43 (dt, *J* = 10.3, 5.8

Hz, 2H), 3.31 – 3.18 (m, 1H), 3.07 (ddd, *J* = 15.2, 11.8, 6.0 Hz, 1H), 2.90 – 2.81 (m, 1H), 2.51 – 2.37 (m, 1H), 1.82 (ddd, *J* = 13.9, 10.9, 7.1 Hz, 1H), 1.56 (dq, *J* = 10.8, 7.4, 6.8 Hz, 1H), 1.09 (t, *J* = 7.5 Hz, 3H), 0.83 – 0.80 (m, 3H).

^{13}C NMR (75 MHz, $CDCl_3$) δ 168.3, 146.2, 137.0, 136.2, 133.4, 131.5, 128.9, 126.7, 124.5, 123.2, 122.4, 119.7, 119.0, 109.8, 109.4, 68.0, 47.6, 40.0, 35.8, 23.2, 22.2, 16.6, 14.1, 11.2.

R_f = 0.65 (1:1 Hex:EtOAc)

HRMS (ESI-Orbitrap, *m*/*z*): calcd for $C_{24}H_{26}N_2O$ $[M + H]^+$ 359.2118; found 359.2128

13,13b-Dibutyl-7,8,13,13b-tetrahydro-5*H*-benzo[1,2]indolizino[8,7-*b*]indol-5-one (**119d**):

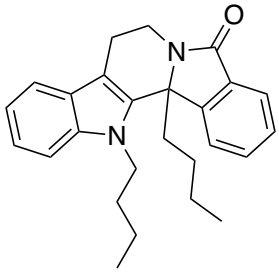

According to GP17, compound **117** (55 mg, 0.2 mmol, 1 equiv.), NaH (60 %) (48 mg, 1.2 mmol, 6 equiv.) and 1-iodobutane (114 μL, 1 mmol, 5 equiv.) in DMF (1 mL, 0.2 M), provided after column chromatography 8:2 Hex:EtOAc the desired product **119d** (55mg, 70.8 % yield) as a light yellow oil.

^{1}H NMR (300 MHz, $CDCl_3$) δ 7.92 (ddd, *J* = 7.4, 1.4, 0.6 Hz, 1H), 7.82 (dt, *J* = 7.9, 0.9 Hz, 1H), 7.61 (td, *J* = 7.6, 1.4 Hz, 1H), 7.53 – 7.45 (m, 2H), 7.29 (d, *J* = 1.0 Hz, 1H), 7.20 (ddd, *J* = 8.3, 6.9, 1.2 Hz, 1H), 7.09 (ddd, *J* = 7.9, 6.8, 1.2 Hz, 1H), 4.76 (ddd, *J* = 12.7, 6.0, 0.9 Hz, 1H), 4.52 – 4.42 (m, 2H), 3.25 (ddd, *J* = 12.7, 11.8, 4.6 Hz, 1H), 3.13 – 3.02 (m, 1H), 2.86 (ddd, *J* = 15.2, 4.6, 0.9 Hz, 1H), 2.47 (ddd, *J* = 14.3, 11.5, 4.7 Hz, 1H), 2.25 (ddd, *J* = 14.3, 11.9, 4.4 Hz, 1H), 1.82 – 1.66 (m, 1H), 1.64 – 1.48 (m, 3H), 1.23 (q, *J* = 7.5 Hz, 2H), 1.04 (d, *J* = 7.0 Hz, 3H), 0.80 (d, *J* = 7.2 Hz, 3H), 0.78 – 0.68 (m, 2H).

^{13}C NMR (75 MHz, $CDCl_3$) δ 168.3, 146.1, 136.9, 136.2, 133.4, 131.5, 128.9, 126.7, 124.5, 123.3, 122.4, 119.6, 119.0, 109.8, 109.5, 68.0, 45.9, 37.5, 35.7, 31.9, 25.2, 22.65, 22.2, 20.3, 14.0, 14.0.

R_f = 0.73 (1:1 Hex:EtOAc)

HRMS (ESI-Orbitrap, *m*/*z*): calcd for $C_{26}H_{30}N_2O$ [M + Na]$^+$ 409.2250; found 409.2258

13,13b-Dihexyl-7,8,13,13b-tetrahydro-5*H*-benzo[1,2]indolizino[8,7-*b*]indol-5-one (**119e**):

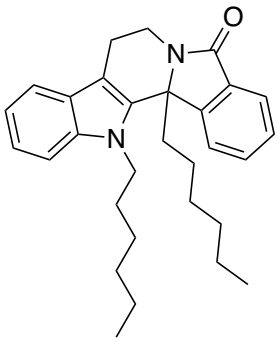

According to GP17, compound **117** (55 mg, 0.2 mmol, 1 equiv.), NaH (60 %) (48 mg, 1.2 mmol, 6 equiv.) and 1-iodohexane (148 μL, 1 mmol, 5 equiv.) in DMF (1 mL, 0.2 M), provided after column chromatography 9:1 Hex:EtOAc the desired product **119e** (22.4 mg, 25.4 % yield) as a light yellow oil.

^{1}H NMR (300 MHz, $CDCl_3$) δ 7.91 (ddd, *J* = 7.4, 1.4, 0.6 Hz, 1H), 7.81 (dt, *J* = 7.8, 0.9 Hz, 1H), 7.60 (td, *J* = 7.5, 1.3 Hz, 1H), 7.54 – 7.45 (m, 2H), 7.28 (t, *J* = 1.0 Hz, 1H), 7.20 (ddd, *J* = 8.2, 6.8, 1.2 Hz, 1H), 7.09 (ddd, *J* = 7.9, 6.8, 1.2 Hz, 1H), 4.83 – 4.70 (m, 1H), 4.46 (dd, *J* = 8.9, 7.3 Hz, 2H), 3.30 – 3.18 (m, 1H), 3.07 (ddd, *J* = 15.2, 11.8, 6.0 Hz, 1H), 2.92 – 2.81 (m, 1H), 2.46 (ddd, *J* = 14.3, 11.3, 4.7 Hz, 1H), 2.25 (ddd, *J* = 14.2, 11.9, 4.2 Hz, 1H), 1.83 – 1.68 (m, 1H), 1.52 (d, *J* = 5.2 Hz, 3H), 1.41 – 1.31 (m, 4H), 1.23 – 1.07 (m, 7H), 0.98 – 0.90 (m, 3H), 0.84 – 0.78 (m, 3H), 0.77 – 0.69 (m, 1H).

^{13}C NMR (75 MHz, $CDCl_3$) δ 168.4, 146.2, 136.9, 136.2, 133.4, 131.5, 128.9, 126.7, 124.5, 123.2, 122.4, 119.7, 119.0, 109.8, 109.5, 68.0, 46.2, 37.8, 35.8, 31.7, 31.6, 29.90, 29.2, 26.7, 23.1, 22.8, 22.6, 22.2, 14.2, 14.1.

R_f = 0.76 (1:1 Hex:EtOAc)

HRMS (ESI-Orbitrap, *m*/*z*): calcd for $C_{30}H_{38}N_2O$ [M + H]$^+$ 443.3057; found 443.3064

13,13b-Diallyl-7,8,13,13b-tetrahydro-5*H*-benzo[1,2]indolizino[8,7-*b*]indol-5-one (**119f**):

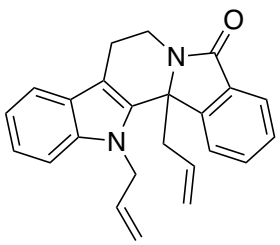

According to GP17, compound **117** (55 mg, 0.2 mmol, 1 equiv.), NaH (60 %) (48 mg, 1.2 mmol, 6 equiv.) and 3-bromoprop-1-ene (87 μL, 1 mmol, 5 equiv.) in DMF (1 mL, 0.2 M), provided after column chromatography 8:2 Hex:EtOAc, the desired product **119f** (16 mg, 23 % yield) as a yellow oil.

^{1}H NMR (300 MHz, $CDCl_3$) δ 7.89 (ddd, *J* = 7.5, 1.4, 0.7 Hz, 1H), 7.80 (dt, *J* = 7.8, 0.9 Hz, 1H), 7.62 – 7.55 (m, 1H), 7.51 – 7.45 (m, 2H), 7.25 – 7.16 (m, 2H), 7.11 (ddd, *J* = 8.0, 6.4, 1.8 Hz, 1H), 5.89 (dddd, *J* = 17.2, 10.1, 5.2, 3.9 Hz, 1H), 5.29 – 5.11 (m, 4H), 5.05 – 4.84 (m, 3H), 4.77 (ddd, *J* = 13.0, 6.1, 1.0 Hz, 1H), 3.32 (ddd, *J* = 13.0, 11.7, 4.7 Hz, 1H), 3.20 (ddt, *J* = 14.8, 6.8, 1.1 Hz, 1H), 3.14 – 3.01 (m, 2H), 2.88 (ddd, *J* = 15.4, 4.7, 1.0 Hz, 1H).

^{13}C NMR (75 MHz, $CDCl_3$) δ 168.3, 145.7, 137.6, 135.4, 133.3, 133.1, 131.7, 130.9, 128.9, 126.7, 124.4, 123.9, 122.7, 120.0, 119.5, 119.0, 117.7, 110.6, 110.5, 67.2, 48.14, 42.4, 35.9, 22.3.

R_f = 0.62 (1:1 Hex:EtOAc)

13,13b-Bis(3-methylbut-2-en-1-yl)-7,8,13,13b-tetrahydro-5*H*-benzo[1,2]indolizino [8,7-*b*]indol-5-one (**119g**):

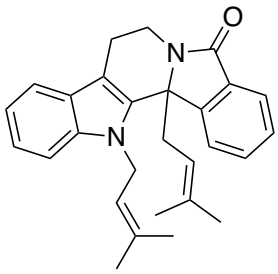

According to GP17, compound **117** (55 mg, 0.2 mmol, 1 equiv.), NaH (60 %) (48 mg, 1.2 mmol, 6 equiv.) and 1-bromo-3-methylbut-2-ene (116 μL, 1 mmol, 5 equiv.) in DMF (1 mL, 0.2 M), provided after column chromatography 9:1 Hex:EtOAc the desired product **119g** (20.8 mg, 25.3 % yield) as a dark orange oil.

^{1}H NMR (300 MHz, $CDCl_3$) δ 7.89 (ddd, *J* = 7.4, 1.4, 0.7 Hz, 1H), 7.79 (dt, *J* = 7.8, 0.9 Hz, 1H), 7.56 (td, *J* = 7.6, 1.4 Hz, 1H), 7.50 – 7.44 (m, 2H), 7.21 – 7.17 (m, 2H), 7.14 – 7.07 (m, 1H), 5.18 (s, 2H), 5.06 – 5.00 (m, 1H), 4.75 (ddd, *J* = 12.9, 6.0, 1.0 Hz, 1H), 4.58 (tt, *J* = 7.0, 1.4 Hz, 1H), 3.30 (ddd, *J* = 13.0, 11.7, 4.7 Hz, 1H), 3.16 (dd, *J* = 15.4, 7.2 Hz, 1H), 3.04 (ddd, *J* = 15.3, 11.6, 6.0 Hz, 2H), 2.91 – 2.80 (m, 1H), 1.94 (d, *J* = 1.3 Hz, 3H), 1.72 (d, *J* = 1.5 Hz, 3H), 1.55 (d, *J* = 1.3 Hz, 3H), 1.49 (d, *J* = 1.4 Hz, 3H).

^{13}C NMR (75 MHz, $CDCl_3$) δ 168.4, 146.5, 137.4, 135.7 (2C), 134.6, 133.1, 131.5, 128.7, 126.7, 124.2, 123.6, 122.5, 121.7, 119.8, 118.9, 116.9, 110.2, 110.2, 67.7, 44.5, 37.0, 36.1, 25.9, 25.6, 22.4, 18.7, 18.4.

R_f = 0.82 (1:1 Hex:EtOAc)

HRMS (ESI-Orbitrap, *m*/*z*): calcd for $C_{28}H_{30}N_2O$ $[M + H]^+$ 411.2431; found 411.2440

13,13b-dibenzyl-7,8,13,13b-tetrahydro-5*H*-benzo[1,2]indolizino[8,7-*b*]indol-5-one (**119h**):

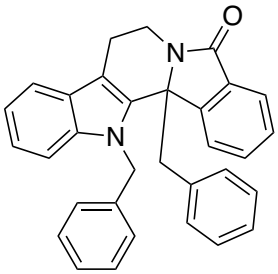

According to GP17, compound **117** (55 mg, 0.2 mmol, 1 equiv.), NaH (60 %) (48 mg, 1.2 mmol, 6 equiv.) and (bromomethyl)benzene (119 μL, 1 mmol, 5 equiv.) in DMF (1 mL, 0.2 M), provided after column chromatography 9:1 Hex:EtOAc the desired product **119h** (31.1 mg, 34.2 % yield) as a light yellow foam.

^{1}H NMR (300 MHz, $CDCl_3$) δ 7.68 – 7.63 (m, 2H), 7.57 – 7.50 (m, 1H), 7.30 – 7.27 (m, 1H), 7.23 – 7.19 (m, 4H), 7.15 – 7.10 (m, 2H), 7.07 – 6.99 (m, 4H), 6.86 (dd, *J* = 4.9, 3.4 Hz, 2H), 6.77 – 6.71 (m, 2H), 6.01 (d, *J* = 17.6 Hz, 1H), 5.89 (d, *J* = 17.6 Hz, 1H), 4.86 – 4.77 (m, 1H), 3.61 (d, *J* = 1.7 Hz, 2H), 3.40 (ddd, *J* = 13.0, 11.6, 4.7 Hz, 1H), 3.11 (ddd, *J* = 15.3, 11.6, 6.0 Hz, 1H), 3.00 – 2.89 (m, 1H).

^{13}C NMR (75 MHz, $CDCl_3$) δ 168.3, 145.1, 137.8, 137.3, 135.8, 134.3, 132.7, 131.1, 130.0 (2C), 128.9 (2C), 128.6, 128.0 (2C), 127.6, 127.1, 126.7, 126.0 (2C), 124.2, 124.0, 123.0, 120.2, 119.0, 111.0, 110.6, 68.2, 49.6, 43.9, 36.2, 22.5.

R_f = 0.6 (1:1 Hex:EtOAc)

HRMS (ESI-Orbitrap, *m*/*z*): calcd for $C_{32}H_{26}N_2O$ $[M + Na]^+$ 477.1937; found 477.1935

13,13b-bis(3-fluorobenzyl)-7,8,13,13b-tetrahydro-5*H*-benzo[1,2]indolizino[8,7-*b*]indol-5-one (**119i**):

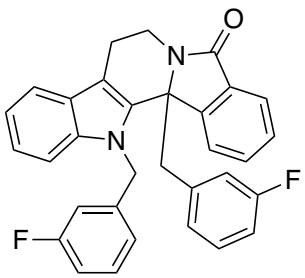

According to GP17, compound **117** (55 mg, 0.2 mmol, 1 equiv.), NaH (60 %) (48 mg, 1.2 mmol, 6 equiv.) and 1-(bromomethyl)-3-fluorobenzene (123 μL, 1 mmol, 5 equiv.) in DMF (1 mL, 0.2 M), provided after column chromatography 8:2 Hex:EtOAc the desired product **119j** (54.3 mg, 55.3 % yield) as a light yellow foam.

^{1}H NMR (300 MHz, $CDCl_3$) δ 7.68 (ddd, *J* = 7.4, 1.5, 0.7 Hz, 1H), 7.62 (dt, *J* = 7.4, 1.0 Hz, 1H), 7.57 – 7.51 (m, 1H), 7.31 (td, *J* = 7.4, 1.1 Hz, 1H), 7.23 (dd, *J* = 7.5, 1.4 Hz, 1H), 7.20 – 7.10 (m, 3H), 7.08 – 6.95 (m, 2H), 6.95 – 6.87 (m, 1H), 6.75 (tdd, *J* = 8.5, 2.6, 1.0 Hz, 1H), 6.62 (ddd, *J* = 7.7, 1.7, 0.9 Hz, 1H), 6.58 – 6.51 (m, 2H), 6.42 (dt, *J* = 9.7, 2.1 Hz, 1H), 5.96 (d, *J* = 17.9 Hz, 1H), 5.87 (d, *J* = 17.8 Hz, 1H), 4.88 – 4.78 (m, 1H), 3.59 (d, *J* = 3.0 Hz, 2H), 3.39 (ddd, *J* = 13.0, 11.6, 4.7 Hz, 1H), 3.12 (ddd, *J* = 15.4, 11.6, 6.0 Hz, 1H), 3.02 – 2.91 (m, 1H).

^{13}C NMR (75 MHz, $CDCl_3$) δ 168.2, 163.4 (d, *J* = 245.6 Hz), 162.3 (d, *J* = 244.5 Hz), 144.6, 140.0 (d, *J* = 6.8 Hz), 137.6, 136.5 (d, *J* = 7.4 Hz), 135.5, 132.8, 131.2, 130.6 (d, *J* = 8.3 Hz), 129.5 (d, *J* = 8.3 Hz), 129.0, 126.8, 125.6 (d, *J* = 3.0 Hz), 124.3, 123.9, 123.4, 121.6 (d, *J* = 2.9 Hz), 120.5, 119.2, 116.8 (d, *J* = 21.5 Hz), 114.7 (d, *J* = 21.1 Hz), 114.2 (d, *J* = 20.9 Hz), 113.1 (d, *J* = 22.5 Hz), 111.4, 110.3, 77.6, 67.8, 49.1 (d, *J* = 1.7 Hz), 43.4 (d, *J* = 1.3 Hz), 36.1, 22.4.

^{19}F NMR (282 MHz, $CDCl_3$) δ -112.1, -113.5.

R_f = 0.6 (1:1 Hex:EtOAc)

HRMS (ESI-Orbitrap, *m*/*z*): calcd for $C_{32}H_{24}F_2N_2O$ $[M + Na]^+$ 513.1749; found 513.1766

13,13b-bis(4-fluorobenzyl)-7,8,13,13b-tetrahydro-5*H*-benzo[1,2]indolizino[8,7-*b*]indol-5-one (**119j**):

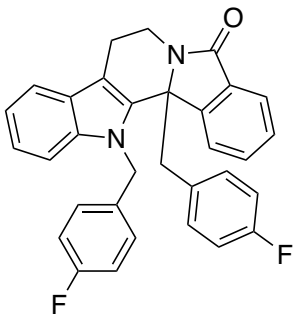

According to GP17, compound **117** (55 mg, 0.2 mmol, 1 equiv.), NaH (60 %) (48 mg, 1.2 mmol, 6 equiv.) and 1-(bromomethyl)-4-fluorobenzene (155 µL, 1 mmol, 5 equiv.) in DMF (1 mL, 0.2 M), provided after column chromatography 8:2 Hex:EtOAc the desired product **119k** (53.3 mg, 54.3 % yield) as a light yellow foam.

^{1}H NMR (300 MHz, $CDCl_3$) δ 7.67 (ddd, *J* = 7.4, 1.4, 0.6 Hz, 1H), 7.59 (dt, *J* = 7.6, 0.8 Hz, 1H), 7.56 – 7.51 (m, 1H), 7.30 (td, *J* = 7.4, 1.0 Hz, 1H), 7.22 (td, *J* = 7.5, 1.4 Hz, 1H), 7.15 – 7.10 (m, 2H), 7.05 – 6.98 (m, 1H), 6.93 – 6.86 (m, 2H), 6.79 (dd, *J* = 8.7,

5.3 Hz, 2H), 6.71 (s, 2H), 6.69 (s, 2H), 5.97 (d, *J* = 16.8 Hz, 1H), 5.84 (d, *J* = 17.5 Hz, 1H), 4.83 (ddd, *J* = 13.0, 5.9, 1.0 Hz, 1H), 3.66 – 3.52 (m, 2H), 3.37 (ddd, *J* = 12.9, 11.6, 4.8 Hz, 1H), 3.10 (ddd, *J* = 15.4, 11.6, 6.0 Hz, 1H), 2.96 (ddd, *J* = 15.4, 4.8, 1.0 Hz, 1H).

^{13}C NMR (75 MHz, $CDCl_3$) δ 168.24, 162.2 (d, *J* = 244.7 Hz), 162.0 (d, *J* = 244.4 Hz), 144.8, 137.5, 135.5, 132.8 (d, *J* = 3.3 Hz), 132.7, 131.4 (d, *J* = 8.0 Hz, 2C), 131.2, 129.9 (d, *J* = 3.4 Hz), 128.9, 127.6 (d, *J* = 8.2 Hz, 2C), 126.8, 124.3, 124.0, 123.2, 120.4, 119.2, 115.9 (d, *J* = 21.8 Hz, 2C), 115.0 (d, *J* = 21.3 Hz, 2C), 111.3, 110.5, 68.0, 49.1, 43.1, 36.1, 22.4.

^{19}F NMR (282 MHz, $CDCl_3$) δ -114.79, -115.27.

R_f = 0.6 (1:1 Hex:EtOAc)

HRMS (ESI-Orbitrap, *m*/*z*): calcd for $C_{32}H_{24}F_2N_2O$ $[M + Na]^+$ 513.1749; found 513.1746

8a,13b-dihexyl-7,8,8a,13b-tetrahydro-5*H*-benzo[1,2]indolizino[8,7-*b*]indol-5-one (**122e**):

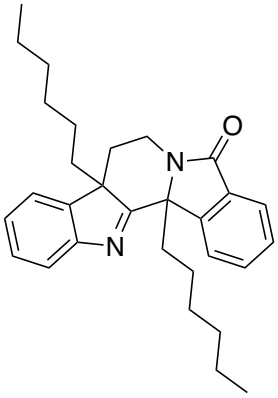

According to GP17, compound **117** (55 mg, 0.2 mmol, 1 equiv.), NaH (60 %) (48 mg, 1.2 mmol, 6 equiv.) and 1-iodohexane (148 μL, 1 mmol, 5 equiv.) in DMF (1 mL, 0.2 M), provided after column chromatography 9:1 Hex:EtOAc the desired product **122e** (11.2 mg, 12.7 % yield) as a colorless oil.

^{1}H NMR (300 MHz, $CDCl_3$) δ 7.87 (ddd, *J* = 7.5, 1.2, 0.7 Hz, 1H), 7.83 (dt, *J* = 7.6, 0.9 Hz, 1H), 7.69 (dt, *J* = 7.8, 0.9 Hz, 1H), 7.61 (td, *J* = 7.5, 1.2 Hz, 1H), 7.49 (td, *J* = 7.4, 1.0 Hz, 1H), 7.35 (ddd, *J* = 7.7, 5.4, 3.4 Hz, 1H), 7.24 – 7.20 (m, 2H), 4.61 (ddd, *J* = 14.1, 9.9, 8.0 Hz, 1H), 3.24 (ddd, *J* = 14.1, 9.5, 3.1 Hz, 1H), 2.67 (ddd, *J* = 14.2, 12.0, 4.5 Hz, 1H), 2.56 (ddd, *J* = 13.3, 9.9, 3.0 Hz, 1H), 2.12 (ddd, *J* = 14.2, 12.0, 4.4 Hz, 1H), 1.72 – 1.44 (m, 3H), 1.24 – 1.07 (m, 6H), 0.98 (td, *J* = 12.0, 5.4 Hz, 1H), 0.84 – 0.73 (m, 5H), 0.68 – 0.49 (m, 7H), 0.43

(dtd, *J* = 14.7, 6.8, 3.9 Hz, 1H), 0.06 (dq, *J* = 18.2, 6.9, 5.4 Hz, 1H), -0.45 (tdd, *J* = 12.8, 7.9, 4.9 Hz, 1H).

^{13}C NMR (75 MHz, $CDCl_3$) δ 187.4, 169.5, 155.0, 145.0, 143.5, 132.6, 131.7, 129.0, 128.2, 126.1, 123.9, 122.5, 121.8, 120.8, 69.2, 58.9, 38.7, 34.9, 33.1, 31.6, 31.1, 31.0, 29.0, 28.8, 24.1, 22.6, 22.4, 22.2, 14.1, 14.0.

R_f = 0.85 (1:1 Hex:EtOAc)

HRMS (ESI-Orbitrap, *m*/*z*): calcd for $C_{30}H_{38}N_2O$ $[M + H]^+$ 443.3057; found 443.3064

8a,13b-diallyl-7,8,8a,13b-tetrahydro-5*H*-benzo[1,2]indolizino[8,7-*b*]indol-5-one (**122f**):

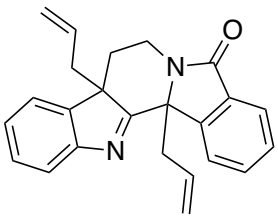

According to GP17, compound **117** (55 mg, 0.2 mmol, 1 equiv.), NaH (60 %) (48 mg, 1.2 mmol, 6 equiv.) and 3-bromoprop-1-ene (87 μL, 1 mmol, 5 equiv.) in DMF (1 mL, 0.2 M), provided after column chromatography 8:2 Hex:EtOAc, the desired product **122f** (11 mg, 15 % yield) as a light yellow oil.

^{1}H NMR (300 MHz, $CDCl_3$) δ 7.93 – 7.85 (m, 2H), 7.72 (dt, *J* = 7.7, 0.9 Hz, 1H), 7.62 (td, *J* = 7.5, 1.3 Hz, 1H), 7.52 (td, *J* = 7.4, 1.1 Hz, 1H), 7.40 (ddd, *J* = 7.8, 6.8, 1.9 Hz, 1H), 7.33 – 7.29 (m, 2H), 5.30 (ddt, *J* = 17.1, 10.0, 7.1 Hz, 1H), 5.09 – 5.00 (m, 1H), 4.95 (ddt, *J* = 10.0, 1.8, 0.9 Hz, 1H), 4.64 (ddd, *J* = 14.1, 9.8, 8.6 Hz, 1H), 4.47 (dddd, *J* = 16.5, 10.1, 8.1, 6.2 Hz, 1H), 4.31 – 4.24 (m, 1H), 4.02 – 3.93 (m, 1H), 3.37 (ddd, *J* = 14.1, 9.5, 2.7 Hz, 1H), 3.28 (ddt, *J* = 14.3, 7.1, 1.1 Hz, 1H), 3.01 (ddt, *J* = 14.2, 7.2, 1.1 Hz, 1H), 2.63 (ddd, *J* = 13.9, 9.8, 2.7 Hz, 1H), 2.42 – 2.31 (m, 1H), 2.14 (dd, *J* = 13.9, 8.1 Hz, 1H), 1.74 (ddd, *J* = 13.9, 9.5, 8.6 Hz, 1H).

^{13}C NMR (75 MHz, $CDCl_3$) δ 185.8, 169.4, 154.4, 144.8, 142.5, 132.7, 131.5, 130.7, 130.4, 129.2, 128.5, 126.3, 123.9, 122.9, 122.4, 120.9, 120.5, 118.4, 68.6, 58.8, 44.0, 38.4, 33.3, 29.9.

R_f = 0.56 (1:1 Hex:EtOAc)

HRMS (ESI-Orbitrap, *m*/*z*): calcd for $C_{24}H_{22}N_2O$ $[M + H]^+$ 355.1805; found 355,1822

8a,13b-Bis(3-methylbut-2-en-1-yl)-7,8,8a,13b-tetrahydro-5*H*-benzo[1,2]indolizino [8,7-*b*]indol-5-one (**122g**):

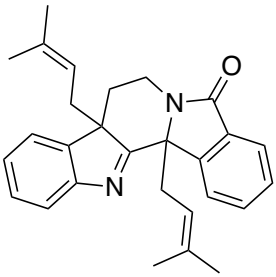

According to GP17, compound **117** (82 mg, 0.3 mmol, 1 equiv.), NaH (60 %) (72 mg, 1.8 mmol, 6 equiv.) and 1-bromo-3-methylbut-2-ene (172 μL, 1.5 mmol, 5 equiv.) in DMF (1.5 mL, 0.2 M), provided after column chromatography 8:2 Hex:EtOAc, the desired product **122g** (11 mg, 15 % yield) as a yellow oil.

^{1}H RMN (250 MHz, $CDCl_3$) δ 7.95 (dt, *J* = 7.6, 0.9 Hz, 1H), 7.85 (ddd, *J* = 7.4, 1.3, 0.8 Hz, 1H), 7.75 (dt, *J* = 7.7, 0.9 Hz, 1H), 7.62 (td, *J* = 7.5, 1.3 Hz, 1H), 7.52 (td, *J* = 7.4, 1.1 Hz, 1H), 7.33 (ddd, *J* = 7.7, 6.6, 2.2 Hz, 1H), 7.24 (dd, *J* = 2.2, 0.9 Hz, 1H), 7.19 (dd, *J* = 7.4, 1.1 Hz, 0H), 5.25 (tt, *J* = 7.1, 1.4 Hz, 1H), 4.50 (ddd, *J* = 13.8, 9.7, 7.6 Hz, 1H), 3.76 – 3.63 (m, 2H), 3.61 – 3.46 (m, 1H), 3.29 (ddd, *J* = 13.8, 9.3, 3.4 Hz, 1H), 2.55 (ddd, *J* = 13.3, 9.6, 3.4 Hz, 1H), 2.29 (dd, *J* = 15.4, 5.6 Hz, 0H), 2.07 (dd, *J* = 14.9, 7.7 Hz, 1H), 1.77 (dd, *J* = 6.0, 1.5 Hz, 1H), 1.62 (d, *J* = 1.2 Hz, 3H), 1.43 (d, *J* = 1.3 Hz, 3H), 1.05 (d, *J* = 1.1 Hz, 6H) ppm.

^{13}C RMN (63 MHz, $CDCl_3$) δ 182.8, 168.6, 155.3, 143.4, 141.6, 137.1, 134.8, 132.8, 132.0, 130.3, 128.1, 126.3, 124.1, 123.8, 122.3, 121.9, 120.5, 117.0, 90.7, 59.8, 57.7, 32.9, 29.8, 28.6, 25.8, 25.3, 18.0, 17.8 ppm.

8a,13b-dibenzyl-7,8,8a,13b-tetrahydro-5*H*-benzo[1,2]indolizino[8,7-*b*]indol-5-one (**122h**):

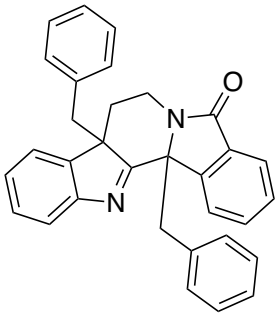

According to GP17, compound **117** (55 mg, 0.2 mmol, 1 equiv.), NaH (60 %) (48 mg, 1.2 mmol, 6 equiv.) and (bromomethyl)benzene (119 μL, 1 mmol, 5 equiv.) in DMF (1 mL, 0.2 M), provided after column chromatography 9:1 Hex:EtOAc, the desired product **122g** (21.5 mg, 23.7 % yield) as a light yellow foam.

^{1}H NMR (250 MHz, $CDCl_3$) δ 7.86 (d, *J* = 7.5 Hz, 1H), 7.74 (d, *J* = 7.5 Hz, 1H), 7.59 (t, *J* = 7.5 Hz, 2H), 7.50 – 7.29 (m, 3H), 7.19 (dd, *J* = 15.0, 7.5 Hz, 2H), 7.09 – 6.93 (m, 4H), 6.90 – 6.76 (m, 3H), 6.66 (t, *J* = 7.5 Hz, 2H), 5.92 (d, *J* = 7.5 Hz, 2H), 4.71

(dt, *J* = 14.0, 9.5 Hz, 1H), 3.59 – 3.42 (m, 2H), 2.88 (d, *J* = 14.0 Hz, 1H), 2.68 – 2.52 (m, 1H), 1.50 (dt, *J* = 14.0, 9.5 Hz, 1H).

^{13}C NMR (63 MHz, $CDCl_3$) δ 184.97, 169.44, 155.22, 145.47, 142.46, 134.75, 134.26, 132.28, 131.38, 130.27, 130.16, 129.11, 129.04, 128.90, 128.46, 128.03, 127.32, 127.19, 126.35, 125.62, 123.86, 123.26, 123.08, 121.01, 69.63, 59.42, 46.77, 39.17, 34.39, 29.04.

R_f = 0.51 (1:1 Hex:EtOAc)

HRMS (ESI-Orbitrap, *m*/*z*): calcd for $C_{32}H_{26}N_2O$ $[M + Na]^+$ 477.1937; found 477.1948

8a,13b-bis(3-Fluorobenzyl)-7,8,8a,13b-tetrahydro-5*H*-benzo[1,2]indolizino[8,7-*b*]indol-5-one (**122i**):

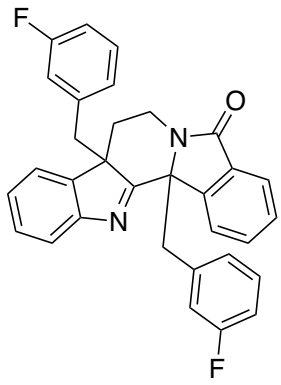

According to GP17, compound **117** (55 mg, 0.2 mmol, 1 equiv.), NaH (60 %) (48 mg, 1.2 mmol, 6 equiv.) and 1-(bromomethyl)-3-fluorobenzene (123 μL, 1 mmol, 5 equiv.) in DMF (1 mL, 0.2 M), provided after column chromatography 8:2 Hex:EtOAc the desired product **122i** (28.3 mg, 28.8 % yield) as a light yellow foam.

^{1}H NMR (300 MHz, $CDCl_3$) δ 7.84 (dt, *J* = 7.6, 0.9 Hz, 1H), 7.77 (ddd, *J* = 7.5, 1.3, 0.7 Hz, 1H), 7.64 – 7.57 (m, 2H), 7.49 (td, *J* = 7.5, 1.0 Hz, 1H), 7.39 (ddd, *J* = 7.7, 6.8, 2.0 Hz, 1H), 7.31 – 7.27 (m, 1H), 7.01 (td, *J* = 8.0, 6.1 Hz, 1H), 6.77 (tdd, *J* = 8.4, 2.6, 1.0 Hz, 1H), 6.62 (dt, *J* = 8.0, 1.5 Hz, 1H), 6.58 – 6.46 (m, 3H), 5.63 (dt, *J* = 7.3, 1.5 Hz, 1H), 5.44 (dt, *J* = 10.0, 2.1 Hz, 1H), 4.71 (dt, *J* = 14.2, 9.6 Hz, 1H), 3.71 (d, *J* = 13.8 Hz, 1H), 3.56 – 3.37 (m, 2H), 2.93 (d, *J* = 13.9 Hz, 1H), 2.73 – 2.57 (m, 2H), 1.56 (dt, *J* = 14.2, 9.5 Hz, 1H).

^{13}C NMR (75 MHz, $CDCl_3$) δ 184.6, 169.4, 162.3 (d, *J* = 244.4 Hz), 161.7 (d, *J* = 243.7 Hz), 154.8, 144.8, 142.2, 137.13 (d, *J* = 7.4 Hz), 136.57 (d, *J* = 7.5 Hz), 132.7, 131.3, 129.51 (d, *J* = 8.3 Hz), 129.50, 128.8, 128.7 (d, *J* = 8.2 Hz), 126.1, 125.9 (d, *J* = 2.9 Hz), 124.6 (d, *J* = 3.0 Hz), 124.1, 123.1, 123.0, 121.2, 117.2 (d, *J* = 21.4 Hz), 115.7

(d, *J* = 21.9 Hz), 114.3 (d, *J* = 21.1 Hz), 113.4 (d, *J* = 20.9 Hz), 69.3, 59.3, 46.11 (d, *J* = 1.2 Hz), 39.1 (d, *J* = 1.2 Hz), 34.2, 29.7.

^{19}F NMR (282 MHz, $CDCl_3$) δ -113.43, -113.69.

R_f = 0.6 (1:1 Hex:EtOAc)

HRMS (ESI-Orbitrap, *m/z*): calcd for $C_{32}H_{24}F_2N_2O$ $[M + Na]^+$ 513.1749; found 513.1753

8a,13b-bis(4-Fluorobenzyl)-7,8,8a,13b-tetrahydro-5*H*-benzo[1,2]indolizino[8,7-*b*]indol-5-one (**122j**):

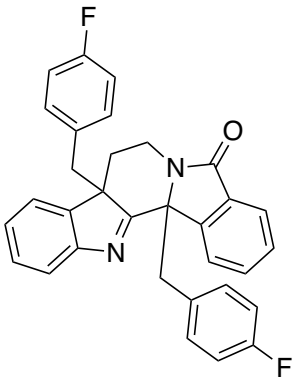

According to GP17, compound **117** (55 mg, 0.2 mmol, 1 equiv.), NaH (60 %) (48 mg, 1.2 mmol, 6 equiv.) and 1-(bromomethyl)-4-fluorobenzene (155 μL, 1 mmol, 5 equiv.) in DMF (1 mL, 0.2 M), provided after column chromatography 8:2 Hex:EtOAc the desired product **122j** (34.9 mg, 35.6 % yield) as a yellow oil.

^{1}H NMR (300 MHz, $CDCl_3$) δ 7.88 (dt, *J* = 7.7, 0.9 Hz, 1H), 7.76 (dt, *J* = 7.5, 1.0 Hz, 1H), 7.66 – 7.57 (m, 2H), 7.49 (td, *J* = 7.5, 1.0 Hz, 1H), 7.42 – 7.36 (m, 1H), 7.30 (dd, *J* = 7.4, 1.1 Hz, 1H), 7.25 – 7.22 (m, 1H), 6.83 – 6.69 (m, 4H), 6.32 – 6.24 (m, 2H), 5.78 – 5.72 (m, 2H), 4.70 (dt, *J* = 14.2, 9.6 Hz, 1H), 3.69 (d, *J* = 14.0 Hz, 1H), 3.54 – 3.40 (m, 2H), 2.89 (d, *J* = 13.9 Hz, 1H), 2.71 – 2.54 (m, 2H), 1.52 (dt, *J* = 14.3, 9.6 Hz, 1H).

^{13}C NMR (75 MHz, $CDCl_3$) δ 185.2, 169.3, 162.1 (d, *J* = 244.7 Hz), 161.4 (d, *J* = 243.8 Hz), 154.2, 144.9, 142.1, 132.6, 131.8 (d, *J* = 8.1 Hz), 131.3, 130.3 (d, *J* = 8.0 Hz), 130.2 (d, *J* = 3.4 Hz), 129.8 (d, *J* = 3.4 Hz), 129.4, 128.9, 126.2, 124.1, 123.3, 123.1, 121.0, 115.1 (d, *J* = 21.3 Hz), 114.2 (d, *J* = 21.1 Hz), 69.5 (d, *J* = 1.5 Hz), 59.6, 45.8, 38.6, 34.3, 29.3.

^{19}F NMR (282 MHz, $CDCl_3$) δ -115.03, -116.20.

R_f = 0.49 (1:1 Hex:EtOAc)

HRMS (ESI-Orbitrap, *m*/*z*): calcd for $C_{32}H_{24}F_2N_2O$ [M + Na]$^+$ 513.1749; found 513.1789

13b-propyl-7,8,13,13b-tetrahydro-5*H*-benzo[1,2]indolizino[8,7-*b*]indol-5-one (**121**):

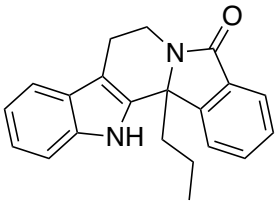

According to GP17, compound **117** (55 mg, 0.2 mmol, 1 equiv.), NaH (60 %) (48 mg, 1.2 mmol, 6 equiv.) and 1-bromopropane (91 μL, 1 mmol, 5 equiv.) in DMF (1 mL, 0.2 M), provided after column chromatography 8:2 Hex:EtOAc, the desired product **121** (30.5 mg, 48.2 % yield) as a white solid.

^{1}H NMR (300 MHz, DMSO-d_6) δ 11.30 (s, 1H), 8.29 – 8.22 (m, 1H), 7.76 – 7.68 (m, 2H), 7.52 (td, *J* = 7.4, 0.9 Hz, 1H), 7.38 (tt, *J* = 6.6, 1.1 Hz, 2H), 7.08 (ddd, *J* = 8.3, 7.1, 1.2 Hz, 1H), 6.97 (ddd, *J* = 7.9, 7.1, 1.0 Hz, 1H), 4.57 – 4.48 (m, 1H), 3.43 – 3.33 (m, 1H), 2.85 – 2.61 (m, 2H), 2.39 (ddd, *J* = 11.9, 10.1, 3.5 Hz, 1H), 2.19 (ddd, *J* = 15.2, 10.8, 5.1 Hz, 1H), 0.98 (dq, *J* = 11.6, 6.6, 6.0 Hz, 1H), 0.81 – 0.74 (m, 3H), 0.69 (dd, *J* = 13.0, 6.5 Hz, 1H).

^{13}C NMR (75 MHz, DMSO) δ 167.7, 147.5, 136.1, 135.2, 132.1, 131.2, 128.6, 125.9, 123.0, 122.8, 121.5, 118.8, 118.3, 111.2, 106.2, 65.1, 35.5, 21.4, 16.4, 13.7.

R_f = 0.56 (1:1 Hex:EtOAc)

HRMS (ESI-Orbitrap, *m*/*z*): calcd for $C_{21}H_{20}N_2O$ [M + Na]$^+$ 339.1468; found 339.1478

*5.4.2. Synthesis of alkoxy-substituted fused β-carboline-isoindolinones (**120**)*

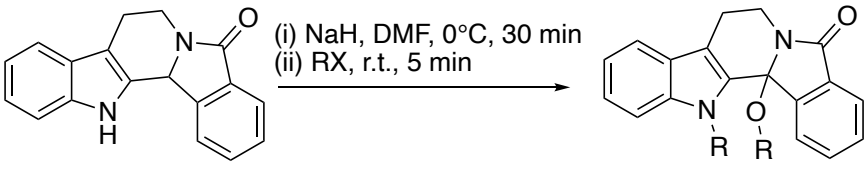

120

120a: R = Me
120b: R = Et
120c: R = benzyl

General procedure for the synthesis of alkoxy-substituted fused β-carboline-isoindolinones (120a-c) GP18

7,8,13,13b-Tetrahydro-5*H*-benzo[1,2]indolizino[8,7-*b*]indol-5-one (**117**) (1 equiv.) and NaH (60 %) (6 equiv.) are added to a round-bottom flask open to air. To this mix, DMF (c = 0.2 M) is added while at 0°C and the mixture is stirred for 30 minutes. When the time is elapsed, the corresponding halide is added and the mixture is stirred for a further 5 minutes at room temperature, then, a saturated solution of NH_4Cl is added and the aqueous phase is extracted 3 times with EtOAc. The combined organic layers are dried over Na_2SO_4 and under reduced pressure. The crude is purified using column chromatography.

13b-Methoxy-13-methyl-7,8,13,13b-tetrahydro-5*H*-benzo[1,2]indolizino[8,7-*b*]indol-5-one (**120a**):

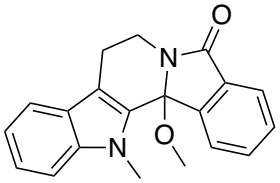

According to GP18, compound **117** (55 mg, 0.2 mmol, 1 equiv.), NaH (60 %) (48 mg, 1.2 mmol, 6 equiv.) and methyl iodide (62 μL, 1 mmol, 5 equiv.) in DMF (1 mL, 0.2 M), provided after column chromatography 8:2 Hex:EtOAc, the desired product **120a** (27 mg, 43 % yield) as a white foam.

^{1}H NMR (250 MHz, $CDCl_3$) δ 7.98 (dt, *J* = 7.5, 1.0 Hz, 1H), 7.90 (ddd, *J* = 7.5, 1.5, 1.0 Hz, 1H), 7.65 (td, *J* = 7.5, 1.5 Hz, 1H), 7.58 – 7.47 (m, 2H), 7.32 (ddd, *J* = 8.5, 1.5, 1.0 Hz, 1H), 7.25 (ddd, *J* = 8.0, 6.5, 1.5 Hz, 1H), 7.10 (ddd, *J* = 8.0, 6.5, 1.5 Hz, 1H), 4.66 (ddd, *J* = 13.0, 5.5, 1.2 Hz, 1H), 4.19 (s, 3H), 3.36 (ddd, *J* = 13.0, 11.5, 4.5 Hz, 1H), 3.09 (s, 3H), 3.01 (ddd, *J* = 17.0, 11.5, 5.5 Hz, 1H), 2.84 (ddd, *J* = 15.5, 4.5, 1.5 Hz, 1H).

^{13}C NMR (63 MHz, $CDCl_3$) δ 168.6, 143.3, 138.6, 132.9, 132.5, 132.4, 130.15, 125.99, 124.35, 123.78, 123.24, 119.81, 119.43, 112.32, 109.57, 90.82, 50.65, 36.65, 33.12, 22.32.

Rf = 0.63 (1:1 Hex:EtOAc)

HRMS (ESI-Orbitrap, *m/z*): calcd for $C_{20}H_{18}N_2O_2$ $[M + Na]^+$ 341.1260; found 341.1260.

13b-Ethoxy-13-ethyl-7,8,13,13b-tetrahydro-5*H*-benzo[1,2]indolizino[8,7-*b*]indol-5-one (**120b**):

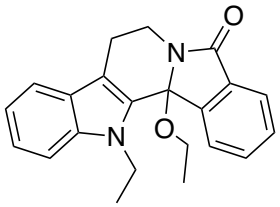

According to GP18, compound **117** (137 mg, 0.5 mmol, 1 equiv.), NaH (60 %) (120 mg, 3 mmol, 6 equiv.) and ethyl iodide (201 μL, 2.5 mmol, 5 equiv.) in DMF (2.5 mL, 0.2 M), provided after column chromatography 8:2 Hex:EtOAc, the desired product **120b** (20 mg, 12 % yield) as a white foam.

^{1}H NMR (250 MHz, $CDCl_3$) δ 7.89 (ddt, *J* = 7.6, 1.6, 0.8 Hz, 2H), 7.64 (td, *J* = 7.5, 1.4 Hz, 1H), 7.56 – 7.45 (m, 2H), 7.36 (dt, *J* = 8.3, 0.9 Hz, 1H), 7.22 (dd, *J* = 8.2, 1.3 Hz, 1H), 7.09 (ddd, *J* = 7.9, 7.0, 1.1 Hz, 1H), 4.81 – 4.56 (m, 3H), 3.46 – 3.23 (m, 2H), 3.18 – 3.02 (m, 1H), 2.97 (dd, *J* = 11.7, 5.3 Hz, 1H), 2.83 (ddd, *J* = 15.5, 4.4, 1.2 Hz, 1H), 1.47 (t, *J* = 7.1 Hz, 3H), 1.16 (t, *J* = 7.0 Hz, 3H).

^{13}C NMR (63 MHz, $CDCl_3$) δ 168.7, 144.0, 137.6, 133.2, 132.9, 132.6, 130.4, 126.9, 124.5, 124.1, 123.3, 120.0, 119.9, 112.5, 110.6, 91.1, 59.1, 41.1, 36.9, 22.7, 15.7, 15.5.

Rf = 0.69 (1:1 Hex:EtOAc)

HRMS (ESI-Orbitrap, *m/z*): calcd for $C_{22}H_{22}N_2O_2$ $[M + Na]^+$ 369.1573; found 369.1581

13-Benzyl-13b-(benzyloxy)-7,8,13,13b-tetrahydro-5*H*-benzo[1,2]indolizino[8,7-*b*]indol-5-one (**120c**):

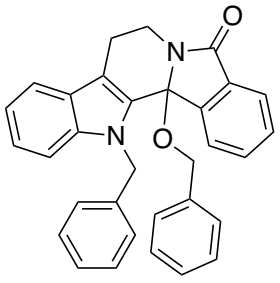

According to GP18, compound **117** (82 mg, 0.3 mmol, 1 equiv.), NaH (60 %) (72 mg, 1.8 mmol, 6 equiv.) and benzyl bromide (178 μL, 1.2 mmol, 5 equiv.) in DMF (1.5 mL, 0.2 M), provided after column chromatography 8:2 Hex:EtOAc, the desired product **120c** (21 mg, 16 % yield) as a white foam

^{1}H NMR (250 MHz, $CDCl_3$) δ 7.95 – 7.88 (m, 1H), 7.58 – 7.34 (m, 4H), 7.29 – 7.27 (m, 1H), 7.25 (d, *J* = 2.1 Hz, 5H), 7.15 (dd, *J* = 6.9, 2.7 Hz, 2H), 7.12 – 7.06 (m, 2H), 7.05 – 6.97 (m, 3H), 6.14 (d, *J* = 17.4 Hz, 1H), 5.70 (d, *J* = 17.4 Hz, 1H), 4.75 – 4.62 (m,

1H), 4.34 (d, *J* = 11.5 Hz, 1H), 4.10 (d, *J* = 11.5 Hz, 1H), 3.43 (ddd, *J* = 12.8, 11.8, 4.4 Hz, 1H), 3.16 – 3.00 (m, 1H), 2.91 (ddd, *J* = 15.6, 4.4, 1.2 Hz, 1H).

^{13}C NMR (63 MHz, $CDCl_3$) δ 168.5, 142.7, 138.3, 137.7, 137.6, 133.6, 132.3, 130.1, 128.7 (2C), 128.5 (2C), 127.7, 127.5 (2C), 127.3, 127.1, 126.6, 126.4 (2C), 124.4, 124.1, 123.4, 120.1, 119.4, 112.8, 111.2, 90.9, 65.4, 49.9, 36.6, 22.5.

Rf = 0.75 (1:1 Hex:EtOAc)

HRMS (ESI-Orbitrap, *m*/*z*): calcd for $C_{27}H_{25}N_3O_2$ $[M + Na]^+$ 493.1887; found 493.1876.

5-oxo-5,13-Dihydrobenzo[1,2]indolizino[8,7-*b*]indol-6-ium (**124**):

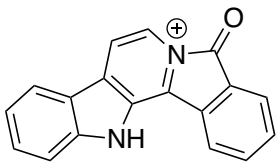

Compound **117** (69 mg, 0.25 mmol, 1 equiv.), NaH (60 %) (60 mg, 1.5 mmol, 6 equiv.) and 1-iodohexane (185 μL, 1.25 mmol, 5 equiv.) in DMF (1.75 mL, 0.2 M), provided after column chromatography 8:2 Hex:EtOAc, compound **124** (9 mg, 14 % yield) as a white solid

^{1}H NMR (250 MHz, $CDCl_3$) δ 8.85 (dd, *J* = 12.0, 7.0 Hz, 3H), 8.67 (d, *J* = 8.0 Hz, 1H), 8.16 (d, *J* = 8.0 Hz, 1H), 8.02 – 7.97 (m, 1H), 7.97 – 7.87 (m, 1H), 7.82 – 7.72 (m, 2H), 7.56 (t, *J* = 7.5 Hz, 1H).

^{13}C NMR (63 MHz, $CDCl_3$) δ 159.6, 145.1, 139.5, 136.1, 134.9, 133.7, 130.8, 130.7, 130.6, 130.2, 129.6, 129.4, 125.5, 125.1, 123.6, 122.6, 117.7, 115.3.

Rf = 0.57 (1:1 Hex:EtOAc)

HRMS (ESI-Orbitrap, *m*/*z*): calcd for $C_{18}H_{11}N_2O^+$ $[M]^+$ 271.0866; found 271.0865.

5.5. BIBLIOGRAPHY

1. V.A. Kovtunenko, Z. V Voitenko. The chemistry of isoindoles. *Rus Chem Rev* **1994**, 63 (12), 997–1018.

2. F.S. Babichev, V.A. Kovtunenko, A.K. Tyltin. Advances in the Chemistry of Isoindole. *Rus Chem Rev* **1981**, 50 (11), 1087–1103.

3. T. Tamaoki, H. Nomoto, I. Takahashi, et al. Staurosporine, a potent inhibitor of phospholipidCa++dependent protein kinase. *Biochem Biophys Res Commun* **1986**, 135 (2), 397–402.

4. S. Omura, Y. Iwai, A. Hirano, et al. A new alkaloid am-2282 of streptomyces origin taxonomy, fermentation, isolation and preliminary characterization. *J Antibiot* **1977**, 30 (4), 275–282.

5. D.E. Williams, V.S. Bernan, F. V. Ritacco, et al. Holyrines A and B, possible intermediates in staurosporine biosynthesis produced in culture by a marine actinomycete obtained from the North Atlantic Ocean. *Tetrahedron Lett* **1999**, 40 (40), 7171–7174.

6. V. Fajardo, V. Elango, B.K. Cassels, M. Shamma. Chilenine: an isoindolobenzazepine alkaloid. *Tetrahedron Lett* **1982**, 23 (l), 39–42.

7. E. Valencia, A.J. Freyer, M. Shamma, V. Fajardo. (±)-Nuevamine, an isoindoloisoquinoline alkaloid, and (±)-lennoxamine, an isoindolobenzazepine. *Tetrahedron Lett* **1984**, 25 (6), 599–602.

8. E. Valencia, V. Fajardo, A.J. Freyer, M. Shamma. Magallanesine: an isoindolobenzazocine alkaloid. *Tetrahedron Lett* **1985**, 26 (8), 993–996.

9. V. Kumar, Poonam, A.K. Prasad, V.S. Parmar. Naturally occurring aristolactams, aristolochic acids and dioxoaporphines and their biological activities. *Nat Prod Rep* **2003**, 20 (6), 565–583.

10. D.B. Mix, H. Guinaudeau, M. Shamma, H. Guinaudeau, H. Guinaudeau. The aristolochic acids and aristolactams. *J Nat Prod* **1982**, 45 (6), 657–666.

11. M.J. Campello(in part), L. Castedo, D. Dominguez, et al. New oxidized isocularine alkaloids from sarcocapnos plants. *Tetrahedron Lett* **1984**, 25 (51), 5933–5936.

12. P. Jayaraj, R. Krishnamoorthy, P. Adhikari, et al. Isoindolinone Derivatives: Synthesis, In Vitro Anticancer, Antioxidant, and Molecular Docking Studies. *ChemistrySelect* **2025**, 10 (15), e202500106.

13. Y.S. Yazıcıoğlu, Ş. Elmas, Z. Kılıç, et al. Synthesis of Novel Isoindolinones: Carbonic Anhydrase Inhibition Profiles, Antioxidant Potential, Antimicrobial Effect, Cytotoxicity and Anticancer Activity. *J Biochem Mol Toxicol* **2025**, 39 (4), e70261.

14. L.A. Sorbera, P.A. Leeson, J. Silvestre, J. Castañer. Pagoclone. Anxiolytic GABa-A/BZD site partial agonist. *Drugs Future* **2001**, 26 (7), 651–657.

15. Z. HUSSEIN, D.J. MULFORD, B.A. BOPP, G.R. GRANNEMAN. Stereoselective pharmacokinetics of pazinaclone, a new non-benzodiazepine anxiolytic, and its active metabolite in healthy subjects. *Br J Clin Pharmacol* **1993**, 36 (4), 357.

16. R. Agarwal, A.D. Sinha, A.E. Cramer, et al. Chlorthalidone for Hypertension in Advanced Chronic Kidney Disease. *N Eng J Med* **2021**, 385 (27), 2507–2519.

17. G.C. Roush, V. Buddharaju, M.E. Ernst, T.R. Holford. Chlorthalidone: Mechanisms of action and effect on cardiovascular events. *Curr Hypertens Rep* **2013**, 15 (5), 514–521.

18. S.H. Zhang, C.Y. Wang, Z.Z. Jiang, et al. Synthesis and Blocking Activities of Isoindolinone- and Isobenzofuranone-Containing Phenoxylalkylamines as Potent α1-Adrenoceptor Antagonists. *Chem Pharm Bull* **2011**, 59 (1), 96–99.

19. W. Kobinger, C. Lillie. Falipamil (AQ-A 39) and UL-FS 49. *Cardiovasc Drug Rev* **1988**, 6 (1), 35–53.

20. S. Ito, Y. Hirata, Y. Nagatomi, et al. Discovery and biological profile of isoindolinone derivatives as novel metabotropic glutamate receptor 1 antagonists: A potential treatment for psychotic disorders. *Bioorg Med Chem Lett* **2009**, 19 (18), 5310–5313.

21. T.R. Belliotti, W.A. Brink, S.R. Kesten, et al. Isoindolinone enantiomers having affinity for the dopamine D4 receptor. *Bioorg Med Chem Lett* **1998**, 8 (12), 1499–1502.

22. K. Wittstein, M. Rascher, Z. Rupcic, et al. Corallocins A-C, Nerve Growth and Brain-Derived Neurotrophic Factor Inducing Metabolites from the Mushroom Hericium coralloides. *J Nat Prod* **2016**, 79 (9), 2264–2269.

23. P. Tapley, F. Lamballe, M. Barbacid. K252a is a selective inhibitor of the tyrosine protein kinase activity of the trk family of oncogenes and neurotrophin receptors. *Oncogene* **1992**, 7 (2), 371–381.

24. R. Fröde, C. Hinze, I. Josten, et al. Isolation and synthesis of 3,4-bis(indol-3-yl)pyrrole-2,5-dicarboxylic acid derivatives from the slime mould Lycogala epidendrum. *Tetrahedron Lett* **1994**, 35 (11), 1689–1690.

25. R. Bonjouklian, T.A. Smitka, L.E. Doolin, et al. Tjipanazoles, new antifungal agents from the blue-green alga Tolypothrix tjipanasensis. *Tetrahedron* **1991**, 47 (37), 7739–7750.

26. N.A.L. Pereira, Â. Monteiro, M. Machado, et al. Enantiopure Indolizinoindolones with in vitro Activity against Blood- and Liver-Stage Malaria Parasites. *ChemMedChem* **2015**, 10 (12), 2080–2089.

27. T.R. Belliotti, W.A. Brink, S.R. Kesten, et al. Isoindolinone enantiomers having affinity for the dopamine D4 receptor. *Bioorg Med Chem Lett* **1998**, 8 (12), 1499–1502.

28. D.A. Skvortsov, M.A. Kalinina, I. V. Zhirkina, et al. From Toxicity to Selectivity: Coculture of the Fluorescent Tumor and Non-Tumor Lung Cells and High-

Throughput Screening of Anticancer Compounds. *Front Pharmacol* **2021**, 12, 713103.

29. C. Chantana, U. Sirion, P. Iawsipo, J. Jaratjaroonphong. Short Total Synthesis of (±)-Gelliusine e and 2,3′-Bis(indolyl)ethylamines via PTSA-Catalyzed Transindolylation. *J Org Chem* **2021**, 86 (19), 13360–13370.

30. D.M. Roll, C.M. Ireland, H.S.M. Lu, J. Clardy. Fascaplysin, an Unusual Antimicrobial Pigment from the Marine Sponge Fascaplysinopsis sp. *J Org Chem* **1988**, 53 (14), 3276–3278.

31. T.I. Oh, Y.M. Lee, T.J. Nam, et al. Fascaplysin Exerts Anti-Cancer Effects through the Downregulation of Survivin and HIF-1α and Inhibition of VEGFR2 and TRKA. *Int J Mol Sci* **2017**, 18 (10), 2074.

32. I. Bryukhovetskiy, I. Lyakhova, P. Mischenko, et al. Alkaloids of fascaplysin are effective conventional chemotherapeutic drugs, inhibiting the proliferation of C6 glioma cells and causing their death in vitro. *Oncol Lett* **2017**, 13 (2), 738–746.

33. T.A. Johnson, L. Milan-Lobo, T. Che, et al. Identification of the First Marine-Derived Opioid Receptor “Balanced” Agonist with a Signaling Profile That Resembles the Endorphins. *ACS Chem Neurosci* **2017**, 8 (3), 473–485.

34. E. Ampofo, T. Später, I. Müller, et al. The Marine-Derived Kinase Inhibitor Fascaplysin Exerts Anti-Thrombotic Activity. *Mar Drugs* **2015**, 13 (11), 6774–6791.

35. S. Manda, S. Sharma, A. Wani, et al. Discovery of a marine-derived bis-indole alkaloid fascaplysin, as a new class of potent P-glycoprotein inducer and establishment of its structure–activity relationship. *Eur J Med Chem* **2016**, 107, 1–11.

36. W. Gul, M.T. Hamann. Indole alkaloid marine natural products: An established source of cancer drug leads with considerable promise for the control of parasitic, neurological and other diseases. *Life Sci* **2005**, 78 (5), 442–453.

37. G. Kirsch, G.M. Köng, A.D. Wright, R. Kaminsky. A New Bioactive Sesterterpene and Antiplasmodial Alkaloids from the Marine Sponge Hyrtios cf. erecta. *J Nat Prod* **2000**, 63 (6), 825–829.

38. S. Mangalaraj, C.R. Ramanathan. Construction of tetrahydro-β-carboline skeletons via Brønsted acid activation of imide carbonyl group: syntheses of indole alkaloids (±)-harmicine and (±)-10-desbromoarborescidine-A. *RSC Adv* **2012**, 2 (33), 12665–12669.

CHAPTER 6. CONCLUSIONS

I. We have synthesised a family of rigid indole-imidazole using the previously described reaction of tryptamines with diazadialkenes, followed by a palladium-catalysed coupling reaction.

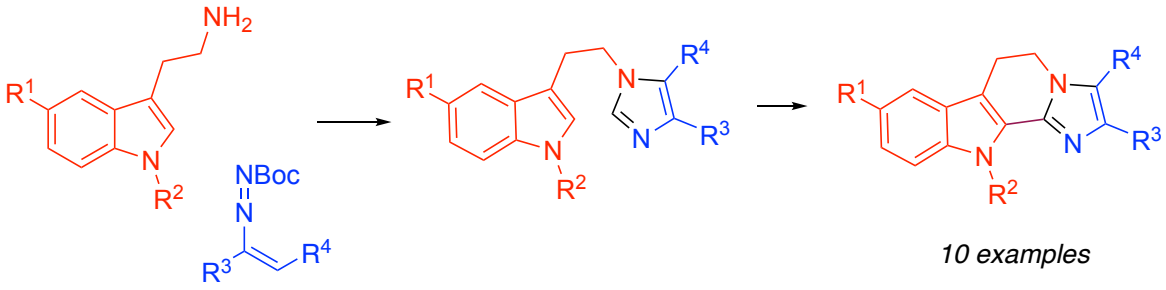

10 examples

II. We have evaluated the biological activity of these compounds, finding one compound with similar activity to the lead compound.

III. The Van Leusen reaction has been evaluated as an alternative for the synthesis of rigid indole-imidazole substituents to increase the variability in R^3 and R^4.

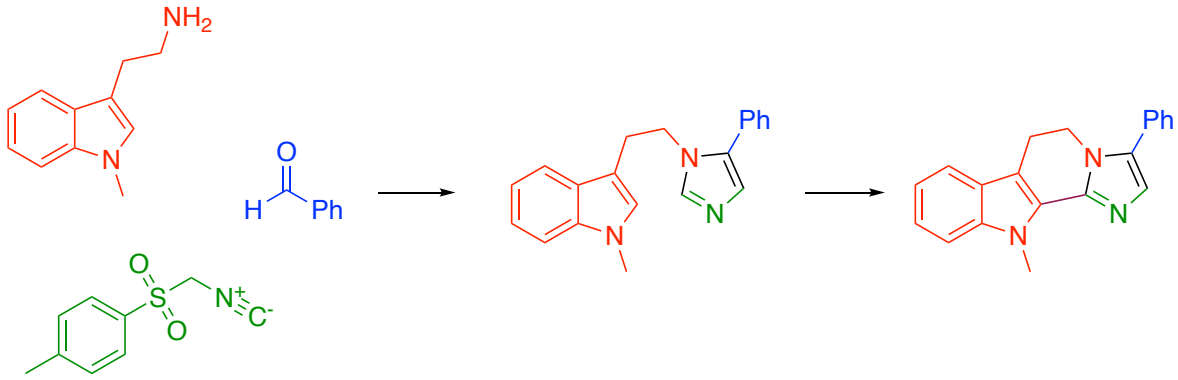

IV. A new synthetic route has been developed and optimised for the synthesis of 3-indolylethylimidazole derivatives, using three different methodologies, providing broader opportunities for introducing structural diversity in the imidazole ring of our fused systems.

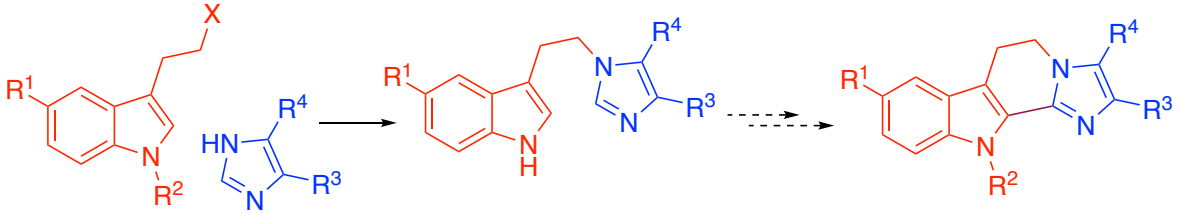

18 examples

V. A wide range of bisindolic compounds from different families of bis (3-indolyl)methanes have been synthesised, including amines, amides, carboxylic acids, esters, glycosylated or tetrasubstituted derivatives.

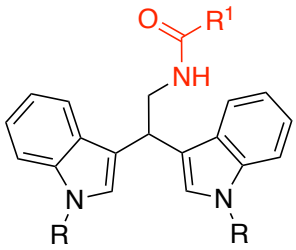

14 examples

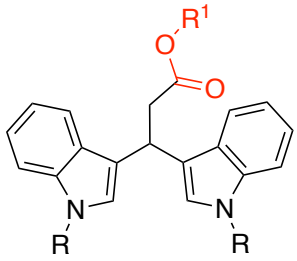

5 examples

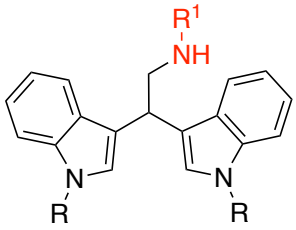

3 examples

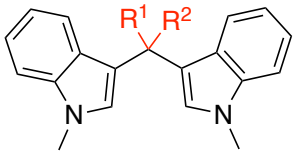

3 examples

VI. These bisindolic compounds have been biologically evaluated against leishmaniasis, providing promising results for some of the derivatives.

VII. Indole-isoindolinone derivatives have been synthesised from phthalic anhydride for future biological evaluation against leishmaniasis. The mechanism of this reaction has been used effectively to synthesise three different families of compounds, all of them containing a quaternary stereocenter: disubstituted compounds, imines and alkoxy derivatives.

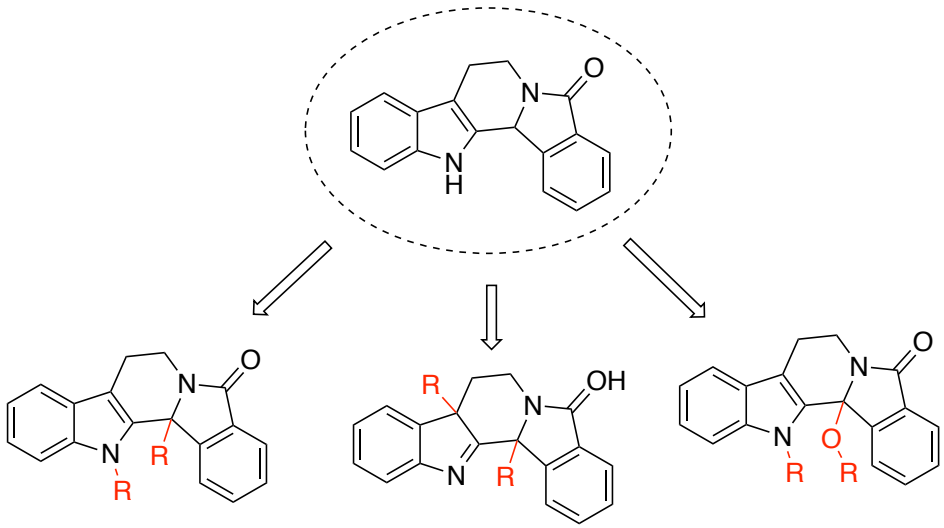

ANNEX

REPRESENTATIVE EXAMPLES OF NMR SPECTRA

CHAPTER 3: INDOLE-IMIDAZOLES

Methyl 1-(2-(5-chloro-1-methyl-1H-indol-3-yl)ethyl)-4-propyl-1*H*-imidazole-5-carboxylate (**66b**)

Methyl 8-chloro-11-methyl-2-propyl-6,11-dihydro-5*H*-imidazo[1',2':1,2]pyrido[3,4-*b*]indole-3-carboxylate (**65b**)

CHAPTER 4: BISINDOLES

2,2-di(1*H*-indol-3-yl)ethan-1-amine (**88b**)

N-(2,2-bis(1-methyl-1*H*-indol-3-yl)ethyl)-4-methoxybenzamide (**89af**)

Methyl 2,2-bis(1-methyl-1*H*-indol-3-yl)acetate (**91a**)

2,2-bis(1-methyl-1*H*-indol-3-yl)propanoic acid (**93a**)

CHAPTER 5: INDOLE-ISOINDOLINONES

13,13b-Diallyl-7,8,13,13b-tetrahydro-5*H*-benzo[1,2]indolizino[8,7-*b*]indol-5-one (**119f**)

8a,13b-Diallyl-7,8,8a,13b-tetrahydro-5*H*-benzo[1,2]indolizino[8,7-*b*]indol-5-one (**122f**)

Methyl 1-(2-(5-chloro-1-methyl-1H-indol-3-yl)ethyl)-4-propyl-1*H*-imidazole-5- carboxylate (**66b**):

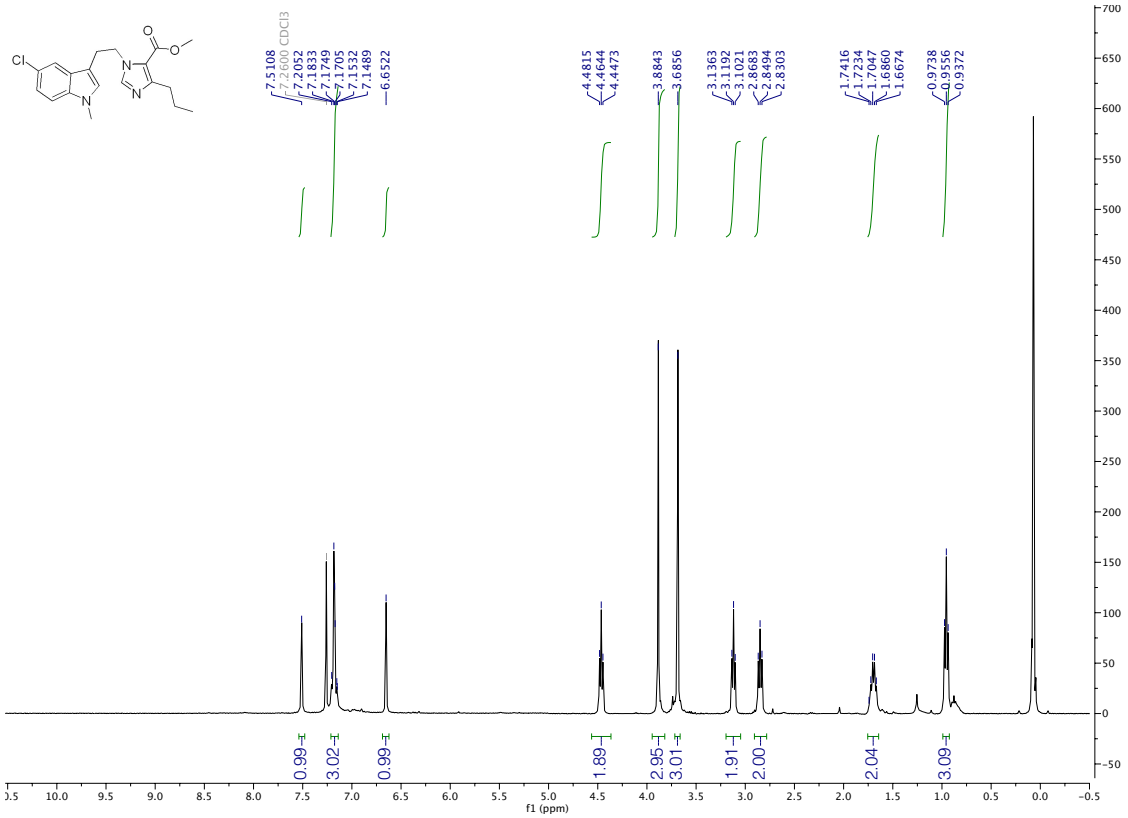

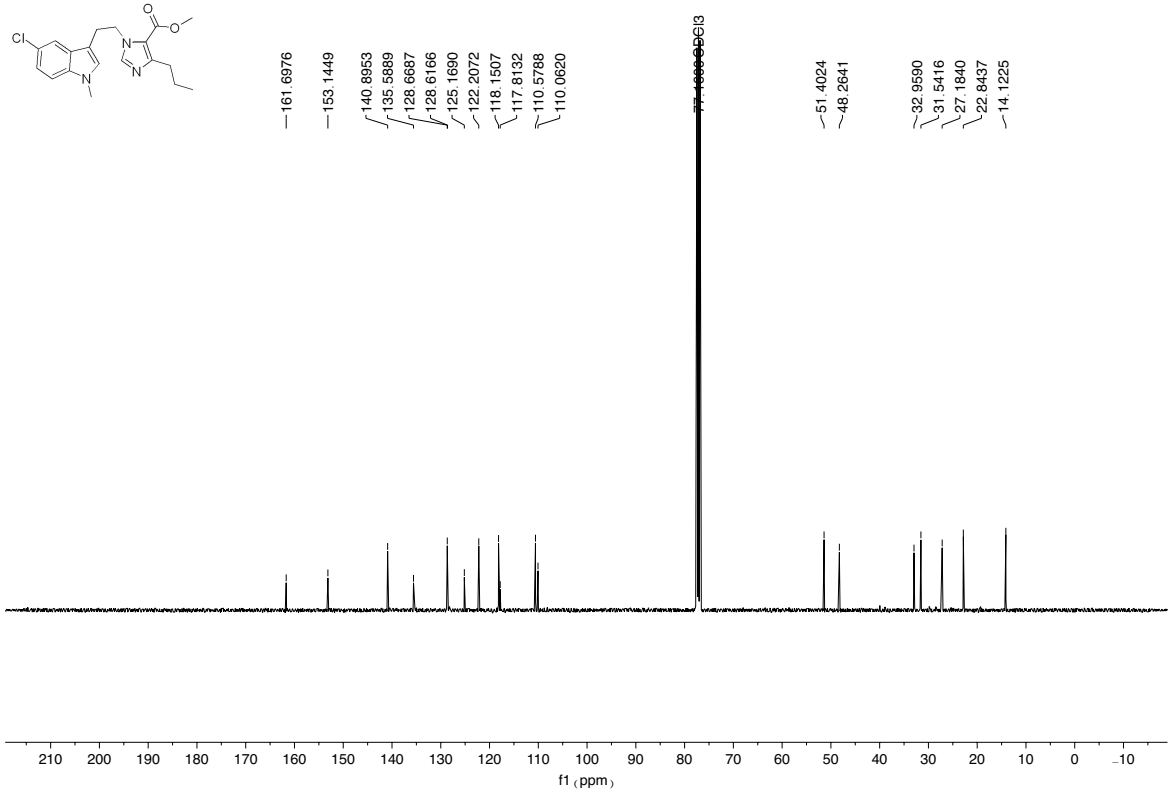

Methyl 8-chloro-11-methyl-2-propyl-6,11-dihydro-5*H*-imidazo[1',2':1,2]pyrido[3,4-*b*]indole-3-carboxylate (**65b**):

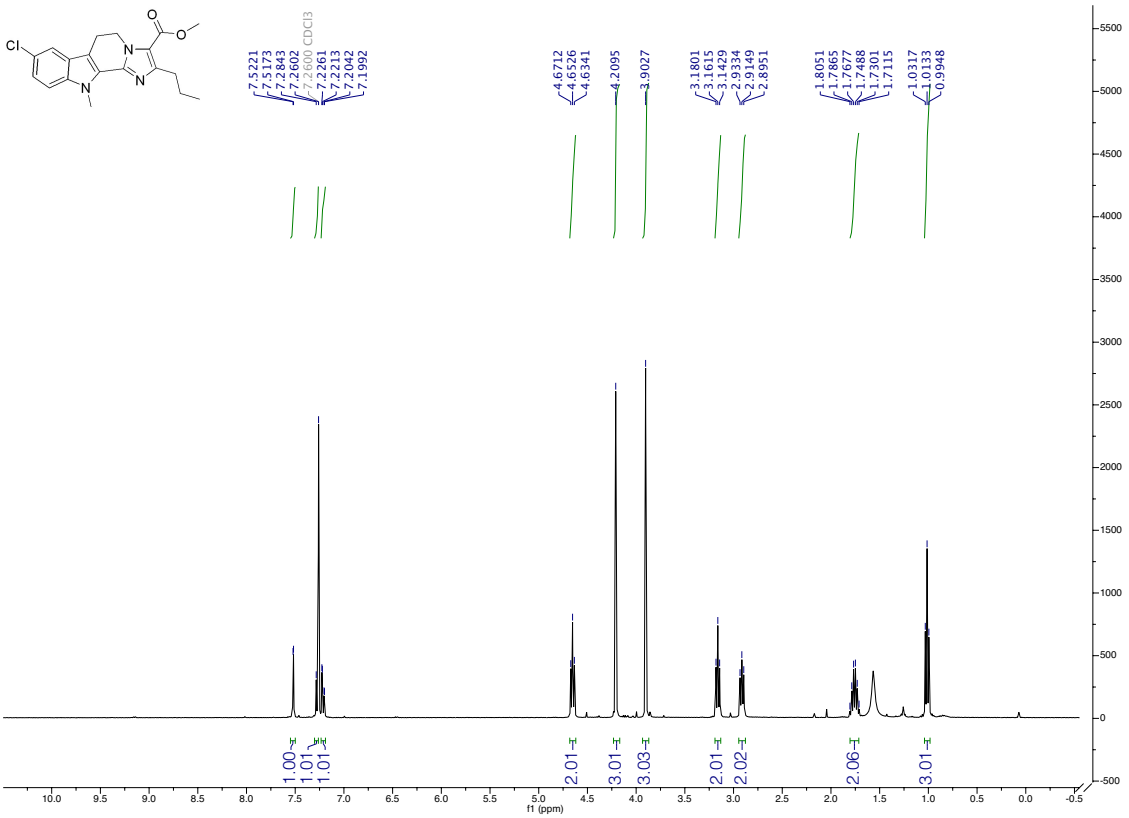

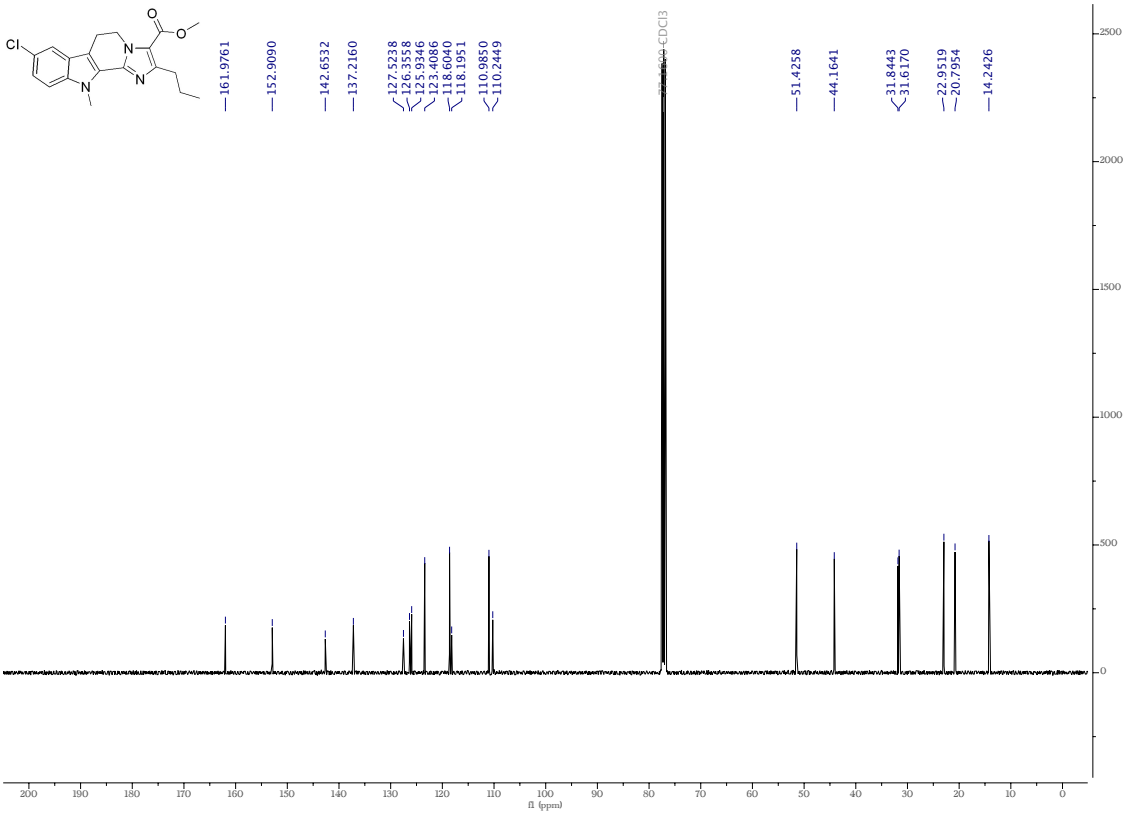

2,2-di(1*H*-indol-3-yl)ethan-1-amine (**88b**):

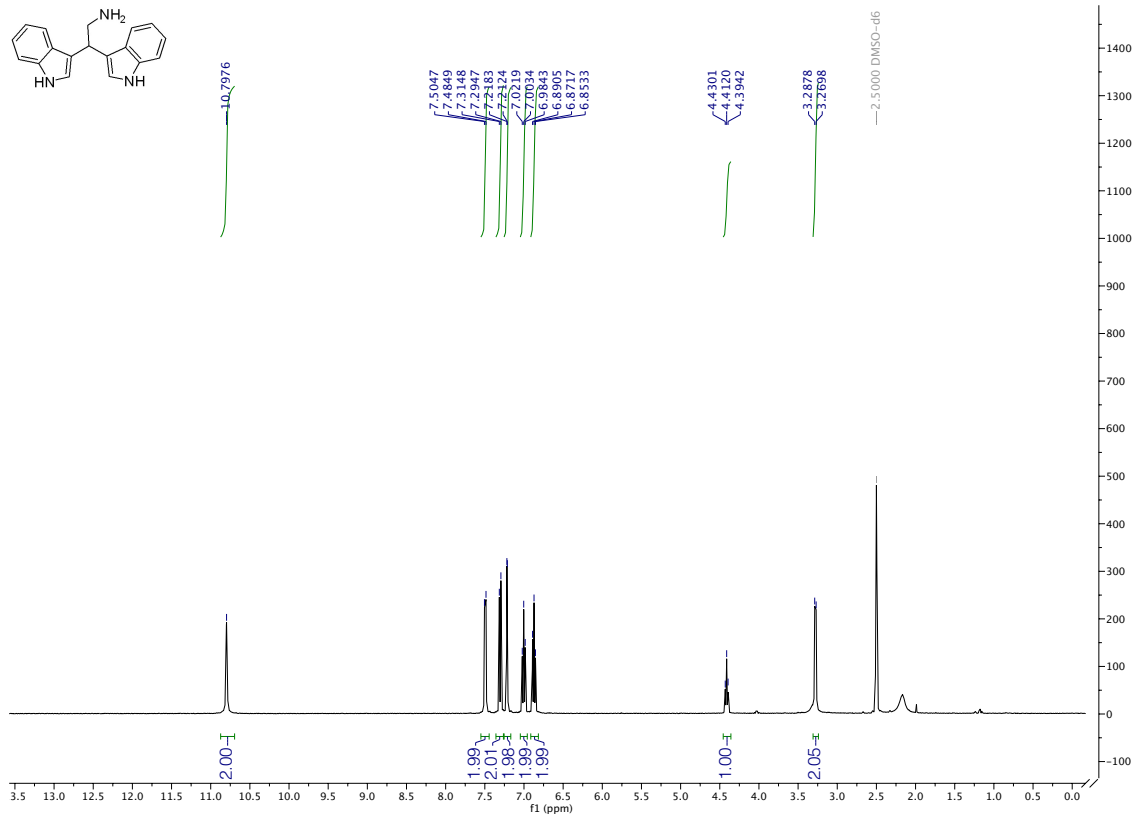

N-(2,2-bis(1-methyl-1*H*-indol-3-yl)ethyl)-4-methoxybenzamide (**89af**):

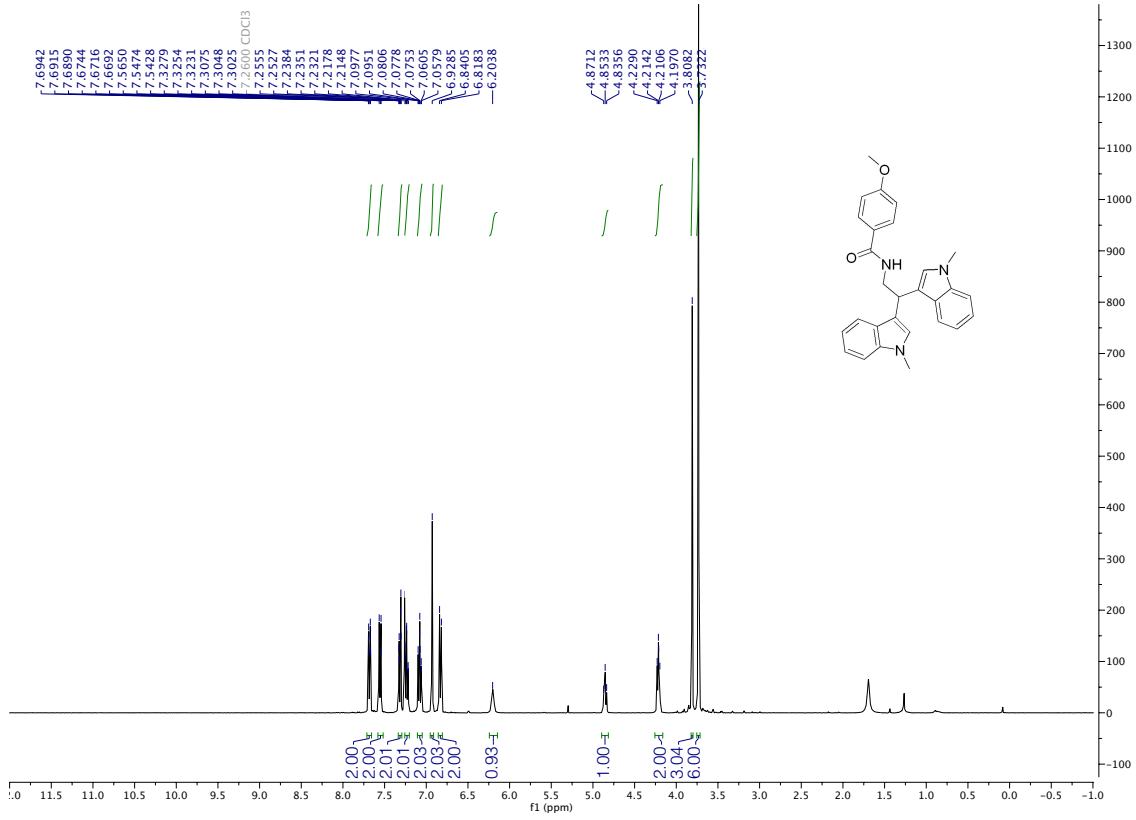

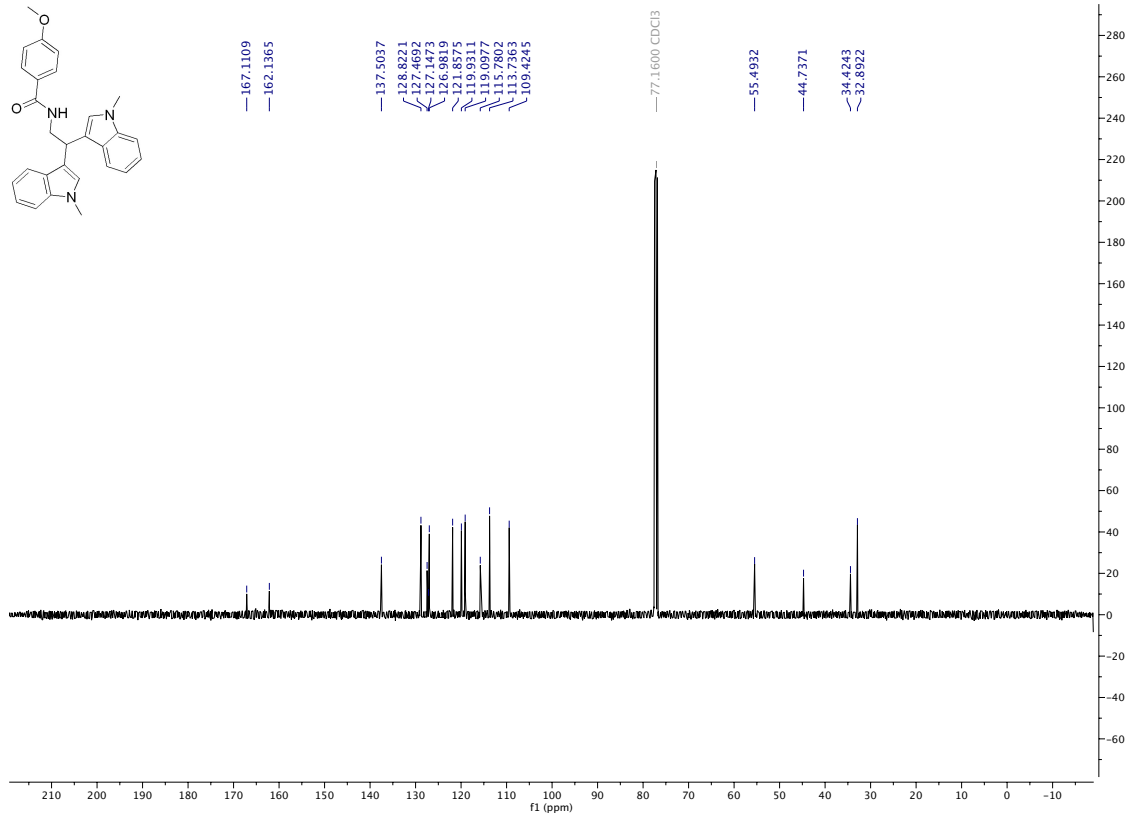

Methyl 2,2-bis(1-methyl-1*H*-indol-3-yl)acetate (**91a**):

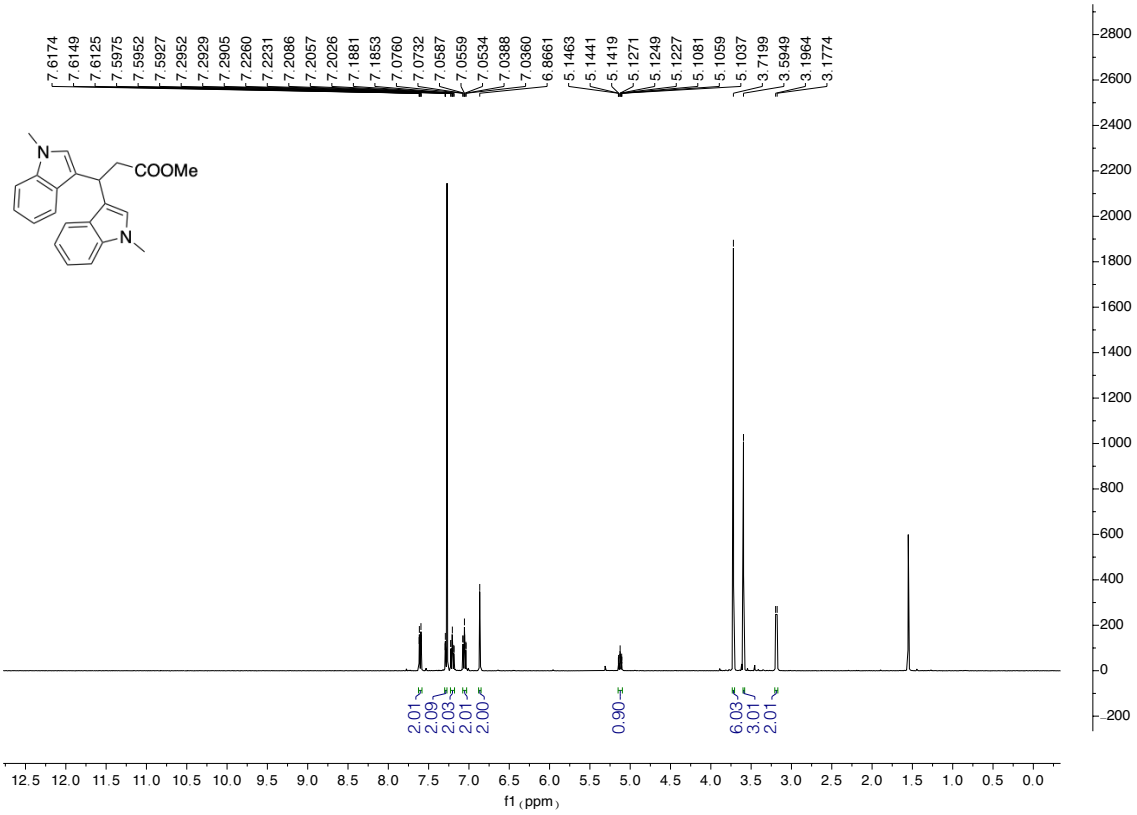

2,2-bis(1-methyl-1*H*-indol-3-yl)propanoic acid (**93a**):

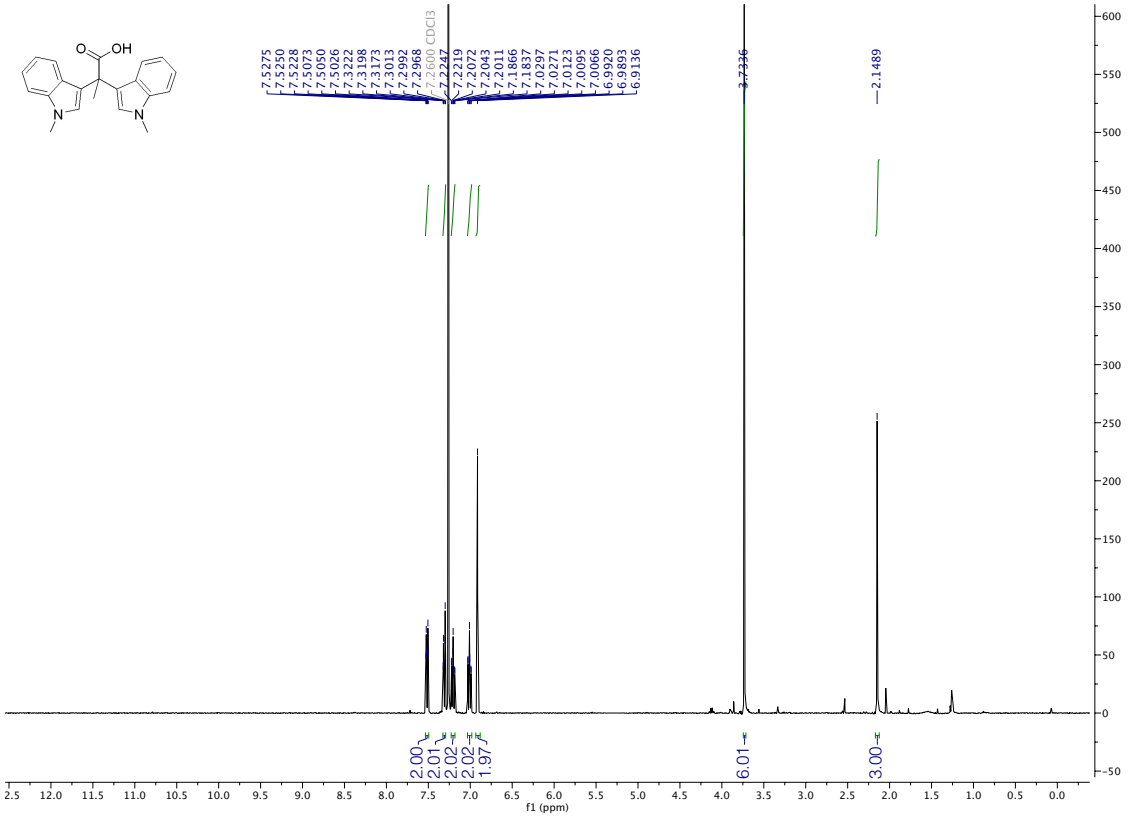

13,13b-Diallyl-7,8,13,13b-tetrahydro-5*H*-benzo[1,2]indolizino[8,7-*b*]indol-5-one (**119f**):

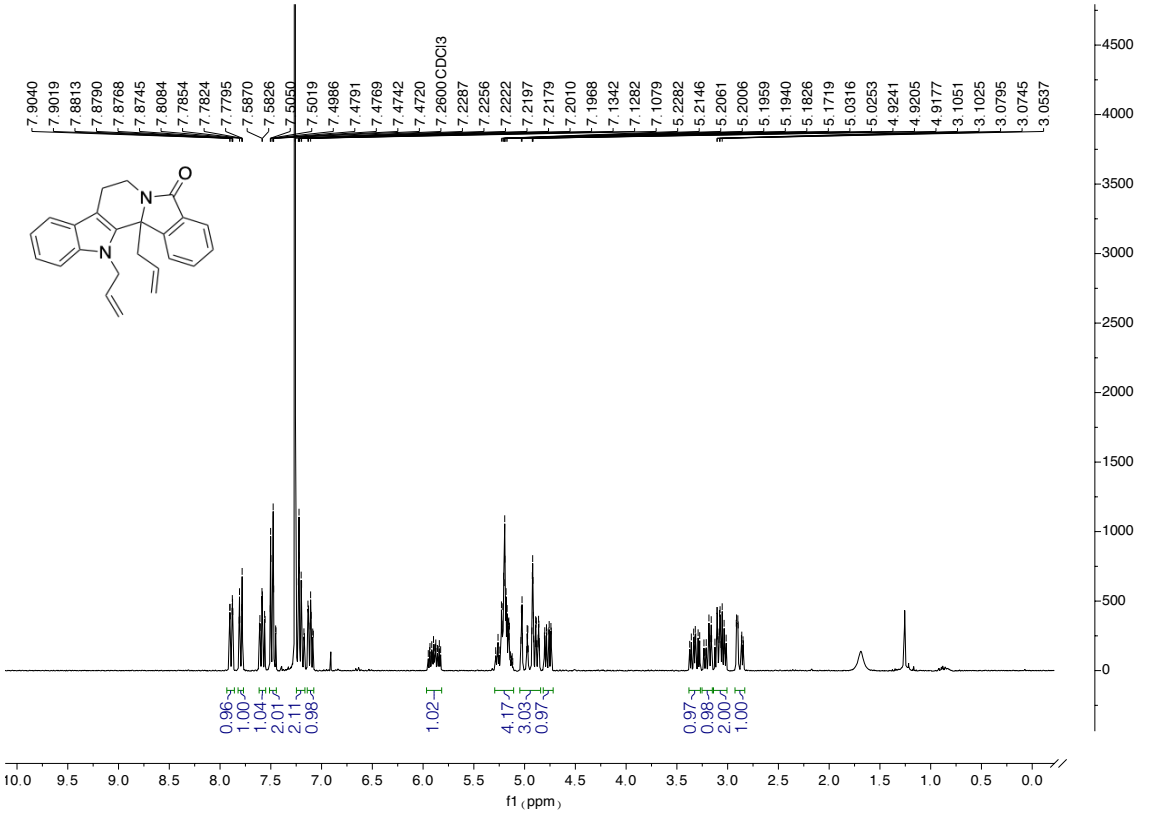

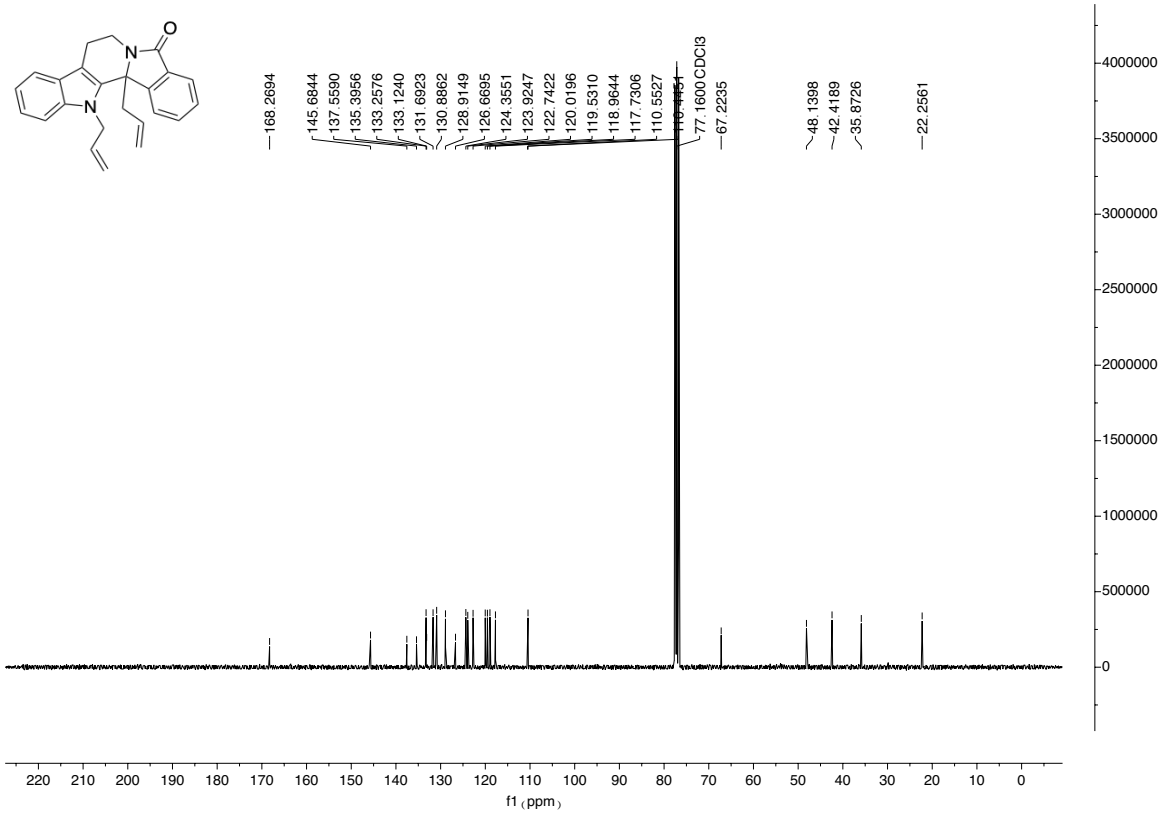

8a,13b-diallyl-7,8,8a,13b-tetrahydro-5*H*-benzo[1,2]indolizino[8,7-*b*]indol-5-one (**122f**):

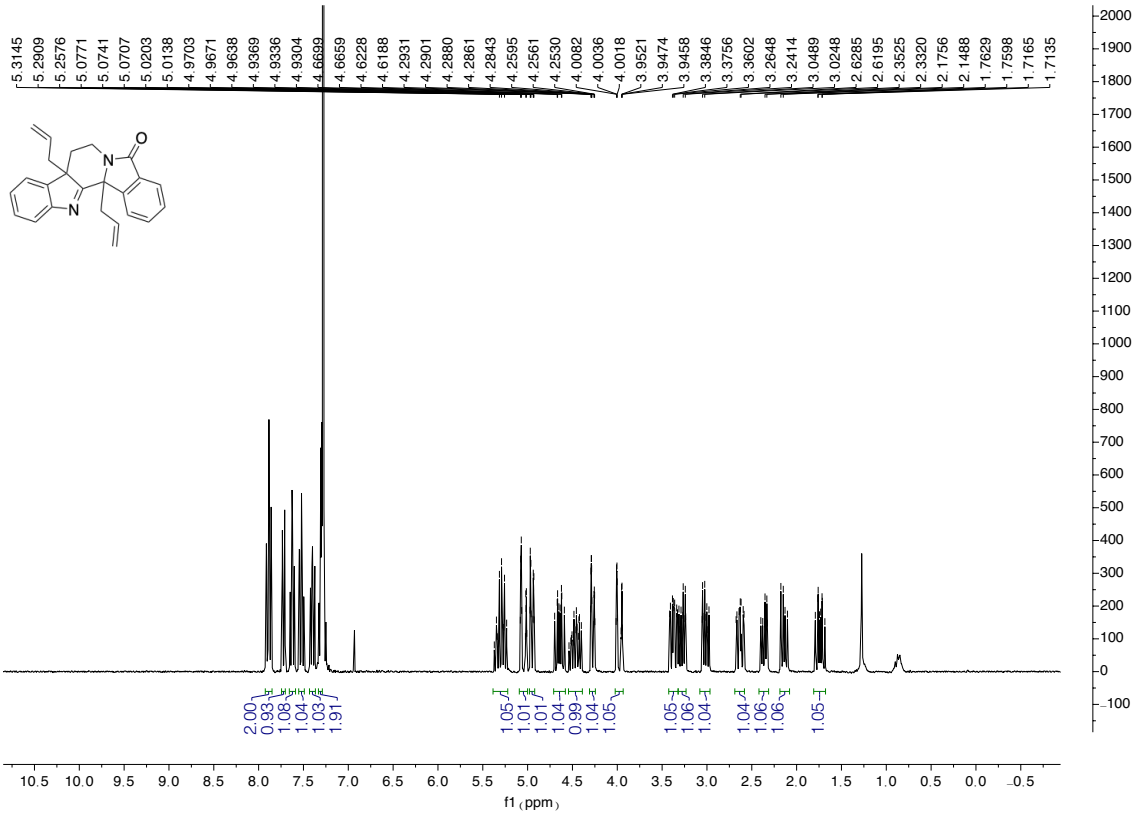

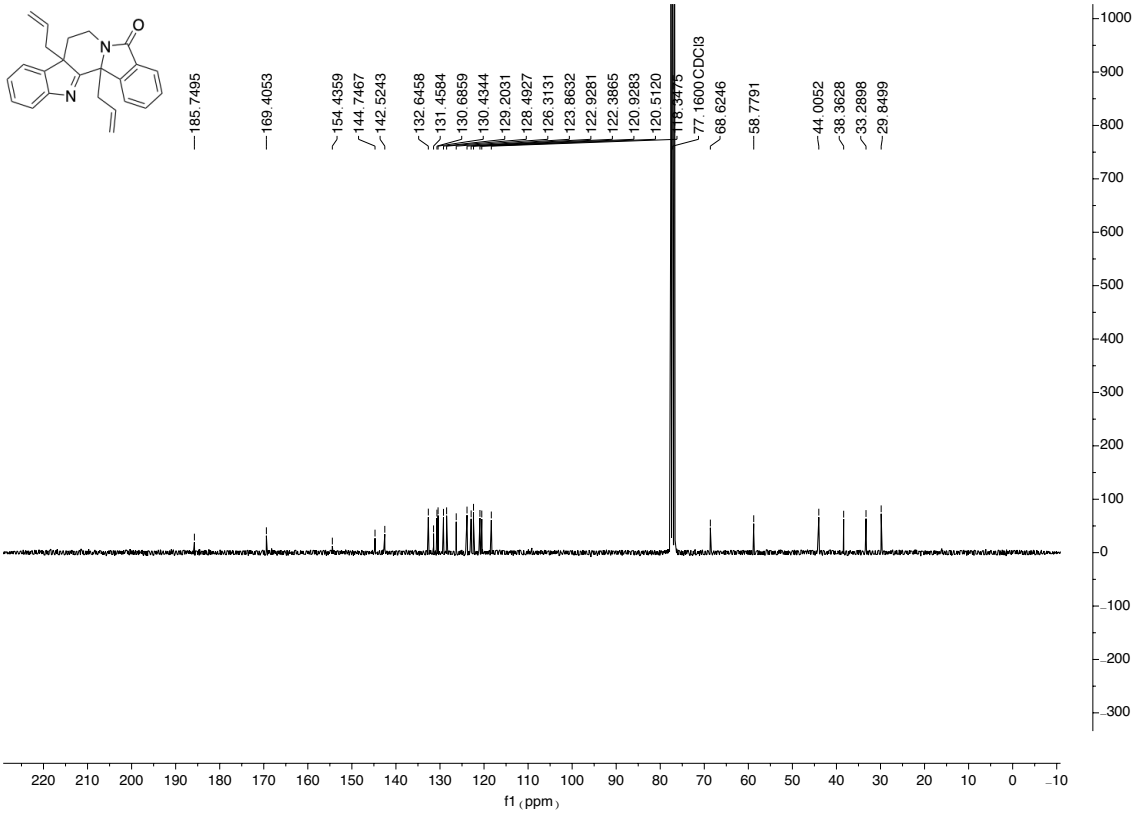

13b-Ethoxy-13-ethyl-7,8,13,13b-tetrahydro-5*H*-benzo[1,2]indolizino[8,7-*b*]indol-5-one (**120b**):